

Compendium

of Sopro cameras articles

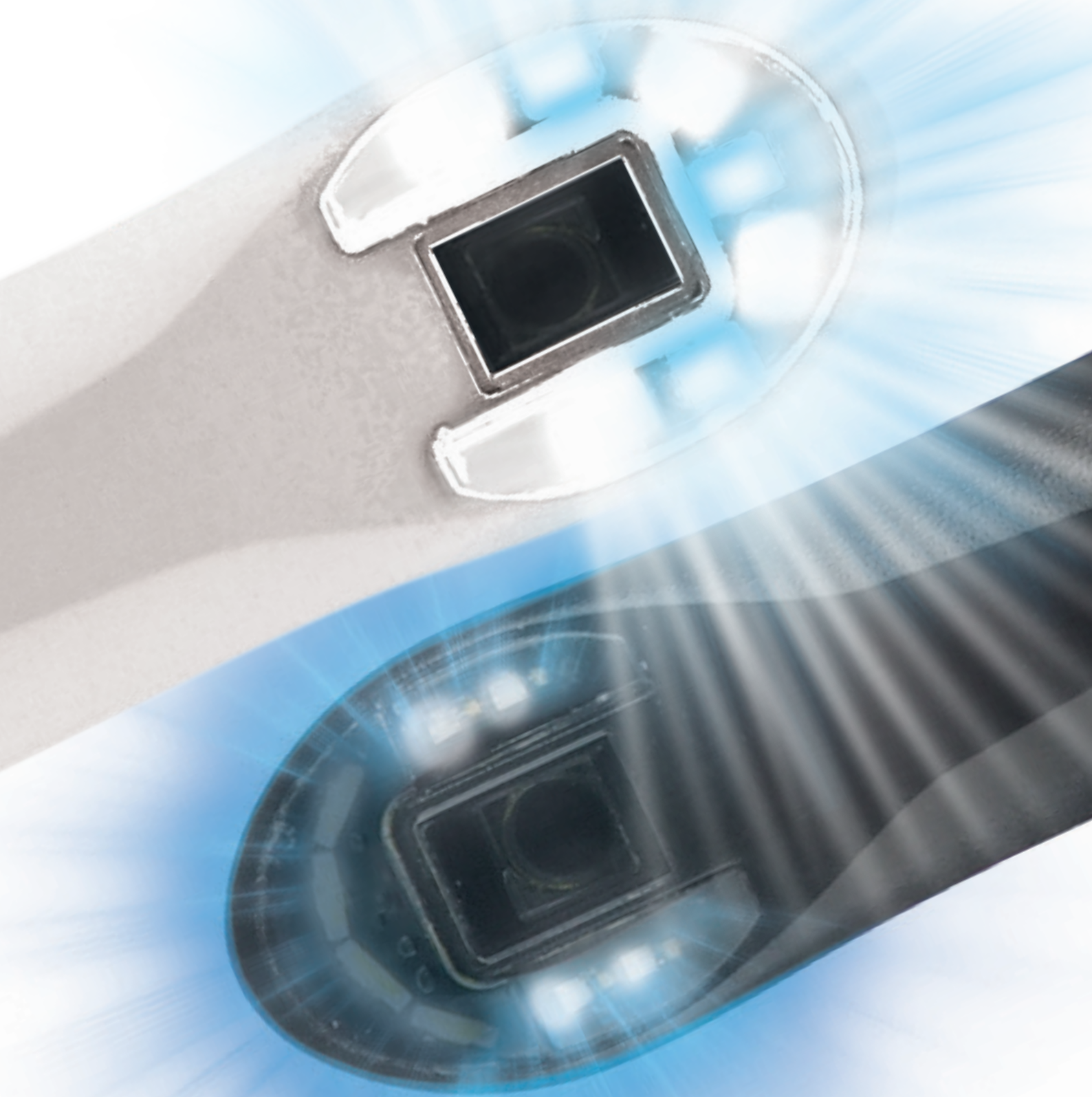


Table of Contents

SOPROLIFE ARTICLES

N° 1. A New Concept in Restorative Dentistry: Light-Induced Fluorescence Evaluator for Diagnosis and Treatment: Part 1 - Diagnosis and Treatment of Initial Occlusal Caries.

E.Terrer, S. Koubi, A. Dionne, G. Weisrock, C. Sarraquigne, A. Mazuir, H. Tassery, in the Journal of Contemporary Dental Practise, 1 November, 2009 **P. 6**

N° 2. A New Concept in Restorative Dentistry: Light-Induced Fluorescence Evaluator for Diagnosis and Treatment: Part 2 - Treatment of Dentinal Caries.

E.Terrer, A. Raskin, S. Koubi, A. Dionne, G. Weisrock, C. Sarraquigne; A. Mazuir; H. Tassery, in the Journal of Contemporary Dental Practise, 1 January 2010..... **P. 18**

N° 3. Naturally aesthetic restorations and minimally invasive dentistry.

G. Weisrock, E. Terrer, G. Couderc, S. Koubi, B. Levallois, D. Manton, H. Tassery, in Journal of Minimum Intervention in Dentistry, 2011 **P. 30**

N° 4. Light induced fluorescence evaluation: A novel concept for caries diagnosis and excavation.

N. Gugnani, IK. Pandit, N. Srivastava, M. Gupta, S. Gugnani, in Journal of Conservative Dentistry, October-December 2011 **P. 42**

N° 5. Molecular structural analysis of carious lesions using micro-Raman spectroscopy.

B. Levallois, E. Terrer, I. Panayotov, H. Salehi, H. Tassery, P. Tramini, F. Cuisinier, in European Journal of Oral sciences, June 2012 **P. 48**

N° 6. In vitro investigation of fluorescence of carious dentin observed with a Soprolife® camera.

I. Panayotov, E. Terrer, H. Salehi, H. Tassery, J. Yachouh, F. J. G.Cuisinier, B. Levallois, in Clin Oral Invert, 10 June, 2012..... **P. 65**

N° 7. Multiphoton imaging of the dentine-enamel junction.

T. Cloitre, I. Panayotov, H. Tassery, C. Gergely, B. Levallois, F. J. G. Cuisinier, in Journal of BioPhotonics, 23 July, 2012..... **P. 72**

N° 8. Suivi orthodontique et concept LIFEDT - La fluorescence au service de la prophylaxie

Michel Blique, Hervé Tassery, Sophie Grosse, Jean-Marc Bondy, dans l'Information Dentaire, n°14, avril 2012..... **P. 81**

N° 9. Functional mapping of human sound and carious enamel and dentin with Raman pectroscopy.

H. Salehi, E. Terrer, I. Panayotov, B. Levallois, B. Jacquot, H. Tassery, F. J. G. Cuisinier, in Journal of BioPhotonics, 20 September, 2012 **P. 86**

N° 10. Use of new minimum intervention dentistry technologies in caries management.

H. Tassery, B. Levallois, E. Terrer, D.J. Manton, M. Otsuki, S. Koubi, N. Gughani, I. Panayotov, B. Jacquot, F. J. G. Cuisinier, P. Rechmann, in Australian Dental Journal, 2013..... **P. 97**

N° 11. Performance of laser fluorescence devices and visual examination for the detection of occlusal caries in permanent molars.

P. Rechmann, D. Charland, B. M. T. Rechmann, J. D. B. Featherstone, in Journal of Biomedical Optics, March 2013..... **P. 116**

N° 12. Gestion thérapeutique de lésions carieuses proximales sur dents adjacentes.

H. Tassery, A. Slimani, A. Lavenant, E. Terrer, dans Réalités Cliniques, Vol.24, 2013..... **P. 133**

N° 13. Decay diagnosis camera: is it a valid alternative?

Kosmas Tolidis, DDS, Christina Boutsouki, DDS, in The international journal of microdentistry **P. 140**

N° 14. In-Vivo Occlusal Caries Prevention by Pulsed CO2-Laser and Fluoride Varnish Treatment—A Clinical Pilot Study

Peter Rechmann, DDS, PhD, Daniel A. Charland, DDS, Beate M.T. Rechmann, Charles Q. Le, and John D.B. Featherstone, MSc, PhD, in Lasers in Surgery and Medicine **P. 145**

N° 15. Performance of a fluorescence device against conventional caries diagnostic methods

K. Tolidis, E. Parasidi, C. Boutsouki, in CED - IADR 2013..... **P. 154**

N° 16. Détection de la carie dentaire : il y a-t-il quelque chose de nouveau ?

Prof. David Manton, in DTI 2013..... **P. 155**

N° 17. Evaluation of Caries Dentin Using Light-Induced Fluorescence: a case report

Lecturer Sebnem Erol, PhD Student Hanife Kamak, Prof. Hülya Erten, in Journal of Clinical and Diagnostic Research 2014..... **P. 158**

N° 18. SOPROLIFE System: An Accurate Diagnostic Enhancer

Prof. Mona Zeitouny, Prof. Mireille Feghali, Prof. Assaad Nasr, Prof. Philippe Abou-Samra, Prof. Nadine Saleh, Prof. Denis Bourgeois, Prof. Pierre Farge, in The Scientific World Journal volume 2014..... **P. 160**

N° 19. Porphyrin involvement in redshift fluorescence in dentin decay

A. Slimani, I. Panayotov, B. Levallois, T. Cloitre, C. Gergely, N. Bec, C. Larroque, H Tassery, F. Cuisinier, in SPIE Belgium 2014 **P. 169**

N° 20. Méthodologie du diagnostic en cariologie Apport des nouvelles technologies

PH. Tassery, A. Slimani, M. Acquaviva, C. Cautain, M.N. Beverini, E. Terrer, in Réalités Cliniques. Vol. 25, n°2, 2014..... **P. 177**

SOPROCARE ARTICLES

N° 1. Democratised fluorescence.

H. Tassery, in L'information Dentaire, 24 October 2012 **P. 187**

N° 2. Contribution of fluorescence and selective chromatic amplification in daily preventive dentistry practise.

M. Blique, S. Grosse, in Dental Asia, May/June 2013 **P. 189**

N° 3. SOPROCARE - 450 nm wavelength detection tool for microbial plaque and gingival inflammation - a clinical study.

P. Rechmann^a, Shasan W. Lioub, Beate M.T. Rechmanna, and John D. B. Featherstone^a
^a Dept. of Preventive and Restorative Dental Sciences; ^b Division of Pediatric Dentistry, School of Dentistry, University of California at San Francisco, San Francisco, CA 94143, SPIE Vol.8929
February 2014 **P. 193**

N° 4. SOPROCARE prophylaxis camera: improved patient communication leads to so much more.

Todd Snyder, DDS in Dental Learning, May/June 2013 **P. 200**

N° 5. La videocamera intraorale, un valido supporto nella pratica clinica.

Dr Gianna Maria Nardi, Dr Fabio Scarano Catanzaro in Hygiene Tribune Italian Edition, April 2014 **P. 203**

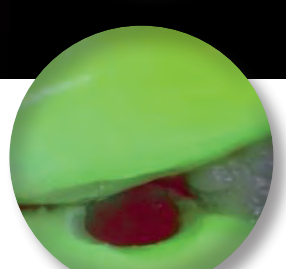
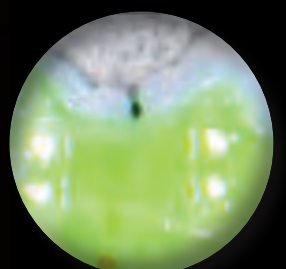
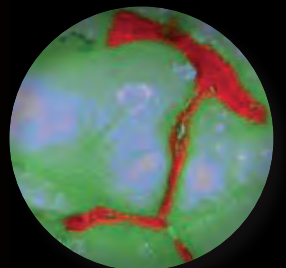
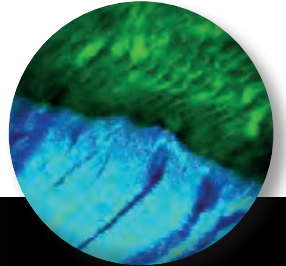
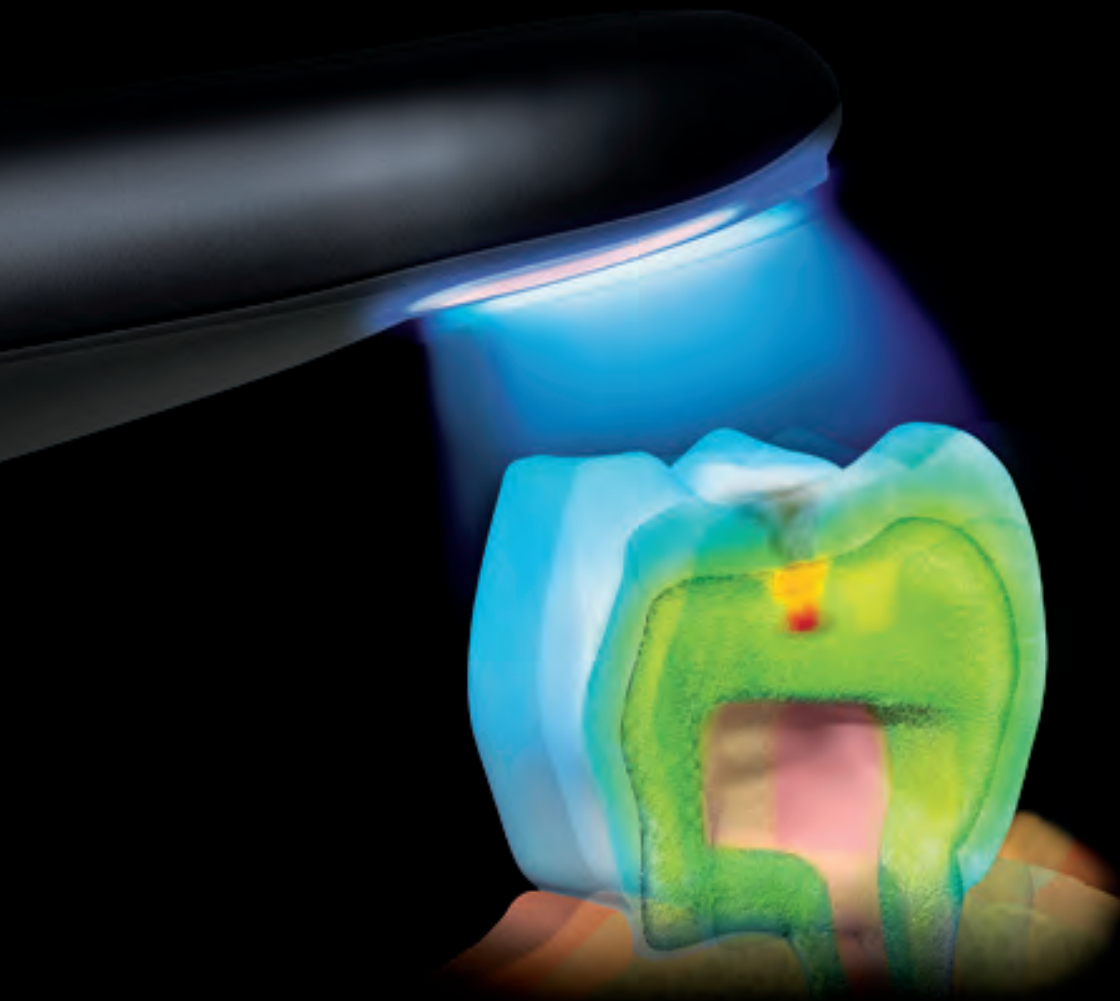
N° 6. Get your hygiene patients «Off the fence»!

M. J. Rosenberg - DDS, Ms J. Papanier - RDH, LLA and Ms B. ABDULLAH - RDH, LLA
in Dentistry Today, 2014 **P. 205**

N° 7. Performance of a light fluorescence device for the detection of microbial plaque and gingival inflammation

Peter Rechmann¹ & Shasan W. Liou² & Beate M. T. Rechmann¹ & John D. B. Featherstone¹
in Springer-Verlag Berlin Heidelberg (outside the USA) 2015, 2015..... **P. 209**

Soprolife articles





A New Concept in Restorative Dentistry: Light-Induced Fluorescence Evaluator for Diagnosis and Treatment: Part 1 – Diagnosis and Treatment of Initial Occlusal Caries

Elodie Terror, DDS; Stephen Koubi, DDS; Alexandro Dionne; Gauthier Weisrock, DDS; Caroline Sarraquigne; Alain Mazuir; Hervé Tassery, DDS, MS, PhD

Abstract

Aim: The objective of this *in vivo* experiment is to propose an innovative therapeutic concept using a light-induced fluorescence evaluator for diagnosis and treatment (LIFEDT) that is based on the imaging and autofluorescence of dental tissues.

Background: Processes with the aim of diagnosing carious lesions in the initial stage with optimum sensitivity and specificity employ a wide variety of technologies, but like the conventional diagnosis tools, they remain either inefficient or too subjective.

Technique: This experiment evaluated a fluorescence light-induced camera that illuminates tooth surfaces within an excitation radiation band of light with a wavelength of 450 nm and facilitates a high magnification image.

Conclusions: An analysis of 50 occlusal grooves revealed three clinical forms of enamel caries: (1) enamel caries on the surface, (2) suspicious grooves with a positive autofluorescent red signal, and (3) suspicious grooves with a neutral fluorescent dark signal. Two decision-making diagrams were proposed in accordance with international recommendations for preventive dentistry, but modified as a result of the accurate information obtained with this new LIFEDT device.

Clinical Significance: The lighting of suspect occlusal grooves with the SoproLife® camera



enables observation of any variations in the optical properties to refine a caries diagnosis and facilitates more than a 50x magnification of occlusal groove anatomy to provide additional information on the carious potential of the tooth surface.

Keywords: Diagnosis, autofluorescence, LIFEDT concept, minimally invasive dentistry.

Citation: Terror E, Koubi S, Dionne A, Weisrock G, Sarraquigne C, Mazuir A, Tassery H. A New Concept in Restorative Dentistry: Light-Induced

Fluorescence Evaluator for Diagnosis and Treatment: Part 1 – Diagnosis and Treatment of Initial Occlusal Caries. J Contemp Dent Pract [Internet]. 2009 Nov; 10(6):086-094. Available from: <http://www.thejcdp.com/journal/view/volume10-issue6-terror>.

Background

Processes with the aim of diagnosing carious lesions in the initial stage with optimum sensitivity and specificity employ a variety of technologies such as laser,^{1,2} fluorescence and autofluorescence,^{3,4,5} electric current, tomographic imaging, and image processing.⁶ Despite the availability of these technologies, their high cost, size, excessive variable sensitivity, and specificity⁷ have prohibited their use on a daily basis like conventional diagnosis tools such as film or digital radiography. These different means of analysis are also dependent on the experience of clinicians and their practice of viewing magnified images using a magnifying glass or microscope.⁸ Conventional diagnosis strategies for caries detection like visual observation or probing with a dental instrument are unfortunately based on subjective criteria such as lesion color and texture. There is a profound need for a fluorescence device that combines magnification and amplification of the visual signal to assist clinicians with the assessment of tooth structure. Defining new diagnostic and treatment strategies and related instrumentation is consistent with the

principles of contemporary restorative dentistry. These principles call for a comprehensive patient approach in terms of caries risk assessment, diagnosis, and appropriate therapies that are consistent with the concepts of minimally invasive dentistry (MID), or minimal Intervention (MI), terms accepted by the Federation Dentaire Internationale in 2000.⁹

Proper caries management dictates that a clinician conduct an analysis of the cariological context of the patient, or their caries risk level, over time. Mount et al.¹⁰ defined caries progression on the basis of lesion site and stage on a scale from 0 to 4. Pitts^{6,11} described the progression of all the stages of dental caries in addition to six levels of severity with the International System for Caries Detection and Assessment (ICDAS) using an iceberg metaphor. Caries risk can be defined in the form of a Cariogram with three levels of caries risk¹² or in accordance with the Caries Management by Risk Assessment (CAMBRA) system¹³ associated with the ICDAS II, which defines four levels of caries risk and describes ad hoc therapies.^{13,14}

The objective of this *in vivo* experiment is to propose an innovative therapeutic concept compliant with international recommendations using a light-induced fluorescence evaluator for diagnosis and treatment (LIFEDT) that is based on the imaging and autofluorescence of dental tissues.

Technique

The SoproLife® Camera

Banerjee et al.³⁻⁵ described an optical property of dental tissues when they are illuminated at a certain wavelength, or autofluorescence. Based on this principle, an experimental LED camera (SoproLife®) was developed and clinically validated in the Department of Restorative Dentistry of the University of the Mediterranean in Marseille, France. The patented technology was developed by Sopro-Acteon Imaging in La Ciotat, France. The technique utilizes an LED camera that can illuminate tooth surfaces within a radiation band (wavelength 450 nm with a bandwidth of 20 nm, centered at ± 10 nm around the excitation wavelength) that is situated in the visible domain. This provides an anatomical image superimposed on an autofluorescence

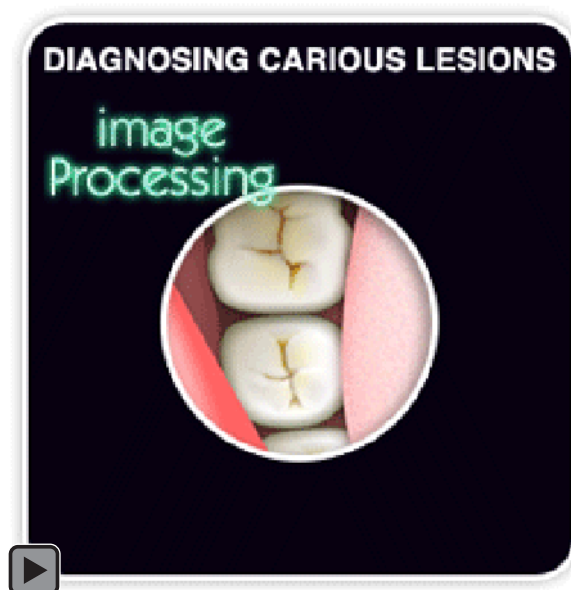




image emitted by the illuminated teeth. This camera can detect and locate differences in density, structure, and/or chemical composition of a biological tissue subjected to continuous lighting in one frequency band while making it generate a fluorescence phenomenon in a second frequency band. The camera is equipped with an image sensor (a 0.25-inch CCD sensor) consisting of a mosaic of pixels covered with filters of complementary colors. The data collected, relating to the energy received by each pixel, enable an image of the tooth to be retrieved. The fluorescence signals corresponding to the more or less damaged parts of a tooth are amplified selectively to accentuate the specificity of the fluorescence images. The wavelength of the autofluorescence signal varies according to the density and chemical composition of the tissue on its surface and subsurface. The different layers of tissue and their characteristics influence its response, the same as for material deposits. As a result, any carious lesion or diseased tissue will be detected by variation in the autofluorescence of its tissues in relation to a healthy area of the same tooth. The camera also provides a magnification range of more than 50x of the tooth surface on a visual screen using three illumination modes: daylight, diagnosis mode, and treatment mode. The images are observed in real time on a big LED screen and can be recorded in a computer using special imaging software (Sopro imaging software Life mode).

The LIFEDT Concept

Except for DIAGNODent (KavoDental, GmbH, Biberach/Riss, Germany), there are only a few

diagnosis tools available for assessment of site 1 stage 0, and 1 or 0 to 3 ICDAS II code lesions that are genuinely usable on a regular basis.^{1,2} These tools provide clinical assistance in the form of an alarm signal in the presence of dentinal caries but have shortcomings in terms of low specificity and false- positive signals. As an alternative, the LIFEDT concept proposes the use of decision-making diagrams in conjunction with the clinical information gathered from the intraoral autofluorescent/LED camera and taking into account international recommendations for caries diagnosis. These diagrams will be discussed later.

The examination of occlusal fissures using a dental mirror and probing should be abolished because it cannot reveal the true complexity, anatomical configuration, and degree of groove fissuration in order to assess the difficulty the patient encounters when attempting to clean them as a part of his or her home care regimen.¹⁵⁻¹⁷ However, a magnification of more than 50x of the occlusal groove anatomy and modifications to the autofluorescence signal via the LED camera produce images of the enamel-dental structures surrounding the groove that provide invaluable information about potential risk of caries infiltration and about the penetration level of the acid front of an advancing lesion. On the other hand, no information is provided via the camera regarding the complex bacterial ecology¹⁸ in terms of lesion composition or interactions.

The LED camera is not a replacement for the clinician's diagnostic capability; it is a device designed to expand the availability of information for the clinician. The camera provides the clinician with a magnified view of occlusal groove anatomy and its complexity, and generates a modified autofluorescent image of carious tissue or hard tissue malformations in relation to an adjacent healthy area of the same tooth.

Methods and Materials

The key principle employed in the use of the SoproLife[®] camera is to observe consistent variation in the enamel-dental tissue autofluorescence in relation to a healthy area of a tooth.

Observation Methods

Without any probing before or after observation, a total of 50 randomly selected dental grooves

Table 1. Distribution of cases of the three forms of enamel caries in this review.

Clinical Form	Description	Number of Cases
1	Enamel caries (presumably on the surface). (Figures 2 and 3)	12
2	Suspicious grooves with a positive autofluorescent signal. The bottom of the groove appears bright red in diagnosis mode. (Figure 6)	18
3	Suspicious grooves with a neutral fluorescent signal, or autofluorescence masking effect. The bottom of the groove appears black in diagnosis mode. (Figure 11)	20

located on the occlusal surfaces of mandibular or maxillary molars were illuminated using the SoproLife® camera and analyzed. The teeth were chosen from 14 female and 11 male dental students using visual inspection with 3.5x magnifying glasses (I.Dentix, Strasbourg, France), a SoproLife® camera in daylight mode, and bitewing radiographs. The mean was two suspicious occlusal grooves per student. The dental students all had favorable socioeconomic backgrounds. The DIAGNOdent was used to establish an average value of its signal as a reference point since any value greater than 20 presupposes the existence of at least enamel-dental caries. The inclusion criteria consisted of all suspicious grooves in terms of color and depth. The exclusion criteria consisted of carious lesions already extending to the dentin and lesions with cavitations.

Results

After analysis of 50 grooves of presumed stages: 0-110 or 0-3 ICDAS11, three clinical forms of enamel caries were observed (Table 1).

Form 1: Enamel Caries.

An example of enamel caries (Form 1) is shown of tooth #18 with caries presumably on the occlusal surface (Figure 1).

Analysis of the acquired data included the following:

- **Radiographic Film Data:** None or uninterpretable.
- **DIAGNOdent Data:** Average value 14–16.

- **SoproLife® Camera Data:** The magnified surface in daylight mode of the occlusal face reveals the extent of the caries (Figure 2), and the diagnostic mode (Figure 3) confirms the presence of a demineralized enamel layer by absorbing the blue signal homothetic to the demineralized surface visible in daylight.

Form 2: Suspicious Grooves with a Positive Autofluorescent Signal.

A radiographic example of a suspicious groove in tooth #17 is shown in Figure 4.

With a positive autofluorescent signal, the bottom of the groove appears bright red in diagnosis mode (Figures 5 and 6).

Analysis of the acquired data included the following:

- **Radiographic Film Data on Tooth #17:** None or uninterpretable.
- **DIAGNOdent Data:** Average value 20.
- **SoproLife® Camera Data:** A red autofluorescent signal appeared in the bottom of the suspicious groove. This localized alarm signal requires a prophylactic cleaning of the groove using a sodium bicarbonate abrasion air process to either confirm or invalidate the area of alarm (Figures 7 and 8).

After cleaning, the groove's anatomy is revealed with the red autofluorescence partially disappearing (Figure 7). Examination of the tissues surrounding the groove does not show any major variation in autofluorescence in relation to the adjacent healthy area with a regular acid green appearance (Figure 8, area A).



Figure 1. Radiography of tooth 18. The yellow circle is the suspicious area.



Figure 4. Periapical radiograph of tooth #17. (The yellow circle identifies the suspicious area.)

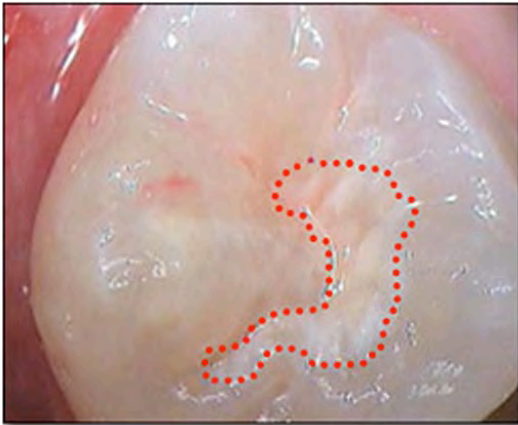


Figure 2. Occlusal surface of tooth #18 in daylight mode.



Figure 5. Occlusal surface of tooth #17 in daylight mode. (A suspicious central groove is shown in the black circle.)

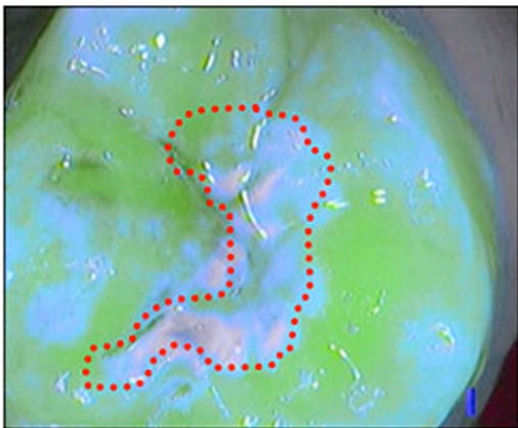


Figure 3. Occlusal surface of tooth #18 in diagnosis mode. (The red dots outline the porous tissue structure.)

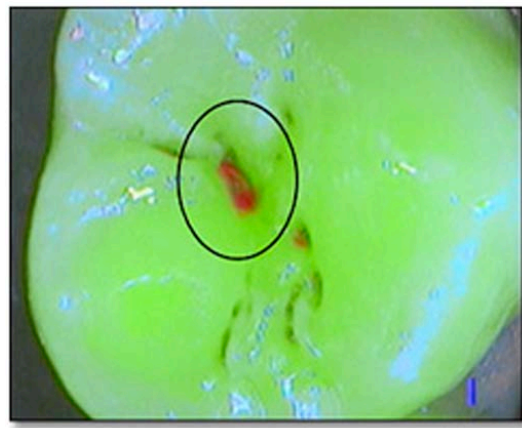


Figure 6. Occlusal surface of tooth #17 in diagnosis mode. A bright red fluorescent signal appears in the central groove.

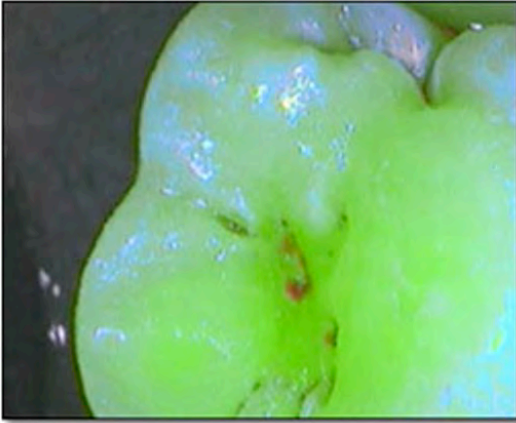


Figure 7. Appearance of the suspicious groove after cleaning with sodium bicarbonate.

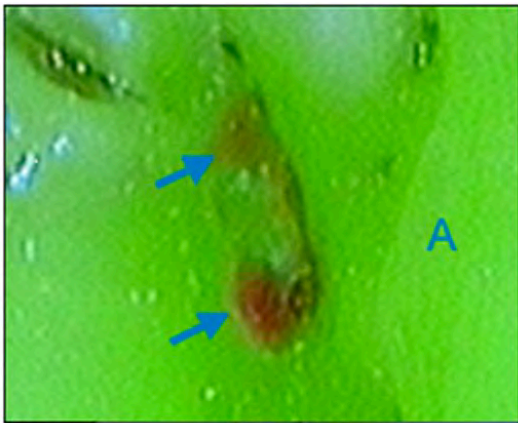


Figure 8. Enlargement of the image (Sopro imaging software). **A.** Healthy area of the tooth. **B.** Arrows identify a low-suspicion area due to its shallowness.



Figure 9. Bitewing radiograph of tooth #27. (The suspicious area is shown in the dark circle.)

Form 3: Suspicious Grooves with a Neutral Fluorescent Signal.

A radiographic example of a suspicious groove in tooth #27 is shown in Figure 9.

With a neutral fluorescent signal, or the presence of autofluorescent masking effect, the bottom of the groove appears black in the diagnostic mode, raising the suspicion of a fissured groove (Figures 10 and 11), meaning that you absolutely need to clean the groove and reuse the camera for reevaluation.

Analysis of the acquired data included the following:

- **Radiographic Film Data on Tooth #27:** None or uninterpretable.
- **DIAGNOdent Data:** Average value 20.
- **SoproLife® Camera Data:** (Figure 11)
 - Absence of a red autofluorescence signal or the presence of a fluorescence masking effect (dark black appearance) with the modified acid green fluorescence taking on a darker appearance.
 - Precise data on groove fissuration.

Localized variation in autofluorescence (Figure 11) from acid green to dark brown is also an alert signal. Air abrasion cleaning with sodium bicarbonate provides useful information on the state of the tissues in the diagnostic mode (Figures 12 and 13).

The option of *in situ* magnification of the image and the autofluorescent signal shows variations in fluorescence in the main groove (Figure 13) that is more pronounced than the reference fluorescence associated with the healthy tissues in area A. There is a hint of the presence of an isthmus between arrows 2 and 3.

Decision-Making Diagram for the LIFEDT Concept

To deal with three kinds of clinical situations, two decision-making diagrams are proposed that are in accordance with the international recommendations for preventive dentistry,^{13,14} and modified because of the additional accurate information provided by the SoproLife® Camera: autofluorescence variations and the magnification.



Figure 10. Fissured, suspicious groove in daylight mode.

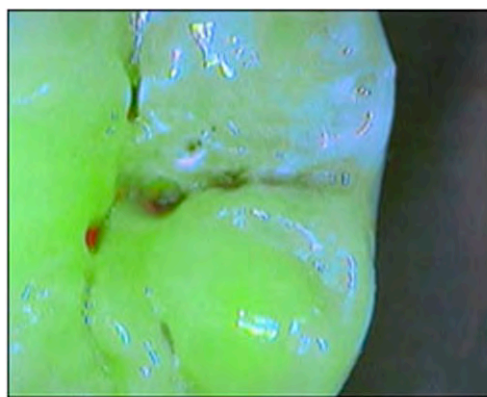


Figure 12. Groove after cleaning in the diagnostic mode.

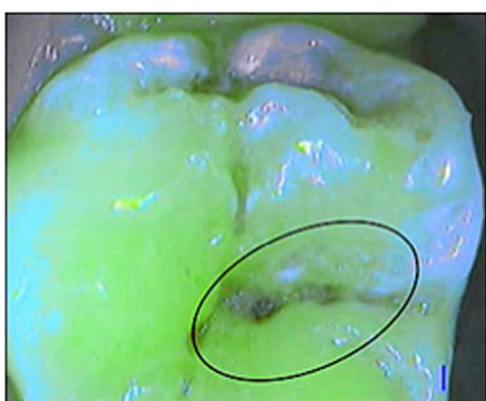


Figure 11. Fissured groove with modified autofluorescence signal (darker appearance) in diagnostic mode.

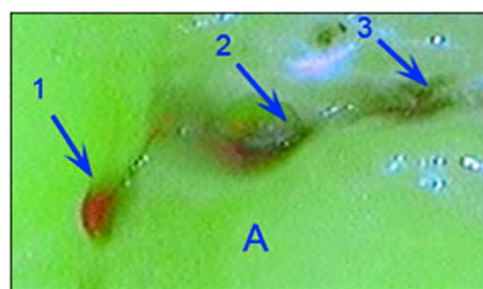


Figure 13. Enlargement of groove with three suspicious areas (arrows 1, 2, 3). Area A indicates a healthy tissue area (diagnostic mode.)

The first diagram is proposed for use with suspected surface enamel lesions (Form 1) and the second diagram is for use with the other two forms of suspicious grooves observed (Forms 2 and 3).

Discussion

The information obtained by the SoproLife[®] camera is interpreted logically according to the caries risk, and the LIFEDT concept suggests therapies in accordance with international recommendations for preventive dentistry, but with greater precision in terms of the system performance, and, of course, its limits. Individuals with visible enamel-dentinal caries, initial enamel lesions (white spots), restorations less than three years old, or with proximal enamel damage (without involvement of the dentin, but

radiographically visible) are considered to be at-risk patients.^{12,13} If oligoptyalism is added to this list, these patients also would be considered a high caries risk.¹³ This would result in four levels of caries risk: low, moderate, high, and extreme. Depending on the social context in many countries, that leaves little room for maneuvering to find a patient with low caries risk. It is difficult to clinically discriminate between these four levels despite the accuracy of different strategies for caries assessment available.^{12,13} For this reason, only two main caries risk levels (low and high risk) and one exceptional risk level (extremely high level, to accommodate oligoptyalism) were included in the two decision-making diagrams. A moderate risk would actually be considered as a high risk in this system.

The recommendation of the CAMBRA concept¹³ is to apply a sealant for up to level 3 of the ICADS II system, but the CAMBRA diagnosis level is limited by the diagnosis tools themselves.²⁰ The potential benefits of the imaging approach

LIFEDT Decision-Making Diagram #1

Form 1: Surface enamel lesions.

High Caries Risk
(Cariogram¹² or CAMBRA analysis¹⁴)

Low Caries Risk
(Cariogram¹² or CAMBRA analysis¹⁴)



LIFEDT Concept

- Professional prophylactic cleaning.
- Care with abrasion air in conjunction with sodium bicarbonate as the crystalline structure is highly unstable.
- Brushing 2–3 times per day: 1.1% NAF toothpaste.
- Xylitol (6 g/day): chewable tablets.
- Application of fluoride varnish (5% NAF); recall every 3–4 months.
- Application of calcium phosphate–based paste (MI plus GC Tooth mousse, GC Tokyo, Japan).
- Mouthwash: 0.05% NAF or 0.12% chlorhexidine: 1 minute every evening.
- Dietary counseling.
- **LIFEDT Concept:** If the LED camera confirms groove fissuration and any variations in fluorescence, a sealant will be applied using a dental dam.

- Professional prophylactic cleaning.
- Care with abrasion air in conjunction with sodium bicarbonate as the crystalline structure is highly unstable.
- Brushing 2–3 times per day with fluoride toothpaste.
- Application of fluoride varnish (5% NAF); patient recall every 6 months.
- Application of calcium phosphate–based paste (optional).
- : If the LED camera confirms groove fissuration and any associated variations in fluorescence, a sealant is recommended.

LIFEDT Decision-Making Diagram #2

Forms 2 and 3: Suspicious grooves with fluorescence altered (red or neutral signal) in relation to a healthy area.

Decision-making criteria for fitting of a sealant:

LIFEDT Concept

- A. See Diagram #1 for either high or low caries risk.
- B. FluoLED camera data:
- Groove fissuration: Positive criterion whatever the caries risk, due to effectiveness of brushing being impossible to monitor.
 - Modification of enamel and dentinal fluorescence of tissues surrounding the groove: Positive criterion whatever the caries risk, as bacterial or acid infiltration is potentially effective.

LIFEDT Concept

- A. **Stage 1:** Fissuration and/or variation in tissue fluorescence require, in a preventive and observation phase, air abrasion cleaning in conjunction with sodium bicarbonate.
- B. **Stage 2:** After cleaning camera data:
- Groove without modified fluorescence.
 - If low risk: sealant^{19,20} and varnish are optional.
 - High risk same as for Diagram #1.
 - Groove with modified fluorescence (Figure 13) must be dealt with as a high risk.

used at present are dependent on assisted clinical decision making. The LIFEDT/SoproLife[®] camera concept, within the limits of the process, can obtain genuine information on groove complexity. Short of using a costly microscope (20x), this information is not accessible by any means currently available. Common magnified vision using magnifying glasses (3.5x) is simply too weak. In reality clinicians are too often working blindly with regard to caries detection. Magnification of more than 50x provides images of the deep structure of the groove that can be viewed live on a big screen monitor. Such images represent an invaluable aid when choosing the best-suited therapies¹⁴ such as the application of a varnish, a transparent protective sealant, or just monitoring the status of a potential carious lesion regardless of the patient's caries risk.

The second source of diagnostic information is provided by the modifications in fluorescence (Figures 6 and 11) observed by the clinician to assess the degree of infiltration of dental caries into an occlusal groove. A recent study²¹ compared the performance of fluorescence-

based methods (FC VistaProof, Dürer Dental, Bietingen-Bissingen, Germany, DIAGNOdent) with a traditional radiograph examination and an ICDAS II visual examination.²² The investigators concluded bitewing radiographs combined with a visual examination ICADII appears to be the best combination for an accurate diagnosis. Unlike the DIAGNOdent, the SoproLife[®] camera provides an overall image of the clinical situation rather than a point-by-point measurement requiring the judgment of the clinician in all cases. The training and clinical experience of the individual dentist remains a critical element in arriving at an accurate diagnosis and treatment strategy. Therefore, the primary usefulness of the SoproLife[®] camera in daily practice might be to improve the diagnostic skill of the dentist, subject, of course, to the inherent limits of the present study. In fact it reveals ultra-structural modifications of enamel and dentin due to the carious process and the resulting optical modifications.⁶ Organic deposits, porosities, crystalline destructuring, and the acid front are all capable of disrupting the autofluorescence signal, discoloring, and modifying the brightness

of the hard tooth structures.^{3-5,23,24} Porous enamel absorbs the incident signal in the blues range of the light spectrum (Figure 3) and the presence of a more complex, deep lesion returns a red (Form 2) or dark brown (Form 3) signal. At present there is no rational explanation of why these two signal types (red or dark brown) are generated, but the presence of organic matter in the bottom of the groove appears to be correlated with the red signal.

Furthermore the system does not address the issue of bacterial ecology. This can be determined using reliable bacterial tests such as GC Saliva Check SM, GC Plaque-check+pH (GC, Tokyo, Japan), and Cariscreen (Oral Biotech, Albany, OR, USA).¹⁸ In the presence of a high-risk oral ecology, any fissured groove and any modification in the natural fluorescence serves as an indication to implement the LIFEDT concept. Until the evidence of dentinal damage by the caries is definitely diagnosed using radiography and the SoproLife[®] camera, the LIFEDT concept, based on the work of Mertz-Fairhurst et al.,²⁵ recommends preventive sealing rather than a conventional irreversible mechanistic approach. This approach also opens up new prospects in terms of monitoring restorations. Indeed, any suspicious modification to the visible tissue fluorescence around existing restoration should facilitate a better diagnosis of recurrent caries.

Conclusion

An analysis of 50 occlusal grooves revealed three clinical forms of enamel caries: (1) enamel caries on the surface, (2) suspicious grooves with a positive autofluorescent red signal, and (3) suspicious grooves with a neutral fluorescent dark signal. Two decision-making diagrams were proposed in accordance with international recommendations for preventive dentistry but modified as a result of the accurate information obtained with this new LIFEDT device.

Clinical Significance

The lighting of suspect occlusal grooves with the SoproLife[®] camera enables observation of any variations in the optical properties to refine a caries diagnosis and facilitates a more than

50x magnification of occlusal groove anatomy to provide additional information on the carious potential of the tooth surface.

References

1. Lussi A. Comparison of different methods for the diagnosis of fissure caries without cavitation. *Caries Res.* 1993; 27(5):409-16.
2. Dommisch H, Peus K, Kneist S, Krause F, Braun A, Hedderich J, Jepsen S, Eberhard J. Fluorescence-controlled Er:YAG laser for caries removal in permanent teeth: a randomized clinical trial. *Eur J Oral Sci.* 2008; 116(2):170-6.
3. Banerjee A, Watson TF, Kidd EA. Dentine caries: take it or leave it? *Dent Update.* 2000; 27(6):272-6.
4. Banerjee A, Yasseri M, Munson M. A method for the detection and quantification of bacteria in human carious dentine using fluorescent *in situ* hybridisation. *J Dent.* 2002; 30(7-8): 359-63.
5. Banerjee A, Kidd EA, Watson TF. *In vitro* validation of carious dentin removed using different excavation criteria. *Am J Dent.* 2003; 16(4):228-30.
6. Pitts N. "ICDAS"—an international system for caries detection and assessment being developed to facilitate caries epidemiology, research and appropriate clinical management. *Community Dent Health.* 2004; 21(3):193-8.
7. Hall A, Girkin JM. A review of potential new diagnostic modalities for caries lesions. *J Dent Res.* 2004; 83 Spec No C:C89-94.
8. Erten H, Üçtasli MB, Akarslan ZZ, Üzun Ö, Semiz M. Restorative treatment decision making with unaided visual examination, intraoral camera and operating microscope. *Oper Dent.* 2006; 31(1):55-9.
9. Tyas MJ, Anusavice KJ, Frencken JE, Mount GJ. Minimal intervention dentistry—a review. FDI Commission Project 1-97. *Int Dent J.* 2000; 50(1):1-12.
10. Mount GJ, Tyas, JM, Duke ES, Hume WR, Lasfargues JJ, Kaleka R. A proposal for a new classification of lesions of exposed tooth surfaces. *Int Dent J.* 2006; 56(2):82-91.
11. Pitts NB. Modern concepts of caries measurement. *J Dent Res.* 2004; 83 Spec No C:C43-7.

12. Bratthall D, Hänsel Petersson G. Cariogram—a multifactorial risk assessment model for a multifactorial disease. *Community Dent Oral Epidemiol.* 2005; 33(4):256-64.
13. Featherstone JD, Domejean-Orliaguet S, Jenson L, Wolff M, Young DA. Caries risk assessment in practice for age 6 through adult. *J Calif Dent Assoc.* 2007; 35(10):703-7, 710-3.
14. Jenson L, Budenz AW, Featherstone JD, Ramos-Gomez FJ, Spolsky VW, Young DA. Clinical protocols for caries management by risk assessment. *J Calif Dent Assoc.* 2007; 35(10):714-23.
15. Ekstrand KR, Ricketts DN, Kidd EA, Qvist V, Schou S. Detection, diagnosing, monitoring and logical treatment of occlusal caries in relation to lesion activity and severity: an *in vivo* examination with histological validation. *Caries Res.* 1998; 32(4):247-54.
16. Ekstrand KR, Ricketts DN, Kidd EA. Occlusal caries: pathology, diagnosis and logical treatment. *Dent Update.* 2001; 28(8):380-7.
17. Ekstrand KR Improving clinical visual detection-potential for caries clinical trials. *J Dent Res* 2004; 83(Spec Iss C) : C67-C71.
18. Walsh LJ, Tsang AK. Chairside testing for cariogenic bacteria: current concepts and clinical strategies. *J Minim Interv Dent.* 2008; 1(2):126-49.
19. Midentistry.com [Internet]. Johannesburg, South Africa: midentistry corp. MI Clinical Dental Practice. Available from: <http://www.midentistry.com/practice.html>
20. Ahovuo-Saloranta A, Hiiri A, Nordblad A, Worthington H, Mäkelä M. Pit and fissure sealants for preventing dental decay in the permanent teeth of children and adolescents. *Cochrane Database Syst Rev.* 2008; (4):CD001830. DOI: 10.1002/14651858.CD001830.pub3.
21. Rodrigues JA, Hug I, Diniz MB, Lussi A. Performance of fluorescence methods, radiographic examination and ICDAS II on occlusal surfaces *in vitro*. *Caries Res.* 2008; 42(4):297-304.
22. Ismail AI, Sohn W, Tellez M, Amaya A, Sen A, Hasson H, Pitts NB. The International Caries Detection and Assessment System (ICDAS): an integrated system for measuring dental caries. *Community Dent Oral Epidemiol.* 2007; 35(3):170-8.
23. Adeyemi AA, Jarad FD, Pender N, Higham SM. Comparison of quantitative light-induced fluorescence (QLF) and digital imaging applied for the detection and quantification of staining and stain removal on teeth. *J Dent.* 2006; 34(7):460-6.
24. Iwami Y, Hayashi N, Yamamoto H, Hayashi M, Takeshige F, Ebisu S. Evaluating the objectivity of caries removal with a caries detector dye using color evaluation and PCR. *J Dent.* 2007 35(9):749-54.
25. Mertz-Fairhurst EJ, Curtis JW Jr, Ergle JW, Rueggeberg FA, Adair SM. Ultraconservative and cariostatic sealed restorations: results at year 10. *J Am Dent Assoc.* 1998; 129(1): 55-66.

About the Authors

Elodie Terrer, DDS



Dr. Terrer is a doctoral student in the Department of Restorative Dentistry of the Marseille Dental School at the University of the Mediterranean. Her major fields of interest are composite restorations and clinical research.

e-mail: elodieterrer83@hotmail.fr

Stephen Koubi, DDS



Dr. Koubi is a professor in the Department of Restorative Dentistry of the Marseille Dental School at the University of the Mediterranean. His major fields of interest are composite restorations, clinical research, and prosthetic dentistry.

Alexandro Dionne

Mr. Dionne is a dental student in the Department of Restorative Dentistry of the Marseille Dental School at the University of the Mediterranean. His major fields of interest are composite restorations and clinical research.

Gauthier Weisrock, DDS



Dr. Weisrock is an Assistant Professor in the Department of Restorative Dentistry of the Marseille Dental School at the University of the Mediterranean. His major fields of interest are composite restorations and clinical research.

Caroline Sarraquigne



Ms. Sarraquigne is a biomedical engineer in Marseille, France, and a clinical development project manager in dental and medical research. Her major field of interest is to define and create product concepts with the potential of leading to the development of groundbreaking products.

Alain Mazuir

Mr. Mazuir is a biomedical engineer in La Ciotat, France, who is an inventor and patent specialist. His major field of interest is the creation of groundbreaking products associated with dental and medical imagery.

Hervé Tassery, DDS, MS, PhD (Corresponding Author)



Dr. Tassery is a professor in the Department of Restorative Dentistry of the Marseille Dental School at the University of the Mediterranean. His major fields of interest are minimally invasive dentistry and clinical research.

e-mail: hervé.tassery@numericable.fr



A New Concept in Restorative Dentistry: LIFEDT— Light-Induced Fluorescence Evaluator for Diagnosis and Treatment: Part 2 – Treatment of Dentinal Caries

Elodie Terror, DDS; Anne Raskin, DDS, MS, PhD; Stephen Koubi, DDS; Alexandro Dionne; Gauthier Weisrock, DDS; Caroline Sarraquigne; Alain Mazuir; Hervé Tassery, DDS, MS, PhD

Abstract

Aim: A new and innovative therapeutic concept using a light-induced fluorescence evaluator for diagnosis and treatment (LIFEDT) of dental caries based on the imaging and autofluorescence of dental tissues is proposed. The aims of this series of *in vivo* experiments are to compare and analyze the brightness variations of sound dentin and active and arrested carious dentin illuminated with an intraoral LED camera and to determine if this new device could be helpful in daily practice to discriminate between caries and sound dentin.

Methods and Materials: A new intraoral LED camera that emits visible blue light was used in this *in vivo* study to illuminate and photograph 15 teeth at high magnification. The magnified images were examined using the free Image J V[®] version 1.41 software. Four standardized rectangular areas were drawn on each picture that included both healthy and pathologic areas to analyze variations in brightness using a brightness formula: $L^* = 0.299 \text{ Red} + 0.587 \text{ Green} + 0.114 \text{ Blue}$.

Results: Statistically significant differences in the brightness were found between active and arrested caries processes in an area of infected dentin designated Z2. Within the limitations of this *in vivo* study, the images created with the intraoral LED camera revealed significant variations in fluorescence between sound dentin and active and arrested caries processes.



Conclusions: The LIFEDT concept provides a therapeutic concept based on these findings of variations in fluorescence between healthy and pathologic tissue.

Clinical Significance: This concept defines a pragmatic clinical and therapeutic approach for treating active and arrested carious lesions based on the interpretation of variations of a fluorescence signal and applying the LIFEDT concept to the treatment of dentin carious lesions.

Keywords: Active caries, arrested caries, dentin fluorescence, caries discrimination, LED camera.

Citation: Terror E, Raskin A, Koubi S, Dionne A,

Weisrock G, Sarraquigne C, Mazuir A, Tassery H. A New Concept in Restorative Dentistry: LIFEDT—Light-Induced Fluorescence Evaluator for Diagnosis and Treatment: Part 2 – Treatment of Dentinal Caries. *J Contemp Dent Pract* [Internet]. 2010 Jan; 11(1):095-102. Available from: <http://www.thejcdp.com/journal/view/volume11-issue1-terror>.

Introduction

In Part 1 of this two-part series,¹ the focus was on the diagnostic potential of the images generated with a new intraoral LED camera. Two decision-making diagrams were proposed in that article based on images observed, while referring to international recommendations.²⁻⁴ The principle employed was to analyze variations in fluorescence of a clinically suspicious carious area in relation to the fluorescence of a healthy area on the same tooth.

Experimentation using the same imaging technology has continued into the treatment phase, i.e., after cavity preparation to remove the carious lesion. In this specific scenario, several caries detection tools are available to discriminate between healthy and carious dentin either *in vivo* or *in vitro* with more or less success in terms of sensitivity or specificity.⁵⁻⁹ These detection tools include the following:

- FACE⁵ (fluorescence-aided caries excavation)
- DIFOTI (digital imaging fiber-optic trans-illumination)
- QLF⁶ (quantitative light fluorescence)
- FC (VistaProof, Dürr Dental, Bietingen-Bissingen, Germany)⁷
- DIAGNOdent (laser)

Other strategies for this purpose involve the use of multiphoton imaging, infrared thermography, infrared fluorescence, optical coherence tomography, ultrasound, and terahertz imaging. Nevertheless, the “take it or leave it” approach, as expressed by Banerjee et al.,¹⁰ is still utilized. Clinicians continue to be confronted with how to identify carious tissue and where to stop the caries excavation process.¹⁰ The inherent problem with existing clinical criteria (hardness, color, and penetration of caries dyes) is a lack of standardization and clinical subjectivity.¹⁰ Recent studies¹¹ based on the CIE 1976 L*a*b* color system stipulated that brightness (L*value)



decreased as the rate of bacterial detection increased and that the L*value was related to the degree of caries progression. Hence, the aims of the series of experiments in the present study were to:

1. Compare and analyze the brightness variations (L*) of sound and carious dentin illuminated with an intraoral LED camera emitting visible blue light without prior distinction of the type of caries process (active or arrested) or brightness variations of dentin within a representative RGB model space.
2. Determine if this new device could be helpful in current practice based on interpretation of the fluorescence signal variation observed.
3. Apply the LIFEDT¹ concept to the treatment of dentinal carious lesions based on images and fluorescence variations observed.

The null hypothesis tested was that the fluorescence of carious dentin, illuminated with the new intraoral LED camera, does not vary between sound dentin and either active or arrested dental caries.

Methods and Materials

This study was designed based on the Patient (or Problem), Intervention, Comparator, and Outcome (PICO) question formulation process,^{12,13} as described below.

Patients (P)

Fifteen teeth among 15 patients with active or arrested caries processes, and with no prior

distinctions, were selected for the study. The stage of each caries process was evaluated using an oral bitewing dental radiograph (Kodak, Rochester, NY, USA) developed in an automatic film processor (Durr Dental System, Bietigheim-Bissingen, Germany). The duration of the study was six months. All patients were recruited at the Centre Gaston Berger, Marseille Dental School, France, and the University of the Mediterranean. All patients were informed in advance of the aim of this trial and signed an approved consent form.

The inclusion criteria were as follows:

- Patient age minimum of 18 years old
- Existence of average to good oral hygiene
- Presence of developing caries at the molar or premolar sites 1, 2 and 3 within lesion sizes 1, 2 and 3¹⁴

The exclusion criteria include those patients with irreversible pulp disease or patients in dental emergency status.

Intervention (I)

The dental treatment steps used in the study were as follows:

1. A dental dam (Dentaldam[®], Bisco, Schaumburg, IL, USA) was placed and the carious lesion was excavated using a hand excavator EXC18H (Hu-Freidy[®], Chicago, IL, USA).
2. A hybrid glass ionomer (Cavity Conditioner[®] and Fuji II.LC[®], GC, Tokyo, Japan) was injected into the cavity preparation as a base material.
3. A nanohybrid dental composite (Adhese System[®] and Tetric EvoCeram[®] cured with a Blue Phase[®] LED curing light at 1200 mW/cm² (Vivadent, Schaan, Liechtenstein) was used to fill the cavity preparation.

For the image analysis, a picture was recorded with the intraoral LED camera at each of the three stages of the clinical procedure:

1. The tooth before preparation
2. The opened cavity
3. Completion of excavation using clinical criteria (color of residual dentin and hardness)

To avoid any interference with the fluorescence of the LED camera, no caries detector dyes were used in this experiment.

Detailed information about the LED camera is presented in Part I of this two-part series.¹

In summary, the Acteon Imaging[®] (Sopro SA, La Ciotat, France) is a patented LED video camera that uses a visible blue light frequency to illuminate the surface of the teeth and provides an anatomic image overlay onto the fluorescent image emitted by the teeth. The illumination occurs at a wavelength of 450 nm with a bandwidth of 20 nm, centered at ± 10 nm around the excitation wavelength. The camera is equipped with an image sensor (a 0.25-inch CCD sensor) consisting of a mosaic of pixels covered with filters of complementary colors. These filters have a greater range of reaction across the light spectrum, compared to the primary colors (RGB).

Comparison (C)

The basic principle of observation and calibration used in this study was to observe consistent variation in the carious dentinal tissue fluorescence/brightness in relation to a healthy area.

Digital photographs of the teeth in the study were taken systematically at the highest magnification (30x) with the LED camera. Images were then transferred to a computer using the SOPRO[®] software (Sopro Imaging[®], Sopro SA, La Ciotat, France) and analyzed using the free Image J V.1.41 software[®] (image processing and analysis in Java, Bethesda, MD, USA). Four standardized rectangular areas were drawn (10 mm long by 10 mm wide) on each picture (150 mm long by 120 mm wide) and labeled as follows:

- Z1, a healthy area of the tooth (Figures 1 and 3)
- Z2 and Z3 (Figures 1 and 3), before excavation
- Z4, in an open area at the end of excavation (Figures 2 and 4)

Area Z2 was associated with infected dentin, Z3 with the infected/affected dentin structure, and Z4 with the affected dentin (end of excavation).

Four levels of brightness (L^*) for each section were obtained and compared: $L^* = 0.299 \text{ Red} + 0.587 \text{ Green} + 0.114 \text{ Blue}$, which were transformed in the RGB color space as L^*_{green} , L^*_{red} , and L^*_{blue} . For each area, the mean and standard deviation of the brightness values were recorded. As for the caries process, the active or arrested status was only determined in teeth with an open cavity.

Outcome (O)

The expected outcome was this new technology



Figure 1. View of the fluorescence of dentin with the cavity opened. Areas (10 mm long by 10 mm wide) are **Z1**, healthy; **Z2**, infected; and **Z3**, infected/affected in an active caries process.

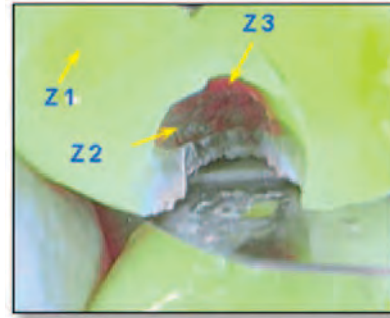


Figure 3. Fluorescence of dentin, cavity opened. Areas (10 mm long by 10 mm wide) are **Z1**, healthy; **Z2**, infected; and **Z3**, infected/affected arrested caries process.

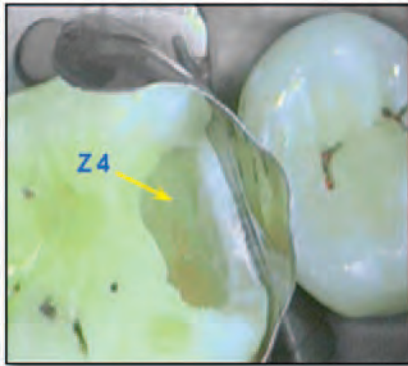


Figure 2. Fluorescence of active caries process at the end of excavation: **Z4**, end of excavation area (10 mm long by 10 mm wide).

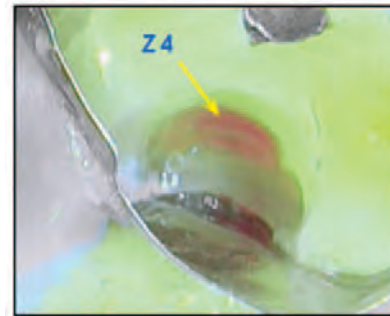


Figure 4. Fluorescence of an arrested caries process at the end of excavation: **Z4**, at the end of the excavation area (10 mm long by 10 mm wide).

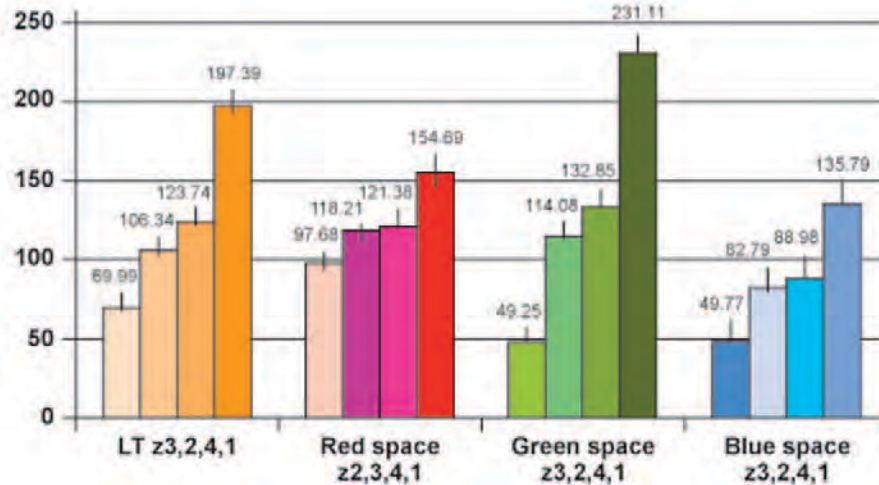
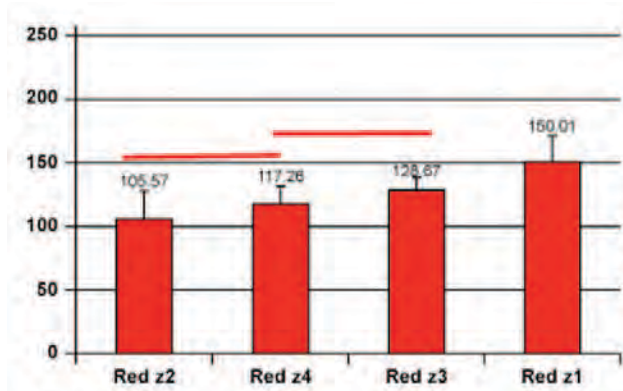
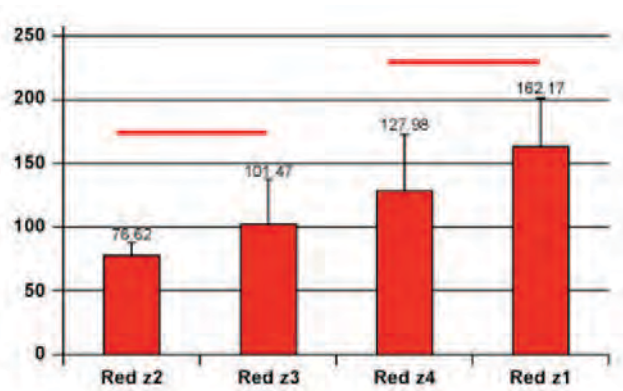


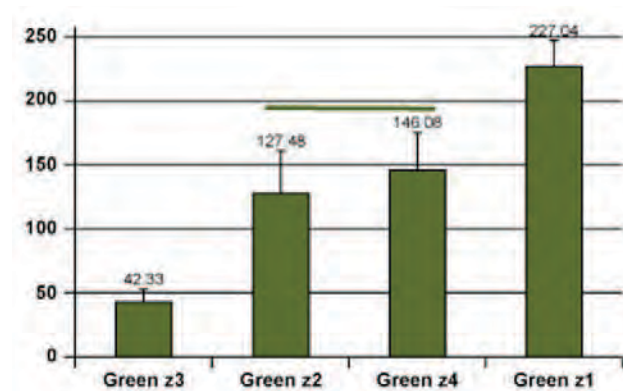
Figure 5. Total brightness (LT) of the four areas and in the red, green, and blue space respectively, independent of the type of carious lesion (mean value). Vertical bars = standard deviation.



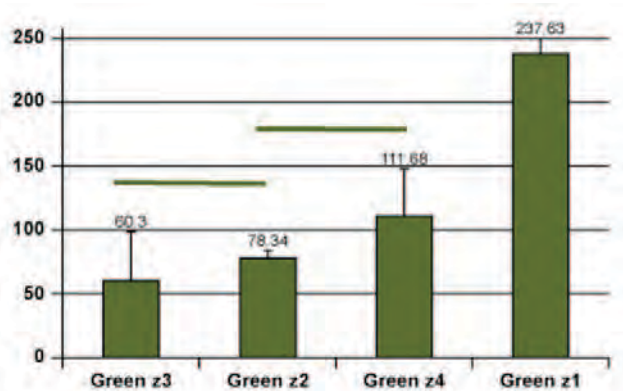
A. L* brightness in the red space. Active caries.



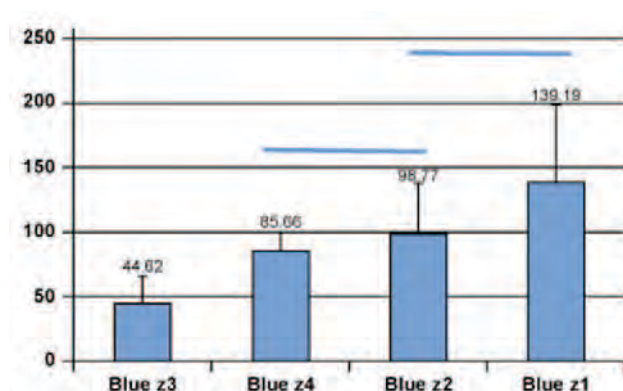
B. L* brightness in the red space. Arrested caries.



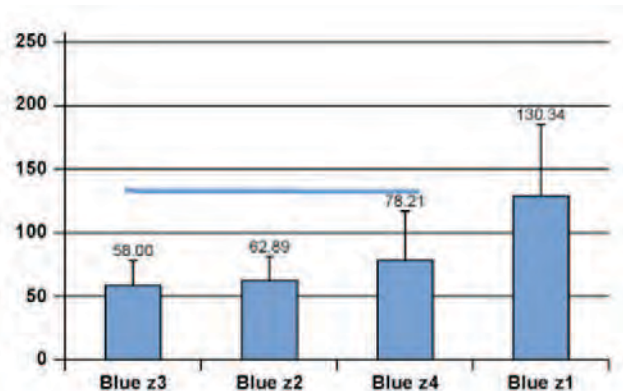
C. L* brightness in the green space. Active caries



D. L* brightness in the green space. Arrested caries



E. L* brightness in the blue space. Active caries.



F. L* brightness in the blue space. Arrested caries.

Figure 6. L* brightness variations in the red (A and B), green (C and D), and blue (E and F) RGB space in active and arrested caries processes, respectively (mean values). Graphs with a horizontal line to link vertical bars did not differ statistically.

would be a reliable aid to clinicians in discriminating and excavating carious dentin.

Statistical Analysis

The Mann-Whitney U and the Wilcoxon signed-rank tests were used for statistical analysis.¹⁵ The Wilcoxon signed-rank test was used to compare the total brightness and the brightness in the

red, green, and blue RGB space between the four different defined areas of the teeth (Z1 to Z4) for the overall experimental group (Figure 5) and then for active caries and for arrested caries (Figure 6).

The Mann-Whitney U test was used to compare active caries and arrested caries for the different parameters tested in the four different defined areas of the teeth (Figure 7).

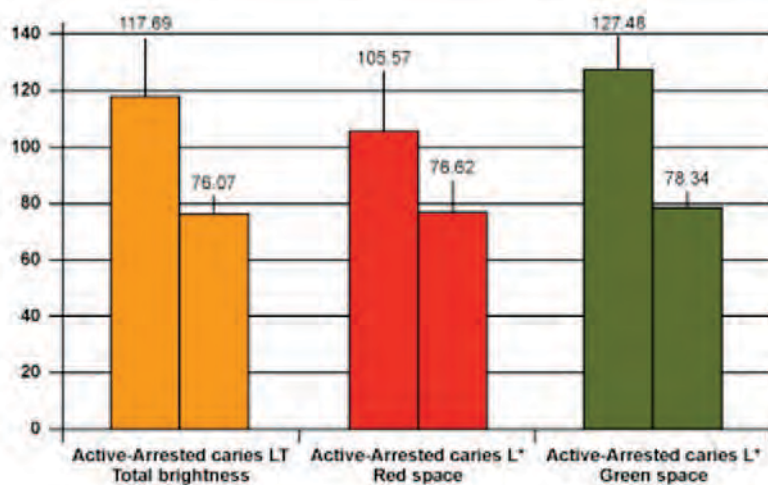


Figure 7. In the Z2 section, total (LT) and L* brightness variations in the red and green RGB space of active versus arrested caries processes respectively (mean value).

Results

Brightness Variations

The brightness variations were analyzed taking into account the total brightness and the brightness in the red, green, and blue RGB space. The first analysis involved all types of caries processes (Figure 5), the second incorporated active and arrested caries processes (Figure 6), and the third focused on active versus arrested caries processes (Figure 7).

The total dentin brightness decreased from Z1 to Z3 and then increased slightly at the end of the excavation (Z4). In the Z3 area using the red RGB space, the brightness increased and the drop in brightness variation decreased a second time. The values in areas Z2 and Z3 did not differ from those in area Z4. In the green RGB space, the brightness dramatically diminished then increased in area Z4. All of the LT and brightness values in the green space were different (Figure 5).

In the blue RGB space, the brightness dramatically diminished in area Z3 then increased in area Z4. The brightness values were the same for areas Z2 and Z4. (Figure 5). In the red RGB space (Figure 6A), the L* variations, even for the active and arrested caries processes, were more linear than in the green/blue space. The red L* slightly increased in the Z3 area (infected/affected level) in contrast to the green L*, which showed the greatest drop (Figure 6C). The green delta values (areas Z1 to Z3) were approximately 185



pixels in active caries processes and around 177 pixels in arrested caries. The same delta values in the red space were only 30 and 60, respectively. In the blue space, the delta values (areas Z1 to Z3) were higher than in the red space but lower than in the green space (Figure 6E).

In a two-by-two comparison (Figure 7), statistical differences were only observed for the Z2 area (infected dentin) in two RGB spaces: red and green. In most cases, the brightness of arrested caries was lower than for active caries. Clinically, healthy area Z1 appeared bright green; however, in the presence of active caries, area Z2 was a dark-green color, area Z3 was bright red (Figure 1), and area Z4 was gray-green, always less bright than area Z1. As for the arrested caries process (Figures 3 and 4), healthy area Z1 looked bright green, Z2 dark green, Z3 red, and Z4 slightly red, but all images were darker than

images of the active caries process. For arrested or slow-progressing lesions, the persistence of saveable intra-tubular or peripulpal tertiary dentin generates a shadowy red fluorescent interface at the bottom of the cavity (Figure 4, arrow).

Discussion

The clinically relevant aspects of this experiment were as follows:

1. Active and arrested caries process areas (Z1, Z2, Z3, and Z4) looked different in terms of fluorescence and brightness.
2. Healthy dentin can also be clearly discriminated from carious dentin as it looks bright green (Z1 area; Figures 1 and 3) at the highest level of brightness (Z1 areas in Figure 6A–F).
3. Any carious lesion could be detected by the variation in the fluorescence of its tissues in relation to a healthy area of the same tooth.
4. The objective of the LIFEDT concept is to adapt these observations in routine clinical practice.

Therefore, it is essential to analyze the brightness and fluorescence variations of dental tissue. In the active caries process, reparative dentin is synthesized mostly without dentinal tubules, in contrast to sclerotic dentin in arrested caries in which the dentinal tubules are full of mineralized deposits. These two types of dentin structure could partially account for the L^* variations. The reason statistical differences were only observed for the Z2 area (infected dentin) in the red and green RGB space remains unclear. A more remarkable observation was the large drop in L^* green in the presence of both active and arrested caries, which accounts for why the Z3 area looked red in active and arrested caries. One of either the organic or inorganic constituents of healthy dentin that emits an acid-green fluorescence partially disappears during the caries process; hence, the red fluorescence appears. Dentinal constituents emitting a red fluorescence seem to be less damaged by the caries process. The Maillard reaction (nonenzymatic browning reaction) with the generation of advanced Maillard products (carboxymethyllysine and pentoside) have been previously described in carious dentin.¹⁶ This phenomenon might partially account for fluorescence variations due to suspected fluorophores in carious dentin such as dityrosine, pentoside, and the Maillard reaction products.

The clinical decision to remove or leave suspicious dental tissue was made with the help of information provided by this new LED camera along with a visual examination. Unlike the VistaProof FC camera⁷ (Dürr Dental, Bietingen-Bissingen, Germany), the LED camera in the present study did not excite the bacterial fluorophore porphyrin in the wavelength between 670 and 700 nm. A recent study⁷ that compared the performance of fluorescence-based methods (FC, DIAGNOdent, radiograph examination, and ICDAS II [International Caries Detection and Assessment System]) concluded that bitewing radiographs combined with an ICDAS II visual examination appears to be the best diagnostic combination to detect caries. Therefore, the judgment of the clinician would still appear to prevail in all cases.

The LED camera, unlike the DIAGNOdent (Kavo, Biberach, Germany), provides an overall image of the clinical situation instead of a point-by-point measurement. The DIAGNOdent has been described as having a good level of sensitivity and low specificity,^{17,18} but it was more useful for caries diagnosis than for caries discrimination, and there were false-positive signals. Moreover, a recent study¹⁹ has revealed that measurements from DIAGNOdent were not strongly correlated with the depth and volume of the cavity preparation and concluded that appropriate visual examination training may provide similar results without the need for additional equipment.

The second aim of this study was to assess the suitability of using this device in daily practice. No prior distinction between the different caries processes was made because the present analysis was the first assessment of this new technology. Every effort was made to avoid introducing any bias into the interpretation of the images as a result of preconceptions. Within the limitations of the number of teeth in this study, the fluorescence of dentin in active and arrested states from Z3 and Z4 looked different enough to be discriminated with appropriate visual training. In the arrested area (Z4), a red shadow persisted at the bottom of the preparation in all cases (Figure 4). Based on the first results of this experiment and despite these limitations, the fluorescence variations between active and arrested caries led to the rejection of the null hypothesis.

Table 1: The LIFEDT concept applied to treatment of dental caries.

Principle	First, analyze a healthy area on the tooth concerned for use as the fluorescence reference during image processing and analysis. (Clinical case: Figure 8)
Active Carious Lesion	<p>Visual signals in fluorescent mode:</p> <ul style="list-style-type: none"> • Healthy dentin: acid green fluorescence. • Infected dentin: green-black fluorescence. • Infected/affected dentin: bright red fluorescence. This tissue is fairly easily eliminated with a manual excavator. • Abnormal dentin at the end of excavation: light green-grey fluorescence, sometimes with a very slight pink transparency (Figure 2, arrow) <p>Clinical considerations: In case of high caries risk—applicable to all lesion types, active or arrested—consider the following:</p> <ul style="list-style-type: none"> • According to depth of lesion: the residual septicity of the dentinal structure is the key factor in the general practitioner’s thinking. • Opt for provisional fitting of a conventional glass ionomer cement, such as Fuji VII (GC, Japan). • Reduce the caries septicity level by applying the recommendations of the Cambra concept.^{3,4} • Perform permanent treatments once the carious disease has stabilized.^{1,3,4} <p>Permanent treatments: In case of low caries risk—applicable to all lesion types, active or arrested—consider the following:</p> <ul style="list-style-type: none"> • Using a dental dam is essential. • Favor manual excavation over mechanical rotary caries removal. • Disinfect the dentin wound with a 5% aqueous solution of chlorhexidine. • If the area is accessible and enables a leak-tight contact, ozone disinfection therapy is feasible. • Favor fitting of a bioactive dentin substitute, such as resin-modified glass ionomer, especially if the enamel edges have disappeared.²¹ • In case of a eugenol-based dressing, opt for an amalgam restoration. • In case of a temporary dentin substitute such as conventional glass ionomer cement, consider the fitting time and the bonding of the adhesive/composite system used with this material. • Consider whether it is necessary to use antiseptic enamel-dentinal adhesives. • Consider the choice of the most appropriate adhesive for the residual dentin structure: destructured tissue, residual minerality, and proximity to pulp.
Arrested Lesion	<p>Visual signals in fluorescent mode:</p> <ul style="list-style-type: none"> • Healthy dentin: acid green fluorescence. • Infected dentin: green-black fluorescence. • Infected/affected dentin: dark red fluorescence. This tissue is more difficult to eliminate with a manual excavator. Surgical treatment of this tissue by rotary milling (tungsten carbide or ceramic) under spray is feasible. • Abnormal dentin at end of excavation: light green-grey fluorescence, with systematically persisting shady pink fluorescence at the bottom of the preparation, opposite the pulpal wall (Figure 4, arrow). <p>Clinical considerations:</p> <ul style="list-style-type: none"> • According to the depth of the lesion: the residual septicity of the dentin structure and activity of the disease are no longer the key factors in the general practitioner’s thinking. • Using a dental dam is essential. • Disinfect the dentin wound with a 5% aqueous solution of chlorhexidine. • If the area is accessible and enables a leak-tight contact, an ozone disinfection therapy is feasible. • Fitting a bioactive dentin substitute such as resin-modified glass ionomer is balanced with the injection of a chemo-polymerizing composite, especially if there are persisting enamel edges around the cervical border of the preparation.²¹ • A lack of residual enamel edges will lead to favoring the use of resin-modified glass ionomer in this specific case.²¹ • In case of a eugenol-based dressing, opt for an amalgam restoration. • Temporary fitting of a conventional glass ionomer cement is not absolutely necessary. • Consider the choice of the most appropriate adhesive for the residual dentin structure: destructured tissue, residual minerality, and proximity to pulp.
Mixed Lesions	In case of a mixed lesion (active and arrested), the carious lesion should be considered active in its entirety.

Whatever the fluorescence variations, magnification of the carious lesions by a factor of 30 greatly enhanced the clinical decision-making process. Even though this aspect was not evaluated during this experiment, a previous study has confirmed the usefulness of the method.²⁰ Moreover, because the Sopro imaging® software provides for the recording of the images from the LED camera, further evaluation of acquired images is facilitated by the software.

Tissue discrimination obtained by observable fluorescence variation has become a precious clinical aid that supplements the practitioner's diagnosis capabilities, and has enabled the development of the LIFEDT concept during the preparation phase of treating dental caries. The more than 30x magnification of the image supplements this advantage. Table 1 summarizes the LIFEDT concept in both active and arrested caries processes with the relevant operative

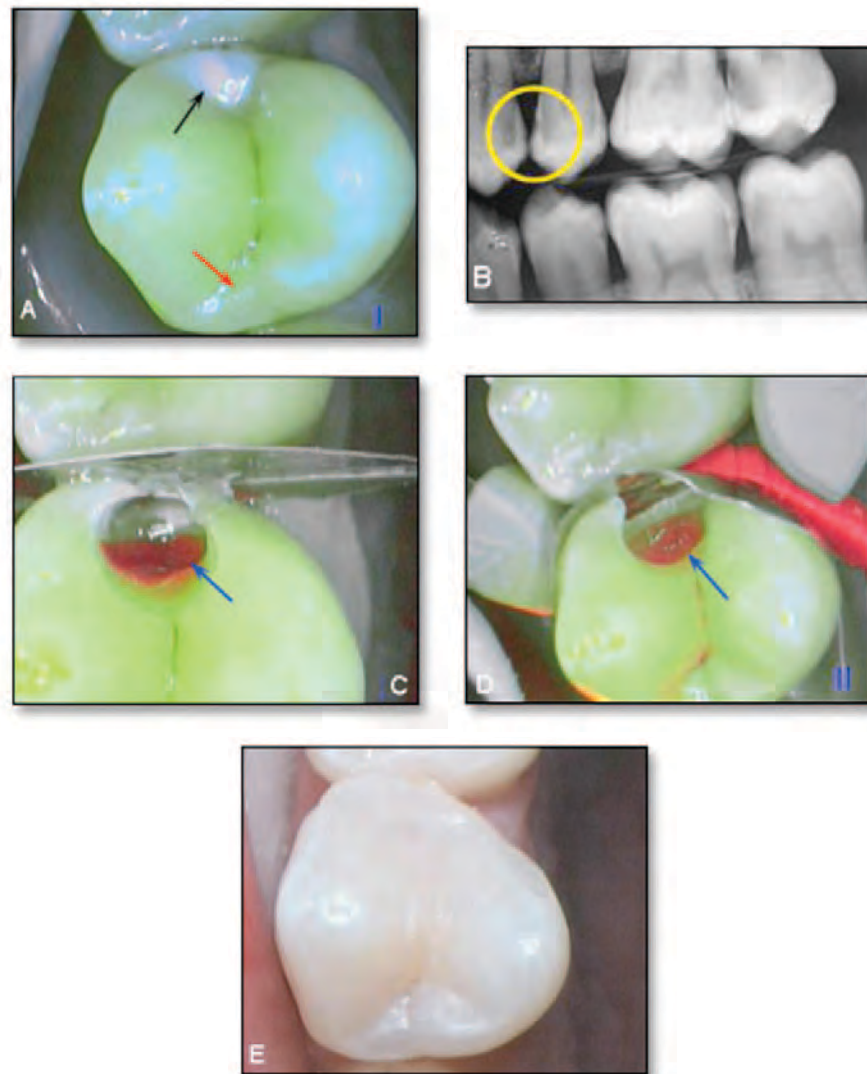


Figure 8. Treatment steps for a carious lesion on the distal aspect of tooth #24. **A.** Observation of marginal ridge destructuring in fluorescent mode (black arrow), as opposed to the opposite ridge (red arrow). **B.** Confirmation of lesion by radiography (yellow circle, distal face of 24). **C.** Shadowy red lesion, showing the infected/affected interface. **D.** End of excavation, with persisting sclerotic dentin (shadowy red fluorescence in the bottom, blue arrow), the sign of a slower rather than a quick lesion. The cervical enamel rim has been preserved. **E.** Completed restoration: Fuji II LC as a dentin substitute, and covered with a nano-hybrid composite (Bleach value: L).

procedures. The visual examination was performed as shown in Figure 8.

Conclusions

The potential benefits of the imaging approach used in the present work lie in the guidance of clinical decision making. Prediction of lesion activity in cases of open cavity types of carious lesions is of great interest and may substantially change traditional operative procedures. Decisions whether to use a bioactive dentin substitute or not could be facilitated. In fact, the bright-red fluorescence of the infected dentin with the intraoral LED camera coincided with the presence of a pale yellow, soft dentin, which is a priori indicative of an active lesion.¹¹

Within the limitations of this *in vivo* study, this new intra-oral LED camera revealed significant variations in fluorescence between sound dentin and active and arrested caries. These findings support the proposed use of the LIFEDT concept as a reasonable clinical protocol for the diagnosis and treatment of dental caries that can be routinely used by clinicians on a daily basis.

Clinical Significance

The use of a more than 30x magnified image to assess the integrity of tooth structure offers the potential for an improved clinical outcome as a result of a more accurate excavation of carious dentin; all finishing procedures are potentially improved. This clinical concept simplifies the everyday work for general practitioners using a pragmatic approach for treating active and arrested carious lesions by enhancing their diagnostic capabilities and, within the limitations of this concept, facilitates their choice of the restorative materials to be used.

References

1. Terrer E, Koubi S, Dionne A, Weisrock G, Sarraquigne C, Mazuir A, Tassery H. A New Concept in Restorative Dentistry: Light-Induced Fluorescence Evaluator for Diagnosis and Treatment: Part 1 – Diagnosis and Treatment of Initial Occlusal Caries. *J Contemp Dent Pract* [Internet]. 2009 Nov; 10(6):086-094. Available from: <http://www.thejcdp.com/journal/view/volume10-issue6-terror>.
2. Bratthall D, Hänsel Petersson G. Cariogram—a multifactorial risk assessment model for a multifactorial disease. *Community Dent Oral Epidemiol*. 2005; 33(4):256-64.
3. Featherstone JDB, Domejean-Orliaguet S, Jenson L, Wolff M, Young DA. Caries assessment in practice for age 6 through adult. *J Calif Dent Assoc*. 2007; 35(10):703-7, 710-3.
4. Jenson L, Budenz AW, Featherstone JD, Ramos-Gomez FJ, Spolsky VW, Young DA. Clinical protocols for caries management by risk assessment. *J Calif Dent Assoc*. 2007; 35(10):714-23.
5. Lennon AM, Attin T, Buchalla W. Quantity of remaining bacteria and cavity size after excavation with FACE, caries detector dye and conventional excavation *in vitro*. *Oper Dent*. 2007; 32(3):236-41.
6. Adeyemi AA, Jarad FD, Pender N, Higham SM. Comparison of quantitative light-induced fluorescence (QLF) and digital imaging applied for the detection and quantification of staining and stain removal on teeth. *J Dent*. 2006; 34(7):460-6.
7. Rodrigues JA, Hug I, Diniz MB, Lussi A. Performance of fluorescence methods, radiographic examination and ICDAS II on occlusal surfaces *in vitro*. *Caries Res*. 2008; 42(4): 297-304.
8. Ismail AI, Sohn W, Tellez M, Amaya A, Sen A, Hasson H, Pitts NB. The International Caries Detection and Assessment System (ICDAS): an integrated system for measuring dental caries. *Community Dent Oral Epidemiol*. 2007; 35(3):170-8.
9. Hall A, Girkin JM. A review of potential new diagnostic modalities for caries lesions. *J Dent Res*. 2004; 83 Spec No C:C89-C94.
10. Banerjee A, Watson TF, Kidd EA. Dentine caries: take it or leave it? *Dent Update*. 2000; 27(6):272-6.
11. Iwami Y, Hayashi N, Yamamoto H, Hayashi M, Takeshige F, Ebisu S. Evaluating the objectivity of caries removal with a caries detector dye using color evaluation and PCR. *J Dent*. 2007; 35(9):749-54.
12. Christenson RH; Committee on Evidence Based Laboratory Medicine of the International Federation for Clinical Chemistry Laboratory Medicine. Evidence-based

laboratory medicine—a guide for critical evaluation of *in vitro* laboratory testing. *Ann Clin Biochem.* 2007; 44(Pt2):111-30.

13. Forrest JL, Miller SA. Enhancing your practice through evidence-based decision making. *J Evid Based Dent Pract* 2001; 1(1):51-7.
14. Mount GJ, Tyas, JM, Duke ES, Hume, WR, Lasfargues JJ, Kaleka R. A proposal for a new classification of lesions of exposed tooth surfaces. *Int Dent J.* 2006; 56(2):82-91.
15. Siegel S, Castellan NL. *Nonparametric statistics for the behavioral sciences.* 2nd ed.; Singapore: McGraw-Hill; 1998.
16. Kleter GA, Damen JJ, Buijs MJ, Ten Cate JM. Modifications of amino acid residues in carious dentin matrix. *J Dent Res.* 1998; 77(3):488-95.
17. Lussi A. Comparison of different methods for the diagnosis of fissure caries without cavitation. *Caries Res.* 1993; 27(5):409-16.
18. Lussi A, Reich E. The influence of toothpastes and prophylaxis pastes on fluorescence measurements for caries detection *in vitro.* *Eur J Oral Sci.* 2005; 113(2):141-4.
19. Hamilton JC, Gregory WA, Valentine JB. DIAGNOdent measurements and correlation with the depth and volume of minimally invasive cavity preparations. *Oper Dent.* 2006; 31(3):291-6.
20. Erten H, Üçtaşlı MB, Akarşlan ZZ, Üzun Ö, Semiz M. Restorative treatment decision making with unaided visual examination, intraoral camera and operating microscope. *Oper Dent.* 2006; 31(1):55-9.
21. Koubi S, Raskin A, Dejou J, About I, Tassery H, Camps J, Proust JP. Effect of dual cure composite as dentin substitute on marginal integrity of class II open-sandwich restorations. *Oper Den.* 2009; 34(2):150-6.

About the Authors

Elodie Terrer, DDS



Dr. Terrer is a doctoral student in the Department of Restorative Dentistry of the Marseille Dental School at the University of the Mediterranean. Her major fields of interest are composite restorations and clinical research.

e-mail: elodieterrer83@hotmail.fr

Anne Raskin, DDS, MS, PhD

Dr. Anne Raskin. DDS, PHD. Department of Biomaterials. IMEB Laboratory. University of Mediterranean. 27 Bd Jean Moulin. 13355 Marseille. His major fields of interest are biomaterials and clinical research.

e-mail: anne.raskin@univmed.fr

Stephen Koubi, DDS



Dr. Koubi is a professor in the Department of Restorative Dentistry of the Marseille Dental School at the University of the Mediterranean. His major fields of interest are composite restorations, clinical research, and prosthetic dentistry.

Alexandro Dionne

Mr. Dionne is a dental student in the Department of Restorative Dentistry of the Marseille Dental School at the University of the Mediterranean. His major fields of interest are composite restorations and clinical research.

Gauthier Weisrock, DDS



Dr. Weisrock is an assistant professor in the Department of Restorative Dentistry of the Marseille Dental School at the University of the Mediterranean. His major fields of interest are composite restorations and clinical research.

Caroline Sarraquigne



Ms. Sarraquigne is a biomedical engineer in Marseille, France, and a clinical development project manager in dental and medical research. Her major field of interest is to define and create product concepts with the potential of leading to the development of groundbreaking products.

Alain Mazuir



Mr. Mazuir is a biomedical engineer in La Ciotat, France, who is an inventor and patent specialist. His major field of interest is the creation of groundbreaking products associated with dental and medical imagery.

Hervé Tassery, DDS, MS, PhD (Corresponding Author)



Dr. Tassery is a professor in the Department of Restorative Dentistry of the Marseille Dental School at the University of the Mediterranean. His major fields of interest are minimally invasive dentistry and clinical research.

e-mail: herve.tassery@numericable.fr

Naturally aesthetic restorations and minimally invasive dentistry

Weisrock G¹, Terrer E¹, Couderc G¹, Koubi S¹,
Levallois B^{3&4}, Manton D², Tassery H^{1&4}

¹Department of Restorative Dentistry of the Marseille Dental School at the University of the Mediterranean. 27 Bd Jean Moulin 13005 Marseille

²Melbourne Dental School. University of Melbourne. 720 Swanston St Victoria 3010 Australia.

³Department of Preventive and Restorative Dentistry of the Montpellier Dental School at the University of the Montpellier 1

⁴LBN Montpellier 1

The risks of iatrogenic actions when we apply therapies to the tooth itself, or to collateral teeth, are potentially high when combined with low sensitivity and specificity of our diagnosis tools. There are therapeutic tools, both for the occlusal and proximal surfaces, in the form of infiltration products, specific inserts for cavity preparation, a fluorescent camera for magnification and early detection, and others; however, preservation of the natural tooth aesthetics also requires early detection of the carious lesion, associated with comprehensive patient care so that our therapies are perpetuated. The purpose of this article is to discuss the advantages and drawbacks of minimally invasive dental techniques, distinguishing those that preserve or reinforce the enamel and enamel-dentine structures (MIT1) from those that require minimum preparation of the dental tissues (MIT2). The discussion is rounded off by an illustration of how the natural tooth aesthetics are preserved in two clinical cases.

Correspondence address:

Pr. Hervé Tassery
Professor and Head of the Department of Preventive and Restorative Dentistry of the Marseille Dental School at the University of the Mediterranean
27 Bd Jean Moulin
13005 Marseille
France
E-mail: herve.tassery@numericable.fr.

Approaches in dentistry unfortunately all too often employ damaging prosthetic techniques, rather than a real philosophy of preserving the dental tissues. The major problem is the ability to inhibit the progression of the carious lesion as early as possible, thereby achieving maximum preservation of the natural tooth aesthetics and structure. This involves gaining a better knowledge of the carious process so as to intercept it better, and determining the therapeutic tools enabling us to treat the carious lesion as early as possible and with minimum invasion. Dental caries is a complex and multifactorial disease resulting in lesions that affect enamel, dentine, pulp, and even cementum if the root portion of the tooth is involved. Caries are accompanied by tissue changes in the affected primary dentine and an inflammatory reaction in the pulp [1]. The development of a carious lesion is an intermittent cause of demineralization interspersed with remineralization. Under unfavorable conditions, the lesion process is referred to as active, with dull, white enamel and soft, yellowish dentine [2,3]. However, under favorable conditions including sensible diet, accurate excavation of the infected tissue, cariostatic sealed restorations, or even with incomplete removal of the carious dentine and good oral hygiene, the process may be reversed, and is referred to as arrested, even in the deep part of the lesion [2-4]. Whatever the type of lesion, depending on the size and pulp proximity of the lesion, various types of caries extension have been described [5,6] which could dramatically interfere with the esthetic goals during the restorative steps. In fact the first main goal and difficulty is to intercept the carious process quickly and to remove all the infected dentine accurately in a complex shaped cavity [7] without injuring sound dentine and pulp, whilst preserving occlusal or proximal dental tissue and the marginal ridge, and providing favorable aesthetic and biological conditions. The caries process can be reversed as long as the surface layer remains intact, and in the case of proximal surfaces, perfect diagnosis of the structural integrity of the enamel layer remains very difficult. Specifically, traditional Class 2 restoration usually leads to reduced tooth stiffness of around 30% [8], and dramatically increases the difficulties of the restorative procedure in terms of acceptable contact areas and natural aesthetics (choice of composite type, shade and shape of restoration) [9]. There are a host of dramatic risks inherent in iatrogenic actions: damaging collateral teeth faces during preparation, excessively mutilating preparation, poor control of dentine excavation, secondary infection due to absence of a dental dam, etc.

A variety of strategies have also been employed to minimize or eliminate microleakage in Class 2 restorations:

- Light-focus-tip polymerization devices concentrating the light to the ends of optical fibers [10].
- Incremental filling methods using self-cure or flow composite, etc. [11].
- Decoupling techniques [12].
- Several soft or pulse delay polymerization devices [13].

All of the above have been identified as strategies, which increase the marginal seal and the degree of conversion of various composite resin restorative materials, but none have gained universal acceptance [14,15].

There are many new products now available with the aim of remineralization and reversing the caries dynamic. Their systematic use should be promoted, since they have the advantage of maintaining and improving aesthetics, being less damaging, and above all, most of their actions are reversible [16,17,18]. The general philosophy of the patient centred approach is also of crucial importance. Indeed, all the techniques described below can only be applied within a medical approach of determining the patient's caries risk via a Cariogram [19], CAMBRA (Caries management by risk assessment) [20,21] or MITP (Minimally Invasive Treatment Plan, GC Europe) [22]. The threshold of intervention seems to be whether there is a cavitated lesion; and we must also have the tools enabling correct detection and diagnosis. The choice between the preventive care advised (PCA) and the preventive and operative care advised (P&OCA) will depend on this decision [6,23,24,25]. Therefore we can divide our preventive and minimalist therapies into 2 groups: the first (Minimally Invasive Treatment 1 or MIT1) for treating enamel and enamel-dentine lesions without any preparation, provided that there is no surface cavitation (radiographic lesion depth classification according to bitewing X-rays from E1 to D1 included). The second group (Minimally Invasive Treatment 2 or MIT2) is for treating early enamel-dentine lesions with surface cavitation (from D1 with cavitation to D2). From D3 onwards, a more conventional therapeutic approach is advisable.

The challenge is to intervene early and on a minimal basis, to achieve maximum preservation of the natural tooth aesthetics.

Regarding the second group, changes in restorative techniques such as the use of micro-burs (e.g. minimally invasive set, Intensive, Grancia, Switzerland; Komet, minimally invasive bur set, Lemgo, Germany), laser technique, air abrasion device, sonic and ultrasonic preparations, could also partly prevent these problems, and facilitate the use of ultraconservative restorations for all carious lesions reaching the first third or the middle third of dentine (Hume and Mount, 1997) with cavitation. If we focus on sonic techniques, both ultrasonic and sonic are useful in minimally invasive procedures. These devices are similar and could be used in combination with other techniques (e.g., air-abrasion, ozone treatment, photoablation, antibacterial therapy, etc.) [27-28].

Another main point is the usefulness of visual aids or other diagnosis tools [29]: indeed, preservation of aesthetics is directly correlated with how early the lesion is detected, especially in the proximal zones, as well as through a minimalist approach in all the restorative phases.

Processes aiming to detect carious lesions in the initial stage with optimum sensitivity and specificity employ a variety of technologies, such as loupes, laser fluorescence and autofluorescence, electric current/impedance, tomographic imaging, and image processing [30].

Despite the availability of these technologies, their high cost, physical size, excessively variable sensitivity and specificity have prohibited their use on a daily basis unlike conventional diagnosis tools, such as film or digital radiography [30].

These different means of analysis are also dependent on the clinicians' experience and proficiency in viewing magnified images using a magnifying glass or microscope. Conventional strategies for caries detection, such as visual observation or probing with a dental instrument, are unfortunately based on subjective criteria [31].

In the present cases, clinical decisions were based on the LIFEDT (Light Induced Fluorescence Evaluator for Diagnosis and Treatment) concept (Table 1) (Soprolife camera, Sopro, La Ciotat, France) which combined magnification, fluorescence and visual signal amplification to assist clinicians with the assessment of tooth structure [32,33]. These principles call for a comprehensive patient approach in terms of caries risk assessment, diagnosis, and appropriate therapies that are consistent with the concepts of minimally invasive dentistry (MID), or Minimal Intervention (MI), terms accepted by the World Dental Federation in 2000 [34].

The present review was undertaken to evaluate the clinical advantages and disadvantages of minimally invasive techniques (MIT) (Table 2) in such a way as to promote natural dental aesthetics whilst preserving dental tissue, and to describe an intermediate operating interval postponing conventional operative and prosthetic dentistry

Clinical reports

There are two kinds of minimally invasive techniques currently available, which achieve maximum tissue preservation whilst preserving the natural tooth aesthetics and structure.

Minimally invasive techniques type 1 (MIT1) incorporates no preparation except tissue conditioning, whilst type 2 (MIT2) incorporates tooth preparation. For the MIT1 techniques, we will limit our proposals to professional products applied in dental practices, though we are aware that so-called self-applied products are an integral part of a comprehensive medical approach (e.g. fluoride toothpastes, mouthwashes, fluoride and Chlorhexidine gel)

MIT1 encompasses all the dental techniques aimed at sterilizing (e.g. ozone therapy), remineralizing, reversing and sealing the carious process. There are many products now available, each with their own advantages and drawbacks (Table 2-3). The relevant clinical case in this review will focus on a new sealing technique using a resin infiltrant called Icon™ [35,36,37]. (DMG, Hamburg, Germany). (Clinical case 1) (Figures 1-7)

Composition of Icon:
Icon™ etch: hydrochloric acid, pyrogenic silicic acid, surface-active substance.
Icon™ dry: 99% ethanol
Icon™-Infiltrant: methacrylate-based resin matrix, initiators, additives.

Clinical case 1

Icon technique in brief

The infiltration of carious lesions with low-viscosity light-curing resins has been shown to inhibit further demineralization *in vitro*.

The infiltration of carious lesions with low-viscosity light-curing resins has been shown to inhibit further demineralization *in vitro*. This micro-invasive method for stabilizing early lesions requires no drilling or anesthesia, and does not alter the tooth's anatomic shape, thereby enhancing natural aesthetic preservation. The principles, after cleaning the area with a gentle abrasive strip, can be divided in four steps (clinical case 1, Figures 1-7):

Esthetic preservation of proximal surface without any preparation except tissue conditioning. Proximal enamel and dentinal lesion without clear cavitation (distal caries on first upper premolar).

Figure 1. Digital X-ray on first upper premolar. (Durr dental X-ray, special Dentsply X-ray, double ring holder)

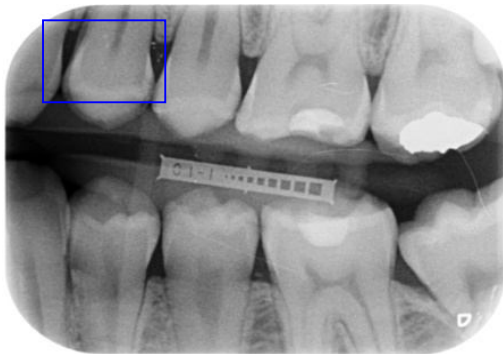


Figure 2. Occlusal surface view (Soprolife camera daylight mode). Visible brown shadow under the enamel marginal ridge.



Figure 3. Visible distal lesion in fluorescence mode (Soprolife camera, mode II). Red shadow in the blue rectangle with no visible cavitation.

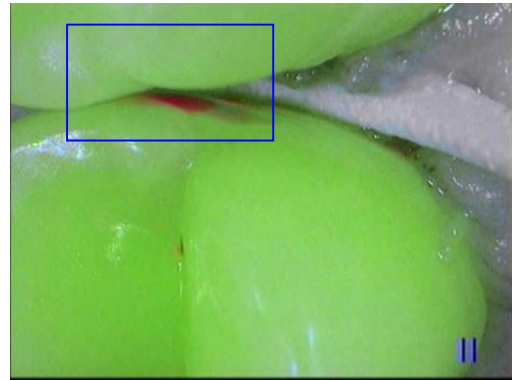


Figure 4. Chlorhydric acid application using a special celluloid matrix. Application time 2 mins.



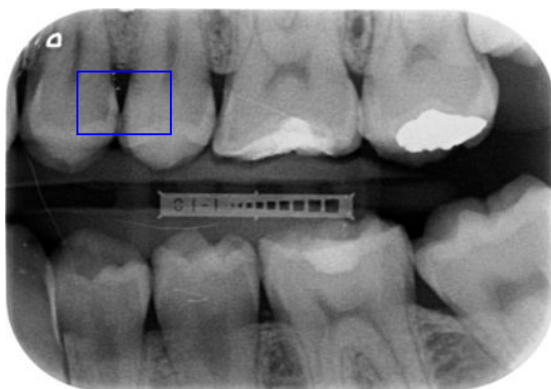
Figure 5. After drying with a 99% alcohol solution, application of the resin infiltrant, Application time 3 mins; followed by multisite photopolymerisation (Bluephase light, Vivadent, 1200 mW, 3 x 20 s).



Figure 6. Final check of the resin infiltrant application. Fluoride varnish is additionally applied on the distal surface. The tooth natural esthetics are preserved.



Figure 7. Digital X-ray after Icon application. (Note that the product is not radio-opaque, blue rectangle) (Durr dental X-ray, special Dentsply X-ray, double ring holder)



Step 1- demineralize the non-cavitated caries with hydrochloric acid for 2 mins, followed by a water rinse for at least 30 s.

Step 2- dry the area with an Icon dry syringe (99% ethanol) solution, followed by drying with oil- and water-free triplex air.

Step 3: infiltrate the suspicious area with an Icon™-Infiltrant syringe and a suitable approximal tip (Figures 4-5). The material will be delivered only on the green side of the approximal tip (Figures 4-5).

Step 4: light cure the resin infiltrant (Bluephase light-curing - Vivadent, Schaan, Lichtenstein), for 20s on the occlusal, vestibular and palatal sides, 1200 mW/cm².

The major difficulty in this technique is associated with the diagnosis of whether cavitation is present in the proximal zones. In this clinical case, we propose separating the tooth as far as possible using

powerful plastic wedges; using the Soprolife™ camera in daylight mode and fluorescent mode so that it becomes possible to view cavitation (if present) in most cases. The presence of cavitation and/or a lesion involving the middle third of the dentine (from D2 onward in terms of caries extension) contra-indicates the use of Icon™, and means that the tissues must be prepared mechanically (clinical case 2, Figures 8 - 15).

Clinical case 2

Minimally invasive technique type 2 (MIT2) (Table 2-4-5): MIT2 involves a series of specific tools, including sonic and ultrasonic inserts, to prepare the relevant tooth minimally without damaging the adjacent tooth, even in case of class 2 preparation. The systematic application of a metal matrix before preparation in order to preserve the adjacent surface is recommended. A slot type preparation is proposed to illustrate the MIT2 clinical case, with maximal preservation of the marginal ridge.

Esthetic preservation of marginal ridge. Proximal enamel and dentinal lesion with clear cavitation on the second upper premolar.

Figure 8. Digital X-rays with Sopix 2 (Sopro, La Ciotat, France). Distal caries on second upper premolar with evidence of cavitation (middle part of dentin involved, blue rectangle).

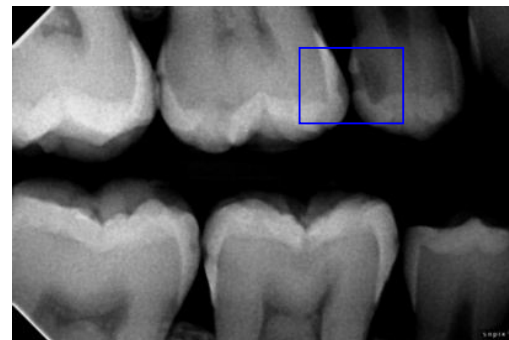


Figure 9. Proximal view with a suspicious red shadow (dark circle, Soprolife camera mode II). Proximal mesial surface of the upper molar with enamel fault (dark arrow).

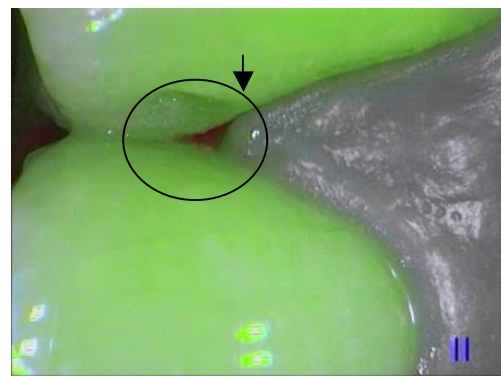


Figure 10. Ultrasonic semi-circular insert (Excavus insert, EX3 half-ball diamond tip) within the preparation. The marginal ridge was preserved. (Soprolife camera, daylight mode).



Figure 11. Treatment fluorescence mode (mode II) viewing the red fluorescence of the infected active caries in the deepest part of the slot cavity.

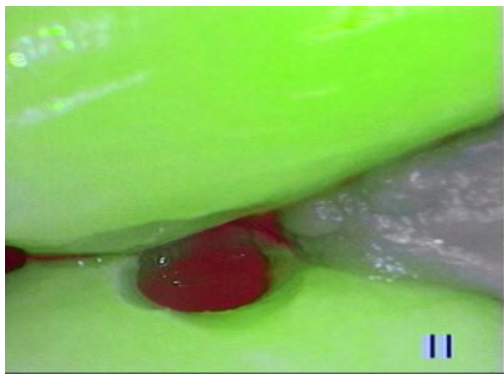


Figure 12. Manual micro-excavator in the deepest part of the cavity (Kotschy set, Hu-Friedy, Chicago, USA). (Soprolife camera, daylight mode).

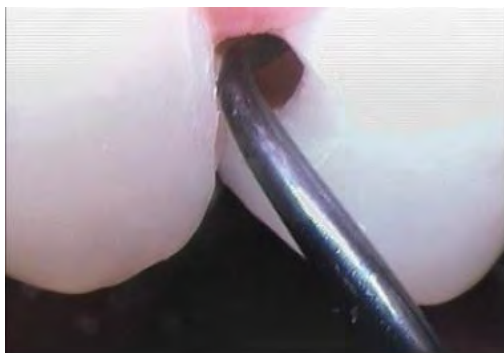


Figure 13. Check that the metal matrix has been properly applied, before injecting the hybrid glass-ionomer cement (Fuji II LC, GC, Tokyo, Japan). (Soprolife camera, daylight mode).



Figure 14. Final esthetic view after shaping and polishing steps of the distal side (blue rectangle). (Soprolife camera, daylight mode).

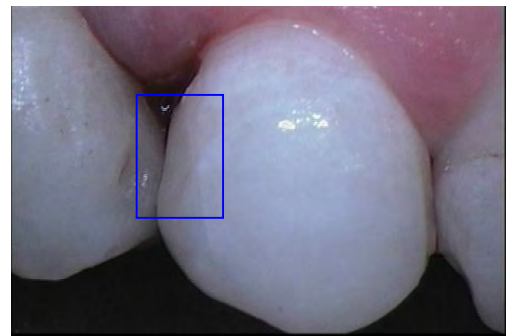
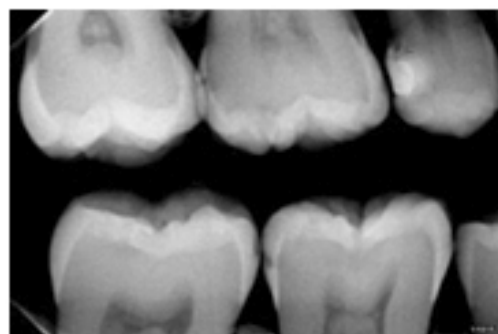


Figure 15. Final digital X-ray check (Sopix 2 digital device, Sopro, la Ciotat, France)



Ultrasonic Devices

The ultrasonic systems (Table 4-5) [28], e.g. EMS (Piezo Cavity System, EMS, Switzerland), Excavus (Acteon, Bordeaux, France), are ergonomically designed. They consist of various autoclavable aluminum cassettes and a selection of semi-circular metallic inserts of different types, with one inactive smooth face free from diamond abrasive. The inserts are held in a water-cooled ultrasonic handpiece which emits ultrasonic vibrations (above 20,000 Hertz).

Depending on the manufacturer, other inserts may be available to bevel the enamel margins and to specifically prepare Class 2 lesions with clear cavitation. The advantages and disadvantages of the ultrasonic system are shown in Table 4. However, these minimal preparations also require systematic use of micro-instrumentation sets developed for minimally invasive dentistry (Kotschy set, Hu-Friedy, Chicago, USA)

Sonic Devices

The sonic insert system (Sonicsys System from Kavo and inserts from Komet, Lemgo, Germany - (Table 4-5) [28]) is also ergonomically designed. It consists of an autoclavable aluminum cassette and a selection of different semi-circular metallic inserts (insert numbers: SF 30-31-32-33) with one inactive smooth face free from diamond abrasive. The inserts are held in a water-cooled handpiece (Kavo 2003, KaVo Biberach, Germany) that emits sonic vibrations (Power 2: 6000 Hertz, oscillation amplitude: 160 µm). The inserts are selected by the defined angularity of each insert, and the working proximal site (mesial or distal surfaces). Others inserts are also available to bevel the enamel margins (Insert numbers: SF28-29).

Steps of clinical case 2 in brief. Figures 8-13:

Step 1: fit a protective metal matrix, and use a micro-bur.

Step 2: prepare the slot cavity at constant pressure using the sonic or ultrasonic insert.

Step 3: fit the dental dam, remove the infected dentine using a Kotschy micro-excavator and monitoring with a Soprolife™ camera, and disinfect the dentine (Tubulicid solution, Schorndorf, Germany).

Step 4: form a metal matrix and inject hybrid glass-ionomer cement.

Step 5: photo-polymerization (3x20s), polishing and application of a fluoride varnish.

Discussion

The apparent simplicity of these techniques is, in most clinical situations, counterbalanced by implementation difficulties and by operating conditions much more complex than they appear [33]. Nevertheless, the objectives are achieved in preserving the natural tooth aesthetics, with preservation of the enamel surface for MIT1 and preservation of the marginal ridge for MIT2, in case of a slot cavity. Of course, this does not mean that the longevity of these restorations is ensured simply through working conscientiously and using a dental dam. However, an intermediate operating interval postponing conventional operative and prosthetic dentistry is achieved. Medical monitoring and implementation of complementary preventive therapies (e.g. fluoride varnishes, calcium technologies such as CPP-ACP etc.) whilst controlling the patient's caries risk should enable this

new operating interval to be maintained over time. There is no lack of caries risk measurement concepts and preventive concepts (Cariogram, MITP, Cambra) [38,39,40,41] with tools adapted to each level of caries risk [42]. As for Icon™ (DMG, Hamburg, Germany), despite its limitations, this product remains attractive in terms of its philosophy, although local application conditions are still difficult to analyze. Indeed, the enamel or enamel-dentine lesion activity is very difficult to analyze without opening the cavity; the absence of visible cavitation depends in particular on the magnifying power of the optical aids used. The camera used in both clinical cases, with a magnification power of more than 50, demonstrated its usefulness perfectly, and confirmed that without visual aid the operator is practically blind. Icon also fills a treatment void in the MIT1 techniques, involving capillary infiltration of the product. Based on available laboratory and clinical studies [35,36,37], it seems that resin infiltration of enamel lesions should reduce (or even stop) the progress of white spot lesions. Combining this ultraconservative restorative approach (which is considered micro-invasive) with a substantial caries remineralization program may provide therapeutic benefits and significantly reduce both long-term restorative needs and costs, thus complementing the overall concept of MID [43].

References

1. Bjorndal L, Mjör AI. Pulp-dentin biology in restorative dentistry. Part 4: Dental caries-Characteristics of lesions and pulp reactions. *Quintessence Int* 2001; 32: 717-36.
2. Silverstone LM, Hicks MJ, Featherstone MJ. Dynamic factors affecting lesion initiation and progression in human dental enamel. The dynamic nature of enamel caries. *Quintessence Int*, 1988; 19: 683-711.
3. Axelsson P. In: *Diagnosis and risk prediction of dental caries*, Vol. 2. Chicago: Quintessence Publishing Co, Inc, 1999.
4. EJ, Curtis JW, Ergle JW, Rueggeberg FA, Adair SM. Ultraconservative and cariostatic sealed restorations: Result at year 10. *JADA* 1998; 129: 55-66.
5. Mount GJ, Hume WR. A revised classification of carious lesions by site and size. *Quintessence Int*, 1997; 28: 301-3.
6. Pitts N. "ICDAS"—an international system for caries detection and assessment being developed to facilitate caries epidemiology, research and appropriate clinical management. *Community Dent Health* 2004; 21: 193-8.
7. Tassery H, Dejou J, Chafaia A, Camps J. *In vivo* diagnostic assessment of dentinal caries by junior and senior students using red acid dye. *Eur J Dent Educ* 2001; 5: 38-42.
8. Rees ES, Messer H, Douglas WH. Reduction in tooth stiffness as a result of endodontic or restorative procedures. *J Endod* 1989; 15: 512-6.

9. Peumans M, Van Meerbeek B, Asscherickx K, Simon S, Abe Y, Lambrechts P, Vanherle G. Do condensable composite help to achieve better proximal contacts? *Dent Mat* 2001; 17: 533-41.
10. Tassery H, de Donato P, Barrès O, Déjou J. *In vitro* assessment of polymerization procedures in class II restorations: Sealing, FTIR, and micro-hardness evaluations. *J Adhesive Dent* 2001; 3: 247-255.
11. Beznos Z. Microleakage at the cervical margin of composite class 2 cavities with different restorative techniques. *Oper Dent* 2001; 26: 60-9.
12. Wilson HF, Cawan A, Unterbrink G, Wilson MA, et al. A clinical evaluation of class II composites placed using a decoupling technique. *J Adhesive Dent* 2000; 2: 319-29.
13. Yoshikawa T, Burrow MF, Tagami J. A light curing method for improving marginal sealing and cavity wall adaptation of resin composite restorations. *Dent Mat* 2001; 17: 359-66.
14. Raskin A, D'Hoore W, Gonther S, Degrange M, et al. Reliability of *in vitro* microleakage tests: a literature review. *J Adhesive Dent* 2001; 3: 295-308.
15. Christenson RH; Committee on Evidence Based Laboratory Medicine of the International Federation for Clinical Chemistry Laboratory Medicine. Evidence-based evaluation of *in vitro* laboratory testing. *Ann Clin Biochem.* 2007; 44: 111-30.
16. MI Compendium of systematic reviews. Minimum Intervention (MI) in Dentistry. www.mi-compendium.org. Edition 1.4: 1-188.
17. Mickenautsch S. Adopting minimum intervention in dentistry: diffusion, bias and the role of scientific evidence. *Int Dent SA* 2009; 11: 16-26.
18. Mickenautsch S. Systematic reviews, systematic error and the acquisition of clinical knowledge *BMC Med Res Methodol* 2010; 10: 53.
19. Bratthall D, Hänsel Petersson G. Cariogram- a multifactorial risk assessment model for a multifactorial disease. *Community Dent Oral Epidemiol* 2005; 33: 256-64.
20. Featherstone JDB, Domejean-Orliaguet S, Jenson L, et al. Caries assessment in practice for age 6 through adult. *J Calif Dent Assoc.* 2007; 35: 703-7.
21. Jenson L, Budenz AW, Featherstone JD, Ramos-Gomez FJ, et al. Clinical protocols for caries management by risk assessment. *J Calif Dent Assoc* 2007; 35: 714-23.
22. Domejean-Orliaguet S, Banerjee A, Gaucher C, Milètic I, et al. Minimal intervention treatment plan. Practical implementation in general dental practice. *J Minim Interv Dent* 2009; 2: 103-123.
23. Ericson D, Kidd E, McCom D, Mjör I, Noak MJ. Minimally Invasive Dentistry- Concepts and techniques in cariology. *Oral Health Prev Dent* 2003; 1: 59-72.
24. Ekstrand KR Improving clinical visual detection-potential for caries clinical trials. *J Dent Res* 2004; 83(Spec Iss C): C67-C71.
25. Ismail AI, Sohn W, Tellez M, Amaya A, SenA, et al. The International Caries Detection and Assessment System (ICDAS): an integrated system for measuring dental caries. *Community Dent Oral Epidemiol* 2007; 35: 170-8.
26. Huguo B, Stassinakis A. preparation and restoration of small interproximal carious lesions with sonic instruments. *Pract Periodontis Aesthet Dent* 1998;10:353-9.
27. Dommisch H, Peus K, Kneist S, Krause F, et al. Fluorescence-controlled Er:YAG laser for caries removal in permanent teeth: a randomized clinical trial. *Eur J Oral Sci* 2008; 116: 170-6.
28. Koubi S, Tassery H. Minimally invasive dentistry using sonic and ultrasonic devices in ultraconservative class 2 restoration. *J Contemp Dent Pract* 2008; 9: 1-11.
29. Erten H, Üçtasli MB, Akarslan ZZ, Üzun Ö, et al. Restorative treatment decision making with unaided visual examination, intraoral camera and operating microscope. *Oper Dent* 2006; 31: 55-9.
30. Hall A, Girkin JM. A review of potential new diagnostic modalities for caries lesions. *J Dent Res.* 2004; 83 Spec No C: C89-94.
31. Rodrigues JA, Hug I, Diniz MB, Lussi A. Performance of fluorescence methods, radiographic examination and ICDAS II on occlusal surfaces *in vitro*. *Caries Res* 2008; 42: 297-304.
32. Terrer E, Koubi S, Dionne A, Weisrock G, et al. A New Concept in Restorative Dentistry: Light-Induced Fluorescence Evaluator for Diagnosis and Treatment: Part 1 -Diagnosis and Treatment of Initial Occlusal Caries. *J Contemp Dent Pract* 2009; 10: 86-94.
33. Terrer E, Raskin A, Koubi S, Dionne A, et al. A new concept in restorative dentistry: LIFEDT-Light Induced Fluorescence Evaluator for Diagnosis and Treatment: Part 2- Treatment of dentinal caries. *J Contemp Dent Pract.* 2010; 11: 1-12.
34. Tyas MJ, Anusavice KJ, Frencken JE, Mount GJ. Minimal intervention dentistry - a review. *FDI Commission Project 1-97.* *Int Dent J* 2000; 50: 1-12.
35. Meyer-Lueckel H, Paris S. Progression of artificial enamel caries lesions after infiltration with experimental light curing resins. *Caries Res* 2008; 42: 117-24.
36. Kugel G, Arsenault P, Papas A. Treatment modalities for caries management, including a new resin infiltration system. *Compend Contin Educ Dent* 2009; 30:1-10.
37. Paris S, Meyer-Lueckel H. Inhibition of caries progression by resin infiltration in situ. *Caries Res* 2010; 44: 47-54.
38. Axelsson P. In: An introduction to risk prediction and preventive dentistry. Other caries-preventive factors. Chapter 7. Quintessence Publishing Co, Inc, 1999: 77-105.
39. Pitts NB. Modern concepts of caries measurement. *J Dent Res.* 2004; 83 Spec No C: C43-7.

40. Walsh LJ, Tsang AK. Chairside testing for cariogenic bacteria: current concepts and clinical strategies. *J Minim Interv Dent* 2008; 1: 126-49.
41. Ahovuo-Saloranta A, Hiiri A, Nordblad A, Worthington H, et al. Pit and fissure sealants for preventing dental decay in the permanent teeth of children and adolescents. *Cochrane Database Syst Rev*. 2008; (4):CD001830. DOI: 10.1002/14651858.CD001830.pub3.
42. <http://www.carifree.com/>
43. Kielbassa AM, Muller J, Gernhardt CR. Closing the gap between oral hygiene and minimally invasive dentistry: a review on the resin infiltration technique of incipient (proximal) enamel lesions. *Quintessence Int* 2009; 40: 663-81.

Table 1. Clinical color guide used with the LIFEDT concept and the Soprolife device.

Color of dental tissue	Active lesion		Arrested lesion	
	Daylight	Fluorescence mode treatment	Daylight	Fluorescence mode treatment
Infected dentine	Yellow-orange	Dark green	Dark brown appearance	Dark green
Infected/affected dentine	Yellow-brown	Bright red	Dark brown	Dark red
Abnormal dentine	Yellow-brown	Grey-green	Brown	Grey-green + red bottom

Table 2. Different types of MIT. MIT1 - no preparation except tissue conditioning, and MIT2 with minimal preparation.

Minimally invasive technique	Type 1: No preparation except tissue conditioning	Type 2: Minimal preparation.
Occlusal, vestibular, lingual or palatal surfaces	Fluoride and chlorhexidine varnish (Vivadent, Voco etc.), Glass ionomer varnish (3M, ESPE) MI paste plus and GC Tooth Mousse (GC, Tokyo, Japan)	Reversed caries process technique (glass-ionomer dentine substitutes, stepwise techniques)
	Ozonotherapy coupled with remineralization solution (Kavo, Biberach, Germany).	Minimally invasive preparation with micro-burs or other techniques (air abrasion, laser, adhesive preparation).
	Sealant application	
Proximal surface	Fluoride and chlorhexidine varnish (Vivadent, Voco etc.), Glass ionomer varnish (3M, ESPE)	Reversed caries process technique (glass-ionomer dentine substitutes, stepwise techniques) with minimally invasive class 2 preparation
	MI paste plus, GC Tooth Mousse (GC, Tokyo, Japan)	
	Icon (DMG, Hamburg Germany)	One step minimally invasive class 2 preparation with micro-burs or other techniques (air laser, adhesive preparation)
		Slot and tunnel cavities with suitable sonic inserts. (Caries scale D1-D2with cavitation)

Table 3. Advantages and drawbacks of MIT1 with regard to the treated surface

MIT 1	Techniques	Advantages	Drawbacks
Occlusal, vestibular, lingual and palatal surfaces	Varnish, MI paste plus, GC Tooth mousse (GC, Tokyo, Japan).	Easy application and protocol.	Efficiency with regard to the caries risk assessment.
	Ozonotherapy (Kavo, Biberach, Germany).	Maximum esthetic results.	Efficiency doubtful for ozone.
	Sealant application.	Reversible actions, non-iatrogenic	
Proximal surface	Varnish* MI paste plus*, GC Tooth mousse* (GC, Tokyo, Japan).	Application not so easy.	Efficiency with regard to the caries risk assessment.
	Icon* (DMG, Hamburg, Germany).	Maximum esthetic results.	Operator-dependent,
	*Needs accessible surfaces.	Reversible actions, non-iatrogenic	New techniques, proof to be confirmed for Icon Accessible surfaces need to be strongly separated when using Icon.

Table 4. Advantages and disadvantages between sonic and ultrasonic cavity preparation systems in case of slot cavity and minimally invasive class 2 preparation.

MIT 2	Ultrasonic	Sonic	Kind of preparation for both
Advantages	<p>Preservation of the adjacent proximal surface.</p> <p>Preservation of the marginal ridge (slot and tunnel cavity).</p> <p>Uses the same ultrasonic handpiece as for periodontal scaling</p> <p>Initial penetration with diamond burs The cavity is required less often</p> <p>Natural aesthetics preserved.</p>	<p>Preservation of the adjacent proximal surface.</p> <p>Preservation of the marginal (slot and tunnel cavity).</p> <p>Low risk of enamel fracture</p> <p>Natural aesthetics preserved.</p>	<p>Tunnel and slot preparations.</p> <p>End steps of minimally class II preparation.</p> <p>Beveling steps.</p>
Drawbacks	<p>Low cost.</p> <p>Information concerning the potential create cracks due to ultrasonic vibrations and their clinical outcomes is not provided by the manufacturer</p> <p>The outer carious dentine is better removed with a round steel bur mounted on a low speed motor or with a manual excavator</p> <p>Preservation of the adjacent proximal surface.</p> <p>Proximal surface is more difficult than with the sonic device with regard to the effectiveness of the ultrasonic vibrations.</p> <p>The effectiveness of the device depends on the hardness of the dental tissue</p> <p>Operator-dependent</p>	<p>Requires a specific water cooled handpiece.</p> <p>High air pressure required.</p> <p>The effectiveness of the device depends on the hardness of the dental tissue</p> <p>Operator-dependent</p>	<p>Efficiency with regard to the caries risk assessment.</p> <p>Operator dependent.</p> <p>Perfect filling remains difficult to control with slot and tunnel cavities.</p> <p>The thickness limit of the marginal ridge remains unknown for tunnel and slot cavities.</p>

Table 5. Advantages and drawbacks of MIT2 techniques

MIT 2	Techniques	Advantages	Drawbacks
Occlusal, vestibular, lingual and palatal surfaces	Micro preparation: preparation is similar to the caries shape.	Easy technique.	Needs visual aid.
	Tools: air abrasion, micro-burs, laser, sonic & ultrasonic inserts.		Oxide silica dust (in case of air abrasion). Laser: Needs visual protection, high cost, could interfere with adhesive technique.
Proximal surface	Adhesive preparation. with no occlusal extension.	Maximum tissue preservation.	Needs visual aid.
	Tunnel cavity (open or closed).	Aesthetic results.	Efficiency with regard to the caries risk assessment.
	Slot cavity.		Perfect filling remains difficult to control.
	Tools: micro-burs, laser, sonic & ultrasonic inserts.		Operator-dependent, Caries spreading difficult to control. (Tunnel and slot cavities).

Article N° 4.

ISSN: 0972-0707

Journal of Conservative Dentistry

Volume 14

Issue 4

Oct - Dec 2011

Official Publication of
**Federation of Operative
Dentistry of India**

Online full text at
www.jcd.org.in

Published by
Medknow Publications

PubMed
Indexed

Light induced fluorescence evaluation: A novel concept for caries diagnosis and excavation

Neeraj Gugnani, IK Pandit, Nikhil Srivastava, Monika Gupta, Shalini Gugnani

Dayanand Anglo-Vedic Dental College, Yamunanagar, Haryana, India

Abstract

In the era of minimal invasive dentistry, every effort should be directed to preserve the maximum tooth structure during cavity preparation. However, while making cavities, clinicians usually get indecisive at what point caries excavation should be stopped, so as to involve only the infected dentin. Apparent lack of valid clinical markers, difficulties with the use of caries detector dyes and chemo mechanical caries removal systems carve out a need for an improved system, which would be helpful to differentiate between the healthy and infected dentin during caries excavation. Light induced fluorescence evaluation is a novel concept implicated for caries detection and for making decisions while cavity preparation. This paper describes a few cases that explain the clinical applicability of this concept, using the Soprolife camera that works on this principle. Autofluorescence masking effect was found to be helpful for caries detection and the red fluorescence in the treatment mode was found helpful in deciding 'when to stop the excavation process.' Light induced fluorescence evaluation – Diagnosis - Treatment concept can be used as a guide for caries detection and excavation. It also facilitates decision making for stopping the caries excavation so as to involve infected dentin only.

Keywords: Dentinal caries; light induced fluorescence; minimal invasive dentistry; soprolife

INTRODUCTION

Once the caries has reached the cavitory stage, the only treatment option left is to restore the lesion, because of the irreversible nature of the disease. Till yester years, cavities were made using GV Black's principles that dictate extension for prevention. This classical approach to treat dentinal lesions mandates removing all the infected and affected dentin. However today, there is paradigm shift in the manner in which the cavitated dentinal lesions are handled.^[1] With changes in the materials and restorative principles, the concept of 'Minimally Invasive Dentistry (MID)' has taken the lead. And, it is now well accepted to extend the cavities only to involve infected dentin and leaving the affected dentin as such.^[2,3] However, while making cavities, it is usually difficult to know at what point caries excavation should be stopped, such as to involve only the infected dentin. This is due to the lack of valid clinical markers to differentiate between the infected and affected dentin.

Many subjective factors like consistency of the tissue and color are being used throughout to differentiate between the healthy and diseased dentinal tissue, and thus serve as a guide for the termination of the excavation process.^[4]

Other methods used to facilitate this excavation process include: use of caries detector dyes; use of chemo mechanical measures; smart prep burs,^[5-8] etc. But there are concerns with their usage, like inadvertent cutting of sound dentin, increased time to excavate etc.^[6,9] Fluorescence has also been used to guide the excavation process.^[10-12] Based on the property of fluorescence of dental tissues, four different fluorescence visions can be observed: green fluorescence indicating healthy tissues; black green fluorescence indicating infected dentin; bright red colour indicting the margin of infected/affected dentin; and, acid green fluorescence indicating sound dentin at the end of excavation. These different fluorescence signals aid in caries detection and decision making during cavity preparation. This concept has been termed as Light Induced Fluorescence Evaluation – Diagnosis - Treatment concept (Life D.T concept).^[13,14]

Recently a new fluorescence based camera system that works on the principle of Life D.T has been launched to aid caries detection and to guide cavity preparation [Soprolife (Sopro, La Ciotat, France)]. The camera captures the images in three different modes that is, daylight, diagnosis and treatment mode.^[13] Capturing in the day light provides a

Address for correspondence:

Dr. Neeraj Gugnani, Dayanand Anglo-Vedic Dental College, Haryana, Yamunanagar – 135 001, India
E-mail: drgugnani@gmail.com

Date of submission: 07.12.2010
Review completed: 11.07.2011
Date of acceptance: 07.09.2011

Access this article online

Quick Response Code:



Website:
www.jcd.org.in

DOI:
10.4103/0972-0707.87216

white light image with a magnification of more than 50 times than the tooth surface. The other two modes of the camera work on the principle of autofluorescence.^[14] In the diagnostic mode, the camera uses a visible blue light frequency (wavelength 450 nm) to illuminate the surface of the teeth, and provides an anatomic image overlay of the green fluorescence image on the “white light” image. This green fluorescence is considered as an indicator of healthy dental tissues; while carious lesions could be detected by variation in the auto fluorescence of its tissues in relation to a healthy area of the same tooth.

In addition to the green fluorescence, red fluorescence may also be seen in some diagnostic mode images. This red fluorescence may represent deep dentinal caries; however, at the same time it might be a false signal coming from the organic deposits covering the tooth. Terrer E. *et al.* found a correlation between this red signal and organic deposits in the bottom of the groove.^[13] Hence, if a red fluorescent signal is encountered in the diagnostic mode images, it needs to be validated. For validation, the area showing the red fluorescence should be washed off with sodium bicarbonate or pumice, and if the fluorescence persists, then only it is considered to be representative of infected dentin. The fluorescence would no longer be there, if the source is simply the organic deposits on the tooth surface.

The third mode is the treatment mode, and the red fluorescence captured in this mode is considered as an indicator to differentiate between infected and affected dentin.^[13,14]

The aim of this paper is to look upon the clinical applicability of the Life D.T concept for caries detection and excavation.

CASE REPORTS

In this paper we present clinical cases done using the principles of Life D.T concept, with SoproLife Camera system. The study involved human volunteers, and was approved by the institutional review board of Dayanand Anglo-Vedic Dental College Yamunanagar, India. An informed consent was sought from the volunteers for participation in the study. The caries in all the experimental teeth were diagnosed, and excavated applying the Life D.T concept, using different fluorescence signals. The clinical implications of the various fluorescence signals have been tabulated in Table 1. An assessment of caries excavation may be explained under following principles:

Table 1: Different fluorescence visions and its interpretations

Healthy dentin	Green fluorescence
Infected dentin	Black green fluorescence
Infected/affected dentin	Bright red fluorescence. This tissue is fairly easily eliminated by manual excavator.

Principle 1:Autofluorescence masking effect

Green fluorescence in the diagnostic mode of the camera is considered an indicator of healthy tooth and loss of green fluorescence (black green fluorescence) indicates infected dentin. This loss of green fluorescence is termed as ‘Autofluorescence masking effect’. In the first patient, the caries in tooth # 36 was scored as International Caries Assessment and Detection System 3 (ICDAS 3) [Figure 1a]; however. The pictures taken with SoproLife camera did show an autofluorescence masking effect in the disto-occlusal aspect of the tooth [Figure 1c], while only slight altered fluorescence was seen on the mesio-occlusal aspect [Figure 1c]. Using the Life D.T guidelines, this autofluorescence masking was indicative of deep dentinal caries. The caries was then excavated by the clinician who was blinded with the fluorescence signals. At the end of excavation, it was observed that a deep cavity had to be made in the Disto Occlusal aspect [Figure 1d]. Thus it might be concluded that “autofluorescence masking” effect can be used as an indicator to diagnose infected dentinal caries.

Principle 2: Excavate till acid green fluorescence is achieved

The second principle dictates that acid green fluorescence is to be achieved at the end of the excavation process, as this is considered as an indicator of sound dentin. In the second series of patients, the excavation was carried out in carious teeth without the guidance of a fluorescence camera. At the end of excavation, images were taken and acid green fluorescence was observed [Figure 1f] in a tooth which was suspected to have dentinal caries, owing to presence of validated red fluorescence, preoperatively [Figure 1e]. Similarly acid green fluorescence was also seen at the end of excavation in other patients [Figure 1b]

Thus, aiming to achieve acid green fluorescence might be used as a guideline for termination of excavation process.

Principle 3: Bright red fluorescence indicates infected/ affected dentin

This principle can only be applied when images are taken in the treatment mode. Terrer E. *et al.* explained that in treatment mode images, sometimes red fluorescence may be seen at the end of excavation instead of acid green fluorescence, and this can be used as an indicator to differentiate between infected and affected dentin.^[14] If bright red fluorescence is seen during cavity making and the area is soft to excavate, it indicates infected dentin, while the in areas which are hard to excavate, it indicates affected dentin. Third patient in our series was scored as ICDAS 3 both in the mesial and distal pits in tooth # 26. The diagnostic mode image showed red fluorescence in both the pits, which was validated even after washing with sodium bicarbonate, indicating infected dentin [Figure 2a]. During excavation, deep dentinal cavities was seen beneath both mesial and distal pits [Figure 2b], and at

the end of cavity preparation, the treatment mode images were captured, and bright red fluorescence was seen in both the pits [Figure 2c]. This bright red fluorescence indicates infected/affected dentin to be confirmed using manual excavator. Applying the Life DT principles, only the areas that were “soft to excavate” were regarded as infected areas, while the “hard to excavate” was left as such. Conclusively, these principles might be helpful in guiding the clinicians to detect initial caries, and also useful to guide caries excavation by differentiating between the infected and affected dentin.

DISCUSSION

Though there is an increased focus on promoting the

detection of non cavitated carious lesions, the irony is that in most of the clinical settings the lesions are detected at the cavitated stage only. And once caries is detected at the cavitation stage, restoration is the only viable option. While making dentinal cavities, clinicians frequently get confronted about where to stop the caries excavation process. Dentinal caries has an outer layer contaminated by bacteria forming a non-remineralizable necrotic collagen matrix, and an inner layer, having the potential to remineralize.^[3]

In an ideal situation, only the layer of carious dentin, which is rich in bacteria, unremineralizable, and has necrotic tissue remaining on its surface, should be removed while leaving the inner remineralizable dentin

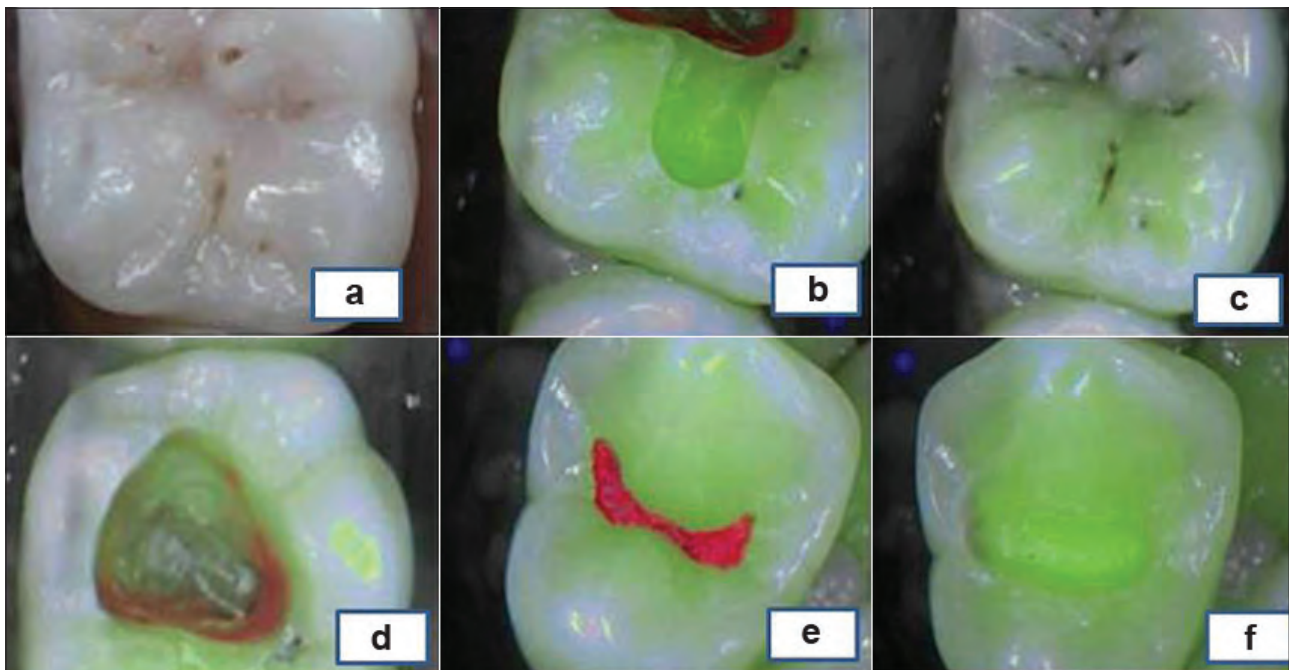


Figure 1: (a) White Light Image of 36, (b) Image showing loss in fluorescence on the Disto Occlusal aspect and green fluorescence on Mesio Occlusal aspect, (c) Image of cavity (A shallow cavity on the Mesio Occlusal aspect), Green fluorescence was achieved at the end of excavation, (d) Image of cavity (A deep cavity on Disto Occlusal aspect), (e) Image with validated red fluorescence. (Another patient), (f) Acid green fluorescence at the end of cavity

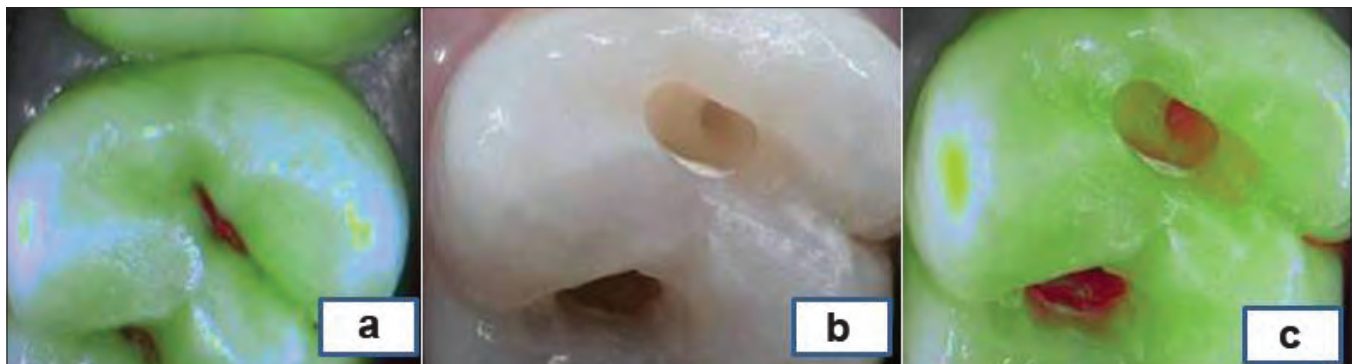


Figure 2: (a) Validated red fluorescence, (b) White light Image after caries excavation, (c) Image during cavity preparation showing bright red fluorescence

(affected dentin) as such.^[4,15] The inherent subjectivity in detecting this excavation boundary results in clinically significant differences in the quality and quantity of dentine removed by different operators. The need of the hour is to shift the restorative dentistry towards MID dentistry, and this requires promoting the use of novel diagnostic equipments, or other such aids that can help us to know 'where to stop the excavation process'. Various concepts that have been used in the past to guide the checkpoint for stopping the caries excavation include: use of caries detector dyes; use of chemomechanical means; and, Fluorescence Aided Caries Excavation. McComb D in a review article emphasized that though caries detector dyes are purported to aid the dentist in differentiation of infected/ affected dentin, these dyes cannot be concluded to be specific for infected dentin.^[16] Literature also raises concerns that the use of these dyes frequently causes the staining of the Circumpulpal dentin or Dentino-enamel junction (DEJ), leading to unnecessary removal of sound tooth structure.^[16,17] Use of chemo-mechanical methods of removal of the caries is also increasing; however, these systems have been found to be much more time consuming than the conventional systems.^[18] Authors have reported left-out carious dentin in DEJ regions when excavation is carried using chemo-mechanical caries removal methods.^[6]

Fluorescence-aided caries excavation (F.A.C.E.) has also been used in past.^[19] Lennon AM *et al.* in their study on F.A.C.E., caries detector, and conventional caries excavation in primary teeth concluded that excavation by using F.A.C.E. is more effective than conventional excavation in removal of the infected primary dentin.^[12] In another study by Lennon *et al.*, it was found that the excavation results on using F.A.C.E. are similar to Conventional excavation; and, superior to Caries Detector dyes and Chemo-mechanical excavation, however, these excavation procedures using F.A.C.E. required a significantly shorter excavation time as compared to the time required by conventional technique.^[11] Life D.T is a novel concept based on the fluorescence property of dental tissues. It employs the principle that the fluorescence signals from the dental tissues can be used for caries detection and excavation, by differentiating between infected and affected dentin. SoproLife is a camera system that is based on Life D.T concept, and claims to help the clinician in diagnosing caries and in decision making during cavity preparation. Terrer E. *et al.* proposed that alteration in the green fluorescence should be considered as the indicator of caries.^[13] This is similar to Quantitative light-induced fluorescence (QLF) system, in which, the loss of fluorescence has been shown to correlate with the degree of demineralization.^[20]

In addition to the green fluorescence, red fluorescence is also observed in images captured in the diagnostic mode of the camera. The red fluorescence, in the diagnostic mode has been proposed to be either due to

infected dentin, or as a false signal coming from organic tooth deposits. This initial red fluorescence needs to be validated. In the treatment mode, the red fluorescence is considered to arise from carious dentin and may be due to the breakdown of organic and inorganic constituents of dentin. This has been attributed to the Maillard reaction,^[14] that is, a non-enzymatic browning reaction in carious dentin that results in the generation of advanced Maillard products (carboxymethyl lysine and pentoside).^[14,21] Terrer E. *et al.* explained this phenomenon to partially account for fluorescence variations due to suspected fluorophores in carious dentin, such as, dityrosine, pentoside and other Maillard reaction products.^[14]

Our aim was to study the clinical applicability of Life D.T principles during caries excavation. The black green fluorescence (autofluorescence masking effect) was shown to be indicative of infected dentin while during cavity preparation, the bright red fluorescence was found to be indicative of infected/affected dentin. This junction was easily differentiated using a manual excavator and the areas which were hard to excavate, were left as such. Thus, different fluorescence signals were a helpful guide for caries detection and excavation. *In vitro* and *in vivo* studies are required both in unison and in comparison to other aids to validate the Life D.T concept.

REFERENCES

1. Carounanidy U, Sathyanarayanan R. Dental caries: A complete changeover (Part III) - Changeover in treatment decisions and treatments. *J Conserv Dent* 2009;13:209-17.
2. Ericson D, Kidd E, McComb D, Mjör I, Noack MJ. Minimally Invasive Dentistry--concepts and techniques in cariology. *Oral Health Prev Dent* 2003;1:59-72.
3. Pai VS, Nadig RR, Jagadeesh T, Usha G, Karthik J, Sridhara K. Chemical analysis of dentin surfaces after Carisolv treatment. *J Conserv Dent* 2009;12:118-22.
4. Banerjee A, Watson TF, Kidd EA. Dentine caries excavation: A review of current clinical techniques. *Br Dent J* 2000;188:476-82.
5. Sato Y, Fusayama T. Removal of dentin by fuchsin staining. *J Dent Res* 1976;55:678-83.
6. Cederlund A, Lindskog S, Blomlöf J. Effect of a chemo-mechanical caries removal system (Carisolv) on dentin topography of non-carious dentin. *Acta Odontol Scand* 1999;57:185-9.
7. van de Rijke J. Use of dyes in cariology. *Int Dent J* 1991;41:111-6.
8. Carounanidy U, Sathyanarayanan R. Dental caries: A complete changeover (Part II)- Changeover in the diagnosis and prognosis. *J Conserv Dent* 2009;12:87-100.
9. Kidd EA, Joyston-Bechal S, Beighton D. The use of a caries detector dye during cavity preparation: A microbiological assessment. *Br Dent J* 1993;174:245-8.
10. Gurbuz T, Yilmaz Y, Sengul F. Performance of laser fluorescence for residual caries detection in primary teeth. *Eur J Dent* 2008;2:176-84.
11. Lennon AM, Buchalla W, Rassner B, Becker K, Attin T. Efficiency of 4 caries excavation methods compared. *Oper Dent* 2006;31:551-5.
12. Lennon AM, Attin T, Martens S, Buchalla W. Fluorescence-aided caries excavation, caries detector, and conventional caries excavation in primary teeth. *Pediatr Dent* 2009;31:316-9.
13. Terrer E, Koubi S, Dionne A, Weisrock G, Sarraquigne C, Mazuir A, *et al.* A new concept in restorative dentistry: Light-induced fluorescence evaluator for diagnosis and treatment. Part 1: Diagnosis and treatment of initial occlusal caries. *J Contemp Dent Pract* 2009;10:E086-94.
14. Terrer E, Raskin A, Koubi S, Dionne A, Weisrock G, Sarraquigne C, *et al.* A new concept in restorative dentistry: LIFEDT-light-induced fluorescence evaluator for diagnosis and treatment: Part 2 - treatment of dental caries. *J Contemp Dent Pract* 2010;11:E095-102.

15. Yip HK, Stevenson AG, Beeley JA. The specificity of caries detector dyes in cavity preparation. *Br Dent J* 1994;176:417-21.
16. McComb D. Caries-detector dyes--how accurate and useful are they? *J Can Dent Assoc* 2000;66:195-8.
17. Stahl J, Zandona A. Rationale and protocol for the treatment of non-cavitated smooth surface carious lesions. *Gen Dent* 2007;55:105-11.
18. Pandit I, Srivastava N, Gugnani N, Gupta M, Verma L. Various methods of caries removal in children: A comparative clinical study. *J Indian Soc Pedod Prev Dent* 2007;25:93-6.
19. Lennon A. Fluorescence-aided caries excavation compared to conventional method. *Oper Dent* 2003;28:341-5.
20. van der Veen MH, de Josselin de Jong E. Application of quantitative light-induced fluorescence for assessing early caries lesions. *Monogr Oral Sci* 2000;17:144-62.
21. Kleter G, Damen J, Buijs M, Ten Cate J. Modification of amino acid residues in carious dentin matrix. *J Dent Res* 1998;77:488-95.

How to cite this article: Gugnani N, Pandit IK, Srivastava N, Gupta M, Gugnani S. Light induced fluorescence evaluation: A novel concept for caries diagnosis and excavation. *J Conserv Dent* 2011;14:418-22.

Source of Support: Nil, **Conflict of Interest:** None declared.

Author Help: Online submission of the manuscripts

Articles can be submitted online from <http://www.journalonweb.com>. For online submission, the articles should be prepared in two files (first page file and article file). Images should be submitted separately.

- 1) **First Page File:**
Prepare the title page, covering letter, acknowledgement etc. using a word processor program. All information related to your identity should be included here. Use text/rtf/doc/pdf files. Do not zip the files.
- 2) **Article File:**
The main text of the article, beginning with the Abstract to References (including tables) should be in this file. Do not include any information (such as acknowledgement, your names in page headers etc.) in this file. Use text/rtf/doc/pdf files. Do not zip the files. Limit the file size to 1024 kb. Do not incorporate images in the file. If file size is large, graphs can be submitted separately as images, without their being incorporated in the article file. This will reduce the size of the file.
- 3) **Images:**
Submit good quality color images. Each image should be less than **4096 kb (4 MB)** in size. The size of the image can be reduced by decreasing the actual height and width of the images (keep up to about 6 inches and up to about 1800 x 1200 pixels). JPEG is the most suitable file format. The image quality should be good enough to judge the scientific value of the image. For the purpose of printing, always retain a good quality, high resolution image. This high resolution image should be sent to the editorial office at the time of sending a revised article.
- 4) **Legends:**
Legends for the figures/images should be included at the end of the article file.

Molecular structural analysis of carious lesions using micro-Raman spectroscopy

**Bernard Levallois¹, Elodie Terrer^{2,3},
Yvan Panayotov¹, Hamideh Salehi¹,
Hervé Tassery^{1,2,3}, Paul Tramini¹,
Frédéric Cuisinier¹**

¹EA 4203, UFR Odontologie, Université Montpellier 1, Montpellier Cedex, France;
²Aix-Marseille-Université, Marseille, France;
³APHM Hôpital Timone, Service Odontologie, Marseille Cedex, France

Levallois B, Terrer E, Panayotov Y, Salehi H, Tassery H, Tramini P, Cuisinier F. Molecular structural analysis of carious lesions using micro-Raman spectroscopy. Eur J Oral Sci 2012; 00: 000–000. © 2012 Eur J Oral Sci

In clinical situations carious dentine tissues can be discriminated by most caries fluorescence detection tools, including a new fluorescence intra-oral camera. The objectives of this study were: (i) to analyze the Raman spectra of sound, carious, and demineralized dentine, (ii) to compare this spectral analysis with the fluorescence variation observed when using a fluorescence camera, and (iii) to evaluate the involvement of the Maillard reaction in the fluorescence variations. The first positive hypothesis tested was that the fluorescence of carious dentine obtained using a fluorescence camera and the Raman spectra variation were closely related. The second was that the variation of fluorescence could be linked with the Maillard reaction. Sound dentine, sound dentine demineralized in aqueous nitric acid solution, carious soft dentine, sound dentine demineralized in lactic acid solution, sound dentine demineralized in aqueous nitric acid solution and immersed in methylglyoxal solution, and sound dentine demineralized in aqueous nitric acid solution and immersed in methylglyoxal and glucose solutions, were studied using micro-Raman spectroscopy. Modifications in the band ratio of amide, phosphate, and carbonate were observed in the decayed and demineralized groups compared with the sound dentine group. The results indicate that a close relationship exists between the Maillard reaction and fluorescence variation.

Hervé Tassery, UFR Odontologie, Université Montpellier 1, 34193 Montpellier Cedex 5, France

Telefax: +336-0-3839119
E-mail: herve.tassery@numericable.fr

Key words: dentine caries; Maillard reaction; Raman spectroscopy

Accepted for publication June 2012

Dental caries involves highly complex odontoblast cell and extracellular matrix modifications, depending on the caries activity and the level of bacteria (1–3). Dental caries activity (i.e. active or arrested) greatly influences the structure and the color of the tissue (4, 5). In daylight, dentine discoloration, the so-called browning reaction, is a common indicator of caries, and thus dentine softness upon probing or excavation and a damp light-brown spot reflect ongoing decay, whereas a hard, shiny dark-brown spot characterizes lesion arrestment. Besides extrinsic staining, collagen destructure (6), one hypothesis for this brown discoloration, takes place, which involves the non-enzymatic glycation of carbohydrate and protein (the so-called Maillard reaction), in which a brownish polymer of cross-linked proteins and advanced glycation end-products (AGEs) (7) is formed. The AGEs accumulate gradually in tissues with aging and in patients with specific diseases, such as diabetes, Alzheimer's disease, and retinal dysfunction (7–11). These AGEs include fructosyllysine, *N*-(carboxymethyl)lysine, *N*-(carboxymethyl)hydroxylysine, and pentosidine (12, 13), a fluorescent cross-link formed between arginine and lysine residues. The Maillard reaction can be studied using methylglyoxal (MGO) as an intermediate glycating agent.

Dentine collagen is likely to link with AGEs over the long term, rendering dentine collagen more resistant to proteolytic breakdown (14). The main organic matrix in dentine is fibrous type I collagen (which has a non-centrosymmetric structure), that, like other intracellular molecules [nicotine adenine dinucleotide, reduced (NADH), flavin adenine dinucleotide (FAD), and aromatic amino acids] can generate fluorescence signals, depending on the excitation wavelength (15, 16). Collagen fluorescence could be used to indicate the condition of the dental tissue (i.e. sound or caries-affected), utilizing the optical property of dental tissues known as autofluorescence, by analyzing collagen using confocal laser-scanning microscopy with blue-light excitation (488 nm) (17–21). The wavelength of the autofluorescence signal varies according to the density and the chemical composition of the tissue on its surface and subsurface. The different layers of tissue and their characteristics influence its response, as found for material deposits. As a result, any carious lesion or affected tissue will be detected by a variation in autofluorescence in comparison with a sound part of the same tooth. The decayed dentine can be discriminated by most caries fluorescence detector tools, such as fluorescence-aided caries excavation (FACE) (ProFace; W&H, Dentalwerk, Bürmoos, Germany), Fluorescent camera

(FC) (VistaProof; Dürr Dental, Bietigheim-Bissingen, Germany), infrared fluorescence, and DIAGNOdent laser (KaVo Dental, Biberach, Germany) (22–25). Based on dentine autofluorescence, a light-emitting diode (LED) camera (SoproLife) was developed (Sopro-Acteon, La Ciotat, France) with an excitation wavelength of around 450 nm (20, 21). The fluorescence signals are amplified selectively to increase the specificity of the images.

The aim of this study was to understand the origin of the fluorescence signals obtained using the SoproLife camera, and thus analyze the Raman spectra of sound, carious, and demineralized dentine, compare this spectral analysis with the fluorescence variation obtained using the SoproLife camera, and assess the involvement of the Maillard reaction in the fluorescence variations.

Regarding the study hypotheses, the first hypothesis assumed a possible relationship between the signals observed using SoproLife and Raman spectroscopy, and the second hypothesis assumed an association with the Maillard reaction.

Material and methods

Samples were prepared *in vitro* to mimic the demineralization and the browning processes occurring during caries. Sound dentine, carious soft dentine (Fig. S1), sound dentine demineralized in aqueous nitric acid solution (Fig. S2 and S3a), sound dentine demineralized in lactic acid solution, sound dentine demineralized in aqueous nitric acid solution and immersed in MGO solution (Fig. S3b), and sound dentine demineralized in aqueous nitric acid solution and immersed in MGO and glucose solutions were studied by micro-Raman spectroscopy. Additionally, pentosidine, an AGE product, was also studied by Raman spectroscopy. Raman spectra of the samples were analyzed and correlated to the fluorescence obtained with the SoproLife camera.

The SoproLife camera

The SoproLife intra-oral camera utilizes two types of LED that can illuminate tooth surfaces in the visible domain, either in the white-light region or in a narrow band (450-nm wavelength with a bandwidth of 20 nm, centered at ± 10 nm around the excitation wavelength). This provides an anatomical image superimposed on autofluorescence. The camera can detect and locate differences in the density, structure, and/or chemical composition of biological tissue subjected to continuous lighting in one frequency band, while making it generate a fluorescence phenomenon in a second frequency band. The camera is equipped with an image sensor [a 0.64 cm charge-coupled device (CCD) sensor] consisting of a mosaic of pixels covered with filters of complementary colors. The data collected, relating to the energy received by each pixel, enable an image of the tooth to be retrieved.

The camera is operated in three modes: (i) daylight mode [four white-light LEDs generate daylight (Fig. S1a)]; and (ii) diagnostic and (iii) treatment modes [for these two modes the light is provided by four blue LEDs (450 nm) (Fig. S1b); the difference between the two modes is due to different CCD settings].

Micro-Raman spectroscopy

Raman spectroscopy is a vibrational spectroscopy technique used to assess light scattered from biological molecules and ions, so that the wavelength difference between scattered and incident light corresponds to molecular vibration, leading to frequency shift bands (labeled in cm^{-1}) in the Raman spectrum (26, 27). Raman spectroscopy has been widely used to investigate the molecular structure of biological tissues and has many benefits: no special treatment is required, analysis can be performed at room temperature, the technique has good reproducibility, and the presence of a molecule to which a spectrum is assigned can be appraised by calculating the spectrum peak.

To investigate the chemical composition of the different dentine samples, Raman spectra were recorded at 298 K using a LabRAM ARAMIS IR² confocal micro-Raman spectrometer (Jobin-Yvon; Horiba, Chilly Mazarin, France) equipped with a BX41 Olympus microscope (Olympus corporation, Tokyo, Japan), an 1,800 grooves mm^{-1} grating, and a CCD detector cooled by a Peltier-effect module. The samples were mounted on an XYZ motorized stage with 0.1- μm step resolution. The microscope lens was a long working distance $\times 50$ objective. The spectral resolution was $\pm 1 \text{ cm}^{-1}$. Raman spectra were obtained by excitation with 632.8-nm wavelength radiation from a He–Ne laser generating $<12 \text{ mW}$ on the samples. Due to fluorescence, the samples were photobleached by laser for 15 min before spectral recording. The acquisition time was 90 s with three accumulations.

The spectra obtained from Raman microscopy were normalized using PEAKFIT v4.12 software (Systat Software, Chicago, IL, USA). For the fluorescence baseline removal, two parametric models were used: linear and power. Power is a non-linear model and is fitted iteratively using the Levenburg–Marquardt algorithm, whereas linear is fitted in a single-step matrix solution. Both models use least-squares minimization. These models remove the fluorescence baselines with respect to the relative peak intensities. We also compared the results with those at auto-baseline, which confirmed the normalization of our data. Regarding the possible drawbacks of photobleaching (vibration saturation and molecule denaturation), because the time recording was equal for all samples, we tended to reduce it. However, the photobleaching effect was needed to reduce the high inner-fluorescence level of all samples, which saturated the analysis. If denaturation occurs it is nearly impossible to find out which molecules in particular are involved, owing to the highly complex composition of the carious dentine. The Gaussian amplitude in the second derivative method was chosen for fitting the peaks (28).

Table S1 collates the different peaks identified in dentine spectra, mainly the bands associated with inorganic components (minerals), which appeared in the spectral range between approximately 959 and $1,070 \text{ cm}^{-1}$, including bands ν_1 phosphate (PO_4^{3-}) and B type mineral carbonate (CO_3^{2-}), and the bands associated with the organic components (collagen). These organic bands appeared in the spectral range near $1,240 \text{ cm}^{-1}$ for (NH) amide III and $1,665 \text{ cm}^{-1}$ for (NH) amide I.

To help understand the spectral variation between the different preparation methods we divided the Raman spectra into three areas. The first spectral area, from 750 to $1,100 \text{ cm}^{-1}$ (Table S2, Figs S4 and S8), contains the CO_3^{2-} and PO_4^{3-} bands; the second spectral area, from $1,100$ to $1,400 \text{ cm}^{-1}$ (Table S3, Figs S5 and S9), primarily concerns amide III bands; and the third spectral area, from $1,400$ to $1,800 \text{ cm}^{-1}$ (Table S4, Figs S6 and S10), corresponds to CH_2 , amide I, pentosidine, and AGE bands.

Pentosidine powder, pure type I collagen powder, and MGO solution were analyzed under the same conditions (Fig. S7).

We also compared the intensities ratios between the different dentine specimens (Table S5) as described below.

Carbonate to phosphate ratio: The presence of a prominent carbonate band around $1,070\text{ cm}^{-1}$ in the Raman spectrum is significant because it shows the degree of carbonate substitution in the lattice structure of the apatite. Raman measures of carbonate-to-phosphate ratios can provide valuable insights into the inorganic chemical composition of dentine. For bone it varies with bone age and mineral crystallinity (29, 30).

Phosphate to CH_2 ratio ($959\text{--}1,450\text{ cm}^{-1}$): The mineral to organic ratio was calculated as the ratio of the phosphate symmetrical stretch-band intensity (at 959 cm^{-1}) to the intensity of vibrations resulting primarily from the CH_2 wagging mode of side-chains of collagen molecules (at $1,450\text{ cm}^{-1}$). This $1,450\text{ cm}^{-1}$ band was chosen for its low sensitivity to molecular orientation compared with amide I at $1,670\text{ cm}^{-1}$ (31, 32).

Carbonate to CH_2 ratio ($1,072\text{--}1,450\text{ cm}^{-1}$): The intensity ratios of CO_3^{2-} at $1,072\text{ cm}^{-1}$ to the CH_2 wagging mode at $1,450\text{ cm}^{-1}$ were calculated to measure the relative differences in phosphate and carbonate (33).

Amide III to CH_2 ratio ($1,243\text{--}1,450\text{ cm}^{-1}$): In dentine the intensity ratios of amide III to CH_2 wagging mode indicate the structural differences. A higher ratio was noted in intertubular dentine than in peritubular dentine, which indicates a higher content of collagen (34).

Cross-link ratio ($1,660\text{--}1,690\text{ cm}^{-1}$): The collagen quality parameter used in Raman spectroscopy is derived from a subset of partially resolved amide I bands, whose relative intensities depend on its secondary structure. Theory supports the use of similar bands, originally developed by infrared spectroscopy of bone, to assess non-reducible to reducible collagen cross-link ratios (of approximately $1,660/1,690\text{ cm}^{-1}$) (35).

Amide I to CH_2 ratio ($1,665\text{--}1,450\text{ cm}^{-1}$): An increase of the amide I band at $1,655\text{ cm}^{-1}$ relative to the CH_2 band at $1,240\text{ cm}^{-1}$ indicates altered collagen quality induced by aging (36), hydration/dehydration (37), or radiologic damage (38).

Specimen preparation

Five teeth freshly extracted for orthodontic reasons (written consent was obtained before extraction) were collected from the University Hospital of Montpellier. The teeth were stored at 4°C in 0.9% PBS (pH 7.4) containing 0.002% sodium azide. Cross-sections, of up to 0.5 mm thickness, were taken in the longitudinal axis of the freshly extracted teeth using an Isomet diamond saw (Isomet 1,000; Buehler, Lake Bluff, IL, USA). The samples were ground to 0.25 mm and then polished on carbide disks and with diamond pastes (6, 1, and $0.25\text{ }\mu\text{m}$) using an Escil polishing machine (Escil, Lyon, France). Finally, the specimens were cleaned for 5 min in an ultrasonic bath with water.

The six different preparation methods were:

- i G0: Sound dentine without preparation or dye application.
- ii G1: Sound dentine demineralized in 2.5% aqueous nitric acid solution (pH 1) until the primary green fluorescence, checked using SoproLife, had totally disappeared. Demineralization solutions were changed every 2 d. The specimens were rinsed in ultrapure water ($18.2\text{ M}\Omega\text{ cm}$, Milli-Q; Millipore) for 5 d.
- iii G3: Sound dentine demineralized in a 4% aqueous solution of lactic acid in carboxymethylcellulose sodium salt (pH 3.5) for 7 d until the primary green fluorescence had partially disappeared (around 7 d). Demineralization solutions were changed every 2 d. The samples were rinsed in ultrapure water for 5 d.
- iv G4: Sound dentine demineralized in 2.5% aqueous nitric acid solution (pH 1) until the primary green fluorescence, checked using SoproLife, had totally disappeared (around 7 d). Demineralization solutions were changed every 2 d. At 7 d, the sample was immersed in PBS containing 10 mM of MGO (an intermediate product of the Maillard reaction) at 37°C for 4 wk. The samples were then rinsed in ultrapure water for 5 d. The solution was changed every 2 d and kept at room temperature.
- v G5: As for method G4, but with an MGO concentration of 1 M to assess the effect of the MGO concentration.
- vi G6: As for method G5, but in the presence of a glucose solution (2 ml glucose/10 ml of PBS) to boost the Maillard reaction.

Carious dentine

Two specimens of carious dentine were also studied (G2 and G2b). The two samples of dark-red decay dentine were collected in vivo from two different patients. To avoid contamination with saliva and blood, a dental dam was fitted and a decayed sample was collected from the carious tooth using a sterile hand excavator. Figures S1a and b were taken with SoproLife in daylight mode (a) and treatment mode (b), providing confirmation of the clinical superimposition between the brown signal and the red signal for both. An understanding and written consent form was signed before excavation of the decayed dentine.

Chemicals

Pentosidine (SC 1535 lot: AW 12130E) was supplied by The Polypeptide Group (Strasbourg, France). Collagen type I (C5483, human collagen type I, acid soluble, powder, approximately 95%), methylglyoxal 1,1-dimethyl acetal (MGO) ($\geq 97\%$, density 0.976 g ml^{-1} at 25°C (lit.), nitric acid, and lactic acid were supplied by Sigma-Aldrich (St Louis, MO, USA). Solutions were prepared in ultra pure water (MilliQ; Millipore). Pentosidine and type I collagen were studied in dry powder.

Results

SoproLife

The two carious dentine samples, G2 and G2b, looked brown in daylight mode and dark red in treatment

mode (Fig. S1a,b), although part of G2b looked lighter red and dark green.

Sound dentine was light yellow in daylight mode and acid green in fluorescence mode (Fig. S2). After incubation for 7 d in nitric acid, the dentine looked transparent and see-through (Fig. S3a). Dentine samples incubated in lactic acid became partially transparent, and in fluorescence mode a partial loss of fluorescence (green) was visible. Demineralized samples immersed in MGO for 1 month (G4) showed a partial recovery of the fluorescence signal (which was red/orange) (Fig. S3b). The green dentine signal in treatment mode was never obtained for nitric acid-demineralized samples in the absence of MGO, even after rinsing in PBS. Samples incubated in pentosidine powder, collagen, and MGO solutions (with and without glucose) did not give any fluorescence signal (green or red) in treatment mode. They remained white or transparent.

Raman spectroscopy

Bands from 750 to 1,100 cm^{-1} : These bands involve mainly the mineral structure $\nu_1 \text{PO}_4^{3-}$ and substituted CO_3^{2-} (Table S2, Figs S3 and S7). The highest peak intensities, for both the phosphate and the carbonate bands, were exhibited for the sound dentine group. In the dark-red carious group the intensity decreased for the ν_1 phosphate band, but the decrease was not as marked as in the nitric acid- and lactic acid-demineralized groups, except for the softer-red dentine sample (G2b, Fig. S8). The peak around 1,002 cm^{-1} was probably linked to $\nu_1 \text{HPO}_4^{2-}$ vibration (Fig. S8). The carbonate mode was clearly identifiable in sound dentine but was absent in all other groups. Dentine samples treated with nitric acid and lactic acid, to a lesser extent, exhibited two peaks (1,050 cm^{-1}) not yet identifiable except for a negative peak shift hypothesis. Demineralization with both nitric acid and lactic acid completely disrupted the mineral structure, and this was more marked in the dark-red dentine group (G2), as a result of the presence of decayed dentine. Concerning the peaks in the range of amino acids in dentine, collagen from 840 to 940 cm^{-1} nitric acid treatment specifically released the CCH aliphatic vibration, as CCH aromatic vibrations were most visible in the lactic acid group; while the CC proline-valine vibration remained stable and higher in sound dentine.

Bands from 1,100 to 1,400 cm^{-1} : These bands involve mainly the organic structure amide III (Table S3, Figs S5 and S9). The dark-red dentine sample, G2b, exhibited broad alteration, with the lowest intensity observed for the two amide III bands. The in-vitro demineralization of the dentine triggered collagen vibrations, demonstrated by a huge, positive shift of the amide III band for the nitric acid group from 1,250 to 1,350 cm^{-1} , and to around 1,300 cm^{-1} also for G6. Addition of MGO to the nitric acid group reduced the intensity of the amide III band. The highest concentration of MGO and the addition of glucose reduced the signal intensities to levels almost as low as the values

obtained for G2. Spectral vibrations of sound dentine and decayed dentine were similar around this band.

Bands from 1,400 to 1,800 cm^{-1} : These bands involve mainly the organic matrix components amide I, CH_2 wagging, and collagen cross-link (Table S4, Figs S6 and S10). With the sound dentine spectrum as a reference, decreases in CH_2 wagging-mode intensity were observed for the dark-red carious dentine samples and the MGO-treated groups (G5, G6). This mode was increased for demineralized dentine (G1 and G3 groups). Amide I band vibrations were also triggered in samples incubated with nitric acid and lactic acid. The main observation was that compared with sound dentine, the intensities around 1,550 cm^{-1} , assigned to pentosidine and AGE (13) modes, clearly increased in the dark-red carious dentine groups G2 compared with sound dentine (Figs S6 and S10).

Ratios: The carbonate to phosphate ratio was similar in dark-red carious dentine (G2) and lactic acid-treated groups. Treatment with nitric acid modified the ratio, which also increased when MGO was added. The carbonate to CH_2 and phosphate to CH_2 ratios were higher in the sound dentine group than in the dark-red dentine group. Demineralization with both nitric acid and lactic acid completely disrupted the mineral structure, to a greater extent than present in the dark-red dentine group (G2). The intensity ratio of amide III to CH_2 increased in the lactic acid-treated group, and MGO also enhanced the ratio, which decreased in the softer red dark-red dentine group (G2b). The ratio of amide I to CH_2 variations was low and similar between the darker-red dentine group (G2) and the lactic acid group. Treatment with nitric acid reduced the ratio close to that of the softer red dark-red dentine group (G2b). The cross-link intensity ratio 1,660/1,690 cm^{-1} decreased in the two carious groups compared with the sound dentine group, and MGO solution modified the ratio according to the concentration. Lactic acid solution did not modify the ratio in relation to the nitric acid solution.

Discussion

Nitric acid was used to totally demineralize the dentine sample in order to gain a proper understanding of the effects of the mineral/organic interactions on dentine fluorescence, while lactic acid was used to mimic dental decay. A solution of MGO was used to mimic the Maillard reaction, as MGO is an intermediate product of this reaction; the Maillard reaction also needs glucose, which was why we included glucose in one group (G6). No caries processes are similar in terms of dynamics, time, activity, bacterial ecology system, oral defense, and dental genetic significance, which mean that it is nearly impossible to statistically average this biological phenomenon.

The major components of dentine have been observed spectroscopically (39), and Raman spectroscopy was

used in this study to appraise any modification in dentine composition caused by the *in vivo* decay and *in vitro* demineralization steps (40, 41). The loss of phosphate and of carbonate (Figs S4 and S8) between the normal dentine group and the carious dentine group was a ratio of around three for the two bands. One sample of carious dentine showed a loss of carbonate but a relatively high phosphate signal. This can be linked to the high solubility of carbonato-apatite. Calcium phosphates structure the collagen fiber, which loses its fluorescence beyond a demineralization threshold (42). Furthermore, analysis of completely demineralized active dentine using Soprolife, showed a tendency for the fluorescence to approach zero (20, 21).

The carbonate/CH₂ ratios showed a large decrease in samples incubated in nitric acid and lactic acid, which was characterized by a marked reduction in the intensity of the fluorescence signal, whereas these ratios remained relatively unchanged in the carious group G2 vs. group G2b. The G2b sample looked softer and darker than the G2 sample, which indicates a higher level of carious activity and demineralization. In fact, the phosphate and respective CH₂ ratio band vibrations of G2b showed a marked decrease, which was not observed for G2 (Tables S2 and S5). Despite not being measured in this study, the mineral/matrix ratio between intertubular dentine (ITD) and peritubular dentine (PTD) differs greatly (34). The content of organic matrix in the PTD is one third of that in the ITD with collagen fibril running across the ITD to PTD, which could partially influence the results (34).

Concerning the organic structure amide III (Figs S5 and S9), the main observation was certainly the huge positive shift of the amide III band from 1,250 to 1,350 cm⁻¹ in the nitric acid-treated group. Amide III vibrations were released as a result of the demineralization. Nitric acid treatment totally demineralized the normal dentine sample and deconstructed the mineral structure surrounding the collagen fibers, making the dentine transparent and translucent, without any signal in fluorescence mode (42). The presence of MGO in groups G4 and G6 (and glucose also in group G6) increased the formation of cross-links, restoring a partial fluorescence signal detectable using Soprolife and a more consistent spectral appearance. A previous study by BONIFACIO & SERGO (43) argued that the intensity ratio of the amide III band is clearly a marker of the orientation of the collagen supramolecular structure (43). This partial loss of order in fibril orientation (aging, caries) influenced the fluorescence signal, and the amide III band ratio in the G2b dark-red group was the lowest, even at 1,234 and 1,275 cm⁻¹, thus providing certain information about the spatial arrangement of collagen structures within tissues and its effect on fluorescence (44).

Compared with the spectrum of pure collagen I, the amide I-CH₂-collagen cross-link (Figs. S6, S7 and S10), with two pronounced bands at around 1,450 cm⁻¹ (caused by the CH₂ wagging mode of the amino acid side chains) and 1,640–1,680 cm⁻¹ (caused

by the presence of amide I from protein, e.g. from dentine and bone), respectively, during this experiment all the groups exhibited a positive or negative variation vs. normal dentine at the same bands; thus providing arguments about the involvement of collagen during fluorescence. This denaturation and modification of the matrix collagen and structure was also confirmed by the CH₂ wagging mode and amide I intensities of matrix collagen, which were both lowest in the carious group. Note that the main acid involved in the caries process is lactic acid, and in fact the matrix ratio of the carious and the lactic acid groups was similar, in contrast to the nitric acid group, in which the samples were totally demineralized and the matrix ratio was disrupted. Incubation of sound dentine samples with nitric and lactic acid solutions specifically modified the collagen amide I and III band vibrations resulting in particular fluorescent effects: the dentine sample incubated with lactic acid had a partially transparent appearance, with a partial loss of fluorescence (green) compared with the dentine sample incubated in nitric acid. The addition of glucose to the MGO solution slightly increased the amide I signal. No explanation was found to interpret the difference in the amide I vibration in relation to the MGO concentration. The vibration levels for pure collagen, pentosidine powder, and MGO solution (1 M) alone were very low (Fig. S7).

The 1,660/1,690 cm⁻¹ ratio of the bands has often been used as a measure of the degree of cross-linking of collagen (45), providing information on collagen quality (46). Our results are in agreement with the work of KLETER *et al.* (14), and thus the physiological cross-link ratio decreased in carious dentine vs. sound dentine (Table S5).

We sought to clarify the purported relationship among dentine caries, matrix protein modification, the browning reaction, and the fluorescence signal. Even though fluorescence cannot serve as absolute proof of the Maillard reaction, mainly because of the molecular patchwork formed in the carious process, the increase of the pentosidine vibrations was encouraging, as this product in particular is a Maillard reaction end-product, in the form of a fluorescence cross-link between arginine and lysine. Pentosidine originates from aldose, which reacts with the epsilon amino group of lysine found in a wide variety of proteins. The arabinose-lysine complex then forms a bond with a cross-arginine residue of a neighboring protein (collagen, in dentine), thereby changing the structure and biological functions.

In the carious group the dark-red signal was perfectly superimposable onto the dark-brown signal that is known to be related to the Maillard reaction (14). The formation of this brown dentine tissue was previously described (1, 4, 5) as sclerotic or reparative dentine gradually formed during quite a low carious process. The formation of brown dentine takes time and involves local conditions and sugar intake, unlike the active carious process, which results in yellow, soft dentine. The respective spectra of the MGO solutions and

pentosidine both exhibited vibrations from 1,400 to 1,800 cm^{-1} . MGO vibrations were located more frequently around 1,580 and 1,650–1,780 cm^{-1} , like the AGE band, but pure pentosidine powder bands (1,430–1,480 cm^{-1}) differed slightly from tissue pentosidine bands (1,550 cm^{-1}). Raman spectroscopy presented the advantage of an overview of the pentosidine signal because the latter is either bound to proteins or is present in the form of soluble peptides (44). This nonenzymatic browning reaction with carbohydrate, seemingly activated in this type of carious process, renders demineralized dentine collagen more resistant to proteolytic breakdown. In fact, clinically, brown dentine looks harder than yellow, soft dentine. Similar results were observed for non-carious cervical lesions (45). Three parameters determine the rate of formation of glycated products: glucose concentration, contact time, and degradation kinetics of the original protein. Therefore, the combination of a high glucose level, a prolonged contact time, and a long protein half-life led us to observe a high level of glycated protein. This is very similar to what happens in a low carious process: slow activity, a high oral concentration of glucose, and a very stable protein structure (collagen). This seemed consistent with denaturation of the collagen layer, which could explain the modification in the fluorescence signal. In a series of deep ultraviolet bone Raman studies, an increase of the amide I bands indicated altered collagen quality (36, 37), and this was the case for lactic acid and nitric acid, respectively. By contrast, the mineral structure of the collagen fibers seems essential for a fluorescence signal, as the signal completely disappeared after 7 d of incubation in nitric acid, and was never recovered except in the dentine samples incubated with MGO solution.

Demineralization of the normal dentine samples triggered the matrix and collagen amide I vibrations (giving high values), and adding MGO (the toxic intermediate product of the Maillard reaction) (47), which produced protein cross-links, seemed to reorganize the matrix framework, resulting in vibrations similar to those of normal dentine. This reorganization was confirmed by the partial recovery of fluorescence after 1 month (determined using SoproLife) and the reddening in groups G5 and G6. Non-collagenous proteins almost certainly contribute to the Raman spectrum, but their low abundance and spectral similarity to collagen make them very difficult to isolate spectroscopically, as already shown for bone tissue (41).

Previous work (20, 21) showed variations in brightness (L^*) and fluorescence of dental tissue during dentine caries. In the active-caries process, reparative dentine is synthesized mostly without dentinal tubules, in contrast to sclerotic dentine in arrested caries, in which the dentinal tubules are full of mineralized deposits, with, in most cases, a browning reaction (dark red sample). A more remarkable observation was the large decrease in L^* green fluorescence in arrested caries, with a more constant L^* red-fluorescence brightness value when analyzing the brightness variation in the RGB space. One of either the organic or inorganic

constituents of sound dentine, which emits an acid-green fluorescence, partially disappears during the caries process, and hence the red fluorescence appears. Dentine constituents emitting a red-dark fluorescence seem to be less damaged by the caries process. The presence of bacteria, such as *Streptococcus mutans*, could also be a prerequisite for the emission of fluorescence from carious lesions; some interaction of bacteria, and specially *S. mutans*, with exposed tooth matrix elements could be required for the generation or unmasking of fluorophores (48–51).

In conclusion, regarding the study hypotheses, the first hypothesis was confirmed; there is indeed a close relationship between the Raman spectra variations in the organic and mineral phases and the variation in the observations visible with SoproLife (loss of green fluorescence). The second hypothesis was also confirmed, because not only is there perfect superimposition, with SoproLife, between the fluorescence in the red and the browning reaction, but everything is correlated to the Raman spectra by intensity variations, specific to the carious group, in the AGEs and pentosidine bands, typical of the Maillard reaction. Our results provide new data on the origin of fluorescence variation in dental caries observed using the SoproLife camera. Parameters such as the presence of bacterial metabolisms must be assessed in the future, as it is clear that destruction of dentine during caries is a complex biological process.

Acknowledgements – We gratefully acknowledge the contribution of Professor Guillaume Penel (Lille, France) for his helpful discussions on Raman modes and his proofreading of this article.

Conflicts of interest – The authors have declared no conflicts of interest.

References

1. Mjör IA. Pulp-dentin biology in restorative dentistry. Part 5: clinical management and tissue changes associated with wear and trauma. *Quintessence Int* 2001; **32**: 771–788.
2. Bjørndal L, Mjör IA. Pulp-dentin biology in restorative dentistry. Part 4: dental caries—characteristics of lesions and pulp reactions. *Quintessence Int* 2001; **32**: 717–736.
3. Heyeraas KJ, Sveen OB, Mjör IA. Pulp-dentin biology in restorative dentistry. Part 3: Pulpal inflammation and its sequelae. *Quintessence Int* 2001; **32**: 611–625.
4. Mjör IA. Pulp-dentin biology in restorative dentistry. Part 7: the exposed pulp. *Quintessence Int* 2002a; **33**: 113–135.
5. Mjör IA, Ferrari M. Pulp-dentin biology in restorative dentistry. Part 6: reactions to restorative materials, tooth-restoration interfaces, and adhesive techniques. *Quintessence Int* 2002b; **33**: 35–63.
6. Banerjee A, Watson TF, Kidd EAM. Dentine caries: take it or leave it? *Dent Update* 2000; **27**: 272–276.
7. Sell DR, Monnier VM. Isolation, purification and partial characterization of novel fluorophores from aging human insoluble collagen-rich tissue. *Connect Tissue Res* 1989; **19**: 77–92.
8. Klein RL, Laimins M, Lopes-Virelle MF. Isolation, characterization, and metabolism of the glycated and non-glycated subfraction of low-density lipoproteins isolated from type 1 diabetic patients and non-diabetics. *Diabetes* 1995; **94**: 1093–1098.
9. Adamis AP, Cunningham JR, Feinsod M, Guyer DR. Inhibition of VEGF prevents retinal ischemia-associated iris

- neovascularisation in a primate. *Arch Ophthalmol* 1996; **114**: 66–71.
10. MIYATA T, TANEDA S, KAWAI R, UEDA Y, HORIUCHI S, HARA M, MAEDA K, MONNIER VM. Identification of pentosidine as a native structure for advanced glycation end products in b2-microglobulin-containing amyloid fibrils in patients with dialysis-related amyloidosis. *Proc Natl Acad Sci USA* 1996; **93**: 2353–2358.
 11. GRAIER WF, KOSTNER GM. Glycated low-density lipoprotein and atherogenesis: the missing link between diabetes mellitus and hypercholesterolaemia? *Eur J Clin Invest* 1997; **27**: 457–459.
 12. PAWLAK AM, GLENN JV, BEATTIE JR, MCGARVEY JJ, STITT AW. Advanced glycation as a basis for understanding retinal aging and noninvasive risk prediction. *Ann N Y Acad Sci* 2008; **1126**: 59–65.
 13. BEATTIE JR, PAWLAK AM, BOULTON ME, ZHANG J, MONNIER VM, MCGARVEY JJ, STITT AW. Multiplex analysis of age-related protein and lipid modifications in human Bruch's membrane. *FASEB J* 2010; **24**: 4816–4824.
 14. KLETER GA, DAMEN JJM, BUIJS MJ, TEN CATE JM. Modification of amino acid residues in carious dentin matrix. *J Dent Res* 1998; **77**: 488–495.
 15. ZOUMI A, YEH A, TROMBERG BJ. Imaging cells and extracellular matrix in vivo by using second-harmonic generation and two-photon excited fluorescence. *Proc Natl Acad Sci USA* 2002; **99**: 1101–1114.
 16. BACHMANN L, ZEZZEL DM, DA COSTARIBEIRO A, GOMES L, ITO AS. Fluorescence spectroscopy of biological tissue – a review. *Appl Spectrosc Rev* 2006; **41**: 575–590.
 17. LUSSI A. Comparison of different methods for the diagnosis of fissure caries without cavitation. *Caries Res* 1993; **27**: 409–416.
 18. KOENIG K, SCHNECKENBURGER H. Laser-induced autofluorescence for medical diagnosis. *J Fluoresc* 1994; **4**: 17–40.
 19. BANERJEE A, YASSERI M, MUNSON M. A method for the detection and quantification of bacteria in human carious dentine using fluorescent in situ hybridization. *J Dent* 2002; **30**: 359–363.
 20. TERRER E, SARRAQUIGNE C, KOUBI S, WEISROCK G, MAZUIR A, TASSERY H. A new concept in restorative dentistry: light induced fluorescence for diagnosis and treatment. Part I: diagnosis and treatment of initial occlusal caries. *J Contemp Dent Pract* 2009; **10**: 86–94.
 21. TERRER E, SARRAQUIGNE C, KOUBI S, WEISROCK G, MAZUIR A, TASSERY H. A new concept in restorative dentistry: LIFEDT-light induced fluorescence for diagnosis and treatment. Part II: treatment of dentinal caries. *J Contemp Dent Pract* 2010; **11**: 95–102.
 22. HALL A, GIRKIN JM. A review of potential new diagnostic modalities for caries lesions. *J Dent Res* 2004; **83**(Spec Iss C): C89–C94.
 23. ADEYEMI AA, JARAD FD, PENDER N, HIGHAM SM. Comparison of quantitative light-induced fluorescence (QLF) and digital imaging applied for the detection and quantification of staining and stain removal on teeth. *J Dent* 2006; **34**: 460–466.
 24. RODRIGUES JA, HUG I, DINI ZMB, LUSSI A. Performance of fluorescence methods, radiographic examination and ICDAS II on occlusal surfaces in vitro. *Caries Res* 2008; **42**: 297–304.
 25. DOMMISCH H, KNEIST S, KRAUSE F, HEDDERICH J, EBERHARD J. Fluorescence-controlled Er: YAG laser for caries removal in permanent teeth: a randomized clinical trial. *Eur J Oral Sci* 2008; **116**: 170–176.
 26. KINOSHITA H, MIYOSHI N, FUKUNAGA Y, OGAWA T, OGASAWARA T, SANO K. Functional mapping of carious enamel in human Raman spectroscopy. *J Raman Spectrosc* 2008; **39**: 655–660.
 27. MORRIS MD, GURJIT SM. Raman assessment of bone quality. *Clin Orthop Relat Res* 2010; **38**: 1607–1617.
 28. BEATTIE JR, GLENN JV, BOULTON ME, STITT AW, MCGARVEY JJ. Effect of signal intensity normalization on the multivariate analysis of spectral data in complex real-world datasets. *J Raman Spectrosc* 2009; **40**: 429–435.
 29. LEGROS R, BALMAIN N, BONEL G. Age-related changes in mineral of rat and bovine cortical bone. *Calcif Tissue Int* 1987; **41**: 137–144.
 30. YERRAMSHETTY JS, LIND C, AKKUS O. The compositional and physicochemical homogeneity of male femoral cortex increases after the sixth decade. *Bone* 2006; **39**: 1236–1243.
 31. FALGAYRAC G, FACQ S, LEROY G, CORTET B, PENEL G. New method for Raman investigation of the orientation of collagen fibrils and crystallites in the Haversian system of bone. *Appl Spectrosc* 2010; **64**: 775–780.
 32. GAMSJAEGER S, MASIC A, ROSCHGER P, KAZANCI M, DUNLOP JWC, KLAUSHOFER K, PASCHALIS EP, FRATZL P. Cortical bone composition and orientation as a function of animal and tissue age in mice by Raman spectroscopy. *Bone* 2010; **47**: 392–399.
 33. KARAN K, YAO X, XU C, WANG Y. Chemical profile of the dentin substrate in non-carious cervical lesions. *Dent Mater* 2009; **25**: 1205–1212.
 34. XU C, WANG Y. Chemical composition and structure of peritubular and intertubular human dentine revisited. *Arch Oral Biol* 2012; **57**: 383–391.
 35. PASCHALIS EP, VERDELIS K, DOTY SB, BOSKEY AL, MENDELSON R, YAMAUCHI M. Spectroscopic characterization of collagen crosslinks in bone. *J Bone Miner Res* 2001; **16**: 1821–1828.
 36. AGER JW, NALLA RK, BREEDEN KL, RITCHIE RO. Deep-ultraviolet Raman spectroscopy study of the effect of aging on human cortical bone. *J Biomed Opt* 2005; **10**: 034012.
 37. AGER JW, NALLA RK, BALOOCH G, KIM G, PUGACH M, HABELITZ S, MARSHALL GW, KINNEY JH, RITCHIE RO. On the increasing fragility of human teeth with age: a deep-UV resonance Raman study. *J Bone Miner Res* 2006; **21**: 1879–1887.
 38. BARTH HD, LAUNEY ME, MACDOWELL AA, AGER JW, RITCHIE RO. On the effect of X-ray irradiation on the deformation and fracture behavior of human cortical bone. *Bone* 2010; **46**: 1475–1485.
 39. TSUDA H, RUBEN J, ARENDS J. Raman spectra of human dentin mineral. *Eur J Oral Sci* 1996; **1042**: 123–131.
 40. SHEA DA, MORRIS MD. Bone tissue fluorescence reduction for visible laser Raman spectroscopy. *Appl Spectrosc* 2002; **56**: 182–186.
 41. PENEL G, DELFOSSE C, DESCAMPS M, LEROY G. Composition of bone and apatitic biomaterials as revealed by intravital Raman microscopy. *Bone* 2005; **36**: 893–901.
 42. BAZIN H, PREAUDAT M, TRINQUET E, MATHIS G. Homogeneous time resolved fluorescence resonance. Energy transfer using rare earth cryptates as a tool for probing molecular interactions. *Spectrochimica Acta A* 2001; **57**: 2197–2211.
 43. BONIFACIO A, SERGO V. Effects of sample orientation in Raman microspectroscopy of collagen fibers and their impact on the interpretation of the amide III band. *Vib Spectrosc* 2010; **53**: 314–317.
 44. ODETTI P, ARAGNO I, GARIBALDI S, VALENTINI S, PRONZATO MA, ROLANDI R. Role of advanced glycation end products in aging collagen. *Gerontology* 1998; **44**: 187–191.
 45. CHANGQI XU, KARAN K, YAO X, WANG Y. Molecular structural analysis of noncarious cervical sclerotic dentin using Raman spectroscopy. *J Raman Spectrosc* 2009; **40**: 1780–1785.
 46. WALLACE JM, GOLCUK K, MORRIS MD, KOHN DH. Inbred strain-specific effects of exercise in wild type and biglycan deficient mice. *Ann Biomed Eng* 2010; **38**: 1607–1617.
 47. SELL DR, MONNIER VM. Structure elucidation of a senescence cross-link from human extracellular matrix. Implication of pentoses in the aging process. *J Biol Chem* 1989; **264**: 21597–21602.
 48. BANERJEE A, GILMOUR A, KIDD E, WATSON T. Relationship between *S. Mutans* and the autofluorescence of carious dentin. *Am J Dent* 2004; **17**: 253–256.
 49. COULTHWAIT L, PRETTY IA, SMITH PW, HIGHAM SM, VERRAN J. The microbiological origin of fluorescence observed in pla-

- que on dentures during QLF analysis. *Caries Res* 2006; **40**: 112–126.
50. LENNON AM, BUCHALLA W, BRUNE L, ZIMMERMANN O, GROSS U, ATTIN T. The ability of selected oral microorganisms to emit red fluorescence. *Caries Res* 2006; **40**: 2–5.
51. SHIGETANI Y, TAKENAKA S, OKAMOTO A, ABU-BAKR N, IWAKU M, OKIJI T. Impact of *Streptococcus mutans* on the generation of fluorescence from artificially induced enamel and dentin carious lesions in vitro. *Odontology* 2008; **96**: 21–25.

Supporting Information

Additional Supporting Information may be found in the online version of this article:

Table S1. Wavenumbers (in cm^{-1}) and band assignments of Raman spectra from normal dentin.

Table S2. Normalized intensity spectra from 750 to $1,100 \text{ cm}^{-1}$.

Table S3. Normalized intensity spectra from $1,100$ to $1,400 \text{ cm}^{-1}$.

Table S4. Normalized intensity spectra from $1,400$ to $1,800 \text{ cm}^{-1}$.

Table S5. Ratio between Raman bands.

Fig S1. Close clinical relationships of the signal with the Sopro-Life camera.

Fig S2. Green fluorescence of the normal dentine sample.

Fig S3. Disappearance of the green fluorescence in nitric acid solution and reddening in 1 mM MGO, with glucose solution.

Fig S4. Representative normalized Raman spectra from 750 to $1,100 \text{ cm}^{-1}$ of normal dentine.

Fig S5. Representative normalized Raman spectra from $1,100$ to $1,400 \text{ cm}^{-1}$ of normal dentine.

Fig S6. Representative normalized Raman spectra from $1,400$ to $1,800 \text{ cm}^{-1}$ of normal dentine.

Fig S7. Representative normalized Raman spectra from $1,400$ to $1,800 \text{ cm}^{-1}$ of pentosidine powder, pure collagen and MGO solution.

Fig S8. Representative normalized Raman spectra of G5, G6, G2 and G2b carious groups from 750 to $1,100 \text{ cm}^{-1}$.

Fig S9. Representative normalized Raman spectra of G5, G6, G2 and G2b carious groups from $1,100$ to $1,400 \text{ cm}^{-1}$.

Fig S10. Representative normalized Raman spectra of G5, G6, G2 and G2b carious groups from $1,400$ to $1,800 \text{ cm}^{-1}$.

Please note: Wiley-Blackwell are not responsible for the content or functionality of any supporting materials supplied by the authors. Any queries (other than missing material) should be directed to the corresponding author for the article.

Supporting Information

Molecular structural analysis of carious lesions using micro-Raman spectroscopy

LEVALLOIS B, TERRER E, PANAYOTOV Y, SALEHI H, TASSERY H, TRAMINI P, CUISINIER F

UFR Odontologie, Université Montpellier 1; Aix-Marseille-Université;
and APHM Hôpital Timone, Marseille, France

- Table S1:** Wavenumbers (in cm^{-1}) and band assignments of Raman spectra from normal dentine.
- Table S2:** Normalized intensity spectra from 750 to 1100 cm^{-1} .
- Table S3:** Normalized intensity spectra from 1100 to 1400 cm^{-1} .
- Table S4:** Normalized intensity spectra from 1400 to 1800 cm^{-1} .
- Table S5:** Ratio between Raman bands.
- Fig. S1:** Close clinical relationships of the signal with the SoproLife camera.
- Fig. S2:** Green fluorescence of the normal dentine sample.
- Fig. S3:** Disappearance of the green fluorescence in nitric acid solution and reddening in 1 mmol/L MGO, with glucose solution.
- Fig. S4:** Representative normalized Raman spectra from 750 to 1100 cm^{-1} of normal dentine.
- Fig. S5:** Representative normalized Raman spectra from 1100 to 1400 cm^{-1} of normal dentine.
- Fig. S6:** Representative normalized Raman spectra from 1400 to 1800 cm^{-1} of normal dentine.
- Fig. S7:** Representative normalized Raman spectra from 1400 to 1800 cm^{-1} of pentosidine powder, pure collagen and MGO solution.
- Fig. S8:** Representative normalized Raman spectra of G5, G6, G2 and G2b carious groups from 750 to 1100 cm^{-1} .
- Fig. S9:** Representative normalized Raman spectra of G5, G6, G2 and G2b carious groups from 1100 to 1400 cm^{-1} .
- Fig. S10:** Representative normalized Raman spectra of G5, G6, G2 and G2b carious groups from 1400 to 1800 cm^{-1} .

Table S1: Wavenumbers^a (in cm^{-1}) and band assignments of Raman spectra from normal dentin (f) probably involved in the dentin fluorescence. ^a s, strong; vs, very strong; m; medium ms, medium; uk, unknown (26, 41).

Wavenumbers (in cm^{-1}) and band assignments of Raman spectra from normal dentin	(cm^{-1})
CCH aliphatic	820
CCH aromatic (Pro, Tyr) (f)	855
CC Proline valine	940
Phosphate ($\nu_1\text{PO}_4^{3-}$)	959 vs
Carbonate	1070 ms
(NH) Amide III (f)	1243 m
(NH) Amide III non-polar triple helix of collagen (f)	1275 ms
CH_2 wagging	1450 m
Amide I (C=O) (f)	1665
Non-reducible crosslink / reducible crosslink ratio (f)	1660/1690
C-H stretching	2943 s
Ratio amide I/ CH_2 wagging (f)	1665/1450
Ratio amide III/ CH_2 wagging (f)	1243/1450
Ratio Carbonate/Phosphate. Mineral ratio	1070/960
Ratio Phosphate/ CH_2 wagging ratio	960/1450
Ratio Carbonate/ CH_2 wagging ratio	1070/1450
Pentosidine (f)	1550 uk
Advanced glycation end products: AGES (f)	1550-1690 uk

Table S2: Normalized intensity spectra from 750 to 1100 cm^{-1} : * lowest values **highest values. (nm : not measurable)

Band assignment cm^{-1}	G0 sound dentine	G1 nitric acid	G2/G2b Red dentine decay	G3 lactic acid	G4 MGO10 mmol/l	G5 MGO 1mol/l	G6 glucose
CCH aliphatic 820	502*	2661**	736/974	1592	1334	694	1012
CCH aromatic (Pro, Tyr) 855 (f)	1254	899	476/424	3906**	2529	55*	862
CC Proline Valine 940	4752**	2928	1806/395	3530	2384	118*	818
Phosphate ($\nu_1\text{PO}_4^{3-}$) 959 (f)	29606**	1590	12500/818	4067	982	nm	192*
Carbonate 1070 (f)	3597**	301	959/327	233*	481	911	651

Table S3: Normalized intensity spectra from 1100 to 1400 cm^{-1} ; * lowest values **highest values.

Band assignment cm^{-1}	G0 sound dentine	G1 nitric acid	G2/G2b Red dentine decay	G3 lactic acid	G4 MGO 10mmol/l	G5 MGO 1mol/l	G6 glucose
(NH) Amide III 1243	2023	4410	1379/201*	4441**	3635	494	1032
(NH) Amide III non polar triple helix of collagen 1275	1475	5521	642/462*	3014	3024**	779	1125

Table S4: Normalized intensity spectra from 1400 to 1800 cm^{-1} ; * lowest values **highest values.

Band assignment cm^{-1}	G0 sound dentine	G1 nitric acid	G2/G2b Red dentine decay	G3 lactic acid	G4 MGO 10 mmol/l	G5 MGO 1mol/l	G6 glucose
1450 – CH ₂ wagging	2226	4207	1072/338	4027**	2970	173*	563
[1550 -1600] Pentosidine	396*	1520	1865**/622	891	729	608	1398
1660 - Non reducible collagen crosslink	2195	3529	1312 /307	4921**	3201	266*	824
1665 – Amide I	2434	3730	1428/314	5452**	3292	278*	877
1690- Reducible collagen crosslink	1613	2096	1286/374	3766**	1697	364*	577

Table S5: Ratio between Raman bands. * lowest values **highest values.

Ratio	G0 sound dentine	G1 nitric acid	G2/G2b Red dentine decay	G3 lactic acid	G4 MGO10 mmol/l	G5 MGO 1mol/l	G6 glucose
Carbonate to Phosphate. Mineral 1070/959	0.12	0.18	0.076/0.39	0.05*	0.4	nm	3.39**
Phosphate to CH ₂ wagging 959/1450	13.3**	0.37	11.06/2.42	1	0.33*	nm	0.34
Carbonate to CH ₂ wagging 1070/1450	1.65	0.07	0.8/0.96	0.05*	0.16	5.26**	1.15
Amide III to CH ₂ wagging 1243/1450	0.9	1.04	1.26/0.59*	4.3**	1.22	2.85	1.83
Crosslink 1660/1690	1.3	1.6	1.02/0.82	1.3	1.8**	0.73*	1.42
Amide I to CH ₂ wagging 1665/1450	1.09	0.8*	1.3/0.92	1.3	1.1	1.60	1.55**

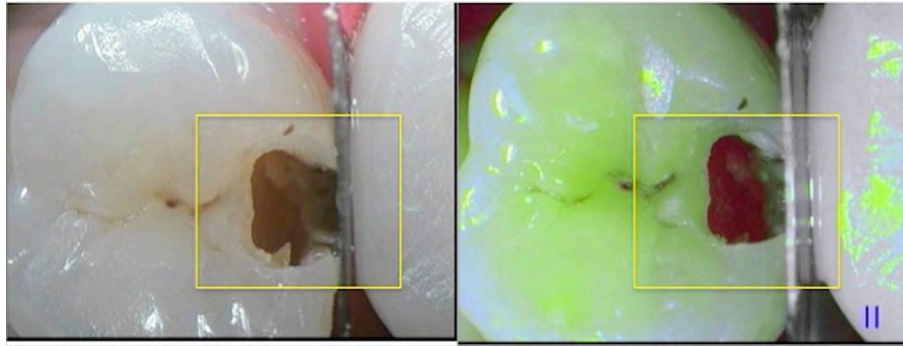


Fig. S1: Close clinical relationships between the browning signal of dental decay in daylight (a) and the red signal in fluorescence mode with the SoproLife camera (b)

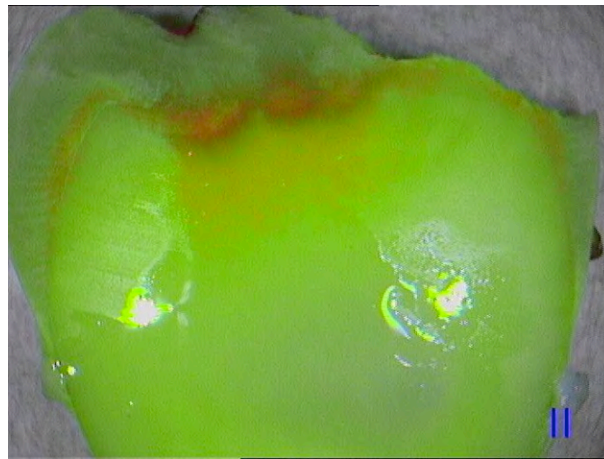


Fig. S2: Green fluorescence of the normal dentine sample (SoproLife in fluorescence mode)

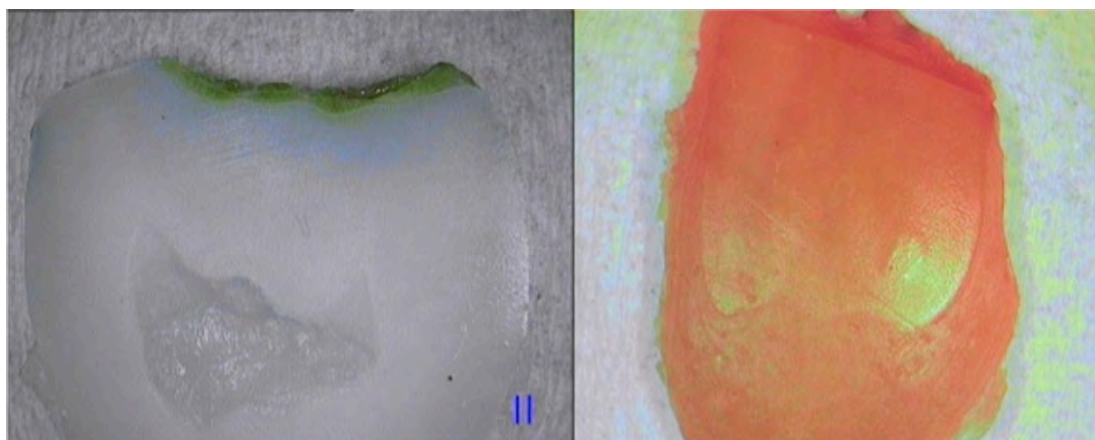


Fig. S3: SoproLife in treatment mode. a: disappearance of the green fluorescence after 7 d in nitric acid solution. b: reddening of nitric acid demineralized dentine after 4 wk in 1 mmol/L MGO, with glucose solution

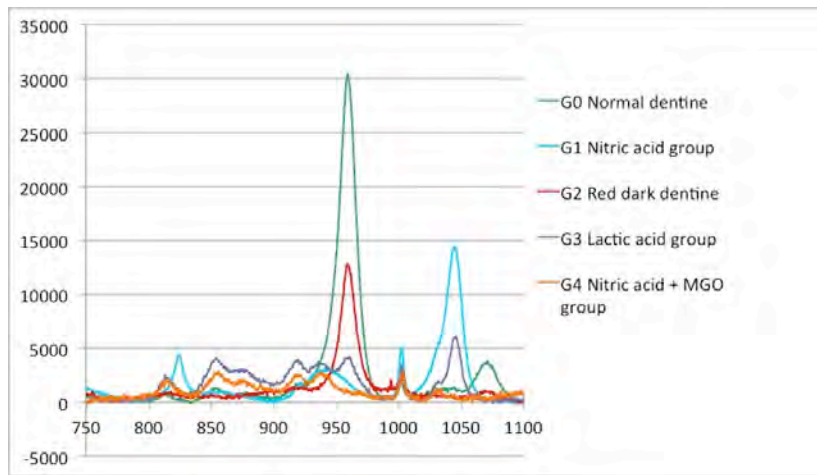


Fig. S4: Representative normalized Raman spectra from 750 to 1100 cm^{-1} of normal dentine, G0, G1, G3, G4 and G2 carious groups

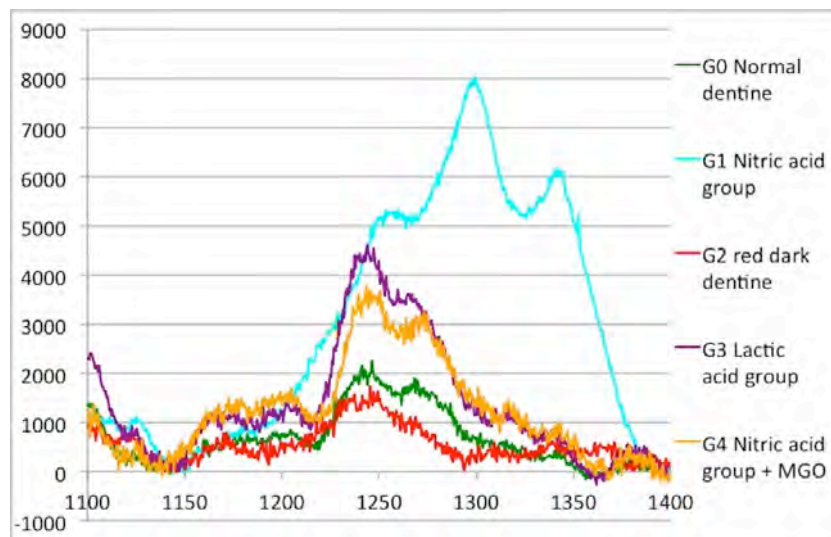


Fig. S5: Representative normalized Raman spectra from 1100 to 1400 cm^{-1} of normal dentine, G0, G1, G3, G4 and G2 carious groups

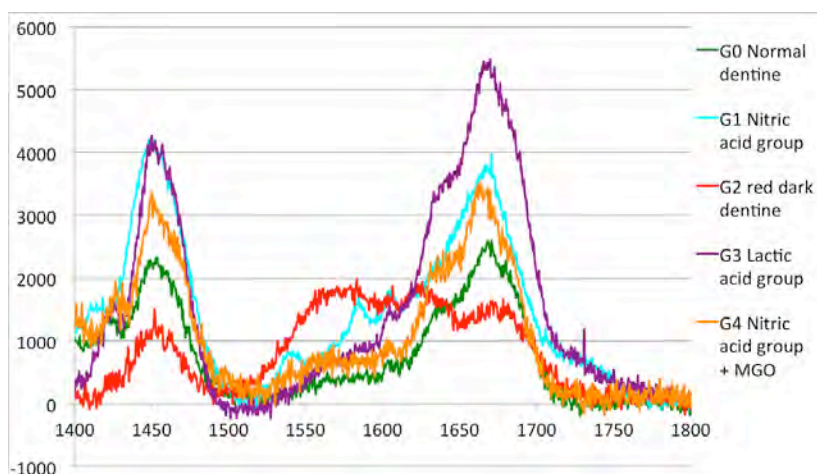


Fig. S6: Representative normalized Raman spectra from 1400 to 1800 cm^{-1} of normal dentine, G0, G1, G3, G4 and G2 carious groups

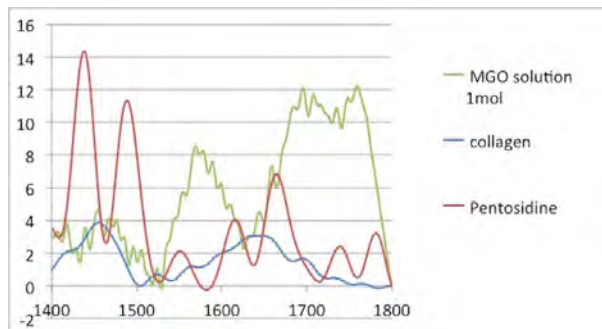


Fig. S7: Representative normalized Raman spectra from 1400 to 1800 cm^{-1} of pentosidine powder, pure collagen and MGO solution

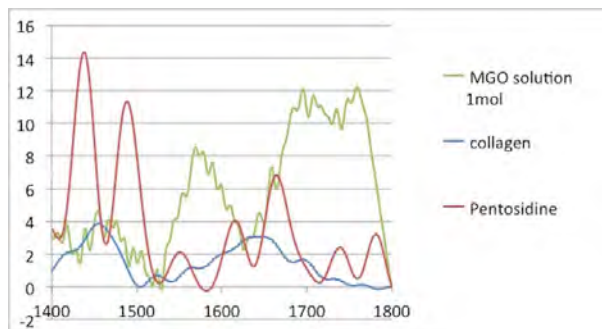


Fig. S8: Representative normalized Raman spectra of G5, G6, G2 and G2b carious groups from 750 to 1100 cm^{-1}

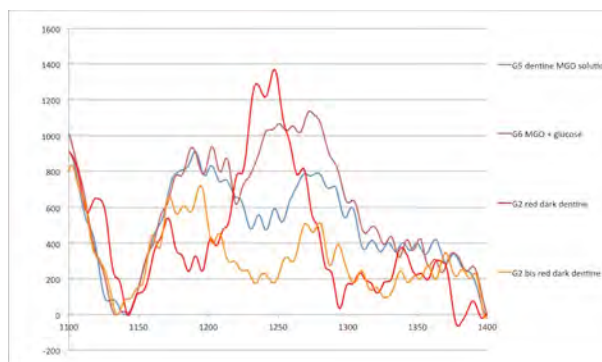


Fig. S9: Representative normalized Raman spectra of G5, G6, G2 and G2b carious groups from 1100 to 1400 cm^{-1}

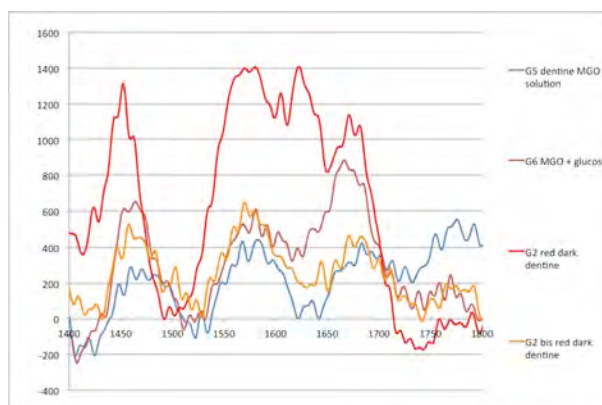


Fig. S10: Representative normalized Raman spectra of G5, G6, G2 and G2b carious groups from 1400 to 1800 cm^{-1}

In vitro investigation of fluorescence of carious dentin observed with a Soprolife® camera

Ivan Panayotov · Elodie Terrer · Hamideh Salehi ·
Hervé Tassery · Jacques Yachouh · Frédéric J. G.
Cuisinier · Bernard Levallois

Received: 4 November 2011 / Accepted: 10 June 2012
© Springer-Verlag 2012

Abstract

Objectives Our aim was to determine the origin of the red fluorescence of carious dentine observed with the Soprolife® camera.

Methods We conducted in vitro studies to evaluate the origin of the red fluorescence using acids and matrix metalloproteinase (MMP) to mimic caries and methylglyoxal (MGO) to evaluate the effect of glycation reactions on the red fluorescence. In every step of these models, we detected the changes of dentin photonic response with Soprolife® in daylight mode and in treatment mode. A Raman spectroscopy analysis was performed to determine the variations of the dentin organic during the in vitro caries processes. Raman microscopy was performed to identify change in the collagen matrix of dentine. **Results** The red fluorescence observed in carious dentine using a Soprolife® camera corresponds to the brownish color observed using daylight. Demineralization using nitric acid induces a loss of the green fluorescence of dentine. The red fluorescence of carious dentine is resistant to acid treatment. Immersion of demineralized dentine in MGO induces a change of color from white to orange-red. This indicates that the Maillard reaction contributes to lesion coloration. Immersion of demineralized dentine in an MMP-1 solution followed by MGO treatment results in a similar red fluorescence. Raman microspectroscopy analysis reveals accumulation of AGE's product in red-colored dentine.

Conclusions Our results provide important information on the origin of the fluorescence variation of dentine observed with the Soprolife® camera. We demonstrate that the red fluorescence of carious dentine is linked to the accumulation of Advanced Glycation End products (AGE).

Clinical relevance The study provides a new biological basis for the red fluorescence of carious dentine and reinforces the importance of the Soprolife® camera in caries diagnostics.

Keywords Dentine · Caries · Maillard reaction · Fluorescence · Raman spectroscopy

Introduction

Proper treatment of dental caries demands detection of carious lesions at an early stage [1]. Because previous caries and caries risk assessments are the best predictors of future caries, the development of a technology to detect and quantify early carious lesions and carious activity may be the best method of identification of patients who require intensive preventive intervention [2]. Several new detection methods based on the fluorescence variation of dentine have been recently developed [3]. Three main imaging techniques based on the fluorescence response of the organic components of teeth have been developed for use in caries detection. The commercially available devices are as follows:

1. Fluorescence system. The DIAGNOdent® (KaVo Dental, Lake Zurich, Ill.), which uses a laser, reacting in part on extrinsic components like porphyrins operating at a fixed wavelength of 655 nm.
2. Combination of camera and fluorescence system: (a) the QLF® (QLF-clin, Inspektor Research Systems BV, Amsterdam, Netherlands), which uses an arc lamp with emission in the wavelength domain of 290–450 nm and

I. Panayotov · H. Salehi · H. Tassery · J. Yachouh ·
F. J. G. Cuisinier (✉) · B. Levallois
EA4203 Laboratory of Biology and Nano-science, Université
Montpellier 1,
Montpellier, France
e-mail: frederic.cuisinier@univ-montp1.fr

E. Terrer · H. Tassery
Preventive and Restorative Department, Mediterranean University,
Marseille, France

looks at the change in transmission from the green fluorescence occurring in the dentin body changed due to micro-porosities in enamel as a result of the acid attack, (b) the Canary® system (Quantum Dental Technologies, Toronto, Canada) is low powered and laser based, which uses a combination of heat and light (Frequency Domain Photothermal Radiometry and Modulated Luminescence (FD-PTR and LUM)) to examine directly the crystal structure of teeth and map the area of tooth decay, and (c) Soprolife® camera (Acteon, La Ciotat, France), which uses an LED light with an excitation wavelength of approximately 450 nm [4–6].

The Soprolife® selectively amplifies fluorescence signals to accentuate the specificity of the fluorescence images. As a result, any carious lesion or diseased tissue is detected based on the variation of its autofluorescence compared to the healthy area of the same tooth. The brown color of caries in daylight is perfectly superimposable over the dark red fluorescence detected with the Soprolife®. Sound dentine fluoresces green, and enamel has no fluorescence, although a bluish color is often observed from the diffusion of the green light emitted by dentine.

Dental caries is generally acknowledged as a process whereby bacterial acids destroy hard dental tissues. It is therefore not surprising that a great deal of caries research has been devoted to the de- and re-mineralization of enamel or dentine. Another notable but less investigated feature of the caries process is the Maillard reaction, which was previously described for dental caries coloration [7]. The Maillard reaction is a sugar–protein reaction of amino acid degradation in the presence of natural monosaccharides and encompasses a huge range of intermediates and products. It is also known as glycation or non-enzymatic browning. Numerous Maillard reaction products have been elucidated; many of which are formed in tissues during ageing and diabetes. Kleter et al. have demonstrated the presence of fluorescent amino acids such as hydroxylslypyridinoline, lysylpyridinoline, pentosidine, and carboxymethyllysine in carious dentine [8].

Based on previous data, the first hypothesis tested in our work was that the fluorescence of carious dentine is caused by demineralization. The second hypothesis was that it is caused by the destruction of the demineralized dentine organic matrix by matrix metalloproteinase (MMP). The third hypothesis tested was that the Maillard reaction-produced advanced glycation end-products (AGEs) of the dentine organic matrix are responsible for the red fluorescence.

The objectives of this study were addressed with a series of experiments intended to investigate the origin of dental tissue fluorescence during caries using the following: (1) in vitro imaging of dental tissues treated with acid and matrix metalloproteinase (MMP) to mimic caries and methylglyoxal (MGO) to evaluate the Maillard reaction using the

Soprolife® camera, (2) Raman microspectroscopy to determine the accumulation of AGE product in dentine appearing red with the Soprolife® camera in fluorescence mode.

Methods

Specimen preparation

Written consent was obtained prior to the extraction of eight healthy wisdom teeth at the University Hospital of Montpellier. In addition, two molars presenting occlusal caries (caries codes 5 and 6, ICDAS, International Caries Assessment and Detection System) were included in the study [9]. Under daylight observation, carious dentine presented a brown color, and a dark red color when observed with the Soprolife® camera in treatment mode.

Freshly extracted teeth were sectioned in the longitudinal axis by means of a diamond saw (Isomet 1000, Buehler, Lake Bluff, USA) with a thickness of up to 0.5 mm. Samples were ground to 0.25 mm and polished on carbide disks using diamond pastes (6, 1, and 0.25 μm) on an Escil polishing machine (Escil, Lyon, France). Finally, specimens were thoroughly cleaned in water with an ultrasonic bath for 5 min. Four samples were demineralized in 2.5 % aqueous nitric acid solution (pH=1) for 9 days. Four samples were demineralized using a four-in 4 % aqueous solution of lactic acid. Demineralization solutions were changed every 2 days.

The nitric acid demineralized samples were then processed as follows:

- Four non-carious samples and two carious samples were incubated for 2 days in a solution of 4 mL of MMP1 (Sigma-Aldrich Corporation, St. Louis, USA) at a concentration of 3 mg mL⁻¹ in phosphate buffered saline (PBS) at room temperature.
- Two demineralized healthy samples were incubated in methylglyoxal (Sigma-Aldrich Corporation, St. Louis, USA) at a concentration of 10 mM in a PBS solution at 37 °C for 4 weeks (Fig. 1).
- Two demineralized healthy samples were incubated in methylglyoxal (Sigma-Aldrich Corporation, St. Louis, USA) at a concentration of 1 M in a PBS solution at 37 °C for 4 weeks (Fig. 1).

Soprolife® camera

The Soprolife® intra-oral camera utilizes two groups of LEDs that can illuminate tooth surfaces in either daylight mode (white light) or blue light mode (wavelength of 450 nm with a bandwidth of 20 nm, centered at ± 10 nm around the excitation wavelength). The camera provides an anatomical image (daylight mode) superimposed on an

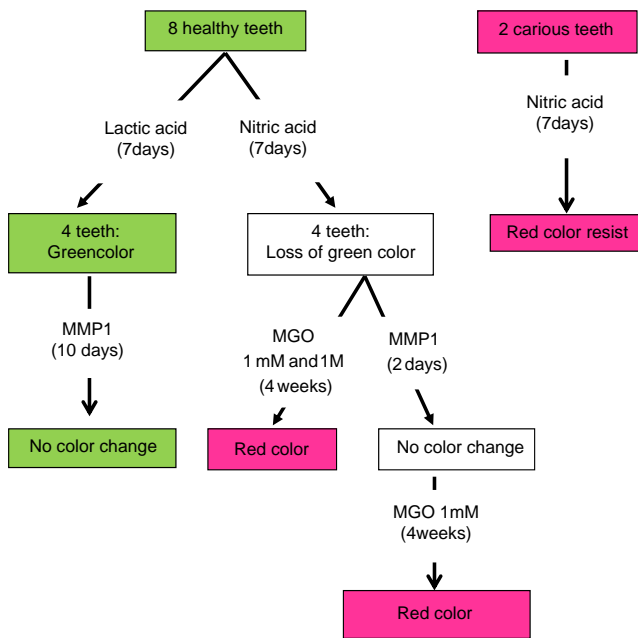


Fig. 1 Sample preparation workflow. Colors indicate the color of dentine observed with the Soprolife® camera in treatment mode after the chemical treatments symbolized by arrows

image produced by the autofluorescence (blue light) of the sample. The camera is equipped with an image sensor (a 0.25-in. CCD sensor) consisting of a mosaic of pixels covered with filters of complementary colors. The collected data, related to the energy received by each pixel, enable an image of the tooth to be retrieved and stored in a computer.

At each stage of analysis, we recorded pictures of the wet samples with the intra-oral fluorescent Soprolife® camera in daylight mode, diagnostic mode, and treatment mode. Daylight mode corresponds to the image registered using the four white light LEDs. Diagnostic and treatment images are produced under blue light from four blue LEDs. The difference between diagnostic and treatment modes involves difference in CCD settings. Treatment mode is designed to increase the red part of the electromagnetic spectrum.

We observed samples in hydrated state to avoid the modifications of teeth that have been previously described [10].

Micro-Raman spectroscopy

To investigate the chemical composition of different dentine samples, Raman spectra were recorded at 298 K with a LabRAM ARAMIS IR² confocal micro-Raman spectrometer (Jobin-Yvon S.A., Horiba, France) equipped with a BX41 Olympus microscope, a 1,800 grooves per mm grating, and a CCD detector cooled by a Peltier effect module. Samples were mounted on an XYZ motorized stage with 0.1-µm step resolution. The microscope lens was a long working distance ×50 objective. The spectral resolution

was ±1 cm⁻¹. Raman spectra were obtained by excitation with 632.8 nm radiations from a He-Ne laser generating less than 12 mW on the samples. Due to fluorescence, samples were under the laser for photobleaching for 15 min before spectral recording. The acquisition time was 90 s with three accumulations.

Spectra obtained from Raman microscopy were normalized using Peakfit v4.12 (USA) software. The Gaussian amplitude in the second derivative method was chosen for fitting the peaks [11].

We also compared modes intensities ratio between and for amide I (1,670 cm⁻¹) and AGE products (1,550–1,600 cm⁻¹) [12, 13]. An increase of this ratio indicates altered collagen quality induced by Maillard reaction.

Results and discussion

Under observation with the Soprolife® intra-oral camera, teeth showing caries appeared acid green in treatment mode, and the carious tissues at the base of the three cavities produced a red color (Fig. 2). Sound dentine fluoresces green, and enamel has no fluorescence, although a bluish color is often observed from the diffusion of the green light emitted by dentine.

More precisely in active and arrested carious lesion, visual signals in fluorescent mode look different depending on the tissue structure [4]. Healthy dentin looks always acid green in fluorescence, as the infected one appears green black. In active caries, infected/affected dentin interface looks bright red fluorescence and yellow brown in daylight. Even caries color is not always a perfect reliable measure; this tissue is fairly easily eliminated with a manual excavator [14, 15]. Abnormal dentin at the end of excavation looks gray-green, sometimes with a very slight pink transparency.

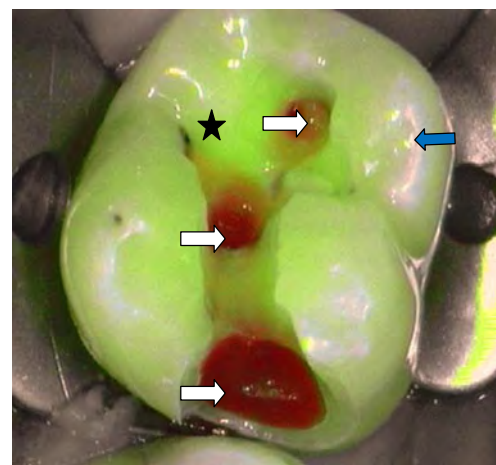


Fig. 2 Aspect of dental caries (ICDAS:5) with Soprolife® camera in treatment mode. Black star healthy dentine, white arrows dentine decay, blue arrows enamel surface

In arrested lesion, the infected/affected interface looks dark red and dark brown in daylight mode. This tissue is more difficult to eliminate with a manual excavator. Abnormal dentin at the end of the excavation looks light gray green with systematically persisting shady pink fluorescence at the bottom of the preparation, opposite the pulpal wall, which don't need to be more removed. It should not be at that time considered as false-positive signal.

In vitro caries model—influence of demineralization

After 9 days of incubation in a 2.5 % aqueous nitric acid solution, tooth sections completely lost their green color (Fig. 3). The loss of fluorescence indicates that dentine fluorescence is not due to collagen alone but to the interplay of calcium phosphate crystals and collagen. During demineralization with lactic acid of a sound tooth observed with the Soprolife® camera in treatment mode, the dentine green fluorescence persists to 7 days (Fig. 4). Enamel persists during these 7 days, showing that demineralization is incomplete. This demineralization is forming pits on dentine surface due to an inhomogeneous acid demineralization. This shows that a complete demineralization as obtained with nitric acid is needed to lose the green fluorescence of dentine. Fluorescence spectroscopy previously performed on sound root dentine also indicated that the strongest emitted fluorescence at a 450-nm excitation is an emission of approximately 500 nm (see Fig. 2 of reference [16]). This property was proposed in a previous fluorescence study using the same excitation light [17]. More recently, using an excitation light of 515 nm, the opposite phenomena were reported, and the authors concluded that the chromophores responsible for the green fluorescence of dentine must be organic in nature [18].

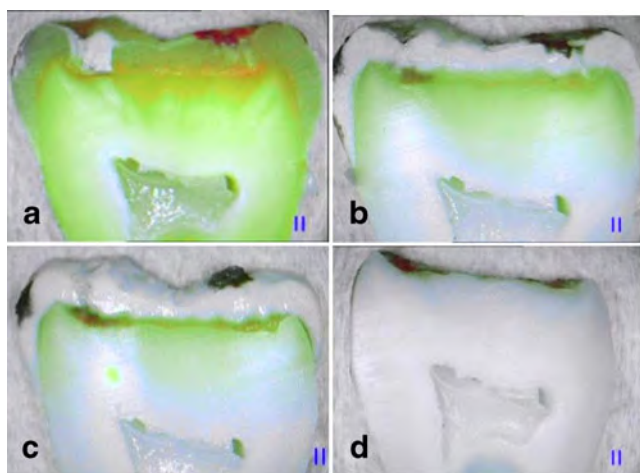


Fig. 3 Kinetics of demineralization with nitric acid of a sound tooth observed with the Soprolife® camera in treatment mode. **a** Day 0, **b** day 3, **c** day 6, **d** day 9. Enamel is absent, and dentine is white

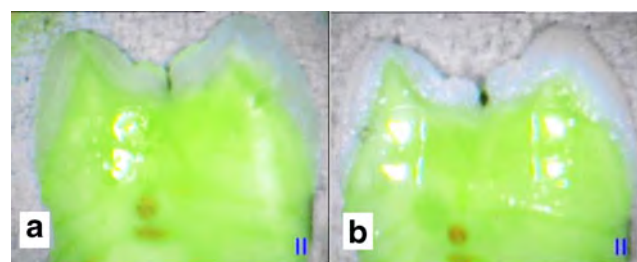


Fig. 4 Kinetics of demineralization with lactic acid of a sound tooth observed with the Soprolife® camera in treatment mode. Dentine green fluorescence persists to 7 days in lactic acid. Surface is irregular with trace of dissolution. **a** Day 0, **b** day 7

These results of sound dentine demineralization didn't explain the strong red fluorescence of caries. The red color of carious dentine observed in the bottom of cavities (Fig. 2) extends deeper into the dentine. We compared dentine fluorescence of sound and caries-affected dentine during nitric acid demineralization (Fig. 5). Comparison between images obtained in daylight mode (Fig. 5a) and treatment mode (Fig. 5b) shows that the red fluorescence corresponds to the brownish color of carious and infiltrated dentine. The green color of dentine is observed under the carious dentine, which has a red color. As for the sound teeth, demineralization in aqueous nitric acid solution induces a loss of dentine's green color when observed with Soprolife® camera in treatment mode. In contrast, the red carious dentine maintains its reddish color following demineralization (Fig. 5d). The loss of the mineral matrix of dentin induces losses of fluorescence of sound dentine and is not responsible of the strong red fluorescence of carious dentin observed with the Soprolife camera in treatment mode. The reason of this red fluorescence must be searched in structural changes of the organic matrix of dentine.

In vitro caries model—Maillard reaction and matrix metalloproteinase

Following demineralization, tooth sections were further treated with MGO and monitored Raman microscopy. After 14 days, the dentine color begins to change to an orange color, and two additional weeks in MGO turn the color of tooth sections homogeneously red. Previous works reported that the Maillard reaction contributes to lesion discoloration [8]. A number of Maillard products, referred to as advanced glycation end-products (AGEs), are formed in tissues during ageing and diabetes [19]. In an in vitro model reaction, demineralized dentine reacted with glucose, acquiring a yellow stain [7]. AGE products are highly fluorescent [20], and the in vitro fluorescence increases as a function of time of incubation, as we observed. The time-dependent color increase reveals the existence of a biochemical reaction leading to accumulation of fluorescent products [21] (Fig. 6).

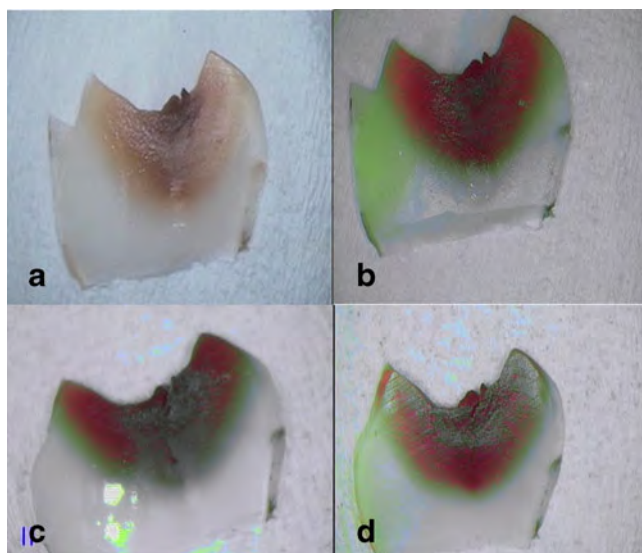


Fig. 5 Carious dentine demineralization in nitric acid observed with the Soprolife® camera. Molar code 6 ICDAS. **a** Day 0, white light mode: carious dentine has a brownish color; **b** day 0, treatment mode: carious dentine is dark red, and sound dentine is green; **c** day 15, treatment mode: carious dentine is dark, still red, and sound dentine is colorless; **d** day 27, treatment mode: carious dentine is still dark red, and sound dentine is colorless

A second experiment with MGO was performed by combining collagen alteration with MMP1 (Fig. 7). This experiment aimed to evaluate whether the orange red color observed during the MGO treatment of demineralized dentine would change. We expected that collagen degradation products would

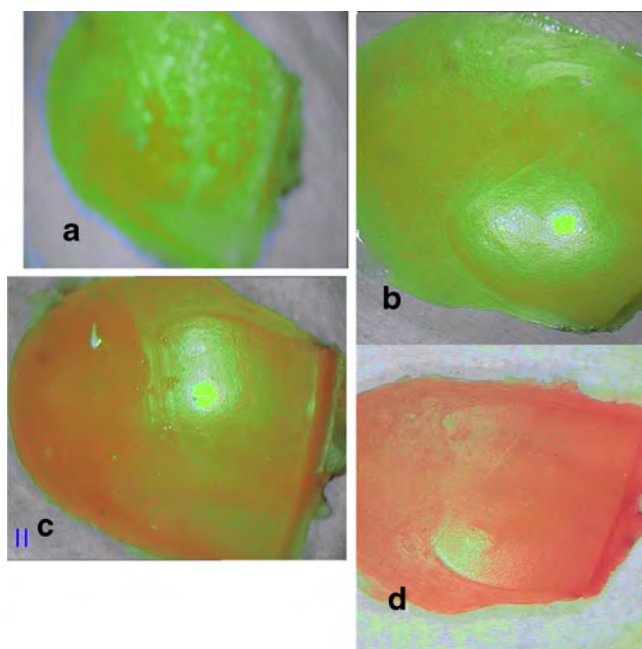


Fig. 6 Nitric acid-demineralized tooth treated with methylglyoxal monitored with the Soprolife® camera in treatment mode. **a** Day 0, **b** day 7, **c** day 14, **d** day 30. After 14 days, the dentine color starts to change to an orange color, which transitions to red by 30 days

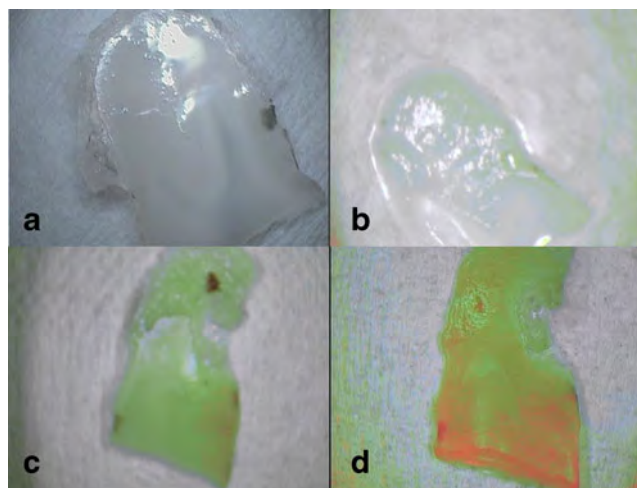


Fig. 7 Combined action of MMP1 and MGO as monitored by Soprolife® camera in treatment mode. **a** Colorless demineralized teeth. **b** After 2 days in MMP1, the specimen is colorless, but its shape was altered due to collagen destruction. **c** After 12 days in MGO, a green color appears. **d** After 19 days in MGO, a red color appears

be more sensitive to non-enzymatic glycation and a red shift would be observed. Following complete demineralization, a tooth section was immersed in an MMP1 aqueous solution for 2 days. Following this treatment, the sample started to lose its original shape, due to collagen degradation. Then, the section was immersed in an MGO solution. After 19 days in this solution, a red color began to appear, similar to the color obtained without collagen degradation.

These two experiments clearly indicate that the end-product of the Maillard reaction (AGE) induces the red color. Albeit, a careful comparison between the red color observed at the bottom of a dental cavity and the orange-red color obtained with the MGO bath indicates that they are different. This difference might be the result of differences in the thickness of the samples or the quantity of AGE products, which would depend on the extent of the Maillard reaction in the samples.

Micro-Raman spectroscopy of carious dentine

As we cannot prove the working mechanism of the camera with the camera as the only objective measure, four dentine samples were studied by Raman spectroscopy. There have been few studies of AGEs using Raman spectroscopy. Sebag et al. used a non-microscopy-based approach to show Raman spectral changes in the human vitreous that were attributed to AGEs [22]. Confocal Raman microscopy was used to quantify AGEs adducts in Bruch membrane [12, 13].

Table 1 gathers the Raman intensities of amide I and AGE's related product bands as well as their ratio. Ratios of this two organic bands increase in carious dentin and also in demineralized dentine treated with methylglyoxal. This

Table 1 AGE's band (1,550–1,600 cm^{-1}) intensity, Amide I band (1,670 cm^{-1}) intensity, and band intensities ratio of AGEs versus Amide I

	Sound dentine	Cariious dentine	MGO 10 mM	MGO 1 M
AGE's band (1,550–1,600 cm^{-1})	399	1,865	729	608
Amide I band (1,670 cm^{-1})	2,434	1,428	3,286	278
Ratio	0.16	1.31	0.22	2.19

gives a second indication that the red color of carious dentine observed with Soprolife® camera is certainly due to an accumulation of AGE product.

Conclusions

The Soprolife® camera selectively amplified the fluorescence signals of carious dentine. The brown signal of caries observed under daylight corresponds to the dark red fluorescence observed with the camera in treatment mode. We demonstrate that the green fluorescence of sound dentine is dependent on demineralization. However, a definitive proof would be to re-create the green fluorescence of a dentine collagen matrix during re-mineralization. As dentine mineralization is a complex process involving different proteins controlling the nature, size, and organization of calcium phosphate crystals [23], such a demonstration will be a challenging task.

The influence of the Maillard reaction on the appearance of a red coloration during caries is suggested. However, it is possible that this reaction is not the only one responsible, as the orange-red color is different from the deep red color observed at the bottom of dental cavities. The influence of bacterial metabolism (e.g., *S. mutans*) in association with Maillard reactions on the generation of the red color remains to be investigated.

Our experiment using MMP1 didn't generate any fluorescence variation. An experimental system closer to reality, using MMP produced by bacteria, might be a more informative approach.

In conclusion, our results provide important information on the origin of fluorescence variation of dental caries observed with the Soprolife® camera. These investigations should be continued and new parameters must be evaluated, as it is clear that destruction of dentine during caries is a complex process with many parameters to consider.

Acknowledgements The authors would like to thank the support of the PHORMOST European network European Network of Excellence and David Bourgogne for the Raman microscopy (Institut Charles Gerhardt, Université Montpellier 2).

Conflict of interest The authors declare that they have no conflict of interest.

References

- Fontana M, Zero DT (2006) Assessing patients' caries risk. J Am Dent Assoc 137:1231–1238
- Zero D, Fontana M, Lennon ÁM (2001) Clinical applications and outcomes of using indicators of risk in caries management. J Dent Educ 65:1126–1131
- Zandoná AF, Zero DT (2006) Diagnostic tools for early caries detection. J Am Dent Assoc 137:1675–1683
- Terrer E, Sarraquigne C, Koubi S, Weisrock G, Mazuir A, Tassery H (2010) A new concept in restorative dentistry: FILEDT—fluorescence induced light for diagnosis and treatment. Part II: treatment of dentinal caries. J Contemp Dent Pract 11:95–101
- Terrer E, Sarraquigne C, Koubi S, Weisrock G, Mazuir A, Tassery H (2009) A new concept in restorative dentistry: FILEDT—fluorescence induced light for diagnosis and treatment. Part 1: diagnosis and treatment of initial occlusal caries. J Contemp Dent Pract 10:86–93
- Weisrock G, Terrer E, Couderc G, Koubi S, Levallois B, Manton D et al (2011) Naturally aesthetic restorations and minimally invasive dentistry. J Mini Interv Dent 4:23–34
- Kleter GA, Damen JJM, Buijs MJ, Ten Cate JM (1998) Modification of amino acid residues in carious dentin matrix. J Dent Res 77:488–494
- Kleter GA (1998) Discoloration of dental carious lesions (a review). Arch Oral Biol 43:629–631
- Ismail A, Sohn W, Tellez M, Amaya A, Sen A, Hasson H et al (2007) The International Caries Detection and Assessment System (ICDAS): an integrated system for measuring dental caries. Community Dent Oral 35:170–178
- Al-Khateeb S, Exterkate RAM, de Jong ED, Angmar-Mansson B, ten Cate JM (2002) Light-induced fluorescence studies on dehydration of incipient enamel lesions. Caries Res 36:25–30
- Beattie JR, Glenn JV, Boulton ME, Stitt AW, McGarvey JJ (2009) Effect of signal intensity normalization on the multivariate analysis of spectral data in complex real-world datasets. J Raman Spectrosc 40:429–435
- Pawlak AM, Glenn JV, Beattie JR, Mc Garvey JJ, Stitt AW (2008) Advanced glycation as a basis for understanding retinal aging and noninvasive risk prediction. Ann N Y Acad Sci 1126:59–65
- Beattie JR, Pawlak AM, Boulton ME, Zhang J, Monnier VM, Mc Garvey JJ et al (2010) Multiplex analysis of age-related protein and lipid modifications in human Bruch's membrane. FASEB J24:4816–4824
- Kuboki Y, Liu CF, Fusayama T (1983) Mechanism of differential staining in carious dentin. J Dent Res 62:713–714
- Ogawa K, Yamashita Y, Ichijo T, Fusayama T (1983) The ultrastructure and hardness of the transparent layer of human carious dentin. J Dent Res 62:7–10
- Buchalla W, Lennon AM, Attin T (2004) Comparative fluorescence spectroscopy of root caries lesions. Eur J Oral Sci 112:490–496
- Araki T, Miyazaki E, Kawata T, Miyata K (1990) Measurements of fluorescence heterogeneity in human teeth using polarization microfluorometry. Appl Spectrosc 44:627–631
- Van der Veen MH, ten Bosch JJ (1996) The influence of mineral loss on the auto-fluorescent behaviour of in vitro demineralised dentine. Caries Res 30:93–99
- Dyer DG, Dunn JA, Thorpe SR, Bailie KE, Lyons TJ, McCance DR et al (1993) Accumulation of Maillard reaction products in skin collagen in diabetes and aging. J Clin Invest 91:2463–2468

20. Sajithlal GB, Chithra P, Chandrakasan G (1999) An in vitro study on the role of metal catalyzed oxidation in glycation and cross-linking of collagen. *Mol Cell Biochem* 194:257–262
21. Pongor S, Ulrich PC, Bencsath FA, Cerami A (1984) Aging of proteins: isolation and identification of a fluorescent chromophore from the reaction of polypeptides with glucose. *Proc Natl Acad Sci U S A* 81:2684–2687
22. Sebag J, Nie S, Reiser K, Charles MA, Yu NT (1994) Raman spectroscopy of human vitreous in proliferative diabetic retinopathy. *Invest Ophthalmol Vis Sci* 35:2976–2980
23. Houle P, Steuer P, Voegel J-C, Cuisinier FJG (1998) Experimental evidence for human dentine crystal formation involving conversion of octacalcium phosphate to hydroxyapatite. *Acta Crystallogr D* 54:1377–1380

FULL ARTICLE

Multiphoton imaging of the dentine-enamel junction

Thierry Cloitre^{1,2}, Ivan V. Panayotov³, Hervé Tassery^{3,4}, Csilla Gergely^{1,2}, Bernard Levallois³, and Frédéric J. G. Cuisinier³

¹ Université Montpellier 2, Laboratoire Charles Coulomb UMR 5221, F-34095, Montpellier, France

² CNRS, Laboratoire Charles Coulomb UMR 5221, F-34095, Montpellier, France

³ EA 4203, UFR Odontologie, Université Montpellier 1, 34193 Montpellier Cedex 5, France

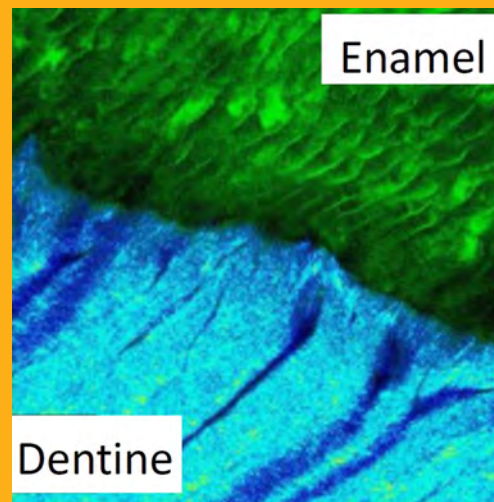
⁴ Aix Marseille Université; Assistance Public Hôpitaux de Marseille, 13354 Marseille, France

Received 9 April 2012, revised 21 June 2012, accepted 22 June 2012

Published online 23 July 2012

Key words: dentine-enamel junction, multiphoton microscopy, second harmonic generation, two photon excited fluorescence, histology, human

Multiphoton microscopy has been used to reveal structural details of dentine and enamel at the dentin-enamel junction (DEJ) based on their 2-photon excited fluorescence (2PEF) emission and second harmonic generation (SHG). In dentine tubule 2PEF intensity varies due to protein content variation. Intertubular dentin produces both SHG and 2PEF signals. Tubules are surrounded by a thin circular zone with a lower SHG signal than the bulk dentine and the presence of collagen fibers perpendicular to the tubule longitudinal axis is indicated by strong SHG responses. The DEJ appears as a low intensity line on the 2PEF images and this was never previously reported. The SHG signal is completely absent for enamel and aprismatic enamel shows a homogeneous low 2PEF signal contrary to prismatic enamel. The SHG intensity of mantle dentine is increasing from the dentine-enamel junction in the first 12 μm indicating a progressive presence of fibrillar collagen and corresponding to the more external part of mantle dentine where matrix metallo-proteases accumulate. The high information content of multiphoton images confirms the huge potential of this method to investigate tooth structures in physiological and pathological conditions.



Dentine-Enamel Junction. Superposition of SHG and 2PEF images showing the relationship of enamel and dentine.

1. Introduction

Attempts to image the dentine-enamel junction (DEJ) follow the history of microscopy. Kohliker (1855) was the one who provided a first view of the

DEJ histology, which appears as a simple line when imaged microscopically [1]. This apparently sharp interface, the ‘optical DEJ’, is thought to represent the original position of the basal membrane between ameloblasts and odontoblasts, where they contact in

* Corresponding author: e-mail: frédéric.cuisinier@univ-montp1.fr, Phone: +33 411 759 225, Fax: +00 411 759 20

the embryological tooth bud. With the appearance of transmission electron microscopy a step toward a precise morphological description of DEJ was achieved [2]. The DEJ itself has a hierarchical microstructure with a three dimensional scalloped appearance along the interface [3]. Developmental studies indicate that DEJ is not restricted to a thin interface and is a transitional zone with spatiotemporal gradient in both tissues [4]. Specifically collagen fibrils in the transitional zone were either perpendicular to the plane of the junction, or converged towards enamel [3]. These coarse fibrils forming bundles of 80–120 nm in diameter appeared to be similar to the “von Korff fibers” [5]. The matrix of bulk dentin consists of an interwoven fibrillar array, in which the majority of fibrils appeared to be either parallel or at angles correspondingly less than 90° to the plane of junction. High resolution electron microscopy (HREM) provides a description of the dentine enamel relationship at the scale of the crystals [6]. Atomic Force Microscopy (AFM) was used to image the dentine-enamel junction but mainly to study microhardness of dentin and enamel on each side of the junction [7]. Synchrotron radiation-based micro computed tomography (SR-CT) measurements were also tested to better understand the inner structure of the collagen fibers [8].

Recently multiphoton microscopy has become an important research tool for noninvasive imaging of thick specimens with cellular resolution using 2-photon excited intrinsic fluorescence (2PEF) [9] and second harmonic generation (SHG) [10]. A number of advantages render multiphoton microscopy a widely used imaging modality in many biomedical applications. The use of near infrared excitation allows deep sample penetration with benign irradiation. The 2PEF and SHG signals in multiphoton microscopy are produced only at the focal point causing less sample photo-damage and enabling sectional imaging. 2PEF image contrast is generated by the excitation of tissue fluorophores. The characteristic 2-photon excited fluorescence (2PEF) provides both morphological and functional information. In addition collagen, microtubules and myosin, are tissue intrinsic and highly non-centrosymmetric molecular assemblies that possess first hyperpolarizabilities large enough to produce SHG signals [10, 11]. The photons interact with the non-centrosymmetric systems producing emission of a coherent light beam at twice the energy of the incident light [12]. As dentine and cement are formed by a calcified collagenous matrix, biphoton microscopy was used to image sound teeth and carious tissue [13–16].

The aim of this work is to provide a multiphotonic description of dentine and enamel structures at the sound dentin-enamel junction. Although multiphoton imaging has been previously applied to investigate dental structures here we present a detailed

study of dentine and enamel structures separated by DEJ, taking advantages of the 2PEF signal of enamel and the strong SHG of dentinal collagen.

2. Materials and methods

2.1 Specimen preparation

Teeth extracted for orthodontic reasons were collected from University Hospital of Montpellier (written consent was signed before extraction). The teeth were stored in 0.9% phosphate buffer saline (PBS) buffer solution (pH = 7.4) containing 0.002% sodium azide at 4 °C. Eight freshly extracted teeth were sectioned in the longitudinal axis by means of an Isomet diamond saw (Isomet 1000, Buehler, Lake Bluff, USA) with a thickness up to 0.5 mm. The samples were grinded to 0.25 mm, polished on carbure disks and using diamond pastes (6, 1 and 0.25 μm) with an Escil polishing machine (Escil, Lyon, France). Specimens were finally thoroughly cleaned up in water with an ultrasound bath for 5 min.

2.2 Multiphoton microscopy (MPM)

MPM images were recorded using a custom-built multiphoton microscope based on a Zeiss Imager Z1 upright microscope. Excitation is provided by 80 MHz femtosecond Ti-sapphire laser system (Tsunami Ti-Sapphire laser, Spectra-Physics, Spectra Physics, Mountain View, USA) operated in pulsed mode (wavelength range 820–890, typically 880 nm, repetition rate 80 MHz, pulse duration 100 fs). The laser beam was fed into the back port of the microscope, deflected by a short pass 670 nm dichroic beamsplitter (Chroma Technology Corp) and focused onto the sample with a 40x, Fluor, N.A. 1.3 oil-immersion microscope objective (Zeiss). Images were created by scanning the sample using an x/y scanning piezostage (P-542-2CD, Physik Instrumente). Two-photon fluorescence was epi-collected through the microscope objective. Fluorescence signal was discriminated from backscattered laser excitation and SHG signal using a short pass dichroic mirror (670 dcspxruv-3p, Chroma Technology Corp) and a combination of long pass, short pass and color glass filters (NT64-625, NT49-822 Edmund Optics and CG BG39 1.0 CVI Melles Griot respectively). This filters combination result in 475–700 nm band-pass for the fluorescence detection channel. Second harmonic signal was dia-collected through a large aperture oil immersion condenser and was discriminated from transmitted laser excitation an fluores-

cence signal using band pass (417–477 nm) and colored glass filters (NT48-074 Edmund Optics and CG BG39 2.0 CVI Melles Griot respectively). Fluorescence and SH signals were synchronously measured using respectively a photomultiplier tube (R928P Hamamatsu) and a photon counting unit (H7422P Hamamatsu). The method enables the acquisition of Z-stacks of 2D images of the sample with a typical Z resolution of 600–800 nm.

2.3 Image analysis

SHG and 2PEF images were viewed using Image J (NIH, Bethesda, MD, USA, <http://rsb.info.nih.gov/ij/>). Lookup tables (LUT) were applied on 2PEF and SHG images, respectively the Green LUT and the 16-colors LUT. Intensity profile plots perpendicular to the dentine-enamel junction were calculated with the same software. SHG image were overlaid on 2PEF images using the co-localization finder plugin of Image J.

3. Results

Images of 8 polished DEJ sections were obtained by measuring second harmonic generation (SHG) and two photon excited fluorescence (2PEF) signals beneath the surface to depths of up to about 70 μm . The 2PEF displays protein intrinsic fluorescence of the sample, whereas the SHG reveals the collagen fibrils due to their non-centrosymmetric structure.

When dentine is imaged in 2PEF and SHG (Figure 1A and B), one can observe a network of low intensity spots corresponding to perpendicular sections of tubules. In the 2PEF image the whole dentin is green fluorescent except some tubules having a

very low 2PEF signal. Other tubules reveal an intense signal (for example the tubule indicated by a black arrow on Figure 1A) indicating the presence of fluorescent material. On the corresponding SHG image (Figure 1B) regardless of the intensity of the 2PEF emission, the tubules (for example the white arrow indicating a tubule with strong 2PEF signal) reveal a very weak SHG indicating the absence of highly noncentrosymmetric molecular assemblies as collagen and microtubules. The mean diameter of the tubules on the 2PEF image is $1.3 \pm 0.1 \mu\text{m}$ whereas on SHG images it is $4.0 \pm 0.2 \mu\text{m}$ on SHG images; this difference will be discussed later. Additionally we have observed variations in the intertubular dentine SHG signal. On the area showing a strong SHG signal (indicated by an orange red color in Figure 1B) tubules are surrounded by a thin circular zone with a lower SHG signal than the bulk dentine.

A series of multiphoton images corresponding to an area including the dentine enamel junction is presented in Figure 2. The upper row of images (Figure 2A–C) depicts 2PEF signals and the bottom row corresponds to the SHG signal. The enamel is situated at the upper right corner of images and dentine tubules end in the close vicinity of the DEJ. Images were recorded at various depths expressed in z values: Figure 2A and D correspond to the same depth; Figure 2B and F are recorded 2 μm under the section presented in Figure 2A and D whereas Figure 2C and G are recorded 2 μm under those depicted in Figure 2B and F. We focus our attention on one tubule indicated by white arrows in the 2PEF images and by black arrows in the SHG images of this z-scan series of images. In Figure 2A the tubule is showing an internal intense 2PEF signal with small isolated non fluorescent areas. On the next image (Figure 2B), 2 μm deeper in Z direction, the 2PEF intensity of the tubule is low and even weaker than the fluorescence of the intertubular dentine. This weak signal is probably due to peritubular dentine with low organic content. In Figure 2C, 2 μm under this area the signal diffuse without clear border and the tubule looks wider than in Figure 2A and B. The corresponding SHG images (Figure 2D–F) show a weak SHG signal for all depth indicating an absence of fibrous collagen in the tubule and in the peritubular area as observed in Figure 1B.

The contact zone between enamel and dentine can be well observed in the 2PEF images as an irregular line of low signal (Figure 3A, black arrow). The average line thickness measured at five spots along the junction is $2.4 \pm 0.4 \mu\text{m}$. The SHG signal is totally absent in the enamel (Figure 3B). The dentine tubules are parallel to the image plan and stop at the vicinity of the DEJ. They appear either with low or with high fluorescence intensity. The superposition of the 2PEF and SHG images enable to clearly

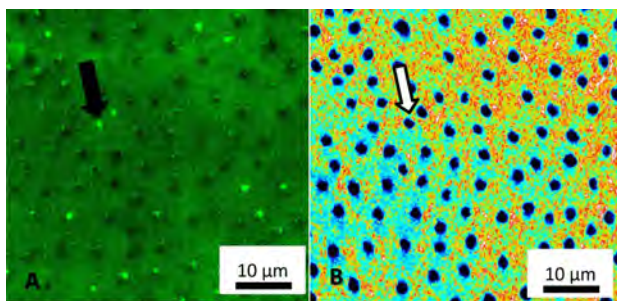


Figure 1 (online color at: www.biophotonics-journal.org) Dentine observed almost perpendicularly to canalicules. (A) 2PEF image. Black arrow: tubule with high fluorescence; (B) SHG image: white arrow: same tubule than in A. The red–orange signal showing the SHG intensity of the collagen framework.

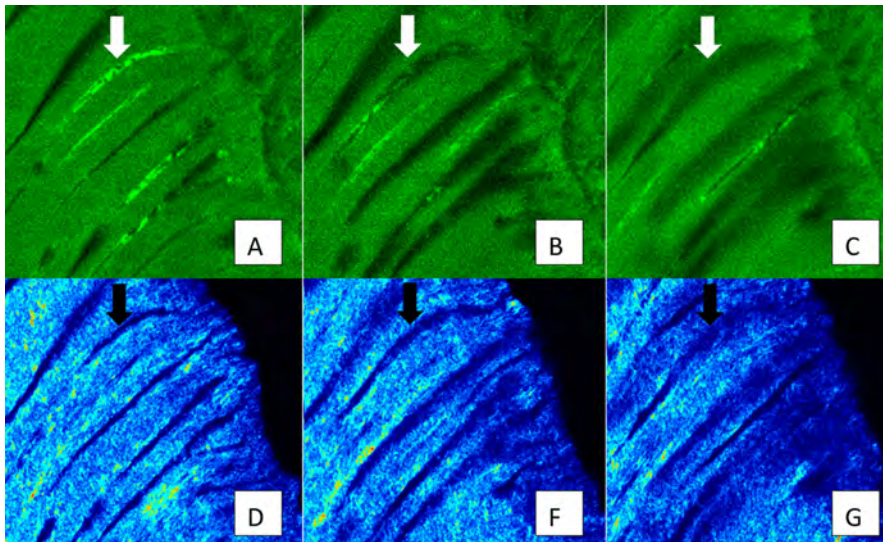


Figure 2 (online color at: www.biophotonics-journal.org) 2PEF and SHG images of DEJ with 2 μm thickness steps. White arrows show the terminal branching of a tubule at different depths in 2PEF images: (A): $z = 0 \mu\text{m}$, (B): $z = -2 \mu\text{m}$, (C): $z = -4 \mu\text{m}$. Dark arrows show the same tubule in the corresponding SHG images at different depths: (D): $z = 0 \mu\text{m}$, (F): $z = -2 \mu\text{m}$, (G): $z = -4 \mu\text{m}$. There is no intense SHG response corresponding to the high fluorescence intensity in the tubule.

visualize the DEJ (Figure 3C). Figure 3D and E are enlargements of Figure 3A and B, respectively. The diameters of tubules in 2PEF images are smaller than in the corresponding SHG images as observed on Figure 3D, E that are enlargement of Figure 3A and B. Strong SHG signals, as the one indicated by a white arrow, are aligned parallel at a constant distance of the tubule (Figure 3E). These strong signals are produced by collagen fibers parallel to the excitation light [12] and they indicate the presence of collagen fibers perpendicular to the tubule longitudinal axis.

A high magnification of the 2PEF image of DEJ (Figure 4) reveals the transitional zone of the enamel. A non-fluorescent line corresponding to the interface between dentin and enamel is observed (dark arrow in Figure 3) indicating the zone of DEJ. En-

amel prism sheaths exhibit a high fluorescence (white arrow in Figure 4). The aprismatic enamel is indicated by a dark bracket. This layer has a homogeneous and lower fluorescence intensity compared to the prismatic enamel. Inside the prisms the fluorescence is weak due to low protein content is noted. The interprismatic space also named enamel prism sheaths stops in the aprismatic enamel layer. The 2PEF intensity of enamel and dentine are similar (Figure 4) which is somehow surprising since dentin contains 30 times more protein than enamel. 2PEF intensity depends of the number of fluorophores, cross sections and quantum yield of the tissue fluorophores. The main fluorescent amino acids are tryptophan, tyrosine and phenylalanine. They fluoresce in the range of 350–280 nm but the objective and the dichroic filter of the microscope cut above 450 nm

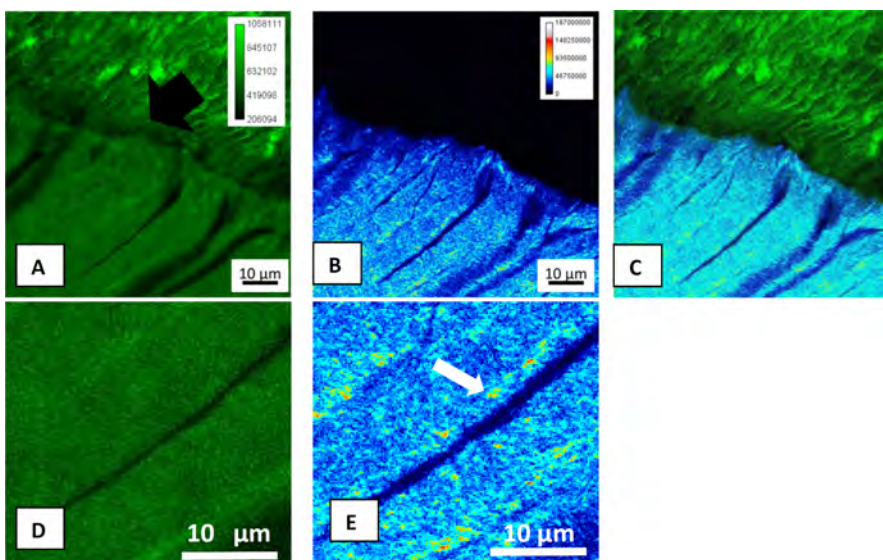


Figure 3 (online color at: www.biophotonics-journal.org) Dentine-enamel junction. (A) 2PEF image. Black arrow: DEJ showing a dark line due to a decrease of 2PEF signal; (B) SHG image: Enamel has no SHG signal. (C) 2PEF/SHG images superposition; (D) Enlargement of A; (E) Enlargement of B: white arrow indicating high intensity SHG signal around the tubule.

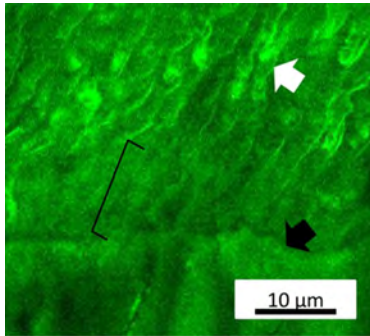


Figure 4 2PEF image of dentine-enamel junction. Black arrow: DEJ; Black left square bracket: inner aprismatic enamel; white arrow: enamel prism sheath with high 2PEF intensity.

and eliminate their contributions. Other intrinsic fluorophores fluorescing at 450 nm are NADH, flavins and porphyrins however these fluorophores are not present in sound enamel. The fluorescence of enamel is really not understood [17]. It was only demonstrated that the one-photon fluorescence of enamel decrease with demineralization. The origins of auto fluorescence generated by dental tissue may be

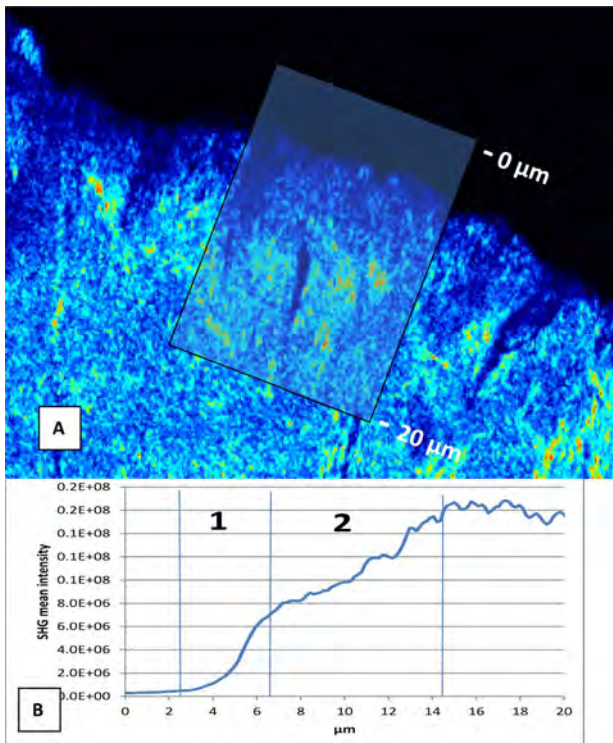


Figure 5 (A) SHG image of DEJ. Enamel gives no SHG signal. The frame is corresponding to the area used to plot SHG intensity. (B) Profile plot of SHG intensity perpendicular to DEJ as indicated by the black frame on A, zone 1 is corresponding to a fast increase of SHG intensity, in zone 2 intensity growth decreases and then reaches a plateau.

quite diverse, and include contributions of both organic and inorganic components [18, 19].

Furthermore we monitored the variation of the SHG signal at the dentine transitional zone of DEJ. As depicted in Figure 5 SHG signal at the dentine transitional zone of DEJ. SHG intensity increases in a two regime rate starting from the DEJ clearly observed as a border line between the dentine and the enamel. Enamel produces no SHG signal. In the dentine we observe a transition zone of 14 μm where the SHG signal varies continuously: in the closest part to the enamel (zone 1) the increase of SHG signal is faster than in zone 2, deeper into the dentin. After 14 μm from the DEJ, SHG intensity reaches a plateau indicating a constant collagen fibrillar structure within the dentine.

4. Discussion

4.1 Dentine tubules

The origin of the observed variations in the 2PEF intensities of dentine tubules is not straightforward. An opposite observation was made by Chen et al. on longitudinal dentin slices [13]. After superposition of 2PEF and SHG images, they found that the collagen composition of the dentinal tubules produces a strong SHG signal.

Our first hypothesis could be that the strong 2PEF emission in the dentine tubules is due to the odontoblast process containing fluorescent proteins. A tubule without fluorescence could point an empty tubule due to the retraction of the odontoblast process as no fixation of dental tissue was performed [20]. The absence of SHG signal in the highly fluorescent tubule is challenging this hypothesis as previous electron transmission studies indicated that odontoblast processes involve a high density of microtubules and microfilaments [21]. Microtubules reveal SHG signal as they are non centrosymmetric [9]. These elements are parallel to the tubules and aim at keeping the odontoblast process elongated. The stability of the microtubules is very weak with an average life spanning from 10 min to 2 hours. Therefore the chance to retrieve SHG signal of microtubules is very low in our experimental conditions. The presence of microtubules would have also been observed by SHG when changing orientation between molecule's axis and incident light. If the elongated molecular elements are parallel to the incident light the SHG signal is weaker [22] and we would expect for SHG images recorded orthogonally to tubules (Figure 2B) that microtubules involved in the odontoblast process have a high signal. However we never detected such a high SHG signal in tubules. Dentine tubule

might also behave as an optical waveguide. In porous media such as porous silicon light confinement was observed [23] when light path was parallel to porous cavities. Similarly to those studies, we never observed a high SHG signal in dentine whatever the light path.

Therefore it seems that the inconstant high 2PEF signal observed in dentine tubule is not related either to the presence of odontoblast processes, neither to an intrinsic property to guide light but is simply due to the presence of intrinsic fluorophores. Irregular electron-dense material within the tubules in absence of cellular processes was reported in dentine studied by transmission electron microscopy (TEM) [24]. The organic periodontoblastic space ie the space between the odontoblast process membrane and the mineralized wall of the tubule is filled by uncalcified collagen fibrils and an amorphous or finely granular ground substance when observed by TEM [25]. Glycosaminoglycan's were localized by staining in the periodontoblastic space [26]. The observed irregular fluorescent materials are certainly this periodontoblastic organic matrix aggregating when the odontoblast process retracts.

4.2 Diameter of dentine tubules

The mean diameter of the tubules in the 2PEF image is $1.3 \pm 0.1 \mu\text{m}$. This value is corresponding to the lumen diameter of tubules measured by scanning electron microscopy [27]. On SHG images tubules have a larger diameter of $4.0 \pm 0.2 \mu\text{m}$. The absence of SHG signals is due to the absence of fibrillar collagen in tubule lumen and in peritubular dentine [28, 29]. The measured dimension corresponds to the outer diameter of peritubular dentine observed by AFM [30]. Peritubular outer diameter determined by SEM is smaller ($2.5 \mu\text{m}$) [31]. The difference between tubule diameters measured in the 2PEF and SHG images corresponds to the thickness of peritubular dentine. The peritubular dentine is characterized by an absence of SHG signal due to its high mineralization and its low content of protein.

We observe a difference also between the 2PEF signals of dentin tubules imaged longitudinally. High 2PEF intensity is corresponding to the central part of the tubule due to an accumulation of intrinsic fluorescent proteins in the tubule. The same tubule, in a different plane, has an aspect of ghost due to diffuse low fluorescence extending in intertubular dentine. This low fluorescence originates in the presence of the peritubular dentine with low organic content. It should be noted that the peritubular dentine is present until the DEJ even in case of Y terminated tubule.

4.3 Variation of intensity of intertubular dentine

It was already described that intertubular dentin produce both SHG and 2PEF signals [13]. Additionally we have observed variations in the SHG signal of the intertubular dentine. In the area exhibiting a strong SHG signal (indicated by an orange red color in Figure 1B) tubules are surrounded by a thin circular zone with a lower SHG signal than the bulk dentine.

Around dentin tubules strong SHG signals are observed when tubules are imaged longitudinally. The observed variation of the SHG signal points towards different orientations of collagen fibrils. When the laser polarization is oriented parallel with the axis of the collagen fibril a maximal SHG signal is produced [12, 32]. Therefore our SHG images indicate the presence of collagen fibers perpendicular to the tubule's longitudinal axis. Our results are in good agreement with previous observations, where groups of fibrils have appeared to follow a circular or oblique course [33]. Such collagen network was also observed by AFM [34].

4.4 Enamel

SHG signal is totally absent in enamel (Figure 2D–F and Figure 3E). Human enamel crystals are poorly crystalline carbonated apatite with a P63/m space group [35]. This space group belongs to the 6/m point group of the hexagonal crystal system. The second-order susceptibility tensor ($\chi(2)$), expressing non-linear phenomena like SHG, vanishes for the 6/m symmetry group [36]. Deviation from the hydroxyapatite hexagonal symmetry of a human tooth enamel crystal observed by high-resolution electron microscopy was reported [37]. Absence of SHG of enamel indicates either that such deviation affects a limited number of crystals either that they are too small to modify the non-linear response of enamel. Mature enamel contains 0.36 per cent of protein [38]. A recent paper has postulated the presence of fiber i.e. non centrosymmetric protein in enamel [39]. The absence of SHG in enamel is also suggesting an absence of non centrosymmetric protein.

4.5 Dentine Enamel Junction

DEJ is indicated as a low intensity line in the 2PEF images. The absence of 2PEF signal at the DEJ was never reported previously. This indicates an absence of endogenous fluorophores at DEJ, contrary to the

dentine where major fluorophores are tryptophan, collagen and elastin [40]. The dark line is certainly indicating a very low concentration of protein at the DEJ. The superposition of the 2PEF and SHG images allow to visualize clearly the DEJ and proves that SHG signals quenches exactly at the level of DEJ.

The invaginations of enamel into dentine provide a scalloped structure with convexities directed towards the dentine and concavities towards the enamel [16, 41, 42]. Aprismatic enamel shows a homogeneous low 2PEF signal contrary to enamel prism. In prismatic enamel the dominant 2PEF contrast comes from the organic-matrix-filled sheaths. The prisms reveal less fluorescence than the sheath due to their lower protein content. Similar enamel images were taken by Chen et al. (2008) using a Third Harmonic Generation (THG) microscopy [43]. Because of the absence of SHG signal of enamel they used THG generated from the interprismatic spaces to reveal the prism structure. In our case we never observed SHG signal at the DEJ. As it is known that strain in crystals can cause the change in symmetry and thus induce SHG [44, 45], the absence of SHG signal in enamel indicates an absence of stress in enamel crystals at the DEJ.

The SHG intensity of mantle dentine is increasing from the level of DEJ towards the dentine. The increase rate is higher in the first 4 μm than in the following 8 μm . This 12 μm zone is corresponding to the more external part of mantle dentine where Von Korf collagen fibrils are present. We pointed three hypotheses to explain this increase. MMP-2 (Gelatinase A) in both pro (~ 72 kDa) and active (~ 68 kDa) forms has been identified in human dentin [46]. MMP-2 is the predominant matrix metalloproteinase in mineralized dentin and may be associated with the collagen matrix but not with hydroxyapatite [46]. Analysis revealed immunoreactivity for MMP-2 throughout human coronal dentin with intense labeling in a 9–10 μm wide zone adjacent to the DEJ [47]. Recently in enamelysin (MMP-20) knockout mice a 10 μm wide hypomineralized area was described [48]. MMP-2 in forming rat incisors may be concentrated in an area adjacent to the dentine-enamel junction [49]. Collagen denaturation decreases SHG intensity and it was demonstrated that collagen degradation with MMP collagenase decrease SHG intensity [50]. Taking into account the accumulation of different MMP's in this zone and the effect of MMP on collagen SHG signal we can hypothesize an influence of MMP's on dentine SHG.

Also the chemical composition profiles (matrix/mineral ratios) determined by Raman spectroscopy change in the first layer of dentine. They increased gradually from nearly zero across the dentin-enamel junction to a constant value in dentine. The width of this transition zone was determined to be in the

range of 5–16 μm [51]. This variation of the Raman peak intensity ratio indicates a progressive increase in protein concentration. Dentine carbonated apatite crystal, as enamel crystal, do not generate SHG. More than ninety percent of the dentine organic matrix is fibrillar collagen type I and collagen is a strong SHG emitter. Our second hypothesis is that SHG intensity is following the matrix/mineral ratio observed by Raman spectroscopy.

The increase of SHG observed in our study can also be explained with reorientation of the collagen fibrils before their interaction with the zone of non-prismatic enamel. Collagen fibrils in the junction area are oriented parallel to each other and perpendicular to the plane of the junction [52]. This is coherent with the increase of SHG observed in our study as it is well known that SHG intensity depends of the respective orientation of the laser light and the fibril [22]. If they are perpendicular, the intensity of the forward SHG emission is low and is high in case of parallel orientation. In contrast to these oriented collagen fibrils entering the enamel, the matrix of bulk dentin was seen to consist of an interwoven fibrillar array, in which the majority of fibrils appeared to be either parallel or at angles correspondingly less than 90° to the plane of the junction [52].

Using multiphoton microscopy it is impossible to select one of these three hypotheses and it is possible that the three mechanisms cooperate to create the SHG increase in the area. However the association of 2PEF and SHG images in our measurements provides a full description of enamel and dentine structures in the DEJ vicinity.

5. Conclusions

In this study we report 2PEF and SHG images recorded by multiphoton microscopy enabling to describe two transitional zones between enamel and dentine reflecting the early developmental stages in first formed enamel and dentin. This technique thereby allows identifying the DEJ and structural characteristic of immediately surrounding tissue characteristics. We found different degrees of organic material in the dentin structure that provokes related changes in the 2PEF and SHG signals. The high quality of images and the simplicity of sample's preparation without any histology treatment render the multiphoton microscopy a powerful methodology to investigate the tooth structures on a sub-micrometric scale. The presented results demonstrate the optical sectioning power of this imaging technique, hence future investigations will aim to describe the differences between normal tooth structures and carious tooth tissues.



Thierry Cloitre received his Ph.D. in physics of condensed matter from the Sciences University of Montpellier, France in 1992. He has turned its research activity from semiconductor physics to biophysics in 2006. He is an assistant professor in the Bionanophotonics team of the Charles Coulomb La-

boratory, Montpellier 2 University. His main contributions rely on his expertise in the field of optical physics for the development of non-linear optical microscopy experimental set-ups and the study of innovative solutions for optical and electrical devices for biosensing applications.



Ivan Vladislavov Panayotov, doctor of dentistry, received his Master of Sciences, Technologies and Health in 2009 at Montpellier 1 University (France). Currently, he is Ph.D. student in EA4203 Laboratory of Nano-science

and assistant professor in endodontic. His research interests are in the functionalization of biomaterials with polyelectrolyte multilayers and specific peptides for medical applications and in the development of new technologies to detected structural changes in mineralized tooth tissues.



Hervé Tassery has received his Ph.D. in biomaterials from Aix Marseille University 2001. Currently, he is professor and head of the Department of Restorative Dentistry of Marseille Dental School at Aix-Marseille University. His major fields of interest are in cariology, fluorescence devices, minimally invasive dentistry and clinical researches. Working in the Laboratory of bionanotechnology of Montpellier 1 University, (EA 4203)

his actual research interest lies in improving the links between fundamental researches, clinical researches and clinical applications.



Csilla Gergely has received her Ph.D. in biophysics from Szeged University, Hungary in 1997. Currently, she is professor in the Charles Coulomb Laboratory of the Montpellier 2 University in France and head of the Bionanophotonics team. Her actual research interest lies in (i) elaborating adhesion peptides for selective bio-functionalization of photonic crystals for elaboration of

semiconductors based biosensing and (ii) developing various microscopic techniques (near-probe and multiphoton microscopy) for functional imaging and follow-up-therapy of cancerous cells.



Bernard Levallois received his doctorate in dentistry in 1986 and his Ph.D. in 1999. He is head of the Operative Dentistry and endodontic department of Montpellier hospital. His research interests are in endodontic, biomaterial and caries diagnostic. He is deputy director of Laboratoire Biologie Santé et nanoscience (EA4203) of Montpellier university.



Frédéric J. G. Cuisinier, professor in Dentistry, received is Ph.D. in 1989 at Strasbourg University under the direction of Pr. Robert Franck. He authored more than 90 papers in High Resolution Electron microscopy of mineralized tissues, in biomineralization, in biosensor and in multilayer film build-up. His current re-

searches concern confocal Raman microscopy of living cells, multiphotonic microscopy of dental tissue and biomaterial interactions with dental pulp stem cells.

References

- [1] A. Kölliker, *Éléments d'histologie humaine: Parties 1 à 5*. Paris: Masson; 1955.
- [2] M. B. Quigley, *J. Dent. Res.* **38**, 558–568 (1959).
- [3] C. P. Lin, W. H. Douglas, and S. L. Erlandsen, *J. Histochem. Cytochem.* **41**, 381–388 (1993).
- [4] J. Meyer, P. Bodier-Houllé, F. Cuisinier, H. Lesot, and J. V. Ruch, *In Vitro Cell. Dev. A* **35**, 159–168 (1999).
- [5] D. B. Scott and M. U. Nysten, *Ann. N.Y. Acad. Sci.* **85**, 133–144 (1960).
- [6] P. Bodier-Houllé, P. Steuer, J. Meyer, L. Bigeard, and F. Cuisinier, *Cell Tissue Res.* **301**, 389–395 (2000).
- [7] H. Fong, M. Sarikaya, S. White, and M. Snead, *Mat. Sci. Eng. C-Bio. S* **7**, 119–128 (2000).
- [8] H. Deyhle, O. Bunk, and B. Müller, *Nanomed-Nanotechnol.* **7**, 694–701 (2011).
- [9] W. Denk, J. Strickler, and W. Webb, *Science* **248**, 73–76 (1990).
- [10] W. Zipfel, R. Williams, R. Christie, A. Nikitin, B. Hyman, and W. Webb, *Proc. Nat. Acad. Sci. USA* **100**, 7075–7080 (2003).
- [11] I. Freund, M. Deutsch, and A. Sprecher, *Biophys. J.* **50**, 693–712 (1986).
- [12] R. Williams, W. Zipfel, and W. Webb, *Biophys. J.* **88**, 1377–1386 (2005).
- [13] M.-H. Chen, W.-L. Chen, Y. Sun, P. T. Fwu, and C.-Y. Dong, *J. Biomed. Opt.* **12**, 40181–40186 (2007).
- [14] J. M. Girkin, A. F. Hall, and S. L. Creanor. Multiphoton imaging of intact dental tissue, in: *Proceedings of the 4th Annual Indiana Conference*, G. K. Stookey, ed. (Indiana University School of Dentistry, Indianapolis, Indiana 1999), pp. 155–168.
- [15] A. Hall and M. Girkin, *J. Dent. Res.* **83**, 89–94 (2004).
- [16] P.-Y. Lin, H.-C. Lyu, C.-Y. S. Hsu, C.-S. Chang, and F.-J. Kao, *Biomed. Opt. Exp.* **2**, 149–158 (2010).
- [17] L. Bachmann, D. M. Zezell, A. da Costa Ribeiro, L. Gomes, and A. S. Ito, *Appl. Spectrosc. Rev.* **41**, 575–590 (2006).
- [18] U. Hafström-Björkman, F. Sundström, and J. J. Ten Bosch, *Acta. Odontol. Scand.* **49**, 133–138 (1991).
- [19] D. Spitzer and J. J. Ten Bosh, *Calcif. Tiss. Res.* **24**, 249–251 (1977).
- [20] R. Frank and P. Steuer, *Arch. Oral. Biol.* **33**, 91–98 (1988).
- [21] R. Frank, *Arch. Oral. Biol.* **1**, 29–32 (1959).
- [22] C. Raub, J. Unruh, V. Suresh, T. Krasieva, T. Lindmo, E. Gratton, B. Tromberg, and S. George, *Biophys. J.* **94**, 2361–2373 (2008).
- [23] M. Martin, G. Palestino, T. Cloitre, V. Agarwal, L. Zimányi, and C. Gergely, *Appl. Phys. Lett.* **94**, (2009).
- [24] G. R. Holland, *J. Anat.* **120**, 169–177 (1975).
- [25] R. M. Frank, *Arch. Oral. Biol.* **11**, 179–192 (1966).
- [26] M. Goldberg and M. Takagi, *Histochem. J.* **25**, 781–806 (1993).
- [27] J. Arends, I. Stikroos, W. Jongbloed, and J. Ruben, *Caries. Res.* **29**, 118–121 (1995).
- [28] L. Bertassoni, K. Stankoska, and M. Swain, *Micron.* **43**, 229–236 (2012).
- [29] L. Schroeder and R. Frank, *Cell Tissue Res.* **2**, 449–451 (1985).
- [30] G. W. Marshall, S. Marshall, J. Kinney, and M. Balooch, *J. Dent.* **25**, 441–458 (1997).
- [31] C.-Y. Chu, T.-C. Kuo, S.-F. Chang, Y.-C. Shyu, and C.-P. Lin, *J. Dent. Sci.* **5**, 14–20 (2010).
- [32] C. Pfeffer, B. Olsen, F. Ganikhanov, and F. Légaré, *J. Struct. Biol.* **164**, 140–145 (2008).
- [33] E. Johansen, *Ann. Ny Acad. Sci.* **131**, 776–785 (1965).
- [34] S. Habelitz, M. Balooch, S. Marshall, G. Balooch, and G. Marshall, *J. Struct. Biol.* **138**, 227–236 (2002).
- [35] E. F. Brès, D. Cherns, R. Vincent, and J.-P. Morniroli, *Acta. Cryst.* **B49**, 56–62 (1993).
- [36] R. Boyd (ed.), *Non linear Optics*: Academic press; 1992.
- [37] E. F. Brès, P. Steuer, J.-C. Voegel, R. M. Frank, and F. J. G. Cuisinier, *J. Microsc.* **170**, 147–154 (1993).
- [38] J. E. Eastoe, *Nature* **187**, 411–412 (1960).
- [39] S. V. Kalinin, B. J. Rodriguez, J. Shin, S. Jesse, V. Grichko, T. Thundat, A. Baddorf, and P. Gruverman, *Ultra-microscopy* **106**, 334–340 (2006).
- [40] M. L. Sinyaeva, A. A. Mamedo, S. Y. Vasilchenko, A. I. Volkova, and V. B. Loschenov, *Laser Phys.* **14**, 1132–1140 (2004).
- [41] D. Whittaker, *J. Anat.* **125**, 323–335 (1978).
- [42] D. Brauer, G. Marshall, and S. Marshall, *J. Dent.* **38**, 597–601 (2010).
- [43] S. Chen, C. S. Hsu, and C. Sun, *Opt. Express* **16**, 11670–11679 (2008).
- [44] I. L. Lyubchanskii, N. N. Dadoenkova, M. I. Lyubchanskii, T. Rasing, J. W. Jeong, and S. C. Shin, *Appl. Phys. Lett.* **76**, 1848–1850 (2000).
- [45] T. Zhao, H. Lu, F. Chen, G. Yang, and Z. Chen, *J. Appl. Phys.* **87**, 7448–7451 (2000).
- [46] S. M. D. L. Heras, A. Valenzuela, and C. Overall, *Arch. Oral. Biol.* **45**, 757–765 (2000).
- [47] L. Boushell, M. Kaku, Y. Mochida, R. Bagnell, and M. Yamauchi, *Arch. Oral. Biol.* **53**, 109–116 (2008).
- [48] E. Beniash, Z. Skobe, and J. Bartlett, *Eur. J. Oral. Sci.* **114**, 24–29 (2006).
- [49] M. Goldberg, D. Septier, K. Bourd, R. Hall, A. George, H. Goldberg, and S. Menashi, *Connect. Tissue Res.* **44**, 143–153 (2003).
- [50] P. C. Stoller, K. M. Reiser, P. M. Celliers, and A. M. Rubenchik, *Proc. SPIE* **4963** 41–51 (2003).
- [51] C. Xu, X. Yao, M. Walker, and Y. Wang, *Calcif. Tissue Int.* **84**, 221–228 (2009).
- [52] C. Lin, W. Douglas, and S. Erlandsen, *J. Hist. Cytochem.* **41**, 381–388 (1993).



Suivi orthodontique et concept LIFEDT

La fluorescence au service de la prophylaxie

Michel Blique, Hervé Tassery, Sophie Grosse, Jean-Marc Bondy

Les traitements orthodontiques fixes compliquent les mesures d'hygiène orale et, de ce fait, augmentent la susceptibilité à la carie de patients qui n'ont pas toujours le degré d'observance nécessaire. Selon les auteurs, la prévalence des lésions blanches durant ces traitements peut varier entre 2 % et 96 % [7]. Parce qu'ils favorisent la rétention des biofilms et l'inflammation gingivale, ils compliquent aussi le diagnostic et les traitements prophylactiques. À travers cette présentation de cas, nous voulons montrer comment une caméra à fluorescence peut aider à mieux prendre en charge ce type de patients.

1. Agé de 13 ans, le patient nous est adressé par son orthodontiste pour mise sous contrôle du risque carieux avant appareillage.

2. De nombreuses lésions initiales (ICDAS 1-3) sont enregistrées.

3. Aux soins prophylactiques conventionnels (ici contrôle de plaque à un mois) est associée la recherche des facteurs favorisant la carie.

4. Etanchéification des lésions et sillons par un CVI à fort taux de relargage de fluor.



Le patient nous est adressé à 13 ans, début 2008, par son orthodontiste, quelques semaines avant d'être appareillé, pour un bilan carieux individuel et la mise en place d'un traitement prophylactique. En effet, il présente de nombreuses lésions carieuses initiales non cavitaires ICDAS [10] 1 à 3 (fig. 1, 2).

Des traitements prophylactiques sont mis en place :

- conventionnels : gestion du risque alimentaire, techniques de brossage et contrôle de la plaque revus et vérifiés (fig. 3) (dentifrice Elmex protection carie® + brosse à dent électrique OralB Professional Care®) ;
- actifs [6] : Nettoyages Prophylactiques Professionnels des Surfaces Dentaires (NPPSD) [4], application de vernis fluorés (Fluor Protector® Vivadent®), étanchéification des sillons et zones de rétention de plaque au moyen de scellements réalisés en ciment verre ionomère à fort niveau de relargage de fluor (GC®Fuji Triage®) (fig. 4).

Après la pose des appareillages maxillaires, puis mandibulaire, le contrôle de plaque est systématiquement revu et adapté. Un NPPSD de maintien est réalisé chaque trimestre avec l'application de vernis fluoré au cabinet et prescription de cures d'un mois de CPP-ACP au domicile [16] (GC® ToothMousse®).

Des synthèses régulières sont faites tant auprès des parents que de l'orthodontiste, qui lui-même nous tient régulièrement informé des étapes du traitement et s'assure que le suivi cariologique est bien réalisé.

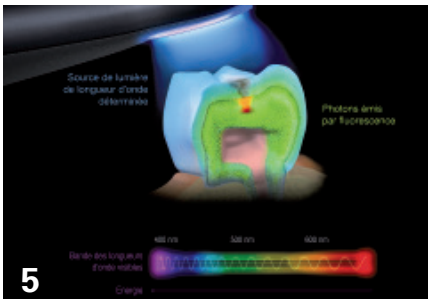
À partir de fin 2009, le diagnostic cariologique habituel est appuyé par le concept LIFEDT, utilisant une

Soprolife® qui génère une fluorescence blanchâtre pour l'émail déminéralisé [13] et rouge pour la dentine cariée [14] (fig. 5). Le dispositif alerte le praticien très précocement sur la présence de lésions de très petite taille (moins de 0,05 mm!), même non cavitaires, et aide à évaluer leur stade d'évolution. Les images en fluorescence recueillies permettent de différencier les tissus sains des tissus affectés ou infectés, déstructurés par la carie [5]. La Soprolife® est à la fois une caméra intrabuccale traditionnelle et un outil de diagnostic. Elle se connecte à un ordinateur (PC ou Macintosh) comportant un logiciel qui acquiert, stocke et gère les images. Un moniteur peut être installé devant le patient, lui permettant de suivre une partie de l'intervention et donnant au praticien l'accès aux images opératoires alors qu'il travaille.

Pendant les deux premières années, malgré des hauts et des bas dans le suivi et la motivation, un rythme de rendez-vous trimestriels est bien suivi. Le patient atteint sa 15e année, sans évolution des lésions carieuses traitées (fig. 7). Le diagnostic cariologique est réalisé avec l'aide de la caméra Soprolife® Acteon®. Le ciblage des traitements locaux s'en trouve facilité (NPPSD, fluoruration topique par vernis, traitements CPP-ACP à domicile) (fig. 6).

Durant l'hiver 2010, le patient doit faire face à des problèmes personnels qui viennent perturber le respect des rendez-vous, l'observance dans les traitements, la régularité et qualité du contrôle de plaque. En quelques mois, des lésions blanches apparaissent

Prophylaxie

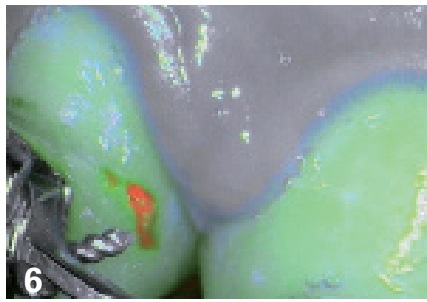


5

5. Principe de fonctionnement de la caméra Soprolife®, selon le concept LIFEDT.

6. La caméra permet de cibler les traitements prophylactiques, notamment au niveau des infiltrations sous la colle orthodontique (en rouge).

7. Le patient franchit le cap des deux ans de traitement orthodontique sans nouvelle lésion.



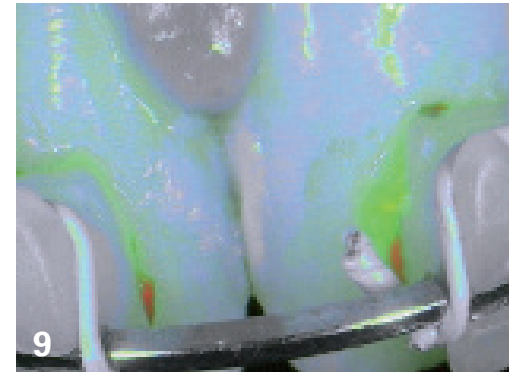
6



7



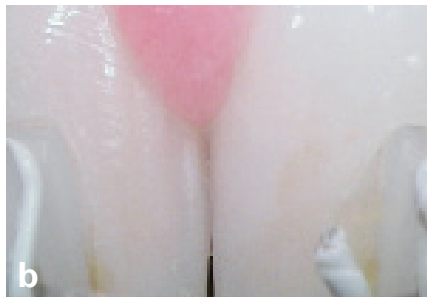
8



9



10a



b



c

8. Après deux années de suivi régulier, le patient (alors 15 ans) perd pied et ne suit plus les traitements régulièrement.

9. La caméra Soprolife® permet de mettre en évidence des lésions de carie interdentaires de l'émail (zone blanchâtre), difficiles à objectiver à l'œil nu tant pour le patient que pour le praticien.

10a. Après quelques mois de brossage et de soins préventifs actifs (verniss fluorés + CPP-ACP), une amélioration est déjà perceptible.

b. La vue en caméra Soprolife® en lumière du jour met en évidence l'excellent contrôle de plaque.

c. La fluorescence confirme la reminéralisation : émail apparaissant bleuté et dentine saine sous-jacente apparaissant en vert.

le long des verrous orthodontiques et au niveau des points de contact des incisives et canines (fig. 8).

L'utilisation de la caméra Soprolife® permet de mettre en évidence des lésions débutantes et de montrer au patient la dégradation des surfaces amélaire dans le temps (fig. 9). En effet, le logiciel SoproImaging rend possible la comparaison des images acquises successivement. De plus, la fluorescence permet de contrôler l'impact des traitements mécaniques et chimiques réalisés au cabinet et l'efficacité de ceux réalisés à la maison (dentifrices fluorés aux fluorures d'amines, dentifrice haute teneur, CPP-ACP) (fig. 10a). En quelques mois, le processus de déminéralisation semble stoppé et les lésions paraissent se reminéraliser (fig. 10a, b, c).

Huit mois plus tard, l'appareillage orthodontique est déposé et la situation paraît totalement sous contrôle (fig. 11, 12). À l'été 2011, soit dix mois plus tard, l'examen clinique confirme que



11

11. Après huit mois, l'appareillage orthodontique est déposé. Les surfaces sous-jacentes ont bien été préservées.



12

12. Vue après huit mois, la SoproLife® en fluorescence confirme la santé des tissus traités.

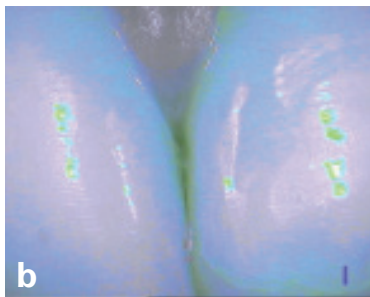


13a

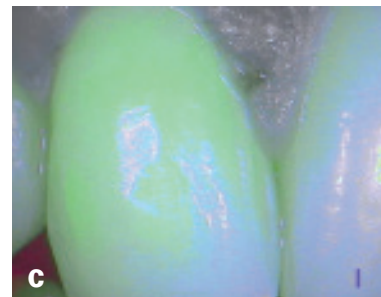
13a. Après quatre ans, le patient semble contrôler sa santé dentaire.

b. Vue en fluorescence de l'espace 11-21, la reminéralisation est confirmée.

c. Vue en fluorescence de l'espace 12-11.



b



c

le processus de guérison des lésions est une réalité confirmée par la fluorescence.

L'examen réalisé début 2012 confirme le succès clinique sans séquelles et la reprise en main de sa santé dentaire par le patient (fig. 13a, b, c).

Discussion

En termes de prophylaxie de la carie, ou de traitement non invasif des lésions, le diagnostic et la prise en charge précoces des lésions (cavitaires ou non) par des solutions thérapeutiques non invasives sont des points essentiels.

Encore faut-il pouvoir diagnostiquer les lésions dès les premiers stades, particulièrement dans le contexte des traitements orthodontiques où accumulation de biofilms autour des verrous et arcs, résines de collage et inflammations gingivales se conjuguent pour rendre difficile le diagnostic visuel et pour créer un environnement propice au maintien d'un pH bas [7].

Lorsque les lésions sont cavitaires et selon leur taille, la mise en œuvre de procédures restauratrices invasives reste nécessaire. Mais pour des lésions débutantes et sans cavitation, des solutions chimiques biologiques ou restauratrices non invasives permettent de restaurer l'intégralité de l'émail et/ou de la dentine lésés par reminéralisation [1].

Pour Basso [3], la « reminéralisation » attendue ne correspond pas à un véritable processus de régénération à l'identique, mais plutôt à une réparation globale du point de vue « macroscopique » (avec restauration de la résistance de l'émail et réduction de l'aspect crayeux); il serait peut-être plus juste de parler de « re-précipitation de minéraux » plutôt que de « reminéralisation ».

Comme dans le cas présenté ici, le phénomène peut être accéléré par des fluorures et/ou des solutions sursaturées de calcium et de phosphate bio-disponibles (CPP-ACP) [11] ainsi que par la modification de certains facteurs salivaires comme le pH

Prophylaxie

(alimentation et déstructuration du biofilm cariogène). Ceci semble permettre la réparation des tissus lésés lors du processus carieux [12]. Jusqu'à présent, ces processus étaient difficiles à mettre en évidence, tant pour réaliser le diagnostic des lésions que pour mettre en évidence l'impact positif des traitements et la reminéralisation des lésions.

Les choses ont changé depuis quelques années [2]. En effet, des dispositifs illuminant les tissus dentaires de façon à exploiter leurs propriétés de fluorescence ont été mis sur le marché pour améliorer la détection et le diagnostic de la carie. C'est cette possibilité qui a été utilisée pour contrôler l'évolution clinique, informer et sensibiliser notre jeune patient sur la nécessité de traiter de façon non invasive les lésions apparues.

Conclusion

La fluorescence peut aider à diagnostiquer tôt les lésions initiales dans le cadre d'un traitement orthodontique, à informer et faire prendre conscience au patient de la nécessité de modifier ses comportements à risque. Elle guide le praticien dans ses actes cliniques prophylactiques et thérapeutiques parfois difficiles à réaliser dans ce contexte de brackets et d'arcs. Elle lui permet de partager avec le patient le suivi de leur impact sur les tissus traités.

Remerciements

Les auteurs remercient les Docteurs Germain Becker et Catherine Boitard, orthodontistes à Luxembourg, pour leur amicale et efficace collaboration dans la gestion de nos cas.

bibliographie

1. Axelsson P. In: Preventive Materials, Methods and Programs, Vol. 4. Chicago: Quintessence Publishing Co, Inc, 2004.
2. Banerjee A, Yasser M, Munson M. A method for the detection and quantification of bacteria in human carious dentine using fluorescent in situ hybridization. *J Dent* 2002; 30: 359-363.
3. Basso M. Active preventive care and induced remineralisation *J Minim Interv Dent* May 2011; 4 (3): 61-64.
4. Blique M. Nettoyage Prophylactique Professionnel des Surfaces Dentaires. Aspects pratiques, 1re Partie et 2e Partie. *Information Dentaire* 1998, 19: 1335-1340 et 22: 1565-1569.
5. Blique M. La fluorescence pour développer une approche de dentisterie peu invasive *Dental Tribune France* novembre 2011; 3: 36-39.
6. Doméjean-Orliaguet S, Banerjee A, Gaucher C, Milétić I, Basso M, Reich E, Blique M, Zalba J, Lavoix L, Roussel F, Khandelwal P. Minimum Intervention Treatment Plan (MITP) – practical implementation in general dental practice. *J Minim Interv Dent* 2009; 2: 103-123.
7. Guzma 'n-Armstrong S, Chalmers J, Warren JJ. White spot lesions: prevention and treatment. *Am J Orthod Dentofacial Orthop* 2010; 138: 690-696.
8. Llana C, Forner L, Baca P. Anticariogenicity of casein phosphopeptide-amorphous calcium phosphate: a review of the literature. *J Contemp Dent Pract.* 2009 May 1; 10 (3): 1-9.
9. Mickenautsch S. Adopting minimum intervention in dentistry: diffusion, bias and the role of scientific évidence. *International Dentistry SA* January 2009; 11 (1): 16-26.
10. Pitts N. "ICDAS"-an international system for caries detection and assessment being developed to facilitate caries epidemiology, research and appropriate clinical management. *Community Dent Health* 2004; 21: 193-198.
11. Robertson MA and coll. MI Paste Plus to prevent demineralization in orthodontic patients: a prospective randomized controlled trial. *American Journal of Orthodontics and Dentofacial* 2011; 140 (5): 660-668.
12. Shen P, Manton DJ, Cochrane NJ, Walker GD, Yuan Y, Reynolds C, Reynolds EC. Effect of added calcium phosphate on enamel remineralization by fluoride in a randomized controlled in situ trial. *Journal of dentistry* 2011; 39: 518-525.
13. Terrer A and coll. A new concept in restorative dentistry: light-induced fluorescence evaluator for diagnosis and treatment: Part 1 – Diagnosis and treatment of initial occlusal caries. *The Journal of Contemporary Dental Practice* 2009; 10 (6): 1-12.
14. Terrer A and coll. A new concept in restorative dentistry: LIFEDT - Light-Induced Fluorescence Evaluator for Diagnosis and Treatment. Part 2 – Treatment of dental caries. *The Journal of Contemporary Dental Practice* 2010; 11 (1) 1-12.
15. Weisrock G, Terrer E, Couderc G, Koubi S, Levallois B, Manton D, Tassery H. Naturally aesthetic restorations and minimally invasive dentistry. *J Minim Interv Dent* 2011; 4 (2): 23-34.
16. Yengopal V, Mickenautsch S. Caries preventive effect of casein phosphopeptide-amorphous calcium phosphate (CPP-ACP): a meta-analysis. *Acta Odontol Scand* 2009 Aug (21): 1-12.

Auteurs

Michel Blique, attaché universitaire, Département d'Odontologie Pédiatrique, Faculté de Nancy

Hervé Tassery, PU-PH, responsable du Département d'Odontologie Restauratrice et Endodontie, Faculté de Marseille

Sophie Grosse, attachée universitaire, Département d'Odontologie Pédiatrique. Faculté de Nancy

Jean-Marc Bondy, pratique privée, Luxembourg

Correspondance

Michel Blique

michel.blique@online.fr

FULL ARTICLE

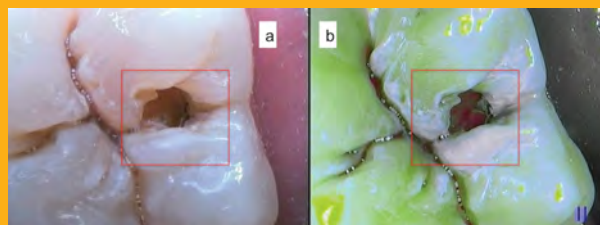
Functional mapping of human sound and carious enamel and dentin with Raman spectroscopy*Hamideh Salehi¹, Elodie Terrer², Ivan Panayotov¹, Bernard Levallois¹, Bruno Jacquot¹, Hervé Tassery^{*,1,2}, and Frédéric Cuisinier¹*¹ Laboratory of Biology and Nano-science, EA4203, Montpellier University 1, 545 av du Pr Viala, 34193 cedex 5, Montpellier, France² Aix-Marseille University, Preventive and Restorative Department of Marseille Dental faculty, 27 bd Jean Moulin, 13005, Marseille France

Received 24 May 2012, revised 22 July 2012, accepted 30 July 2012

Published online 20 September 2012

Key words: enamel and dentine caries, Maillard reaction, Raman spectroscopy, SoproLife[®]

The goals of this trial were, first, to produce a Raman mapping of decay and sound dentin samples, through accurate analysis of the Raman band spectra variations of mineral and organic components. The second goal was to confirm the correlation between the Raman signal and the signal of a fluorescent camera, by assaying the concentration of pentosidine and natural collagen fluorescent crosslink using reverse phase high-pressure liquid chromatography. The first correlation assumed a possible relationship between the signal observed with the camera and Raman spectroscopy. The second correlation assumed an association with the Maillard reaction. Absence of a correlation for this trial was that no association could be found be-



Dentin decay in daylight and fluorescence light.

tween Raman spectra characteristics, fluorescence variation and the HPLC assay. Our results void this absence.

1. Introduction

The dental caries process involves highly complex cell activities modification to synthesize tertiary (or sclerotic dentin depending on the caries activity [1–3]. Dental caries activity, i.e. active or arrested, greatly influences histology and color of the affected tissue [4, 5]. In daylight, dentine discoloration is a common indicator of caries, thus a soft, damp light-brown spot indicates ongoing decay, whereas a hard, shiny dark brown spot characterizes lesion arrestment. Besides extrinsic stains [6], the so-called browning reaction is one hypothesis. This reaction initiates a cascade known as the Maillard reaction, which ultimately

forms a brownish polymer, crosslinked proteins and AGEs (advanced glycation end products) whose pentosidine product [7]. The main component of the dentin organic matrix is the fibrous type-I collagen, a noncentrosymmetric structure, which like other intracellular molecules (NADH, FAD, aromatic amino acid) can generate, depending on the excitation wavelength, autofluorescence signals [8, 9].

An LED camera (SoproLife[®]) was developed (Sopro-Acteon Imaging in La Ciotat, France) with an excitation wavelength of around 450 nm [10, 11]. The fluorescence signals of the tooth are amplified selectively to increase the specificity of the fluorescence images. The autofluorescence emission wave-

* Corresponding author: e-mail: herve.tassery@numericable.fr; Phone: +33 6 86 46 56 99

Table 1 Wave number (in cm^{-1}) and band assignments of Raman spectra from normal dentin. (f): bands probably involved in the dentin fluorescence. (Modified data from Penel et al. [14].)

Wave number (in cm^{-1}) and band assignments of Raman spectra from sound enamel and dentine	Enamel (cm^{-1})	Dentin (cm^{-1})
ν_2 Phosphate (PO_4^{3-})	433	432
ν_4 Phosphate (PO_4^{3-})	(579–608)	(580–610)
ν_1 Phosphate (PO_4^{3-})	959	959
B type ν_1 Carbonate (CO_3^{2-})	1071	1069
A type ν_1 Carbonate (CO_3^{2-})	1103	1102
(NH) Amide III (f)		1243
(NH) Amide III nonpolar triple helix of collagen (f)		1275
CH (deformation)		1450
Amide I (C=O) (f)		1665
Nonreducible crosslink/reducible crosslink ratio (f)		1660/1690
C–H bending		2943
Ratio amide I/CH. Matrix (f)		1665/1450
Ratio amide III/CH. Matrix (f)		1243/1450
Ratio Carbonate/Phosphate. Mineral ratio	1070/959	1070/959
Ratio Phosphate/CH Matrix deformation		959/1450
Ratio Carbonate/CH Matrix deformation		1070/1450
Pentosidine (f)		1550
AGEs (f)		1550–1690
OH Stretch	3513	

length varies according to the density and chemical composition of the tissue on its surface and subsurface. The different tissue layers and their characteristics influence its response, the same as for material deposits [11]. As a result, any carious lesion or affected tissue will be detected by an autofluorescence variation in comparison to a sound part of the same tooth. Thus, the brown signal in daylight is perfectly superimposable over the SoproLife[®] dark red one. More precisely in active and arrested carious lesion, visual signals in fluorescent mode look different depending on the tissue structure. Healthy dentin always looks acid green in fluorescence, and the infected one appears green black. In active carious infected/affected dentin interface looks bright red fluorescence and yellow brown in daylight. Abnormal dentin at the end of excavation looks gray-green with sometimes a very slight pink transparency [11].

Several studies have already reported Raman spectra of tooth substances [12, 13]. In most of them, the data focus was on the most intense peak of tooth, which is the ν_1 phosphate (PO_4^{3-}) symmetric stretching vibrational mode at 960 cm^{-1} . But dental caries involves highly complex acid tissue destruction of organic (collagen, noncollagenic proteins) and mineral tissues, meaning that analysis should not be reduced to a phosphate band; furthermore, other phosphate bands have been previously described [14] (Table 1). The goals of this trial were, first, to produce a Raman mapping of decay and sound dentin samples, through accurate analysis of the Raman band spectra variations of mineral and organic com-

ponents. The second goal was to confirm the correlation between the Raman signal and the fluorescence signal of SoproLife[®] (red or not red), by assaying the concentration of pentosidine and natural collagen fluorescent crosslink using reverse-phase high-pressure liquid chromatography (HPLC). The null hypothesis would be true if there is an absence of a correlation between Raman spectra characteristics, fluorescence variation and the HPLC assay. Finding a correlation could increase the understanding of the diagnosis and treatment steps (e.g. endpoint of the dentin excavation) in restorative dentistry and lead to a better understanding of the caries process as a whole.

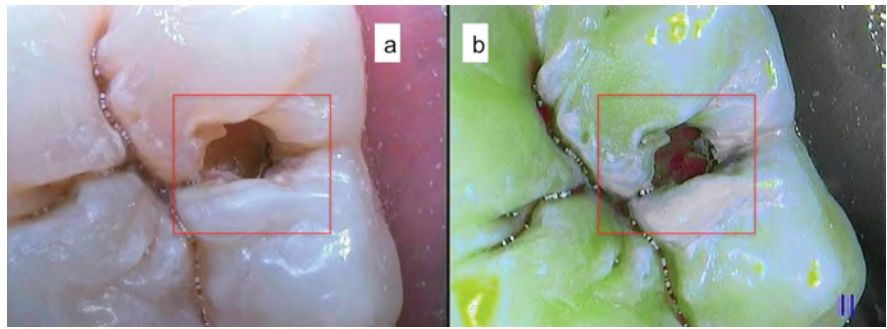
2. Experimental

2.1 SoproLife[®] data

The intraoral camera utilizes two series of LED camera that can illuminate tooth surfaces within the visible domain. This provides an anatomical image superimposed with autofluorescence. The camera is equipped with an image sensor (a 0.25-inch CCD sensor) consisting of a mosaic of pixels covered with filters of complementary colors. The data collected, relating to the energy received by each pixel, enable an image of the tooth to be retrieved.

The camera operates in three modes: 1 daylight and 2 fluorescence modes.

Figure 1 (online color at: www.biophotonics-journal.org) (a), (b) Occlusal caries observed with SoproLife[®] camera. (a) in daylight mode; (b) in treatment mode. A clinical superposition between the brown signal (a) and red fluorescent signal (b) is observed (inside the red rectangle).



- Daylight mode: 4 white-light LEDs generate daylight.
- Fluorescence modes: Diagnostic and treatment modes: For these two modes the light is provided by 4 blue LEDs (wavelength 450 nm with a bandwidth of 20 nm, centered at ± 10 nm around the excitation wavelength for the fluorescence); the difference between the two modes is due to different CCD settings. In this experimentation only the treatment mode was used.

The tooth sample was filmed with the SoproLife[®] camera, and the pictures stored in the Sopro imaging software (PNG file). The camera provides anatomical images (daylight mode) (Figure 1a) and fluorescent images in treatment mode (Figure 1b). The treatment mode is designed to increase the red part of the electromagnetic spectrum.

2.2 Micro-Raman microscopy

To investigate the chemical composition of the different enamel and dentin areas, Raman spectra (Table 1) were recorded at 298 K with a LabRAM ARAMIS IR² confocal micro-Raman spectrometer (Jobin-Yvon S.A., Horiba, France) equipped with an BX41 Olympus microscope, an 1800 grooves per mm grating and a CCD detector cooled by a Peltier effect module. The samples were mounted on an XYZ motorized stage with 0.1 μm step resolution. The microscope lens was a long working distance $\times 20$. The spectral resolution was $\pm 1 \text{ cm}^{-1}$. Raman spectra were obtained by excitation with 632.8 nm radiation from a He–Ne laser generating less than 12 mW on the samples. Due to fluorescence, the samples were under the laser for photobleaching for 10 min before spectral recording. The acquisition time was 90 s with 3 accumulations.

2.3 Spectra normalization

The obtained Raman spectra have different baselines for different intensities reflected from samples.

For comparison purposes, a fixed baseline was calculated using Peakfit v4.12 software (Systat Software, San Jose, CA 95110, USA). The baselines differed according to the data-linear, exponential and power fittings chosen. The Peakfit software automatically selected the best baseline. The Gaussian amplitude in the second derivative method was chosen for fitting the peaks [15]. In addition to the analysis of the main band assignments (Table 1), we also compared the intensities ratio (Table 4):

- Carbonate to phosphate ratio: The presence of a prominent carbonate band around 1070 cm^{-1} in the Raman spectrum is significant because it shows the degree of carbonate substitution in the lattice structure of the apatite. Raman measurements of carbonate-to-phosphate ratios can provide valuable insights into the chemical inorganic composition of dentin. For bone it varies with bone age, and mineral crystallinity [16, 17].
- Phosphate to CH_2 ratio (960 to 1450 cm^{-1}). The mineral to organic ratio was calculated as the ratio of the ν_1 phosphate band intensity (at 960 cm^{-1}) to the intensity of vibrations resulting primarily from the CH_2 wagging mode of collagen molecule side-chains (at 1450 cm^{-1}). This 1450 cm^{-1} band was chosen due to its low sensitivity to molecular orientation compared to the amide I band at 1670 cm^{-1} [18, 19].
- Carbonate to CH_2 ratio (1072 to 1450 cm^{-1}). The CO_3^{2-} at 1072 cm^{-1} to CH_2 wagging mode at 1450 cm^{-1} intensity ratios were calculated to measure the relative differences in the phosphate and carbonate [20].
- Amide III to CH_2 ratio (1243 to 1450 cm^{-1}). In dentin the intensity ratio of amide III to the CH_2 wagging mode indicates the structural differences. A higher ratio was noted in intertubular dentin than in peritubular dentin, indicating higher collagen content [21].
- Crosslink ratio (1660 to 1690 cm^{-1}). The collagen quality parameter used in Raman spectroscopy is derived from a subset of partially resolved amide I bands, whose relative intensities depend on its secondary structure. How-

ever, the theory supports the use of similar bands originally developed by bone infrared spectroscopy to assess nonreducible to reducible collagen crosslink ratios [22].

- Amide I to CH₂ ratio (1665 to 1450 cm⁻¹). An increase relative to the CH₂ band at 1240 cm⁻¹ of the amide I band at 1655 cm⁻¹ indicates altered collagen quality induced by aging [23], hydration/dehydration [24] or radiological damage [25].
- Amide III and I/AGEs ratios. We use these two ratios to get an overview of the glycation reaction versus collagen scaffolding.

2.4 Reverse-phase high-pressure liquid chromatography (HPLC)

Reverse-phase HPLC was chosen for the determination of the dentin pentosidine and natural fluorescent crosslink collagen content. Although recent studies using specific ELISA for pentosidine have given results comparable with those obtained using HPLC assay, the latter is a more accurate and acceptable method for measuring the total pentosidine content, because ELISA methods may not recognize pentosidine on the interior of proteins, and require chemical hydrolysis and enzymatic digestion of protein, which may alter the epitope recognized by the antibodies. In this study, HPLC was used as described originally by Odetti et al. [26] for assay of naturally fluorescent collagen bridging molecules [13]: Pyridinoline (PYD), Deoxypyridinoline (DPD), and assay of one of the main AGE products: pentosidine (PEN). Each dentin samples (approx. 1 g), from sound dentin and from a red fluorescent decay dentin were pulverized in a grinder in liquid nitrogen. Each sample was demineralized by a solution of 0.5 M EDTA 0.05 M in TRIS pH 7.4, for 72 h at 4 °C. The insoluble collagen fraction was separated from the dissolved mineral by centrifuging, and then washed thoroughly in ultra-pure water, and freeze-dried. The insoluble collagen in each sample was hydrolyzed in 6 M hydrochloric

acid for 20 h at 110 °C in a dry bath. Each hydrolyzate obtained will be pretreated on an SPE Chromabond Crosslinks column to concentrate the collagen bridging molecules and to eliminate the contaminating amino acids.

PYD, DPD and PEN were separated by a reverse-phase high-pressure liquid chromatography (HPLC) technique, and the collagen bridging molecules was be quantified by fluorimetry. The collagen contents of the dentin samples were estimated by reverse-phase HPLC assay of after precolumn derivatization and colorimetric detection. The concentrations of PYD, DPD and PEN are expressed in mmole/mole of collagen.

2.5 Specimen

Written consent was obtained prior to the extraction of 4 teeth at the University Hospital of Montpellier.

Two teeth presenting occlusal caries (caries codes 5 and 6, ICDAS, International Caries Assessment and Detection System) were included in the study.

The teeth were stored in 0.9% phosphate buffer saline (PBS) buffer solution (pH = 7.4) containing 0.002% sodium azide at 4 °C. Cross sections in the longitudinal axis of the freshly extracted teeth were taken by means of a low speed diamond saw (Isomet 1000, Buehler, Lake Bluff, USA), with a thickness up to 0.5 mm. The samples were ground to 0.25 mm, polished on carbide disks and polished with diamond pastes (6 μm, 1 μm and 0.25 μm) using a polishing machine (Escil, Lyon, France). 6 areas were determined: 1, sound enamel (SE); 2, enamel decay (ED); 3, Black fluorescence (no green or red signals) dentin decay (BFDD); 4, tertiary dentine, which faces the decay, looks red when clinically test in fluorescence mode with SoproLife® (TD); 5 sclerotic dentin, face the pulp horn (SCD); 6, sound dentin (SD) (Figure 2).

Two other samples of decayed dentin with red fluorescence when illuminated with SoproLife®, were collected in vivo from 2 different patients. Sam-

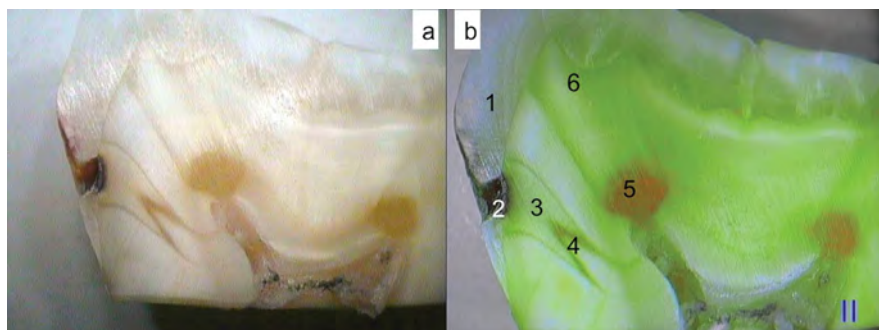


Figure 2 (online color at: www.biophotonics-journal.org) (a), (b) Mapping point of the Raman analysis in daylight (1) and fluorescent mode (2): 1, sound enamel; 2, carious enamel; 3, dark fluorescent dentin decay; 4, tertiary dentin; 5, sclerotic dentin; 6, sound dentin.

Table 2 HPLC results between sound and red fluorescent dentin.

Dentin samples	Fluorescent collagen crosslinks		Maillard products
	Pyridinoline (PYD) mmol/mol collagen	Desoxypyridinoline (DPY) mmol/mol collagen	Pentosidine (PEN) mmol/mol collagen
Sound dentin	455	97	8.3
Red fluorescent dentin	490	87	16

ples were conserved at 4 °C and analyzed the day following. To avoid saliva and blood contamination, a dental dam was fitted and decayed samples were collected with a sterile hand excavator from the carious tooth.

3. Results and discussion

3.1 SoproLife® result

In clinical conditions the carious dentine sample looks brown in daylight (Figure 1a), and red in fluorescence mode (Figure 1b). In daylight the sound dentin of a tooth slice sample looks pale yellow and green in fluorescence, whereas sound enamel looks white and blue, respectively. The dentin decay area looks dark in daylight, and dark with a red shadow in fluorescence (Figures 2a and b).

3.2 HPLC results

Figure 3 shows a caries selected for HPLC analysis. Concentrations of physiological fluorescent collagen crosslink (PYD and DPY products) from sound and red fluorescent dentin decay were similar. The Maillard reaction product (PEN, pentosidine) had a near-twofold objective increase from sound sample to decay dentin (8.3 to 16 mmol/mol collagen). The concentration of pentosidine in sound dentin was noteworthy.

3.3 Confocal Raman microscopy results

Areas of interest were selected after imaging the caries with the SoproLife® (Figure 4a). An optical image (Figure 4b) was registered of the orange rectangle area, see Figure 4a, before using the confocal



Figure 3 (online color at: www.biophotonics-journal.org) (a) Distal groove of second upper molar ICDAS code 4/5 on daylight mode. (b) Opening of the distal groove. Caries appearing yellow-brown in daylight on daylight mode. (c) Active caries appearing red in fluorescence mode.

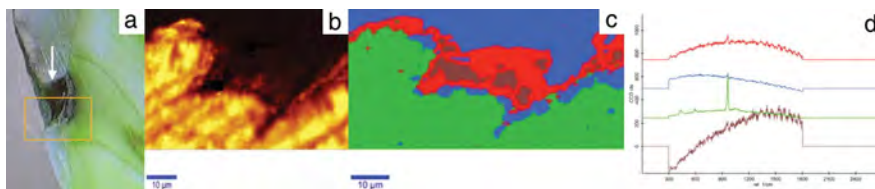


Figure 4 (online color at: www.biophotonics-journal.org) (a) Border between sound and enamel decay in fluorescence mode. White arrow: enamel decay. Orange rectangle area: Raman measured surface. (b) Optical microscope image of the enamel border $\times 20$ in the orange rectangle area, Figure 4a. (c) Colored map of the different mineral intensities based on Figure 4b: green, sound enamel; Red, blue and brown: carious enamel border. (d) ν_1 , ν_2 , ν_4 PO_4^{3-} peak vibrations in the red, blue, green and brown enamel areas.

Raman microscope and acquired Raman spectra. Spectral images of the sound and decay enamel border involving the phosphate and carbonate peaks (Figures 4a–d).

Spectra of the green area (sound enamel) showed clear vibrations around ν_2 PO_4^{3-} (433 cm^{-1}), ν_2 (579 cm^{-1} to 608 cm^{-1}), ν_1 PO_4^{3-} (959 cm^{-1}) and $\nu_1\text{CO}_3^{2-}$ (B type 1071 cm^{-1} and A type 1103 cm^{-1}). The value of ν_1 PO_4^{3-} was around 10 times higher than the other mineral vibrations. The shape of the transition border between the sound (green) and decay areas (blue, red and brown) was rough, but contrasted in terms of vibration drops. The brown decay fragment inside the red area showed a high level of fluorescent signal masking the main vibrational bands. The blue and red fragments maintained a weak peak of ν_1 PO_4^{3-} (959 cm^{-1}) vibration. The other spectra were not visible, being masked due to the high level of inner fluorescence. (Figures 4a–d).

3.3.1 Bands from 300 to 3600 cm^{-1} for decayed enamel (area 2) and dark fluorescent decayed dentin (area 3)

The high level of the fluorescence signal in these 2 areas masked the specific vibrations, even for the mineral and organic part. The values were not objectively measurable even with a long-time bleaching effect. Both spectra shapes looked very similar.

3.3.2 Band vibrations from 300 to 1700 cm^{-1} (areas 1, 4, 5, 6, red dentine decay) (Figure 5)

This vibration range concerns all the major inorganic and organic bands.

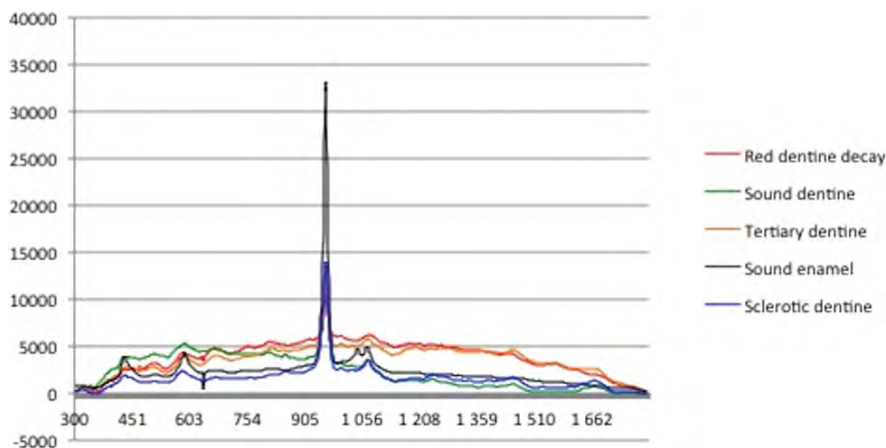


Figure 5 (online color at: www.biophotonics-journal.org) Representative normalized Raman spectra from 300 to 1700 cm^{-1} of sound, red, tertiary, sclerotic dentin and sound enamel.

3.3.2.1 Phosphate bands from 300 to 959 cm^{-1} (Table 3)

In the sound enamel the intensity ratio between ν_2 , ν_4 PO_4^{3-} and ν_1 PO_4^{3-} was around 10. In the dentine ν_1 PO_4^{3-} vibrations were relatively stable, while the red dentin value was the lowest. ν_2 and ν_4 PO_4^{3-} in the tertiary dentin and red dentin were similar, whereas the sound dentin exhibited the highest value and the sclerotic dentin (area 6) the lowest for both vibrations.

3.3.2.2 Carbonate bands from 1069 to 1103 cm^{-1}

Variations of carbonate bands (A and B type $\nu_1\text{CO}_3^{2-}$) were around 2 times higher in the red dentin and tertiary dentin. Carbonate bands intensities of sound and sclerotic dentins are almost similar.

3.3.2.3 Pentosidine and AGE bands

The signal of the pentosidine bands, even low ones (blue arrow, Figure 5) were clearly higher in the red dentin decay and tertiary dentin, around 10 times the sound dentin value (Table 3). Sclerotic dentin also exhibited an increase in Pentosidine and AGEs but to a lesser extent. For AGEs the band values increased about three- or four-fold in the red dentin and tertiary dentin.

3.3.2.4 Organic and amide vibrations

For both amide III vibrations (1243 and 1275 cm^{-1}), tertiary dentin and red fluorescent dentin values were close, and higher than for the sclerotic and

Table 3 Normalized dentin intensity spectra: SE, sound enamel; TD, tertiary dentin; SCD, sclerotic dentin; SD, sound dentin; RFD, red fluorescent dentin. (*lowest value, **highest value).

Wave numbers (cm ⁻¹)	1, SE	4, TD	5, SCD	6, SD	7, RFD
Band assignments ≈ wave number (in cm ⁻¹)	SE	TD	SCD	SD	RFD
ν_2 Phosphate (PO ₄ ³⁻) Enamel ≈ 433	3781				
ν_2 Phosphate (PO ₄ ³⁻) Dentin ≈ 432		830	1945*	3944**	2697
ν_4 Phosphate (PO ₄ ³⁻) Enamel ≈ 579–608	3572				
ν_4 Phosphate (PO ₄ ³⁻) Dentin ≈ 580–610		3336	1747*	4804**	3914
ν_1 Phosphate (PO ₄ ³⁻) Enamel ≈ 959	33193				
ν_1 Phosphate (PO ₄ ³⁻) Dentin ≈ 959		12931	13925**	12733	10475*
B type ν_1 Carbonate (CO ₃ ²⁻) Enamel ≈ 1071	4975				
A type ν_1 Carbonate (CO ₃ ²⁻) Enamel ≈ 1103	2809				
B type ν_1 Carbonate (CO ₃ ²⁻) Dentin ≈ 1069		5784	3612	3548*	6160**
A type ν_1 Carbonate (CO ₃ ²⁻) Dentin ≈ 1102		4803	2107*	2142	5507**
(NH) Amide III (f) Dentine ≈ 1243		4829	1945	1500*	5191**
(NH) Amide III nonpolar triple helix of collagen (f) Dentin ≈ 1275		4816	1797	1239*	4864**
CH (deformation) Dentin ≈ 1450		4655**	1684	1043*	4200
Amide I (C=O) (f) Dentin ≈ 1665		2641**	1408	772*	1993
C–H wagging ≈ 2948	191	2342	3148**	2465	370*
O–H wagging ≈ 2998	164	799	932**	863	252*
Pentosidine (f) Dentin ≈ 1550		3213	651	233*	3168**
AGEs (f) Dentin ≈ 1550–1690		2145**	976	509*	1725
OH Stretch Enamel ≈ 3513	24				

sound dentin. The results were similar in the amide I, CH₂ (1450 cm⁻¹ wagging) bands, while red fluorescent dentin revealed the lowest values for C–H and O–H wagging (2948 and 2998 cm⁻¹), while sclerotic dentine had the highest.

3.3.2.5 Band intensity ratio results (Table 4)

Band intensity ratio values confirmed the similarity of the tertiary dentin and red fluorescent dentin groups. Mineral ratios confirmed an increase in carbonate vibrations in the same 2 groups, while the or-

ganic ratio (amide I/CH₂, amide III/CH₂) decreased. Sound dentin exhibited the highest value of ratio amide I & III/pentosidine, and the specific ratios involving pentosidine followed the same variation as tertiary and fluorescent dentin, due to the huge rise in the pentosidine signal. The crosslink ratios were similar.

For the analysis of Maillard reaction-related amino acids and crosslinks in collagen, ion-exchange HPLC was performed. This method is advantageous in requiring no prior clean-up of samples, enabling more reliable results. The reverse-phase HPLC results agreed with the work of Kleter et al. [13], showing an increase in the fluorescent pentosidine amino

Table 4 Normalized dentin ratio intensities spectra: TD, tertiary dentin; SCD, sclerotic dentin; SD, sound dentin; RFD, red fluorescent dentin. (*Lowest value, **highest value).

Wave number (in cm ⁻¹) and band assignments of Raman spectra from sound enamel and dentin.	TD	SCD	SD	RFD
Amide I/CH ₂ matrix wagging ratio (f) 1665/1450	0.5	0.8**	0.7	0.4*
Amide III/CH ₂ matrix wagging ratio (f) 1243/1450	1.03*	1.15	1.4**	1.2
Carbonate/Phosphate ratio 1070/960	0.4	0.2*	0.2*	0.5**
Phosphate/CH ₂ matrix wagging ratio 960/1450	2.7	8.2	12.2**	2.4*
Carbonate/CH ₂ matrix wagging ratio 1070/1450	1.2*	2.1	3.4**	1.4
Amide III/Pentosidine ratio 1243/1550	1.5*	2.9	6.4**	1.6
Amide I/Pentosidine ratio 1665/1550	0.8	2.1	3.1**	0.6*
Nonreducible crosslink/reducible crosslink ratio (f) 1660/1690	1.2	1.3**	1.3**	1.1*

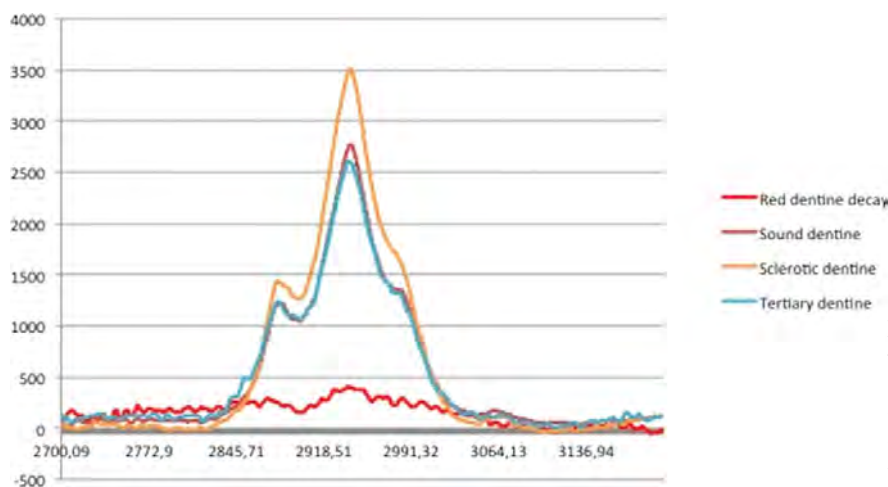


Figure 6 (online color at: www.biophotonics-journal.org) Representative normalized Raman spectra from 2700 to 3300 cm^{-1} of sound, red, tertiary, sclerotic dentin.

acids and AGEs during the caries process. In our trial the HPLC and Raman results both showed an increase in pentosidine but, unexpectedly, a relative stability of the fluorescent crosslink (pyridinoline and desoxypyridinoline) between sound and carious dentine. The same reduction was previously observed by Kleter et al. [13], which concluded that two opposite reactions probably occur in caries: a decrease in physiological crosslinks, and the formation of new crosslinks in the advanced stages of the Maillard reaction.

The SoproLife[®] wavelength of around 450 nm was close to the excitation/emission pairs of post-translational as well as chemical and/or age-related fluorophores [27]. Illuminated with the fluorescent camera, sound dentin appeared acid-green, while the appearance was black-gray-green in the case of highly infected dentin tissue, bright red in affected active caries and dark red in arrested caries [11]. Destruction of the 3D noncentrosymmetric collagen structure, accumulation of pentosidine, AGE products and new crosslink formation during the carious process modified the 3-dimensional supramolecular collagen scaffolding, causing a palpable effect on the fluorescence spectra and temperature dependence of collagen-bound fluorophores [28]. Nevertheless, to some extent the collagen dentinal network remains practically unaffected in the early stage, when analyzed with synchrotron-based X-ray scattering [29], though collagen fluorescence seemed to show a binary response: yes or no. In fact even in the early stage of decay, the fluorescence signal of the dentin illuminated with SoproLife[®] is modified: loss of green and appearance of red signal.

Collagen fibers are highly integrated in the mineral structure, and calcium phosphates structure the collagen fiber, which loses its fluorescence beyond a demineralization threshold. Energy transfer (FRET) had already been demonstrated between bone collagen and synthetic hydroxyapatite [30],

which could also reveal for dentin the existence of true molecular interactions between collagen and mineral structures. The carbonate/phosphate ratio showed an increase in carbonate (A and B type) vibrations during the caries process with a relative stability of phosphate vibrations in dentin. Intensity values in these particular bands of tertiary and decayed dentin with red fluorescence were also similar. It should be noted that sclerotic dentin exhibited the lowest intensity values for ν_2 and ν_4 PO_4^{3-} bands, whereas sound dentin normally exhibited the highest values. The mineral/organic ratio confirmed the matrix disorganization in the decay groups, which, combined with the carbonate mineral modification, certainly influenced the fluorescence signal.

Concerning the organic structure the main observation was the amide III vibrations released thanks to the demineralization in the decayed dentin with red fluorescence and tertiary dentin group. A previous study by Bonifacio and Sergio [31] argued that the intensity ratio of the amide III band is clearly a marker of the orientation of collagen supramolecular structure [28]. This partial loss of order in fibrils orientation (aging, caries) influenced the fluorescence signal, thus providing certain information about the spatial arrangement of collagen structures within tissues and the fluorescence [32–34]. Concerning the organic structures amide I and CH_2 : caries denaturation and modification of the matrix collagen were also confirmed by a vibration release for these respective bands. The amide I/matrix CH_2 ratio, gave the lowest values in the two carious groups, which greatly influenced their respective ratios.

The vibration bands around 2940 cm^{-1} were related to the CH_2 , CH_3 stretching mode from the amino acid side chains of proteins. The dentin included much more collagen type I protein than noncollagen protein (e.g. Sibling proteins). The denaturation of this specific protein structure indicated by these par-

ticular vibrations was remarkable in the decayed dentin with red fluorescence. On the other hand, nonreducible and reducible crosslinks clearly increased in the decayed dentin with red fluorescence and tertiary dentin, compared to sound and sclerotic dentin, but the crosslink ratio 1660/1690, which provided information on the collagen quality [35], remained stable whatever the dentin sample, meaning that the intrinsic strength of the collagen persists in these specific samples. The HLPC assay and crosslink ratio of sound dentine versus red decayed dentin (PY and DPY) confirm the high resistance level of the molecular conformation of collagen, especially in the case of mild decay [29].

In our trial, the intensity bands of AGEs and pentosidine increased greatly (Table 3) in red dentin decay, but in the black area (area 3, Figure 2b) the autofluorescence totally masked these specific vibrations. Increases of pentosidine concentrations in the dentin were confirmed by HPLC experimentation. Fluorescence spectra of dental hard tissues vary due to alterations in the chemical composition of pathological areas and in the optical properties [36–41]. Previous analysis of the color intensity variations in the red-green-blue (RGB) space (free software ImageJ, image processing and analysis in Java) of sound and dentin decay samples described a huge drop of the green signal in the dentin caries, and a slight increase of the red signal, giving an average red signal in the caries sample [11]. Using laser-induced fluorescence spectroscopy (LIF) with a 360–1000 nm wavelength range, Thomas et al. [36] confirmed a reduction of the overall fluorescence intensity in the caries lesion, which is always less bright than the sound dentin [10, 11]. The mean LIF spectra, normalized at 500 nm, close to the 450 nm of the SoproLife[®], exhibited an increased fluorescence spectral intensity in the red wavelength region, clinically visible.

Concerning the involvement of endogenous porphyrins (protoporphyrin IX, mesoporphyrin and coproporphyrin in bacteria) in the red signal retrieved with the SoproLife[®], it seems to depend on the bacteria species; the excited wavelengths were around 404 nm and 620–635 nm [36]. However, *Streptococcus mutans* and *lactobacilli* [42–45] seemed to have a weaker or no porphyrin fluorescence in the red wavelength region. The red signal certainly involved the Maillard product [46–48] and in part the bacteria species, which formed a highly complex ecosystem, depending on the activity and depth of decay, with variable excitation wavelengths.

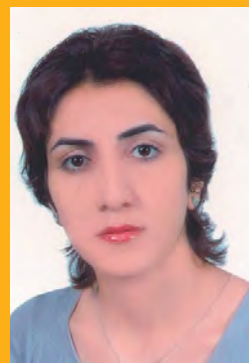
4. Conclusion

Regarding the work hypotheses, the first correlation assumed a possible relationship between the signal

observed with SoproLife[®] and Raman spectroscopy. This correlation is positive, indeed there is a close relationship between the Raman spectra variations in the organic and mineral phases, and the variation in the observations visible with SoproLife[®] (red fluorescence). There are two clearly differing groups, the first involved in the caries process (tertiary dentin and red dentin), and the second comprising sound dentin and sclerotic dentin. The second correlation assumed an association with the Maillard reaction. This second point is positive, since not only is there perfect superimposition, with SoproLife[®], between the red fluorescence and the browning reaction, but everything is correlated in Raman spectra by intensity variations specific to the carious group in the AGEs and pentosidine bands, typical of the Maillard reaction. Our results provide new data on the origin of fluorescence variation of dental caries observed with the SoproLife[®] camera. Absence of a correlation for this trial was that no association could be found between Raman spectra characteristics, fluorescence variation and the HPLC assay. Our results void this absence. Parameters such as the presence of bacterial metabolisms should be evaluated in the future, as it is clear that destruction of dentin during caries is a complex biological process.

Acknowledgements We gratefully acknowledge the contribution of Didier Bourgogne to this article, for the helpful discussions on Raman modes.

Conflict of interest No potential conflicts of interest could be identified for any of the authors.



Hamideh Salehi is a Ph.D. student in the EA4203 Laboratory of Biology and Nano-science, Université Montpellier 1. She obtained a B.Sc. in Atomic and Molecular Physics – Laser and Fiber Optics in 2001 and an MSc in Solid State Physics on “Development of software for designing photonic crystals with certain properties” in 2004 in Teheran. She obtained a second MSc

on “Shape Memory Polymers” at ParisTech, France, in 2010.



Elodie Terror graduated from Marseille University (France) Dental School in 2008. In 2007, she joined the laboratory of AFMB (Architectures and Functions of Macromolecules Biologies, UMR 6098, CNRS). She maintained a private practice around Cosmetic Dentistry and Endodontology in Aix en Provence until 2009. In 2010, she got a Hospitalo-Universitary Assistant post

to the Marseille Dental Faculty, in charge of Pathologic Anatomy and Preventive-Restorative Odontology. Her current research interests concern the relationship between Raman spectroscopy, the fluorescent intraoral camera (the SoproLife® camera) and the involvement of the Maillard reaction in the fluorescence variations.



Ivan Vladislavov Panayotov, doctor of dentistry, received his Master of Sciences, Technologies and Health in 2009 at Montpellier 1 University (France). Currently, he is a PhD student in EA4203 Laboratory of Nano-science

and assistant professor in endodontic. His research interests are in the functionalization of biomaterials with polyelectrolyte multilayers and specific peptides for medical applications and in the development of new technologies to detected structural changes in mineralized tooth tissues.



Bernard Levallois received his doctorate in dentistry in 1986 and his Ph.D. in 1999. He is head of the Operative Dentistry and Endodontic Department of Montpellier hospital. His research interests are in endodontic, biomaterial and caries diagnostic. He is deputy director of the Laboratoire Biologie Santé et Nanoscience (EA4203) of Montpellier University.



Bruno Jacquot graduated from Nancy University (France) Dental School in 1978. He maintained a private practice around cosmetic dentistry in Nancy until 2002. In 1996 he joined the Dental Faculty of Nancy as a Part-time Senior Lecturer. In 2006, he moved to Montpellier Dental Faculty, in charge of Dental Biomaterials Science. His current

research interests concern the relationship between tooth and dental biomaterials by Raman spectroscopy and multiphoton microscopy.



Hervé Tassery received his Ph.D. in biomaterials from Aix-Marseille University 2001. Currently, he is professor and head of the Department of Restorative Dentistry of Marseille Dental School at Aix-Marseille University. His major fields of interest are in cariology, fluorescence devices, minimally invasive dentistry and clinical researches. Working in the Laboratory of Bionanotechnology of Montpellier 1 University, (EA 4203) his actual

research interest lies in improving the links between fundamental studies, clinical studies and clinical applications.



Frédéric J. G. Cuisinier, professor in Dentistry, received his PhD in 1989 at Strasbourg University under the direction of Pr. Robert Franck. He has authored more than 90 papers in high-resolution electron microscopy of mineralized tissues, in biomineralization, in biosensors and in multi-layer film build-up. His current

researches concern confocal Raman microscopy of living cells, multiphotonic microscopy of dental tissue and biomaterial interactions with dental pulp stem cells.

References

- [1] I. A. Mjör, *Quintessence Int.* **32**, 771–788 (2001).
- [2] L. Bjørndal and I. A. Mjör, *Quintessence Int.* **32**, 717–736 (2001).
- [3] K. J. Heyeraas, O. B. Sveen, and I. A. Mjör, *Quintessence Int.* **32**, 611–625 (2001).
- [4] I. A. Mjör, *Quintessence Int.* **33**, 113–135 (2002).
- [5] I. A. Mjör and M. Ferrari, *Quintessence Int.* **33**, 35–63 (2002).
- [6] A. Banerjee, T. F. Watson, and E. A. M. Kidd, *Dent. Update* **27**, 272–276 (2000).
- [7] D. R. Sell and V. M. Monnier, *J. Biol. Chem.* **264**, 21597–21602 (1989).
- [8] A. Zoumi, A. Yeh, and B. J. Tromberg, *Proc. Natl. Acad. Sci.* **99**, 11014–1101 (2002).
- [9] L. Bachmann, D. M. Zezell, A. da Costa Ribeiro, L. Gomes, and A. S. Ito, *Appl. Spectrosc. Rev.* **41**, 575–590 (2006).
- [10] E. Terrer, C. Sarraquigne, S. Koubi, G. Weisrock, A. Mazuir, and H. Tassery, *Dent. Pract.* **10**, 86–94 (2009).
- [11] E. Terrer, C. Sarraquigne, S. Koubi, G. Weisrock, A. Mazuir, and H. Tassery, *J. Contemp. Dent. Pract.* **11**, 95–102 (2010).
- [12] H. Kinoshita, N. Miyoshi, Y. Fukunaga, T. Ogawa, T. Ogasawara, and K. Sano, *J. Raman. Spectrosc.* **39**, 655–660 (2008).
- [13] G. A. Kleter, J. J. M. Damen, M. J. Buijs, and J. M. Ten Cate, *J. Dent. Res.* **77**, 488–495 (1998).
- [14] G. Penel, C. Delfosse, M. Descamps, and G. Leroy, *Bone* **36**, 893–901 (2005).
- [15] J. R. Beattie, J. V. Glenn, M. E. Boulton, A. W. Stitt, and J. J. McGarvey, *J. Raman Spectrosc.* **40**, 429–435 (2009).
- [16] R. Legros, N. Balmain, and G. Bonel, *Calcif. Tissue Int.* **41**, 137–144 (1987).
- [17] J. S. Yerramshetty, C. Lind, and O. Akkus, *Bone* **39**, 1236–1243 (2006).
- [18] G. Falgayrac, S. Facq, G. Leroy, B. Cortet, and G. Penel, *Appl. Spectrosc.* **64**, 775–780 (2010).
- [19] S. Gamsjaeger, A. Masic, P. Roschger, M. Kazanci, J. W. C. Dunlop, K. Klaushofer, E. P. Paschalis, and P. Fratzl, *Bone* **47**, 392–399 (2010).
- [20] Karan, X. Yao, C. Xu, and Y. Wang, *Dent. Mater.* **25**, 1205–1212 (2009).
- [21] C. Xu and Y. Wang, *Arch. Oral Biol.* **11** [Epub ahead of print] (2011).
- [22] E. P. Paschalis, K. Verdelis, S. B. Doty, A. L. Boskey, R. Mendelsohn, and M. Yamauchi, *J. Bone Miner. Res.* **16**, 1821–1828 (2001).
- [23] J. W. Ager, R. K. Nalla, K. L. Breeden, and R. O. Ritchie, *J. Biomed. Opt.* **10**, 034012 (2005).
- [24] J. W. Ager, R. K. Nalla, G. Balooch, G. Kim, M. Pugach, S. Habelitz, G. W. Marshall, J. H. Kinney, and R. O. Ritchie, *J. Bone Miner. Res.* **21**, 1879–1887 (2006).
- [25] H. D. Barth, M. E. Launey, A. A. MacDowell, J. W. Ager, and R. O. Ritchie, *Bone* **46**, 1475–1485 (2010).
- [26] P. Odetti, I. Aragno, S. Garibaldi, S. Valentini, M. A. Pronzato, and R. Rolandi, *Gerontology* **44**, 187–191 (1998).
- [27] V. M. Monnier, R. R. Kohon, and A. Cerami, *Proc. Natl. Acad. Sci. USA* **81**, 583–587 (1984).
- [28] J. M. Menter, *Photochem. Photobiol. Sci.* **5**, 403–410 (2006).
- [29] H. Deyle, O. Bunk, and B. Müller, *Nanomedicine* **7**, 694–701 (2011).
- [30] H. Bazin, M. Paudat, E. Trinquet, and G. Mathis, *Spectrochim. Acta A* **57**, 2197–2211 (2001).
- [31] A. Bonifacio and V. Sergo, *Vib. Spectrosc.* **53**, 314–317 (2010).
- [32] X. U. Changqi, K. Karan, X. Yao, and Y. Wang, *J. Raman. Spectrosc.* **40**, 1780–1785 (2009).
- [33] M. D. Morris and S. M. Gurjit, *Clin. Orthop. Relat. Res.* **38**, 1607–1617 (2010).
- [34] D. A. Shea and M. D. Morris, *Appl. Spectrosc.* **56**, 182–186 (2002).
- [35] J. M. Wallace, K. Golcuk, M. D. Morris, and D. H. Kohn, *Ann. Biomed. Eng.* **38**, 1607–1617 (2010).
- [36] S. S. Thomas, J. L. Jayanthi, N. Subhash, J. Thomas, R. J. Mallia, and G. N. Aparna, *Lasers Med. Sci.* **26**, 299–305 (2011).
- [37] S. Al-Khateeb, R. A. M. Exterkate, E. D. de Jong, B. Angmar-Mansson, and J. M. ten Cate, *Caries Res.* **36**, 25–30 (2002).
- [38] A. Banerjee, M. Yasseri, and M. Munson, *J. Dent.* **30**, 359–363 (2002).
- [39] K. Koenig and H. J. Schneckenburger, *Fluorescence* **4**, 17–40 (1994).
- [40] H. Tsuda, J. Ruben, and J. Arends, *Eur. J. Oral Sci.* **1042**, 123–131 (1996).
- [41] A. Hall and J. M. Girkin, *J. Dent. Res.* **83** (Special Issue C), C89–C94 (2004).
- [42] A. Banerjee, A. Gilmour, E. Kidd, and T. Watson, *J. Dent.* **17**, 253–256 (2004).
- [43] L. Coulthwaite, I. A. Pretty, P. W. Smith, S. M. Higham, and J. Verran, *Caries Res.* **40**, 112–116 (2006).
- [44] A. M. Lennon, W. Buchalla, L. Brune, O. Zimmermann, U. Gross, and T. Attin, *Caries Res.* **40**, 2–5 (2006).
- [45] Y. Shigetani, S. Takenaka, A. Okamoto, N. Abu-Bakr, M. Iwaku, and T. Okiji, *Odontology* **96**, 21–25 (2008).
- [46] R. L. Klein, M. Laimins, and M. F. Lopes-Virelle, *Diabetes* **94**, 1093–1098 (1995).
- [47] T. Miyata, S. Taneda, R. Kawais, Y. Ueda, S. Horiihii, M. Hara, K. Maeda, and V. M. Monnier, *Proc. Natl. Acad. Sci.* **93**, 2353–2358 (1996).
- [48] A. M. Pawlak, J. V. Glenn, J. R. Beattie, J. J. McGarvey, and A. W. Stitt, *Ann. NY Acad. Sci.* **1126**, 59–65 (2008).

Use of new minimum intervention dentistry technologies in caries management

H Tassery,*† B Levallois,* E Terrer,*† DJ Manton,‡ M Otsuki,§ S Koubi,† N Gugnani,¶
I Panayotov,* B Jacquot,* F Cuisinier,* P Rechmann**

*UFR Odontologie, Université Montpellier 1, LBN 4203, Montpellier Cedex, France.

†UFR Odontologie Marseille, Preventive and Restorative Department, Aix-Marseille-Université, Marseille Cedex, France.

‡Elsdon Storey Chair of Child Dental Health, Melbourne Dental School, The University of Melbourne.

§Cariology and Operative Dentistry, Graduate School of Medical and Dental Sciences, Tokyo Medical and Dental University, Yushima, Bunkyo-ku Tokyo, Japan.

¶Department of Pedodontics and DAV Dental College, Yamuna Nagar, Haryana, India.

**Division of Prosthodontics, Director Clinical Sciences Research Group, Department of Preventive and Restorative Dental Sciences, School of Dentistry, University of California at San Francisco, USA.

ABSTRACT

Preservation of natural tooth structure requires early detection of the carious lesion and is associated with comprehensive patient dental care. Processes aiming to detect carious lesions in the initial stage with optimum efficiency employ a variety of technologies such as magnifying loupes, transillumination, light and laser fluorescence (QLF[®] and DIAGNOdent[®]) and autofluorescence (Soprolife[®] and VistaCam[®]), electric current/impedance (CarieScan[®]), tomographic imaging and image processing. Most fluorescent caries detection tools can discriminate between healthy and carious dental tissue, demonstrating different levels of sensitivity and specificity. Based on the fluorescence principle, an LED camera (Soprolife[®]) was developed (Sopro-Acteon, La Ciotat, France) which combined magnification, fluorescence, picture acquisition and an innovative therapeutic concept called light-induced fluorescence evaluator for diagnosis and treatment (LIFEDT). This article is rounded off by a Soprolife[®] illustration about minimally or even non-invasive dental techniques, distinguishing those that preserve or reinforce the enamel and enamel-dentine structures without any preparation (MIT1 – minimally invasive therapy 1) from those that require minimum preparation of the dental tissues (MIT2 – minimally invasive therapy 2) using several clinical cases as examples. MIT1 encompasses all the dental techniques aimed at disinfection, remineralizing, reversing and sealing the caries process and MIT2 involves a series of specific tools, including microburs, air abrasion devices, sonic and ultrasonic inserts and photo-activated disinfection to achieve minimal preparation of the tooth. With respect to minimally invasive treatment and prevention, the use of lasers is discussed. Furthermore, while most practices operate under a surgical model, Caries Management by Risk Assessment (CaMBRA) encourages a medical model of disease prevention and management to control the manifestation of the disease, or keep the oral environment in a state of balance between pathological and preventive factors. Early detection and diagnosis and prediction of lesion activity are of great interest and may change traditional operative procedures substantially. Fluorescence tools with high levels of magnification and observational capacity should guide clinicians towards a more preventive and minimally invasive treatment strategy.

Keywords: Caries, fluorescence, minimally invasive dentistry, LIFEDT concept.

Abbreviations and acronyms: CaMBRA = Caries Management by Risk Assessment; CRE = caries removal effectiveness; ECC = early childhood caries; ICDAS = International Caries Detection and Assessment System; LIFEDT = light-induced fluorescence evaluator for diagnosis and treatment; MID = minimum intervention dentistry; MIP = minimal invasive potential; MIT1 = minimally invasive therapy 1; MIT2 = minimally invasive therapy 2; NIR = near infrared radiation; OCT = optical coherence tomography; PS-OCT = polarized sensitive optical coherence tomography.

INTRODUCTION

Appropriate treatment of dental caries demands detection of carious lesions at an early stage. Previous caries experience is the best predictor of future caries. Additionally, a caries risk assessment can help to

determine the caries risk status of an individual. The development of technology to detect and quantify early carious lesions as well as caries activity may help to identify patients who require intensive preventive interventions best.^{1–3} All methods for detection and quantification of dental caries require certain

conditions: they have to meet all safety regulations; detect early shallow lesions; differentiate between shallow and deep lesions; give a low proportion of false positive readings; present data in a quantitative form so that caries activity can be monitored; be precise so that measurements can be repeated by several operators; be cost-effective and user-friendly.⁴ Many new caries classifications have been published, and the main issues are to be certain that the diagnosis device and the classification used fits within the framework of the daily dental practice routine.⁵ The introduction of a caries management system in correlation with the caries risk assessment, Caries Management by Risk Assessment (CaMBRA) and evidence based management options for non-cavitated and cavitated lesions might depend on these new diagnostic technologies. The goal of this review is to give an overview of these new minimum intervention dentistry (MID) technologies assigned to diagnose and treat caries in a pre-cavitated or cavitated stage using a medical approach.

New detection methods can be based on light transmission, light fluorescence and other systems such as ultrasound and near infrared illumination.

Light transmission

Fibre optic transillumination (FOTI[®], DIFOTI, Electro-Optical Sciences, Irvington, NY, USA), and the more recent digitized DIFOTI[®] technique, use light transmission through the tooth.^{4,6-8} The images can be stored and re-examined later. Fibre optic transillumination with a camera from KaVo[®], the DIAGNOcam[®] (KaVo Dental, Lake Zurich, IL, USA) is a new system developed recently, also based on simple transillumination (excitation wavelength of 780 nm) (Fig. 1). So far only limited research has been

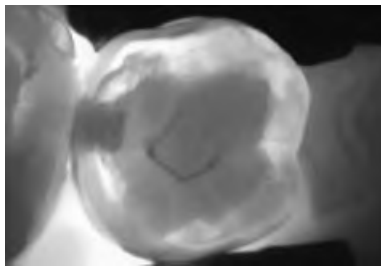


Fig. 1 Tooth picture taken with the DIAGNOcam camera.

published. The DIAGNOcam[®] is placed directly on the tooth, the transilluminating light positioned either side of the tooth and the picture captured; the software allows storage of the picture.

Light fluorescence

The imaging techniques based on the fluorescent response of organic components of teeth have been developed for use in caries detection. Commercially available devices include fluorescence systems, a combination of camera and fluorescence systems, optical coherence tomography, and electrical impedance and conductivity.

Fluorescence systems

The DIAGNOdent[®] (DIAGNOdent 2095, DIAGNOdent 2190, KaVo Dental, Lake Zurich, IL, USA), which uses a laser at a wavelength of 655 nm, creating fluorescence in components such as porphyrins, and the intensity of the emitted fluorescent light is measured.¹³⁻¹⁵ DIAGNOdent[®] values guide clinical decision making (Table 1). After calibration of the tool on a ceramic disc or sound adjacent enamel, the detection handpiece is placed on the tooth surfaces and the device provides a value which can be recorded.

Fluorescence Aided for Caries Excavation (FACE, SIROInspect[®], Sirona Dental Systems GmbH, Germany) (Fig. 2 and 3) has an excitation wavelength of around 405 nm. The practitioner needs to use specific glasses to see the fluorescence in dentine.^{16,17} Limited information is presently available. No images can be recorded with either system. The Midwest Caries ID unit (Dentsply, York, PA, USA) uses LED illumination and feedback relating to caries status is provided via audible 'beeps'. Very little information or research is available.

Combination of camera and fluorescence systems

The QLF[®] (QLF, Inspektor Research Systems BV, Amsterdam, Netherlands), with emission in the wavelength region of 290–450 nm, uses a xenon arc lamp and looks at the change in transmission from the green fluorescence occurring in the dentine body due

Table 1. Laser fluorescence scores and clinical recommendations

DIAGNOOpen score	Interval 1	Interval 2	Interval 3
Occlusal and pits	0–12	13–24	>25
Histological interpretation	Healthy tissue	Demineralized enamel	Dentine involved
Recommended therapy	Normal prophylactic care	Intensive prophylactic care	Minimally invasive operative care
Proximal area	0–7	8–15	>16
Recommended therapy	Normal prophylactic care	Intensive prophylactic care	Minimally invasive operative care



Fig. 2 SIROInspect® (from Sirona website).

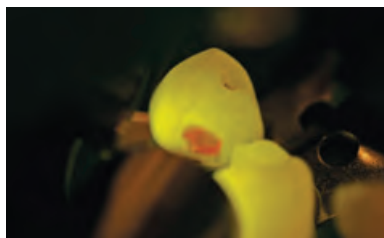


Fig. 3 Red fluorescence emission of dentine after excitation with SIRO-Inspect (from Sirona website. Buchalla W).

to microporosities in enamel as a result of the caries acid attack.^{18–21} In brief, the QLF system's ability is to accurately determine mineral content of enamel.

The Canary® (Quantum Dental Technologies Inc. Ontario, Canada) is a laser-based system that uses a combination of heat and light (Frequency Domain Photothermal Radiometry and Modulated Luminescence; FD-PTR and LUM) claiming to examine the crystal structure of teeth and map areas of tooth decay directly.^{22–25} The Canary uses a low power, pulsating laser light to scan teeth for the presence of dental caries. The tooth absorbs the laser light and two phenomena are observed and measured: the laser light is absorbed and then consequently a release of heat occurs. This heat will not harm the tooth. By varying the pulse of the laser beam, a depth profile of the tooth can be created to permit detection of decay as deep as 5 mm from the tooth surface and as small as 50 microns in size. Simultaneous measurement of the reflected heat and light provides information on the presence and extent of tooth decay below the tooth surface before being detected by dental radiographs. The device is supposed to provide early detection of small cavities, and thus is more advantageous in comparison to traditional approaches for detection and monitoring early stage tooth decay. This might reduce the cost barriers to dental services by treating emerging 'cavities' before invasive and more expensive treatments are required. The handpiece is applied on the tooth, pictures and 'Canary' values are given by the system. Protective glasses are recommended.

The Soprolife® camera (Acteon, La Ciotat, France)^{3,4,26–31} is an intraoral camera that utilizes two types of LEDs that illuminate tooth surfaces in the visible domain, either in the white light region or in a

narrow band (wavelength 450 nm with a bandwidth of 20 nm). This provides an anatomical image superimposed on an autofluorescence image. The device can detect and locate differences in density, structure and/or chemical composition of biological tissue by continuously illuminating with one frequency band while it generates a fluorescence phenomenon in a second frequency band. The camera is equipped with an image sensor (0.25-inch CCD sensor) consisting of a mosaic of pixels covered with filters of complementary colours. The data collected, relating to the energy received by each pixel, allows retrieval of an image of the tooth. The camera operates in three modes: for daylight mode four white light LEDs are engaged; for the diagnostic and treatment modes the light is provided by four blue LEDs (450 nm). A new camera, the Soprocure®, also provides three clinical modes: daylight, caries and periodontal mode. The caries mode focuses on enamel and dentine caries, and the periodontal mode on periodontal inflammation. Table 2 gives an overview of the fluorescence signals for coronal caries and Table 3 focuses on the observed dentine signal.

The LIFEDT concept^{26,27} (light induced fluorescence evaluator for diagnosis and treatment) is linked to the fluorescence camera. The principles are: (1) the occlusal surfaces of the tooth of interest are cleaned; (2) the tooth can be observed in daylight and fluorescence mode with a high level of magnification; (3) any modification of the reflected light from dentine or enamel in comparison to a healthy area can be noted; (4) clinical decisions are not linked to numerical values but the system improves visual inspection and helps in decision making.

Soproimaging® software makes it possible to record and compare the pictures. The camera is positioned on the tooth, with magnification and mode (daylight or fluorescence) selected. Pictures are recorded with the specific Soproimaging® software.

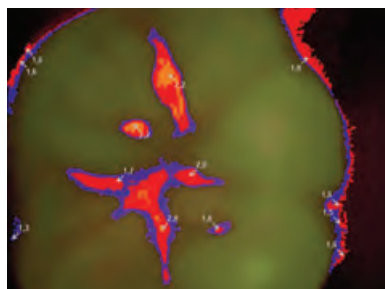
The VistaCam® camera (Classic, CL and IX) is an intraoral fluorescence camera (Dürr Dental, Bietigheim-Bissingen, Germany) that illuminates teeth with a violet light (405 nm) and captures the reflected light as a digital image (Fig. 4). The reflected light is filtered for light below 495 nm and contains the green-yellow fluorescence of normal teeth with a peak at 510 nm, as well as the red fluorescence of bacterial metabolites with a peak at 680 nm. The software (DBSWIN version 5.3) quantifies the green and red components of the reflected light on a scale from 0 to 3 as a ratio of red to green (Table 3), showing the areas with a higher than healthy tooth ratio. A new version, the VistaCam CL-IX® with removable head cameras, wireless and a light cure function, has just been launched.^{32,33} The camera is placed on the tooth, pictures are recorded with specific software, which then reveals the caries scores.

Table 2. Soprolife® in daylight and blue fluorescence codes for coronal caries according to Rechmann et al.⁴ Treatment decision proposition

Code. Visual inspection	Description in daylight after cleaning	Description in fluorescence after cleaning	DIAGNOdent versus Spectra Caries (VistaCam®) detection. Average value (±SD)	Treatment decision proposition
0	Sound, no visible change in the fissure	Sound, no visible change in enamel (rarely a graphite-pencil-coloured thin shine/line can be observed) shiny green fissure	5.7 (±4.3) 0.7 (±0.68)	MIT1 + CAMBRA recommendations
1	Centre of the fissure showing whitish, slightly yellowish change in enamel, limited to part or all of the base of the pit and fissure system	Tiny, thin red shimmer in the pits and fissure system, can come up the slopes, no red dots visible	13.3 (±11.8) 1.26 (±0.61)	MIT1 + CAMBRA recommendations
2	Whitish change comes up the slopes (walls) toward the cusps; the change is wider than the confines of the fissure, seen in part or all of the pit and fissure system, no enamel breakdown is visible	In addition to tiny, thin red shimmer in pits and fissures, possibly coming up the slopes darker red spots confined to the fissure are visible	2.2 (±17.5) 1.6 (±0.51)	MIT1 + CAMBRA recommendations
3	Fissure enamel is rough and slightly open with beginning slight enamel breakdown; changes are confined to the fissure and do not necessarily come up the slopes, no visual signs of dentinal involvement	Dark red extended areas confined to the fissures; slight incipient roughness	40.6 (±24.6)/ 1.95(±0.57)	MIT1 + CAMBRA recommendations
4 Reasonable cut-off point	Caries process is not confined to the fissure width; appears much wider than the fissure; changed area has a 'mother-of-pearl' glossy appearance	Dark red or orange areas wider than fissures; surface roughness occurs, possibly grey or rough grey zone visible		MIT2 Operative steps
5	Enamel breakdown with visible open dentine	Obvious wide openings with visible dentine		MIT2 Operative steps

Table 3. Clinical dentine colour guide used with the LIFEDT concept and the Soprolife® device^{3,26,27}

Camera. Visual inspection	Healthy dentine	Infected dentine	Affected dentine. Active process (soft-yellow-tissue)	Affected dentine. Arrested process (brown-tissue, quite hard)
Soprolife® Soprocure®	Acid green Grey	Dark grey Dark grey	Bright red Bright red	Dark red Dark red

**Fig. 4** VistaCam® picture of occlusal decay with their respective caries ratios.

All these devices can be used specifically for diagnostics or treatment, but at this time only Soprolife® can be used for both.

Optical coherence tomography

Optical coherence tomography (OCT, Dental Imaging System, Lantis Laser, Denville, NJ, USA) is a non-ionizing imaging technique that can produce cross-section images of biological tissues using an infrared light at 1310 nm. Only *in vitro* studies are available, and often the images are limited to the depth of

enamel. The polarized sensitive OCT (PS-OCT) can be correlated with the degree of demineralization and lesion severity. Monitoring *in vivo* carious lesion changes could be helpful with this device.^{34–36} A combination of near infrared radiation (NIR) imaging with PS-OCT was also described to acquire depth-resolved images. Combining this technology with a short-pulsed CO₂ laser ablation system would allow for the selective removal of dental caries.

Electric impedance and conductivity

The Electronic Caries Monitor (ECM®; Lode Diagnostics, Groningen, the Netherlands) is based on tissue electroconductivity and CarieScan® on electric impedance. The CarieScan® (Dundee, Scotland) technique originates from the theory that sound dental hard tissue exhibits high electrical resistance or impedance. The more demineralized the tissue, the lower the resistance becomes. *In vitro* and *in vivo* studies were performed, showing moderate sensitivity and specificity.^{9–12} Measures are linked with a scale number giving information about the supposed severity of the decay (Table 5). The metallic probe of the CarieScan® is

Table 4. VistaCam scores and colour scales versus the histological scale

0–1	1–1.5	1.5–2	2–2.5	2.5 >3
Healthy enamel	Initial enamel demineralization	Deep enamel decay	Dentine caries	Deep dentine caries

Table 5. CarieScan® score versus ICDAS II classification and histological classification

CarieScan site status Reference standard <i>validated by Micro-CT plus visual examination</i>	CarieScan code	ICDAS code <i>validated by clinical visual examination</i>	ICDAS site status <i>validated by histological examination</i>
Sound	0	0	Sound
Sound-outer 1/3 enamel caries interface	1–20	0	Sound
Enamel caries <i>outer 1/3 enamel</i>	21–30	1	Enamel caries
<i>middle 1/3 enamel</i>	31–50	2	<i>outer 1/2 enamel</i>
<i>inner 1/3 enamel</i>	51–90	2	<i>inner 1/2 enamel</i>
Enamel and enamel – dentine junction / outer half dentine caries	91–99	2	<i>inner 1/2 enamel</i> <i>outer 1/3 dentine</i>
Established dentine caries <i>inner 1/2 dentine</i>	100	3, 4, 5, 6	Dentine caries <i>middle 1/3 dentine</i> <i>inner 1/3 dentine</i>

directly placed on the tooth and the caries values are given by the system. A lip hook is needed.

Other systems

Other systems include ultrasound, near-infrared illumination, Raman spectroscopy and terahertz imaging. Further research is still required before these systems can clinically be used. Sensitivity, specificity and advantages of the main different devices are summarized in Tables 6 and 7.

Illustrations with clinical cases

Clinical recommendation for the diagnosis step

For caries diagnostics the use of a combination of diagnostic aids is still recommended.³⁷ Whatever numerical values given by the device,^{35,36} visual inspection remains an essential component in making the final decision: to drill or not to drill. Indeed it is more the complexity of the shape, depth and the width of the grooves which governs clinical decision, meaning that before the diagnostic step the pits need to be perfectly clean. Regarding the treatment, after the diagnosis has been established, many new products are now available with the aim of remineralization and reversing the caries process. Their systematic use should be promoted.^{38–40} The general philosophy of the patient-centred approach is of importance. Indeed, all the techniques described below should be applied within a modern medical approach of

determining and managing the patient's caries risk by applying the CaMBRA system.^{41,42} The threshold of invasive intervention is given at a lesion with first visible enamel breakdown (ICDAS score 3). The choice between advising preventive care and the preventive with operative care, respectively will be based on this decision.^{43,44} Consequently, preventive and minimal invasive therapies can be divided into two groups: the first (minimally invasive treatment 1 or MIT1) for treating enamel and enamel-dentine lesions without any preparation ('non-invasive'), provided that there is no surface cavitation. The second group (minimally invasive treatment 2 or MIT2) is for treating early enamel-dentine lesions with surface cavitation. From ICDAS score 3 onwards, a more conventional therapeutic approach is advisable (Table 2).^{3,4,26,27}

CaMBRA: a paradigm shift in dentistry

Dental caries is the most prevalent infectious disease in children in the USA.⁴⁵ Caries is five times more common than asthma and seven times more likely than hay fever in children.⁴⁶ More than 40% of children have tooth decay by the time they reach kindergarten.⁴⁷ Recent research has shown that early preventive dental visits (by age 1) are effective at preventing early childhood caries (ECC, or severe tooth decay in children under 5) and can reduce total dental costs.⁴⁸

Caries results from an overgrowth of specific organisms (*Streptococcus mutans*, lactobacillus species) that are part of normally occurring human dental flora. Infant colonization with *S. mutans* commonly occurs through vertical transmission from mother to child. Children of mothers with high caries rates are at higher risk of ECC.⁴⁹ Other factors which contribute to the overgrowth of cariogenic organisms include frequent ingestion of fermentable carbohydrates and reduced salivary function.

The caries process is most effectively managed by assessing each patient's individual risk factors (the balance/imbalance of protective factors and pathological factors) and by prescribing appropriate non-surgical interventions. The conventional restorative approach alone will not eliminate the disease of caries.⁵⁰

Table 6. Sensitivity and specificity of the main different devices^{4,37}

Devices	Sensitivity	Specificity
Electronic caries monitor [®]	0.65	0.73
Visual inspection	0.6	0.73
Fibre optic transillumination [®]	0.21	0.88
Bitewing	0.19	0.80
QLF [®]	0.5–0.68	0.7–0.9
Spectra [®] or VistaCam [®]	0.92	0.37
SiroInspect	0.94	0.83
DIAGNOdent [®]	0.87	0.5
SoproLife [®]	0.93	0.63

Table 7. Main advantages of the respective devices

Main devices	VI	Numerical value	Magnification	Picture recording	Treatment steps	Activity assessment
QLF [®]	+	+	+	+++	+	+/-
DIAGNOcam [®]	+	-	++	+++	-	-
DIAGNOdent [®]	-	+	-	-	-	-
VistaProof [®]	++	+	++	+++	?	+
Vistascan IX [®]		+	++	+++	?	+
Canary system [®]	+/-	+	+/-	++	-	+
SiroInspect [®] (FACE)	+	-	-	-	+	+
SoproLife [®]	+++	-	++++	+++	+++	+++

Currently, the majority of dental practices operate under a surgical model. Caries Management by Risk Assessment (CaMBRA) encourages a paradigm shift from this methodology to one based on a medical model of disease prevention and management.

Caries can be largely prevented in nearly all populations by encouraging a regimen of oral hygiene protocols that control the manifestation of the disease, or keep the oral environment in a state of balance between pathological and preventive factors. CaMBRA is an approach to caries management that uses evidence-based treatment decisions based on the caries risk status of the individual. If a patient's caries risk is assessed, then appropriate interventions that are consistent with CaMBRA clinical protocols are implemented in order to influence caries progression. An imbalance towards either pathological or protective factors will determine whether caries progresses, halts or reverses.

The principles of CaMBRA are modification of the oral flora to favour health; patient education and informed participation in preventing oral disease; remineralization of non-cavitated lesions of enamel and dentine/cementum; and minimal operative intervention of cavitated lesions and defective restorations.

At the dental visit, the practitioner will conduct a clinical exam to assess the caries status. On the basis of saliva tests (to determine bacterial levels) and a validated risk assessment questionnaire,⁵¹ caries risk status will be determined as low, moderate, high or extreme high.⁵²

The UCSF School of Dentistry has conducted a three-year study where the overall study objective was to provide clinical evidence that scientifically based caries risk assessment, in conjunction with aggressive preventive measures and conservative restorative treatment, resulted in a dramatic reduction in future caries incidence. The study group who received restorative treatment alone showed after a slight decrease, an increase in caries-causing bacteria over time, but the group who received restorative and preventive interventions combined showed a decrease. The intervention group had a statistically significantly 24% lower mean caries increment than the control group ($p = 0.020$). Overall, caries risk reduced significantly in intervention versus control over two years.⁵⁰

Lasers for minimally invasive preparation and caries prevention

Lasers of the Erbium family (Er:YAG emission wavelength 2970 nm, ErCr:YSGG laser 2780 nm wavelength) are considered safe for ablation of dental hard tissues,^{53–56} as well as for removal of composite resins.^{57–59} Whether caries removal with lasers is as efficient as using a regular drill is up for discussion⁶⁰ but using lasers for instance in paediatric dentistry is

widely considered as advantageous.⁶¹ The ability of hard tissue lasers to reduce or eliminate vibrations, the audible whine of drills, microfractures, and some of the discomfort that many patients fear and commonly associate with high-speed handpieces has been described as impressive.⁶²

High caries prevalence in occlusal pits and fissures has warranted the search for novel prevention methods. The capability of lasers to modify enamel surface properties has promised a new type of caries prevention therapy. Erbium lasers have been shown to produce acid resistance *in vitro*,⁶³ but currently there is no information available showing the clinical uses of those lasers for caries prevention.

Specific carbon dioxide (CO₂) lasers – wavelength 9.6 or 9.3 μm, short pulsed in the microsecond range – have been better studied for caries prevention. *In vivo* an 86% reduction in smooth surface demineralization following short-pulsed 9.6 μm CO₂-laser irradiation was recently reported.^{64,65} In a consequent study using the International Caries Detection and Assessment System (ICDAS-II) and the Soprolife Light-Induced Fluorescence Evaluator, it was shown that irradiating fissures of second molars with this specific CO₂-pulsed laser markedly inhibited caries progression in pits and fissures in comparison to fluoride varnish use alone over 12 months. Soprolife evaluations confirmed the ICDAS results.⁶⁶ To achieve acid resistance of the fissure system of a tooth, the fissure and the adjacent enamel next to the fissure area is covered with the 9.6 μm CO₂-laser irradiation. The laser emits laser pulses with a repetition rate of 20 Hz (20 pulses per second), the laser spot size is roughly 0.8 mm and the laser is applied with an angulated laser handpiece. To achieve caries resistance, the goal is to irradiate each enamel spot with 20 overlapping laser pulses, resulting in a superficial temperature rise of roughly 800 °C (just below enamel melting) in an enamel layer of less than 100 μm thickness. The average treatment time for a molar fissure is around 1.5 minutes and results in driving out the carbonated phase from the typical natural carbonated hydroxyapatite. Getting rid of the carbonated phase changes enamel into the more acid resistant, less soluble hydroxyapatite. Adding fluoride immediately afterwards results in the even more acid resistant and least soluble fluorapatite. These short-pulsed CO₂-lasers will represent the next generation of hard tissue lasers for caries removal^{67,68} as well as hard tissue cutting.⁶⁹

Common clinical steps

Professional prophylactic cleaning

This step currently remains one of the most complicated. In fact an *ad hoc* diagnosis assumed that the

deepest part of the groove was perfectly cleaned without injury to the infected enamel, providing an overview of an area around 0.1 mm wide in dry conditions. Without clear evidence, we simply limited our purposes to clinical advice. As the crystalline structure is highly unstable and the average width of the pits is around 0.1 mm, the use of sharp probe and burs is strictly forbidden, and cleaning with a rotating brush in combination with prophylactic paste could disturb the values ratio given by the different diagnosis devices. One reasonable clinical proposition is to treat with an air polishing device in conjunction with sodium bicarbonate (Kavoprophy[®], AirNGO[®], EMS[®] air flow handy). The use of slightly harder calcium carbonate powder (Pearl powder[®], Acteon Satelec, France, Kavoprophy[®] prophylactic powder, Germany) is also advisable. Precautions are needed to reduce the overflow of the powder (high suction, dental dam set up). In case of a high-risk patient with no monitoring possibilities, the decision can be made to seal the groove. Syc[®] powder (OSSpray, Abbottstown, USA) in this particular case selectively removed the infected enamel, but a special nozzle was needed due to the extreme hardness of the powder.^{70,71}

In case 1 sandblasting was undertaken with a calcium carbonate powder (Fig. 5–13). In case 2 sandblasting was undertaken with a bioactive glass. (Syc[®] powder) (Fig. 14–17).

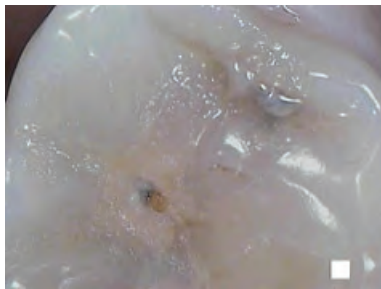


Fig. 5 Occlusal view, daylight mode before cleaning: dental plaque concealing possible decay.



Fig. 6 View of the occlusal decay and the obvious proximal decay after cleaning (Pearl power, AirNGo system, Acteon, Bordeaux France, Soprocure[®], daylight view) (black arrows).

Minimally invasive treatment type 1

Minimally invasive treatment type 1 (MIT1) encompasses all the dental techniques aimed at sterilizing/disinfecting (e.g. ozone therapy), remineralizing, reversing and sealing the carious process. Nowadays there are many products available, each with their own advantages and disadvantages (Table 8).³

The LIFEDT concept applied to treatment of enamel caries

The challenge is early diagnosis of enamel decay before cavitation occurs, and consequently to manage your clinical decision depending on the individual caries risk of the patient. A combination of the CaMBRA approach^{41,42} and LIFEDT could certainly help to better understand this clinical approach (Table 9). Based



Fig. 7 Red fluorescence confirming the decay (ICDAS 5) (Soprocure[®], Cario mode) (black arrows).



Fig. 8 Illustration of the occlusal and proximal decay of the same tooth during preparation. (Soprolife[®], treatment mode).

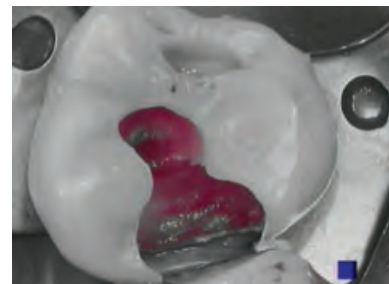


Fig. 9 The same tooth in caries mode during preparation (Soprocure[®]).

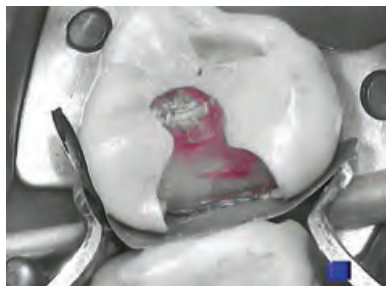


Fig. 10 End of the excavation steps of the occlusal and Class II area (caries mode Soprocure®).



Fig. 14 Occlusal view. ICDAS⁴⁹ score 4 or 5. Old sealant visible. Soprocure® daylight mode.



Fig. 11 The same tooth in daylight.

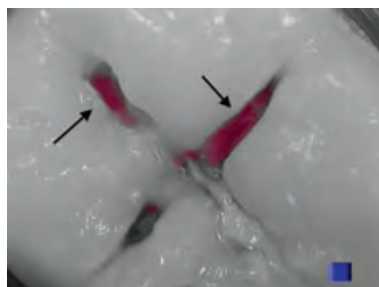


Fig. 15 Open pits after Sylec® sandblasting. Red signal revealing the dentine decay. Soprocure® caries mode (black arrows).

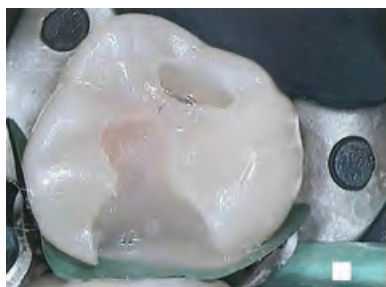


Fig. 12 Dentine substitute (3M, flow composite, V3 ring matrix, USA).

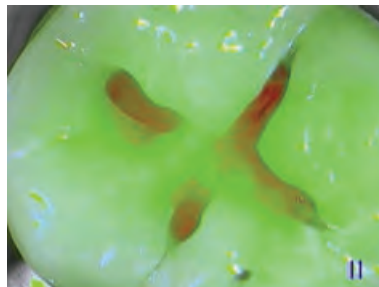


Fig. 16 Soprolife® view at the end point of excavation with Sylec powder. Red shadow revealed hard sclerotic dentine remaining.



Fig. 13 Occlusal and proximal areas rebuilding (HrI composite, Micerium, Italy).

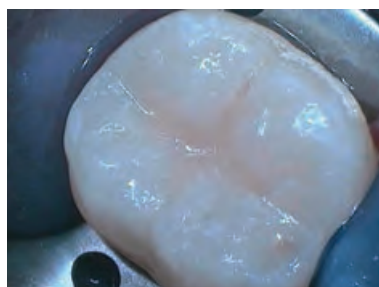


Fig. 17 Occlusal restoration with a nanohybrid composite.

on daylight and fluorescence observations, coupled with the high magnification, a decision-making diagram is as follows. With a smooth surface, use of a polishing cup with prophylaxis paste which removes discolourations, plaque and polishes the tooth surface. Choose a fine grit, as the crystalline structure is highly unstable, to avoid causing any unnecessary abrasion

of the tooth's structure and restoration surfaces. Some pastes contain fluoride and should be free of known allergens (e.g. Flairesse® prophylaxis paste, DMG, Germany).

Furthermore, the LIFEDT system does not address the issue of bacterial load. This can be determined using bacterial tests such as GC Saliva Check SM®, GC Plaque-check® + pH (GC, Tokyo, Japan), and

Table 8. Advantages and disadvantages of MIT1 with regard to the treated surface^{3,26,27}

MIT1	Techniques	Advantages	Disadvantages	Diagnosis aided
Occlusal, vestibular, lingual and palatal surfaces	Varnish, MI paste plus, GC Tooth Mousse (GC, Tokyo, Japan). Ozonotherapy (Kavo, Biberach, Germany). Sealant application.	Easy application and protocol. Optimum aesthetic results. Reversible actions, non-iatrogenic.	Efficiency with regard to the caries risk assessment and the sensitivity and specificity of the diagnosis aid. Efficiency doubtful for ozone.	Fluorescence/picture device: ++++ Fluorescence device: ++ Laser device: ++ Electric device: ++ Transillumination: +
Proximal surface	Varnish* MI Paste Plus*, GC Tooth Mousse* (GC, Tokyo, Japan). Icon* (DMG, Hamburg, Germany). *Needs accessible surfaces.	Application not so easy. Optimum aesthetic results. Reversible actions, non-iatrogenic.	Efficiency with regard to the caries risk assessment and the sensitivity and specificity of the diagnosis aid. Operator-dependent. New techniques proof to be confirmed for Icon. Accessible surfaces need to be strongly separated when using Icon.	Fluorescence/picture device: ++++ Fluorescence device: ++ Laser device: +++ Electric device: ++ Transillumination device: +++

Table 9. Combination of CaMBRA and LIFEDT in case of enamel lesions

Type of lesion	High risk	Low risk
Smooth surface enamel lesion. Active smooth surface showed blueish cast in diagnostic mode and looks rough and matt in daylight mode.	Professional prophylactic cleaning. • Brushing 2–3 times per day: 1.1% (5000 ppm) NAF toothpaste. Xylitol (6 g/day): chewable tablets. Application of fluoride varnish (5% NAF); recall every 3–4 months. Application of calcium phosphate-based paste (MI Plus [®] GC Tooth Mousse [®] , GC Tokyo, Japan). Mouthwash: 0.12% chlorhexidine: 1 minute every evening for 1 week per month. Dietary counselling.	Brushing 2–3 times per day with 1100 ppm fluoride toothpaste); Patient recall every 6 months. (Application of calcium phosphate-based, paste (optional). (MI Plus [®] GC Tooth Mousse [®] , GC Tokyo, Japan).
Pits or complex shape grooves. After cleaning: Suspicious grooves with fluorescence altered (red signal) from a healthy area. Code ⁴ 1–3 (Table 2)	LIFEDT Concept: If the diagnostic aided (fluorescence, laser, electric monitor) confirm groove fissuration and any variations in fluorescence, a sealant will be applied using a dental dam, due to effectiveness of brushing being impossible to monitor. (Note that red fluorescence of the grooves might be related with the activity of the decay).	Groove without modified fluorescence. Sealant and varnish are optional. Groove with modified fluorescence: a sealant is recommended.
Products available	Fluoride varnish: Fluoroprotector [®] (Vivadent, Schaan, Leichtenstein), Flairesse varnish [®] (DMG, Germany).	Sealants: VOCO, 3M, Vivadent.

Cariscreen[®] (Oral Biotechnologies, Albany, OR, USA). In the presence of a high-risk oral ecology, any fissured groove and any modification in the natural fluorescence serves as an indication to implement the LIFEDT concept. Until the evidence of dentinal damage by caries is definitely diagnosed using radiography and other diagnosis aiding cameras, the LIFEDT concept, based on the work of Mertz-Fairhurst *et al.*,⁷² recommends preventive sealing rather than a conventional irreversible mechanistic approach of drilling.^{3,73} This approach also opens up new prospects in terms of monitoring restorations if a transparent sealant is applied (experimental sealant, Voco, Germany). Indeed, any suspicious variation of the tissue fluorescence around existing restorations should facilitate better diagnosis of recurrent caries.

The LIFEDT concept applied to treatment of dentinal caries

In terms of the MID philosophy, the minimally excavating technique entails evaluating the caries removal effectiveness (CRE) and minimal invasive potential (MIP) of the different available techniques for removing infected dentine (Table 10). Neves *et al.*⁷⁴ reported that rotary/oscillating caries removal may lead to over-excitation when combined with Caries Detector (Kuraray, Japan). Despite the original intention, the Er:YAG-laser aided by light induced fluorescence has been described as a non-selective caries removal technique. A tendency of under-preparation was observed with ceramic burs (CeraBur, KISM, Komet-Brasseler, Lemgo, Germany) and Cariex, an air scaler with

Table 10. LIFEDT concept for dentine^{4,26,27}

Principle	First analyse a healthy area on the tooth concerned for use as a fluorescence reference during image processing and analysis
Active carious lesion	<p>Visual signals in fluorescent mode</p> <ul style="list-style-type: none"> • healthy dentine: acid green fluorescence • infected dentine: green-black fluorescence • infected/affected dentine: bright red fluorescence. This tissue is fairly easily eliminated with a manual excavator. <p>Clinical considerations In case of high caries risk-applicable to all lesion types, active or arrested, consider the following:</p> <ul style="list-style-type: none"> • according to depth of lesion: the residual septicity of the dentinal structure is the key factor in the general practitioner's thinking. Opt for provisional fitting of a conventional glass ionomer, such as Fuji VII® (GC Japan). • perform permanent treatments once the carious disease has stabilized. <p>Permanent treatments In case of low caries risk-applicable to all lesion types, active or arrested, consider the following:</p> <ul style="list-style-type: none"> • using a dental dam is essential • favour manual excavation over mechanical rotary caries removal • disinfect the dentine wound with a 5% aqueous solution of chlorhexidine or use the PAD® technique (photo of activated disinfection with tolonium chloride solution)⁵⁵ • if the area is accessible and enables a leak-tight contact, ozone disinfection therapy is feasible • favour fitting a bioactive dentine substitute, such as resin-modified glass ionomer, especially if the enamel edges have disappeared²¹ • in case of a eugenol-based dressing, opt for an amalgam restoration • in case of a temporary dentine substitute such as conventional glass ionomer cement, consider the fitting time and the bonding of the adhesive/composite system used with this material. A change in fluorescence could help with this decision • consider whether it is necessary to use antiseptic enamel-dentinal adhesives (e.g. Clearfil Protect Bond®, Kuraray, Japan) • consider the choice of the most appropriate adhesive for the residual dentine structure (total etch, self etch, etc).
Arrested lesion	<p>Visual signals in fluorescent mode</p> <ul style="list-style-type: none"> • healthy dentine: acid green fluorescence • infected dentine: green-black fluorescence • infected/affected dentine: dark red fluorescence. This tissue is more difficult to eliminate with a manual excavator. Surgical treatment of this tissue by rotary milling (tungsten carbide or ceramic) under spray is feasible • abnormal dentine at end of excavation: light green-grey fluorescence with systematically persisting shady pink fluorescence at the bottom of the preparation, opposite the pulpal wall. <p>Clinical considerations</p> <ul style="list-style-type: none"> • according to the depth of the lesion: the residual septicity of the dentine structure and activity of the disease are no longer the key factors in the general practitioner's thinking. Using a dental dam is essential • disinfect the dentine wound with a 5% aqueous solution of chlorhexidine or use the PAD® technique⁵⁵ (photo-activated-disinfection with tolonium chloride solution) • if the area is accessible and enables a leak-tight contact, an ozone disinfection therapy is feasible • fitting a bioactive dentine substitute such as resin-modified glass ionomer is balanced with the injection of a chemo-polymerizing composite, especially if there are persisting enamel edges around the cervical border of the preparation • in case of a eugenol-based dressing, opt for an amalgam restoration • temporary fitting of a conventional glass ionomer is not absolutely necessary • consider the choice of the most appropriate adhesive for the residual dentine structure (total etch, self etch, etc).
Mixed lesions	In case of a mixed lesion (active and arrested), the carious lesion should be considered active in its entirety.

coupled tungsten-carbide oscillating tips. Finally, the tungsten-carbide bur use gave good results when used alone, and the best technique with regards to CRE and MIP remained the chemomechanical methods with the new experimental enzyme-based caries-removal gels (exp. SFC and VIII, 3M-ESPE, Seefeld, Germany), coupled with a metal spoon excavator which is not yet on the market. Time use should be more precisely evaluated with these kinds of techniques. Specifically removing the layer of carious dentine which is rich in bacteria, unremineralizable and has necrotic tissue remaining on its surface, remains a challenge, depending on the CRE and MIP concept.^{74–77} The end point of the excavation process still remains hazy. The use of caries dyes can be useful for training purposes⁷⁸ but in clinical practice will definitely lead to unnecessary removal of sound tooth structure. Use of chemomechanical methods of caries removal is also increasing but the main drawbacks are time consumption and a tendency of under-preparation.⁷⁴ Concerning the fluorescence aids for caries excavation device (FACE[®]), Lennon *et al.* in their study^{16,17} on FACE[®] versus caries detector and conventional caries excavation concluded that excavation using FACE[®] is more effective than conventional excavation in removing infected primary dentine and superior to caries detector dyes and chemomechanical excavation. Among the different caries detection devices, only those combining fluorescence signals with pictures are useful. Soprolife[®], unlike DIAGNOdent[®] (KaVo, Biberach, Germany), provides an overall image of the clinical situation instead of a point-by-point measurement. DIAGNOdent[®] has been described as having a good level of sensitivity and low specificity, but it was more useful for caries diagnosis than for caries discrimination, and there were false-positive signals. Moreover, a recent study¹⁵ has revealed that measurements from DIAGNOdent[®] were not strongly correlated with the required depth and volume of the cavity preparation. Authors concluded that appropriate visual examination training may provide similar results without the need for additional equipment.

The LIFEDT concept applied to occlusal decay

When evaluating occlusal fissure areas with Soprolife[®] in daylight and fluorescent modes, three clinical forms (Code 1, 2, 3) were previously described^{26,27} dependent on information given by the fluorescence signal and the magnification. In a more recent study, Rechmann *et al.*⁴ gave an accurate score description from zero to five for daylight and fluorescence mode (Table 2). Discussions about an appropriate cut-off point to determine an operative intervention deserve our attention, but it seems reasonable to treat from a score of 4/5 depending on the width, depth and cavity shape, as well as the fluorescence information

retrieved. The sensitivity and specificity of each device will shift this cut-off point; therefore, the principle is first to gently clean the pits (applicable for all devices) and then observe any modification of the structure and shape of the pits in daylight and fluorescence mode. Systems giving caries scores with no visual inspection can be used complementarily. (Illustrations in Fig. 5–9 and Fig. 14–17. See also Tables 11 and 12.)

The LIFEDT concept applied to approximal cavities

The major difficulty in the approximal tooth area is associated with the possible presence of a caries lesion in the approximal zones. Even though bitewing radiographs give relatively good information, mistakes are sometimes unforeseeable (Fig. 18). In some clinical situations, we propose separating the teeth as far as possible using powerful plastic wedges. When using the Soprolife[®] camera in daylight mode and fluorescent mode it might be possible in most cases to view cavitations (if present). Transilluminations with DIAGNOcam[®] could also be helpful. The presence of cavitation and/or a lesion involving the middle third of the dentine contraindicates the use of the resin infiltrant technique and means that the tissues must be prepared mechanically. To objectively balance your clinical decision between MIT1 and MIT2 in proximal areas, a combination of X-rays, fluorescence, laser and magnification could help to achieve better identification (Tables 11 and 12.)

Treatment decision making

In preventive care decision making, depending on the extent of demineralization, suspicion of the enamel breakdown and lesion accessibility, the clinical treatment choice should be balanced between monitoring, application of fluoride varnish and sealing with resin infiltrant (Icon[®], DMG, Germany) (Tables 8 and 9). Operative decision making in regards to the marginal crest should take into account the traditional Class II restoration, tunnel or slot preparation. When the marginal crest is non-recoverable, the fluorescence emission is blueish with a very low green emission (Fig. 22). In that particular case, only traditional Class II preparation is recommended.

Approximal caries lesions without cavitation

MIT1 illustration of a sealant infiltration (resin infiltrant Icon[®], DMG).

The presence of cavitation and/or a lesion involving the middle third of the dentine (from D2 onward in terms of caries extension) contraindicates the use of Icon, and means that the tissues must be prepared mechanically.

Table 11. Advantages and disadvantages between sonic and ultrasonic cavity preparation system in case of slot cavity and minimally invasive Class II preparation³

MIT2	Ultrasonic	Sonic	Preparations
Advantages	<p>Preservation of the adjacent proximal surface.</p> <p>Preservation of the marginal ridge (slot and tunnel cavity).</p> <p>Uses the same ultrasonic handpiece as for periodontal scaling.</p> <p>Initial penetration with diamond burs. The cavity is required less often.</p> <p>Natural aesthetics preserved.</p>	<p>Preservation of the adjacent proximal surface.</p> <p>Preservation of the marginal ridge (slot and tunnel cavity).</p> <p>Uses the same sonic handpiece as for periodontal scaling.</p> <p>Natural aesthetics preserved.</p>	<p>Tunnel and slot preparations.</p> <p>End steps of minimally invasive Class II preparation.</p> <p>Bevelling steps.</p>
Disadvantages	<p>Information concerning the potential to create cracks due to ultrasonic vibrations and their clinical outcomes is not provided by the manufacturer.</p> <p>The outer carious dentine is better removed with a round steel bur mounted on a low speed motor or with a manual excavator.</p> <p>Proximal surface is more difficult to preserve than with the sonic device with regard to the effectiveness of the ultrasonic vibrations.</p> <p>The effectiveness of the device depends on the hardness of the dental tissue.</p> <p>Operator-dependent.</p>	<p>Requires specific type of water cooled handpiece.</p> <p>The effectiveness of the device depends on the hardness of the dental tissue.</p> <p>Operator-dependent.</p>	<p>Efficiency with regard to the caries risk assessment.</p> <p>Operator dependent.</p> <p>Perfect filling remains difficult to control with slot and tunnel cavities.</p> <p>The thickness limit of the marginal ridge remains unknown for tunnel and slot cavities.</p>

Table 12. Different types of MIT1 (no preparation except tissue conditioning) and MIT2 with minimal preparation^{3,57}

Minimally invasive technique	Type 1: No preparation except tissue conditioning	Type 2: Minimal preparation
Occlusal, vestibular, lingual or palatal surfaces	<p>Fluoride and chlorhexidine varnish (Vivadent, Voco etc.), Glass ionomer varnish (3M, ESPE) MI Paste Plus[®] and GC Tooth Mousse[®] (GC, Tokyo, Japan)</p> <p>Ozonotherapy coupled with remineralization solution (KaVo, Biberach, Germany). Sealant application</p>	<p>Reversed caries process technique (glass ionomer dentine substitutes, stepwise techniques).</p> <p>Minimally invasive preparation with micro-burs or other techniques (air abrasion, laser, sonic or ultrasonic inserts, adhesive preparation).</p>
Proximal surface	<p>Fluoride and chlorhexidine varnish (Vivadent, Voco etc.), Glass ionomer varnish (3M, ESPE) MI Paste Plus[®], GC Tooth Mousse[®] (GC, Tokyo, Japan)</p> <p>Resin Infiltrant: Icon[®] (DMG, Hamburg Germany)</p>	<p>Reversed caries process technique (glass-ionomer dentine substitutes, stepwise techniques) with minimally invasive Class II preparation.</p> <p>One-step minimally invasive Class II preparation with micro-burs or other techniques (air abrasion, laser, sonic or ultrasonic inserts, adhesive preparation).</p> <p>Slot and tunnel cavities with suitable sonic inserts. (Caries scale D1-D2 with cavitation).</p>
Diagnosis and treatment aids	<p>Fluorescence: +++; Laser: +++;</p> <p>Electric: ++</p>	<p>Fluorescence/picture: ++++; Transillumination: ++; Laser: -Electric: -</p>

Clinical steps in brief

The following steps should be followed³: (1) demineralize the non-cavitated caries with hydrochloric acid for 2 minutes (Fig. 26), followed by a water rinse for at least 30 seconds; (2) dry the area with an Icon dry

syringe (99% ethanol) solution (Fig. 30), followed by drying with oil- and water-free triplex air; (3) infiltrate the suspicious area with an Icon[®] infiltrant syringe and a suitable approximal tip (Fig. 28). The material will be delivered only on the green side of

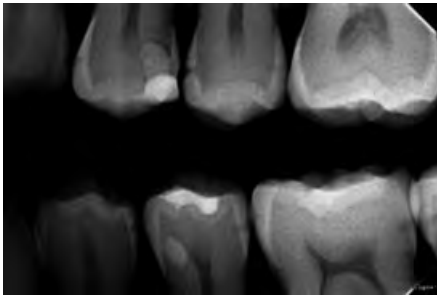


Fig. 18 Proximal mesial decay on the second upper premolar. Minor cavitation of the enamel layer is visible.

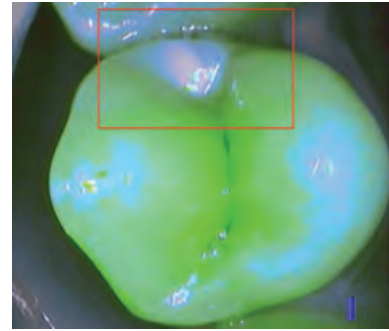


Fig. 22 Blue marginal crest revealing complete destruction of the underlying dentine (red rectangular).



Fig. 19 Soprolife® daylight picture in macro focus mode of the same tooth. The clinical view showed a more complex situation with a plaque stagnation area, a large demineralized enamel area, and two points of entry with one cavitated.

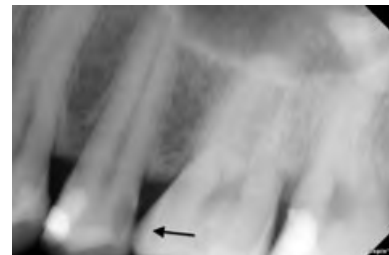


Fig. 23 Enamel decay (black arrow) on mesial side of the first upper molar face the distal one of the second upper premolar. Poor X-ray information.



Fig. 20 Early proximal decay with a visible enamel crack. Soprolife® diagnosis mode.

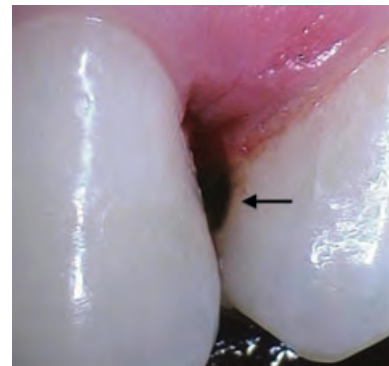


Fig. 24 Front view of proximal decay of a demineralized area of enamel (daylight mode Soprolife®).

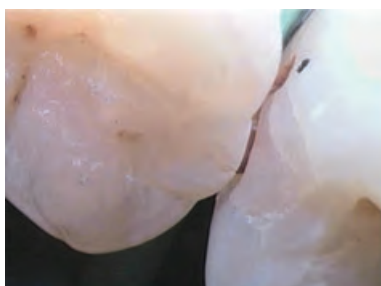


Fig. 21 Enamel cracks and visible enamel breakdown detected due to the high magnification on a proximal distal area.

the approximal tip; (4) light cure the resin infiltrant for 20 seconds, on the occlusal, vestibular and palatal sides, power required 1200 mW/cm²) (Fig. 29).

Minimally invasive treatment type 2

Minimally invasive treatment type 2 (MIT2)^{3,80,81} involves a series of specific tools, including sonic and ultrasonic inserts, to prepare the relevant tooth minimally without damaging the adjacent tooth, even in the case of Class II preparations. The systematic application of a

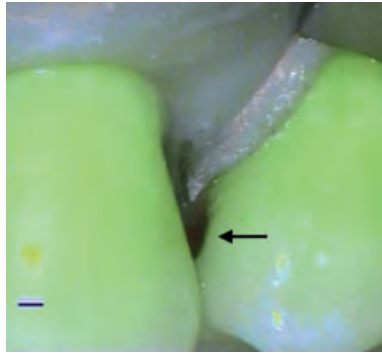


Fig. 25 Confirmation of the green signal fluorescence modification to dark signal (dark arrow) (diagnostic mode Soprolife®).



Fig. 28 Injection of the resin infiltrant through the microporosities of the celluloid matrix.



Fig. 26 Application of hydrochloric acid for 2 minutes with the adapted celluloid matrix.



Fig. 29 Final checking of the nanohybrid composite and the resin infiltration.



Fig. 27 Rinsed and dried with alcohol.

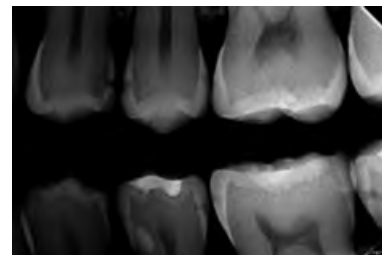


Fig. 30 Numeric bitewing X-ray (Sopix 2®, Soprolife, la Ciotat, France).

metal matrix (Fenderwedge, V ring matrix, USA) before preparation in order to preserve the adjacent surface is recommended even for slot or Class II preparations. The advantages and disadvantages of the ultrasonic system are shown in Table 11. However, these minimal preparations also require systematic use of micro-instrumentation sets developed for minimally invasive dentistry (Kotschy set, Hu-Friedy, Chicago, USA).

Ultrasonic devices

The ultrasonic systems consist of various autoclavable aluminium cassettes and a selection of semi-circular

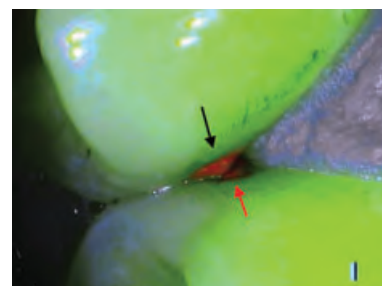


Fig. 31 Palatal view in focus macro-mode (Diagnosis mode, Soprolife®). Black arrow showing the plaque stagnation area, and red arrow showing the visible cavitation of the distal area.

metallic inserts of different types, with one inactive smooth face free of diamond abrasive.^{80,81} The inserts are mounted in a water-cooled ultrasonic handpiece

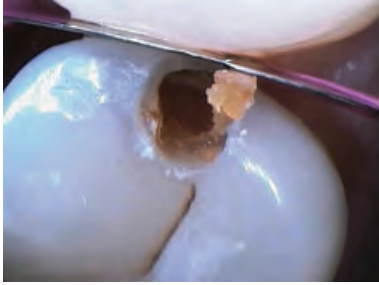


Fig. 32 View of the preparation in daylight mode.



Fig. 33 View of the preparation in fluorescent mode.

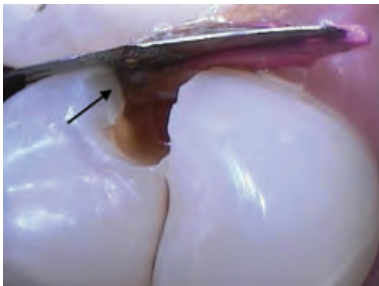


Fig. 34 Observation of the vestibular spreading of the decay under magnification (black arrow).

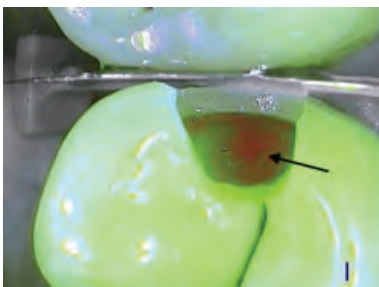


Fig. 35 End of the excavation step. Red fluorescence shadow of sclerotic dentine remained (black arrow).

which emits ultrasonic vibrations (above 20 000 Hertz) (Table 11).

Sonic devices

The sonic insert system is also ergonomically designed.^{80,81} It consists of an autoclavable aluminium



Fig. 36 Proximal area rebuilt with a nanohybrid composite (Empress® composite L shade, Vivadent, Schaan, Liechtenstein).

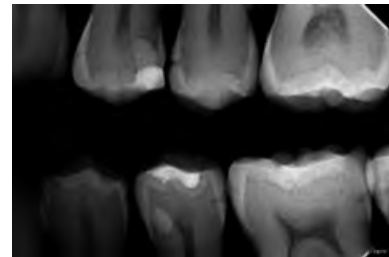


Fig. 37 Numeric bitewing checking (Sopix 2®, Sopro, La Ciotat, France).

cassette and a selection of different semi-circular metallic inserts with one inactive smooth face free of diamond abrasive. The inserts are mounted in a water-cooled handpiece (Kavo® 2003, KaVo Biberach, Germany) that emits sonic vibrations (Power 2; 6000 Hertz, oscillation amplitude: 160 µm). The inserts are selected by the defined angularity of each insert, and the working proximal site (mesial or distal surfaces) (Table 11).

Clinical illustrations

Case 1 minimally invasive Class II preparation

Illumination of the marginal ridge in fluorescence mode gives information about the dentine structure beneath the enamel layer (Fig. 30–37). If the medium third or inner third of the dentine is decayed, the marginal crest reveals a blue reflection most of the time (Fig. 22). In that case, conventional Class II preparation is beneficial.

Case 2 slot preparation^{80,81}

If the fluorescence of the marginal crest remains green, slot or tunnel preparation (Fig. 38–48) can be considered (Fig. 40) subject to the presence of enamel cracks, the residual thickness and the operative difficulties. Fluorescence can also give information about the direction of the decay's point of entry (Fig. 40 and 41). That greatly influences your clinical decision and the operative steps.

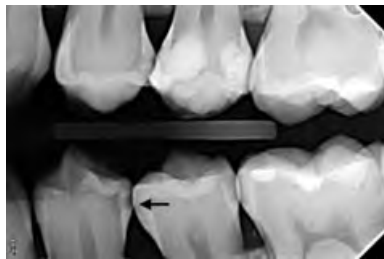


Fig. 38 Bitewing X-rays showing the distal proximal decay on the first lower molar (black arrow).



Fig. 39 Orange-brown shadow revealing the decay through the marginal crest thickness (black arrow).

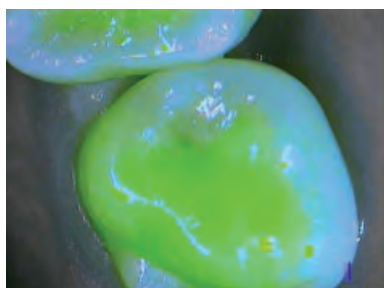


Fig. 40 Fluorescence of the marginal crest appears similar to the healthy one.

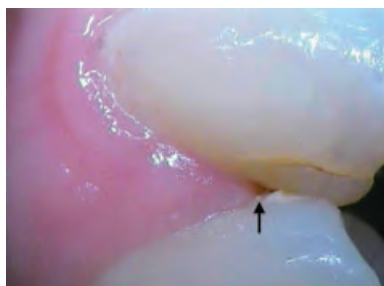


Fig. 41 Vestibular point of entry with a dental plaque accretion.

Operative steps for slot preparation

Slot preparation involves the following steps: (1) fit a protective metal matrix, and use a micro-bur (circular microburs, Komet, France); (2) prepare the slot cavity

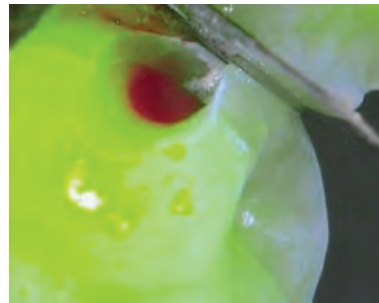


Fig. 42 Infected decay in the heart of the slot preparation looking red when light in fluorescence mode.



Fig. 43 Sonic or ultrasonic diamond insert in action (semi-circular insert, Komet[®], Excavus[®], KaVo[®]).

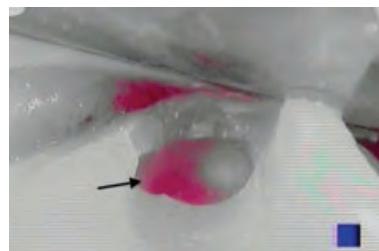


Fig. 44 Half-way checking of the excavation with the Soprocure[®] mode caries. Part of the infected dentine still needed to be removed (Soprocure[®] view, caries mode).

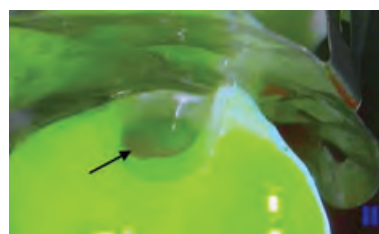


Fig. 45 End step of excavation of the infected dentine. Red fluorescent dentine was partially removed with the combination of ceramic burs (Komet[®]) and sharp hand excavator.

at constant pressure using the sonic or ultrasonic diamond insert; (3) fit the dental rubber dam, remove the infected dentine using a Kotschy micro-excavator, monitoring with a Soprolife[®] camera, and disinfect the dentine (Tubulicid[®] solution, Schorndorf,



Fig. 46 Possible sterilization of the affected dentine with tolonium chloride application for 60 seconds and light activated (60 seconds irradiation) (PAD[®] or photoactivated-disinfection, Dentfotex, UK).⁵⁵



Fig. 47 Lingual view of the slot preparation filled with a hybrid glass ionomer (Fuji II LC[®], GC, Japan) one week later.



Fig. 48 Final check, numeric bitewing X-ray (Sopix 2[®], Acteon; Bordeaux, France).

Germany); (4) form a metal matrix and inject hybrid glass-ionomer cement; and (5) photo-polymerization (3 x 20 seconds), polishing and application of a fluoride varnish.

CONCLUSIONS

The apparent simplicity of these techniques is, in most clinical situations, counterbalanced by implementation difficulties and by operating conditions which are much more complex than they appear. Without the different diagnostic and treatment aids, as described, the work could be even more difficult than expected. Nevertheless, the objectives of preserving the natural tooth structure are achieved by preservation of the

enamel surface for MIT1 intervention and with preservation of the marginal ridge for MIT2 interventions, if a slot cavity could be prepared. Of course longevity of these restorations is ensured simply by working conscientiously, applying the LIFEDT concept and using a dental rubber dam for instance, but would be better accomplished by also applying CaMBRA principles. Nevertheless, more invasive treatments can successfully be delayed by minimal intervention dental therapies. Engaging a fluorescence caries detection camera in clinical cases providing a magnification power of more than 50 demonstrated its usefulness and confirmed that without visual aid the operator reduced his own sensitivity and specificity during the visual inspection. Combining the ultraconservative, restorative approach (which is considered micro-invasive) with a substantial caries risk assessment and caries management with remineralization programme (CaMBRA) may provide therapeutic benefits and will significantly reduce both long-term restorative needs and costs, thus complementing the overall concept of MID.

DISCLOSURE

The authors have no conflicts of interest to declare.

REFERENCES

1. Axelsson P. In: Diagnosis and risk prediction of dental caries. Volume 2. Chicago: Quintessence Publishing Co. Inc., 1999:32–40.
2. Silverstone LM, Hicks MJ, Featherstone MJ. Dynamic factors affecting lesion initiation and progression in human dental enamel. The dynamic nature of enamel caries. *Quintessence Int* 1988;19:683–711.
3. Weisrock G, Terrer E, Couderc G, *et al.* Naturally aesthetic restorations and minimally invasive dentistry. *J Minim Interv Dent* 2011;4:23–35.
4. Rechmann P, Charland D, Rechmann BMT, Featherstone JDB. Performance of laser fluorescence devices and visual examination for the detection of occlusal caries in permanent molars. *J Biomed Optics* 2012;17:036006:1-15.
5. Fisher J, Glick M. A new model for caries classification and management. *The FDI World Dental Federation Caries Matrix*. *JADA* 2012;143:546–551.
6. Mitropoulos CM. The use of fibre-optic transillumination in the diagnosis of posterior approximal caries in clinical trials. *Caries Res* 1985;19:379–384.
7. Deery C, Care R, Chesters R, Huntington E, Stelmachonoka S, Gudkina Y. Prevalence of dental caries in Latvian 11- to 15-year-old children and the enhanced diagnostic yield of temporary tooth separation, FOTI and electronic caries measurement. *Caries Res* 2000;34:2–7.
8. Cortes DF, Ellwood RP, Ekstrand KR. An *in vitro* comparison of a combined FOTI/visual examination of occlusal caries with other caries diagnostic methods and the effect of stain on their diagnostic performance. *Caries Res* 2003;37:8–16.
9. Kuhnisch J. An *in vitro* comparison between two methods of electrical resistance measurement for occlusal caries detection. *Caries Res* 2006;40:104–111.

10. Rock WP, Kidd EA. The electronic detection of demineralisation in occlusal fissure. *Br Dent J* 1988;164:243–247.
11. Verdonchot EH, Wenzel A, Truin GJ. Performance of some diagnostic systems in examinations for small occlusal carious lesions. *Caries Res* 1992;26:59–64.
12. Huysmans MC, Longbottom C, Hintze H. Surface-specific electrical occlusal caries diagnosis: reproducibility, correlation with histological lesion depth, and tooth type dependence. *Caries Res* 1998;32:330–336.
13. Lussi A. Comparison of different methods for the diagnosis of fissure caries without cavitation. *Caries Res* 1993;27:409–416.
14. Lussi A, Reich E. The influence of toothpastes and prophylaxis pastes on fluorescence measurements for caries detection *in vitro*. *Eur J Oral Sci* 2005;113:141–144.
15. Hamilton JC, Gregory WA, Valentine JB. DIAGNOdent measurements and correlation with the depth and volume of minimally invasive cavity preparations. *Oper Dent* 2006;31:291–296.
16. Lennon AM, Buchalla W, Rassner B, Becker K, Attin T. Efficiency of 4 caries excavation methods compared. *Oper Dent* 2006;31:551–555.
17. Lennon AM, Attin T, Martens S, Buchalla W. Fluorescence-aided caries excavation, caries detector, and conventional caries excavation in primary teeth. *Pediatr Dent* 2009;31:316–319.
18. Hafström-Björkman U, Sundström F, de Josselin de Jong E, Oliveby A, Angmar-Månsson B. Comparison of laser fluorescence and longitudinal microradiography for quantitative assessment of *in vitro* enamel caries. *Caries Res* 1992;26:241–247.
19. Emami Z, al-Khateeb S, de Josselin de Jong E, Sundström F, Trollsås K, Angmar-Månsson B. Mineral loss in incipient caries lesions quantified with laser fluorescence and longitudinal microradiography. A methodologic study. *Acta Odontol Scand* 1996;54:8–13.
20. al-Khateeb S, ten Cate JM, Angmar-Månsson B, *et al.* Quantification of formation and remineralization of artificial enamel lesions with a new portable fluorescence device. *Adv Dent Res* 1997;11:502–506.
21. al-Khateeb S, Oliveby A, de Josselin de Jong E, *et al.* Laser fluorescence quantification of remineralisation *in situ* of incipient enamel lesions: influence of fluoride supplements. *Caries Res* 1997;31:132–140.
22. Garcia J, Mandelis A, Abrams SH, Matvienko A. Photothermal radiometry and modulated luminescence: application to dental caries detection. In: J Popp, VV Tuchin, A Chiou, SH Heineemann, eds. *Handbook of Biophotonics. Volume 2. Photonics for Health Care.* Wiley-VCH, 2011:1047–1052.
23. Hellen A, Mandelis A, Finer Y, Amaechi BT. Quantitative remineralization evolution of artificially demineralized human enamel using photothermal radiometry and modulated luminescence. *J Biophotonics* 2011;4:788–804.
24. Hellen A, Mandelis A, Finer Y, Amaechi BT. Quantitative evaluation of simulated human enamel caries kinetics using photothermal radiometry and modulated luminescence. *J Biomed Optics* 2011;16:071406:1-13.
25. Hellen A, Matvienko A, Mandelis A, Finer Y, Amaechi BT. Optothermophysical properties of demineralized human dental enamel determined using photothermally generated diffuse photon density and thermal-wave fields. *Appl Opt* 2010;49:6938–6951.
26. Terrer E, Koubi S, Dionne A, *et al.* A new concept in restorative dentistry: light-induced fluorescence evaluator for diagnosis and treatment: Part 1 – diagnosis and treatment of initial occlusal caries. *J Contemp Dent Pract* 2009;10:86–94.
27. Terrer E, Raskin A, Koubi S, *et al.* A new concept in restorative dentistry: LIFEDT–light induced fluorescence evaluator for diagnosis and treatment. Part 2 – treatment of dentinal caries. *J Contemp Dent Pract* 2010;11:1–12.
28. Salehi H, Terrer E, Panayotov I, *et al.* Functional mapping of human sound and carious enamel and dentin with Raman spectroscopy. *J Biophotonics* 2012 Sept 19. doi: 10.1002/jbio.201200095:1-11. [Epub ahead of print.]
29. Levallois B, Terrer E, Panayotov Y, *et al.* Molecular structural analysis of carious lesions using micro-Raman spectroscopy. *Eur J Oral Sci* 2012;120:444–451.
30. Panayotov I, Terrer E, Salehi H, Tassery H, Yachouh J, Cuisinier FJ, Levallois B. *In vitro* investigation of fluorescence of carious dentin observed with a Soprolife® camera. *Clin Oral Investig* 2012 Aug 2. [Epub ahead of print.]
31. Gugnani N, Pandit IK, Srivastava N, Gupta M, Gugnani S. Light induced fluorescence evaluation: a novel concept for caries diagnosis and excavation. *J Conserv Dent* 2011;14:418–422.
32. Jablonski-Momeni A, Liebegall F, Stoll R, Heinzel-Gutenbrunner M, Pieper K. Performance of a new fluorescence camera for detection of occlusal caries *in vitro*. *Lasers Med Sci* 2012 Mar 21. [Epub ahead of print.]
33. Seremidi K, Lagouvardos P, Kavvadia K. Comparative *in vitro* validation of VistaProof and DIAGNOdent pen for occlusal caries detection in permanent teeth. *Oper Dent* 2012;37:234–245.
34. Fried D, Xie J, Shafi S, *et al.* Imaging caries lesions and lesion progression with polarization sensitive optical coherence tomography. *J Biomed Opt* 2002;7:618–627.
35. Jones RS, Staninec M, Fried D. Imaging artificial caries on the occlusal surfaces with polarization-sensitive optical coherence tomography. *Caries Res* 2006;40:81–89.
36. Jones RS, Fried D. Remineralization of *in vitro* dental caries assessed with polarization-sensitive optical coherence tomography. *J Biomed Opt* 2006;11:014016.
37. Hall A, Girkin JM. A review of potential new diagnostic modalities for caries lesions. *J Dent Res* 2004;83 Spec No C:89–94.
38. Domejean-Orliaguet S, Banerjee A, Gaucher C, *et al.* Minimal intervention treatment plan. Practical implementation in general dental practice. *J Minim Interv Dent* 2009;2:103–123.
39. Midentistry cc. MI compendium of systematic reviews. Available at: www.mi-compendium.org.
40. Mickenautsch S. Adopting minimum intervention in dentistry: diffusion, bias and the role of scientific evidence. *Int Dent SA* 2009;11:16–26.
41. Mickenautsch S. Systematic reviews, systematic error and the acquisition of clinical knowledge. *BMC Med Res Methodol* 2010;10:53–62.
42. Featherstone JDB, Domejean-Orliaguet S, Jenson L, *et al.* Caries assessment in practice for age 6 through adult. *J Calif Dent Assoc* 2007;35:703–707.
43. Jenson L, Budenz AW, Featherstone JD, Ramos-Gomez FJ, Spolsky VW, Young DA. Clinical protocols for caries management by risk assessment. *J Calif Dent Assoc* 2007;35:714–723.
44. Ekstrand KR. Improving clinical visual detection-potential for caries clinical trials. *J Dent Res* 2004;83(Spec Iss C):C67–C71.
45. Ismail AI, Sohn W, Tellez M, Amaya *et al.* The International Caries Detection and Assessment System (ICDAS): an integrated system for measuring dental caries. *Community Dent Oral Epidemiol* 2007;35:170–178.
46. Beltran-Aguilar ED, Barker LK, Canto MT, *et al.* Surveillance for dental caries, dental sealants, tooth retention, edentulism and enamel fluorosis—United States, 1988–1994 and 1999–2002. *MMWR Surveill Summ* 2005;54.
47. Bentley LP. Disparities in children’s oral health and access to care. *J Calif Dent Assoc* 2007;35:618–623.
48. Kopycka-Kedzierawski DT, Bell CH, Billings RJ. Prevalence of dental caries in Early Head Start children as diagnosed using teledentistry. *Pediatr Dent* 2008;30:329–333.

Journal of Biomedical Optics

SPIDigitalLibrary.org/jbo

Performance of laser fluorescence devices and visual examination for the detection of occlusal caries in permanent molars

Peter Rechmann
Daniel Charland
Beate M. T. Rechmann
John D. B. Featherstone

Performance of laser fluorescence devices and visual examination for the detection of occlusal caries in permanent molars

Peter Rechmann,^a Daniel Charland,^b Beate M. T. Rechmann,^a and John D. B. Featherstone^a

^aUniversity of California at San Francisco, School of Dentistry, Department of Preventive and Restorative Dental Sciences, San Francisco, California 94143

^bUniversity of California at San Francisco, Division of Pediatric Dentistry, School of Dentistry, San Francisco, California 94143

Abstract. The aim of this study was to evaluate the diagnostic capabilities of a laser fluorescence tool DIAGNOdent (KaVo, Biberach, Germany) and two light-emitting diode fluorescence tools—Spectra Caries Detection Aid (AIR TECHNIQUES, Melville, NY), and SOPROLIFE light-induced fluorescence evaluator in daylight and blue fluorescence mode (SOPRO, ACTEON Group, La Ciotat, France)—in comparison to the caries detection and assessment system (ICDAS-II) in detection of caries lesions. In 100 subjects (age 23.4 ± 10.6 years), 433 posterior permanent unrestored teeth were examined. On the occlusal surfaces, up to 1066 data points for each assessment method were available for statistical evaluation, including 1034 ICDAS scores (intra-examiner kappa = 0.884). For the SOPROLIFE tool, a new caries-scoring system was developed. Per assessment tool each average score for one given ICDAS code was significantly different from the one for another ICDAS code. Normalized data linear regression revealed that both SOPROLIFE assessment tools allowed for best caries score discrimination followed by DIAGNOdent and Spectra Caries Detection Aid. The area under the receiver operating characteristics curve calculations showed the same grading sequence when cutoff point ICDAS codes 0-1-2 were grouped together. Sensitivity and specificity values at the same cutoff were calculated (DIAGNOdent 87/66, Spectra Caries Detection Aid 93/37, SOPROLIFE 93/63, SOPROLIFE blue fluorescence 95/55.) © 2012 Society of Photo-Optical Instrumentation Engineers (SPIE). [DOI: 10.1117/1.JBO.17.3.036006]

Keywords: caries detection; in vivo; precavitated lesions; fluorescence; ICDAS II; DIAGNOdent; Spectra Caries Detection Aid; SOPROLIFE daylight and blue fluorescence.

Paper 11667 received Nov. 12, 2011; revised manuscript received Dec. 29, 2011; accepted for publication Dec. 29, 2011; published online Mar. 22, 2012.

1 Introduction

Current commonly used caries detection methods in the United States include visual inspection, tactile use of the explorer, and radiographs. Studies in Europe have shown that the explorer is only correct less than 50% of the time.¹ Radiographs are good for interproximal caries, but ineffective in detecting occlusal caries before it is well into the dentin due to the amount of sound tissue attenuating the beam.² By the time an occlusal caries lesion is detectable radiographically, it is too large to be remineralized. If carious lesions are detected early enough, intervention methods, such as fluoride application, sealants, preventive resin restorations, laser treatment, and antibacterial therapy, can be applied to reverse the caries process.²

To successfully apply Caries Management by Risk Assessment (CAMBRA)³⁻⁹ the correct diagnosis of the demineralization status (caries level) of the tooth is required. In its early stage, caries detection and diagnosis remain difficult.

Visual inspection can be subjective based on clinician experience and training. Standardized visual inspection systems should be adopted to avoid inconsistencies amongst diagnoses from different dentists. The International Caries Detection and Assessment System (ICDAS) provides a standardized method of lesion detection and assessment, leading to caries diagnosis.¹⁰

Longitudinal monitoring of lesions has been difficult due to the lack of appropriate diagnostic techniques, i.e., techniques with high sensitivity and specificity that accurately reflect the slow lesion progression. The aim is to arrest or reverse the disease process and to intervene before operative restorative dentistry is needed.

All methods for detection and quantification of dental caries require certain conditions: they have to meet all safety regulations; detect early shallow lesions; differentiate between shallow and deep lesions; give a low proportion of false positive readings; present data in a quantitative form so that activity can be monitored; be precise so that measurements can be repeated by several operators; be cost-effective and user-friendly.

There are several novel early caries detection methods of which some are commercially available. Fiber-optic transillumination (FOTI) is a technique that uses light transmission through the tooth¹¹⁻¹³ and has been available on the market for more than 40 years. A recently marketed method based upon the same principles as FOTI is the digitized DIFOTI method. The images can be stored for later retrieval and comparative examination. Only limited research has so far been performed.¹⁴⁻¹⁶

Fluorescence is a property of some manmade and natural materials that absorb energy at certain wavelengths and emit light at longer wavelengths. Several caries detection methods engage fluorescence. When a caries lesion in enamel and dentin

Address all correspondence to: Peter Rechmann, University of California, School of Dentistry, 707 Parnassus Avenue, San Francisco, California 94143. Tel: +415 514 3225; Fax: 415 476 0858; E-mail: rechmannp@dentistry.ucsf.edu.

is illuminated with, for instance, red laser light (655 nm), organic molecules that have penetrated porous regions of the tooth, especially metabolites from oral bacteria, will create an infrared (IR) fluorescence. The enamel is essentially transparent to red light. The IR fluorescence is believed to originate from porphyrins and related compounds from oral bacteria.^{17–20}

In case of the DIAGNOdent tool (KaVo) the emitted light is channeled through the handpiece to a detector and presented to the operator as a digital number. A higher number indicates more fluorescence and by inference a more extensive lesion below the surface. The system has shown good performance and reproducibility for detection and quantification of occlusal and smooth surface carious lesions in *in vitro* studies,^{17,21,22} but with somewhat more contradictory results *in vivo*, both in the primary and permanent dentition.^{23–29} It has also been tried for longitudinal monitoring of the caries process and for assessing the outcome of preventive interventions.³⁰

The phenomenon of tooth auto fluorescence has long since been suggested to be useful as a tool for the detection of dental caries.³¹ An increased porosity due to a subsurface enamel lesion, occupied by water, scatters the light either as it enters the tooth or as the fluorescence is emitted, resulting in a loss of its natural fluorescence. Consequently the demineralized area appears opaque. The strong light scattering in the lesion leads to shorter light path than in sound enamel, and the fluorescence becomes weaker. The quantitative light-induced fluorescence (QLF) method that recently came on the market (Inspektor™ Pro) in several countries can readily detect lesions to a depth of approximately 500 μm on smooth and occlusal enamel surfaces. The QLF method has been tested in several *in vitro*,^{32–34} *in situ*,³⁵ and *in vivo*^{36–41} studies for smooth surface caries lesions. The possibility of adapting the QLF method for occlusal caries diagnosis is under investigation.⁴²

The Spectra Caries Detection Aid system aids in the detection of caries using fluorescence technology light-emitting diodes (LED) projecting high-energy light onto the tooth surface causing cariogenic bacteria to fluoresce red and healthy enamel green.

The SOPROLIFE system is thought to combine the advantages of a visual inspection method (high specificity) with a high-magnification oral camera and a laser fluorescence device (high reproducibility and discrimination). This technique is based on the light-induced fluorescence evaluator, diagnostic and treatment (LIFE DT) concept.^{43,44}

The electronic caries measurement (ECM) technique is centered on the theory that sound dental hard tissue, especially the enamel, shows high electrical resistance or impedance. Demineralized enamel becomes porous, and the pores fill with saliva, water, microorganisms, etc. The more demineralized the tissue, the lower the resistance becomes. Site-specific measurements have been evaluated in a number of *in vitro* studies^{45–48} and *in vivo* studies.^{49,50} Surface-specific electrical conductance measurements have been investigated under *in vitro* conditions,⁵¹ which showed moderate sensitivity and specificity.

Optical coherence tomography (OCT) is a nonionizing imaging technique that can produce cross-section images of biologic tissues such as ocular, intravascular, gastrointestinal, epidermal, soft oral tissues, and teeth.^{52–56} OCT can produce two- or three-dimensional images of demineralized regions in dental enamel. When a tooth with a carious lesion is illuminated with infrared light at 1310 nm, OCT technology can produce a quantitative image of the subsurface lesion to the full depth of the enamel.^{57,58} Polarized sensitive OCT (PS-OCT)

can be correlated with the degree of demineralization and lesion severity.^{57,59} A potential utility for the system is monitoring *in vivo* caries lesion changes.

Up to now all available caries diagnostic tools have limitations due to low sensitivity, specificity, or usefulness. The aim of the study presented here was to evaluate the diagnostic capabilities of three successfully marketed caries lesion detection tools—a laser fluorescence tool (DIAGNOdent) and two LED fluorescence tools (Spectra Caries Detection Aid system and SOPROLIFE daylight and blue fluorescence tool)—in comparison to the ICDAS II system in detection of caries lesions.

2 Materials and Methods

2.1 Study Inclusion and Exclusion Criteria

Approval for the study was obtained from the Committee on Human Research at UCSF (IRB approval number: 10-01869). Prior to enrollment of each subject into the study, an independent dental examiner, not otherwise involved in the study, conducted a clinical examination to assess caries status and to determine an appropriate treatment plan (treatment decisions will not be reported in this paper). An intraoral exam, review of intraoral radiographs, medical history, and definitive dental history were also completed.

Inclusion criteria to be eligible for the study were a subject age of 13 years and older, having no occlusal restorations and fissure sealants on at least one molar or bicuspid, and having at least one untreated molar or bicuspid surface presenting an ICDAS II score zero to five (one tooth with ICDAS II score six was included).

Subjects had to be healthy and willing to sign the “Authorization for Release of Personal Health Information and Use of Personally Unidentified Study Data for Research” form. There were no gender restrictions.

Subjects were excluded from the study if they were suffering from systemic diseases, had a significant past or medical history with conditions that may affect oral health (i.e., diabetes, HIV, heart conditions that require antibiotic prophylaxis), or were taking medications that may affect the oral flora (e.g., antibiotic use in the past three months).

Subjects who met the selection criteria were asked to provide verbal/written assent/consent themselves and/or their parent/guardian.

One hundred subjects were recruited for the study, comprising 58 females and 42 males with an average age of 23.4 ± 10.6 years, ranging from 13.0 to 58.3 years. Fifty percent of the subjects were aged 13 to 20, 28% were 21 to 30, and 22% were 31 to 60 years old. Figure 1 demonstrates the age distribution.

In the 100 enrolled subjects, 433 posterior teeth were examined, including 90 bicuspid and 343 molars. On each tooth, if a score could be given up to five fissure areas were separately evaluated per tooth, comprising the mesial, central, and distal parts of the fissure as well as lingual and buccal fissure areas.

2.2 Tooth Cleaning

Before evaluating the occlusal surfaces, the 433 teeth were cleaned with a sodium-bicarbonate powder-cleaning tool (Air Max air-polisher with ProphyPen; SATELEC, ACTEON Group, Merignac, France) for five to 10 sec per tooth and then carefully rinsed to remove the powder remnants from

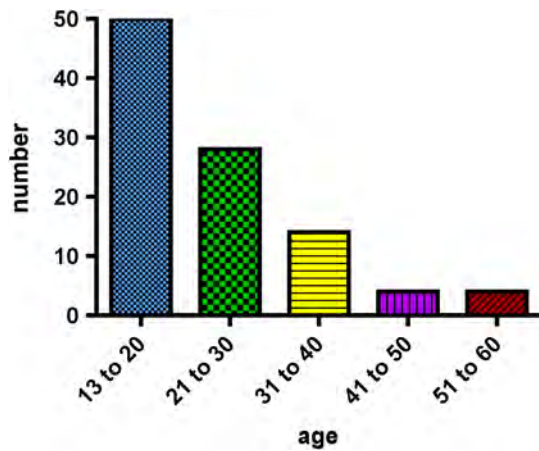


Fig. 1 Age distribution of 100 subjects: 50 subjects were 13 to 20 years old; 28 subjects were 21 to 30 years; 14 subjects were 31 to 40 years; four subjects were 41 to 50 years; and four subjects were 51 to 60 years old.

the fissure with an air-water spray. Cotton roles were placed and the occlusal surface was shortly air-dried (three seconds per tooth) immediately before performing an assessment.

2.3 Caries Lesion Assessment

In this study five different caries assessments were performed. The applied carious lesion assessment methods and number of scores given per tool were as follows:

2.3.1 Visual examination and assessment using ICDAS II criteria

The ICDAS II provides a standardized method of lesion detection and assessment, leading to caries diagnosis.¹⁰ ICDAS II assigns scores to lesions based on apparent caries status and lesion severity of plaque-free teeth when visualized wet and when air-dried.¹⁰

Of particular interest to this study were the coronal primary caries detection criteria. The two examiners (DC, PR) were blinded to each other's evaluation results. After independently scoring for ICDAS II, the examiners discussed their findings and agreed on one ICDAS II score per different areas of the tooth. A total of 1034 ICDAS II scores were agreed on for all 433 examined teeth.

2.3.2 Bitewing digital radiographs

On 176 available digital bitewing radiographs (Kodak 2200 Intraoral x-ray system, dental x-ray position indicating device, Kodak RVG 6100 Digital Radiography System by Kodak Dental System, Carestream Health, Atlanta, GA; image storage on Dell Optiplex 755, Dell, Round Rock, TX), a total of 519 areas could be evaluated. Evaluated areas on the x-rays were the mesial and distal approximal and the occlusal areas. Noted was no caries, caries up to 50% in enamel in direction to the dentin enamel junction (DEJ), caries deeper than 50% to the DEJ, caries in dentin up to 50% into dentin (halfway to the pulp), and deeper than 50% into dentin.

2.3.3 DIAGNOdent laser fluorescence

The DIAGNOdent Classic tool (KaVo, Biberach, Germany) emits a red laser light (wavelength 655 nm) and measures

the returning fluorescence in the spectral region >680 nm wavelength. Before assessing a new subject the tool was calibrated according to manufacturer's instruction.

The highest score per evaluated fissure area was noted (scores ranged from zero to 99). About 1041 DIAGNOdent scores were registered from the 433 occlusal surfaces (DC and PR agreed-on scores).

2.3.4 Spectra Caries Detection Aid

The Spectra Caries Detection Aid system uses six blue-violet LEDs emitting at 405-nm wavelength to produce fluorescence pictures. The fluorescence from the tooth is collected by a camera system. Depending on the fluorescence intensity, an on-screen color and a number scale are assigned by the system (Spectra Visix score). The displayed colors are green, blue, red, orange, and yellow; the displayed numbers range from 1.0 (blue) to >3.0 (yellow); the numbers collected in the study ranged from 1 to 3.9; no number given by the system for an examined fissure was scored as zero. A 10-mm distance spacer and the Spectra handpiece disposable camera covers were used (both AIR TECHNIQUES). To collect and store the images and Spectra Visix scores the Visix imaging software was used. A HP 620 Notebook (HP, Palo Alto, CA; Windows 7, Microsoft Redmond, WA) was used to collect the data. A total of 1039 Spectra Visix scores were noted for the 433 occlusal surfaces.

2.3.5 SOPROLIFE light induced fluorescence evaluator

The SOPROLIFE light induced fluorescence evaluator system operates in daylight and in blue fluorescence mode. In the daylight mode, the system uses four white LEDs; in the fluorescence mode it uses four blue LEDs emitting a wavelength of 450 nm. The handpiece allows for collecting pictures at different distances to a tooth resulting in different magnifications (from lowest to highest magnification: extra-oral, intra-oral, LIFE, macro preset position). In this study the system was used in the LIFE magnification mode with daylight or fluorescence detection mode I—diagnosis aid mode—utilizing the disposable intraoral protection sheets and the intraoral tip. The images were recorded with the SOPRO IMAGING software. A HP 620 Notebook was used to collect the data.

At total of 1066 SOPROLIFE daylight mode scores and 1064 SOPROLIFE blue fluorescence mode scores were assigned to the 433 occlusal surfaces. The newly developed scoring system will be explained in the result section.

2.4 Statistical Analyses

The data were analyzed by multiple statistical methods (One-way ANOVA, Newman-Keuls multiple comparison test, linear regression analysis, area under the receiver operating characteristics (AROC), sensitivity and specificity calculations with regards to cutoff points) to compare results from the laser fluorescence device (DIAGNOdent), the SOPROLIFE daylight and fluorescence mode evaluation, the Spectra Caries Detection Aid system, with the visual inspection method (ICDAS II) and digital bitewing x-rays.

The inter-examiner reliability (DC, PR) for the ICDAS II scoring was assessed with a kappa = 0.884, SE of kappa = 0.017, 95% confidence interval from 0.851 to 0.917, 571 observations. The strength of agreement is considered to be "very good."⁶⁰ The weighted Kappa was calculated at

kappa = 0.905 using linear weighting. Assessed this way, the strength of agreement is considered to be “very good.”⁶⁰

3 Results

All results from caries assessment tool will first be presented separately. Then the relationship between ICDAS II scores and all findings will be described in terms of average score of the tool per ICDAS II code, followed by linear regression fits. Last, area under the receiver operating characteristics curves for overall sensitivity of each detection tool and sensitivity and specificity calculations will be presented.

3.1 Evaluated Scores

3.1.1 ICDAS II scores distribution

On the occlusal surfaces of the 433 evaluated teeth, 110 areas in pits and fissures were scored as sound (code 0). ICDAS II code 1 was given for 450 spots and code 2 for 314 lesions, presenting a total of 764 precavitated lesions. Early cavitation with first visual enamel breakdown—ICDAS code 3—was diagnosed in 107 cases, more progressed carious lesions with code 4 as well as code 5 were each noted 26 times. (One lesion scored with an ICDAS II code 6 was included into the code 5 group when averages were performed; when not, it was left separately [see figure axis].) Figure 2 shows the distribution of ICDAS II score.

3.1.2 Digital bitewing radiographs

On 176 available bitewings, 519 areas were evaluated; 491 of those 519 evaluated areas showed no radiographically detectable caries. Twelve lesions located in the approximal areas in enamel extended less than 50% to the DEJ, one lesion extended further than 50% to the DEJ. Three lesions reached 50% into dentin (two approximal, two occlusal), and 12 reached deeper than 50% into dentin halfway to the pulp (three approximal lesions, nine occlusal areas).

3.1.3 DIAGNOdent laser fluorescence

On the occlusal surfaces of the 433 evaluated teeth in 1041 pits and fissure areas, DIAGNOdent evaluations were performed. Measured values ranged from zero to 99. In the majority of cases (424) values between zero and 10 were recorded, followed by 291 measured spots with values between 11 and 20. The remaining 326 measurements covered values between 21 and

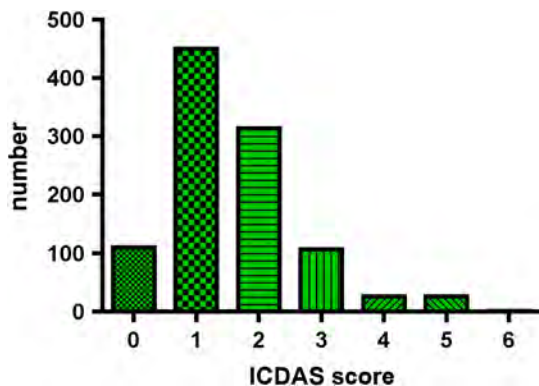


Fig. 2 Distribution of ICDAS II scores, representing 110 sound pits and fissure areas, 764 precavitated lesion scores and 134 progressed lesions.

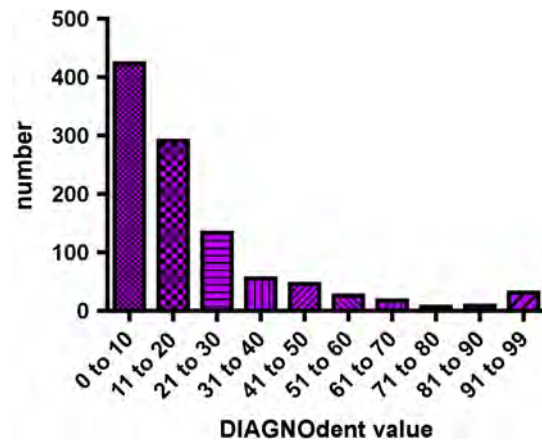


Fig. 3 Distribution of DIAGNOdent values measured in 1041 pits and fissure areas.

99, including 31 areas with a DIAGNOdent value of 99. Figure 3 shows grouping and the detailed distribution of DIAGNOdent scores.

3.1.4 Spectra Caries Detection Aid system

A total of 1039 Spectra Visix scores was noted. A Spectra Visix value of 0 (no value depicted by the Spectra System) was observed 114 times. Values between 1.0 and 1.9 were 739 times displayed, 172 times a value of 2.0 to 2.9 was registered, and 14 times a value between 3.0 and 3.9 was shown with 3.9 as the highest value measured. The Spectra Visix score distribution is depicted in Fig. 4.

3.1.5 SOPROLIFE scores for occlusal fissure areas

From each evaluated tooth, SOPROLIFE daylight and SOPROLIFE blue fluorescence pictures were picked, evaluated for sharpness, and then a categorization was attempted. SOPROLIFE daylight and SOPROLIFE fluorescence pictures for occlusal fissure areas could both be categorized into six different groups each—code 0 to code 5. The categorization followed appearance criteria of the lesion and was performed independently from the registered ICDAS II code. The categorization was led by the idea that width of a lesion related to the confines

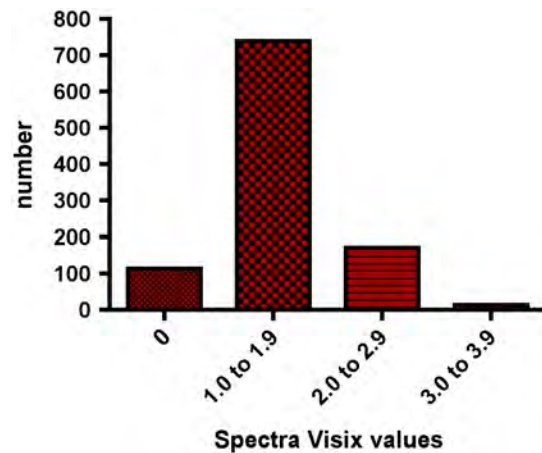


Fig. 4 Distribution of Spectra Visix values measured, with 71% of measured values in the range of 1.0 to 1.9.



Fig. 5 (a) and (b) SOPROLIFE daylight code 0; no visible change in the fissure.

of fissures, difference in color, and intensity of the registered color expressions as well as roughness of the enamel structure, break in enamel with first enamel loss, and finally visible dentin would go along with the progression of a caries lesion. Thus precavitated and cavitated lesions and their development levels were categorized.

SOPROLIFE daylight mode score description and examples. When evaluating occlusal fissure areas in SOPROLIFE daylight mode, code 0 was given for sound enamel with no changes in the fissure area [Figs. 5(a) and 5(b)]. Code 1 was selected if the center of the fissure showed whitish or slightly yellowish change in the enamel. In code 1 change is limited to part or all the base of the pit and fissure system [Figs. 6(a)–6(c)]. For a code 2 the whitish change extends the base of the pit and fissure system and comes up the slopes (walls) of the fissure system toward the cusps. The change is wider than the confines of the fissure and can be seen in part of or all the pit and fissure system. No enamel breakdown is visible [Figs. 7(a)–7(c)]. Code 3 describes fissures with rough and slightly open areas depicting a beginning slight enamel breakdown. Changes are confined to the fissure and do not need to come up the slopes. There are no visual signs of dentin involvement [Figs. 8(a)–8(c)]. In code 4 the caries process is not confined to the fissure width anymore and presents itself much wider than the fissure; the due to caries changed areas have a “mother-of-pearl” glossy appearance [Figs. 9(a)–9(c)]. If there is obvious enamel breakdown with visible dentin code 5 was given [Figs. 10(a)–10(c)]. Table 1

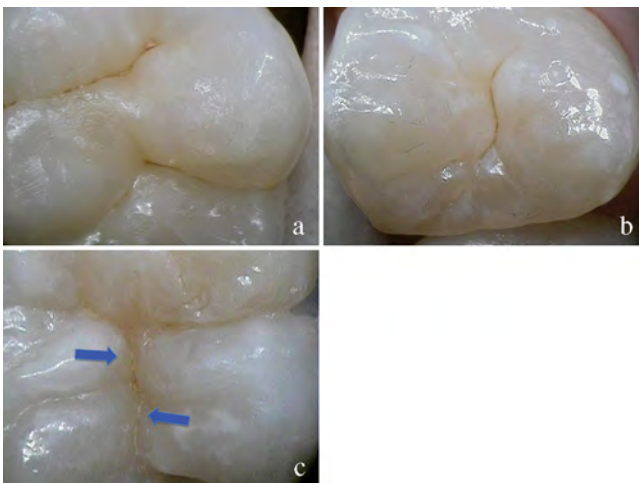


Fig. 6 (a), (b), and (c) SOPROLIFE daylight code 1; center of the fissure showing whitish, slightly yellowish change in enamel, limited to part or all of the base of the pit and fissure system (see blue arrows).

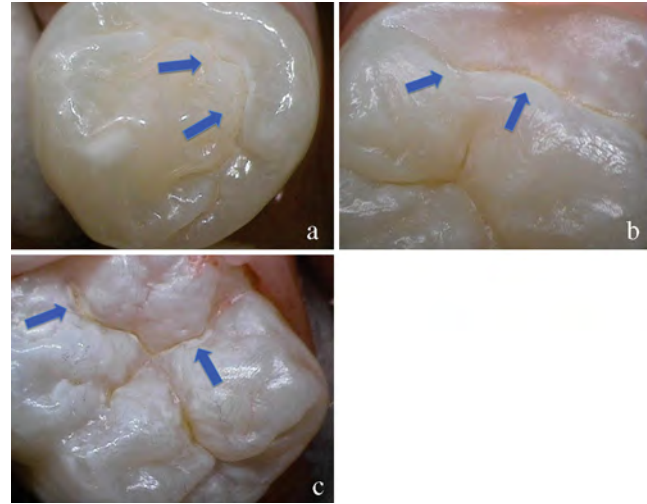


Fig. 7 (a), (b), and (c) SOPROLIFE daylight code 2; whitish change comes up the slopes (walls) toward the cusps; the change is wider than the confines of the fissure, seen in part or all the pit and fissure system, no enamel breakdown is visible (blue arrows mark the changes coming up the slopes).

summarizes the observed changes and the corresponding codes for the SOPROLIFE daylight mode.

SOPROLIFE blue fluorescence mode score description and examples. When evaluating occlusal fissure areas in SOPROLIFE blue fluorescence mode, code 0 was given when the fissure appears shiny green, the enamel appears sound, and there are no visible changes [Fig. 11(a)]. Rarely a graphite-pencil-colored thin shine/line can be observed [Fig. 11(b)]. Code 1 was selected if a tiny, thin red shimmer in the pits and fissure system is observed, which can slightly come up the slopes (walls) of the fissure system. No red dots are visible [Figs. 12(a) and 12(b)]. At code 2, in addition to the tiny, thin red

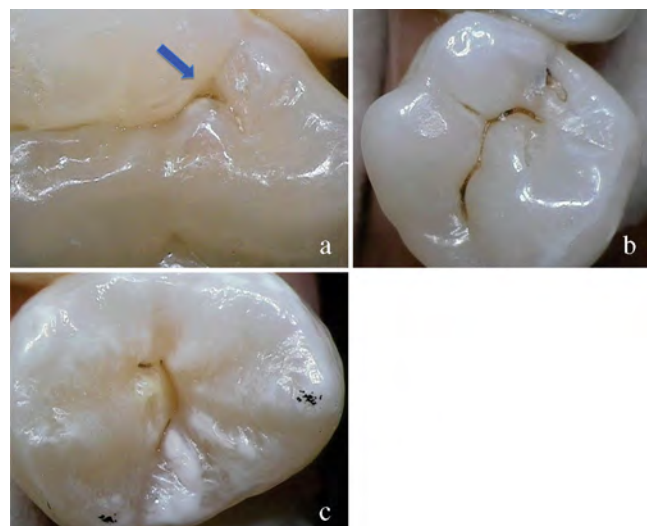


Fig. 8 (a), (b), and (c) SOPROLIFE daylight code 3; fissure enamel is rough and slightly open with beginning slight enamel breakdown; changes are confined to the fissure and do not need to come up the slopes, no visual signs of dentin involvement (blue arrow marks slight enamel loss).

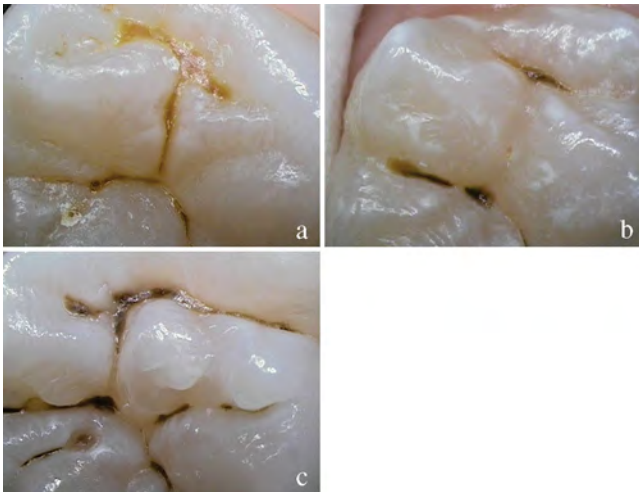


Fig. 9 (a), (b), and (c) SOPROLIFE daylight code 4; caries process is not confined to the fissure width; presents itself much wider than the fissure; changed area has a “mother-of-pearl” glossy appearance.

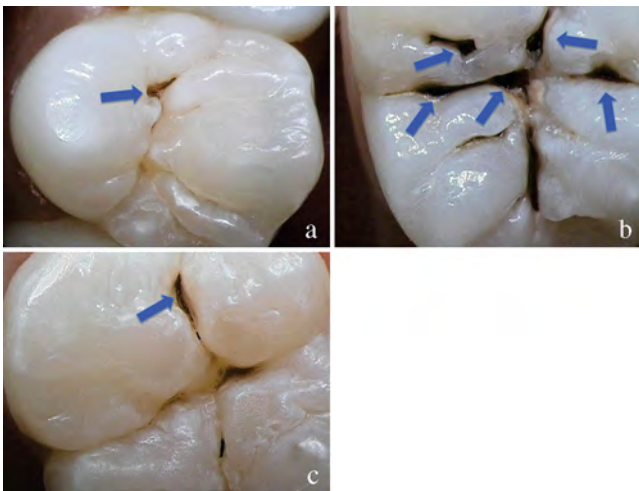


Fig. 10 (a), (b), and (c) SOPROLIFE daylight code 5; enamel breakdown with visible open dentin (arrows mark open dentin).

Table 1 SOPROLIFE daylight codes for coronal caries.

Code	Description
0	Sound, no visible change in the fissure
1	Center of the fissure showing whitish, slightly yellowish change in enamel, limited to part or all of the base of the pit and fissure system
2	Whitish change comes up the slopes (walls) toward the cusps; the change is wider than the confines of the fissure, seen in part or all the pit and fissure system, no enamel breakdown is visible
3	Fissure enamel is rough and slightly open with beginning slight enamel breakdown; changes are confined to the fissure and do not need to come up the slopes, no visual signs of dentinal involvement
4	Caries process is not confined to the fissure width; presents itself much wider than the fissure; changed area has a “mother-of-pearl” glossy appearance
5	Enamel breakdown with visible open dentin

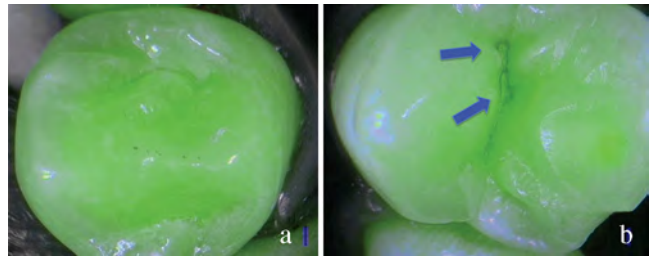


Fig. 11 (a) and (b) SOPROLIFE blue fluorescence code 0; no visible change in enamel (rarely a graphite pencil colored thin shine can be observed—blue arrow mark)

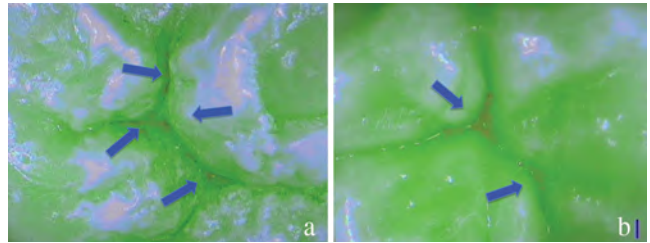


Fig. 12 (a) and (b) SOPROLIFE blue fluorescence code 1; tiny, thin red shimmer in the pits and fissure system can come up the slopes, no red dots visible; arrows mark tiny, thin red shimmer.

shimmer in pits and fissures possibly coming up the slopes, darker red spots confined to the fissure are visible [Figs. 13(a) and 13(b)]. For code 3 dark red spots have extended as lines into the fissure areas but are still confined to the fissures. A slight beginning roughness of the more lined red areas can be visible [Figs. 14(a) and 14(b)]. If the dark red (or red-orange) extends wider than the confines of the fissures, a code 4 was given [Figs. 15(a) and 15(b)]. Surface roughness occurs, possibly grey and/or rough grey zone are visible [Figs. 15(c) and 15(d)]. Code 5 was selected if obvious openings of enamel were seen with visible dentin [Figs. 16(a) and 16(b)]. Table 2 summarizes the observed changes and the corresponding scores for the SOPROLIFE blue fluorescence mode.

Results SOPROLIFE daylight mode. 1066 SOPROLIFE daylight mode scores were assigned to the occlusal surfaces of the 433 study teeth using the newly developed scoring system. The SOPROLIFE daylight scores were assigned evaluating the stored SOPROLIFE pictures from each subject on a MacBookPro 17-inch-screen laptop.

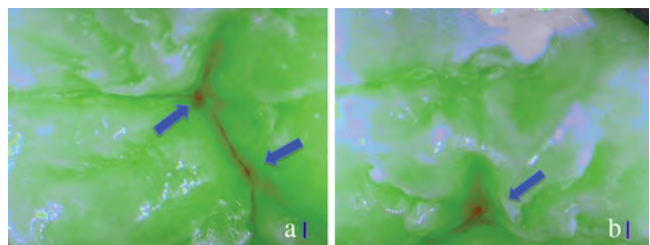


Fig. 13 (a) and (b) SOPROLIFE blue fluorescence code 2; in addition to tiny, thin red shimmer in pits and fissures possibly coming up the slopes darker red spots confined to the fissure are visible; no surface roughness; arrows mark dark red spots.

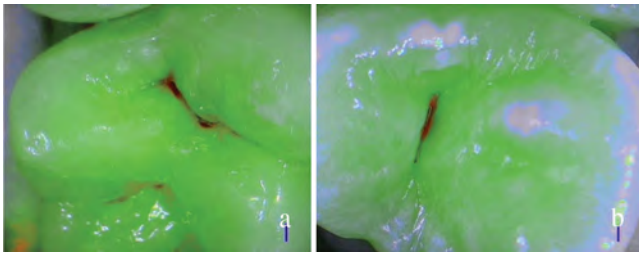


Fig. 14 (a) and (b) SOPROLIFE blue fluorescence code 3; dark red extended areas confined to the fissures; slight beginning roughness possible.

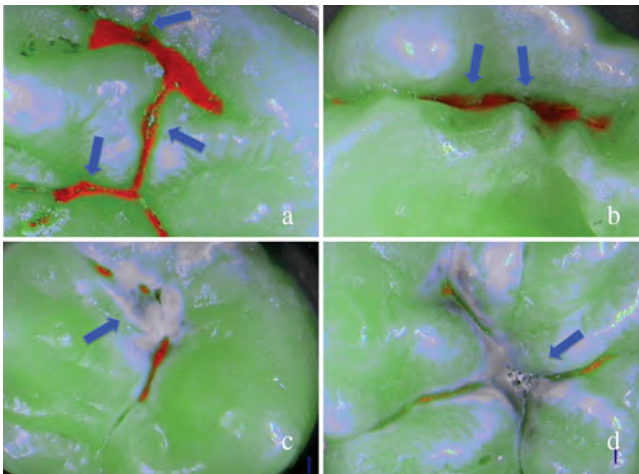


Fig. 15 (a), (b), (c), and (d) SOPROLIFE blue fluorescence code 4; dark red or orange areas wider than fissures; surface roughness occurs, possibly grey or rough grey zone visible; arrows mark surface roughness.

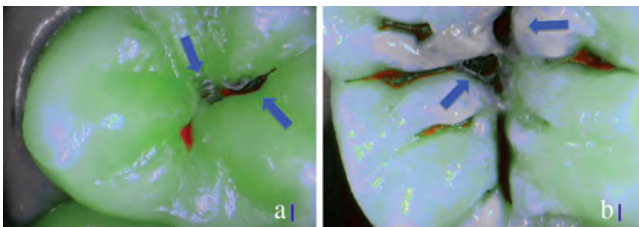


Fig. 16 (a) and (b) SOPROLIFE blue fluorescence code 5; obvious wide openings with visible dentin (arrows).

Table 2 SOPROLIFE blue fluorescence codes for coronal caries.

Code	Description
0	Sound, no visible change in enamel (rarely a graphite-pencil-colored thin shine/line can be observed) shiny green fissure
1	Tiny, thin red shimmer in the pits and fissure system, can come up the slopes, no red dots visible
2	In addition to tiny, thin red shimmer in pits and fissures possibly coming up the slopes darker red spots confined to the fissure are visible
3	Dark red extended areas confined to the fissures; slight beginning roughness
4	Dark red or orange areas wider than fissures; surface roughness occurs, possibly grey or rough grey zone visible
5	Obvious wide openings with visible dentin

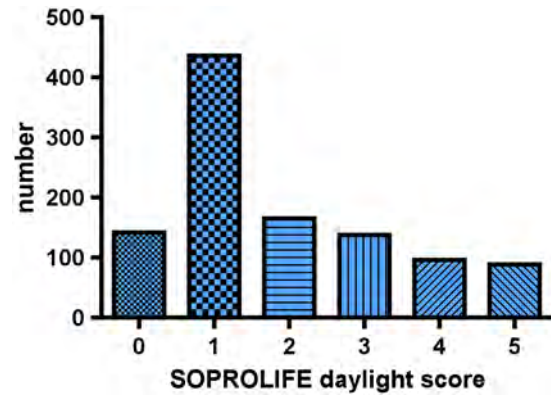


Fig. 17 Distribution of SOPROLIFE daylight scores 0 to 5.

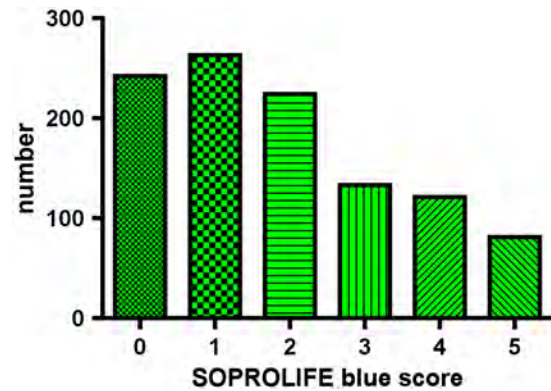


Fig. 18 Distribution of SOPROLIFE blue fluorescence scores.

142 pits and fissure areas were scored as score zero, 436 as score 1, 165 as score 2, 138 as score 3, 96 as score 4, and 89 as score 5 (Fig. 17).

Results SOPROLIFE blue fluorescence mode. 1064 SOPROLIFE fluorescence mode scores were assigned to the occlusal surfaces of the study teeth with the newly developed scoring system. The SOPROLIFE blue fluorescence pictures were also scored on a MacBookPro 17-inch screen. As depicted by Fig. 18, 242 times score zero was given, 263 times score 1 was assigned, 224 times score 2, 133 times score 3, 121 times score 4, and 81 times score 5 was given by the two independent examiners.

3.2 Relationship Between ICDAS II and Other Caries Assessment Scores

The following calculations and graphs demonstrate the score distribution of the different caries assessment tools in relation to the ICDAS II score.

3.2.1 Relationship between ICDAS II and DIAGNOdent values

Figure 19 shows the average registered DIAGNOdent values per each ICDAS II score. ICDAS II scores 0 for “sound” receives an average DIAGNOdent value of 6 ± 4 (mean \pm SD); scores one and two—precavitated lesions—showed DIAGNOdent values of 13 ± 12 and 22 ± 18 , respectively. Cavitated lesions—ICDAS II score three and five—demonstrated average

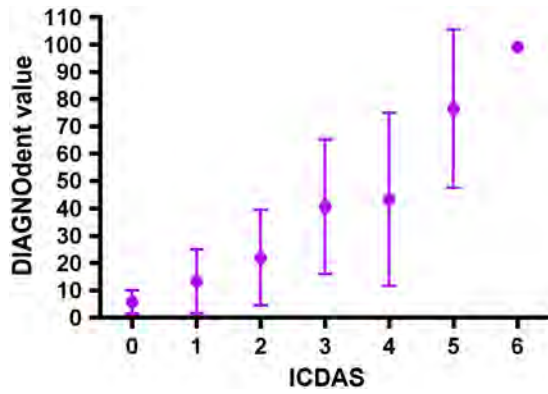


Fig. 19 Distribution of average DIAGNOdent values per ICDAS II score, (mean ± SD).

DIAGNOdent values of 41 ± 25 and 77 ± 29 , respectively. ICDAS II code 4 shows with 43 ± 32 , a similar average value as code 3.

The one-way ANOVA test with Newman-Keuls Multiple Comparison Test revealed that all average DIAGNOdent values for ICDAS II 0, 1, 2, 3, and 5 were statistically significant different from each other with a P value of $P < 0.001$. Only the average DIAGNOdent values comparing ICDAS II score 3 to 4 were not statistically significant different.

3.2.2 ICDAS II and Caries Detection Aid system Spectra Visix values

Figure 20 demonstrates the distribution of the average Spectra Visix values per ICDAS II score. ICDAS II score 0 shows an average Spectra Visix value of 0.7 ± 0.7 (mean ± SD). ICDAS II score 1 and 2 demonstrate average Spectra Visix values of 1.3 ± 0.6 and 1.6 ± 0.5 , respectively. Occlusal surfaces with an ICDAS II score 4 show average values of 2.0 ± 0.6 , and ICDAS II score 5 pits and fissures demonstrate a Spectra Visix value of 2.6 ± 0.6 .

Spectra Visix average values are significantly different from each other for ICDAS II score 0, 1, 3, and 5 with $P < 0.001$, and for score 2 and 4 with $P < 0.05$. Spectra Visix scores for ICDAS II score 3 do not statistically significant differ from those given for ICDAS II score 4.

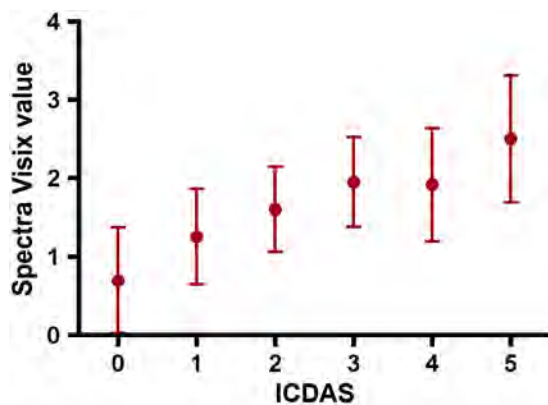


Fig. 20 Distribution of average Spectra Visix per ICDAS II score, (mean ± SD).

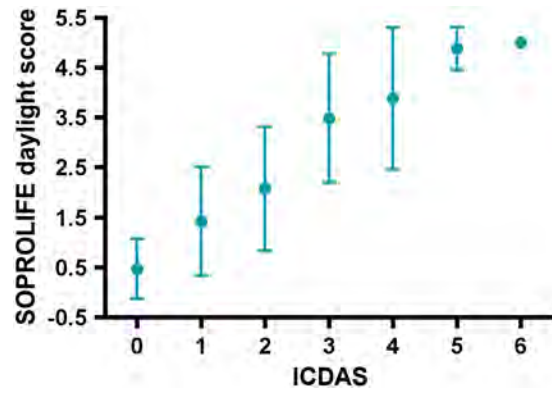


Fig. 21 Distribution of average SOPROLIFE daylight scores per ICDAS II score, (mean ± SD).

3.2.3 Relationship between ICDAS II and SOPROLIFE daylight scores

Figure 21 demonstrates the different ICDAS II scores and the corresponding distribution of the assigned SOPROLIFE daylight scores.

For surfaces, which were scored with ICDAS II code 0—“sound”—a SOPROLIFE daylight average score of 0.47 ± 0.6 (mean ± standard deviation) was given. For precavitated lesions—ICDAS II code 1 and 2—a SOPROLIFE daylight average score of 1.4 ± 1.1 and 2.1 ± 1.2 , respectively, was given.

More severe caries lesions (cavitated) received significant higher scores. An ICDAS II score 3—first visible breakdown of enamel—received a 3.5 ± 1.3 SOPROLIFE daylight score and a carious lesion with visible dentin exposure was scored with an average 4.9 ± 0.4 SOPROLIFE daylight score. The one-way ANOVA test with Newman-Keuls multiple comparison test revealed that all mean SOPROLIFE daylight scores for ICDAS 0, 1, 2, 3, and 5 were statistically significant different from each other with a P value of $P < 0.001$. The average SOPROLIFE daylight score for ICDAS II score 4 (3.9 ± 1.4) was not significantly different from the average for ICDAS score 3 but still significantly different from the average given for ICDAS II score 5 ($P < 0.01$).

3.2.4 Relationship between ICDAS II and SOPROLIFE blue fluorescence scores

Figure 22 demonstrates the different ICDAS II scores and the corresponding distribution of the assigned SOPROLIFE blue fluorescence scores. The distribution patterns are very close

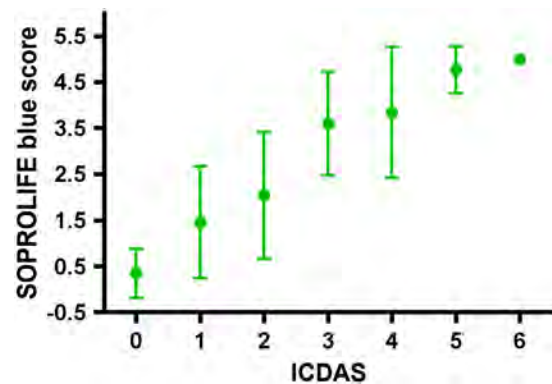


Fig. 22 Distribution of average SOPROLIFE blue fluorescence scores per ICDAS II score, (mean ± SD).

to the above-described patterns for the average SOPROLIFE daylight scores. The average SOPROLIFE blue fluorescence scores differed minimally or not at all from the SOPROLIFE daylight average scores for the different ICDAS II score groups.

An ICDAS II score 0 received an average SOPROLIFE blue fluorescence score of 0.35 ± 0.5 (mean \pm standard deviation)—slightly lower than the SOPROLIFE daylight score (lower by 0.13). For precavitated lesions—ICDAS II score 1 and 2—the SOPROLIFE blue fluorescence scores of 1.5 ± 1.2 and 2.0 ± 1.4 , respectively, were given. The average SOPROLIFE blue fluorescence score for ICDAS II score 3 lesions was 3.6 ± 1.1 . Caries lesions with visible dentin exposure (ICDAS II score 5) were scored with an average 4.8 ± 0.5 score. Again, the one-way ANOVA test with Newman-Keuls Multiple Comparison Test revealed that all mean SOPROLIFE blue fluorescence scores for ICDAS 0, 1, 2, 3, and 5 were statistically significant different from each other with a value of $P < 0.001$.

Similar to the SOPROLIFE daylight scores the average SOPROLIFE blue fluorescence score for ICDAS II score 4 (3.8 ± 1.4) was not significantly different from the average for ICDAS score 3 but still significantly different from the average given for ICDAS II score 5 ($P < 0.01$).

3.3 Linear Regression Fits for Caries Assessment Tools in Relation to ICDAS II Scores

To evaluate for each assessment method the discrimination between two different scores of a system, regression curves were calculated for each caries assessment tool.

The following graph (Fig. 23) combines the linear regression fit for all four assessment tools—DIAGNOdent, SOPROLIFE daylight and blue fluorescence, and Spectra Caries Detection Aid—in relation to the ICDAS scores in one plot. In order to produce this overview, data had to be normalized to achieve a y-axis value range between 0 and 5 (DIAGNOdent values were adjusted with a factor of 0.04x; the other values were not adjusted).

The slopes of the regression lines for all tools are significantly nonzero (SOPROLIFE daylight $P < 0.0001$ and blue fluorescence $P = 0.0002$, DIAGNOdent $P = 0.0022$, Spectra Caries Detection Aid $P = 0.0010$). The slopes of the regression lines are the highest/steepest for both SOPROLIFE assessment methods, followed by DIAGNOdent and Spectra Caries Detection Aid. The slopes of the regression lines are 0.8809 for SOPROLIFE daylight (± 0.04984) and SOPROLIFE blue

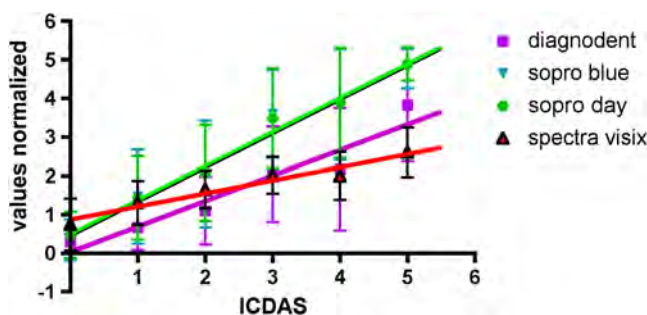


Fig. 23 Linear regression fit for SOPROLIFE daylight and blue fluorescence, DIAGNOdent and Spectra Visix values in respect to ICDAS II scores, all data are normalized.

fluorescence (± 0.06866), 0.6600 (± 0.09479) for DIAGNOdent, and 0.3357 (± 0.03849) for Spectra Caries Detection Aid.

The goodness of fit for SOPROLIFE daylight was $r^2 = 0.9874$, for SOPROLIFE blue fluorescence 0.9763, for DIAGNOdent 0.9238 and for Spectra Visix 0.9501.

3.4 Area Under the Receiver Operating Characteristics Curves

To quantify the overall ability of the different applied caries detection tools to discriminate between those individuals with the disease and those without the disease, we have looked at different ICDAS scores and grouping of ICDAS scores to evaluate the area under the receiver operating characteristics curves (AROC) for DIAGNOdent, SOPROLIFE blue fluorescence, and Spectra Caries Detection Aid.

In the past, caries lesions have typically only been defined as “cavity,” thus our basic approach was to sum all ICDAS values corresponding to no or precavitated lesions together as “healthy” and compare them to the remaining “disease” scores. Thus in the following calculations the values for the different detection tools related to the ICDAS II codes 0, 1, and 2 are placed into one group to represent healthy conditions. Values defined by ICDAS code 3 (first visible enamel breakdown) and higher will be grouped together to represent carious lesions.

In a second approach, values derived only from ICDAS II code 0 locations were compared to all other values. Furthermore, values originated from ICDAS II scores 0 and 1 were summed together in one group as healthy. None of those additional approaches delivered superior results over placing values from ICDAS code 0, 1, and 2 locations into one group. Thus we will only present ROC curves for values originated from summing ICDAS II score 0, 1, and 2 together in one group (ICDAS 0-1-2).

The area under the ROC curve was interpreted by using the following classification:⁶¹ 0.60 to 0.75 = fair; 0.75 to 0.90 = good; 0.90 to 0.97 = very good; and 0.97 to 1.00 = excellent.

The highest area under the ROC curve value, thus the highest overall ability to discriminate between “carious” and “noncarious,” is achieved for the SOPROLIFE blue fluorescence tool with AROC = 0.8854 ± 0.01400 (SE), and a 95% confidence interval of 0.8580 to 0.9128 and a P value < 0.0001 (Fig. 24). This is followed by the SOPROLIFE daylight assessment with an area under the curve value of 0.8779 ± 0.01505 .

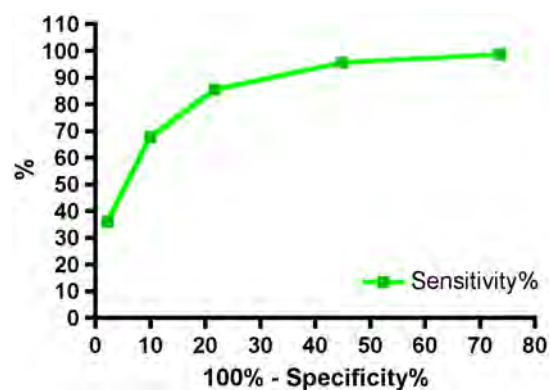


Fig. 24 AROC curve for SOPROLIFE blue fluorescence is 0.8854 ± 0.01400 (SE), 0.8580 to 0.9128 (95% confidence interval) with a P value < 0.0001 .

For the DIAGNOdent tool, the area under the ROC curve was slightly smaller with 0.8700 ± 0.01410 (Fig. 25). The Spectra Visix receives the smallest area under the ROC curve with 0.8186 ± 0.01939 (Fig. 26). Table 3 shows additionally confidence intervals and *P* values for all diagnostic methods.

Using the grouping of ICDAS II code 0-1-2 as “healthy” results in the highest area under the ROC value for the all four diagnostic methods. All methods received an area under the curve value, which is regarded as a “good” overall sensitivity of the diagnostic method.⁶¹

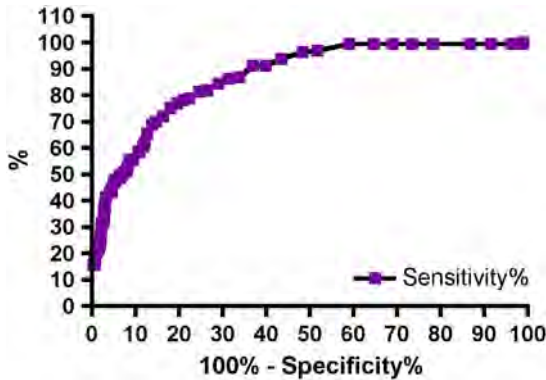


Fig. 25 AROC curve for the DIAGNOdent is 0.8700 (SE), 0.8423 to 0.8976 (95% confidence interval), with a *P* value <0.0001.

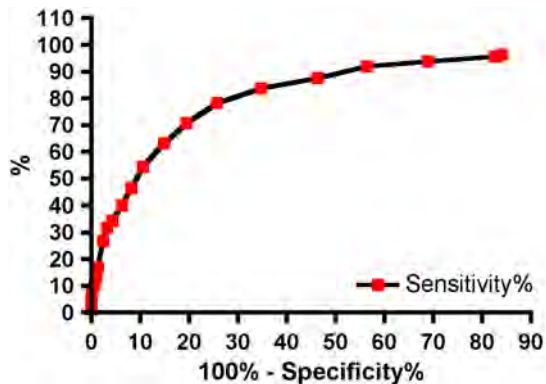


Fig. 26 AROC curve for Spectra Visix is 0.8186 ± 0.01939 (SE), 0.7806 to 0.8566 (95% confidence interval) with a *P* value <0.0001.

3.5 Sensitivity and Specificity of Caries Assessment Tools at Different ICDAS Cutoff Points

In a next step, sensitivity and specificity of all four caries detection systems were calculated. As cutoff point, the corresponding value for ICDAS grouping of score 0, 1, and 2 together as healthy and noncavitated lesions was chosen (Figs. 27–29). Table 4 shows in addition to the average scores (mean \pm standard deviation) for each diagnostic method for the grouping of code 1, 2, and 3 together as overview the average values for ICDAS code 1, 2, and 3, separately. If the value for grouping ICDAS code 0, 1, and 2 is chosen as cutoff point for the sensitivity calculation, the average value for DIAGNOdent is 15.5 with a corresponding sensitivity of 87% and a specificity of 66%. With the same ICDAS cutoff, Spectra Caries Detection Aid at its corresponding cutoff value of 1.3 achieves a sensitivity of 92%, but the specificity is only 37%. SOPROLIFE in daylight mode with an equivalent cutoff value of 1.54 presents a sensitivity of 93% and specificity of 63%, while SOPROLIFE blue fluorescence with cutoff value of 1.52 shows a sensitivity of 95%, but the specificity is down to 55%. Table 5 summarizes the specific tool cutoff values for grouping ICDAS 0 with 1 and 2 as “healthy,” the sensitivity and specificity at this cutoff, confidence intervals, and likelihood ratio.

4 Discussion

Over the years diverse caries detection systems have been used, all of them using different definitions and description terms; consequently communication across different dental fields has been difficult. The visual method known as the International Caries Detection and Assessment System II (ICDAS II) has been developed with the purpose of bridging the gap of communication between fields of dental epidemiology, clinical caries research, and clinical caries management.¹⁰

ICDAS criteria are based on enamel properties of translucency and microporosity. With numerous demineralization events, the microporosity of enamel subsurface increases, which leads to changes in its refractive index. The first sign of carious alteration is a change in translucency and light refraction of the enamel surface. If demineralization is allowed to continue, the enamel microporosity increases, which then leads to further decrease in the refractive index of enamel.⁶²

Ekstrand et al.^{46,63,64} validated ICDAS by demonstrating an association between the severity of caries lesions (as described by ICDAS codes) and the lesions’ histological depth. Other authors have confirmed a close relationship between ICDAS scoring, and the histological depth of the caries lesion especially in precavitated but also in slightly cavitated stages.^{65,66} These

Table 3 Area under the ROC curve for SOPROLIFE, DIAGNOdent, and Spectra Caries Detection Aid.

	Area under ROC curve value (SE)	95% confidence interval	<i>P</i> value
SOPROLIFE blue fluorescence	0.8854 ± 0.01400	0.8580 to 0.9128	<i>P</i> < 0.0001
SOPROLIFE daylight	0.8779 ± 0.01505	0.8484 to 0.9074	<i>P</i> < 0.0001
DIAGNOdent	0.8700 ± 0.01410	0.8423 to 0.8976	<i>P</i> < 0.0001
Spectra Caries Detection Aid	0.8186 ± 0.01939	0.7806 to 0.8566	<i>P</i> < 0.0001

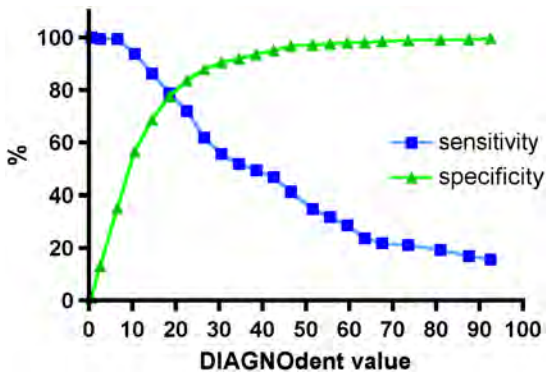


Fig. 27 Sensitivity and specificity of the DIAGNOdent; cutoff point at the grouping of ICDAS code 0, 1, and 2 together.

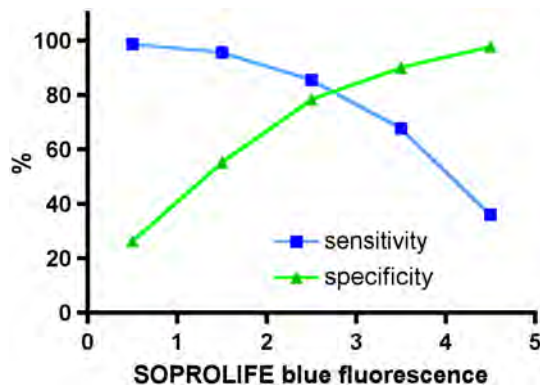


Fig. 28 Sensitivity and specificity of the SOPROLIFE blue fluorescence; cutoff point at the grouping of ICDAS code 0, 1, and 2 together.

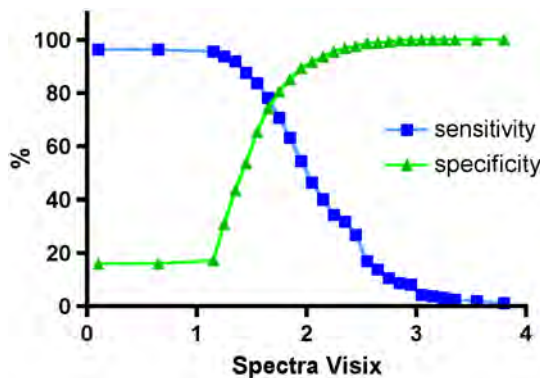


Fig. 29 Sensitivity and specificity of the Spectra Caries Detection Aid; cutoff point at grouping of ICDAS code 0, 1, and 2 together.

studies again endorsed a relationship between the visual topography at surface level and the histological lesion depth.

ICDAS II code and relation to histological lesion depth has been reported as: code 1, lesion depth in pits/fissures was 90% in the outer enamel with only 10% into dentin; code 2, lesion depth was 50% into the inner enamel and 50% into the outer 1/3 dentin; code 3, lesion depth was 77% in dentin; code 4, lesion depth was 88% into dentin; code 5, lesion depth was 100% in dentin.⁶³

Due to the validated relationship between ICDAS codes and the histological depth of a carious lesion, ICDAS II was used as “gold standard” in the present study. ICDAS II ratings were

compared to four other caries assessment tools, including DIAGNOdent, SOPROLIFE daylight and blue fluorescence, and Spectra Caries Detection Aid. Digital bitewings are not discussed further here since they only showed occlusal lesions in nine cases, therefore not detecting occlusal lesions in the bulk of the teeth examined and were only successful in detecting approximal lesions.

In this study 433 posterior teeth in 100 subjects were examined and up to 1066 data points for each assessment method were available for statistical evaluation. Using 1066 SOPROLIFE daylight and 1064 blue fluorescence areas of interest led to the development of a new SOPROLIFE daylight and blue fluorescence scoring system with six distinct codes for each detection mode. Developing those codes enabled us to compare the diagnostic abilities of the SOPROLIFE system with ICDAS II as well as the other caries assessment tools.

Examining the relationship between the ICDAS II scores and the scores derived from the different assessment tools revealed that for each ICDAS II code, each diagnostic tool provides a distinct average score. Per assessment tool each average score for one given ICDAS II code was significantly different from the one for another ICDAS II code. Interestingly, for all tools there was a difference in average values for ICDAS II code 3 versus code 4 with the average for code 4 higher, but that difference was not statistically significant. One explanation could be that only 25 lesions were scored with ICDAS II code 4.

DIAGNOdent as a spot fluorescence measurement tool has been previously discussed for its clinical validity.²³⁻²⁹ The discussion about an appropriate cutoff point to determine an operative intervention (filling) is ongoing.⁶⁷⁻⁷¹ The company recommends a cutoff point between 15 and 30 depending on caries risk. Eakle et al. recommended as cutoff point a DIAGNOdent value of 25 to 30.⁷² If an ICDAS code 3—first visualized breakdown of enamel—is considered as reason for an operative intervention, according to our study the equivalent DIAGNOdent value is located around 40, while for code 2 it is around 22.

ICDAS II code 0—“sound”—accumulated a very low SOPROLIFE daylight average score of 0.47 ± 0.6 (mean \pm standard deviation). Noncavitated lesions (ICDAS II code 1 and 2, respectively) provided significantly higher SOPROLIFE daylight scores of 1.4 ± 1.1 and 2.1 ± 1.2 , respectively. More severe, already slightly cavitated caries lesions with first visible enamel breakdown (ICDAS II code 3) received significant higher scores with 3.5 ± 1.3 , and when even dentin was visibly exposed (ICDAS II code 5) the SOPROLIFE daylight climbed to a 4.9 ± 0.4 score. For SOPROLIFE blue fluorescence the distribution pattern as well as the values for average scores were similar and close to the SOPROLIFE daylight assessments.

The absolute value differences between those average scores are high enough to allow the conclusion that the difference between each code is not only statistically but clinically significant. Thus the new SOPROLIFE daylight and blue fluorescence codes can serve as a distinct classification for sound, precavitated and cavitated caries lesions allowing the prediction of the histological depth of caries lesions.

Last, when comparing average Spectra Visix values for each ICDAS II code, the differences in values for each ICDAS II code are statistically significant, but the absolute value differences are relatively small. Those small differences in value for each lesion

Table 4 Average values for DIAGNOdent, SOPROLIFE, and Spectra Caries Detection Aid at different ICDAS scores and grouping of ICDAS 0, 1, and 2 together.

ICDAS score	DIAGNOdent (mean \pm SD)	SOPROLIFE daylight (mean \pm SD)	SOPROLIFE blue (mean \pm SD)	Spectra Caries Detection Aid (mean \pm SD)
0	5.7 \pm 4.3	0.47 \pm 0.60	0.35 \pm 0.53	0.70 \pm 0.68
1	13.3 \pm 11.8	1.43 \pm 1.08	1.46 \pm 1.22	1.26 \pm 0.61
2	22 \pm 17.5	2.07 \pm 1.24	2.03 \pm 1.36	1.60 \pm 0.54
3	40.6 \pm 24.6	3.48 \pm 1.29	3.59 \pm 1.14	1.95 \pm 0.57
grouping 0–1–2	15.5 \pm 14.6	1.54 \pm 1.20	1.52 \pm 1.32	1.31 \pm 0.66

Table 5 Sensitivity and specificity at the cutoff value for DIAGNOdent, SOPROLIFE, and Spectra Caries Detection Aid, 95% confidence interval and likelihood ratio.

Tool	Cutoff value	Sensitivity %	95% confidence interval	Specificity %	95% CI	Likelihood ratio
DIAGNOdent	15.5	87	81 to 92%	66	63 to 69%	2.6
Spectra Caries Detection Aid	1.31	92	87 to 96%	37	34 to 40%	1.5
SOPROLIFE daylight	1.54	93	88 to 96%	63	59 to 66%	2.5
SOPROLIFE blue	1.52	95	91 to 98%	55	52 to 59%	2.1

class might not be clinically significant to help in differentiating between sound, precavitated or cavitated lesions.

The linear regression fits for caries assessment tools in relation to average ICDAS II scores revealed that for all different caries assessment tools all line fits were significantly nonzero. In other words with a known value on the x -axis, a distinct value on the y -axis can be calculated. The slope of the line determines the discrimination. On a flat curve two different values on the y -axis are not easy to discriminate. In contrast, on a steep curve the difference between two values on the y -axis is much higher and thus easier to discriminate. The goodness of fit r^2 was very high for all linear regression fit calculations.

Using normalized data the linear regression fit for all caries assessment tools revealed that both SOPROLIFE caries assessment tools present the highest slope values of all, demonstrating the steepest slope with 0.8809. The slope for the DIAGNOdent linear regression fit is lower with 0.6600, while the Spectra Visix slope is 0.3357. From this point of view, SOPROLIFE daylight and SOPROLIFE blue fluorescence allow for the best discrimination followed by DIAGNOdent and Spectra Caries Detection Aid. Using SOPROLIFE a judgment call for classification of a lesion into sound, precavitated or cavitated, even with sublevels per class, is easier to make than with the other tools.

With respect to the overall ability of the different applied caries assessment tools to discriminate between healthy and diseased the AROC achieved similar high values for each tool. The best AROC values were accomplished when ICDAS code 0 and precavitated lesions (codes 1 and 2) were grouped together as “healthy” and all other codes were gathered as “caries” representing in a traditional way cavitated lesions. No other grouping of codes resulted in higher AROC values; no higher overall ability to discriminate between carious and noncarious could be achieved.

When sensitivity and specificity were calculated, the grouping of no lesion/healthy and precavitated lesions together appeared again to be the best cutoff point for each detection method to determine sensitivity and specificity of each method. Selecting this cutoff point DIAGNOdent achieved a sensitivity of 87% with a specificity of 66%. At the same cutoff point, SOPROLIFE in daylight mode showed with 93% a slightly higher sensitivity and a slightly lower specificity (63%). In the blue fluorescence mode the sensitivity of the tool was slightly higher, up to 95%, but the specificity drops to 55%. The Spectra Visix achieved a similar high-sensitivity value at this cutoff (92%), but the specificity was extremely low at 37%. Only for the DIAGNOdent tool, a wide range of reports is available, but the sensitivity values range widely from 19% to 100%. The specificity values exhibit a similar pattern, ranging from 52% to 100%.⁷³ In comparison with visual assessments Bader et al. (2004) state in a systematic review that the DIAGNOdent exhibits a sensitivity value that was always higher and a specificity value that was always lower.⁷³

The DIAGNOdent and DIAGNOdent pen have been compared with the Spectra Caries Detection Aid *in vitro*,⁷⁴ and the *in vitro* sensitivity and specificity of the tool against the gold standard histology has also been evaluated. Sensitivity was reported between 57% and 94%, while specificity was calculated between 50% and 78%, depending on chosen diagnostic threshold/cutoff points and selected data sets.⁷⁵ In another *in vitro* study when using the cutoff points recommended by the manufacturer, sensitivity values showed a high variance ranging from 0.04 to 0.86, and specificity values were between 0.32 and 0.99.⁷⁶

DIAGNOdent scores were relatively high on precavitated lesions. Contrary to DIAGNOdent and Spectra Caries Detection Aid with the SOPROLIFE system, the lesion and its real

topography can be seen in a magnified enlarged view. The lesion extension in terms of confinement of the lesion to the fissure, extending from the base of the fissure up the slopes etc., as well as the physical surface topography with roughness and with first enamel loss or even open dentin, can clearly be seen. This helps in scoring a lesion in daylight mode. Adding the blue fluorescence an additional prediction can be made from the “color scheme,” especially intensity and spread of the fluorescence color, which are reflected in the new SOPROLIFE blue fluorescence score. We assume from our observations in this study that the fluorescence signal and expression are most probably triggered and modified by bacteria and bacterial byproducts. The blue light transmits through healthy enamel and evokes a green fluorescence of the dentin core. The green fluorescence light coming back from the dentin core then leads to a red fluorescence from bacteria and bacterial byproducts like porphyrins. The prediction of lesion depth and stage is guided by scoring details like tiny shiny red fluorescence, red dots confined to the fissure, dark red fluorescence confined to the fissure, intense red wider than the fissure confinement possibly including grey areas wider than the fissure, and additional roughness. Both evaluation modes allow the definition of the lesion width as well as an assumption of the histological lesion depth.

The additional observation with the SOPROLIFE camera might also prevent unnecessary operative interventions based on high fluorescence scores due to the better visibility. The fluorescence camera system allows picturing where the fluorescence signal comes from and, especially, what the reason for an unexpected high fluorescence value might be. Due to that “visibility” of the lesion, the interpretation of a higher fluorescence answers is easier. The observation capacity of the SOPROLIFE system should guide the clinician toward a more preventive and minimally invasive treatment strategy with monitoring lesion progression or remineralization over time and not tempt him/her to overtreat a lesion.⁷⁷

5 Conclusion

All fluorescence tools were able to differentiate between distinct ICDAS II scores. For all tools the AROC depicting the overall capability to discriminate between healthy and diseased achieved similar high values with the SOPROLIFE tool in daylight as well as blue fluorescence mode having the highest values. Furthermore, the linear regression fits for the caries assessment tools in relation to ICDAS II codes revealed that both SOPROLIFE assessment tools with the highest slope values allow for the best caries lesion discrimination followed by DIAGNOdent. Spectra Caries Detection Aid demonstrates a relatively flat curve with low discrimination ability. At a cutoff point grouping healthy teeth and precavitated lesions together, DIAGNOdent shows a sensitivity of 87% and specificity of 66%, followed by SOPROLIFE daylight with sensitivity to specificity 93% to 63%, SOPROLIFE blue fluorescence with 95% to 55%, and Spectra Caries Detection Aid with 92% to 37%. Engaging those fluorescence tools, specifically those with observational capacity should guide clinicians toward a more preventive and minimally invasive treatment strategy and will allow monitoring lesions for success of prevention measures over time.

Acknowledgment

This work was supported by ACTEON, France.

References

1. A. Lussi, “Validity of diagnostic and treatment decisions of fissure caries,” *Caries Res.* **25**(4), 296–303 (1991).
2. J. D. Featherstone, “Caries detection and prevention with laser energy,” *Dent. Clin. North Am.* **44**(4), 955–969, ix (2000).
3. D. A. Young, J. D. Featherstone, and J. R. Roth, “Curing the silent epidemic: caries management in the 21st century and beyond,” *J. Calif. Dent. Assoc.* **35**(10), 681–685 (2007).
4. D. A. Young et al., “Caries management by risk assessment: implementation guidelines,” *J. Calif. Dent. Assoc.* **35**(11), 799–805 (2007).
5. L. Jensen et al., “Clinical protocols for caries management by risk assessment,” *J. Calif. Dent. Assoc.* **35**(10), 714–723 (2007).
6. S. Domejean-Orliaguet, S. A. Gansky, and J. D. Featherstone, “Caries risk assessment in an educational environment,” *J. Dent. Educ.* **70**(12), 1346–1354 (2006).
7. J. D. B. Featherstone et al., “Chlorehexidine and fluoride therapy reduces caries risk,” *J. Dent. Res.* **84A** (2005).
8. C. I. Hoover et al., “Effect of a caries management regimen on cariogenic bacterial population,” *J. Dent. Res.* **83A** (2004).
9. J. D. Featherstone, “The caries balance: the basis for caries management by risk assessment,” *Oral Health Prev. Dent.* **2**, Suppl 1, 259–264 (2004).
10. ICDAS and Foundation, “International Caries Detection & Assessment System,” <http://www.icdas.org>.
11. C. M. Mitropoulos, “The use of fibre-optic transillumination in the diagnosis of posterior approximal caries in clinical trials,” *Caries Res.* **19**(4), 379–384 (1985).
12. C. Deery et al., “Prevalence of dental caries in Latvian 11- to 15-year-old children and the enhanced diagnostic yield of temporary tooth separation, FOTI and electronic caries measurement,” *Caries Res.* **34**(1), 2–7 (2000).
13. D. F. Cortes, R. P. Ellwood, and K. R. Ekstrand, “An *in vitro* comparison of a combined FOTI/visual examination of occlusal caries with other caries diagnostic methods and the effect of stain on their diagnostic performance,” *Caries Res.* **37**(1), 8–16 (2003).
14. D. A. Young and J. D. Featherstone, “Digital imaging fiber-optic transillumination, F-speed radiographic film and depth of approximal lesions,” *J. Am. Dent. Assoc.* **136**(12), 1682–1687 (2005).
15. J. Vaarkamp et al., “Quantitative diagnosis of small approximal caries lesions utilizing wavelength-dependent fiber-optic transillumination,” *J. Dent. Res.* **76**(4), 875–882 (1997).
16. A. Schneiderman et al., “Assessment of dental caries with Digital Imaging Fiber-Optic Transillumination (DIFOTI): *in vitro* study,” *Caries Res.* **31**(2), 103–110 (1997).
17. A. Lussi et al., “Performance and reproducibility of a laser fluorescence system for detection of occlusal caries *in vitro*,” *Caries Res.* **33**(4), 261–266 (1999).
18. A. Lussi, R. Hibst, and R. Paulus, “DIAGNOdent: an optical method for caries detection,” *J. Dent. Res.* **83C**, C80–83 (2004).
19. E. H. Verdonshot and M. H. van der Veen, “Lasers in dentistry 2. Diagnosis of dental caries with lasers,” *Ned Tijdschr Tandheelkd* **109**(4), 122–126 (2002).
20. K. König, G. Flemming, and R. Hibst, “Laser-induced autofluorescence spectroscopy of dental caries,” *Cell Mol. Biol. (Noisy-le-grand)* **44**(8), 1293–1300 (1998).
21. X. Q. Shi, U. Welander, and M. B. Angmar, “Occlusal caries detection with KaVo DIAGNOdent and radiography: an *in vitro* comparison,” *Caries Res.* **34**(2), 151–158 (2000).
22. X. Q. Shi, S. Tranaeus, and B. Angmar-Mansson, “Validation of DIAGNOdent for quantification of smooth-surface caries: an *in vitro* study,” *Acta Odontol. Scand.* **59**(2), 74–78 (2001).
23. R. O. Rocha et al., “*In vivo* effectiveness of laser fluorescence compared to visual inspection and radiography for the detection of occlusal caries in primary teeth,” *Caries Res.* **37**(6), 437–441 (2003).
24. A. Astvaldsdottir, W. P. Holbrook, and S. Tranaeus, “Consistency of DIAGNOdent instruments for clinical assessment of fissure caries,” *Acta Odontol. Scand.* **62**(4), 193–198 (2004).
25. S. Tranaeus et al., “*In vivo* validity and reliability of IR fluorescence measurements for caries detection and quantification,” *Swed. Dent. J.* **28**(4), 173–182 (2004).

26. M. Bamzahim, A. Aljehani, and X. Q. Shi, "Clinical performance of DIAGNOdent in the detection of secondary carious lesions," *Acta Odontol. Scand.* **63**(1), 26–30 (2005).
27. V. Angnes et al., "Clinical effectiveness of laser fluorescence, visual inspection and radiography in the detection of occlusal caries," *Caries Res.* **39**(6), 490–495 (2005).
28. A. Reis et al., "Performance of methods of occlusal caries detection in permanent teeth under clinical and laboratory conditions," *J. Dent.* **34**(2), 89–96 (2006).
29. S. Akarsu and H. Koprulu, "In vivo comparison of the efficacy of DIAGNOdent by visual inspection and radiographic diagnostic techniques in the diagnosis of occlusal caries," *J. Clin. Dent.* **17**(3), 53–58 (2006).
30. M. J. Altenburger et al., "The evaluation of fluorescence changes after application of casein phosphopeptides (CPP) and amorphous calcium phosphate (ACP) on early carious lesions," *Am. J. Dent.* **23**(4), 188–192 (2010).
31. H. C. Benedict, "A note on the fluorescence of teeth in ultraviolet rays," *Science* **67**(1739), 442 (1928).
32. U. Hafstrom-Bjorkman et al., "Comparison of laser fluorescence and longitudinal microradiography for quantitative assessment of in vitro enamel caries," *Caries Res.* **26**(4), 241–247 (1992).
33. Z. Emami et al., "Mineral loss in incipient caries lesions quantified with laser fluorescence and longitudinal microradiography. A methodologic study," *Acta Odontol. Scand.* **54**(1), 8–13 (1996).
34. S. al-Khateeb et al., "Quantification of formation and remineralization of artificial enamel lesions with a new portable fluorescence device," *Adv. Dent. Res.* **11**(4), 502–506 (1997).
35. S. al-Khateeb et al., "Laser fluorescence quantification of remineralisation *in situ* of incipient enamel lesions: influence of fluoride supplements," *Caries Res.* **31**(2), 132–140 (1997).
36. E. de Josselin de Jong et al., "A new method for *in vivo* quantification of changes in initial enamel caries with laser fluorescence," *Caries Res.* **29**(1), 2–7 (1995).
37. S. Al-Khateeb et al., "A longitudinal laser fluorescence study of white spot lesions in orthodontic patients," *Am. J. Orthod. Dentofacial Orthop.* **113**(6), 595–602 (1998).
38. S. Tranaeus et al., "Application of quantitative light-induced fluorescence to monitor incipient lesions in caries-active children. A comparative study of remineralisation by fluoride varnish and professional cleaning," *Eur. J. Oral Sci.* **109**(2), 71–75 (2001).
39. S. Tranaeus et al., "In vivo repeatability and reproducibility of the quantitative light-induced fluorescence method," *Caries Res.* **36**(1), 3–9 (2002).
40. I. A. Pretty and R. P. Ellwood, "Comparison of paired visual assessment and software analyses of changes in caries status over six months from fluorescence images," *Caries Res.* **41**(2), 115–120 (2007).
41. W. Yin et al., "Reliability of quantitative laser fluorescence analysis of smooth surface lesions adjacent to the gingival tissues," *Caries Res.* **41**(3), 186–189 (2007).
42. A. G. Ferreira Zandona et al., "An *in vitro* comparison between laser fluorescence and visual examination for detection of demineralization in occlusal pits and fissures," *Caries Res.* **32**(3), 210–218 (1998).
43. E. Terrer et al., "A new concept in restorative dentistry: light-induced fluorescence evaluator for diagnosis and treatment. Part 1: Diagnosis and treatment of initial occlusal caries," *J. Cont. Dent. Pract.* **10**(6), E086–094 (2009).
44. E. Terrer et al., "A new concept in restorative dentistry: LIFEDT-light-induced fluorescence evaluator for diagnosis and treatment: part 2—treatment of dental caries," *J. Cont. Dent. Pract.* **11**(1), E095–102 (2010).
45. G. E. White, A. Tsamtsouris, and D. L. Williams, "Early detection of occlusal caries by measuring the electrical resistance of the tooth," *J. Dent. Res.* **57**(2), 195–200 (1978).
46. K. R. Ekstrand, D. N. Ricketts, and E. A. Kidd, "Reproducibility and accuracy of three methods for assessment of demineralization depth of the occlusal surface: an *in vitro* examination," *Caries Res.* **31**(3), 224–231 (1997).
47. D. N. Ricketts et al., "Histological validation of electrical resistance measurements in the diagnosis of occlusal caries," *Caries Res.* **30**(2), 148–155 (1996).
48. J. Kuhnisch, "An *in vitro* comparison between two methods of electrical resistance measurement for occlusal caries detection," *Caries Res.* **40**(2), 104–111 (2006).
49. W. P. Rock and E. A. Kidd, "The electronic detection of demineralisation in occlusal fissures," *Br. Dent. J.* **164**(8), 243–247 (1988).
50. E. H. Verdonshot et al., "Performance of some diagnostic systems in examinations for small occlusal carious lesions," *Caries Res.* **26**(1), 59–64 (1992).
51. M. C. Huysmans et al., "Surface-specific electrical occlusal caries diagnosis: reproducibility, correlation with histological lesion depth, and tooth type dependence," *Caries Res.* **32**(5), 330–336 (1998).
52. D. Huang et al., "Optical coherence tomography," *Science* **254**(5035), 1178–1181 (1991).
53. A. F. Fercher et al., "In vivo optical coherence tomography," *Am. J. Ophthalmol.* **116**(1), 113–114 (1993).
54. G. J. Tearney et al., "In vivo endoscopic optical biopsy with optical coherence tomography," *Science* **276**(5321), 2037–2039 (1997).
55. B. W. Colston, Jr. et al., "Imaging of hard- and soft-tissue structure in the oral cavity by optical coherence tomography," *Appl. Opt.* **37**(16), 3582–3585 (1998).
56. J. G. Fujimoto et al., "High-resolution *in vivo* intra-arterial imaging with optical coherence tomography," *Heart* **82**(2), 128–133 (1999).
57. D. Fried et al., "Imaging caries lesions and lesion progression with polarization sensitive optical coherence tomography," *J. Biomed. Opt.* **7**(4), 618–627 (2002).
58. R. S. Jones et al., "Imaging artificial caries on the occlusal surfaces with polarization-sensitive optical coherence tomography," *Caries Res.* **40**(2), 81–89 (2006).
59. R. S. Jones et al., "Remineralization of *in vitro* dental caries assessed with polarization-sensitive optical coherence tomography," *J. Biomed. Opt.* **11**(1), 014016-1–014016-9 (2006).
60. GraphPad, "Quantify Agreement with Kappa: Assess how well two observers classify subjects into groups," Q. A. w. Kappa, QuickCalcs Online Calculators for Scientists, GraphPad Software Incorporated (2011), <http://www.graphpad.com/quickcalcs/kappa1.cfm>.
61. J. A. Swets, "Measuring the accuracy of diagnostic systems," *Science* **240**(4857), 1285–1293 (1988).
62. Rationale and Evidence for the International Caries Detection and Assessment System (ICDAS II) International Caries Detection and Assessment System (ICDAS) Coordinating Committee (September 2005).
63. K. R. Ekstrand et al., "Relationship between external and histologic features of progressive stages of caries in the occlusal fossa," *Caries Res.* **29**(4), 243–250 (1995).
64. S. Tranaeus et al., "In vivo validity and reliability of IR fluorescence measurements for caries detection and quantification," *Swed. Dent. J.* **28**(4), 173–182 (2004).
65. F. M. Mendes et al., "Performance of DIAGNOdent for detection and quantification of smooth-surface caries in primary teeth," *J. Dent.* **33**(1), 79–845 (2005).
66. A. Astvaldsdottir, W. P. Holbrook, and S. Tranaeus, "Consistency of DIAGNOdent instruments for clinical assessment of fissure caries," *Acta Odontol. Scand.* **62**(4), 193–198 (2004).
67. A. Jablonski-Momeni et al., "Performance of laser fluorescence at tooth surface and histological section," *Lasers Med. Sci.* **26**(2), 171–178 (2011).
68. A. Goel, "Comparison of validity of DIAGNOdent with conventional methods for detection of occlusal caries in primary molars using the histological gold standard: an *in vivo* study," *J. Indian Soc. Pedod. Prev. Dent.* **27**(4), 227–234 (2009).
69. W. Zhang, C. McGrath, and E. C. Lo, "A comparison of root caries diagnosis based on visual-tactile criteria and DIAGNOdent *in vivo*," *J. Dent.* **37**(7), 509–513 (2009).
70. K. C. Huth et al., "Clinical performance of a new laser fluorescence device for detection of occlusal caries lesions in permanent molars," *J. Dent.* **36**(12), 1033–1040 (2008).
71. V. Anttonen, L. Seppa, and H. Hausen, "Clinical study of the use of the laser fluorescence device DIAGNOdent for detection of occlusal caries in children," *Caries Res.* **37**(1), 17–23 (2003).
72. S. Eakle et al., "Clinical Evaluation of the DIAGNOdent Device," in *Early Detection of Dental Caries III Indiana. Conference 2003* G. Stookey, ed., Indiana University Press, Indiana (2005).

73. J. D. Bader and D. A. Shugars, "A systematic review of the performance of a laser fluorescence device for detecting caries," *J. Am. Dent. Assoc.* **135**(10), 1413–1426 (2004).
74. M. S. De Benedetto et al., "Comparing the reliability of a new fluorescence camera with conventional laser fluorescence devices in detecting caries lesions in occlusal and smooth surfaces of primary teeth," *Lasers Med. Sci.* **26**(2), 157–162 (2011).
75. A. Jablonski-Momeni et al., "Impact of measuring multiple or single occlusal lesions on estimates of diagnostic accuracy using fluorescence methods," *Lasers Med. Sci.* **27**(2), 343–352 (2011).
76. A. Jablonski-Momeni et al., "Performance of a fluorescence camera for detection of occlusal caries in vitro," *Odontology/the Society of the Nippon Dental University* **99**(1), 55–61 (2011).
77. A. C. Pereira et al., "Validity of caries detection on occlusal surfaces and treatment decisions based on results from multiple caries-detection methods," *Eur. J. Oral Sci.* **117**(1), 51–57 (2009).

49. Weintraub JA. Prevention of early childhood caries: a public health perspective. *Community Dent Oral Epidemiol* 1998;26:32–34.
50. Zhan L, Tan S, Den Besten P, Featherstone JD, Hoover CI. Factors related to maternal transmission of mutans streptococci in high-risk children—pilot study. *Pediatr Dent* 2012;34:86–91.
51. Featherstone JD, White JM, Hoover CI, *et al.* A randomized clinical trial of anticaries therapies targeted according to risk assessment (caries management by risk assessment). *Caries Res* 2012;46:118–129.
52. Domejean S, White JM, Featherstone JD. Validation of the CDA CAMBRA caries risk assessment—a six-year retrospective study. *J Calif Dent Assoc* 2011;39:709–715.
53. Featherstone JD, Domejean-Orliaguet S, Jenson L, Wolff M, Young DA. Caries risk assessment in practice for age 6 through adult. *J Calif Dent Assoc* 2007;35:703–707.
54. Keller U, Hibst R. Histological findings of pulpal changes after Er:YAG laser irradiation. *J Dent Res* 1995;74:435–438.
55. Keller U, Hibst R. The pulp reaction following Er:YAG laser application. In: O'Brien SJ, Dederich DN, Wigdor HA, Trent AM, eds. Bellingham, Washington: SPIE, 1991:127–133.
56. Keller U, Hibst R. Effects of Er:YAG laser in caries treatment: a clinical pilot study. *Lasers Surg Med* 1997;20:32–38.
57. Dostalova T, Jelinkova H, Krejsa O, *et al.* Dentin and pulp response to Erbium:YAG laser ablation: a preliminary evaluation of human teeth. *J Clin Laser Med Surg* 1997;15:117–121.
58. Dostalova T, Jelinkova H, Kucerova H, *et al.* Noncontact Er:YAG laser ablation: clinical evaluation. *J Clin Laser Med Surg* 1998;16:32–38.
59. Correa-Afonso AM, Pecora JD, Palma-Dibb RG. Influence of pulse repetition rate on temperature rise and working time during composite filling removal with the Er:YAG laser. *Photomed Laser Surg* 2008;26:221–225.
60. Hibst R, Keller U. Removal of dental filling materials by Er:YAG laser radiation. In: O'Brien SJ, Dederich DN, Wigdor HA, Trent AM, eds. Bellingham, Washington: SPIE, 1991:120–126.
61. Jacobsen T, Norlund A, Englund GS, Tranaeus S. Application of laser technology for removal of caries: a systematic review of controlled clinical trials. *Acta Odont Scand* 2011;69:290–297.
62. Olivi G, Genovese MD. Laser restorative dentistry in children and adolescents. *Eur Arch Paediatr Dent* 2011;12:68–78.
63. van As G. Erbium lasers in dentistry. *Dent Clin North Am* 2004;48:1017–1059.
64. Hossain M, Kimura Y, Nakamura Y, Yamada Y, Kinoshita JJ, Matsumoto K. A study on acquired acid resistance of enamel and dentin irradiated by Er, Cr:YSGG laser. *J Clin Laser Med Surg* 2001;19:159–163.
65. Rechmann P, Fried D, Le CQ, *et al.* Caries inhibition in vital teeth using 9.6- μm CO₂-laser irradiation. *J Biomed Opt* 2011;16:071405.
66. Rechmann P, Fried D, Le CQ, *et al.* Inhibition of caries in vital teeth by CO₂ laser treatment. In: Rechmann P, Fried D, eds. *Lasers in Dentistry XIV*: SPIE, 2008.
67. Rechmann P, Charland DA, Rechmann BMT, Le CQ, Featherstone JDB. *In vivo* occlusal caries prevention by pulsed-CO₂ laser and fluoride varnish treatment. *J Dent Res* 2010;17:036006.
68. Konishi N, Fried D, Staninec M, Featherstone JDB. Artificial caries removal and inhibition of artificial secondary caries by pulsed CO₂ laser irradiation. *Am J Dent* 1999;12:213–216.
69. Fried D, Ragadio J, Akrivou M, Featherstone JD, Murray MW, Dickenson KM. Dental hard tissue modification and removal using sealed transverse excited atmospheric-pressure lasers operating at $\lambda = 9.6$ and 10.6 μm . *J Biomed Opt* 2001;6:231–238.
70. Staninec M, Darling CL, Goodis HE, *et al.* Pulpal effects of enamel ablation with a microsecond pulsed $\lambda = 9.3$ - μm CO₂ laser. *Lasers Surg Med* 2009;41:256–263.
71. Banerjee A, Hajatdoost-Sani M, Farrell S, Thompson I. A clinical evaluation and comparison of bioactive glass and sodium bicarbonate air-polishing powders. *J Dent* 2010;38:475–479.
72. Sauro S, Watson TF, Thompson I. Dentine desensitization induced by prophylactic and air-polishing procedures: an *in vitro* dentine permeability and confocal microscopy study. *J Dent* 2010;38:411–422.
73. Mertz-Fairhurst EJ, Curtis JW Jr, Ergle JW, Rueggeberg FA, Adair SM. Ultraconservative and cariostatic sealed restorations: results at year 10. *J Am Dent Assoc* 1998;129:55–66.
74. Pitts N. ICDAS – an international system for caries detection and assessment being developed to facilitate caries epidemiology, research and appropriate clinical management. *Community Dent Health* 2004;21:193–198.
75. Neves Ade A, Coutinho E, De Munck J, Van Meerbeek B. Caries-removal effectiveness and minimal-invasiveness potential of caries-excitation techniques: a micro-CT investigation. *J Dent* 2011;39:154–162.
76. Banerjee A, Watson TF, Kidd EA. Dentine caries excavation: a review of current clinical techniques. *Br Dent J* 2000;188:476–482.
77. Yip HK, Stevenson AG, Beeley JA. The specificity of caries detector dyes in cavity preparation. *Br Dent J* 1994;176:417–421.
78. McComb D. Caries-detector dyes—how accurate and useful are they? *J Can Dent Assoc* 2000;66:195–198.
79. Tassery H, Déjou J, Chafaie A, Camps J. *In vivo* diagnostic assessment of dentinal caries by junior and senior students using red acid dye. *Eur J Dent Educ* 2001;5:38–42.
80. Williams JA, Pearson GJ, Colles MJ, *et al.* Determine the effective parameters for PAD™ treatment in a caries model. A detailed study to determine the effective parameters for PAD™ treatment in a caries model. *Caries Res* 2004;38:530–536.
81. Koubi S, Tassery H. Minimally invasive dentistry using sonic and ultrasonic devices in ultraconservative Class 2 restorations. *J Contemp Dent Pract* 2008;9:1–11.
82. Huguo B, Stassinakis A. Preparation and restoration of small interproximal carious lesions with sonic instruments. *Pract Periodontol Aesthet Dent* 1998;10:353–359.

Address for correspondence:

Dr Hervé Tassery

8 allée canto cigalo

30400 Villeneuve les Avignon

France

Email: herve.tassery@numericable.fr

Gestion thérapeutique de lésions carieuses proximales sur dents adjacentes

H. TASSERY, A. SLIMANI, A. LAVENANT, E. TERRER

RÉSUMÉ

La gestion thérapeutique des lésions carieuses proximales postérieures se heurte à plusieurs complexités tant diagnostiques que techniques. La multiplicité des matériaux commercialisés et la difficulté d'évaluer aussi l'activité carieuse résiduelle compliquent le choix du substitut dentinaire à utiliser, spécialement lors de lésions actives. La transition entre une restauration a minima de type 1, sans aucune préparation ou de type 2, avec préparation tissulaire demeure ténue. Les bases des traitements proposés dans ce report de cas dérivent du concept LIFEDT ou light induced fluorescence for diagnosis and treatment. Cet exposé se propose de traiter deux lésions carieuses proximales (Site 2) contiguës, l'une de stade 3 et l'autre de stade 1.

Hervé Tassery

Université d'Aix-Marseille,
Département d'odontologie
conservatrice et restauratrice,
Université de Montpellier 1,
Laboratoire de biologie
et Nano-science LBN 4203

Amel Slimani

Université de Montpellier 1,
Laboratoire de biologie
et Nano-science LBN 4203

Adrien Lavenant

Université d'Aix-Marseille,
Département d'odontologie
conservatrice et restauratrice

Elodie Terrer

Université d'Aix-Marseille,
Département d'odontologie
conservatrice et restauratrice
Laboratoire de biologie
et Nano-science LBN 4203

**Les auteurs déclarent
ne pas avoir de lien d'intérêt**

La gestion thérapeutique des lésions carieuses proximales postérieures se heurte à plusieurs difficultés tant diagnostiques que techniques. En effet, bien souvent, l'image radiologique sous-évalue l'extension de la lésion et la restauration d'un contact proximal efficient constitue une réelle difficulté technique. La multiplicité des matériaux commercialisés et la difficulté d'évaluer aussi l'activité carieuse résiduelle compliquent le choix du substitut dentinaire à utiliser spécialement lors de lésions actives. La transition entre une restauration a minima de type 1, sans aucune préparation ou de type 2, avec préparation tissulaire (1) demeure ténue. Cela dépend exclusivement de la sensibilité des outils de diagnostic utilisés ou à disposition par l'omnipraticien, lui-même supposé être

formé aux techniques de la dentisterie a minima

La dentisterie a minima de type 1 est représentée par l'ensemble des techniques préventives sans préparation excepté le conditionnement tissulaire jusqu'à l'infiltration résineuse inclus. La dentisterie a minima de type 2 est représentée par toutes les techniques de préparation avec conservation maximale des tissus.

Parmi tous les outils récents d'aide au diagnostic, le Diagnopen®, le Cariscann®, la Vistacam®, et le SironInspect® sont plus spécifiques aux évaluations carieuses des faces occlusales comparativement au Diagnocam® (Kavo), qui paraît plus adapté aux détections carieuses des lésions proximales.



Fig. 1 - Image numérique Sopix®2 (Acteon). Carie en mésiale de la 25 et carie amélaire en distale de 24.

Fig. 2 - Image mode diagnostique (carré rouge ou aplomb de la zone cariée).



Les systèmes basés sur la fluorescence tissulaire dont les caméras Soprolife® et Soprocare®, sous réserve de leur sensibilité et spécificité, permettent d'observer tant les faces occlusales que proximales (2) en s'aidant d'astuces cliniques. Pour cette présentation l'essentielle des images ont été prises à l'aide de ces deux types de caméras en mode jour, mode diagnostique ou mode traitement pour la caméra Soprolife® et en mode carie pour la caméra Soprocare®.

Les bases des traitements proposés dans ce report de cas dérivent du concept LIFEDT ou light induced fluorescence for diagnosis and treatment (1, 2).

Cet exposé se propose de traiter deux lésions carieuses proximales (Site 2) contiguës, l'une de stade 3 (dent 25) et l'autre de stade 1 (dent 24).

PRÉSENTATION DU CAS CLINIQUE

Le patient 25 ans, sans pathologie générale, présente deux lésions proximales dent 25 stade 3 et 24 stade 1. Les lésions semblent anciennes, le patient n'a pas consulté depuis 3 ans. Il n'y a pas d'autres lésions carieuses. Le risque carieux est évalué comme modéré et pris en charge classiquement en renforçant les mesures d'hygiène orale.

TRAITEMENT DE LA CARIE MÉSIALE SUR 25

L'examen clinique et l'observation de la face occlusale en mode diagnostique confirment les informations obtenues avec le cliché rétrocoronaire (fig. 1, cercle rouge). La modification de la fluorescence de la crête marginale (fig. 2, carré rouge) indique la destruction de la dentine sous-jacente et implique l'impossibilité de sa conservation. En effet, un blanchiment de la texture de la crête marginale révèle une disparition de la dentine sous-jacente donc une diminution du signal fluorescent. Cette modification de la fluorescence est caractéristique d'une lésion active impliquant l'usage d'un substitut dentinaire bioactif type ciment verre ionomère modifié par apport de résine (ex Fuji II LC, GC).

Phase chirurgicale : accès, curetage et finition de la préparation

Après mise en place d'un Fenderwedge® ou Wedge-guard® (Wam, France) assurant un écartement et une protection efficace de la face distale de la 24, la préparation est réalisée à l'aide d'une fraise boule ou poire diamantée (0,8. Komet®) (fig. 3).

Le traitement chirurgical de la dentine infectée se fait préférentiellement à l'aide d'excavateur (GC ou Hu-Friedy) (fig. 4) de petite taille ou de fraise céramique type K1SM® (Komet) sous contrôle en lumière fluorescente (mode traitement), permettant d'évaluer la structure de la dentine résiduelle infectée ou affectée. Celle-ci émet une fluorescence rouge et le geste clinique doit se concentrer



Fig. 3 - Ouverture de la préparation à l'aplomb de la zone bleutée (carré rouge fig. 2).

Fig. 4 - Eviction de la couche de dentine infectée (Excavateur Hu-Friedy®) (mode traitement Soprolife®).



Fig. 5 - Visualisation de la dentine tertiaire, couleur rouge (mode carie Soprocure®).

Fig. 6 - Révélation de la plaque interdentaire par photoactivation Blue LED et colorant fluorescine (Newtron® P5XS, Actéon).



uniquement sur cette interface colorée (fig. 5). La réaction de Maillard dite de brunissement est en partie responsable de cette coloration après excitation en lumière bleue (450 nm) (5).

•La finition de la préparation peut se faire à ce stade avec des inserts diamantés activés par ondes sonores (Kavo®, Komet®) ou ultrasonores (Actéon Newtron® et Système Excavus®, EMS®). L'application d'un colorant fluorescent type fluorescine dans l'espace interdentaire couplé au système Newtron, activé par lumière bleue permet de bien visualiser les dépôts et donc leur élimination avant finalisation de la préparation (fig. 6).

Contact interproximal

L'étape suivante consiste à rétablir l'aire de contact interproximal et l'architecture proximale. Une fois le champ opératoire mis en place (Dental Dam®, Bisico, France), l'utilisation d'une matrice métallique limite le risque d'échec dans la réalisation du point de contact. Notre choix se porte sur les matrices V3Ring®, SuperCurve® (Wam, France) et Composi-Tight3D® (Bisico, Garrison) (fig. 7) couplant anneaux écarteurs, coins plastiques puissants et matrices métalliques. Certaines (Slick bands®, Garrison) sont recouvertes sur leur face interne,



Fig. 7 - Restauration du contact interproximal. Slick band® et anneau de Garrison® (Bisico, France).



Fig. 8 - Restauration de la face occluso-proximale selon la technique du composite-up. Composite nano-hydride universel type Empress direct® (Ivoclar) ou Hri® (Bisico), teinte bleach L ou UE2 amélaire.

d'un revêtement de téflon pour faciliter la mise en place et l'éviction. Une fois la matrice positionnée, on prendra soin de brunir la face interne de la matrice vers le point de contact pour finaliser sa position. L'aide de digue liquide (Bisidam®, Bisico) pour stabiliser l'ensemble et plaquer la matrice en proximal n'est pas superflue. L'emploi d'une pince type matrix forceps (Bisico) sera une aide précieuse pour enlever la matrice en fin de soins.

Réalisation de la restauration

Cette étape essentielle implique deux étapes :

1. la désinfection de la plaie,
2. le choix pertinent du système adhésif et des matériaux de restauration.

- **La phase de désinfection** est réalisée par un nettoyage soigneux de la plaie dentinaire soit, avec du Tubulicid®, soit avec de la chlorhexidine à 2 %. Cette dernière ayant de plus un effet protecteur contre l'activation de MMPs dentinaires par le pH acide du système adhésif.

- **Le choix de l'adhésif** : parmi tous les adhésifs commercialisés, seul le Clearfil Protect Bond® (Kuraray, Japon) revendique un effet bactérien (monomère type MDBP). Sinon, on privilégiera les SAM 1 et surtout 2, en cas de proximité pulpaire et les MR3 ou 2 pour les autres situations. Quel que soit le système utilisé, il est recommandé de mordancer l'émail avec de l'acide phosphorique pendant 15 secondes au moins pour compléter le conditionnement tissulaire des SAM2 et surtout des SAM1.

Lorsque le recours à un substitut dentinaire s'impose, il demeure toujours important de vérifier la compatibilité de l'adhésif avec le substitut utilisé, surtout si ce dernier est dual. D'autre part, il faut rapidement et bien photopolymériser l'adhésif pour réduire l'effet membrane semi-perméable du fait de l'acidité des adhésifs. Les systèmes adhésifs modernes type Excite DSC® (Vivadent),

Universal Bond® (Bisico), XTR® (SAM2, Kerr) et autres ont l'avantage d'être dual et de laisser le choix au praticien entre les techniques du mordantage total, partiel (amélaire) ou sans mordantage à l'acide phosphorique. La proximité pulpaire est l'un des facteurs déterminants quant au choix de la technique.

Choix du substitut dentinaire

Le substitut permet de réduire la masse du composite à incrémenter, le facteur C, et si possible d'avoir un effet bioactif sur le tissu dentinaire résiduel. La fluorescence peut aider l'omnipraticien dans ce choix. En effet, une lésion à marche lente apparaîtra rouge foncé en début d'excavation et verte avec des ombres rouges marquées en fin d'excavation et une lésion active rouge vif en début d'excavation et vert gris en fin d'excavation. Dans ce cas précis, la dent étant asymptomatique avec une carie active et profonde notre choix s'est porté sur un substitut dentinaire bioactif type verre ionomère.

Mais de façon générale deux cas de figures apparaissent :

- si la lésion est active et de progression rapide : notre choix se portera sur l'utilisation de verres ionomères modifiés par apport de résine (de type Fuji II LC® (GC, Japon), Riva light Cure® (SDI) etc)
- si la lésion est à progression lente : le choix est plus vaste entre les composites photos et dual. De nombreux matériaux sont à disposition, dont : Multicore flow dual® (Vivadent), Bisfil 2B® (Bisco), LuxaCore® dual (DMG) etc. SDR flow® (Dentsply), X-Tra® (Voco) etc.

En cas de lésion moyennement profonde, il est également possible d'utiliser des composites type Bulk (TetricBulk®, Vivadent) et autres, mais le recul clinique sur l'usage de ces matériaux récents reste encore insuffisant.

Reconstruction occluso-proximale

- La reconstruction de la face occlusale est réalisée selon la technique dite du composite-up (fig. 8), au-dessus du substitut dentaire selon la technique du sandwich ouvert. La présence d'une bordure amélaire nous permet d'utiliser aussi des composites en zone cervicale. Néanmoins la forte activité carieuse nous fait préférer le CVIMAR.

Le composite-up est réalisé en 2 temps :

- restauration de la face proximale : après avoir plaqué la matrice métallique vers le point de contact à l'aide d'un fouloir, 1 apport de composite est apposé et positionné à la spatule de bouche pour être sculpté secondairement à l'aide d'une sonde ou d'un instrument type PK Thomas,
- reconstruction des cuspidés vestibulaires et palatines, chacune figée 3 secondes séparément puis photopolymérisée 40 secondes (puissance minimale 1200mW/cm²) sur la totalité.

Finition et polissage

La finition de la restauration composite, après réglage de l'occlusion s'effectue en plusieurs étapes :

- élimination des excès de composite et d'adhésif dans la zone proximale avec une lame 15 et des disques (Opti-disc®, Kerr),



- dégrossissage avec une fraise olive bague rouge sous spray,
- finition avec des brosses type Occlubrush® (Kerr ou Vivadent) et pointes siliconées Optrapol® (Vivadent) ou identoflex Diamond® (Kerr), Jiffy Hishine® (Bisico),
- le coffret de polissage Enamel plus Shiny® (Bisico) complète ces dernières propositions de produits.

Une étanchéification secondaire pourra être réalisée à l'aide d'adhésif, par application d'un film résineux protecteur ou coat (type GC coat® ou Biscover LV®) placé en très fine couche et parfaitement photopolymérisée. Cependant, l'intérêt de cette procédure sur la longévité des restaurations composites reste à confirmer.

TRAITEMENT DE LA CARIE DISTALE SUR 24

La présence d'une lésion débutante collatérale à une classe II est courante et demeure bien compliquée à traiter dans de nombreux cas. Le nœud de décision est la présence ou pas d'une cavitation et son ampleur indiquant un traitement a minima de type MID1 ou MID2 (1). L'observation sous lumière fluorescente des lésions amélares type « white spot » est souvent améliorée. Dans cet exemple clinique, la lésion amélaire contiguë à la classe 2 précédente (fig. 9) est certes parfaitement visible en mode lumière du jour (Soprolife®), mais aucune cavitation ne semble visible. La même surface observée en mode diagnostique révèle un début de cavitation quasiment invisible à la radiographie et à l'inspection visuelle (fig. 10). Le choix de traitement, avant obturation de la lésion adjacente, se fera entre l'application d'un vernis fluoré, une infiltration résineuse ou une micropréparation par insert diamanté (Kavo®, coffret Excavus®, Actéon). La faible profondeur et l'accessibilité de la lésion ont été déterminantes quant au choix du traitement: l'infiltration résineuse par résine fluide type Icon® (DMG, Allemagne). Les premiers résultats encourageants décrits dans la littérature ne soustraient pas à la pose d'un champ opératoire.

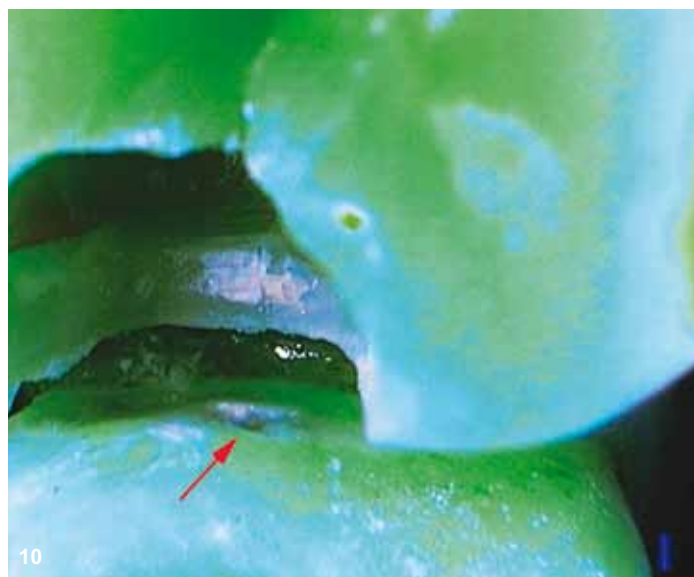


Fig. 9 - Observation en lumière du jour de l'atteinte amélaire.

Fig. 10 - Observation en mode diagnostique. Visualisation de la cavitation par fluorescence (flèche rouge).

Fig. 11 - Application du gel acide via la membrane semi-perméable du porte-matrice.

Dans le cas présent, celui-ci étant déjà posé dans le cadre du traitement de la 25, la lésion est traitée d'après les recommandations du fabricant selon les étapes suivantes (1):

- mordantage acide pendant 2 minutes (fig. 11),
- déshydratation alcoolique 30 secondes,
- infiltration résineuse pendant 3 minutes suivie d'une photopolymérisation pendant 40 secondes (fig. 12, 13).

La restauration ocluso-proximale mésiale de la 25 est alors réalisée (chapitre ci-dessus).



Fig. 12 - Cavitation comblée par la résine Icon® (flèche rouge). Mode diagnostique (Soprolife®).

Fig. 13 - Vérification radiologique postopératoire des deux traitements. Notez que l'Icon® n'est pas radio-opaque.

CONCLUSION

Face à la présence de lésions carieuses proximales, le praticien doit rechercher les facteurs de risque carieux locaux et généraux afin de les contrôler autant que faire se peut et de diminuer leur impact sur la santé orale du patient. Vient ensuite la décision de s'orienter vers un traitement interceptif non invasif ou vers un traitement chirurgical avec réalisation d'une restauration proximo-triturante. Souvent, comme dans le cas clinique présenté, des lésions présentant différents stades de sévérité coexistent. La gestion de ces lésions proximales, tant par technique classique que par infiltration, est faussement facile. Les nombreux pièges devront être parfaitement analysés avant toute thérapeutique. Les aides visuelles comme les caméras basées sur la fluorescence sont des aides précieuses non seulement pour affiner le diagnostic, mais aussi pour gérer les étapes du traitement. Enfin, les procédures opératoires adhésives, de comblement des pertes de substance et de finition doivent être mises en œuvre avec rigueur. Le succès thérapeutique dépend du respect de l'ensemble de ces paramètres.

Mots clés

Fluorescence, classe II, excavation dentinaire

Keywords

Fluorescence, class 2, dentin excavation

AUTO-ÉVALUATION

1. Le diagnostic d'une lésion carieuse :

- a. implique l'usage systématique de radios bitewing
- b. doit être complété par des radios rétroalvéolaires
- c. suppose l'usage systématique d'outils complémentaires de diagnostic

2. Les outils de diagnostic basés sur la fluorescence, notamment la Soprolife :

- a. augmentent la sensibilité et la spécificité de l'observation
- b. sont utilisables aussi bien pour le traitement que le diagnostic
- c. permet un grossissement majeur de l'image

3. Le substitut type CVIMAR :

- a. assure une bonne biocompatibilité
- b. une étanchéité convenable
- c. est recommandé surtout en cas de lésion à marche lente

4. La reconstruction du point de contact sur molaire :

- a. doit se faire avec des matrices métalliques
- b. en utilisant de préférence des anneaux écarteurs
- c. en privilégiant des composites de haute viscosité

Réponses

1a, b ; 2a, b, c ; 3a, b ; 4a, b

RÉFÉRENCES

1. Tassery H, Levallois B, Terrer E, Manton D, Otsuki M, Koubi S, Gugnani N, Panayotov I, Jacquot B, Cuisinier F, Rechmann P. Use of new minimum intervention dentistry technologies in caries management. *Aust Dent J.* 2013 Jun; 58 Suppl 1: 40-59.
2. Terrer E, Raskin A, Koubi S, Dionne A, Weisrock G, Sarraquigne C, Mazuir A, Tassery H. A new concept in restorative dentistry: LIFEDT-light-induced fluorescence evaluator for diagnosis and treatment: part 2 - treatment of dentinal caries. *J Contemp Dent Pract.* 2010; 11: 95-102.
3. Neves A de A, Coutinho E, De Munck J, Van Meerbeek B. Caries-removal effectiveness and minimal-invasiveness potential of caries-excitation techniques: a micro-CT investigation. *J Dent.* 2011; 39: 154-162.
4. Banerjee A, Cook R, Kellow S, Shah K, Festy F, Sherriff M, Watson T. A confocal microendoscopic investigation of the relationship between the microhardness of carious dentine and its autofluorescence. *Eur J Oral Sci.* 2010; 118: 75-79.
5. Levallois B, Terrer E, Panayotov Y, Salehi H, Tassery H, Tramini P, Cuisinier F. Molecular structural analysis of carious lesions using micro-Raman spectroscopy. *Eur J Oral Sci.* 2012; 120: 444-451.

Correspondance :

Hervé Tassery

Université d'Aix-Marseille

Département d'odontologie conservatrice et restauratrice

27 bd Jean Moulin 13005 Marseille

Email : hervé.tassery@univ-amu.fr

ABSTRACT

THERAPEUTIC MANAGEMENT OF PROXIMAL CARIOUS LESIONS ON ADJACENT TEETH

The therapeutic management of posterior proximal carious lesions faces encounters both diagnostic and technical difficulties. The multiplicity of materials on the market and the difficulty of assessing residual caries activity also complicate the choice of dentine substitute to use, especially in the case of active lesions. The transition between a Type 1 minimal restoration, without any preparation, or a Type 2 restoration with cavity preparation, remains tenuous. The treatment bases proposed in this case report are derived from the LIFEDT (Light Induced Fluorescence for Diagnosis and Treatment) concept. This paper proposes to deal with two contiguous proximal carious lesions (Site 2), one Stage 3 and the other Stage 1.

RESUMEN

UN EJEMPLO DE GESTIÓN TERAPÉUTICA DE LESIONES CARIOSAS PROXIMALES EN DIENTES ADYACENTES

La gestión terapéutica de las lesiones cariosas proximales posteriores se enfrenta a varias dificultades, tanto diagnósticas como técnicas. La multiplicidad de los materiales comercializados y la dificultad de evaluar además la actividad cariosa residual, complican la elección del sustituto dentinario que debe usarse, especialmente cuando hay lesiones activas. La transición entre una restauración mínima de tipo 1, sin ninguna preparación, o de tipo 2, con preparación tisular, sigue siendo tenue. Las bases de los tratamientos propuestos en este informe de caso derivan del concepto LIFEDT (fluorescencia inducida por luz para diagnóstico y tratamiento). Esta ponencia pretende tratar 2 lesiones cariosas proximales (Sitio 2) contiguas, una en fase 3 y la otra en fase 1.



Les blogs de la santé orale
www.idweblogs.com

C'est parti !

Consultez et commentez GRATUITEMENT des articles originaux
Endodontie - Occlusion
Implantologie et prothèse - Esthétique...

DECAY DIAGNOSIS CAMERA: IS IT A VALID ALTERNATIVE?

Kosmas Tolidis, DDS¹, Christina Boutsiouki, DDS²

Early occlusal or hidden caries is generally difficult to detect. A visual examination is augmented with a number of diagnostic aids. The most common aid is radiography either conventional or digital, with or without enhancement. Less commonly used are laser fluorescent devices, fiber optic transillumination devices, electrical resistance devices and caries detector dyes. This article demonstrates the efficacy of a light induced fluorescence evaluator for diagnosis and treatment using SoproLife, SOPRO, Acteon Imaging at various clinical stages of caries formation. Clinical photos before and after intervention are compared using 50X magnification. The case reports show the importance of imaging with the camera during progressive caries removal. To assure the proper diagnosis and complete removal of the caries, the light induced fluorescence evaluator should be used along with visual inspection and radiography.

*INT J MICRODENT 2012;3:**-***

INTRODUCTION

Several methods are used to detect occlusal enamel and dentine caries. The sensitivity of different clinical examination methods, i.e the ability to recognize diseased surfaces as diseased, varies between very low to very high^{1,2} and are more useful in the identification of carious lesions involving the dentine of primary teeth.³ Generally, bite-wing radiography provides a more reliable result than visual inspection with or without magnification and probing in both deciduous and permanent teeth.⁴ While it does not enhance detection of initial occlusal enamel caries,² it increases the number of false-positive diagnosis⁵ and the risk of x-ray overexposure. Probing on the other hand, gives no reliable indication of a lesion, can be traumatic on an intact surface area with weakened subsurface, and can carry bacteria from one site to another.^{6,7} Laser fluorescent devices show the highest sensitivity in dentine caries detection.³ But a very high sensitivity is obtained at

the expense of reduced specificity. A combination of clinical examination first, with laser fluorescent device or bite-wing radiography is suggested.^{2,8} Hidden caries, demineralization of the dentine combined with intact occlusal surface, can be detected by visual examination after careful cleaning and drying of teeth and by use of bite-wing radiographs, but it is often very difficult and may lead to an incorrect diagnosis.⁹ Electrical resistance measurements and fiber-optic transillumination devices have a comparatively good performance in occlusal caries diagnosis.¹⁰ However, having results from multiple methods may lead the dentist to a more invasive treatment.¹¹ Ultimately, the clinician's experience in detecting and choosing how to treat caries is of utmost importance.^{5,12} It is important that overtreatment or undertreatment be avoided. As a result, neither healthy enamel nor dentine will be lost because of a false positive result of the detection method used, nor will carious tissue be left without treatment.

¹ Assistant Professor, Department Operative Dentistry, Aristotle University of Thessaloniki, Greece

² Dentist, DDS, Aristotle University of Thessaloniki, Greece

Correspondence to:

Dr. Christina Boutsiouki
Kallidopoulou 11, 54642, Thessaloniki, Greece
Email: christinaboutsiouki@gmail.com



Fig 1a and 1b Case 1: Cavity prepared on tooth #36. Mode II shows of the presence of a carious lesion by a contrast of luminosity or at least a contrast of colors (red-orange colored shadow in contrast to acid green healthy dentine).

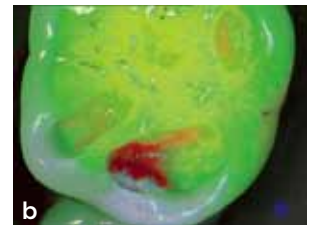


Fig 2a and 2b Case 2: Tooth 36 shows extensive wear due to abrasion and attrition. After opening it can be seen that fissures that are easily self-cleaned, show no signs of caries, under blue light. In the mesial fissure, a plaque accumulation area has been formed indicating the evolution of caries. Moreover, the marginal ridge fractures (black arrows), are signs of undermining caries.

Fig 3a to 3c Case 3: This case presents the importance of 50X magnification under white light in caries detection. Following the opening, the alert is confirmed in Mode II, as dentine shows signs of decay.

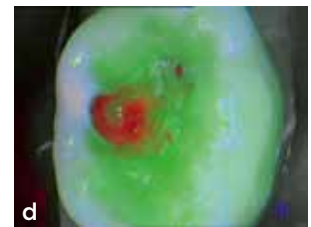


Fig 4a to 4h Case 4(4a to 4d), Case 5(4e to 4h): Large carious lesions on teeth #75 and #74 in a young patient, which have cavitated the occlusal surfaces in both cases, as is demonstrated under white light. Under blue light a grey-white area is pointed out around the cavity, which is a sign of demineralization. As the preparation is begun, the LIFEDT function is confirmed on primary teeth, as decay is clearly visualized as vivid red area at the bottom of the prepared cavity. When carious dentine is removed, color turns to darker red, indicating the presence of sclerotic dentine on #75.

METHOD

A light induced fluorescence evaluator for diagnosis and treatment (LIFEDT) was used in this study. This camera illuminates tooth surfaces within an excitation radiation

band of light of 450nm wavelength to induce fluorescence and facilitates a high magnification image. The SoproLife camera reveals three types of enamel caries: 1) enamel caries on the surface, 2) suspicious grooves with positive red signal and 3) suspicious

grooves with neutral dark signal.¹³

Photos of suspicious for carious lesion tooth surface, were taken in both I and II modes of SoproLife camera. Mode I (Diagnosis Mode) makes decay detection possible at various clinical stages, without loss of consistency and

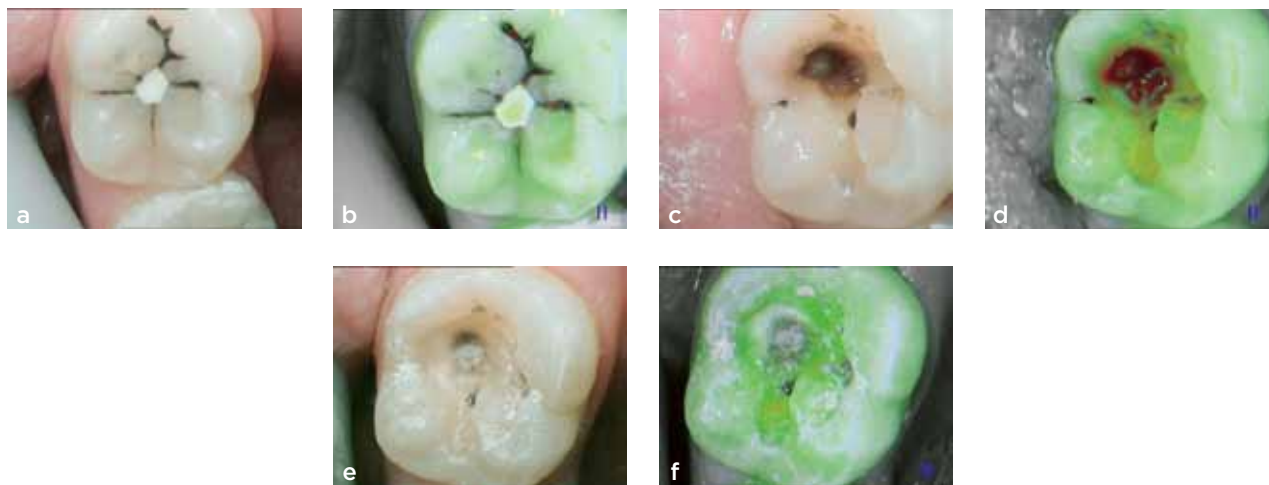


Fig 5a to 5f Case 6: Under white light, a carious infiltration is visible on all fissures of tooth #36. In Mode II the lesion is confirmed by a drastic variation of the fluorescence (from acid green to black). After preparation, the large underlying carious lesion appears in red. The completely decayed tissues appear in wet black. The infected and non conservable dental tissues are removed. The cavity is controlled again in Mode II until full removal of the caries. When caries removal was finished, the dentine looks acid green in Mode II. This case shows the poor caries prevention in failed pit-and-fissure sealants. The fluorescence of pit-and-fissure sealant material under blue light is remarkable.

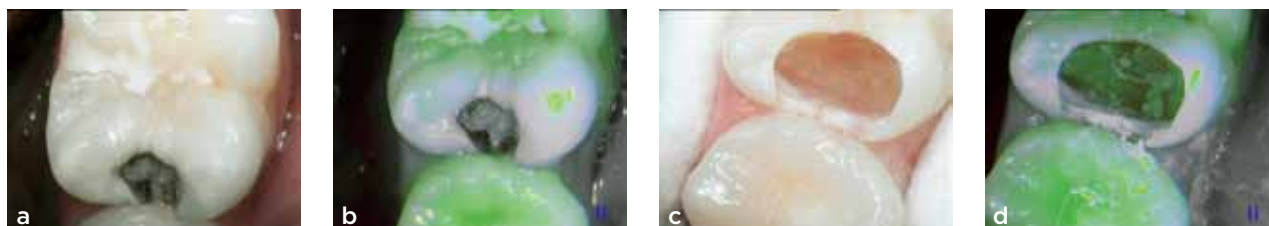


Fig 6a to 6d Case 7: Unlike Case 6, the pit-and-fissure sealant is better preserved but there is a large cavitation on occluso-mesial surface of tooth #36. No sign of caries is shown under blue light, due to plaque accumulation in the cavity. Caries removal is finished and a large cavity is prepared. However, the hard brownish-red, sclerotic dentine is not systematically necessary to remove.

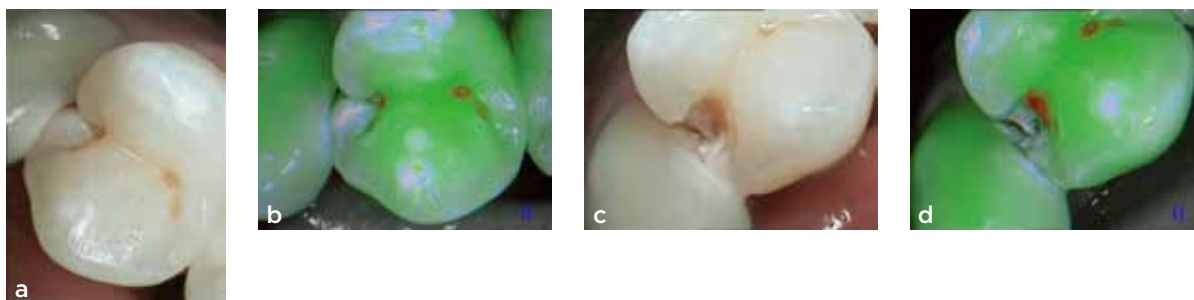


Fig 7a to 7d Case 8: Under white light the inspection of the occlusal surface gives no hints on tooth #14. This is a case of hidden caries. Blue-light inspection confirms caries presence with both contrast of luminosity and contrast of colors. At the opening, the demineralized enamel is characterized in opaque grey-white, while at the bottom of the cavity preparation, the bright red color indicates the presence of an infected/affected interface. This case marks the importance of premolar, mesial fissure morphology in caries propagation.



Fig 8a to 8e Case 9: Under white light nothing appears suspect, except from the grayish shadow on the occluso-mesial surface. Under blue light, a grey-white limited area is observed on the marginal ridge indicating the need to treat this lesion. Next, the pictures show the beginning of the preparation that confirms the presence of caries and the control of caries removal in Mode II throughout the preparation process.



Fig 9a to 9d Case 10: White light inspection shows that tooth #26 exhibits carious lesions on both mesial and distal pits on the occlusal surface, undermining the oblique ridge. The alert is confirmed under blue light, but plaque accumulation in the pit makes it impossible to determine the extent of the lesion. The preparation begins and the alert at the distal pit is confirmed in Mode II with contrast of colors of dentine.

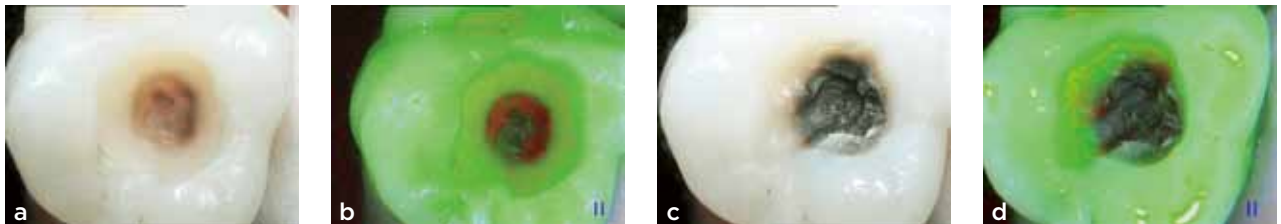


Fig 10a to 10d Case 11: The mesial pit of tooth #16 is opened and decay formation is confirmed. The exeresis goes on until dentine is green, less luminous than healthy dentine, or presents a dark brownish-red shadow, indicating the presence of sclerotic dentine.

in very high resolution. Fluorescence Mode II (Treatment Mode) enables actual spatial mapping of unbroken tissue areas that are suspect, making it easier for the dentist to specify the limits of exeresis of dentinal tissue. Photos of the cavity were taken to prove the existence of caries. The cavity preparation was extended to the extent of the caries and was monitored by consecutive photo shots by SoproLife camera.

CLINICAL CONCLUSIONS

The lighting of the occlusal grooves with the SoproLife camera, enabled observation of any variations in the optical properties of dental tissues at a 50X magnification. It provided a definitive caries diagnosis and provided additional information on the carious potential of

the specific surface and treatment options. Therefore, it is considered an effective and versatile real-time tissue differentiation device, for preserving dental structures and speeding up the daily diagnostic procedures employed by dentists.

REFERENCES

1. Wenzel A, Larsen M, Fejerskov O. Detection of occlusal caries without cavitation by visual inspection, film radiographs, xeroradiographs, and digitized radiographs. *Caries Res.* 1991;25(5):365-71.
2. Nytnun R, Raadal M, Espelid I. Diagnosis of dentine involvement in occlusal caries based on visual and radiographic examination of the teeth. *Scand J Dent Res.* 1992 Jun;100(3):144-8.
3. Lussi A, Francescut P. Performance of conventional and new methods for the detection of occlusal caries in the deciduous teeth. *Caries Res.* 2003 Jan-Feb;37(1):2-7.
4. Poorterman J, Weerheijm K, Groen H, Kalsbeek H. Clinical and radiographic judgement of occlusal caries in adolescents. *Eur J Oral Sci.* 2000 Apr;108(2):93-8.
5. Espelid I, Tveit A, Fjelltveit A. Variations among dentists in radiographic detection of occlusal caries. *Caries Res.* 1994;28(3):169-75.
6. Ekstrand K, Qvist V, Thylstrup. A light microscope study of the effect of probing in occlusal surfaces. *Caries Res.* 1987;21:368-74.
7. Hennequin M, Lasfarges JJ. La demarche diagnostique en cariologie. *Realites Cliniques.* 1999 ;10 :515-39.
8. Chu C, Lo E, You D. Clinical diagnosis of fissure caries with conventional and laser-induced fluorescence techniques. *Lasers Med Sci.* 2010 May;25(3):355-62. Epub 2009 Mar 4.
9. Ricketts D, Kidd E, Weerheijm K, De Soet H: Hidden Caries: What is it? Does it exist? Does it matter? *Int Dent J.* 1997 Oct;47(5):259-65.
10. le Y, Verdonschot E: Performance of diagnostic system in occlusal caries detection compared. *Community Dent Oral Epidemiol.* 1994 Jun;22:187-191.
11. Pereira AC, Eggertsson H, Martinez-Mier EA, Mialhe FL, Eckert GJ, Zero DT. Validity of caries detection on occlusal surfaces and treatment decisions based on results from multiple caries-detection methods. *Eur J Oral Sci.* 2009 Feb;117(1):51-7.
12. Swenson E, Hennessy B. Detection of occlusal carious lesions: an in vitro comparison of clinicians' diagnostic abilities at varying levels of experience. *Gen Dent.* 2009 Jan-Feb;57(1):60-6; quiz 67-8, 95-6.
13. Terrer E, Koubi S, Dionne A, Weisrock G, Sarraquigne C, Mazuir A, Tassery H. A new concept in restorative dentistry: light-induced fluorescence evaluator for diagnosis and treatment. Part 1: Diagnosis and treatment of initial occlusal caries. *J Contemp Dent Pract.* 2009 Nov 1;10(6):E086-94.

In-Vivo Occlusal Caries Prevention by Pulsed CO₂-Laser and Fluoride Varnish Treatment—A Clinical Pilot Study

Peter Rechmann, DDS, PhD,*¹ Daniel A. Charland, DDS,² Beate M.T. Rechmann,¹ Charles Q. Le,¹ and John D.B. Featherstone, MSc, PhD¹

¹Department of Preventive and Restorative Dental Sciences, School of Dentistry, University of California at San Francisco, 707 Parnassus Avenue, San Francisco, California, 94143

²Department of Orofacial Sciences, School of Dentistry, University of California at San Francisco, 707 Parnassus Avenue, San Francisco, California, 94143

Background and Objectives: High caries prevalence in occlusal pits and fissures warrants novel prevention methods. An 86% reduction in dental enamel smooth surface demineralization *in-vivo* following short-pulsed 9.6 μm -CO₂-laser irradiation was recently reported. The objective of this study was to conduct a blinded 12-month-pilot clinical trial of occlusal pit and fissure caries inhibition using the same CO₂-laser irradiation conditions.

Study Design/Materials and Methods: Twenty subjects, average age 14 years, were recruited. At baseline, second molars were randomized into test and control groups, assessed by International Caries Detection & Assessment System (ICDAS-II), SOPROLIFE light-induced fluorescence evaluator in daylight and blue-fluorescence mode and DIAGNOdent. An independent investigator irradiated test molars with a CO₂-laser, wavelength 9.6 μm , pulse-duration 20 μs , pulse-repetition-rate 20 Hz, beam diameter 800 μm , average fluence $4.5 \pm 0.5 \text{ J/cm}^2$, 20 laser pulses per spot. At 3-, 6- and 12-month recall teeth were assessed by ICDAS, SOPROLIFE and DIAGNOdent. All subjects received fluoride varnish applications at baseline and 6-month recall.

Results: All subjects completed the 3-month, 19 the 6-month and 16 the 12-month recall. At all recalls average ICDAS scores had decreased for the test and increased for the control fissures (laser vs. control, 3-month: -0.10 ± 0.14 , 0.30 ± 0.18 , $P > 0.05$; 6-month: -0.26 ± 0.13 , 0.47 ± 0.16 , $P = 0.001$; 12-month: -0.31 ± 0.15 , 0.75 ± 0.17 , $P < 0.0001$; mean \pm SE, unpaired *t*-test) being statistically significantly different at 6- and 12-month recalls.

SOPROLIFE daylight evaluation revealed at 6- and 12-months statistically significant differences in changes between baseline and recall for test and control molars, respectively (laser vs. control, 6-month: 0.22 ± 0.13 , 0.17 ± 0.09 , $P = 0.02$; 12-month: 0.28 ± 0.19 , 0.25 ± 0.17 , $P = 0.03$). For SOPROLIFE blue-fluorescence evaluation mean changes in comparison to baseline for the control and the laser treated teeth were also statistically significant for the 6- and 12-month recall.

Conclusion: Specific microsecond short-pulsed 9.6 μm CO₂-laser irradiation markedly inhibits caries progression

in pits and fissures in comparison to fluoride varnish alone over 12 months. *Lasers Surg. Med.* © 2013 Wiley Periodicals, Inc.

Key words: CO₂-laser; microsecond pulsed; *in vivo* occlusal caries prevention; occlusal fissures; fluoride varnish; randomized prospective clinical pilot study

INTRODUCTION

Studies investigating the enhancement of the acid resistance of dental enamel were reported within a few years of the invention of the first laser. Studies from the 1970s to the early 2000s aimed at reducing the acid dissolution of enamel by the use of CO₂-lasers, mostly at 10.6 μm [1–10], all successfully showing various levels of demineralization inhibition of smooth enamel surfaces in the laboratory [11,12]. Other laser wavelengths have been investigated in laboratory studies including Nd:YAG- [13–16], Er:YAG - [17–20], Er,Cr:YSGG- [21–23] as well as argon lasers [24–29] with and without additional topical fluoride application. Small scale *in-vivo* studies using an argon laser around orthodontic brackets [30] or Nd:YAG-laser treatment coupled with initiation dye and acidulated fluoride application in children with the effects assessed by following the development of white spot lesions or fissure caries [31] were reported.

Featherstone et al. [9,10,32] have shown, in several studies, that enhancement of caries resistance of enamel can be achieved in the laboratory by irradiation with short-

Conflict of interest Disclosures: All authors have completed and submitted the ICMJE Form for Disclosure of Potential Conflicts of Interest and none were reported.

Contract grant sponsor: NIH/NIDCR; Grant number: DE09958
*Correspondence to: Peter Rechmann DDS, PhD, Department of Preventive and Restorative Dental Sciences, School of Dentistry, University of California at San Francisco, 707 Parnassus Avenue, San Francisco, CA 94143.

E-mail: rechmannp@dentistry.ucsf.edu

Accepted 9 April 2013
Published online in Wiley Online Library
(wileyonlinelibrary.com).
DOI 10.1002/lsm.22141

pulsed CO₂-lasers under well-specified irradiation conditions using much lower energy levels than those reported in most of the above studies. The wavelengths most strongly absorbed in dental enamel are the 9.3 and 9.6 μm CO₂-laser wavelengths with up to a 10× higher absorption coefficient compared to a 10.6 μm CO₂-laser [33]. In addition using microsecond instead of millisecond pulses allows a well-defined energy application without harmful side effects. The loss of the carbonate phase from the enamel crystals due to the irradiation heat is reported to be responsible for the reduction in acid dissolution of enamel [34,35]. Using the same laser irradiation conditions in a “pulpal safety study” on teeth in humans evidence was provided that there is no harm to the pulpal tissue of those irradiated teeth [36].

Rechmann et al. [37] used an orthodontic bracket model and showed, for the first time *in-vivo*, in a single blind, prospective clinical trial that enhancing enamel demineralization resistance can be achieved by irradiation with a CO₂ 9.6 μm laser, emitting laser pulses in the microsecond range [38]. The quantitative assessment of demineralization by cross sectional microhardness testing of laser treated enamel revealed that using a 9.6 μm CO₂-laser irradiation significantly inhibited the formation of carious lesions around orthodontic brackets. For the first time in vital teeth in humans it was shown that the laser irradiation reduced enamel mineral loss by up to 46% over a time period of 4 weeks. Evaluating the caries resistance enhancing capacity of this CO₂-laser treatment over 12 weeks revealed an 87% reduction in mineral loss in comparison to the control surfaces, which was speculated to be also related to an enhancement of demineralization following the laser irradiation [38].

The study presented here was a single blind, controlled, randomized prospective clinical pilot trial, assessing treatment effects within-person thereby controlling for genetic, nutritional, hygiene, and oral environment factors. The hypothesis to be tested was that the use of a microsecond pulsed 9.6 μm CO₂-laser with additional fluoride varnish applications will significantly inhibit the formation of carious lesions in fissures of molars *in vivo* in comparison to a non-irradiated control tooth in the same arch over a 1 year observation interval.

MATERIALS AND METHODS

Study Inclusion and Exclusion Criteria

The Committee on Human Research at UCSF (IRB# 10-03431) approved the study. Prior to enrolling into the study an independent dental examiner, not otherwise involved in the study, conducted a clinical exam to assess caries status and to determine any treatment needs. An intraoral exam, review of intraoral radiographs, medical history and definitive dental history were performed.

Inclusion criteria for the study were a subject age of 10–17 years, high caries risk status, and having at least two fully erupted second molars in the same arch (contralateral) with untreated, non-carious occlusal surfaces (ICDAS code 0, 1, 2 were allowed; see below). Subjects

had to be willing to comply with all study procedures and protocols. They had to be residents of San Francisco or other nearby local communities with water fluoridation (to eliminate water fluoridation as a potential confounding variable). Subjects had to be healthy and subjects/parent had to be willing to sign the “Authorization for Release of Personal Health Information and Use of Personally Unidentified Study Data for Research” form. There were no gender restrictions.

Subjects were excluded from the study if they were suffering from systemic diseases, had a significant past or medical history with conditions that may affect oral health (i.e., diabetes, HIV, heart conditions that require antibiotic prophylaxis), were taking medications that may affect the oral flora or salivary flow (e.g., antibiotic use in the past 3 months, drugs associated with dry mouth/xerostomia), had in-office fluoride treatment within the last 3 months prior to being enrolled in the study, were not willing to stop the use of any mouth rinse or other oral hygiene product during the duration of the study, or were planning to leave the area and would not be available for recall visits.

Subjects who met the selection criteria were asked to provide verbal assent/consent and their parent/guardian to provide written informed consent.

Twenty subjects were recruited for the study, comprising six females and 14 males with an average age of 14.2 ± 1.2 years.

The right or left second molar was randomly selected for laser treatment—the tooth on the opposite site in the same jaw served as control. In six subjects the upper and in 14 the lower jaw was available for selection. Randomization resulted in the laser treatment of nine teeth on the right and 11 teeth on the left side. The randomization list was created by a random number generator (QuickCalcs online random numbers by GraphPad Software, Inc.).

Study Procedure

After enrollment, before evaluating the occlusal surfaces the second molars were cleaned with a disposable tapered rotating brush (Denticator, Earth City, MO) 10–20 seconds per tooth and then rinsed with an air–water spray. Prophyl paste was not used. Cotton rolls were placed and the occlusal surface was briefly air-dried (3 seconds per tooth) immediately before performing a caries lesion assessment (detailed description below). Then the study tooth was laser treated and the lesion assessment was repeated. The participants were instructed to brush twice daily with a dentifrice containing 1,100 ppm F as NaF for 1 minute each brushing.

All subjects received fluoride varnish applications (Omni Vanish fluoride varnish, Omni Preventive Care, West Palm Beach, FL) at baseline and 6-month recall.

For caries lesion assessment recalls were scheduled at 3-, 6-, and 12 months after laser treatment.

As entrance criteria only subjects with no caries or precavitated lesions (ICDAS code 0, 1, 2) were allowed into the study. If at any recall appointment a higher ICDAS code was registered a sealant or filling was placed and the subject’s participation in the study was terminated. At the

end of the study the control and test teeth were sealed with a sealant (Helioseal, Ivoclar Vivadent, Amherst, NY).

Laser Settings

The laser used in the study was a CO₂-laser, Pulse System, Inc (PSI) (Model #LPS-500, Los Alamos, NM), wavelength 9.6 μm, pulse duration 20 μseconds, pulse repetition rate 20 Hz, beam diameter at focus approximately 800 μm delivered through a contra-angle hand piece specifically custom made for this study. The goal was to irradiate each spot of the irradiation area with 20 laser pulses. The laser fluence used in this study-averaged $4.5 \pm 0.5 \text{ J/cm}^2$ per pulse (range 4.3–5.9 J/cm²). The average treatment time per tooth was 95 ± 20 seconds (range 63–134 seconds).

The area of the surface to be irradiated (fissure and adjacent 1 mm surface to each side) was measured and the number of laser pulses and the irradiation time respectively were calculated. High volume evacuation was used and a water coolant was not applied.

Assessment Tools Used

The occlusal surfaces of the study second molars were visually assessed for decalcification using the ICDAS II criteria (International Caries Detection and Assessment System) [39], the SOPROLIFE Light Induced Fluorescence Evaluator system (SOPRO, ACTEON Group, La Ciotat, France) and the DIAGNOdent (KaVo, Biberach, Germany). For each tooth a specific area of interest was noted for the reevaluations, thus at baseline and at all recalls all three assessments occurred exactly at the same point of interest.

Visual Examination and Assessment Using ICDAS Criteria

The ICDAS criteria (International Caries Detection and Assessment System) [39] were applied for assessing the degree of decalcification of the fissure areas of the study teeth. The two examiners (DC, PR) were blinded to each other's evaluation results. On each tooth a specific area of interest was defined and noted for the reevaluations. After independently scoring for ICDAS, the examiners discussed their findings and agreed on one ICDAS score per tooth.

The inter-examiner reliability (DC, PR) for the ICDAS scoring was assessed with a $\kappa = 0.884$, SE of $\kappa = 0.017$, 95% confidence interval from 0.851 to 0.917, at 571 observations in a study occurring before [40]. The strength of agreement is considered to be "very good [41]. The weighted Kappa was calculated at $\kappa = 0.905$ using linear weighting. Assessed this way, the strength of agreement is again considered to be "very good [41].

SOPROLIFE Light Induced Fluorescence Evaluator

The SOPROLIFE Light Induced Fluorescence Evaluator system operates in daylight and in blue fluorescence mode. In the daylight mode the system uses four white LEDs, in the fluorescence mode it uses four blue LEDs emitting a

wavelength of 450 nm. In this study the system was used in the LIFE magnification mode with daylight or fluorescence detection mode I—diagnosis aid mode. The hand-piece allows for collecting pictures. The images were recorded with the SOPRO IMAGING software. A HP 620 Notebook (HP, Palo Alto, CA; Windows 7, Microsoft Redmond, WA) was used to collect the data for independent evaluation. A lately introduced scoring system was utilized [40,42] to evaluate the images by two independent examiners (BR, PR). The same areas of interest as chosen for the ICDAS scoring were used for the SOPROLIFE scoring. After independently evaluating SOPROLIFE daylight and blue fluorescence scores, the examiners discussed their findings and agreed on one SOPROLIFE daylight and one blue fluorescence score per tooth.

DIAGNOdent Laser Fluorescence

The DIAGNOdent Classic tool (KaVo, Biberach, Germany) emits a red laser light (wavelength 655 nm) and measures the returning fluorescence in the spectral region >680 nm wavelength. Before assessing a new subject the tool was calibrated according to manufacturer's instruction.

The highest score per evaluated fissure area of interest was noted (scores ranged from 3 to 64 in this study).

RESULTS

ICDAS Visual Examination and Assessment—Results

A total of 20 subjects were recruited into the study from which all subjects completed the 3-month recall. At the 6-month recall appointment one subject and at the 12-month recall two subjects were no-shows despite multiple reminders, thus 19 subjects completed the 6-month and 16 the 12-month recall.

One subject presented at the 6-month recall with an ICDAS code 3 lesion in the control tooth, consequently received fissure sealants on the study molars, and was withdrawn from further participating in the study. At the 12-month recall 4 other subjects had developed ICDAS code 3 lesions in their control teeth.

Figure 1 shows the average ICDAS scores for control and laser treated teeth. At baseline the average ICDAS scores were not statistically significant different between the control and the laser group with 1.0 ± 0.18 (mean \pm SE) and 1.15 ± 0.15 , respectively (unpaired *t*-test, $P > 0.5$). At the 3-month recall the average ICDAS score for the control increased to 1.30 ± 0.15 and the score for the laser slightly decreased (1.05 ± 0.14) but they were still not statistically significant different ($P = 0.2$). At the 6- and the 12-month recall the average ICDAS score for the control increased to 1.53 ± 0.19 and 1.69 ± 0.27 , respectively. On the contrary, at these recalls the mean ICDAS scores for the laser treated molars had decreased below the starting average to 0.95 ± 0.14 for the 6-month and 0.88 ± 0.16 for the 12-month recall. The differences between control and laser treated scores were statistically significant at both time

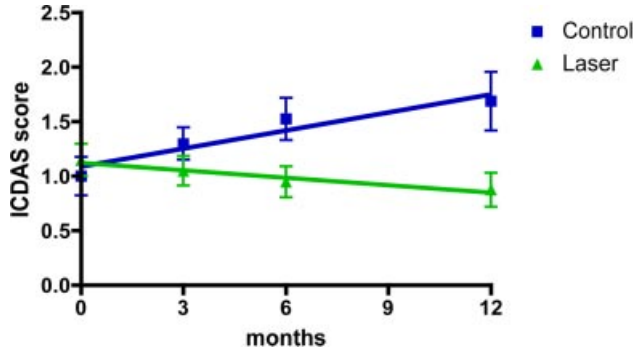


Fig. 1. Average ICDAS scores at baseline, 3-, 6-, and 12-month recall (mean \pm SE) for laser treated and control teeth with statistically significant differences at 6- and 12-month recall; linear regression fits being significantly non-zero with a positive slope (increasing—demineralization) for the controls and a negative slope (decreasing—remineralization) for laser treated teeth.

points ($P = 0.021$ at 6-month; $P = 0.016$ at 12-month recall).

Figure 1 also shows the linear regression fit for the average ICDAS scores for control and laser treated teeth. The slopes of the regression lines are significantly non-zero (control $P = 0.048$, laser treated $P = 0.034$) indicating that differences between each average score exist with a goodness of fit of r^2 0.91 and 0.93 for control and laser treated molars, respectively. Furthermore the slope of the regression line for the control teeth is positive (0.06 ± 0.01) and the slope for the laser treated teeth is negative (-0.03 ± 0.004).

Considering average changes of the ICDAS scores between baselines and the 3-, 6- and 12-month recall reveals at the 3-month recall that the laser treated teeth showed a slightly negative ICDAS change while the controls showed slightly positive changes but the differences were not statistically significant (laser treated -0.10 ± 0.14 vs. control 0.30 ± 0.18 , mean \pm SE; $P = 0.09$). For 6-month and the 12-month recall the tendency continued (6-month: laser treated -0.26 ± 0.13 vs. control 0.47 ± 0.16 ; 12-month: laser treated -0.31 ± 0.15 vs. control: 0.75 ± 0.17). Those differences in ICDAS changes were statistically significant (6-month $P = 0.001$ and 12-month $P < 0.0001$, unpaired t -test).

SOPROLIFE Light Induced Fluorescence Evaluator

SOPROLIFE daylight mode—results. In addition to the ICDAS assessment system the fissure systems of the study teeth were evaluated with the SOPROLIFE system and scored with a recently introduced scoring system developed for the SOPROLIFE light induced fluorescence evaluator for daylight and for the blue fluorescence mode [40,42]. For the control as well as the laser treated teeth the SOPROLIFE scores ranged between 0 and 3 at baseline.

At baseline the SOPROLIFE daylight scores were not statistically significant different for the two groups (laser 1.45 ± 0.19 , control 1.6 ± 0.23 (mean \pm SE); unpaired t -test $P > 0.05$). At all recall times using the SOPROLIFE daylight evaluation the control molars showed in average more severe and/or extended lesion while the laser treated teeth exhibited less severe or same lesion scores (3-month: laser 1.70 ± 0.23 , control 1.35 ± 0.18 ; 6-month: laser 1.22 ± 0.22 , control 1.83 ± 0.23 ; 12-month: laser 1.22 ± 0.26 , control 1.87 ± 0.27). Nevertheless at each recall time point differences between control and laser teeth were not statistically significant ($P > 0.05$). A linear fit calculation revealed that the deviation from zero for each linear regression line was not significant.

Calculating the changes in SOPROLIFE daylight scores between baseline and each recall (Fig. 2) revealed an increased daylight score for the controls and a decreased score for the laser treated fissures. Those differences were statistically significant for the 6- and 12-month recall (6-month: control 0.17 ± 0.09 vs. laser -0.22 ± 0.13 , unpaired t -test $P = 0.02$; 12-month: control 0.25 ± 0.11 vs. laser -0.28 ± 0.19 , $P = 0.03$).

SOPROLIFE blue fluorescence mode—results.

When evaluating the SOPROLIFE blue fluorescence average scores for baseline and the 3-, 6- and 12-month recall as with the SOPROLIFE daylight scores a similar tendency of increasing control and decreasing laser treated fissure scores was observed (except for the 12-month recall laser group). Nevertheless for each time point the average scores for control and laser treated teeth were statistically not different ($P > 0.05$) (baseline: laser 1.16 ± 0.21 , control 1.4 ± 0.3 ; 3-month: laser 1.05 ± 0.19 , control 1.5 ± 0.29 ; 6-month: laser 1.0 ± 0.24 , control

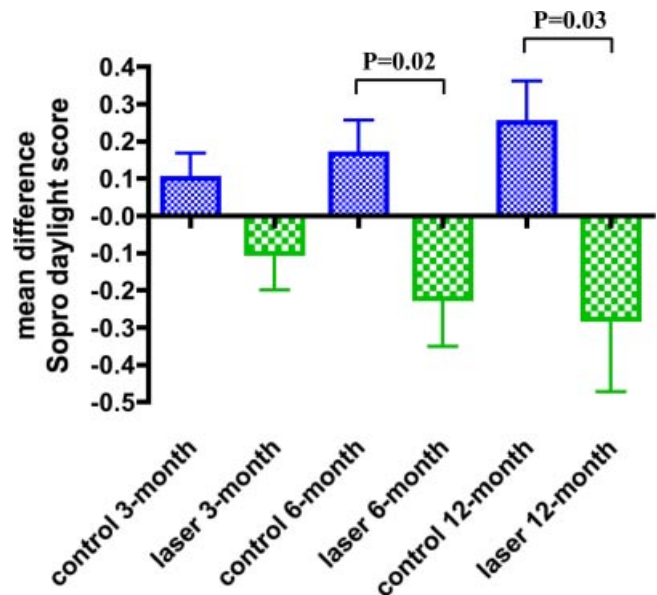


Fig. 2. Average changes of the SOPROLIFE daylight scores for laser treated and control teeth between baseline and the 3-, 6-, and 12-month recall (mean \pm SE) with statistically significant differences at the 6- and 12-month recall.

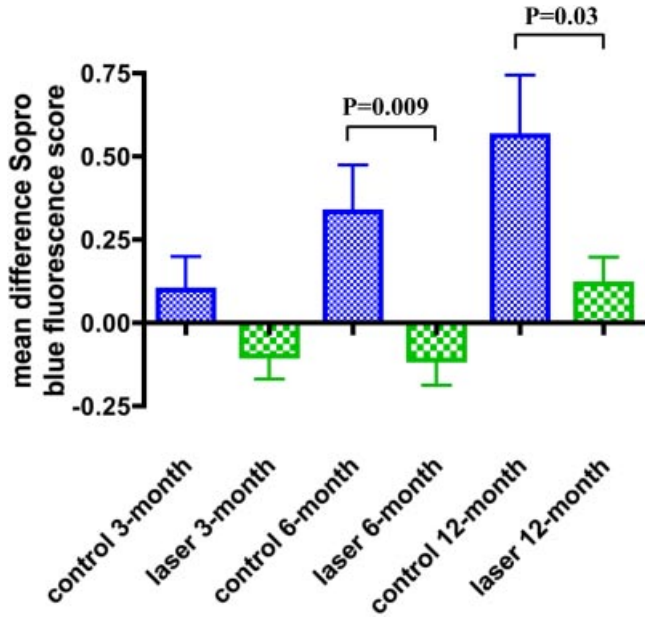


Fig. 3. Average changes of the SOPROLIFE blue fluorescence scores for laser treated and control teeth between baseline and the 3-, 6-, and 12-month recall (mean ± SE) with statistically significant differences at the 6- and 12-month recall.

1.6 ± 0.29; 12-month: laser 1.31 ± 0.24, control 1.8 ± 0.31).

Calculating the changes in SOPROLIFE blue fluorescence scores between baseline and each recall point (Fig. 3) revealed a similar pattern to that for the SOPROLIFE daylight evaluation an increasing average score for the controls, the laser treated teeth showed a score reduction for the 3- and 6-month observation and then slightly increased to the level the control teeth had demonstrated at the 3-month recall. The mean changes in comparison to baseline for the control and the laser treated teeth were statistically significant for the 6- and 12-month recall (Fig. 3) (3-month: control 0.1 ± 0.1 vs. laser -0.1 ± 0.07, unpaired *t*-test *P* = 0.1; 6-month: control 0.33 ± 0.14 vs. laser -0.11 ± 0.08, *P* = 0.009; 12-month: control 0.56 ± 0.18 vs. laser 0.12 ± 0.08, *P* = 0.03).

Figures 4 and 5 are examples of daylight and blue fluorescence pictures of one control and one laser treated tooth of the same subject at baseline and at the 6-month recall. Both molars show obvious changes in the fissure system, which are very distinct in the distal groove. While the area of demineralization in the control tooth appears wider in daylight mode and fluorescence mode after 6 months in the laser treated tooth the demineralization and the red fluorescence, respectively disappeared (left side baseline, right side 6-month recall).

DIAGNOdent—Results

At baseline the DIAGNOdent average values for the control fissures were 23.7 ± 16 and for the laser group 22.4 ± 11.9 (mean ± SD). Over the observation time the

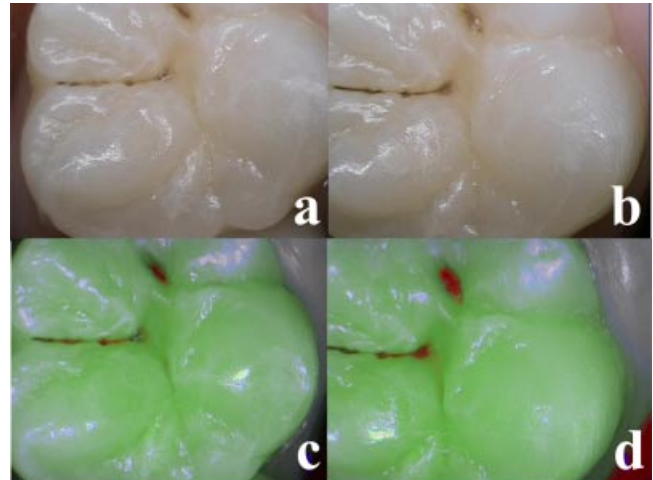


Fig. 4. Example of daylight and blue fluorescence pictures of a control tooth of a subject at baseline and at the 6-month recall. The area of demineralization in the control tooth appears wider in daylight mode and fluorescence mode after 6 month (a: daylight, c: blue fluorescence mode at baseline; b and d: at 6-month recall).

average DIAGNOdent values for the controls slightly increased to 25.1 ± 17.8, the value for the laser treated teeth at 12-month recall stayed around 21.0 ± 13.9 (Fig. 6 shows mean ± SE).

Figure 6 also shows a linear regression fit for the average DIAGNOdent scores for control and laser treated teeth over time. The slopes of the regression lines do not deviate significantly from zero indicating that there is no significant change over time for the DIAGNOdent scores. Comparing changes in DIAGNOdent average scores between baseline and each recall point revealed no statistically significant differences for either group.

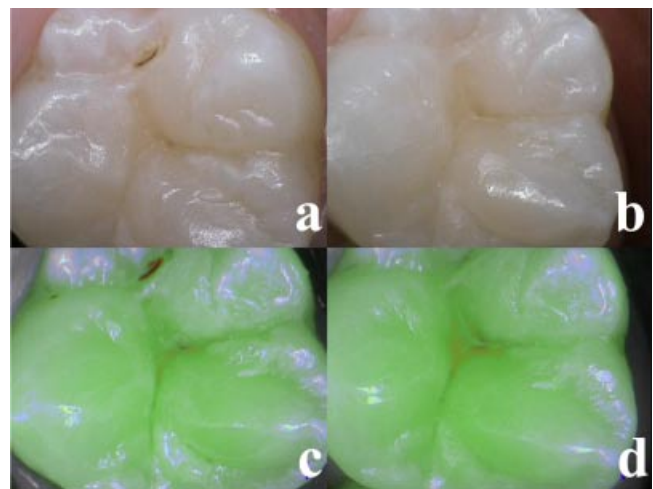


Fig. 5. Daylight and blue fluorescence pictures of the laser treated tooth (same subject as in Fig. 4) at baseline and at the 6-month recall. In the distal fossa of the laser treated tooth in daylight mode and fluorescence mode the demineralization zone and the red fluorescence, respectively is not visible anymore (a: daylight and c: blue fluorescence mode at baseline; b and d: at 6-month recall).

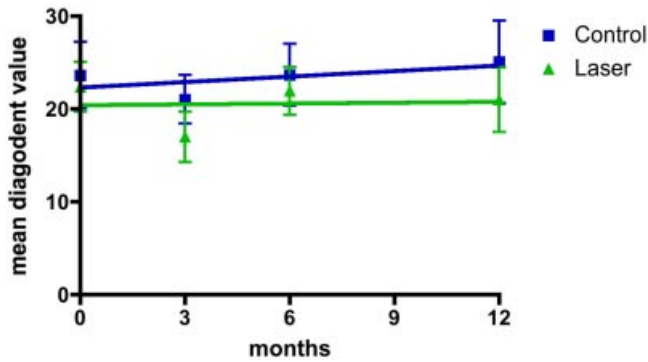


Fig. 6. Average DIAGNOdent scores at baseline, 3-, 6-, and 12-month recall (mean \pm SE) for laser treated and control teeth statistically not different at all time points; linear regression fits do not deviate significantly from zero indicating that there is no significant change over time for the DIAGNOdent scores.

DISCUSSION

In the past, several laboratory studies have shown that enhancing enamel demineralization resistance can be achieved by irradiation with microsecond pulsed CO₂-lasers [9,32]. The wavelengths absorbed most strongly in dental enamel are the 9.3 and 9.6 μ m CO₂-laser wavelengths [33]. The loss of the carbonate phase from the enamel crystals due to the irradiation heat is responsible for the reduction in acid dissolution of enamel [34,43] transforming carbonated hydroxyapatite into the more acid resistant hydroxyapatite. Adding fluoride at this time leads to the formation of fluorapatite, which is even less acid soluble [44].

Lately we reported that using a 9.6 μ m CO₂-laser irradiation (20 μ seconds pulse duration) significantly inhibits the formation of carious lesions around orthodontic brackets [38]. Our study showed for the first time in vital teeth in humans that the applied irradiation scheme reduced enamel mineral loss by up to 46% over a time period of 4 weeks and due to enhanced remineralization up to 87% over a 12 weeks period. At the same time demineralization for the controls, as expected, continued to become more severe [38]. This *in-vivo* orthodontic bracket model study confirmed that caries inhibition demonstrated in numerous models and experiments in the laboratory [9,45–47] can also be achieved in humans in vital teeth using short-pulsed 9.6 μ m CO₂-laser irradiation.

In this orthodontic bracket model study the test teeth had to be extracted to perform the cross sectional microhardness testing. In the study presented here we irradiated, for the first time, occlusal pits and fissures of second molars in the mouth and assessed a change in mineralization status by visual methods using the International Caries Detection & Assessment System—ICDAS, SOPRO-LIFE in daylight and in fluorescence mode and the DIAGNOdent tool. The intent of the study was to demonstrate caries inhibition in fissures of molars and this included the additional challenge of irradiating

normal fissures as well as deep fissures. In order to reach and irradiate the walls of deep fissures we designed and used a contra-angle laser handpiece specifically custom made for this study.

This single blind, controlled, randomized clinical pilot trial showed that using a microsecond pulsed 9.6 μ m CO₂-laser with additional fluoride varnish applications significantly inhibits the formation of carious lesions in fissures of molars *in vivo* in comparison to a non-irradiated control tooth in the same arch over a 1 year observation interval.

However, DIAGNOdent as a spot fluorescence measurement tool, illuminating with a red laser light (655 nm) and creating an infrared fluorescence originated from porphyrins and related compounds from oral bacteria [48–51], was not able to confirm this positive result due to the system's inherent limited capacity of caries detection at the enamel level. The system has shown good performance and reproducibility for detection and quantification of occlusal and smooth surface carious lesions in *in-vitro* studies [48,52,53], but with somewhat more contradictory results *in vivo*, both in the primary and permanent dentition [54–60]. It has also been tried for longitudinal monitoring of the caries process, and for assessing the outcome of preventive interventions [61].

In this laser caries prevention study the average DIAGNOdent score at baseline was 23.0 (\pm 13.9, SD) and thus below the discussed cut-off points for operative interventions (filling) [62–64]. Even if for the controls the value slightly increased over time, those differences were not significant and not expected. All visually observed changes were at a precavitated level or at most a first enamel breakdown (ICDAS code 3) was observed in this study. Thus significant dentin involvement with consequently increased porphyrin levels in dentin did not occur and thus no significant changes in the DIAGNOdent assessments took place. The DIAGNOdent measures the uptake of organic bacterial by-products and does not measure demineralization or remineralization directly.

The International Caries Detection and Assessment System provides a standardized method of lesion detection and assessment, leading to caries diagnosis [39]. ICDAS criteria are based on enamel properties of translucency and microporosity. With numerous demineralization events the microporosity of enamel subsurface increases, which leads to changes in its refractive index. The first sign of carious alteration is a change in translucency and light refraction of the enamel surface. If demineralization continues the enamel microporosity increases, which then leads to further decrease in the refractive index of enamel [65].

Ekstrand et al. [66–68] validated ICDAS by demonstrating an association between the severity of caries lesions (as described by ICDAS codes) and the lesions' histological depth. Other authors have confirmed a close relationship between ICDAS scoring and the histological depth of the caries lesion, especially in precavitated but also in slightly cavitated stages [55,69], endorsing a relationship between the visual topography at surface level and the histological lesion depth.

In this present short-pulsed CO₂-laser caries prevention study only subjects presenting teeth with no caries at all (ICDAS code 0) or with precavitated lesions (code 1, 2) were allowed to participate. Any tooth exhibiting a higher score at any recall received fissure sealants and lead to the withdrawal of the subject from further participating in the study.

One subject presented at the 6-month recall with an ICDAS code 3 lesion—first visible enamel loss—at the control tooth, and at the 12-month recall four other subjects had developed ICDAS code 3 lesions at their control teeth. Thus in total during the observation time of 12 months 5 out of 20 subjects had developed caries lesions at ICDAS 3 code level—all on the non-irradiated control teeth. None of the laser treated teeth changed into ICDAS 3 code.

Regarding the ICDAS score development over time the score for the control teeth constantly increased depicting more severe mineral loss while in the control teeth the ICDAS scores constantly decreased, demonstrating some mineral gain. Comparing average ICDAS scores for each time point and average changes of the ICDAS scores between baselines and the 3-, 6- and 12-month recall showed statistically significant levels at 6- and 12-month and that over the observation period of 1 year the control teeth increased the ICDAS score by almost $\frac{3}{4}$ of an ICDAS score from an average ICDAS code 1 to an ICDAS 1.7 code. At the same time the laser treated fissures at the contralateral side of the mouth showed for a similar ICDAS code at study start (average code 1.05) a reduction of almost $\frac{1}{5}$ of an ICDAS score, down to an average ICDAS 0.88 code.

These trends were confirmed by the linear regression fit, depicting for both groups regression lines significantly deviating from zero with a positive slope (increase) for the control and a negative (decrease) for the laser treated teeth. In the *in-vivo* orthodontic bracket model laser study using short-pulsed 9.6 μm CO₂-laser irradiation the same trends were observed with a lower mineral loss or even mineral gain at the 12-week in comparison to the 4-week interval for the laser treated teeth [38]. From this present study and the orthodontic bracket study the assumption is supported that driving out the carbonated phase from the enamel crystal due to the irradiation decreases demineralization of the modified hydroxyapatite in an acid environment. The transformed hydroxyapatite also appears to be prone to higher remineralization specifically when fluoride is present. This phenomenon was observed in this study over a period of 12 months.

Fluorescence is a property of some materials that absorb energy at certain wavelengths and emit light at longer wavelengths. Several caries detection methods engage fluorescence. The SOPROLIFE system is thought to combine the advantages of a visual inspection method (high specificity) with a high magnification oral camera and a laser fluorescence device (high reproducibility and discrimination). In the daylight mode the system uses four white, and in the fluorescence mode it uses four blue LEDs. The fluorescence signal and expression is most probably

triggered and modified by bacteria and bacteria by-products. The blue light transmits through healthy enamel and evokes a green fluorescence of the dentin core. The green fluorescence light coming back from the dentin core then leads to a red fluorescence from bacteria and bacterial byproducts like porphyrins [40].

A recently published SOPROLIFE daylight and blue fluorescence scoring system with six distinct codes for each detection mode [40,42] was used to evaluate the teeth in this laser study. As with the ICDAS scores SOPROLIFE daylight as well as blue fluorescence scoring showed over time increasing average scores for the control teeth and decreasing scores for the laser treated fissures. The differences became significant for the 6- and 12-month recall intervals. The trends were obvious for the daylight evaluation, which in the scoring codes strongly correlates with the ICDAS [42] and thus confirmed the ICDAS results for this study. The SOPROLIFE blue fluorescence evaluation despite showing the same significant differences between baseline and follow up for the 6- and 12-month evaluation time points revealed a slightly increased average score at the 12-month recall for the laser treated teeth. Nevertheless the variations in the average code change for the fluorescence codes for the laser treated fissures were extremely low with only around $\frac{1}{10}$ of a score while the control teeth showed more prominent average changes of $\frac{6}{10}$ of a score. The mechanism as to how porphyrin fluorescence might change over time, specifically in superficial enamel lesions related to remineralization is still not completely understood.

This clinical study has verified that microsecond short pulsed 9.6 μm CO₂-laser irradiation in combination with biannual application of fluoride varnish can, over a 1 year period, efficiently enhance caries resistance of laser treated fissures in comparison to non-treated fissures. The study revealed that using the same laser irradiation conditions, which in a pulpal safety study on teeth in humans had provided evidence that there is no harm to the pulpal tissue of those irradiated teeth [36], even leads to remineralization of the irradiated enamel proven by ICDAS and SOPROLIFE daylight and fluorescence assessments.

Further larger scale clinical studies to ascertain the efficiency of treating fissures and gingival smooth surfaces to reduce demineralization with the short-pulsed CO₂-laser are needed.

REFERENCES

1. Stern RH, Sognnaes RF. Laser inhibition of dental caries suggested by first tests in vivo. *J Am Dent Assoc* 1972;85 (5):1087–1090.
2. Stern RH, Vahl J, Sognnaes RF. Lased enamel: Ultrastructural observations of pulsed carbon dioxide laser effects. *J Dent Res* 1972;51(2):455–460.
3. Beeking PO, Herrmann C, Zuhrt R. Examination of laser-treated tooth surfaces after exposure to acid. *Dtsch Stomatol* 1990;40(12):490–492.
4. Nammour S, Renneboog-Squilbin C, Coomans D, Dourou N. The resistance of the dentine to acid following vaporisation of the caries by CO₂ laser. In: Melcer J, editor. *The Impact of Lasers on Dental Science*. Paris: ITBM Journal; 1990. p 96.

5. Fox JL, Yu D, Otsuka M, Higuchi WI, Wong J, Powell GL. Combined effects of laser irradiation and chemical inhibitors on the dissolution of dental enamel. *Caries Res* 1992;26:333–339.
6. Nammour S, Renneboog-Squilbin C, Nyssen-Behets C. Increased resistance to artificial caries-like lesions in dentin treated with CO₂ laser. *Caries Res* 1992;26(3):170–175.
7. Hsu J, Fox JL, Wang Z, Powell GL, Otsuka M, Higuchi WI. Combined effects of laser irradiation/solution fluoride ion on enamel demineralization [published erratum appears in *J Clin Laser Med Surg* 1998 Oct; 16(5) 294–295]. *J Clin Laser Med Surg* 1998;16(2):93–105.
8. Hossain M, Nakamura Y, Kimura Y, Ito M, Yamada Y, Matsumoto K. Acquired acid resistance of dental hard tissues by CO₂ laser irradiation. *J Clin Laser Med Surg* 1999;17(5):223–226.
9. Featherstone JD, Barrett-Vespone NA, Fried D, Kantorowitz Z, Seka W. CO₂ laser inhibitor of artificial caries-like lesion progression in dental enamel. *J Dent Res* 1998;77(6):1397–1403.
10. Kantorowitz Z, Featherstone JD, Fried D. Caries prevention by CO₂ laser treatment: Dependency on the number of pulses used. *J Am Dent Assoc* 1998;129(5):585–591.
11. Hsu CY, Jordan TH, Dederich DN, Wefel JS. Effects of low-energy CO₂ laser irradiation and the organic matrix on inhibition of enamel demineralization. *J Dent Res* 2000;79(9):1725–1730.
12. Hsu CY, Jordan TH, Dederich DN, Wefel JS. Laser-matrix-fluoride effects on enamel demineralization. *J Dent Res* 2001;80(9):1797–1801.
13. Tagomori S, Morioka T. Combined effects of laser and fluoride on acid resistance of human dental enamel. *Caries Res* 1989;23:225–231.
14. Huang GF, Lan WH, Guo MK, Chiang CP. Synergistic effect of Nd:YAG laser combined with fluoride varnish on inhibition of caries formation in dental pits and fissures in vitro. *J Formos Med Assoc* 2001;100(3):181–185.
15. Hashimoto M. Effects of Nd:YAG laser irradiation on acid resistance of defective rat enamel. *Shoni Shikagaku Zasshi* 1990;28(4):956–967.
16. Hossain M, Nakamura Y, Kimura Y, Yamada Y, Kawanaka T, Matsumoto K. Effect of pulsed Nd:YAG laser irradiation on acid demineralization of enamel and dentin. *J Clin Laser Med Surg* 2001;19(2):105–108.
17. Kayano T, Ochiai S, Kiyono K, Yamamoto H, Nakajima S, Mochizuki T. Effects of Er:YAG laser irradiation on human extracted teeth. *Kokubyo Gakkai Zasshi* 1989;56(2):381–392.
18. Hossain M, Nakamura Y, Kimura Y, Yamada Y, Ito M, Matsumoto K. Caries-preventive effect of Er:YAG laser irradiation with or without water mist. *J Clin Laser Med Surg* 2000;18(2):61–65.
19. Delbem AC, Cury JA, Nakassima CK, Gouveia VG, Theodoro LH. Effect of Er:YAG laser on CaF₂ formation and its anticariogenic action on human enamel: An in vitro study. *J Clin Laser Med Surg* 2003;21(4):197–201.
20. Bevilacqua FM, Zezell DM, Magnani R, da Ana PA, Eduardo Cde P. Fluoride uptake and acid resistance of enamel irradiated with Er:YAG laser. *Lasers Med Sci* 2008;23(2):141–147.
21. Hossain M, Kimura Y, Nakamura Y, Yamada Y, Kinoshita JI, Matsumoto K. A study on acquired acid resistance of enamel and dentin irradiated by Er, Cr:YSGG laser. *J Clin Laser Med Surg* 2001;19(3):159–163.
22. Moslemi M, Fekrazad R, Tadayon N, Ghorbani M, Torabzadeh H, Shadkar MM. Effects of Er, Cr:YSGG laser irradiation and fluoride treatment on acid resistance of the enamel. *Pediatr Dent* 2009;31(5):409–413.
23. de Freitas PM, Rapozo-Hilo M, Eduardo Cde P, Featherstone JD. In vitro evaluation of erbium, chromium:Yttrium-scandium-gallium-garnet laser-treated enamel demineralization. *Lasers Med Sci* 2010;25(2):165–170.
24. Westerman GH, Hicks MJ, Flaitz CM, Blankenau RJ, Powell GL, Berg JH. Argon laser irradiation in root surface caries: In vitro study examines laser's effects. *J Am Dent Assoc* 1994;125(4):401–407.
25. Flaitz CM, Hicks MJ, Westerman GH, Berg JH, Blankenau RJ, Powell GL. Argon laser irradiation and acidulated phosphate fluoride treatment in caries-like lesion formation in enamel: An in vitro study. *Pediatr Dent* 1995;17:31–35.
26. Hicks MJ, Flaitz CM, Westerman GH, Blankenau RJ, Powell GL, Berg JH. Enamel caries initiation and progression following low fluence (energy) argon laser and fluoride treatment. *J Clin Pediatr Dent* 1995;20(1):9–13.
27. Haider SM, White GE, Rich A. Combined effects of argon laser irradiation and fluoride treatments in prevention of caries-like lesion formation in enamel: An in vitro study. *J Clin Pediatr Dent* 1999;23(3):247–257.
28. Westerman GH, Flaitz CM, Powell GL, Hicks MJ. Enamel caries initiation and progression after argon laser irradiation: In vitro argon laser systems comparison. *J Clin Laser Med Surg* 2002;20(5):257–262.
29. Vlacic J, Meyers IA, Kim J, Walsh LJ. Laser-activated fluoride treatment of enamel against an artificial caries challenge: Comparison of five wavelengths. *Aust Dent J* 2007;52(2):101–105.
30. Hicks J, Winn D II, Flaitz C, Powell L. In vivo caries formation in enamel following argon laser irradiation and combined fluoride and argon laser treatment: A clinical pilot study. *Quint Int* 2004;35(1):15–20.
31. Zezell DM, Boari HG, Ana PA, Eduardo Cde P, Powell GL. Nd:YAG laser in caries prevention: A clinical trial. *Lasers Surg Med* 2009;41(1):31–35.
32. Featherstone JD, Nelson DG. Laser effects on dental hard tissues. *Adv Dent Res* 1987;1(1):21–26.
33. Fried D, Zuerlein MJ, Le CQ, Featherstone JD. Thermal and chemical modification of dentin by 9–11 microns CO₂ laser pulses of 5–100 microns duration. *Lasers Surg Med* 2002;31(4):275–282.
34. Zuerlein MJ, Fried D, Featherstone JD. Modeling the modification depth of carbon dioxide laser-treated dental enamel. *Lasers Surg Med* 1999;25(4):335–347.
35. Featherstone JDB, Nelson DG. Recent uses of electron microscopy in the study of physico-chemical processes affecting the reactivity of synthetic and biological apatites. *Scan Microsc* 1989;3:815–827.
36. Goodis HE, Fried D, Gansky S, Rechmann P, Featherstone JD. Pulpal safety of 9.6 μ TEA CO₂ laser used for caries prevention. *Lasers Surg Med* 2004;35(2):104–110.
37. Gorton J, Featherstone JD. In vivo inhibition of demineralization around orthodontic brackets. *Am J Orthod Dentofacial Orthop* 2003;123(1):10–14.
38. Rechmann P, Fried D, Le CQ, Nelson G, Rapozo-Hilo M, Rechmann BM, Featherstone JD. Caries inhibition in vital teeth using 9.6-μm CO₂-laser irradiation. *J Biomed Opt* 2011;16(7):071405.
39. Foundation I. International Caries Detection & Assessment System www.icdas.org.
40. Rechmann P, Charland D, Rechmann BM, Featherstone JD. Performance of laser fluorescence devices and visual examination for the detection of occlusal caries in permanent molars. *J Biomed Opt* 2012;17(3):036006.
41. GraphPad Software. *Quantify agreement with Kappa Quick-Calcs Online Calculators for Scientists* GraphPad Software Incorporated; www.graphpad.com/quickcalcs/kappa1/, 2013.
42. Rechmann P, Rechmann BM, Featherstone JD. Caries detection using light-based diagnostic tools. *Compend Contin Educ Dent* 2012;33(8):582–584 586, 588–593; quiz 594, 596.
43. Featherstone JD, Nelson DG. Recent uses of electron microscopy in the study of physico-chemical processes affecting the reactivity of synthetic and biological apatites. *Scan Microsc* 1989;3(3):815–827 discussion 827-818.
44. Takagi S, Liao H, Chow LC. Effect of tooth-bound fluoride on enamel demineralization/ remineralization in vitro. *Caries Res* 2000;34(4):281–288.
45. Featherstone JD. Lasers in dentistry 3. The use of lasers for the prevention of dental caries. *Ned Tijdschr Tandheelkd* 2002;109(5):162–167.
46. Featherstone JDB, Barrett-Vespone NA, Fried D. CO₂ laser inhibition of artificial caries-like lesions progression. *J Dent Res* 1995;74(470):70.

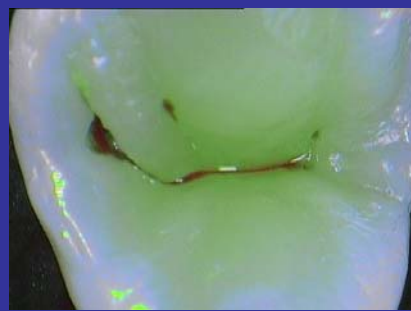
47. Fried D, Ragadio J, Akrivou M, Featherstone JD, Murray MW, Dickenson KM. Dental hard tissue modification and removal using sealed transverse excited atmospheric-pressure lasers operating at $\lambda = 9.6$ and 10.6 microm. *J Biomed Opt* 2001;6(2):231–238.
48. Lussi A, Imwinkelried S, Pitts N, Longbottom C, Reich E. Performance and reproducibility of a laser fluorescence system for detection of occlusal caries in vitro. *Caries Res* 1999;33(4):261–266.
49. Lussi A, Hibst R, Paulus R. DIAGNOdent: An optical method for caries detection. *J Dent Res* 2004;83 (Spec No C): C80–C83.
50. Verdonschot EH, van der Veen MH. Lasers in dentistry 2. Diagnosis of dental caries with lasers. *Ned Tijdschr Tandheelkd* 2002;109(4):122–126.
51. König K, Flemming G, Hibst R. Laser-induced autofluorescence spectroscopy of dental caries. *Cell Mol Biol (Noisy-legrand)* 1998;44(8):1293–1300.
52. Shi XQ, Welander U, Angmar MB. Occlusal caries detection with KaVo DIAGNOdent and radiography: An in vitro comparison. *Caries Res* 2000;34(2):151–158.
53. Shi XQ, Tranaeus S, Angmar-Mansson B. Validation of DIAGNOdent for quantification of smooth-surface caries: An in vitro study. *Acta Odontol Scand* 2001;59(2):74–78.
54. Rocha RO, Ardenghi TM, Oliveira LB, Rodrigues CR, Ciamponi AL. In vivo effectiveness of laser fluorescence compared to visual inspection and radiography for the detection of occlusal caries in primary teeth. *Caries Res* 2003;37(6):437–441.
55. Astvaldsdottir A, Holbrook WP, Tranaeus S. Consistency of DIAGNOdent instruments for clinical assessment of fissure caries. *Acta Odontol Scand* 2004;62(4):193–198.
56. Tranaeus S, Lindgren LE, Karlsson L, Angmar-Mansson B. In vivo validity and reliability of IR fluorescence measurements for caries detection and quantification. *Swed Dent J* 2004;28(4):173–182.
57. Bamzahim M, Aljehani A, Shi XQ. Clinical performance of DIAGNOdent in the detection of secondary carious lesions. *Acta Odontol Scand* 2005;63(1):26–30.
58. Angnes V, Angnes G, Batistella M, Grande RH, Loguercio AD, Reis A. Clinical effectiveness of laser fluorescence, visual inspection and radiography in the detection of occlusal caries. *Caries Res* 2005;39(6):490–495.
59. Reis A, Mendes FM, Angnes V, Angnes G, Grande RH, Loguercio AD. Performance of methods of occlusal caries detection in permanent teeth under clinical and laboratory conditions. *J Dent* 2006;34(2):89–96.
60. Akarsu S, Koprulu H. In vivo comparison of the efficacy of DIAGNOdent by visual inspection and radiographic diagnostic techniques in the diagnosis of occlusal caries. *J Clin Dent* 2006;17(3):53–58.
61. Altenburger MJ, Gmeiner B, Hellwig E, Wrbas KT, Schirmermeister JF. The evaluation of fluorescence changes after application of casein phosphopeptides (CPP) and amorphous calcium phosphate (ACP) on early carious lesions. *Am J Dent* 2010;23(4):188–192.
62. Jablonski-Momeni A, Ricketts DN, Rolfsen S, Stoll R, Heinzl-Gutenbrunner M, Stachniss V, Pieper K. Performance of laser fluorescence at tooth surface and histological section. *Las Med Sci* 2011;26(2):171–178.
63. Huth KC, Neuhaus KW, Gygax M, Bucher K, Crispin A, Paschos E, Hickel R, Lussi A. Clinical performance of a new laser fluorescence device for detection of occlusal caries lesions in permanent molars. *J Dent* 2008;36(12):1033–1040.
64. Eakle S, Gansky S, Zhan L, Featherstone JDB. Clinical evaluation of the diagnodent device. In: Stookey G, editor. *Early detection of dental caries III Indiana conference 2003*. Indiana: Indiana University Press; 2005.
65. Rationale and Evidence for the International Caries Detection and Assessment System (ICDAS II) International Caries Detection and Assessment System (ICDAS) Coordinating Committee September 2005.
66. Ekstrand KR, Kuzmina I, Bjorndal L, Thylstrup A. Relationship between external and histologic features of progressive stages of caries in the occlusal fossa. *Caries Res* 1995;29(4):243–250.
67. Ekstrand KR, Ricketts DN, Kidd EA. Reproducibility and accuracy of three methods for assessment of demineralization depth of the occlusal surface: An in vitro examination. *Caries Res* 1997;31(3):224–231.
68. Tranaeus S, Lindgren LE, Karlsson L, Angmar-Mansson B. In vivo validity and reliability of IR fluorescence measurements for caries detection and quantification. *Swedish Dent J* 2004;28(4):173–182.
69. Mendes FM, Siqueira WL, Mazzitelli JF, Pinheiro SL, Bengtson AL. Performance of DIAGNOdent for detection and quantification of smooth-surface caries in primary teeth. *J Dent* 2005;33(1):79–84.

INTRODUCTION:

Early caries detection is essential in treatment planning and crucial in discrimination between preventive, therapeutic and intervention decisions in general dental practice. Subjectivity, low sensitivity and high specificity of clinical and radiographic examination generate the need for additional caries diagnostic tools.

PURPOSE:

Evaluation of the efficacy of a laser fluorescence device for caries diagnosis (SOPROLIFE, Sopro - Acteon Group) in caries detection. Thus, ICDAS II scores, digital radiography and SOPROLIFE fluorescence mode (SFM) were compared in detection of occlusal lesions. Tissue examination of sectioned teeth was used as a gold standard for caries detection.



METHODS:

Ninety-six pit or fissure areas were randomly selected on forty-five posterior teeth. Specimens were evaluated with a) ICDAS II scores, b) radiographic examination (Xmind, Satelec Acteon Group, 70kV, 4 mA, 0.080 sec), c) SFM d) tissue examination in stereomicroscope (Zeiss) after sectioning in microtome. Findings were classified in scale 0-4 by three examiners. Score 0 was regarded as healthy for all examination methods. Each observation was repeated for fifteen times (one every two days) in order to check intra-examiner and inter-examiner reliability (Intraclass Correlation Coefficient). The caries detection methods were compared by means of sensitivity, specificity, and were correlated against tissue examination. SPSS 20.0 and DBMMRMC 2.32 Build 3 statistic softwares were used. Statistical significance was set at $p < 0.05$.

RESULTS:

Intra-rater and inter-rater reliability for radiographic evaluation and SFM evaluation were excellent ($p < 0.001$). Stronger positive correlation was exhibited between ICDAS II scores and SFM ($\rho = 0.688$, $p < 0.001$) or between SFM and tissue examination ($\rho = 0.556$, $p < 0.001$) than when radiographic evaluation was correlated with the same ($\rho = 0.372$, $\rho = 0.395$ respectively, $p < 0.001$). Sensitivity and specificity values are as follows:

TREATMENT	INDEX	VALUE
ICDAS II	sensitivity	0.91
	specificity	0.57
Radiographic Evaluation	sensitivity	0.54
	specificity	0.24
SOPROLIFE fluorescence mode	sensitivity	0.92
	specificity	0.47

DISCUSSION:

Occlusal imaging with SFM allows for better caries lesion discrimination than radiographic examination, however the camera identifies more precisely a decayed tooth as decayed. Presenting sensitivity and specificity values similar to clinical examination, it cannot replace clinical examination, but it can be regarded as a useful technological aid in caries diagnosis also helping in monitoring caries lesion behaviour.

References:

- Celiberti P, Leamari VM, Imparato JCP, Braga MM, Mendes FM. In vitro ability of a laser fluorescence device in quantifying approximal caries lesions in primary molars. J Dent 2010;38:666-70
- Jablonski-Momeni A, Stachniss V, Ricketts DN, Heinzl-Gutenbrunner M, Pieper K. Reproducibility and accuracy of the ICDAS-II for detection of occlusal caries in vitro. Caries Res 2008;42(2):79-87.
- Gomez J, Zakian C, Salsone S, Pinto SCS, Taylor A, Pretty IA, Ellwood R. In vitro performance of different methods in detecting occlusal caries lesions. J Dent 2013;41(2):180-6.
- Rechmann P, Charland D, Rechmann BM, Featherstone JD. Performance of laser fluorescence devices and visual examination for the detection of occlusal caries in permanent molars. J Biomed Opt. 2012;17(3):036006.

DENTAL TRIBUNE

— The World's Dental Newspaper —

News France



Transillumination avec lumière de diagnostic SDI et collimateur. (DTI/Photo : University of Melbourne, Australie)

1 nov. 2013 | News France

Détection de la carie dentaire : il y a-t-il quelque chose de nouveau ?

by Pr David J. Manton, Australie

La carie dentaire est encore dans le monde, l'une des maladies les plus répandues, bien qu'évitable. Il y a de plus en plus de preuves que ceux qui ont des problèmes de santé orale ont aussi des problèmes de santé générale. Qu'il y ait un lien de causalité ou une association avec d'autres cofacteurs est encore à déterminer.

was written by:



Même si une grande partie de la population des pays développés a vu une amélioration de leur santé bucco-dentaire au cours des trois ou quatre dernières décennies, les personnes appartenant à certains groupes, tels que les groupes socio-économiques inférieurs et médicalement compromis, ont un risque élevé de développer des caries dentaires. Il y a eu un changement de philosophie sur ce qui est considéré comme étant un traitement approprié, avec l'abandon du modèle chirurgical en faveur d'un modèle de gestion de la maladie, souvent qualifié de dentisterie à intervention minimale. À la suite d'une diminution de l'incidence des

Prof. David Manton

caries, la sensibilité du diagnostic des caries a aussi été réduite. Un diagnostic précoce est essentiel, car il permet une intervention pour reminéraliser ou guérir la lésion carieuse, tout en considérant également les facteurs de risque de caries et en entreprenant des actions préventives, telles que le scellement des fissures.

La carie dentaire est une source de confusion pour beaucoup en raison du milieu médical, qui utilise le même terme pour désigner à la fois le processus de la maladie et le résultat de ce processus. Une distinction doit être faite entre les trois processus, distincts mais liés entre eux : le diagnostic de la carie dentaire, la détection d'une lésion carieuse et l'évaluation de cette lésion. Bien que le diagnostic des caries comprenne l'évaluation globale de l'individu, compte tenu de tous les facteurs de risque de caries, tels que les facteurs personnels et sociaux, les facteurs environnementaux oraux et les facteurs quotidiens qui contribuent directement au risque de carie chez l'individu et sur la surface de la dent spécifique, la détection des caries implique l'utilisation d'un instrument objectif pour détecter la maladie sous la forme de lésions carieuses, avec évaluation pour caractériser et quantifier l'étendue et l'état de la maladie.

Le développement de l'International Caries Detection and Assessment System (ICDAS) ou système international de détection et d'évaluation des lésions carieuses, a récemment fourni une méthode valable pour évaluer et quantifier les lésions. La création récente d'un système de gestion associé, l'International Caries Classification and Management System (ICCMS) ou système international de classification et de gestion des caries, offre des options de gestion pour les différentes étapes de la lésion carieuse, tenant en compte les circonstances individuelles. L'ICDAS évalue les lésions, leur donnant une note entre 1, la première étape, où la dent doit être séchée pour identifier une tache de décalcification, et 6, qui représente une lésion avancée. Un logiciel éducatif est disponible (www.icdas.org) et un logiciel pour aider à utiliser l'ICDAS dans les enquêtes épidémiologiques est maintenant disponible : www.icdas.org/software-tools.

Utiliser une sonde de détection pour les caries est toujours chose commune dans la pratique clinique et l'enseignement dentaire de premier cycle, mais elle peut endommager la couche superficielle de l'émail déminéralisé, augmentant la probabilité qu'une intervention réparatrice soit nécessaire. Sonder ne fournit aucun avantage par rapport à d'autres méthodes de détection, même lorsqu'utilisé en conjonction avec elles. Il est donc recommandé que seule une sonde à bout sphérique soit utilisée, en particulier pour vérifier l'intégrité/la rugosité de la surface de l'émail.

La sensibilité d'une méthode de détection est liée à sa capacité à détecter la maladie lorsqu'elle est présente, et sa spécificité est liée à sa capacité à détecter l'absence de la maladie quand elle n'est pas présente. La détection de la carie occlusale est compliquée cliniquement due à la morphologie de la surface, l'exposition au fluorure dans le passé, la topographie de la fissure anatomique et la présence de plaque et de taches. Les méthodes couramment utilisées sont l'inspection visuelle et tactile, la radiographie, la transillumination et la fluorescence laser. Cette dernière, à savoir le DIAGNOdent (KaVo), est encouragée pour la détection de lésions à la fois occlusales et interproximales. Sa technologie est basée sur la fluorescence de porphyrines excitées par une lumière laser, à une longueur d'onde de 655 nm. La sensibilité et la spécificité de la fluorescence laser pour détecter les lésions intra-dentaire varie considérablement, avec des faux positifs, problème principal de la technologie. Afin d'obtenir les meilleurs résultats, l'angulation de la pointe doit être consistante et les résultats devraient être évalués avec d'autres méthodes de détection.

Les systèmes les plus récents de fluorescence induite par la lumière quantitative (y compris QLF, Inspektor Research Systems, et SOPROLIFE, Actéon) utilisent des différences dans l'auto-fluorescence entre le son et l'émail et la dentine déminéralisée. L'émail déminéralisé paraît plus sombre que la structure de la dent saine adjacente, et la dentine cariée apparaît en rouge en fonction des filtres utilisés. L'utilisation du QLF (longueur d'onde 405 nm) permet la détection

précoce de la déminéralisation de l'émail et il peut être utilisé pour distinguer entre la dentine affectée et infectée. Comme le DIAGNOdent, la technologie QLF est tributaire de techniques standardisées, en particulier du contrôle de la lumière ambiante, et les résultats doivent être considérés en conjonction avec d'autres méthodes. Le SOPROLIFE utilise une longueur d'onde de 450 nm, et présente les paramètres pour le diagnostic de la dentine cariée ainsi qu'un mode de traitement, ce qui aide à déterminer quelle dentine doit être supprimée.

Un nouveau système, récemment présenté, utilise la radiométrie photothermique à base de laser (The Canary System, Quantum Dental Technologies), en détectant la luminescence et le changement de la température, pour quantifier les changements de minéralisation. Des recherches supplémentaires sont nécessaires pour cette technologie.

Le procédé de la transillumination par fibre optique est basé sur le principe que la structure de la dent saine a un indice plus élevé de transmission de la lumière qu'une dent cariée. Des unités, telles que la pointe de diagnostic SDI pour l'unité de photopolymérisation SDI ou la pièce à main de transillumination NSK sont simples à utiliser. La source de lumière est placée sur la face vestibulaire ou linguale de la dent. La transillumination est principalement utilisée pour la détection des lésions carieuses proximales, bien que des études aient montré qu'elle peut aussi améliorer la détection visuelle des lésions occlusales. Les lésions carieuses limitées à l'émail apparaissent comme des teintes grises, et celles de la dentine apparaissent comme des teintes de brun-orange ou de bleu.

L'utilisation de la radiographie numérique est devenue monnaie courante chez de nombreux praticiens. Les capacités de détection de la radiographie numérique sont sensées être semblables à celles des méthodes à base de film, et ont l'avantage de réduire l'exposition aux rayonnements et la capacité de transférer facilement les images.

Le développement récent de gels révélateurs multitons (Tri Plaque ID Gel, GC Corporation) peut faciliter la détection des caries, car la plaque vieille et cariogène peut être identifiée assez facilement et les taches de décalcification ont tendance à se produire sous la plaque, de sorte que les zones à considérer peuvent être ciblées après élimination du gel. Ces produits sont potentiellement bons pour l'éducation des patients, car la zone à risque peut être facilement montrée au patient.

L'obtention de la reproductibilité du diagnostique entre les praticiens est difficile, puisqu'ils ont tendance à développer des concepts individuels, basés sur leur expérience en matière de détection des caries et des options de prévention ou traitement qui en découlent. Leur expérience est aussi un facteur important, car les praticiens expérimentés ont une plus grande sensibilité, spécificité et une plus grande reproductibilité, que ceux moins expérimentés. En raison de l'absence d'une méthode de détection unique qui fournisse à la fois une grande sensibilité et une spécificité élevée, la combinaison d'un certain nombre de méthodes est recommandée pour augmenter la précision de la détection. Par exemple, il peut s'agir de combiner les résultats des DIAGNOdent ou SOPROLIFE avec des images visuelles et radiographiques directes. Plusieurs facteurs, tels que l'éclairage fluorescent, peuvent perturber les résultats des méthodes de détection à base de fluorescence, donc un bon contrôle de l'éclairage ambiant et la standardisation de la méthodologie sont impératifs lors de l'utilisation de ces nouvelles méthodes de détection.

Le développement de nouvelles technologies pour aider à la détection et au diagnostic de la carie peut fournir une fiabilité accrue, mais elles doivent être utilisées dans le cadre d'une évaluation visuelle et radiographique traditionnelle, qui sont toujours les règles d'or des soins à l'heure actuelle. Le développement actuel de l'ICCMS par un groupe mondial de cariologistes utilisera l'ICDAS et la base de données actuelles, pour donner des informations aux praticiens sur les caractéristiques des lésions et risques de caries, leur permettant ainsi de formuler des décisions thérapeutiques valables.

Evaluation of Caries Dentin Using Light-Induced Fluorescence: A Case Report

SEBNEM EROL¹, HANIFE KAMAK², HÜLYA ERTEN³

ABSTRACT

Minimal invasive therapy has been becoming more important day by day in dentistry. In minimally invasive dentistry, only the infected dentin is removed and the affected dentin is left behind while preparing to repair a cavity. Healthy enamel and dentin have particular fluorescence properties, compared to demineralized dental tissues, which absorb less light and thereby have a lower level of fluorescence properties. It helps clinicians detect caries and apply the most appropriate treatment strategy during cavity preparation. This study investigated the efficacy of the SoproLife camera system which is a novel light-induced fluorescence camera system.

Keywords: Dentinal caries, Light-induced fluorescence, SoproLife, Minimally invasive dentistry

CASE REPORT

Patients And Methods

This study investigated the efficacy of the SoproLife camera system (Sopro-Acteon, La Ciotat, France) in three males, one female range 18-24 years four patients with initial occlusal decay of the lower molar tooth, who were admitted to Gazi University, Faculty of Dentistry, Department of Conservative Dentistry. In this study, patients had no caries and no symptoms. They came for a routine check. The patients were informed about the study and informed consent was obtained from the participants. Camera images of the occlusal caries were obtained before treatment [Table/Fig-1a, 2a, 3a, 4a]. A #5 round diamond bur with water-cooled high speed hand piece was used for cavity preparation. Camera images of the cavities were re-taken when no caries were observed in visual examination. Then, the presence of demineralized dentin was examined. Demineralized dentin as shown by the red signal in the image was cleared by a micromotor with a #5 round steel bur. The images of the cavities were re-taken [Table/Fig-1b, 2b, 3b, 4b]. This procedure was repeated until no red signal was produced.

An adhesive resin (Tetric, Ivoclar, North America, USA) was applied into the cavities. The cavities were restored by a composite resin (Tetric, Ivoclar, North America, USA) using the layering technique. Polishing discs (Sof-Lex; 3M ESPE, St. Paul, MN, USA) were used and the procedure was completed. No complications, such as tenderness or discolouration, were observed at one month, three months, and one year. Radiographic findings did not suggest secondary caries.

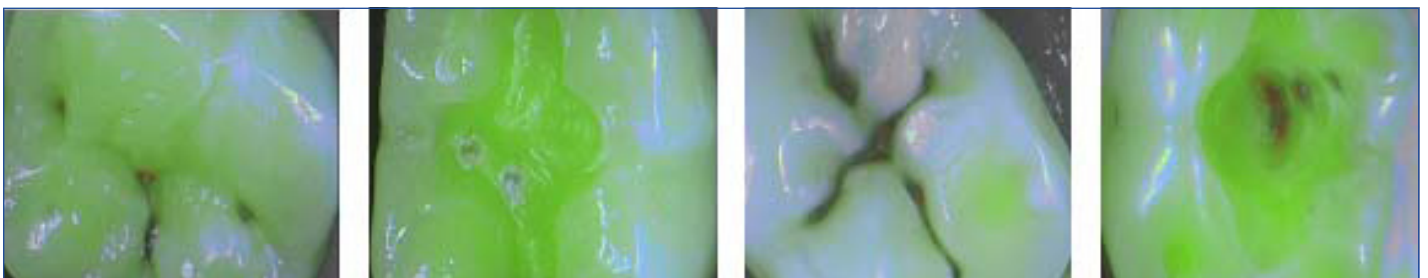
DISCUSSION

The concept of minimally invasive dentistry refers to early detection

of lesions, evaluation of possible risk factors, planning preventive care, and patient education [1]. Therefore, remineralization of the demineralized enamel and dentin without a caries cavity after the infection is cleared and taking necessary precautions on a regular basis in high-risk patients are the cornerstones of minimally invasive dentistry. In the case of demineralized enamel and dentin with a caries cavity, the primary goal of the treatment is to conserve maximum tooth structure during cavity preparation [1].

In minimally invasive dentistry, only the infected dentin is removed and the affected dentin is left behind while preparing to repair a cavity. However, clinicians are usually indecisive regarding the timing of the excavation to remove the infected dentin only during cavity preparation [1,2]. Subjective approaches may be helpful for the evaluation of the stiffness and colour of dentin (stiff dentin in the clinical examination using a probe and dark colour appearance in visual examination) [3]. Air-abrasion, ultrasonic devices and laser are the recent methods to facilitate the removal process of caries. On the other hand, these methods have several disadvantages such as possibility of removal of the healthy dentin and prolonged duration of the procedure [1,4].

Fluorescence is often used as a guide for caries excavation. The principle of fluorescence is based on the absorption of the light at a particular wavelength and the emission of light of a longer wavelength [1]. Healthy enamel and dentin have particular fluorescence properties, compared to demineralized dental tissues, which absorb less light and thereby have a lower level of fluorescence properties [1,5]. In addition, the colour of the dental tissues may vary according to the fluorescence properties. This helps clinicians detect caries and apply the most appropriate treatment strategy during cavity preparation.

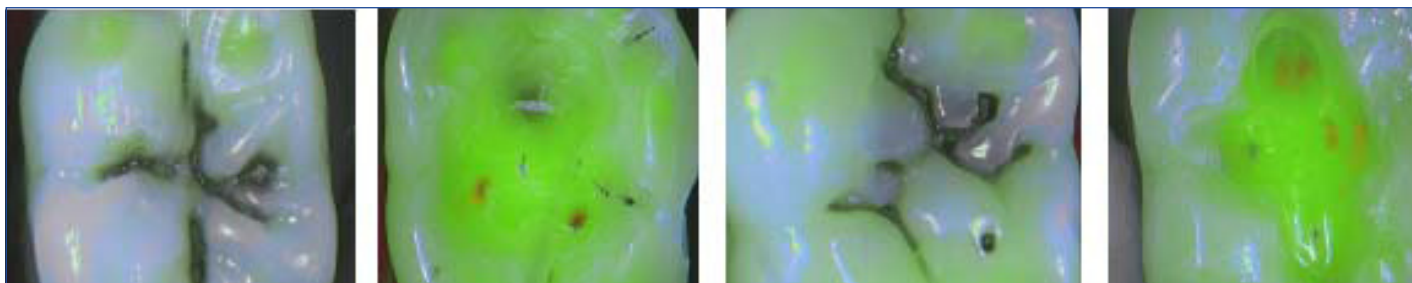


[Table/Fig-1a]: Camera images of cavities before treatment

[Table/Fig-1b]: Camera images of cavities after first preparations

[Table/Fig-2a]: Camera images of cavities before treatment

[Table/Fig-2b]: Camera images of cavities after first preparations



[Table/Fig-3a]: Camera images of cavities before treatment

[Table/Fig-3b]: Camera images of cavities after first preparations

[Table/Fig-4a]: Camera images of cavities before treatment

[Table/Fig-4b]: Camera images of cavities after first preparations

Light-induced fluorescence is a novel technique used for detection of caries [6]. The Soprolife system, which is a novel light-induced fluorescence camera system, seems to be advantageous for visual examination thanks to its intra-oral camera with a high level of magnification and laser fluorescence device. This system works based on the principle of diagnosis and treatment of dental caries (LIFE DT) [4,7].

Soprolife captures the images in three modes: daylight mode, diagnostic aid mode, and treatment aid mode [5-8]. Firstly, the daylight mode offers a white light image with a magnification of more than 50 times than the dental surface. Secondly, the diagnostic aid mode and treatment aid mode work on the principle of auto fluorescence. The diagnostic aid mode works with a visible blue light frequency (wavelength 450 nm) for the illumination of the dental surface and produces an overlapping image of the green fluorescence image on the image of the white light. The green fluorescence image is considered an indicator of healthy dental tissues. On the other hand, auto fluorescence variations of the healthy area of the same tooth are useful to detect carious lesions. In addition, caries can be easily detected by dark red fluorescence of the diagnostic mode of the camera in the daylight. The colour of the fluorescence signal is green when the dentin is healthy. The healthy enamel is blue due to the scattered green light of the dentin, despite the lack of a fluorescence signal [5]. The third mode is the treatment aid mode. The red fluorescence signal in this mode is considered an indicator to differentiate between infected and affected dentin [5].

Traditional modalities for the diagnosis of caries and removal of the infected dentin during cavity preparation depend on subjective criteria such as colour or structure of the lesion. The current study obtained images using the Soprolife camera system, once the infected dentin was completely removed. A red fluorescence signal was obtained, which indicated dental caries in that area. The

infected dentin was removed and the caries were re-cleared until no red signal was produced.

CONCLUSION

The Soprolife was helpful in the detection of the infected dentin. This system was also useful for the magnification of the signs and visualization of the cavity elaborately, as well as deep dental caries. In conclusion, the study results suggest that the novel Soprolife system is effective in the differentiation between infected and affected dentin during cavity preparation. In this study, Soprolife used a few teeth and also only young patients. Furthermore, Comparison did not made with other devices which used for diagnosis to caries dentin. Therefore, further in vivo and in vitro studies are required to confirm these findings.

REFERENCES

- [1] Korkut B, Arslantunali Tagtekin D, Çaliskan Yanikoglu F. Early diagnosis of dental caries and new diagnostic methods: QLF, Diagnodent, Electrical Conductance and Ultrasonic System. *EUDFD*. 2011; 32; 55-67.
- [2] Zangoeei Booshehry M, Fasihinia H, Khaesi M, Gholami L. Dental Caries Diagnostic Methods. *DHJ*. 2011; 2(1).
- [3] Kisbet S, Ölmez A. Current approaches in chemomechanical caries removal methods. *Cumhuriyet Dent J*. 2012; 15(4): 364-72.
- [4] Neeraj Gugnani, IK Pandit, Nikhil Srivastava, Monika Gupta, and Shalini Gugnani. Light induced fluorescence evaluation: A novel concept for caries diagnosis and excavation. *J Conserv Dent*. 2011; 14(4): 418-22.
- [5] Panayotov I, Terrer E, Salehi H, Tassery H, Yachouh J, Frédéric JG, Cuisinier, Levallois B. In vitro investigation of fluorescence of carious dentin observed with a Soprolife® Camera. *Clin Oral Invest*. Doi 10.1007/S00784-012-0770-9.
- [6] Lussi A, Megert B, Longbottom C, Reich E, Francescut P. Clinical performance of a laser fluorescence device for detection of occlusal caries lesions. *Eur J Oral Sci*. 2001; 109: 14-19.
- [7] Terrer E, Koubi S, Dionne A, Weisrock G, Sarraquigne C, Mazuir A Tassery H. A new concept in restorative dentistry: light-induced fluorescence evaluator for diagnosis and treatment: Part 1 – Diagnosis and treatment of initial occlusal caries. *The Journal of Contemporary Dental Practice*. 2009; 10(6).
- [8] Sopralife And Life-D.T. Method Light Induced Fluorescence Diagnosis And Treatment. Pr Hervé Tassery, Caroline Sarraquigne, Alain Mazuir And Coll. 2008.

PARTICULARS OF CONTRIBUTORS:

1. Lecturer, Department of Restorative Dentistry, Gazi University Faculty of Dentistry, Block-B, Street No. 8, Emek/Ankara, Turkey.
2. PhD Student, Department of Restorative Dentistry, Gazi University Faculty of Dentistry, Block-B, Street No. 8, Emek/Ankara, Turkey.
3. Professor, Department of Restorative Dentistry, Gazi University Faculty of Dentistry, Block-B, Street No. 8, Emek/Ankara, Turkey.

NAME, ADDRESS, E-MAIL ID OF THE CORRESPONDING AUTHOR:

Dr. Sebnem Erol,
Gazi University Faculty of Dentistry, Department of Restorative Dentistry, Block-B, Street No. 8, Emek/Ankara, Turkey.
Phone: +905327851631, E-mail: sebnem_erol@hotmail.com

FINANCIAL OR OTHER COMPETING INTERESTS: None.

Date of Submission: **Oct 31, 2013**

Date of Peer Review: **Nov 14, 2013**

Date of Acceptance: **Dec 15, 2013**

Date of Publishing: **Jan 12, 2014**

Clinical Study

SOPROLIFE System: An Accurate Diagnostic Enhancer

Mona Zeitouny,¹ Mireille Feghali,¹ Assaad Nasr,¹ Philippe Abou-Samra,¹ Nadine Saleh,² Denis Bourgeois,³ and Pierre Farge⁴

¹ Department of Aesthetic and Restorative Dentistry, Dental School, Lebanese University, Hadath, Lebanon

² Faculty of Nursing and Health Sciences, Notre Dame University, Beirut, Lebanon

³ Department of Public Health, Faculty of Odontology, University of Lyon 1, 69008 Lyon, France

⁴ Department of Endodontics and Dentistry, Faculty of Odontology, University of Lyon 1, 69008 Lyon, France

Correspondence should be addressed to Mona Zeitouny; ezeitouny@hotmail.com

Received 2 May 2014; Revised 8 September 2014; Accepted 12 September 2014; Published 21 October 2014

Academic Editor: Romeo Umberto

Copyright © 2014 Mona Zeitouny et al. This is an open access article distributed under the Creative Commons Attribution License, which permits unrestricted use, distribution, and reproduction in any medium, provided the original work is properly cited.

Objectives. The aim of this study was to evaluate a light-emitting diode fluorescence tool, the SOPROLIFE light-induced fluorescence evaluator, and compare it to the international caries detection and assessment system-II (ICDAS-II) in the detection of occlusal caries. **Methods.** A total of 219 permanent posterior teeth in 21 subjects, with age ranging from 15 to 65 years, were examined. An intraclass correlation coefficient (ICC) was computed to assess the reliability between the two diagnostic methods. **Results.** The results showed a high reliability between the two methods (ICC = 0.92; IC = 0.901–0.940; $P < 0.001$). The SOPROLIFE blue fluorescence mode had a high sensitivity (87%) and a high specificity (99%) when compared to ICDAS-II. **Conclusion.** Compared to the most used visual method in the diagnosis of occlusal caries lesions, the finding from this study suggests that SOPROLIFE can be used as a reproducible and reliable assessment tool. At a cut-off point, categorizing noncarious lesions and visual change in enamel, SOPROLIFE shows a high sensitivity and specificity. We can conclude that financially ICDAS is better than SOPROLIFE. However SOPROLIFE is easier for clinicians since it is a simple evaluation of images. Finally in terms of efficiency SOPROLIFE is not superior to ICDAS but tends to be equivalent with the same advantages.

1. Introduction

Dental caries is a preventable and reversible infectious disease process [1, 2] to which people are susceptible throughout their lifetime [2]. Despite the benefits of its prevention through fluorides, toothpastes, sealants, improvements in diet, oral health education, and dental care [3], dental caries still remains a major problem worldwide [4] affecting 60–90% of schoolchildren and the vast majority of adults [5, 6]. Its prevalence is around 80% worldwide [7]. Molars and premolars are the most vulnerable teeth of caries attack related to the morphology of their occlusal surfaces [8] and the difficulty of plaque removal [9]. Many dentists continue to intervene when caries are still at enamel level [10]. For that reason, accurate preoperative diagnosis of caries depths and early occlusal caries detection are important to establish adequate preventive measures and avoid premature tooth treatment by restoration [9].

To date, there are two major techniques aimed at helping clinicians in detecting caries on occlusal surfaces [11] represented by visual examination and by light-based caries diagnostic tools as fiber optic transillumination (FOTI), DIAGN-ODent tool (KaVo), and SOPROLIFE. Visual examination of caries has progressed by establishing the international caries detection and assessment system (ICDAS) [12]; indeed, ICDAS-II, the second version, was improved and developed to provide a standardized system [13] to enable clinicians to diagnose and detect the first visual change in enamel leading to better information for clinical management [14, 15].


All diagnostic tools for detection and quantification of dental caries have to obey safety regulations, detect and differentiate shallow and deep lesions, and make monitoring possible by taking precise and quantitative measurement; in addition they have to be cost-effective and user-friendly [13].

The principle of FOTI is used since the seventies [16]. This technique uses a narrow beam of bright white light

TABLE 1: International caries detection and assessment system criteria used in visual examination [11].

Six-point scale categories	Criteria	Clinical lesions
0	Sound tooth surface.	
1	First visual change in enamel.	
2	Distinct visual change in enamel.	
3	Microcavitation in enamel.	
4	Underlying dark shadow from dentine with or without cavitation.	

TABLE I: Continued.

Six-point scale categories	Criteria	Clinical lesions
5	Distinct cavity with visible dentine.	
6	Extensive distinct cavity with visible dentine.	

that is directed across areas of contact between the proximal surfaces and the disruption of crystal structure that deflects the light beam and thus produces shadows [1]. The DIAGNODent tool is based on laser fluorescence and detects porphyrins involvement areas; it appears to measure caries lesion rather than crystalline demineralization [17]. SOPROLIFE is a more recently released device using a light-induced fluorescence evaluator for diagnostic and treatment (LIFE D.T); it was developed and based on the imaging and autofluorescence of dental tissues [18, 19].

Till now, no study has looked at the reproducibility of the SOPROLIFE in the detection and assessment of occlusal caries. Therefore we designed a clinical study with the aim of evaluating the clinical sensitivity and specificity rates of SOPROLIFE as opposed to ICDAS for the detection of initial occlusal caries in noncavitated enamel in permanent premolars and molars.

2. Materials and Methods

2.1. Sample Patients' Selection. This study was conducted over 2 months from March 7 to May 10, 2013. Twenty-one patients were randomly selected (based on their arrival order) from all patients attending the Aesthetic and Restorative Dentistry Department of the Dental School of Lebanese University. Inclusion criteria were age between 15 and 65 years, with no gender restriction, and patients with fully unrestored dental arches.

Exclusion criteria were patients with posterior restorations on molars or premolars or poor oral health with chronic or acute dental infection. In addition patients with a significant past or current medical problem history were not considered for the study, that is, patients with conditions that may affect oral health or oral flora (i.e., diabetes, HIV, and heart conditions which require antibiotic prophylaxis) or taking medication that may affect the oral flora or salivary flow; pregnant or breastfeeding women were also excluded. The subjects who met the criteria were informed of the purpose of the study and verbal consent from the patient was obtained before the examination session.

Examiners start evaluating patients using the ICDAS. After finishing all the samples, they did the work using

SOPRO. One should note that patients ID was hidden when working with SOPRO.

2.2. Observers. Two independent dentists (Mona Zeitouny and Mireille Feghaly) specialized in restorative and aesthetic dentistry randomly examined each tooth by two different methods of caries assessments consecutively and without knowing the results of each method: the visual examination and assessment using the ICDAS-II criteria (Table 1) [20] and the use of the light fluorescence device SOPROLIFE (SOPRO, ACTEON Group, La Ciotat, France). This method involves an intraoral LED light-emitting diode camera offering the ability to detect and locate differences in density, structures, and/or chemical composition of a biological tissue.

Twenty days prior to the initiation of the study, calibration sessions were arranged for the 2 operators and the two methods separately in the examination site. Observers were trained using 100 premolars and molars cleaned without sealants or restorations. Each observer examined each tooth and noted the results. Then, the observers compared the results between them and reviewed the discrepancy cases for calibration until the two observers reach a full concordance rate.

2.3. Tooth Cleaning. Before examination, the occlusal surfaces of each tooth were cleaned for 10 seconds with a water powder jet cleaner and sodium bicarbonate powder (EMS) (ProphyFlex II, KaVo and Biberach; Germany) and then rinsed by an air water spray for another 10-second period in order to remove any powder remnants from the fissure. Following this preparation step of the tooth surfaces, all examinations were conducted under standard conditions in a professional dental light with a front-surface dental mirror and an oil-free air syringe for drying teeth during 5 seconds. The drying procedure is a requisite both for the ICDAS-II evaluation and for the use of the SOPRO device.

2.4. Visual Examination. The visual examination was performed using the ICDAS-II criteria, which provides a standardized method of lesion detection. The ICDAS-II detection codes for coronal caries range from 0 to 6 depending on the

TABLE 2: Scores of SOPROLIFE in blue fluorescence mode [13].


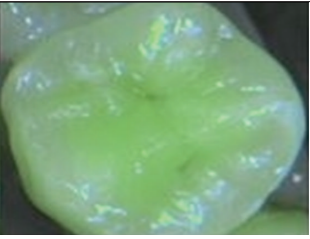

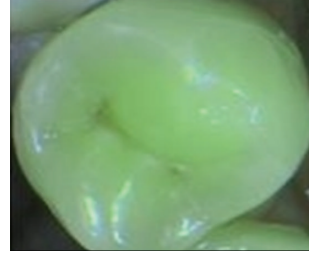
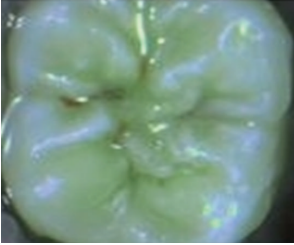
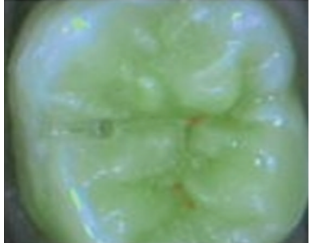
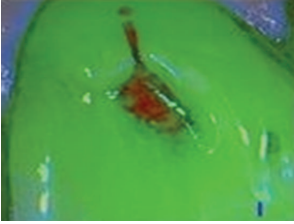


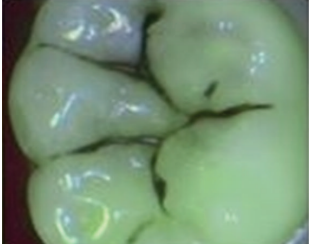


Five-point scale categories	Criteria	Clinical lesions	
0	Fissure appears as shiny green; enamel appears sound. A graphite-pencil-colored thin shine/line is rarely observed.		
1	Tiny, thin red shimmer in the pit and fissure system is viewed. No red dots appeared.		
2	In addition to tiny, thin red shimmer in pits and fissures possibly coming up the slopes darker red spots confined to the fissure are visible. There was no surface roughness.		
3	Dark red extended areas are confined to the fissures. Slight roughness is possible.		
4	Dark red areas are wider than fissures. Surface roughness occurs. Possibly grey or rough grey zone may be visible.		
5	Obvious enamel breakdown with visible dentine was observed.		

TABLE 3: Characteristics of the study population.

Characteristics	N (%) or mean (SD)
Patients age	30.61
Male patients	11 (52.4%)
Female patients	10 (47.6%)
Permanent molars	98 (44.7%)
Permanent premolars	121 (55.3%)

severity of the lesion with the corresponding clinical views (Table 1).

In this study, we used the SOPROLIFE light-induced fluorescence evaluator system (SOPRO, ACTEON Group, La Ciotat, France) operating in the blue fluorescence mode, in which the system uses four white LEDs, and the magnification mode I with the disposable intraoral protection sheets and the intraoral tip. The blue LED, selected by the device, emits at a 450 nm-wavelength which excites a light fluorescence signal re-transmitted by dentine. The spectrum of the fluorescence signal is green when the dentine is healthy and dark red when the dentine is infected (according to the SOPROLIFE manufacturer's instructions). The images were recorded with the SOPRO IMAGING software. An HP 620 Notebook was used to collect the data.

When evaluating occlusal fissure areas in the SOPROLIFE blue fluorescence mode, we used the SOPROLIFE blue fluorescence mode score description as presented in Table 2.

Code 0 was given when the fissure appears shiny green, the enamel appears sound, and there are no visible changes. Code 1 was selected if a tiny, thin red shimmer in the pits and fissure system is observed, which can slightly come up the slopes (walls) of the fissure system. No red dots appeared. At code 2, darker red spots confined to the fissure are visible. For code 3 dark red spots have extended as lines into the fissure areas but remain confined to the fissures. A slight beginning roughness of the more lined red areas can be visible. If the dark red (or red-orange) extends wider than the confines of the fissures, code 4 was given. Code 5 was selected if obvious openings of enamel were seen with visible dentin [13].

2.5. Data Collection. Each tooth was evaluated and scored for lesions severity using a seven-category scale (0–6) according to ICDAS-II and a six-category scale (0–5) according to SOPROLIFE.

2.6. Statistical Analysis. Data were analyzed using the SPSS program (version 17, SPSS Inc., Chicago, IL, USA). In all analyses, a P value < 0.05 was considered significant. Demographic data are presented as mean \pm one standard deviation (SD). Interobserver reproducibility with each examination method and between methods was assessed using intraclass correlation coefficients (ICCs). ICC values equal to 0 represent agreement equivalent to that expected by chance, while 1 represents full agreement. ICC values between 0 and

0.2 indicate poor agreement, values between 0.3 and 0.4 indicate fair agreement, values between 0.41 and 0.6 indicate moderate agreement, values between 0.61 and 0.8 indicate strong agreement, and values greater than 0.8 indicate almost perfect agreement. In addition, a Bland and Altman analysis was done to show graphically the difference between the two methods. Sensitivity and specificity of the new diagnostic system for detecting caries in noncavitated lesions were calculated by reference to the ICDAS-II values. Since we are interested in noncavitated lesions, the calculation was made by dividing scores of the two diagnostic methods into two groups: group 1 which included scores 0 representing healthy teeth without caries and group 2 which included scores 1 and 2 both representing visual change in enamel.

3. Results

This study compared the SOPROLIFE device (in blue fluorescence mode) to the ICDAS-II in the detection of caries lesions. Twenty-one patients were evaluated in this study and a total of 219 teeth (98 permanent molars and 121 permanent premolars), without sealants or restoration, were examined. The patient sample consisted of 10 women and 11 men with age ranging from 15 to 65 and involved mostly young adult patients in their thirties (Table 3).

3.1. ICDAS-II and SOPROLIFE Scores Distribution. The recorded data by each observer are presented in Table 4. Most lesions were noted in the 0 to 2 range of ICDAS-II criteria or in the 0 to 5 range of SOPRO blue fluorescence codes.

3.2. Interobserver Reproducibility. The reproducibility of measurements by each observer was first calculated by the means of ICC for each observer and for each diagnostic method (ICDAS-II and SOPROLIFE) as shown in Table 5. The level of interobserver agreement was found to be high both for visual ICDAS-II scored examination (ICC = 0.972; $P < 0.001$) and for SOPROLIFE (ICC = 0.979; $P < 0.001$).

3.3. Agreement between ICDAS-II and SOPROLIFE Methods. Since each observer examined and scored the same teeth by both ICDAS-II and SOPROLIFE, the means of the two measurements done by each observer were calculated for each tooth and diagnostic method and used to determine agreement and reliability between the two methods. The reliability between methods was computed using the intraclass correlation scale; here we considered the ICDAS-II and SOPROLIFE scales as quantitative variables. Means values for each method (ICDAS II mean = 1.69 ± 1.48 and SOPROLIFE mean = 1.56 ± 1.52) did not differ significantly and a high intraclass correlation coefficient was found (ICC = 0.92; CI = 0.901–0.940; $P < 0.001$). Thus, our results showed a high agreement between the two methods of caries detection.

Figure 1 shows the Bland-Altman analysis. The x -axis shows the mean of the results of the two methods ($(\text{SOPRO} + \text{ICDAS-II})/2$), whereas the y -axis represents the absolute

TABLE 4: Distribution of the ICDAS-II and SOPROLIFE blue fluorescence mode scores by both observers.

Method	Observer	0 (n)	1 (n)	2 (n)	3 (n)	4 (n)	5 (n)	6 (n)
ICDAS-II score (n = 219)	1	56	56	61	16	10	20	—
	2	45	59	60	20	10	21	—
SOPROLIFE blue fluorescence score (n = 219)	1	51	57	64	16	10	21	—
	2	68	52	60	11	7	21	—

TABLE 5: Interobserver repeatability among the two observers.

Type of examination	ICC* (CI† 95%)
ICDAS-II	0.972‡ (0.964–0.979)
SOPROLIFE	0.979‡ (0.972–0.984)

*ICC = intraclass coefficients.

† CI = confidence interval.

‡ P value < 0.001.

difference between the two methods ([SOPRO – ICDAS-II]). Our results showed an acceptable discrepancy between methods (Figure 1).

3.4. *Sensitivity and Specificity for the SOPROLIFE.* In this study we further attempted to estimate both sensitivity and specificity of the SOPROLIFE blue light irradiation in regard to the visual examination score ICDAS-II used as a reference. Sensitivity was measured as the proportion of actual caries lesions which are correctly diagnosed by SOPROLIFE in regard to ICADS-II, whereas specificity was measured as the proportion of noncariou lesions which were correctly diagnosed by SOPROLIFE in regard to that of ICADS-II. For this purpose, we considered the following two groups: the noncariou (sound tooth surface) lesion group that comprised the 0 scores for each method and the visual change in enamel group that included both score 1 and score 2 groups for each method. These results showed that SOPROLIFE detects noncariou lesions in 88% (specificity measurement) of the cases diagnosed by ICDAS-II. Visual change in enamel was detected by SOPROLIFE in 93% (sensitivity measurement) of the cases detected by ICDAS-II (Table 6).

4. Discussion

The present study assessed and compared the newly marketed caries lesion detection tool SOPROLIFE diagnostic mode to the ICDAS-II system.

The results of this study found an almost perfect agreement among the two methods of caries detection with no statistical significant differences between scoring with visual examination and LED fluorescence. This indicates that the diagnosis made with visual examination is roughly the same as the diagnosis made by SOPROLIFE. In addition, according to our results, the number of teeth with 0 score was greater when using fluorescence LED with no statistical difference.

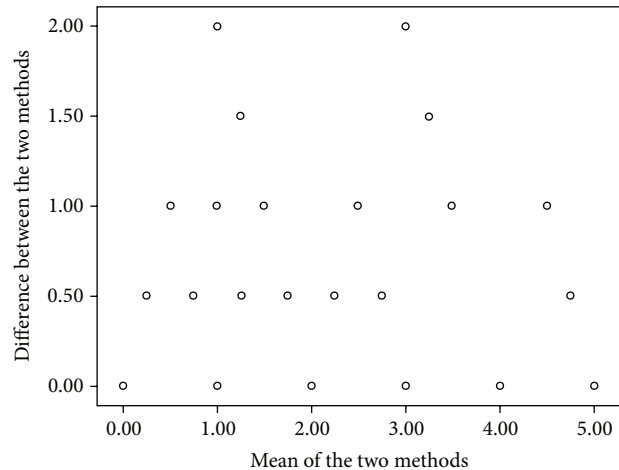


FIGURE 1: Bland-Altman analysis.

The perfect agreement between the two techniques found in our study has been demonstrated in previous study [13]. The visual examination is routinely used for detecting caries in dental clinics and was also used in recent studies comparing the efficacy of various visual aids. It has the benefit that it is quick and easy to perform, does not need expensive equipment, and can be completed without unnecessary radiation or fluorescence [14]. On the other hand, in the results from *in vitro* study conducted to determinate which nondestructive diagnostic method is clinically applicable and reliable at resolving early enamel changes in occlusal fissure caries created in the laboratory, SOPROLIFE demonstrated only additional light scattering due to the demineralization process [21]. *In vitro* and *in vivo* studies showed that different fluorescence signals emitted by SOPROLIFE were a helpful guide for caries detection and excavation [19].

Despite the clinical comparable results between the two diagnostic methods found in our study and in literature, the visual examination presents many limitations in its use. Indeed, one of its limitations is that it requires subjective evaluations to be made by the practitioner; lesions can go undetected because teeth are typically examined by the naked eye. In addition, studies showed that training dental examiners is an essential component of good quality control in dental research [22]. The examiners should be experienced dentists with an interest in cariology and the teeth should be well cleaned for a better visual examination [23]. Stained sites, areas of fluorosis, or developmental defects could be incorrectly scored as caries [9]. By meticulously examining clean

TABLE 6: Validity of the SOPROLIFE regarding ICDAS-II.

Tools	Group 1* % (n) of teeth scored as noncarious and non cavitated	Group 2† % (n) of teeth scored as carious and non cavitated	Sensitivity‡§b	Specificity¶ b
ICDAS-II	25.5 (56)	53.3 (117)		
SOPROLIFE	29 (64)	52 (114)	93%	88%

* Group 1: including score 0.

† Group 2: including scores 1 and 2.

‡ Sensitivity and specificity calculated by taking the ICDAS-II as a gold standard.

§ Sensitivity measured the proportion of actual caries lesions which are correctly diagnosed by SOPROLIFE regarding ICDAS-II.

¶ Specificity measured the proportion of noncarious lesions which are correctly diagnosed by SOPROLIFE regarding ICDAS-II.

b True negative results = 46; true positive results = 104; false negative results = 8; false positive results = 6.

dry teeth, sensitivity of a visual examination can be improved after a short training period [9]. Furthermore, meticulous visual inspection with a good operation light, a dry tooth, and a probe can render good sensitivity and specificity values [14]. The readings may also be influenced by several factors such as calculus, plaque and prophylactic pastes, and nonconsistent cleaning procedures [12]. Therefore, caries detection by eyesight is better at an advanced stage than early and presents many limitations related to the experience of the examiner and to the preparation procedure of the teeth examined. Consequently, diagnosis of the caries process by visual inspection is partial and auxiliary methods are needed as adjunct to conventional examination for identifying and quantifying such lesions [12, 24]. In addition, one other disadvantage of ICDAS-II is that no images can be taken in order to save the findings for longitudinal monitoring.

In contrast, with SOPROLIFE system, the lesion and its real topography can be seen in a magnified enlarged view [13]. Several studies have shown that the additional observation with the SOPROLIFE camera might also prevent unnecessary operative interventions based on high fluorescence scores due to the better visibility [23, 25]. Due to that “visibility” of the lesion, the interpretation of higher fluorescence answers is easier [26]; the observation capacity of the SOPROLIFE system should guide the clinician toward a more preventive and minimally invasive treatment strategy with monitoring lesion progression or remineralisation over time and not tempt him/her to overtreat a lesion [27].

When comparing the measurements between the two examiners for both methods, our results demonstrated a high reproducibility among the two methods of diagnosis. These results indicated similarity in diagnosis among the 2 observers with both techniques. Despite the different degrees of experience in detecting caries between the two observers, this high interobserver agreement could result from the fact that the observers were from the same department and had a suitable training and calibration session before starting teeth's examination.

In the current study, ICDAS-II was set as “gold standard” [14] due to validated relationship between its codes and the histological depth of a carious lesion as in many other studies [13, 28]. In addition, several studies have shown good reproducibility and accuracy of ICDAS-II for occlusal caries

detection in permanent teeth [29] especially caries lesions in the outer half of the enamel [29].

Our results show a high sensitivity and specificity of SOPROLIFE blue fluorescence mode consistently with other studies [13], probably due to its better visibility.

Finally sensitive caries diagnostic tools can serve not only for early detection but also for monitoring of caries lesions to confirm the success of prevention and remineralisation efforts. In order to limit diagnostic errors resulting not only from failure to detect caries, but also from unnecessary preparing of healthy fissures, it is vital to enhance the visual examination (ICDAS-II method) with other sensitive and specific methods as the SOPROLIFE system.

5. Conclusion

Compared to the most used visual method in the diagnosis of occlusal caries lesions, the finding from this study suggests that SOPROLIFE can be used as a reproducible and reliable assessment tool. At a cut-off point, categorizing noncarious lesions and visual change in enamel, SOPROLIFE shows a high sensitivity and specificity. We can conclude that financially ICDAS is better than SOPROLIFE. However SOPROLIFE is easier for clinicians since it is a simple evaluation of images. Finally in terms of efficiency SOPROLIFE is not superior to ICDAS but tends to be equivalent with the below advantages.

- (i) High-resolution fluorescence images are likely to provide reliable scores. The better visibility of such images could prevent unnecessary operative intervention.
- (ii) We can compare images (before and after).

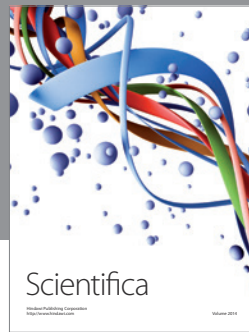
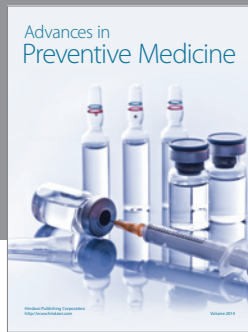
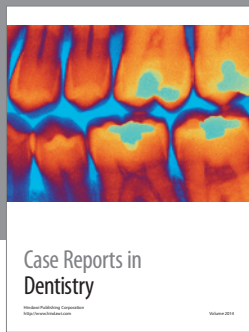
SOPROLIFE may suffer from interference since it is light based. It might also give false positive results if images are magnified above a certain threshold. Both effects are not elaborated within this study.

Conflict of Interests

The authors declare that there is no conflict of interests regarding the publication of this paper.

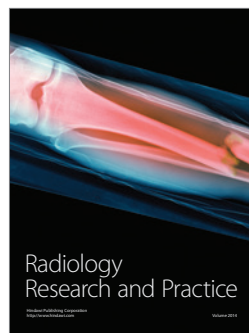
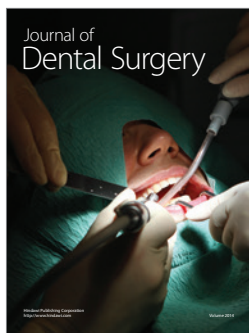
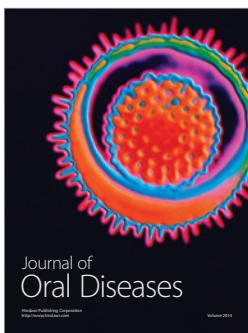
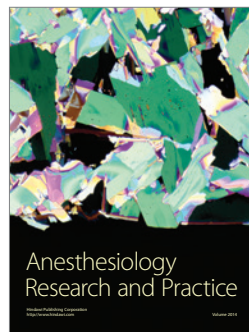
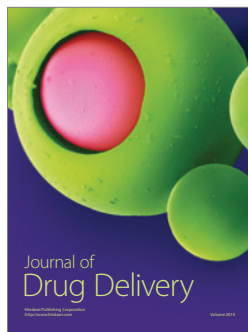
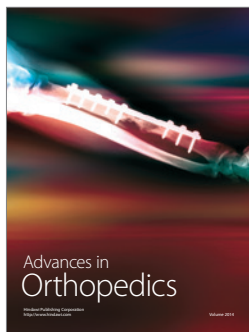
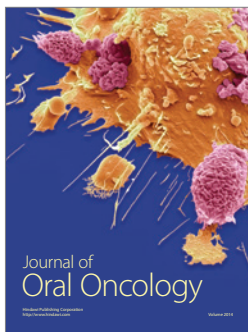
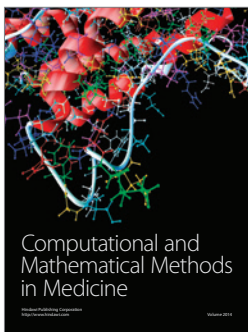
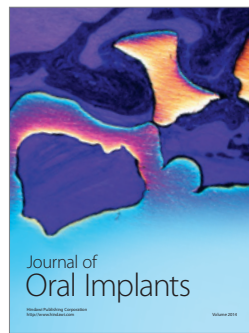
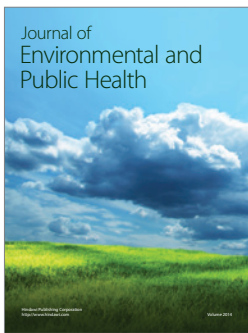
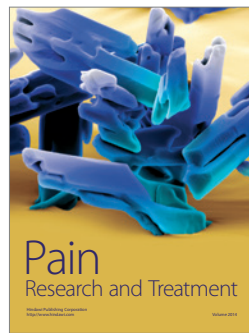
References

- [1] G. M. Davies, H. V. Worthington, J. E. Clarkson, P. Thomas, and R. M. Davies, "The use of fibre-optic transillumination in general dental practice," *British Dental Journal*, vol. 191, no. 3, pp. 145–147, 2001.
- [2] R. H. Selwitz, A. I. Ismail, and N. B. Pitts, "Dental caries," *The Lancet*, vol. 369, no. 9555, pp. 51–59, 2007.
- [3] R. A. Bagramian, F. Garcia-Godoy, and A. R. Volpe, "The global increase in dental caries. A pending public health crisis," *The American Journal of Dentistry*, vol. 22, no. 1, pp. 3–8, 2009.
- [4] P. E. Petersen, "World Health Organization global policy for improvement of oral health—World Health Assembly 2007," *International Dental Journal*, vol. 58, no. 3, pp. 115–121, 2008.
- [5] P. E. Petersen and M. A. Lennon, "Effective use of fluorides for the prevention of dental caries in the 21st century: the WHO approach," *Community Dentistry and Oral Epidemiology*, vol. 32, no. 5, pp. 319–321, 2004.
- [6] T. M. Marthaler, "Changes in dental caries 1953–2003," *Caries Research*, vol. 38, no. 3, pp. 173–181, 2004.
- [7] D. Bandyopadhyay, B. J. Reich, and E. H. Slate, "A spatial beta-binomial model for clustered count data on dental caries," *Statistical Methods in Medical Research*, vol. 20, no. 2, pp. 85–102, 2011.
- [8] F. Bromo, A. Guida, G. Santoro, M. R. Peciarolo, and S. Eramo, "Pit and fissure sealants: review of literature and application technique," *Minerva stomatologica*, vol. 60, no. 10, pp. 529–541, 2011.
- [9] A. Jablonski-Momeni, D. N. J. Ricketts, S. Rolfsen et al., "Performance of laser fluorescence at tooth surface and histological section," *Lasers in Medical Science*, vol. 26, no. 2, pp. 171–178, 2011.
- [10] D. B. Rindal, V. V. Gordan, J. L. Fellows et al., "Differences between reported and actual restored caries lesion depths: results from the dental PBRN," *Journal of Dentistry*, vol. 40, no. 3, pp. 248–254, 2012.
- [11] B. Shikha, G. Munish, V. Shweta, D. Surya, and J. Vikas, "Diagnostic modalities of early caries detection," *Indian Journal of Dental sciences*, vol. 3, pp. 45–49, 2011.
- [12] K. W. Neuhaus, J. A. Rodrigues, I. Hug, H. Stich, and A. Lussi, "Performance of laser fluorescence devices, visual and radiographic examination for the detection of occlusal caries in primary molars," *Clinical Oral Investigations*, vol. 15, no. 5, pp. 635–641, 2011.
- [13] P. Rechmann, D. Charland, B. M. T. Rechmann, and J. D. B. Featherstone, "Performance of laser fluorescence devices and visual examination for the detection of occlusal Caries in permanent molars," *Journal of Biomedical Optics*, vol. 17, no. 3, Article ID 036006, 2012.
- [14] A. I. Ismail, W. Sohn, M. Tellez et al., "The International Caries Detection and Assessment System (ICDAS): an integrated system for measuring dental caries," *Community Dentistry and Oral Epidemiology*, vol. 35, no. 3, pp. 170–178, 2007.
- [15] A. Jablonski-Momeni, D. N. J. Ricketts, M. Heinzl-Gutenbrunner, R. Stoll, V. Stachniss, and K. Pieper, "Impact of scoring single or multiple occlusal lesions on estimates of diagnostic accuracy of the visual ICDAS-II system," *International Journal of Dentistry*, vol. 2009, Article ID 798283, 7 pages, 2009.
- [16] S. Tranæus, X.-Q. Shi, and B. Angmar-Månsson, "Caries risk assessment: methods available to clinicians for caries detection," *Community Dentistry and Oral Epidemiology*, vol. 33, no. 4, pp. 265–273, 2005.
- [17] I. A. Pretty and G. Maupomé, "A closer look at diagnosis in clinical dental practice: part 5. Emerging technologies for caries detection and diagnosis," *Journal of the Canadian Dental Association*, vol. 70, no. 8, article 540, 2004.
- [18] H. Tassery, B. Levallois, E. Terrer et al., "Use of new minimum intervention dentistry technologies in caries management," *Australian Dental Journal*, vol. 58, no. 1, pp. 40–59, 2013.
- [19] N. Gugnani, I. K. Pandit, N. Srivastava, M. Gupta, and S. Gugnani, "Light induced fluorescence evaluation: a novel concept for caries diagnosis and excavation," *Journal of Conservative Dentistry*, vol. 14, no. 4, pp. 418–422, 2011.
- [20] M. B. Diniz, J. A. Rodrigues, I. Hug, R. De Cássia Loiola Cordeiro, and A. Lussi, "Reproducibility and accuracy of the ICDAS-II for occlusal caries detection," *Community Dentistry and Oral Epidemiology*, vol. 37, no. 5, pp. 399–404, 2009.
- [21] D. Charland, C. Fulton, B. Rechmann et al., "Enhancing caries resistance in occlusal fissures with a short-pulsed CO₂ 9.6 μm laser—an in vitro pH-cycling study—preliminary results," in *Lasers in Dentistry XVII*, Proceedings of SPIE, January 2011.
- [22] D. W. Banting, B. T. Amaechi, J. D. Bader et al., "Examiner training and reliability in two randomized clinical trials of adult dental caries," *Journal of Public Health Dentistry*, vol. 71, no. 4, pp. 335–344, 2011.
- [23] A. Jablonski-Momeni, J. F. Busche, C. Struwe et al., "Use of the international caries detection and assessment system two-digit coding method by predoctoral dental students at philipps university of Marburg, Germany," *Journal of Dental Education*, vol. 76, no. 12, pp. 1657–1666, 2012.
- [24] A. F. Zandoná, E. Santiago, G. Eckert, M. Fontana, M. Ando, and D. T. Zero, "Use of ICDAS combined with quantitative light-induced fluorescence as a caries detection method," *Caries Research*, vol. 44, no. 3, pp. 317–322, 2010.
- [25] A. Jablonski-Momeni, D. N. J. Ricketts, K. Weber et al., "Effect of different time intervals between examinations on the reproducibility of ICDAS-II for occlusal caries," *Caries Research*, vol. 44, no. 3, pp. 267–271, 2010.
- [26] J. D. Bader, D. A. Shugars, and A. J. Bonito, "Systematic reviews of selected dental caries diagnostic and management methods," *Journal of Dental Education*, vol. 65, no. 10, pp. 960–968, 2001.
- [27] A. C. Pereira, H. Eggertsson, E. A. Martinez-Mier, F. L. Mialhe, G. J. Eckert, and D. T. Zero, "Validity of caries detection on occlusal surfaces and treatment decisions based on results from multiple caries-detection methods," *European Journal of Oral Sciences*, vol. 117, no. 1, pp. 51–57, 2009.
- [28] S. Tranæus, L.-E. Lindgren, L. Karlsson, and B. Angmar-Månsson, "In vivo validity and reliability of IR fluorescence measurements for caries detection and quantification," *Swedish Dental Journal*, vol. 28, no. 4, pp. 173–182, 2004.
- [29] M. B. Diniz, L. M. Lima, G. Eckert, A. G. F. Zandona, R. C. L. Cordeiro, and L. S. Pinto, "In Vitro evaluation of icdas and radiographic examination of occlusal surfaces and their association with treatment decisions," *Operative Dentistry*, vol. 36, no. 2, pp. 133–142, 2011.



Hindawi

Submit your manuscripts at
<http://www.hindawi.com>



Porphyrin involvement in redshift fluorescence in dentin decay

A. Slimani ^a, I. Panayotov ^a, B. Levallois ^a, T. Cloitre ^c, C. Gergely ^c, N. Bec ^d, C. Larroque ^d, H. Tassery ^{a,b}, F. Cuisinier ^a.

- a) Laboratoire Nanoscience et Biosanté EA4203, Université Montpellier 1, 34193 Montpellier Cedex 5, France.
- b) Assistance publique AP-HM, Marseille ; Aix-Marseille-Université, 13284, Marseille, France.
- c) Université Montpellier2, Laboratoire Charles Coulomb UMR5221, F-34095, Montpellier, France.
- d) IRCM, INSERM, F-34298 U896, Montpellier, France;

ABSTRACT

The aim of this study was to evaluate the porphyrin involvement in the red fluorescence observed in dental caries with Soprolife[®] light-induced fluorescence camera in treatments mode (SOPRO, ACTEON Group, La Ciotat, France) and Vistacam[®] camera (DÜRR DENTAL AG, Bietigheim-Bissingen, Germany). The International Caries Detection and Assessment System (ICDAS) was used to rank the samples. Human teeth cross-sections, ranked from ICDAS score 0 to 6, were examined by epi-fluorescence microscopy and Confocal Raman microscopy. Comparable studies were done with Protoporphyrin IX, Porphyrin I and Pentosidine solutions. An RGB analysis of Soprolife[®] images was performed using ImageJ Software (1.46r, National Institutes of Health, USA). Fluorescence spectroscopy and MicroRaman spectroscopy revealed the presence of Protoporphyrin IX, in carious enamel, dentin and dental plaque. However, the presence of porphyrin I and pentosidine cannot be excluded. The results indicated that not only porphyrin were implicated in the red fluorescence, Advanced Glycation Endproducts (AGEs) of the Maillard reaction also contributed to this phenomenon.

Keywords: Caries detection, Fluorescence spectroscopy, Raman spectroscopy, Porphyrin, Maillard reaction, Soprolife[®]/Vistacam[®] cameras, ICDAS.

1. INTRODUCTION

Variation of dentin autofluorescence was observed during the caries process^{1,2}, and to explain the underlying phenomena various hypotheses were suggested³: modification of the collagen fibers, non-centrosymmetric structure with fluorescence properties and/or accumulation of specific decay products and bacterial biofilm formation with specific endogenous porphyrin. The best known of the decay products are the so-called Maillard reaction products. The Maillard reaction forming a brownish polymer of crosslinked proteins and advanced glycation end-products (AGEs).^{4,5} AGEs accumulate gradually in tissues with aging or caries and include fructolysine (FL), N-(carboxymethyl) lysine (CML), N-(carboxymethyl) hydrolysine (CMhL) and pentosidine.⁶ Dentin collagen fibers are likely to link with AGEs over the long term, rendering dentin collagen more resistant to proteolytic breakdown and modifying its intrinsic fluorescence.⁵ Previous studies also focused on porphyrin and its derivatives in an attempt to link the autofluorescence signal of dentin decay and porphyrin sediment.^{3,7} Nevertheless, porphyrin is a generic term that refers to a huge range of molecules, not only bacterial derivatives. Porphyrins are aromatic tetrapyrrole macrocycles, and they are abundant in nature⁸.

2. MATERIALS AND METHODS

2.1 ICDAS classification

The International Caries Detection and Assessment System was used to rank the samples.^{9,10} The ICDAS codes range from sound surfaces (code 0), through primary carious lesions in enamel (codes 1–3) to primary carious lesions in dentin (codes 4–6).

2.2 Fluorescence dental devices

2.2.1 Vistacam[®] camera

Vistacam[®] (Classic, CL and IX) is an intraoral fluorescence camera (Dürr Dental, Bietigheim-Bissingen, Germany) that emits at 405 nm and captures a digital image. The software (DBSWIN version 5.3) quantifies the green and red components of the reflected light on a scale from 0 to 3 as a ratio of red to green, the carious areas having a higher ratio.^{11,12}

2.2.2 Soprolife[®] camera

The Soprolife (Acteon, La Ciotat, France) intra-oral camera has two types of LED that can illuminate tooth surfaces in the visible domain, either in the white-light region or in a narrow band (450 nm wavelength with a bandwidth of 20 nm, centered at ± 10 nm around the excitation wavelength).¹³⁻¹⁸

Soprolife[®] images were analyzed with ImageJ Software (1.46r, National Institutes of Health, USA) to measure intensity variations in red, blue and green color (RGB space) and analyze in detail the red fluorescence signal variation.

2.3 Sample preparation

2.3.1 Teeth

Nine teeth, freshly extracted, were collected from Montpellier University Health Center, the subjects having signed written informed consent. The teeth were ranked according to ICDAS classification (score 0 to 6), cleaned with an air polishing device with added sodium bicarbonate powder (Air N Go, classic powder, Actéon, Bordeaux, France)¹⁹ and stored in water at 4°C. Cross-sections of 1 mm thick were prepared using an Isomet diamond saw (Isomet 1,000; Buehler, Lake Bluff, IL, USA) and polished on carbide disks (Escil, Lyon, France). Each tooth cross-section was kept in a separate box.

2.3.2 Dental plaque

The red fluorescent dental plaque from an upper molar [Fig. 2] observed with a Soprolife[®] camera was collected. The molar was first isolated with a rubber dam and the plaque removed with a sterilized probe #17. The sample was then stored in physiological serum at 4°C and analyzed within 48 H.

2.4 Chemicals

Protoporphyrin IX (PpIX) (Sigma Aldrich, France), porphyrin I (PI) (Sigma Aldrich, France) and pentosidine (Polypeptide Group, Strasbourg, France) were observed separately with a Soprolife[®] camera. Protoporphyrin IX and porphyrin I powders were prepared in absolute ethanol and pentosidine in PBS at a concentration of 0.2 mg/ml.

2.5 Fluorescence spectroscopy:

Emission fluorescence spectral characteristics of teeth cross sections with carious dentin and enamel were examined by epi-fluorescence microscopy (Nikon Eclipse TE 2000) with a range of excitation wavelengths of λ_{ex} 380-420 nm, a spectrometer (Acton SP215i-CCD PIXI400B) and Winspect Software.

2.6 Micro-Raman spectroscopy:

Raman spectra were collected using a LabRAM ARAMIS IR2 confocal micro-Raman spectrometer. Raman spectra were recorded on teeth cross-sections, dental plaque and chemicals as well.

2.7 Imaging mass spectrometry

Matrix-assisted laser desorption/ionization time-of-flight imaging mass spectrometry (MALDI-TOF IMS) on teeth cross-sections were performed using the 4800 Plus MALDI TOF/TOFTM analyzer, 4800 Imaging Tool and TissueView softwares.

3. RESULTS

3.1 Clinical case

The figure 1 represents a clinical case of a proximal dentin caries. The dentin caries appeared bright red in the cavity before full excavation [Fig. 1 (B)]. Once the cavity cleaned, shadowy red fluorescence represented the sclerotic dentin [Fig. 1 (C)].

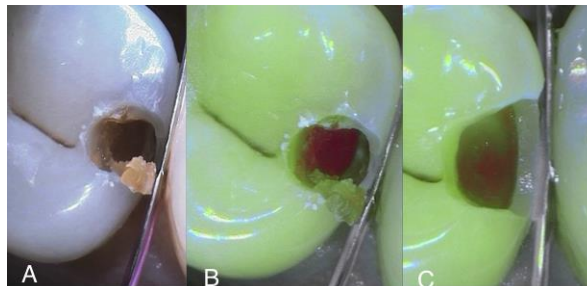


Figure 1. Optical (A) and fluorescence images (B-C) of a dentin caries using the Soprolife[®] camera

3.2 Enamel

3.1.1 Fluorescence images with Soprolife[®] and Vistacam[®]

The ICDAS 1 sample represents an early stage of decay that affects enamel only. Carious enamel appeared opaque white in daylight and more whitish with Soprolife[®]. In the Vistacam[®] image, the infected area was red color-coded with enamel caries up to enamel/dentin border which indicated a carious activity with a positive porphyrin-like signal. The cross-section ICDAS 2 showed an enamel and dentin carious activity. The Soprolife[®] image showed a dark red fluorescent dentin at the upper layer, followed by a color-gradient of grey/green fluorescence from the brown lesion. In the Vistacam[®] image carious enamel and dentin were clustered into the same area with the same color-code.

3.1.2 Fluorescence spectroscopy

Protoporphyrin IX solution revealed two main characteristic peaks in the red spectral range: 620 nm and 675 nm. Comparable fluorescence emission maxima have been observed for dental calculus and carious enamel.^{3,21} The emission spectra of porphyrin I solution had three peaks at around 510 nm, 645 nm and 680 nm. These peaks are weaker than the protoporphyrin IX peaks, and the presence of porphyrin I can be masked for this reason. The fluorescence intensity of the pentosidine solution is weak compared to protoporphyrin IX, and porphyrin I and exhibited two large peaks centered around 510 nm and 680 nm.

Sound enamel (ICDAS 0) had a single peak in the green spectral region at around 470 nm. Carious enamel revealed one main peak in the green spectral range and two peaks in the red spectral range (620 nm and 670 nm). Fluorescence spectra of ICDAS 2 enamel showed two peaks (610 nm and 675 nm) with higher intensities than ICDAS 1.

3.1.3 Micro-Raman spectroscopy

To reveal underlying structural modifications for the score ICDAS 2 sample, a specific enamel spot was investigated in the tooth cross-section with Micro-Raman spectroscopy. The Raman spectra of the ICDAS 2 sample showed two bands C-C (1345cm⁻¹) and CH₂ (1578cm⁻¹). These bands were also present in the Raman spectrum of the protoporphyrin IX powder.

The red fluorescent dental plaque was collected on a molar fissure [Fig. 2]. The micro-Raman spectrum of this dental plaque showed a high fluorescence signal, and two main bands (1330 cm^{-1} and 1570 cm^{-1}) were observable [Fig. 3].

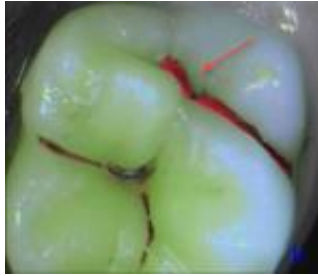


Figure 2. Soprolife® image of an in vivo upper molar; the excited dental plaque appeared bright red (red arrow).

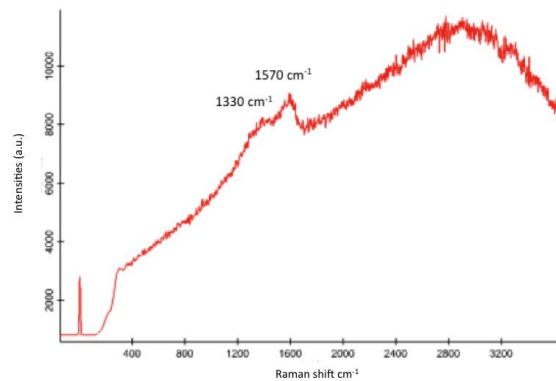


Figure 3. In vivo dental plaque Raman spectrum

3.3 Dentin

3.2.1 Fluorescence spectroscopy

The ICDAS 6 sample is an extensive dentin caries with no enamel left. The Vistacam® camera did not detect a color-coded fluorescence on carious dentin, even with various imaging distances, backgrounds and camera orientations. The image taken with Soprolife® showed a red dark fluorescence.

The fluorescence spectra up to ICDAS 5 did not give any specific porphyrin-like spectral pathway. All these spectra showed a main peak in the green spectral range, centered around 480-500 nm, and their relative intensities as well as their positions varied. The red shift increased as ICDAS scores increased, with the relative fluorescence intensities falling. On the other hand, the ICDAS 6 sample exhibited two porphyrin-like peaks at 620 nm and 675 nm [fig. 4]. It was the sample that gave the most accurate porphyrin-like spectra. The double peaks decreased while the main peak in the green spectral range increased as the measuring spot migrated to less infected areas.

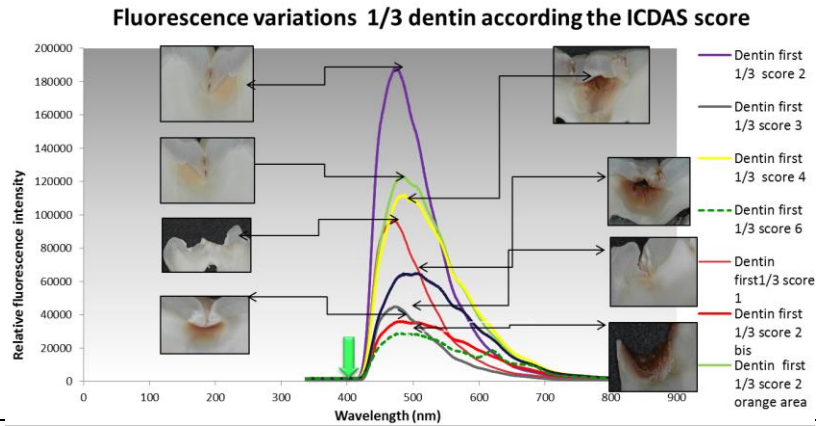


Figure 4. Fluorescence spectra of different ICDAS scores on the first layer of dentin.

3.2.2 RGB analysis

An RGB analysis was performed on the ICDAS 2 cross-section at different spots to evaluate the green and red proportions in the Soprolife[®] fluorescence image.

The green value prevailed in the measurement taken on the sound dentin. The red was dominant in the infected dentin while the green greatly decreased to almost reach the blue value, as the measurement migrated to the affected dentin, again indicating a dominant green color but still less bright.^{18,21} The blue color roughly followed the green variations.

3.4 Imaging mass spectrometry

This preliminary study allowed achieving a mapping of the spatial distribution of Protoporphyrin IX (m/z 562.6) in teeth cross-sections [Fig. 5].

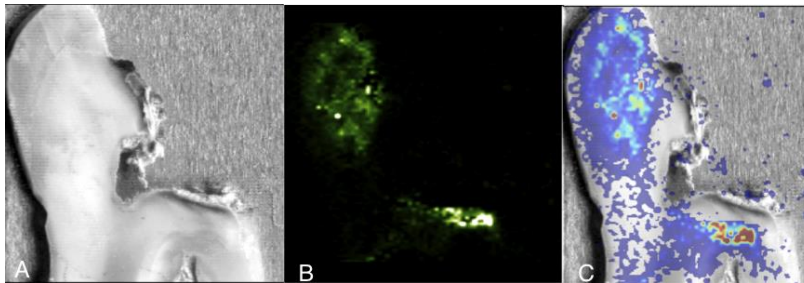


Figure 5. Optical image (A), ionic image m/z 562.6 (\pm 0.4) and an overlay of MALDI and ionic images of the distribution of protoporphyrin IX.

4. DISCUSSION

Healthy dentin could be also clearly discriminated from carious dentin, as it appeared bright green at the highest level of brightness. Any carious lesion could be detected by the variation in the fluorescence of its tissues in relation to a healthy area of the same tooth. Both tertiary and sclerotic dentin structures could partially account for the brightness (L^*) variations, but they are centripetal scar tissue with a constantly low level of brightness and modified fluorescence color.^{18,21} The RGB histograms and RGB plots confirmed the huge drop of the green signal in carious dentin, showing a residual red signal. One of either the organic or inorganic constituents of healthy dentin that emits an acid-green fluorescence partially disappears during the caries process; hence, the red fluorescence appears.^{15,18,21} The hypothesis of a modification of the non-centrosymmetric structure of collagen 1 was previously described^{14,16}, and dentinal constituents emitting a red fluorescence seem to be less damaged by the caries process. The spectral data acquired with the various spots can be correlated to the carious activity: spot #3 represented the infected dentin

and appeared red, while spots #4 and #5 represented the affected areas which had fewer bacteria, and produced an increasing green fluorescence signal.

In fact, porphyrin is claimed to be of bacterial origin, yet few cariogenic bacteria produce it, and if it were the case we should observe a porphyrin gradient, and this is not the case. The numerical value for red given by the Vistacam[®] camera never indicated a porphyrin gradient. Threshold detection seemed to control the color code. Porphyrins are part of our biological system, they are responsible for a variety of biological functions.⁸ The most important fluorophores are protoporphyrin IX, coproporphyrin III, uroporphyrin III, and hematoporphyrin IX.⁵ Protoporphyrin IX was the most investigated in dental caries fluorescence but other types of porphyrins could be involved in addition to AGEs (Maillard reaction). In contrast, on ICDAS 6, no porphyrin signal was revealed, which is often observed in clinical situations. Previous studies aimed to examine whether *Streptococcus mutans* is implicated in the generation of the fluorescence detected in carious lesions. The results demonstrated that *S. mutans* induced enamel and dentin lesions exhibited, and increased fluorescence in the red and green spectral regions, with a stronger signal in the red region. But neither bacterial cells nor culture media generated any fluorescence^{22,23}. Our study confirmed this result only for enamel but diverged for dentin. In fact, *S. mutans* penetration in dentin should give a similar porphyrin gradient signal, which was not observed with the Vistacam[®] device. The specific red gradient signal observed with Soprolife[®] was previously described as a result of the AGEs and Maillard reaction.^{14,16} About the similar Raman signals observed in the infected enamel, protoporphyrin IX chemical and the *in vivo* plaque debris, our hypothesis was that the measurement was taken on a specific bacterium at this precise spot, which allowed a positive Raman signal to be detected (bacteria PpIX bands). Despite the huge fluorescence background noise observed in the Raman spectra of dental plaque, the two specific Raman vibrations were detected as a typical signature of *in vivo* plaque debris²⁴. No such Raman vibrations were observed in the dentin decay, as they were certainly masked by the vibrations of AGEs products.

Observations of the fluorescence spectra on various tooth tissues most of the time showed the same variations. A clear reduction of the intensities, similar to the brightness reduction and flattening spectra, were observed from the sound to the infected area. On the other hand, the spectra apexes, except for ICADS 6, were mainly centered in the green spectral range (500 nm) regardless of the additional visible color. The balance between red and green signal was in favor of the red signal as soon as the spectra shifted close to 600 nm. The fluorescence image recorded with Soprolife[®] did not detect a fluorescence signal in the early stage of carious enamel (ICDAS 1), probably due its weak fluorescence emission. In fact, enamel has 20-30x less organic material than dentin. Therefore, in the different ICDAS scores, enamel fluorescence spectra exhibited lower relative intensities compared to dentin fluorescence. In the Vistacam[®] image of an ICDAS 1 sample, the infected area revealed a positive porphyrin-like signal and correlated with emission fluorescence spectra of the same area: two porphyrin-like spectra with low relative intensities and similar pathway, in addition to the main peak in the green spectral range, were observed. The ICDAS 6 sample gave specific protoporphyrin IX-like spectra with different intensities. This carious area at the last ICDAS score was dark, which implied extensive scattering and absorption phenomena. This process could explain the weak fluorescence intensity on the infected area.

The two specific vibration bands (1345 cm^{-1} and 1578 cm^{-1}) observed with Raman spectroscopy had never been described before in enamel and *in vivo* dental plaque samples. They were specific to the protoporphyrin IX and similar excitations were more difficult to observe with the other fluorescence molecules. In dentin decay, these signals were overlapped by the fluorescence signal. This strengthens our hypothesis that the porphyrin signals were more visible in the upper layer of the decay, and non-existent or masked in the deepest decay layer. As for the involvement of AGEs produced by Maillard reactions^{14,15,25} For the ICDAS 2 sample, fluorescence emission spectra of enamel showed the PpIX-like double peaks around 620 nm and 680 nm. There is a positive correlation between this result and the Vistacam[®] image.

5. CONCLUSION

This study provided a comparison between the different stages of dental decay and its red shifted fluorescence emission spectra. It also provided a correlation study of the single photon fluorescence spectroscopy and micro-Raman spectroscopy of various teeth areas with fluorescence images using Soprolife[®] and Vistacam[®] cameras. Our results suggested that protoporphyrin IX contributed to the red shift fluorescence observed in carious tissues. Protoporphyrin IX was not systematically detected in carious dental hard tissues. Our data allowed us to conclude that protoporphyrin contributed to the red shift fluorescence of dentin and enamel decay, but AGEs probably also participated in this complex biological reaction.

However, this study achieved its objectives by successfully recording more than 200 spectra (fluorescence and Raman) and images (microscopic, optical and fluorescence) recorded with intra-oral cameras. This study led to a descriptive panel of fluorescence changes at all stages of dental decay. Current work is ongoing using mass spectrometry imaging to define a mapping of teeth cross-sections to identify and localize specific metabolites such as protoporphyrin IX and various AGEs.

REFERENCES

- [1] Bjørndal L. and Mjör I. A., “Pulp-dentin biology in restorative dentistry. Part 4: Dental caries--characteristics of lesions and pulpal reactions,” *Quintessence Int. Berl. Ger. 1985* **32**(9), 717–736 (2001).
- [2] Mjör I. A., “Pulp-dentin biology in restorative dentistry. Part 5: Clinical management and tissue changes associated with wear and trauma,” *Quintessence Int. Berl. Ger. 1985* **32**(10), 771–788 (2001).
- [3] Buchalla W, Lennon A. M. and Attin T., “Fluorescence spectroscopy of dental calculus,” *J. Periodontol Res.* **39**(5), 327–332 (2004).
- [4] Sell D. R. and Monnier V. M. , “Isolation, purification and partial characterization of novel fluorophores from aging human insoluble collagen-rich tissue,” *Connect. Tissue Res.* **19**(1), 77–92 (1989).
- [5] Kleter G. A., Damen J. J., Buijs M. J. and Ten Cate J. M., “Modification of amino acid residues in carious dentin matrix,” *J. Dent. Res.* **77**(3), 488–495 (1998).
- [6] Kleter G. A., “Discoloration of dental carious lesions (a review),” *Arch. Oral Biol.* **43**(8), 629–632 (1998).
- [7] Buchalla W., Lennon A. M. and Attin T., “Comparative fluorescence spectroscopy of root caries lesions,” *Eur. J. Oral Sci.* **112**(6), 490–496 (2004).
- [8] Hu Y., Geissinger P. and Woehl J. C., “Potential of protoporphyrin IX and metal derivatives for single molecule fluorescence studies,” *J. Lumin.* **131**(3), 477–481 (2011).
- [9] Ismail A. I., Sohn W. Tellez M., Amaya A., Sen A., Hasson H. and Pitts N. B., “The International Caries Detection and Assessment System (ICDAS): an integrated system for measuring dental caries,” *Community Dent. Oral Epidemiol.* **35**(3), 170–178 (2007).
- [10] Ismail A. I., Sohn W., Tellez M., Willem J. M., Betz J. and Lepkowski J., “Risk indicators for dental caries using the International Caries Detection and Assessment System (ICDAS),” *Community Dent. Oral Epidemiol.* **36**(1), 55–68 (2008).
- [11] Jablonski-Momeni A., Liebegall F., Stoll R., Heinzl-Gutenbrunner M. and Pieper K., “Performance of a new fluorescence camera for detection of occlusal caries in vitro,” *Lasers Med. Sci.* **28**(1), 101–109 (2013).
- [12] Seremidi K., Lagouvardos P., and Kavvadia K., “Comparative in vitro validation of VistaProof and DIAGNOdent pen for occlusal caries detection in permanent teeth,” *Oper. Dent.* **37**(3), 234–245 (2012).
- [13] Rechmann P., Charland D., Rechmann B. M. T., and Featherstone J. D. B., “Performance of laser fluorescence devices and visual examination for the detection of occlusal caries in permanent molars,” *J. Biomed. Opt.* **17**(3), 036006 (2012).
- [14] Levallois B., Terrer E., Panayotov I., Salehi H., Tassery H., Tramini P. and Cuisinier F., “Molecular structural analysis of carious lesions using micro-Raman spectroscopy,” *Eur. J. Oral Sci.* **120**(5), 444–451 (2012).
- [15] Salehi H., Terrer H., Panayotov I., Levallois B., Jacquot B., Tassery H. and Cuisinier F., “Functional mapping of human sound and carious enamel and dentin with Raman spectroscopy,” *J. Biophotonics* **6**(10), 765–774 (2013).
- [16] Panayotov I., Terrer E., Salehi H., Tassery H., Yachouh J., Cuisinier F. J. G. and Levallois B., “In vitro investigation of fluorescence of carious dentin observed with a Soprolife® camera,” *Clin. Oral Investig.* **17**(3), 757–763 (2013).
- [17] Gugnani N., Pandit I., Srivastava N., Gupta M. and Gugnani S., “Light induced fluorescence evaluation: A novel concept for caries diagnosis and excavation,” *J. Conserv. Dent. JCD* **14**(4), 418–422 (2011).
- [18] Terrer E., Raskin A., Koubi A., Dionne A., Weisrock G, Sarraquigne C, Mazuir A and Tassery H., “A new concept in restorative dentistry: LIFEDT-light-induced fluorescence evaluator for diagnosis and treatment: part 2 - treatment of dentinal caries,” *J. Contemp. Dent. Pract.* **11**(1), E095–102 (2010).
- [19] Tassery H., Levallois B, Terrer E., Manton D. J., Otsuki M., Koubi S., Gugnani N., Panayotov I., Jacquot B., et al., “Use of new minimum intervention dentistry technologies in caries management,” *Aust. Dent. J.* **58** **Suppl 1**, 40–59 (2013).
- [20] Lennon A. M., Buchalla W., Rassner B., Becker K., and Attin T., “Efficiency of 4 caries excavation methods compared,” *Oper. Dent.* **31**(5), 551–555 (2006).

- [21] Terrer E., Koubi S., Dionne A., Weisrock G., Sarraquigne C., Mazuir A. and Tassery H., "A new concept in restorative dentistry: light-induced fluorescence evaluator for diagnosis and treatment. Part 1: Diagnosis and treatment of initial occlusal caries," *J. Contemp. Dent. Pract.* **10**(6), E086–094 (2009).
- [22] Shigetani Y., Takenaka S., Okamoto A., Abu-Bakr N., Iwaku M. and Okiji T., "Impact of *Streptococcus mutans* on the generation of fluorescence from artificially induced enamel and dentin carious lesions in vitro," *Odontol. Soc. Nippon Dent. Univ.* **96**(1), 21–25 (2008).
- [23] Lennon A. M., Buchalla W., Brune L., Zimmermann O., Gross U. and Attin T., "The ability of selected oral microorganisms to emit red fluorescence," *Caries Res.* **40**(1), 2–5 (2006).
- [24] Koenig K., Hibst R., Meyer H., Flemming G. and Schneckenburger H., "<title>Laser-induced autofluorescence of carious regions of human teeth and caries-involved bacteria</title>," 170–180 (31 December 1993).
- [25] Kleter G. A., Damen J. J., Buijs M. J. and J. M. Ten Cate, "The Maillard reaction in demineralized dentin in vitro," *Eur. J. Oral Sci.* **105**(3), 278–284 (1997).

Méthodologie du diagnostic en cariologie

Apport des nouvelles technologies

H. TASSERY, A. SLINAMI, M. ACQUAVIVA, C. CAUTAIN, M.N. BEVERINI
E. TERRER

Hervé Tassery¹

PU-PH

Amel Slinami²

Docteur en Chirurgie Dentaire

Michèle Acquaviva³

Docteur en Chirurgie Dentaire

Responsable du service

Maxillo-Facial, Hôpital d'Avignon

Cécile Cautain³

AHU

Marie-Noëlle Beverini³

AHU

Elodie Terrer¹

AHU

¹Université d'Aix-Marseille,
Département d'odontologie
conservatrice et restauratrice
Université de Montpellier 1,
Laboratoire de biologie
et nanoscience, EA4203

²Université de Montréal,

³Université d'Aix-Marseille,
Département d'odontologie
conservatrice et restauratrice

**Les auteurs déclarent
ne pas avoir de lien d'intérêt**

RÉSUMÉ

L'approche médicale des lésions carieuses dentaires requiert une détection de ces lésions à un stade le plus précoce possible. Les nouvelles méthodes de détection sont basées sur: la transmission de lumière, la fluorescence (systèmes de fluorescence uniquement, combinaison de caméra et système de fluorescence), l'impédance électrique et la conductivité. Le diagnostic établi sera plus ou moins fiable et précis selon l'aide visuelle utilisée et l'expérience de l'opérateur. Ces techniques nous permettent d'établir un diagnostic de lésions précoces et par conséquent de réaliser des traitements préventifs et *a minima* afin de conserver au maximum les tissus sains ou de contrôler l'évolution de lésions débutantes en cas d'abstention thérapeutique.

IMPLICATION CLINIQUE

La gestion du risque carieux et les technologies pour détecter et quantifier les caries précoces ainsi que l'activité carieuse sont des outils pour identifier des patients nécessitant une intervention préventive intensive.

L'approche médicale des lésions carieuses dentaires requiert une détection de ces lésions à un stade le plus précoce possible. La gestion du risque carieux et le développement de technologies pour détecter et quantifier ces caries précoces ainsi que l'activité carieuse seront des outils pour identifier des patients nécessitant une intervention préventive intensive (1). Ces méthodes de détection et quantification des lésions carieuses nécessitent certaines conditions: des contrôles réguliers, être capable de détecter des lésions précoces, de différencier des lésions superficielles de celles plus profondes (haute sensibilité), présenter si possible des données quantitatives de sorte que l'activité puisse être surveillée; être précis afin que les mesures puissent être répétées par plusieurs opérateurs, être rentables et faciles à utiliser.

De nouvelles classifications sont apparues (ICDAS, Univiss) et la principale requête est d'être sûr que le dispositif de diagnostic et la classification utilisée soient parfaitement adaptables à une pratique quotidienne (2).

L'introduction d'un système de gestion du risque carieux en corrélation avec l'évaluation des risques et la gestion des caries (cavitaires ou non) fondées sur des preuves pourrait dépendre de ces nouvelles technologies d'aides au diagnostic.

LES DIFFÉRENTES TECHNOLOGIES UTILISÉES: INTÉRÊTS ET INDICATIONS

Les nouvelles méthodes de détection sont basées sur la transmission de lumière et la fluorescence.



Fig. 1
a) Lésion proximale observée par transillumination avec le DIAGNOcam® posé à cheval sur la dent.
b) Caméra DIAGNOcam®.

Transmission de lumière

a) **transillumination par fibre optique** (Foti®, Difoti®, Electro-Optical Sciences) et plus récemment une technique numérisée Difoti® qui utilise la transmission de la lumière à travers la dent. Ainsi les images peuvent être stockées et réexaminées plus tard (3, 4, 5).

b) **Camera Kavo®: DIAGNOcam®** (Kavo Dental): un nouveau système développé récemment par Kavo est également basé sur le niveau élevé de transillumination et une longueur d'onde proche de l'infrarouge. Seulement, peu de recherches ont été effectuées pour l'instant et le système semble plus adapté au diagnostic des lésions carieuses proximales avec des résultats prometteurs (1) (fig. 1).

Tableau 1 - Scores du DIAGNOOpen et recommandations.			
score DIAGNOOpen	niveau 1	niveau 2	niveau 3
Occlusal et sillon	0-12	13-24	> 25
Interprétation histologique	tissu sain	Email déminéralisé	Dentine atteinte
Thérapeutique recommandée	Soin prophylactique normal	Soin prophylactique intensif	Soin invasif <i>a minima</i>
Surface proximale	0-7	8-15	>16
Thérapeutique recommandée	Soin prophylactique normal	Soin prophylactique intensif	Soin invasif <i>a minima</i>

Instructions: DIAGNOcam® est placé directement sur la dent, la lumière est envoyée sur la surface dentaire et l'image est récupérée par le logiciel. Les images sont enregistrées directement et la prise de vidéo est possible.

La fluorescence

Les techniques d'imagerie basées sur la réponse de fluorescence des composants organiques des dents ont été développées pour être utilisées dans la détection des caries (1). Les dispositifs disponibles dans le commerce sont les suivants:

Systèmes de fluorescence uniquement

a) **le DIAGNOdent®** (DIAGNOdent 2095, DIAGNOdent 2190, Kavo Dental), qui utilise un laser, réagissant avec des composés extrinsèques comme les porphyrines et fonctionnant à une longueur d'onde fixe de 655 Nm (6). Les scores obtenus avec le DIAGNOdent vont guider les décisions cliniques (7, 8, 9) (tableau 1).

b) **le dispositif FACE** (Fluorescence Aided for Caries Excavation) (SIROIconcept®) qui nécessite l'utilisation de lunettes filtrantes spécifiques. Peu d'informations sont disponibles sur ce sujet. Pour les deux systèmes, aucune image ne peut être récupérée (10,11).

Instructions: DIAGNOdent: après un étalonnage sur un plot de céramique, le laser est placé sur les surfaces et le dispositif donne un score selon le degré d'atteinte carieuse.

FACE: l'outil éclaire directement la dent concernée et le tissu carié apparaît rouge au travers des lunettes.

Combinaison de caméra et système de fluorescence

a) **le système QLF®** (Quantitative light fluorescence) (QLF-clin, Inspektor Research Systems), avec une émission de longueur d'onde de 290-450 Nm. Ce système permet de contrôler les lésions amélaire. Quelques essais décrits dans la littérature ont été réalisés sur la dentine (12, 13, 14).

b) **le système Canary®** (Quantum Dental Technologies) est un laser de faible puissance, qui utilise une combinaison de chaleur et lumière (Frequency Domain Photothermal Radiometry and Modulated Luminescence (FD-PTR and LUM) afin d'examiner directement la structure cristalline des dents et cartographier la carie. Pour la dentine des essais sont en cours (15, 16, 17, 18).

Instructions : le laser est posé sur la dent. Le système fournit conjointement des images et des valeurs prédictives de caries. Des lunettes de protection sont recommandées.

c) **la caméra VistaCam®** (Classic, CL and IX) est une caméra intra-orale à fluorescence (Dürr Dental) qui illumine les dents avec une lumière ultraviolette (405 Nm) et capte la lumière réfléchiée sous forme d'image numérique. Cette lumière est filtrée par la lumière au-dessous de 495 Nm et contient la fluorescence jaune-vert des dents normales avec un pic à 510 Nm ainsi que la fluorescence rouge des métabolites bactériens avec un pic à 680 Nm. Un logiciel (version 5.3 DBSWIN) quantifie la composante verte et rouge de la lumière réfléchiée sur une échelle de



Fig. 2

a) Image VistaCam® d'une carie occlusale avec leurs ratios respectifs de valeur carieuse.

b) Caméra VistaCam® avec 3 têtes interchangeables (mode jour, mode fluorescence, mode macro).

3

Fig. 3 - Caméra Soprocure® et Soprolife®.

Fig. 4 a et b - Image Soprocure® en mode jour (carré blanc) et caries (carré bleu).

0 à 3 avec un rapport du rouge au vert, en montrant les zones où le rapport est supérieur à celui d'une zone saine. Une nouvelle Vista Cam CL-IX® avec des caméras à tête amovible, sans fil et une fonction de photopolymérisation, vient d'être commercialisée (**tableau 2**) (**fig. 2**).

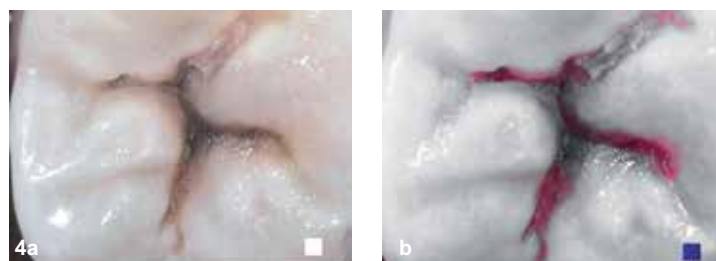
Instructions : la caméra est appliquée sur la dent, les images sont enregistrées dans un logiciel spécifique en fonction des valeurs de caries.

d) Soprolife® camera (Actéon) (19, 20, 21) La caméra intra-orale utilise deux types de LED qui peuvent illuminer les surfaces de la dent dans le domaine du visible, soit dans la région de la lumière blanche ou dans une bande étroite (longueur d'onde 450 Nm avec une bande passante de 20 Nm, centrée à ± 10 Nm autour de la longueur d'onde d'excitation). Une image anatomique est recueillie sur laquelle se superpose une autofluorescence. La caméra peut détecter et localiser des différences de densité, de structure et/ou de composition chimique d'un tissu biologique soumis à un éclairage continu dans une bande de fréquences, tout en le rendant apte à générer un phénomène de fluorescence dans une seconde bande de fréquences. La caméra est équipée d'un capteur d'image (un capteur CCD de 0,25 pouce) constitué d'une mosaïque de pixels couverts avec des filtres de couleurs complémentaires. Les données recueillies, relatives à l'énergie reçue par chaque pixel, permettent de recueillir une image de la dent. La caméra est utilisée dans trois modes grâce à 2 boutons-pression et une large gamme de grossissements est disponible :

- le mode jour : 4 LED à lumière blanche génèrent la lumière,
- les modes de diagnostic et de traitement : pour ces deux modes, la lumière provient de 4 LED à lumière bleue (450 Nm).

Une nouvelle caméra, appelée la Soprocure® (**fig. 3**) (caméra blanche) possède 3 modes cliniques : le mode jour, le mode carie et le mode pério. L'avant-dernier met en évidence l'émail et la dentine cariée et le dernier, l'inflammation gingivale (**fig. 4**).

La caméra à fluorescence est liée au concept LIFEDT (Light Induced Fluorescence Evaluator for Diagnosis and Treatment). Les principes en sont les suivants :



- éclairer la dent en mode jour et en mode fluorescence avec un fort grossissement,
- noter toute modification de la lumière réfléchi sur la dentine ou de l'émail comparativement à une zone saine,
- nettoyer soigneusement la zone suspecte par air pulsé type Air-Ngo (Actéon), Kavoprophy (Kavo),

Tableau 2 - Les scores et échelles de couleur de la VistaCam® par rapport à la lecture histologique.

0-1	1-1.5	1.5-2	2-2.5	2.5 >3
Email sain	Déminéralisation initiale de l'émail	Lésion profonde de l'émail	Lésion dentinaire	Lésion profonde de la dentine

- éclairer à nouveau la dent, tout signal rouge résiduel, signe la présence d'une carie ou d'une zone suspecte,
- les décisions cliniques ne sont pas liées à des valeurs numériques, mais à l'amplification de l'inspection visuelle.

Le logiciel de Soproimaging® permet d'enregistrer, de comparer et de modifier les images (**tableaux 3, 4, 5**) (5, 6, 22, 23, 24, 25).

Tableau 3 - Guide des couleurs obtenues en clinique utilisé avec le concept LIFEDT et la Soprolife®/Soprocare®.

Caméra. Inspection visuelle	Dentine saine	Dentine infectée	Dentine affectée processus actif (tissu jaune clair)	Dentine affectée Processus arrêté (tissu marron, très dur)
Soprolife®	Vert	Gris foncé	Rouge vif	Rouge sombre
Soprocare®	Gris	Gris foncé	Rouge vif	Rouge sombre

Tableau 4 - La sensibilité et la spécificité des différents principaux appareils (5,6,22-25).

Outils/Technologies	Sensibilité	Spécificité
Inspection visuelle	0,6	0,73
Radiographie rétro-coronaire	0,19	0,80
Moniteur® électronique de caries	0,65	0,73
Transillumination® par fibres optiques	0,21	0,88
QLF®	0,5 – 0,68	0,7 – 0,9
Spectra® ou VistaCam®	0,9	0,37
DIAGNOdent®	0,87	0,5
Soprolife®	0,68	0,93

Tableau 5 - Les principaux avantages des différents dispositifs

Principaux dispositifs	Inspection visuelle	Valeur numérique	Grossissement	Enregistrement d'images	Etapes de traitement	Evaluation de l'activité
QLF®	+	+	+	+	+	+/-
DIAGNOcam®	+	-	+	+	-	-
DIAGNOdent®	-	+	-	-	-	-
VistaProof® VistaCam IX®	++ ++	++ +	++ +++	+++ +++	? ?	+ +
Canary system®	+/-	+	+/-	++	?	?
FACE®	++	-	-	-	++	?
Soprolife® Soprocare®	+++ +++	- -	++++ ++++	+++ +++	+++ +++	+++ +++

Instructions : la caméra est posée sur la dent, le grossissement et le mode (jour ou fluorescence) sont choisis. Les images sont stockées dans un logiciel spécifique appelé Soproimaging®. La prise de la vidéo est possible.

Technologies non ionisantes

La tomographie par cohérence optique (OCT, système d'imagerie dentaire) est une technique d'imagerie non ionisante qui peut produire des images en coupe des tissus biologiques en utilisant une lumière infrarouge à 1310 Nm. Seules, les études *in vitro* sont disponibles et souvent limitées à la profondeur de l'émail. L'OCT polarisée (PS-OCT) de dernière génération peut être corrélée avec le degré de déminéralisation et de la gravité de la lésion.

Impédance électrique et conductivité (23, 26, 27, 28, 29): Electronic caries Monitor (ECM, Diagnostics Lode) est basée sur la conductivité électrique des tissus et le CarieScan sur l'impédance électrique. Plus précisément la technique du CarieScan® (Dundee) est basée sur la théorie que les tissus durs dentaires montrent une forte résistance électrique ou impédance électrique. Plus le tissu est déminéralisé, plus la résistance devient faible. Des études ont été réalisées *in vitro* et *in vivo*, montrant une sensibilité et spécificité modérées. Les mesures sont liées à une échelle de nombres donnant des informations sur l'atteinte carieuse.

Instructions : la sonde métallique du CarieScan® se place directement sur la dent et les valeurs de caries sont données par le système. Le crochet à lèvres est nécessaire.

Autres systèmes : ultrasons, imagerie infrarouge, spectroscopie Raman, imagerie tetrahertz. D'autres recherches sont encore nécessaires pour utiliser cliniquement ces systèmes.

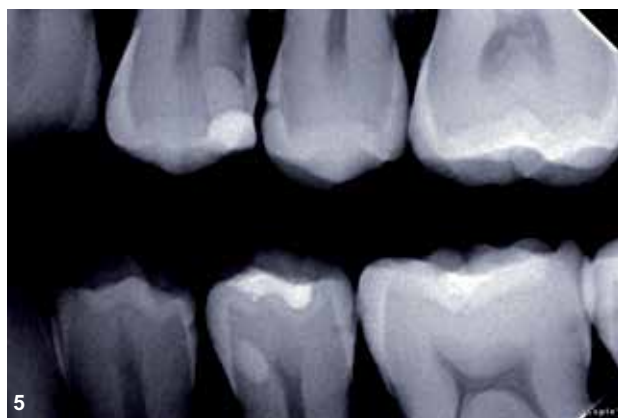
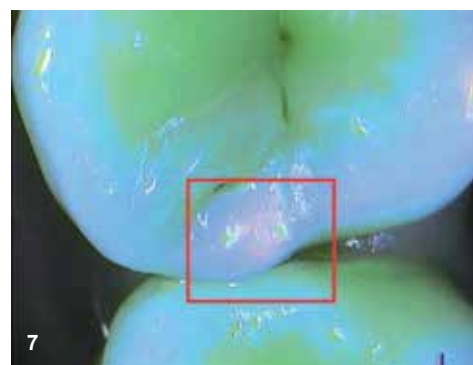


Fig. 5 - Radiographie rétrocoronaire carie mésiale sur une deuxième prémolaire supérieure. Petite cavitation de l'émail visible.



Fig. 6
 a) Image obtenue avec la Soprolife® en mode plein jour et focus macro. Cliniquement, nous voyons une situation plus complexe avec une zone de stagnation de la plaque dentaire, une zone de l'émail déminéralisée, et deux points d'entrée dont l'une avec cavitation.
 b) Carie proximale précoce avec fissure visible de l'émail. Soprolife® en mode diagnostic.
 c) Fissure visible de l'émail grâce à un fort grossissement dans la zone distale.

Fig. 7 - La crête marginale bleue révèle une destruction complète de la dentine sous-jacente. Image Soprolife®.



RECOMMANDATIONS CLINIQUES, LIMITES ET ERREURS À ÉVITER

Recommandations cliniques pour l'étape de diagnostic

L'utilisation des aides diagnostiques est recommandée. Mais, quelle que soit la valeur numérique donnée par le dispositif, l'inspection visuelle demeure essentielle dans la prise de décision finale : doit-on fraiser ou non ? En effet, la complexité de la forme, la profondeur et la largeur de la carie vont influencer la décision clinique et pour ce faire, nous avons absolument besoin de nettoyer parfaitement les surfaces avant l'étape de diagnostic. À propos du traitement, suivant les étapes de diagnostic, beaucoup de nouveaux produits sont maintenant disponibles dans le but de reminéraliser et de reverser les caries. Leur utilisation systématique devrait être encouragée, car ils ont l'avantage de ne pas être invasifs, et par-dessus tout, leurs actions sont le plus souvent réversibles. La philosophie générale de l'approche centrée sur le patient est réellement importante. En effet, toutes les techniques décrites ci-après devraient être appliquées dans une approche médicale globale dont le risque carieux du patient serait déterminé par une approche médicale moderne telle que le système CAMBRA (Caries management by risk assessment) (6) (**tableau 6**).

Le seuil d'intervention correspond à une rupture de l'émail visible (score ICDAS 3) (**fig. 5, 6, 7**). Le choix entre les soins préventifs et purement opératoires sera déterminé par la précision du diagnostic. Par conséquent, nos thérapies préventives et d'intervention *a minima* peuvent être divisées en 2 groupes : le premier (traitement invasif *a minima* type 1 ou MIT1) pour le traitement de l'émail et des lésions émail-dentine ne nécessitant aucune préparation, à condition qu'il n'y ait pas de cavitation de surface (classification de la profondeur de la lésion radiographique après bitewing de E1 à D1). Le deuxième groupe (traitement invasif *a minima* type 2 ou MIT2) pour le traitement des lésions émail-dentine avec cavitation de surface (de D1 avec cavitation de D2). À partir de D3, une approche thérapeutique plus classique est envisageable.

Tableau 6 - Combinaison de CAMBRA et LIFEDT (6, 19–21)		
Type de lésion	Haut risque	Faible risque
Surface lisse de l'émail. Surface active, rugueuse et mate montrant un bluissement en mode diagnostique.	Nettoyage prophylactique professionnel. • brossage 2–3 fois par jour: 1.1% NAF toothpaste. • Xylitol (6 g/day): tablettes de chewing gum. • Application de vernis fluoré (5% NAF); Reconduit tous les 3-4 mois. • Application pâtes de calcium phosphate (MI plus GC Tooth mousse, GC). • bain de bouche: 0.05% NAF ou 0.12% Chlorhexidine: 1 minute tous les soirs. • Conseils alimentaires.	Brossage 2–3 fois par jour avec un dentifrice fluoré. • Application de vernis fluoré (5% NAF); Reconduit tous les 6 mois. • Application de pâte de calcium phosphate (optionnel). (MI plus GC Tooth mousse, GC).
Puits et sillons de forme complexe. Après nettoyage: sillons suspects avec fluorescence altérée (signal rouge) en comparaison avec une zone saine. Code 1-3	Concept LIFEDT: si la caméra LED confirme la complexité des sillons et les variations de fluorescence, un sealant pourra être appliqué sous digue. Notez que la fluorescence rouge des sillons semble être liée à l'activité de la carie et doit être considérée comme un critère positif quel que soit le risque de carie.	Sillon sans modification de fluorescence. Sealant et vernis sont facultatifs. Tout sillon avec modification de fluorescence doit être traité comme un risque élevé : un sealant est recommandé.

Tableau 7 - Détection des caries occlusales à l'aide de la SoproLife® en mode lumière du jour et mode diagnostic (6). Proposition de décision de traitement.

Code	Description en mode plein jour après nettoyage	Description en mode fluorescence après nettoyage	Diagnodent versus Vistacam Valeur moyenne (±SD)	Proposition de décision de traitement
0	Saine, pas de changement visible des sillons	Saine, pas de changement visible de l'émail, sillons verts.	5.7(±4.3)/0.7 (±0.68)	Recommandations MIT1 + CAMBRA
1	Centre du sillon blanchâtre, légèrement jaunâtre avec changement visible de l'émail, limité à une partie ou la totalité de la base du sillon.	Pas de point rouge visible	13.3 (±11.8)/1.26 (±0.61)	Recommandations MIT1 + CAMBRA
2	Changement blanchâtre des sillons, pas de fissures visibles de l'émail.	Coloration rouge sombre limitée au sillon	22 (±17.5)/1.6 (±0.51)	Recommandations MIT1 + CAMBRA
3	Fissure de l'émail changement limité à la zone fissurée, pas d'atteinte dentinaire visible.	Coloration rouge foncée au niveau des fissures	40.6(±24.6)/1.95(±0.57)	MIT1 + CAMBRA recommandations
4 "cut off point" Prise de décision de préparer la lésion	Le processus carieux ne se limite pas à la zone du sillon, l'atteinte carieuse est beaucoup plus large, avec une apparence brillante	Coloration rouge foncée étendue		Etapes opératoires MIT2
5	Email fissuré avec ouverture visible de la dentine	Large ouverture avec atteinte dentinaire visible		Etapes opératoires MIT2

Le nettoyage prophylactique professionnel

Cette étape clinique commune à tous les systèmes de diagnostic reste en fait l'une des plus compliquées. En fait, un diagnostic précis présuppose d'avoir nettoyé parfaitement la partie la plus profonde du sillon sans léser l'émail affecté et être en mesure d'observer la zone autour sur une largeur de 0,1 mm dans des conditions optimales. Sans preuve évidente, nous nous limitons simplement à des conseils cliniques. Comme la structure cristalline est très instable et la largeur moyenne des puits est d'environ 0,1 mm, l'utilisation d'une sonde et de fraises est strictement interdite et le nettoyage à l'aide d'une brosse rotative et d'une pâte prophylactique pourrait perturber le rapport des valeurs données par les différents dispositifs de diagnostic. Une proposition clinique raisonnable est de nettoyer avec de l'air pulsé couplé à du bicarbonate de sodium (Kavoproph[®], AirNGO[®], AirFlow[®]). L'utilisation de poudre de carbonate de calcium : poudre Pearl[®], (Actéon Satelec) ou Kavoproph[®] prophylaxie poudre (Kavo) légèrement plus abrasive est également conseillée. Des précautions sont nécessaires pour réduire l'excédent de poudre (aspiration forte, digue dentaire). Si le patient est à très haut risque carieux sans possibilité de contrôle, la décision d'ouvrir les sillons peut être envisagée avec une poudre plus abrasive type bioverre ou Syc[®] en poudre (OSSpray). Pour les lésions proximales, la combinaison caméra et écartement puissant des dents à l'aide de coins en plastique permet dans la majeure partie des situations cliniques, une observation directe de la lésion (**tableau 7**).

Les limites

- Ne pas se baser uniquement sur la sensibilité et spécificité annoncées par le fabricant, en effet la réalité clinique est souvent tout autre.
- Il existe un risque permanent de faux positifs, car l'architecture complexe des sillons limite souvent l'efficacité du nettoyage.
- Le praticien a l'obligation de s'adapter à l'outil utilisé. Pour les systèmes basés sur la fluorescence, le mode lumière du jour permet cela.

Les erreurs à éviter

- Ne pas ou mal nettoyer la surface de la dent est souvent une source d'erreur de diagnostic.
- Utiliser une brosse à dents ou des mini-brossettes rotatives pour nettoyer les sillons.
- L'usage de pâte de nettoyage peut perturber le signal fluorescent ou masquer les informations.
- Surestimer la lésion carieuse du fait du grossissement de l'image.
- Sous-estimer la lésion carieuse en se basant uniquement sur le diagnostic radiologique.

Les aides visuelles sont un apport considérable à l'élaboration d'un diagnostic cariologique juste et précis. Cependant, nous devons également garder en considération notre bon sens clinique. Le diagnostic établi sera plus ou moins

Mots clés

Diagnostic, traitement, carie, aide visuelle

Keywords

Diagnosis, treatment, decay, visual aid

fiable et précis selon l'aide visuelle utilisée et l'expérience de l'opérateur. Ces techniques nous permettent d'établir un diagnostic de lésions précoces et, par conséquent, de réaliser des traitements préventifs et *a minima* afin de conserver au maximum les tissus sains ou de suivre l'évolution de lésions débutantes en cas d'abstention thérapeutique.

CONCLUSION

Ces différents systèmes et leurs grandes diversités permettent à l'omnipraticien d'améliorer son diagnostic et donc sa prise de décision. Les possibilités de prendre des images et de les conserver sont un atout non négligeable qui orienteront l'omnipraticien dans ses choix de système d'aide au diagnostic.

AUTO ÉVALUATION

1. Les aides visuelles, généralités :

- Les nouvelles méthodes de détection sont basées sur la transmission de lumière et la fluorescence
- Lorsque le DIAGNOpen indique une valeur comprise entre 13 et 24 dans un sillon occlusal, le traitement doit être de type invasif
- L'utilisation des aides visuelles permet de s'affranchir de l'inspection visuelle
- Les surfaces dentaires doivent être parfaitement nettoyées avant d'utiliser les aides visuelles
- Le nettoyage des surfaces dentaires se fait avec de l'air pulsé couplé à du bicarbonate de sodium

2. La fluorescence : la caméra Soprolife

- La caméra Soprolife possède 3 modes : le mode jour, le mode carie et le mode pério
- La dentine saine en mode diagnostic de la Soprolife, apparaît de couleur verte
- Une crête marginale bleue en mode diagnostic de la Soprolife, indique une dentine saine sous-jacente et de ce fait, la possibilité de conserver la crête marginale

3. Le traitement :

- Le seuil d'intervention opératoire correspond à une rupture de l'émail visible
- S'il n'y a pas de cavitation de surface de l'émail, le traitement sera préventif uniquement
- S'il y a cavitation de surface de l'émail, le traitement sera opératoire

ABSTRACT

CARIES DIAGNOSTIC TECHNIQUES: THE CONTRIBUTION OF NEW TECHNOLOGIES

The medical approach to dental caries lesions requires detection of carious lesions at the earliest possible stage. The new detection methods are based on light transmission, fluorescence (fluorescence only systems or a combination of camera systems and fluorescence), electrical conductivity and impedance. The reliability of the diagnosis is more or less accurate and precise depending on the visual aids employed and the experience of the operator. These techniques allow early lesions to be diagnosed and thus the implementation of preventive treatment or minimal interventions to conserve healthy tissue or to control the development of early lesions in the absence of therapy.

RESUMEN

METODOLOGÍA DEL DIAGNÓSTICO EN CARIOLOGÍA. APORTACIÓN DE LAS NUEVAS TECNOLOGÍAS

El enfoque médico de las lesiones cariosas requiere una detección de éstas en una fase lo más precoz posible. Los nuevos métodos de detección están basados en: la transmisión de la luz, la fluorescencia (sistemas de fluorescencia sola o combinación de cámara y sistema de fluorescencia), la impedancia eléctrica y la conductividad. El diagnóstico establecido será más o menos fiable y preciso según la ayuda visual utilizada y la experiencia del operador. Estas técnicas nos permiten establecer un diagnóstico de lesiones precoces y, por consiguiente, realizar tratamientos preventivos a mínima para conservar al máximo los tejidos sanos o controlar la evolución de las lesiones iniciales en caso de abstención terapéutica.

Réponses

1. a : vrai, b : faux, c : faux, d : vrai, e : vrai
2. a : faux, b : vrai, c : faux
3. a : faux, b : vrai, c : vrai

RÉFÉRENCES

1. Tassery H, Levallois B, Terrier E, Manton D, Otsuki M, Koubi S, Gugnani N, Panayotov I, Jacquot B, Cuisinier F, Rechmann P. Use of new minimum intervention dentistry technologies in caries management. *Aust Dent J*. 2013 Jun;58 Suppl 1:40-59.
2. Fisher J, Glick M, FDI World Dental Federation Science Committee. A new model for caries classification and management: the FDI World Dental Federation caries matrix. *J Am Dent Assoc*. 2012 Jun;143(6):546-51.
3. Mitropoulos CM. The use of fibre-optic transillumination in the diagnosis of posterior approximal caries in clinical trials. *Caries Res*. 1985;19(4):379-84.
4. Deery C, Care R, Chesters R, Huntington E, Stelmachonoka S, Gudkina Y. Prevalence of dental caries in Latvian 11- to 15-year-old children and the enhanced diagnostic yield of temporary tooth separation, FOTI and electronic caries measurement. *Caries Res*. 2000 Feb;34(1):2-7.
5. Côrtes DF, Ellwood RP, Ekstrand KR. An *in vitro* comparison of a combined FOTI/visual examination of occlusal caries with other caries diagnostic methods and the effect of stain on their diagnostic performance. *Caries Res*. 2003 Feb;37(1):8-16.
6. Rechmann P, Charland D, Rechmann BMT, Featherstone JDB. Performance of laser fluorescence devices and visual examination for the detection of occlusal caries in permanent molars. *J Biomed Opt*. 2012 Mar;17(3):036006.
7. Lussi A. Comparison of different methods for the diagnosis of fissure caries without cavitation. *Caries Res*. 1993;27(5):409-16.
8. Lussi A, Reich E. The influence of toothpastes and prophylaxis pastes on fluorescence measurements for caries detection *in vitro*. *Eur J Oral Sci*. 2005 Apr;113(2):141-4.
9. Hamilton JC, Gregory WA, Valentine JB. DIAGNODent measurements and correlation with the depth and volume of minimally invasive cavity preparations. *Oper Dent*. 2006 Jun;31(3):291-6.
10. Lennon AM, Buchalla W, Rassner B, Becker K, Attin T. Efficiency of 4 caries excavation methods compared. *Oper Dent*. 2006 Oct;31(5):551-5.
11. Lennon AM, Attin T, Martens S, Buchalla W. Fluorescence-aided caries excavation (FACE), caries detector, and conventional caries excavation in primary teeth. *Pediatr Dent*. 2009 Aug;31(4):316-9.
12. Hafström-Björkman U, Sundström F, de Josselin de Jong E, Oliveby A, Angmar-Månsson B. Comparison of laser fluorescence and longitudinal microradiography for quantitative assessment of *in vitro* enamel caries. *Caries Res*. 1992;26(4):241-7.
13. Emami Z, al-Khateeb S, de Josselin de Jong E, Sundström F, Trollsås K, Angmar-Månsson B. Mineral loss in incipient caries lesions quantified with laser fluorescence and longitudinal microradiography. A methodologic study. *Acta Odontol Scand*. 1996 Feb;54(1):8-13.
14. al-Khateeb S, ten Cate JM, Angmar-Månsson B, de Josselin de Jong E, Sundström G, Exterkate RA, Oliveby A. Quantification of formation and remineralization of artificial enamel lesions with a new portable fluorescence device. *Adv Dent Res*. 1997 Nov;11(4):502-6.
15. Garcia J, Mandelis A, Abrams S, Matvienko A. Photothermal radiometry and modulated luminescence: application to dental caries detection. *Handbook of biophotonics*. Jüegen Popp; 2011. p. 1047-52.
16. Hellen A, Mandelis A, Finer Y, Amaechi BT. Quantitative remineralization evolution kinetics of artificially demineralized human enamel using photothermal radiometry and modulated luminescence. *J Biophotonics*. 2011 Nov;4(11-12):788-804.

17. Hellen A, Mandelis A, Finer Y, Amaechi BT. Quantitative evaluation of the kinetics of human enamel simulated caries using photothermal radiometry and modulated luminescence. *J Biomed Opt.* 2011 Jul;16(7):071406.
18. Hellen A, Matvienko A, Mandelis A, Finer Y, Amaechi BT. Opto-thermo-physical properties of demineralized human dental enamel determined using photothermally generated diffuse photon density and thermal-wave fields. *Appl Opt.* 2010 Dec 20;49(36):6938-51.
19. Weisrock G, Terrer E, Couderc G, Koubi S, Levallois B, Manton D, Tassery H. Naturally aesthetic restorations and minimally invasive dentistry. *J Minim Interv Dent.* 2011;4(2):23-34.
20. Terrer E, Koubi S, Dionne A, Weisrock G, Sarraquigne C, Mazuir A, Tassery H. A new concept in restorative dentistry: light-induced fluorescence evaluator for diagnosis and treatment. Part 1: Diagnosis and treatment of initial occlusal caries. *J Contemp Dent Pract.* 2009;10(6):86-94.
21. Terrer E, Raskin A, Koubi S, Dionne A, Weisrock G, Sarraquigne C, Tassery H. A new concept in restorative dentistry: LIFEDT-light-induced fluorescence evaluator for diagnosis and treatment: part 2 - treatment of dentinal caries. *J Contemp Dent Pract.* 2010;11(1):E095-102.
22. Seremidi K, Lagouvardos P, Kavvadia K. Comparative *in vitro* validation of Vista-Proof and DIAGNOdent pen for occlusal caries detection in permanent teeth. *Oper Dent.* 2012 Jun;37(3):234-45.
23. Kühnisch J, Heinrich-Weltzien R, Tabatabaie M, Stösser L, Huysmans MCDNJM. An *in vitro* comparison between two methods of electrical resistance measurement for occlusal caries detection. *Caries Res.* 2006;40(2):104-11.
24. Rock WP, Kidd EA. The electronic detection of demineralisation in occlusal fissures. *Br Dent J.* 1988 Apr 23;164(8):243-7.
25. Verdonschot EH, Bronkhorst EM, Burgersdijk RC, König KG, Schaeken MJ, Truin GJ. Performance of some diagnostic systems in examinations for small occlusal carious lesions. *Caries Res.* 1992;26(1):59-64.
26. Rock WP, Kidd EA. The electronic detection of demineralisation in occlusal fissures. *Br Dent J.* 1988 Apr 23;164(8):243-7.
27. Pitts NB, Longbottom C, Hall A, Czajczynska-Waszkiewicz A, Los P, Masalski M, Biecek P, Christie AM. Diagnostic accuracy of an optimised AC impedance device to aid caries detection and monitoring. *Caries research.* 2008;(42):185-238.
28. Pitts NB, Longbottom C, Ricketts D, Czajczynska-Waszkiewicz A. Hidden dental caries detection using a novel electrical impedance device. Available from: http://iadr.confex.com/iadr/2008Toronto/techprogram/abstract_108999.htm
29. Guimerà A, Calderón E, Los P, Christie AM. Method and device for bio-impedance measurement with hard-tissue applications. *Physiol Meas.* 2008 Jun;29(6):S279-290.

Correspondance :

Hervé Tassery

Université d'Aix-Marseille

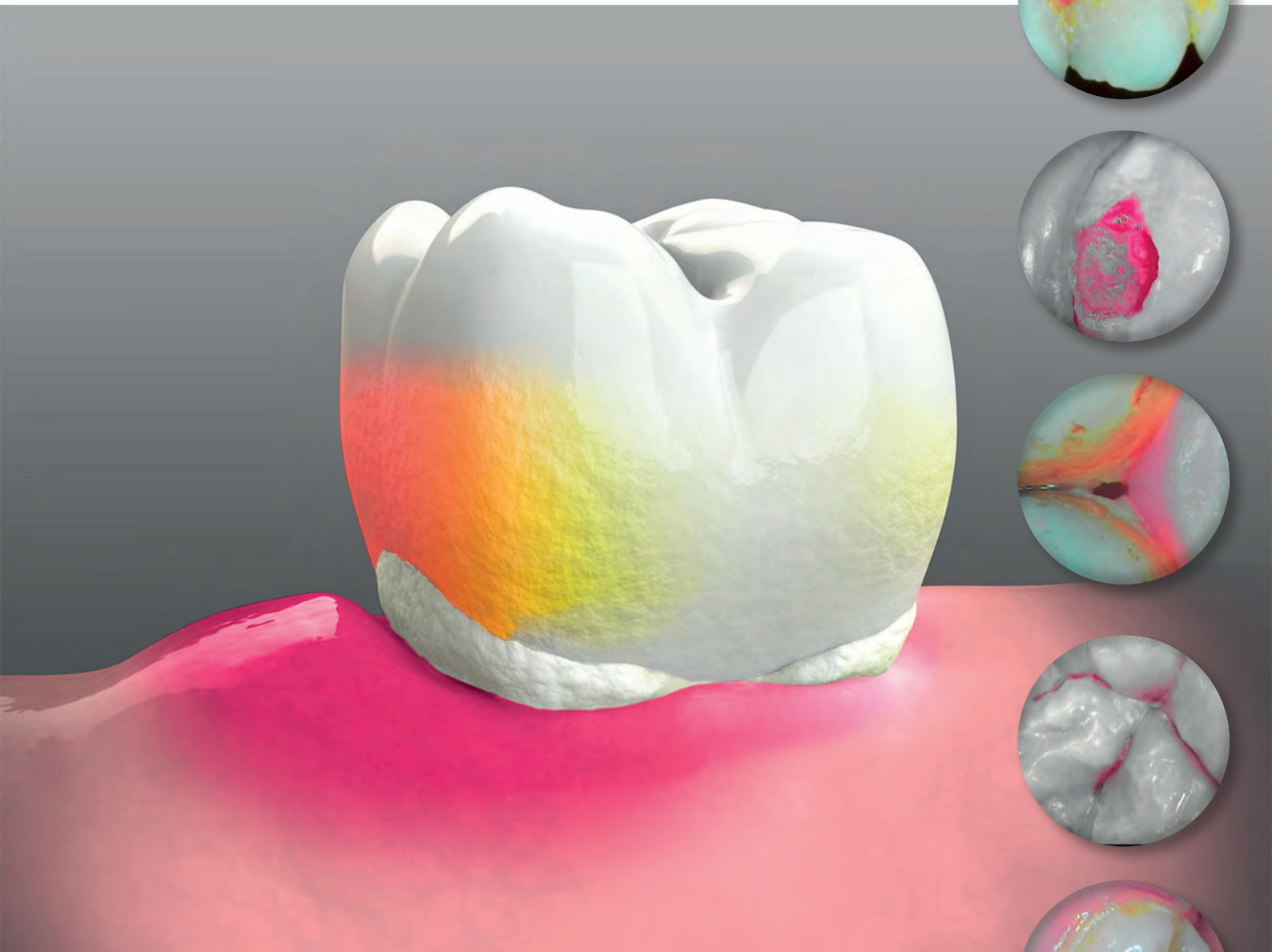
Département d'odontologie conservatrice et restauratrice

27 bd Jean Moulin 13005 Marseille

Email : herve.tassery@univ-amu.fr



Soprocure articles



Democratised fluorescence

Pr Hervé Tassery

Professor and Head of Department of Preventive and Restorative Dentistry, Dental School, Aix-Marseille University



Fig 1. View in CARIO mode, ICDAS code 5 buccal surface of 27



Fig 2. Close-up visualisation of marginal inflammation and deposits in PERIO mode

An accurate diagnosis in periodontics is the result of several factors, including in-depth knowledge of biology and histology, complex medical knowledge and a high level of technical expertise. However, the essential medical approach to diagnosing means that dental practitioners need to be provided with the appropriate and necessary tools to minimise loss of opportunity, especially enabling them to make an early diagnosis.

Modern tools such as bacterial tests and plaque disclosing solutions reinforce this approach, but are often merely another source of information that complements visual examination and probing. This visual examination, a cornerstone of diagnosing, tells us about the structure of tissues, their typology, the level of inflammation, etc., but is still dependent on the practitioner's visual acuity, the quality of the lighting and the time available.

Building on experience acquired in the areas of imaging, cariology and tissues characterized by auto fluorescence via SOPROLIFE®, the new tool SOPROCARE® (SOPRO®, Acteon Group®) consists of an LED camera fitted with a specific CCD sensor.



Fig 3a. Observation of the occlusal surface of 37 in DAYLIGHT mode



Fig 3b. Detection of a carious enamel-dentine lesion of 37 in CARIO mode

SOPROCARE enables caries to be detected in CARIO mode (Figure 1) as well as dental plaque in PERIO mode (Figure 2), by illuminating the tooth surfaces in a wavelength bandwidth located in the visible (blue) spectrum and by supplying an auto-fluorescence image superimposed over a natural anatomical image.



Fig 4a. Observation of the lingual surfaces of 33 and 34 in DAYLIGHT mode

Fig 4b. Observation of Figure 4a. in PERIO mode with tartar, plaque and inflammation highlighted.

Furthermore, SOPROCARE® provides a means of highlighting gingival inflammation in PERIO mode (Figure 5), thanks to the combination of blue light absorption by soft tissues and selective chromatic amplification. This means that SOPROCARE® modifies the natural colour and amplifies the visibility of all areas of tissue inflammation.

SOPROCARE® additionally offers between 30 and 115 times magnification (MacroVision) of the tooth and its surroundings. The early diagnosis carried out by the dental practitioner avoids the usual constraints associated with visual acuity, difficulty of access or interpretation of findings.

Combining SOPROCARE® with Sopro Imaging® software provides practitioners with a dedicated module that allows personalised patient follow-up (Figures 6). Direct visualisation of soft and hard tissues in the three available modes actually aids interactivity and communication between dentist or hygienist and the patient. Furthermore, the facility to store image documents in a preferred format will prove a considerable asset. Finally, the prophylactic follow-up that is essential to any medical approach is made easier by the speed with which a dental image survey can be done and by the possibility provided by Sopro Imaging® of saving and comparing images at any time. (Figures 4)

Therefore SOPROCARE® is a tool to aid diagnosis, follow-up and communication which can be smoothly integrated into everyday dental practice. In a single camera SOPROCARE® makes it possible to detect caries, dental plaque and gingival inflammation easily and instantly (Figure 5), even in the early stage (Figures 3), without the need to wear protective glasses or any other additional constraint.

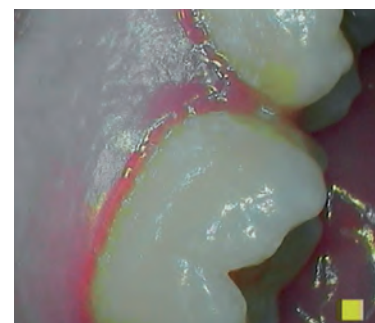


Fig 5. Plaque, tartar and inflammation in PERIO mode, buccal surface of 26

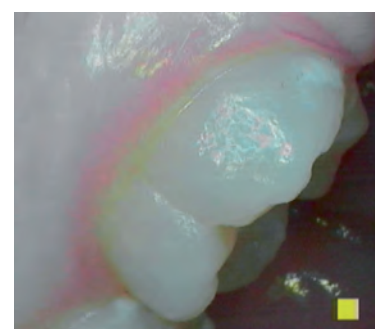


Fig 6a. and 6b. Gingival inflammation, lingual surface of 47 (DAYLIGHT mode and PERIO mode) (D0)

Fig 6c. View after scaling and polishing (AIR-N-GO, classic powder) (D0)

Fig 6d. View after 21 days. Check of improvement in the area (PERIO mode)

userreport

by Dr Michel Blique and Dr Sophie Grosse

Contribution of fluorescence and selective chromatic amplification in daily preventive dentistry practise

Caries can be diagnosed earlier by means of intraoral cameras that utilise the fluorescence of dental tissues. New technologies such as fluorescence together with selective chromatic amplification now make it possible to intervene even earlier, in other words during prophylactic treatments.

Highlighting with stains and evaluating the biofilms that lead to disease of dental and periodontal tissues have been described for some time (Axelsson 1999). The simplest method is to use “bacterial plaque disclosing dyes” which are applied to the surfaces being checked, then rinsed off to remove excess. The dental practitioner then observes and assesses the situation with the patient, either using a mirror or on a photograph. They are used relatively infrequently in current practise because they take time and require tooth cleaning after application (Fig. 1).

To overcome these objections, systems using fluorescein (barely visible in natural light) exposed to light devices with a specific wavelength have also been proposed (Faller 2000), but their use remains very unofficial. The development of intraoral cameras comprising diodes that enable dental tissues to fluoresce (Banerjee 2002) led to the “SOPROCARE” concept. In practical terms this resulted in the creation of an intraoral camera by the company SOPRO® from the ACTEON® group, which can be connected to all versions of digital image management

Fig. 2: The SOPROCARE® camera



Fig. 1: Revelation by application of erythrosine. The Plaque disclosing solution has to be applied, take effect and be cleaned off and it can mask inflammation of gingival tissues.



Fig. 3a: “PERIO” mode Schematic illustration of the colours produced:
 • At the neck, white colour: soft deposits
 • Above that, orange to yellow colour: calcified deposits and tartar
 • On the gum, magenta colour: inflamed areas



Fig. 3b: “CARIO” mode Schematic illustration of the colours produced: The areas warning of carious activity appear Red

Fig. 4: Examination in white light (4a) then in fluorescence and selective chromatic amplification (“Perio” mode) (4b)



Fig. 4a: View of a molar interdental space in “DAYLIGHT” white light

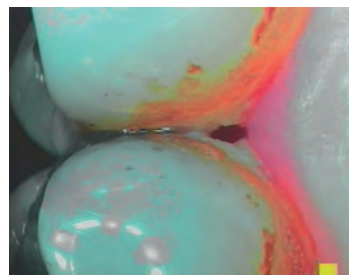


Fig. 4b: View in fluorescence with selective chromatic amplification (“PERIO” mode)

Fig. 4b:
 • Whitish areas: “soft” bacterial deposits or “dental plaque”
 • Orange-coloured areas: “calcified” bacterial deposits and tartar sub-layer
 • “Purplish pink” gingival area: gingival inflammation
 Clinical implication: this patient “brushes” his teeth but not effectively enough for 1.5 mm around the neck. He uses interdental brushes or sticks of the wrong diameter. This results in slight marginal inflammation which is more severe in the interdental spaces with damage to the papilla.

Fig. 5: Examination of a class 1 composite in white light then in fluorescence, "CARIO" mode: minimal repair of the margins may be considered.



Fig. 5a: Partial view of the occlusal surface of a molar in white light: check of an existing filling and "Suspicious" grooves.



Fig. 5b: "CARIO" mode Highlights "warning" areas which appear red

Fig. 6: Communication between patient and dental practitioner. A few Pictures in "PERIO" mode are enough to observe the Dental plaque before, then after scaling/cleaning/polishing, to show the results or assess what was done before corrections.



Fig. 6a: Pre-treatment view in white light (DAY- LIGHT mode)

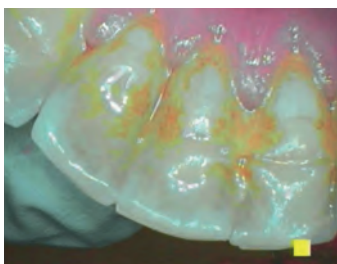


Fig. 6b: Pre-treatment view in "PERIO" mode



Fig. 6c: View in "PERIO" mode, check of clean- ing: a few calcified (orange-coloured) deposits still need to be removed

Fig. 7: Patient motivation and plaque control:



Fig. 7a: 1st visit clinical situation of 41-31 in a 23-year-old male before patient motivation and brushing instructions



Fig. 7b: View of area 41-31 in white light (DAYLIGHT mode)

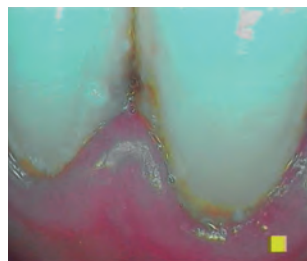


Fig. 7c: View of area 41-31 in "PERIO" mode: the inflamed areas are accentuated, the soft bacterial deposits (white) are substantial, orange-yellow areas are assumed to be under lying tartar

software. After using this device for several hundred clinical situations, we wanted to illustrate in this article how this technology is becoming a new tool in the daily practise of preventive dentistry.

Technology used: fluorescence and selective chromatic amplification. Operating principle

The device used is a high-performance intraoral camera (zoom with magnification up to around 100x) (Fig 2), fitted with white LEDs and blue LEDs whose light is absorbed by dental tissues and reproduced in the form of fluorescence. This fluorescence is selected then chromatically amplified, allowing characterisation of hard and soft tissues.

Named "SOPRO CARE®" by its manufacturer SOPRO® from the ACTEON® group, it uses the properties of tissue autofluorescence as well as those of selective chromatic

amplification in order to reveal enamo-dentinal caries, calcified or non-calcified dental plaque and gingival inflammation. It is the first and only system to combine these two photonics technologies in a single intra- oral camera.

The camera illuminates the dental tissues with a wavelength between 440 and 680 nm. The excited material absorbs the energy and reconstitutes it as fluorescent light. This means the image obtained can be superimposed over the natural anatomical image and the nuances that are invisible in white light can be revealed in real time for each tissue. Figures 3a and 3b, simplified image obtained by fluorescence with selective chromatic amplification ("PERIO" mode 3a and "CARIO" mode 3b).

Using blue light absorption properties, selective chromatic amplification increases the colouring of certain tissues, such as gingival inflammation. Figures 4a & 4b show the image obtained after exposure to white light (on

Fig. 8: Patient motivation and plaque control:



Fig. 8b: 2nd visit Clinical situation of 41-31 for assessment of patient's motivation and compliance with brushing instructions after 3 weeks



Fig. 8b: View of area 41-31 in white light (DAYLIGHT mode)



Fig. 8c: View of area 41-31 in "PERIO" mode: the inflamed areas are accentuated, the soft bacterial deposits (white) are reduced the tartar concretions appear orange-yellow

Fig. 9: Earlier detection of lesions, for less invasive treatment



Fig. 9a: Partial view of the occlusal surface of 36: "questionable" grooves, view in white light (DAYLIGHT mode)

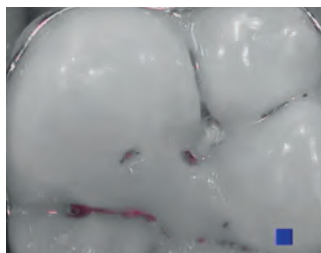


Fig. 9b: "CARIO" mode identifies "warning" areas which appear red



Fig. 9c: After removal of organic plugs and cleaning by air-polishing ("DAYLIGHT" mode)



Fig. 9d: After removal of organic plugs and cleaning by air-polishing, the carious areas are indicated (view in "CARIO" mode)



Fig. 9e: After preparation by air-abrasion with 27µ aluminium oxide (view in "DAYLIGHT" mode)



Fig. 9f: After preparation by air-abrasion with 27µ aluminium oxide, the red areas have disappeared (view in "CARIO" mode)



Fig. 9g: Conventional dental photograph After therapeutic sealing with a glass ionomer cement, before finishing work

the left) then a blue and white light with selective chromatic amplification ("PERIO" mode); similarly for caries and "CARIO" mode in Figures 5a & 5b.

Many possible uses:

1-Communication between patient and dental surgeon (Fig. 6a and 6c)

Dental surgeons know that the "first consultation is decisive". They therefore have to identify the clinical signs but also the risk factors. The best approach is to make a "codiagnosis" combining what the patient notices himself with what the dental professional observes. This could be done by explaining the image seen in a mirror. X-rays then made it possible to share what was "invisible" with the patient. The use of intraoral cameras subsequently provided a simple way of sharing images in which carious lesions were highly magnified (Mary 1997). Patients gradually discovered their mouth and teeth as they were seen by their dental practitioner.

A camera such as SOPROCARE® expands the information-sharing possibilities. In one or two clicks, it offers ease of use, a wide choice of magnification levels (from macro- vision, Fig. 4 0 – to several teeth, Fig. 6) and fluorescence with selective chromatic amplification, which make it possible to identify suspected carious areas (Fig. 5) or periodontal lesions (highlighting soft or calcified deposits and marginal inflammation) –Fig. 7.

2-Patient motivation and plaque control:

Nowadays dentists can no longer pretend to be unaware of the presence and extent of bacterial biofilms on the dental, interdental or juxta-gingival surfaces they are going to treat. They know patients have to be told about these biofilms in order to make them active partners in their own treatment (Rozenzweig 1988). Explaining the whys and wherefores of oral hygiene at home, monitoring whether it is being done and checking how effective it is become simple if it can be shown and demonstrated. (Fig. 7abc and 8abc)

Fig. 10: Peri-operative check of removal of soft and calcified biofilms during professional preventive cleaning of dental surfaces or scaling.

Fig 10a to 10e: Different stages of prophylactic cleaning of a molar neck

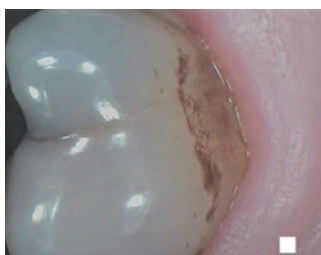


Fig. 10a: Initial condition in "DAYLIGHT" mode

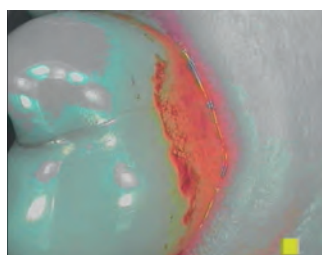


Fig. 10b: Initial condition of calcified residues in "PERIO" mode appears yellow and orange-coloured. The marginal inflammation appears "purplish pink"

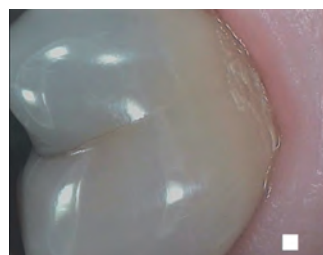


Fig. 10c: After removal of soft deposits with prophylactic paste in white light

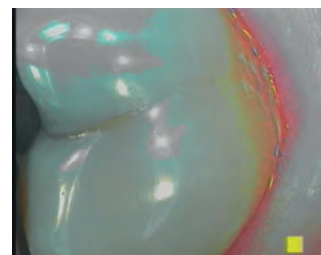


Fig. 10d: After removal of soft deposits with a prophylactic paste in "PERIO" mode, calcified residues appear yellow and orange-coloured. The marginal inflammation appears "purplish pink"

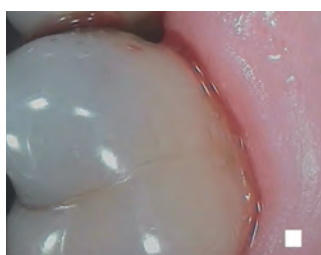


Fig. 10e: After removal of calcified deposits with an air-polisher in white light mode

The images are saved and managed by all the commercially available imaging software packages or by dedicated image management software ("SOPRO-Imaging[®]"). This makes it possible to look back at previous patient visits and compare those images with the current clinical condition, to assess the progress made, encourage the patient and target the patient's efforts.

3- Earlier detection of lesions, for less invasive treatment

Fluorescence facilitates very early diagnosis (first stages of enamel demineralisation) so that preventive or minimally invasive treatment of lesions is possible (Terrer et al. 2009).

SOPROCARE[®] is first of all an educational and motivational tool because the patient is able to "see" the early stages of his lesions and even follow as the dentist checks the tissues that have been treated.

This highlights the importance of brushing and home treatment of the identified early lesions (for example, with fluoride toothpaste, ACP-CPP, etc.) and of course the minimally invasive treatment carried out by the dental surgeon (professional preventive cleaning, treatment with fluoride varnish, sealant or minimal filling). (Fig 9a to 9g)

4-Peri-operative check of removal of soft and calcified biofilms during professional preventive cleaning of dental surfaces or scaling. (Fig. 6abc and 10a to 10e)

The removal of soft and calcified biofilms during professional preventive cleaning of supragingival or

subgingival tooth surfaces or scaling by a dental hygienist is an essential part of caries or periodontal prophylactic treatment (Goodson et al. 2004). The camera enables the practitioner to check the treatments being performed peri-operatively. "PERIO" mode and the choice of magnification allow faster and more precise examination of the areas being treated.

Conclusion

This new device expands the standard usage of intraoral cameras. Processing the image obtained by fluorescence by means of selective chromatic amplification provides a tool for early diagnosis of caries and gingival inflammation. Soft or calcified bacterial deposits can be highlighted. These have to be removed by brushing or by preventive chair-side treatments. The device offers a means of involving patients in their treatment at a very early stage helps in the implementation and acceptance of a prophylactic approach and, in all cases, makes it possible to nip any disease in the bud. **DA**

About the authors



Dr Michel Blique
 • Graduate of Faculty of Dental Surgery, Nancy
 • University Associate in Paediatric Dentistry at the Faculty of Dental Surgery, Nancy
 • Private practice in France and Luxembourg, limited to minimally invasive and preventive dentistry and to periodontal medicine
 • michel.blique@online.fr



Dr Sophie Grosse
 • Graduate of Faculty of Dental Surgery, Nancy
 • University Associate in Paediatric Dentistry at the Faculty of Dental Surgery, Nancy
 • Private practice in NANCY, France

SOPROCARE – 450 nm wavelength detection tool for microbial plaque and gingival inflammation - a clinical study

P. Rechmann^{*a}, Shasan W. Liou^b, Beate M.T. Rechmann^a, and John D. B. Featherstone^a

^aDept. of Preventive and Restorative Dental Sciences; ^bDivision of Pediatric Dentistry, School of Dentistry, University of California at San Francisco, San Francisco, CA 94143

ABSTRACT

Gingivitis due to microbial plaque and calculus can lead over time if left untreated to advanced periodontal disease with non-physiological pocket formation. Removal of microbial plaque in the gingivitis stage typically achieves gingival health. The SOPROCARE camera system emits blue light at 450 nm wavelength using three blue diodes. The 450 nm wavelength is located in the non-ionizing, visible spectral wavelength region and thus is not dangerous. It is assumed that using the SOPROCARE camera in perio-mode inflamed gingiva can easily be observed and inflammation can be scored due to fluorescence from porphyrins in blood. The assumption is also that illumination of microbial plaque with blue light induces fluorescence due to the bacteria and porphyrin content of the plaque and thus can help to make microbial plaque and calculus visible. Aim of the study with 55 subjects was to evaluate the ability of the SOPROCARE fluorescence camera system to detect, visualize and allow scoring of microbial plaque in comparison to the Turesky modification of the Quigley and Hein plaque index. A second goal was to detect and score gingival inflammation and correlated the findings to the Silness & Løe gingival inflammation index. The study showed that scoring of microbial plaque as well as gingival inflammation levels similar to the established Turesky modified Quigley Hein index and the Silness & Løe gingival inflammation index can easily be done using the SOPROCARE fluorescence system in perio-mode. Linear regression fits between the different clinical indices and SOPROCARE scores in fluorescence perio-mode revealed the system's capacity for effective discrimination between scores.

Keywords: 450nm wavelength, gingival inflammation, microbial plaque, detection, clinical study, SOPROCARE

1. INTRODUCTION

Gingival inflammation due to microbial plaque and calculus can lead over time [1, 2] to advanced periodontal disease with non-physiological pocket formation.[3] If left untreated, loss of attachment with bone loss are the consequences. Nevertheless, removal of microbial plaque in the gingivitis stage typically achieves gingival health.[4, 5]

Illumination with blue light inducing fluorescence due to the bacteria and porphyrin content of the plaque might help to make microbial plaque and calculus visible. Consequently, using a fluorescence detection tool like SOPROCARE may allow indexing of the plaque level on a tooth surface similar to a clinically scalable plaque index. In addition inflammation of the gingiva might become more visible due to more fluorophores present in inflamed tissue.

The hypothesis to be tested in this study was that using the SOPROCARE camera in fluorescence perio-mode allows detecting, visualizing and scoring of microbial plaque. It also allows a comparison to the Turesky modification of the Quigley Hein plaque index. Furthermore, the use of the system permits detecting, visualizing and scoring of gingival inflammation with scoring comparable to a clinical scoring using the Silness & Løe gingival inflammation index.

* Corresponding author email: rechmannp@dentistry.ucsf.edu

2. MATERIALS AND METHODS

2.1 Study Subjects, Inclusion and Exclusion Criteria, Stratified Recruitment

Approval for the study was obtained from the Committee on Human Research at UCSF (IRB approval number: 13-10575). Inclusion criteria to be eligible for the study were a subject age of 13 years and older, having a dentition with at least 6 anterior teeth. Subjects were excluded if they had multiple front teeth crowned, major areas of the buccal surfaces filled, or frank caries lesions on buccal tooth surfaces on several teeth. Subjects had to be healthy and willing to sign the “Authorization for Release of Personal Health Information and Use of Personally Unidentified Study Data for Research” form. There were no gender restrictions. Subjects who met the selection criteria were asked to provide verbal/written assent/consent themselves and/or their parent/guardian.

Fifty-five subjects were recruited for the study, comprising 23 females and 32 males with an average age of 36.9 ± 17.8 years, ranging from 14.0 to 83.4 years.

In order to recruit subjects with representative various amounts of plaque we performed a stratified recruitment based on a clinical screening of the presented plaque amount on the front teeth (no, low, moderate, high amount of plaque). Through the stratified recruitment we achieved a relatively even distribution of subjects with different levels of microbial plaque, and consequently all stages of gingival inflammation (Table 1).

Table 1: Recruiting goal and actual recruited number of subjects per level of plaque amount.

Plaque amount level clinical screening	Recruiting goal	Number of subjects recruited
no	5 to 10	18
low	5 to 10	16
moderate	5 to 10	10
high	5 to 10	11

2.2 Study Tests

As clinical indices the Turesky modification of the Quigley Hein plaque index (T-QH) and the Silness & Løe (GI) gingiva inflammation index were recorded. In addition pictures were recorded with the SOPROCARE system in fluorescence perio-mode. Finally, regular digital photographs were taken. All recorded pictures were later on assessed using the same criteria as described for the plaque and the gingival inflammation index. Details of the indices are explained below.

2.2.1 Turesky Modification of the Quigley Hein Plaque Index (T-QH)

A plaque index was performed to register the amount of microbial plaque on the study teeth. The Turesky modification of the Quigley Hein plaque index (T-QH)[6] does not use a plaque disclosing agent. Clinically the T-QH index is performed by carefully probing over the tooth surface while beginning from the tip of the tooth in direction to the gingival margin. The moment when plaque occurs at the probe tip is registered and the according score is assigned (Table 2).

Table 2: Criteria for Turesky modification of the Quigley and Hein plaque index.

Scores	Criteria
0	No plaque
1	Separate flecks of plaque at the cervical margin of the tooth.
2	A thin continuous band of plaque (up to one mm) at the cervical margin of the tooth.
3	A band of plaque wider than one mm but covering less than one-third of the crown of the tooth.
4	Plaque covering at least one-third but less than two-thirds of the crown of the tooth.
5	Plaque covering two-thirds or more of the crown of the tooth

2.2.2 Gingival Index (GI) - Silness & Løe

The Silness & Løe gingival index (19, 20) is assigned to register the degree of gingival inflammation. Using this index the absence of inflammation and three levels of gingival inflammation, respectively were registered for the facial surface of each study tooth (Table 3).

Table 3: Criteria for Silness & Løe Gingival Index.

Scores	Criteria
0	Normal, healthy gingival with sharp, non-inflamed margins.
1	Marginal gingivitis with minimal inflammation and edema at the free gingival. No bleeding on probing.
2	Moderate gingivitis with a wider band of inflammation and bleeding upon probing.
3	Advanced gingivitis with severe inflammation, tendency to spontaneous bleeding.

2.2.3 SOPROCARE Fluorescence Perio-mode and Daylight Pictures

The SOPROCARE camera system in fluorescence perio-mode emits blue light at the 450 nm wavelength using three blue diodes (SOPRO Acteon Imaging, La Ciotat, France). The tooth fluoresces due to the blue light illumination and is simultaneously illuminated with four white LEDs. The handpiece allows for collecting pictures at different distances to a tooth resulting in different magnifications. In this study the system was used in the intra-oral mode imaging 3 teeth (canine to central incisor) in one picture. The images were recorded with the SOPRO imaging software. A HP 620 Notebook (HP, Palo Alto, CA; Windows 7, Microsoft Redmond, WA) was used to collect the data.

2.3 Statistical Analyses

The data were analyzed by multiple statistical methods (One-way ANOVA, Newman-Keuls Multiple Comparison Test, Linear Regression Analysis) to compare results from the SOPROCARE fluorescence perio-mode evaluation with the clinical indices.

3. RESULTS

In the result section the clinically evaluated indices Turesky modified Quigley Hein and Silness & Løe are presented for all subjects. Linear regression fits for each index for clinical scoring in comparison to scoring with SOPROCARE in fluorescence perio-mode are also presented.

3.1 Turesky Modified Quigley Hein Plaque Index

The average plaque score clinically evaluated with the Turesky modified Quigley Hein criteria for all subjects was 1.1 ± 1.2 (Mean \pm Standard Deviation [SD]). The plaque scoring with SOPROCARE in perio-mode led to a slightly higher average score (1.4 ± 1.2). The difference was statistically not significant ($P > 0.05$) (Figure 1).

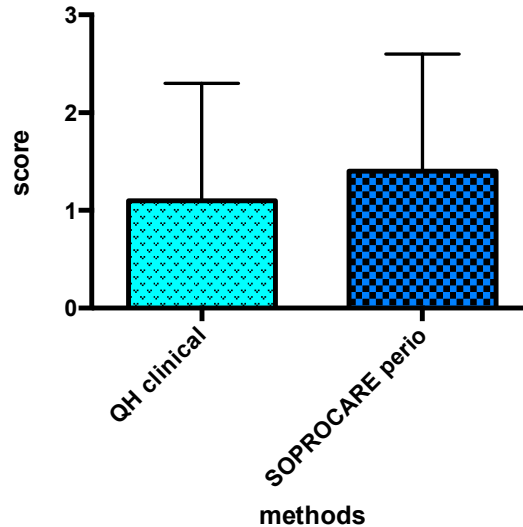


Figure 1: Average Turesky modified Quigley Hein plaque index; clinically registered, and scored on SOPROCARE perio-mode pictures (Mean \pm SD); difference is statistically not significant ($P > 0.05$).

To evaluate for the fluorescence assessment method the capacity for discrimination between two different consecutive scores linear regression fit curves were calculated.

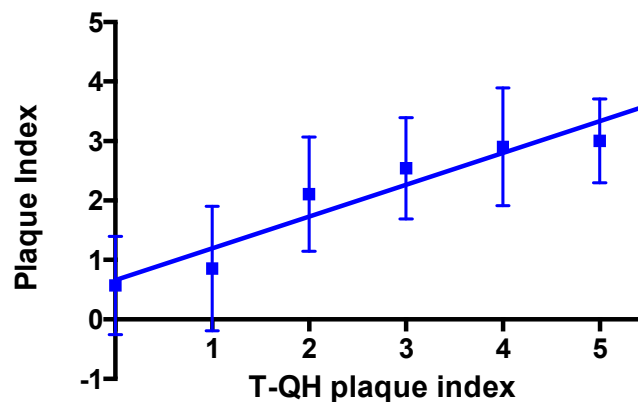


Figure 2: Linear Regression fit for Turesky modified Quigley Hein plaque index and the plaque index evaluated by SOPROCARE perio-mode (Mean \pm SD).

Figure 2 shows the linear regression fit for the clinical evaluated T-QH plaque index versus SOPROCARE perio-mode scores. The linear regression fit was significantly different from zero with goodness for fit of 0.9152 for the SOPROCARE perio-mode assessment. The slope for the fit representing the capacity to discriminate between two consecutive scores was relatively steep with 0.5344 ± 0.08134 .

The linear regression also showed that there was a “set-off”. The Y-axis intercept was at 0.66 ± 0.25 for the SOPROCARE perio-mode evaluation. Thus the fluorescence assessment method led to higher scoring values than the clinical T-QH values.

3.2 Silness & Løe Gingival Inflammation Index

638 teeth were available for evaluating the Silness & Løe gingival inflammation index (S&L). For all subjects the average gingival inflammation index was 0.7 ± 0.9 (Mean \pm SD). Figure 3 depicts a comparison between the clinical evaluated Silness & Løe gingival index and the results of the SOPROCARE perio-mode evaluation. The SOPROCARE perio-mode gingival index was with 0.6 ± 0.9 (Mean \pm SD) slightly lower than the clinical evaluated Silness & Løe plaque index. The observed difference was not statistically significant.

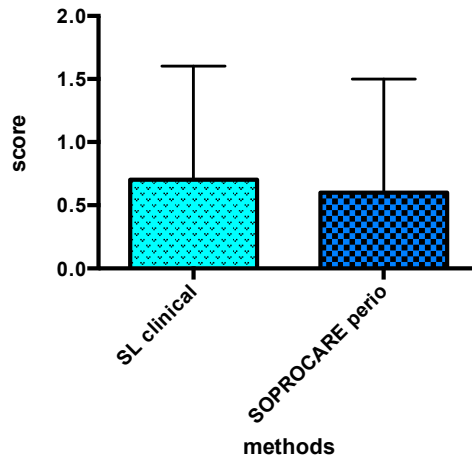


Figure 3: Average gingival inflammation index evaluated clinically as Silness & Løe gingival index and with the SOPROCARE system in perio-mode; in average the SOPROCARE tool showed a slightly lower index but the observed difference was not statistically significant (Mean \pm SD).

To evaluate for the fluorescence method the discrimination between two different consecutive scores, again a linear regression fit was calculated. The following graph (Fig. 4) shows the linear regression fit for the SOPROCARE perio assessment.

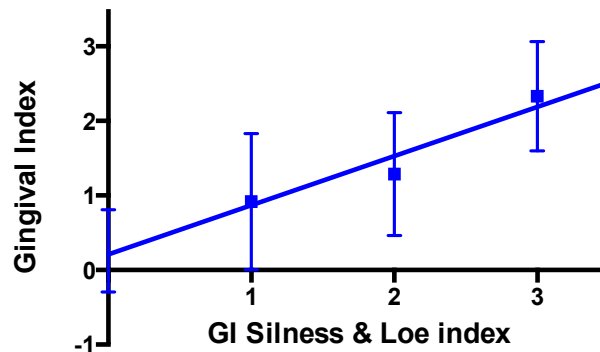


Figure 4: Linear Regression fit for Silness & Løe Gingival Index scores versus and the gingival index evaluated by SOPROCARE perio-mode (Mean \pm SD).

The linear regression fit was significantly different from zero with goodness for fit of 0.9631 for the SOPROCARE perio-mode tool. The slope for the fit, representing the capacity to discriminate between two scores, was again relatively high for the SOPROCARE perio-mode evaluation (0.6598 ± 0.09135). The linear regression confirms that there was

only a slight “set-off”. The Y-axis intercept for the SOPROCARE perio evaluation was slightly elevated with 0.21 ± 0.17 .

Figure 5 shows typical pictures captured with the SOPROCARE fluorescence tool in perio-mode. The Turesky modified Quigley Hein scores and the Silness & Løe gingival inflammation scores are noted, accordingly. The values are always noted for the 3 scored teeth from left to right.



T-QH scores 3,3,1 S&L 2,2,2

T-QH scores 3,4,3, S&L 3,2,1

T-QH scores 1,1 S&L 1,2

Figure 5. Typical pictures captured with the SOPROCARE fluorescence tool in perio-mode. T-QH and S&L scores noted for the 3 scored teeth from left to right.

4. DISCUSSION

Evaluating the SOPROCARE fluorescence perio-mode detection camera system in comparison to a typical clinical plaque indexing method revealed the capacity of the SOPROCARE fluorescence perio-mode system to assess and score microbial plaque levels accordingly. With the SOPROCARE fluorescence perio-mode method the plaque levels are detected in average at a slightly higher score level than clinically but the differences are not statistically significant. Nevertheless this slight overestimation might be useful in patient education and motivation.

The study also showed that the SOPROCARE camera system in perio-mode not only allows detection and scoring of microbial plaque but also correlating of these scores with the Turesky modified Quigley Hein microbial plaque index. The linear regression fit comparing SOPROCARE perio-mode with the clinical index showed the regression fit was significantly different from zero and its slope was relatively steep. A steep slope indicates the capacity of the tool to differentiate between two consecutive scores. As with the total average plaque score the linear regression fit revealed that the fit is slightly set-off in positive direction. Again the linear regression fit underlines that the SOPROCARE perio assessment tool evaluates the plaque level only at a slightly elevated level.

The clinical study also showed the ability of the SOPROCARE fluorescence camera system to detect gingival inflammation and its help in scoring the inflammation. The clinical Silness & Løe gingival inflammation indexing showed a slightly higher average than the SOPROCARE perio-mode scoring. Nevertheless the differences were not statistically significant. The linear regression fit for the SOPROCARE fluorescence evaluated index in relation to the clinical gingival inflammation index was significantly different from zero with a high goodness of fit and a steep slope. This again demonstrated the capacity of the tool to differentiate between two consecutive scores.

5. CONCLUSION

The SOPROCARE fluorescence assessment tool in perio-mode allows for reliable judgment of microbial plaque and gingival inflammation levels similar to the established Turesky modified Quigley Hein index and the Silness & Løe Gingival Inflammation index.

As a major advantage these scoring judgments can be performed on stored pictures, which can be used for patient education and motivation but also can be consulted and compared at a patient recall visit.

REFERENCES

- [1] I. Brook, "Microbiology and management of periodontal infections," *Gen Dent*, 51(5), 424-8 (2003).
- [2] A. L. Neely, T. R. Holford, H. Loe *et al.*, "The natural history of periodontal disease in man. Risk factors for progression of attachment loss in individuals receiving no oral health care," *Journal of Periodontology*, 72(8), 1006-15 (2001).
- [3] M. Schatzle, H. Loe, W. Burgin *et al.*, "Clinical course of chronic periodontitis. I. Role of gingivitis," *Journal of Clinical Periodontology*, 30(10), 887-901 (2003).
- [4] H. Loe, E. Theilade, and S. B. Jensen, "Experimental Gingivitis in Man," *The Journal of periodontology*, 36, 177-87 (1965).
- [5] E. Theilade, W. H. Wright, S. B. Jensen *et al.*, "Experimental gingivitis in man. II. A longitudinal clinical and bacteriological investigation," *Journal of Periodontal Research*, 1, 1-13 (1966).
- [6] S. Turesky, N. D. Gilmore, and I. Glickman, "Reduced plaque formation by the chloromethyl analogue of vitamin C," *Journal of Periodontology*, 41(1), 41-3 (1970).



SoproCARE Prophylaxis Camera: *Improved Patient Communication Leads to So Much More*

Todd Snyder, DDS

It is wonderful to watch the rapid evolution of technology within dentistry that enables dentists and their staff to be far more productive than ever and provide better care for their patients. The ideal technology should begin with improved patient communication, which then leads to many other clinical opportunities for both clinicians and patients.

The SoproCARE prophylaxis camera (ACTEON North America, Mount Laurel, NJ) is a perfect example of this type of technology; it improves patient communication by allowing patients to see the problem at hand so they can better understand the diagnosis, treatment options, and cost of care.

SoproCARE is the most recent innovation to SOPRO's dental imaging system and diagnosis tool that started with the SoproLIFE in 2010. Using autofluorescence and chromatic amplification to reveal caries, dental plaque, and tartar, SoproCARE is the only product on the market to reveal gingival inflammation in real time.

Improved Patient Communication

SoproCARE allows dentists, hygienists, or assistants to capture a thorough and rapid assessment of a patient's oral health by implementing 3 clinical modes:

1. PERIO Mode: Highlights dental plaque and gingival inflammation, even at the earliest stages (Figure 1). Clinicians see and show patients where the lack of proper dental hygiene is, which creates the need for more involved in-office periodontal therapy. The system can highlight and reinforce a patient's need for additional attention or tools to better manage the condition at home.

2. CARIO Mode: Helps detect enamo-dental caries easily (Figure 2), from stage 1 (code ICDAS II), so that mini-

mally invasive dental care can be performed to maintain as much of the tooth as possible.

3. DAYLIGHT Mode: Macrovision makes imperceptible flaws visible and allows clinicians to watch the stability of microlesions and their evolution (Figure 3).

This improved patient communication leads to all the ways SoproCARE can benefit a dental practice—increased case acceptance, early diagnosis, less invasive treatment



Figure 1. PERIO Mode



Figure 2. CARIO Mode

SoproCARE Prophylaxis Camera: *Improved Patient Communication Leads to So Much More*

options, increased office efficiency and production, and marketing opportunities.

Increased Case Acceptance

Patient engagement and involvement increases dramatically when patients can actually see and perceive what a dentist, hygienist, or staff member is trying to communicate. SoproCARE offers a unique benefit—the ability for virtually everyone in the practice to offer an improved level of service to patients. With SoproCARE, patients can now see the problem, understand the recommended treatment, recognize the time needed to resolve the issue, and acknowledge the financial impact of the treatment.

Patients can see the problem in the operatory as the clinician discovers it, then when they move to the treatment coordinator, the assistant can explain the areas of concern. By using visual aids, patients are again reminded of the problem and see the issue while it is being discussed.

As the treatment coordinator solidifies the financial aspects of care, there is no miscommunication regarding the necessary treatment and the fees incurred. In addition, the office can use the images to assist in possibly gaining better reimbursement rates from dental insurance carriers. The visual communication from the dentist to staff members can be seamless, improving the patient experience and increasing case acceptance.

Early Diagnosis and Minimally Invasive Treatment

A simple explorer is about 50% accurate in finding decay, and radiographs are not much better as they are approximately 68% accurate. SoproCARE provides both



Figure 3. CARIO Mode

dentists and hygienists with enhanced diagnostic capabilities, allowing for early diagnosis and typically less invasive treatment, including remineralization therapies and earlier intervention with oral hygiene care.

With SoproCARE's early diagnosis capabilities, clinicians can offer more minimally invasive protocols to treat various dental conditions. If traditional treatment is deemed necessary, then patients can benefit from clinicians finding pathology when it is smaller.

The ideal technology should begin with improved patient communication, which then leads to many other clinical opportunities for both clinicians and patients.

In addition to the CARIO Mode, the PERIO Mode allows the hygienist and hygiene department to better demonstrate and educate patients on the health of their gum tissues and the accumulation of plaque and calculus on their teeth. The educational discussion of gum disease becomes more relevant and personal when patients can see firsthand the level of their oral health. Less invasive therapies are then possible with earlier diagnosis.

Increased Office Efficiency and Productivity

SoproCARE's 3 modes allow dentists and hygienists to quickly and accurately evaluate various surfaces of teeth, integrity/patency of restorations, and periodontal health. Capturing images using SoproCARE can be delegated to dental assistants or hygienists, accelerating the diagnosis process so dentists can be more productive. This streamlined examination process can help move the patient toward treatment acceptance more quickly.

With SoproCARE, dentists can delegate more procedures to staff members, improving efficiency that can be a huge advantage to the bottom line of the dental practice. SoproCARE's small, portable system can be cleaned easily and moved from operatory to operatory, allowing each clinician



to implement it with virtually no down time.

In addition, the front office staff, armed with this technology, can refer to the images any time there is a discussion regarding treatment and recommendations for management.

Marketing

SoproCARE can be implemented into a marketing campaign outside of the practice through various traditional media outlets as well as the practice's website and social media. Modern technology that offers sensory feedback to patients can become an instant marketing platform and referral system for a dental office.

Many patients seek a secondary consultation; a practice that offers services that others do not can be a great way to create new patient opportunities. Using marketing tactics, a practice can explain SoproCARE's features and benefits, which patients may not have seen in other practices.

A common patient concern is whether recommended treatment is truly necessary. Without visual aids at other dental practices, patients typically do not see the actual problem and are not sold on the treatment. When patients seek a dentist for a second opinion, they may be more receptive to a practice that has optimized its Internet presence with tools that can answer patients' questions. With an

informative online presence, a practice has a better opportunity to acquire new patients.

Conclusion

The ability to offer patients a better understanding of their oral health condition through a visual presentation offers many benefits to patients, staff members, and dentists. Earlier diagnosis as a result of using SoproCARE leads to more noninvasive or minimally invasive options that might not be available because of finding the pathology later in the process. When patients visually perceive their problems, it allows for a quicker response to necessary care. Finally, a faster implementation process for staff members, while having the time to see more patients, can allow the entire dental office to be more productive.

Further Reading

1. Rechmann P, Charland D, Rechmann BMT, et al. Performance of laser fluorescence devices and visual examination for the detection of occlusal caries in permanent molars. *J Biomed Opt.* 2012;17(3):036006.
2. Tassery H, Levallois B, Terrer E, et al. Use of new minimum intervention dentistry technologies in caries management. *Aust Dent J.* 2013;58(suppl1):49-59.
3. Terrer E, Koubi S, Dionne A, et al. A new concept in restorative dentistry: light-induced fluorescence evaluator for diagnosis and treatment: Part 1: Diagnosis and treatment of initial occlusal caries. *J Contemp Dent Pract.* 2009;10(6):E086-94.

La videocamera intraorale, un valido supporto nella pratica clinica

Gianna Maria Nardi*, Fabio Scarano Catanzaro**

*RUC, Dipartimento di Scienze odontoiatriche e maxillofacciali, Sapienza Università di Roma.

**Medico Odontoiatra, libero professionista in Bari

Una buona comunicazione è alla base del protocollo operativo di prevenzione primaria secondaria e terziaria. La comunicazione digitale, attraverso l'utilizzo di strumenti informatici come la videocamera, diventa strumento essenziale per l'osservazione clinica del cavo orale, permettendo un'efficace esplorazione intraorale, un esatto screening dei rischi alla patologia e favorisce la condivisione della

diagnosi e l'accettazione del piano di trattamento alle terapie di prevenzione da parte del paziente.

Case report

Si presenta alla nostra attenzione un paziente di anni 27 di sesso maschile, che riferisce una attenta e scrupolosa igiene orale domiciliare, ma lamenta frequente sensibilità sugli elementi dentari posteriori superiori ed infe-

riori. All'esame clinico obiettivo si riscontra la presenza di biofilm batterico e tartaro sulle superfici linguali degli incisivi inferiori, nella zona compresa tra gli elementi 3.2, 4.2. (Fig. 1). Inoltre, a livello delle superfici vestibolari dei primi molari superiori, denti sui quali il paziente ci riferisce una sensibilità aumentata, evidenziamo aree di demineralizzazione. Indagando sulla storia clinica del paziente, il

quale riferisce di un trattamento ortodontico eseguito precedentemente, è perciò plausibile pensare a un danno da imputarsi alla difficile detersione delle superfici nella zona compresa tra la banda ortodontica e la superficie dentale. Eseguiamo dunque un esame approfondito avvalendoci della fotocamera Acteon SoproCare™ che permette, tramite led appositi, di evi-

denziare in modo rapido ed accurato le zone di demineralizzazione e le aree infiammate, e di mostrarle al paziente in real time rendendolo attivamente partecipe e consapevole dell'eventuale danno (Fig. 2). La stessa telecamera in modalità Perio, ha evidenziato invece la presenza di placca dentale e infiammazioni gengivali, presenti in uno stadio iniziale specialmente nella regione linguale e palatale degli incisivi superiori e inferiori. Le immagini



Fig. 1



Fig. 2



Fig. 3a

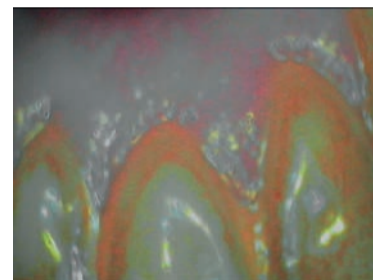


Fig. 3b

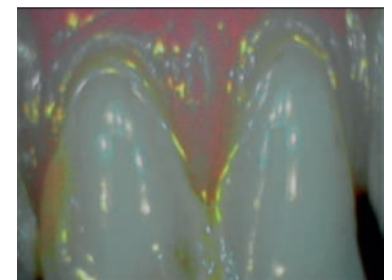


Fig. 3c



Fig. 4a



Fig. 4b

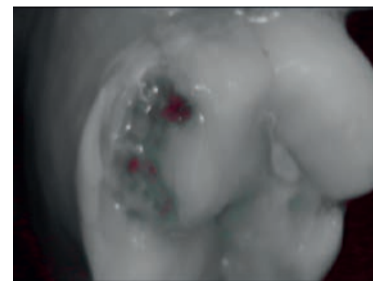


Fig. 5

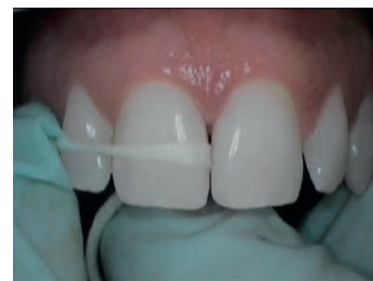


Fig. 6a

ottenute attraverso l'analisi della fluorescenza vengono sovrapposte alle immagini anatomiche creando una rappresentazione delle condizioni del tessuto, di semplice e immediata comprensione anche per il paziente, altrimenti non percettibili con il semplice utilizzo della luce bianca. I tessuti irradiati vengono rappresentati con una mappatura cromatica di semplice e immediata interpretazione come mostrato nelle figure 3a, 3b e 3c. In modalità Daylight con luce bianca ed ingrandimento a 100X, abbiamo evidenziato una cospicua perdita di smalto dovuta a un precontatto sulla parete mesiale della superficie occlusale del 4.6 e una lesione aftosa

> pagina 27



Fig. 6b



HELBO

è efficace contro le infezioni batteriche



La terapia HELBO è un trattamento supplementare ottimale per curare i Vostri pazienti da tutte le infiammazioni parodontali e perimplantari, che non produce effetti collaterali od interazioni, e previene future ricadute.

Siete interessati ad integrare la terapia HELBO alla vostra prassi quotidiana per il benessere dei vostri pazienti?

Per maggiori informazioni visitate il sito <http://helbo.bredent-medical.com> o chiamate il numero 0471 / 469576.



Applicazione del fotosensibilizzatore HELBO®Blue.

Esposizione al laser HELBO®TheraLite.



bredent group



Fig. 7a



Fig. 7b

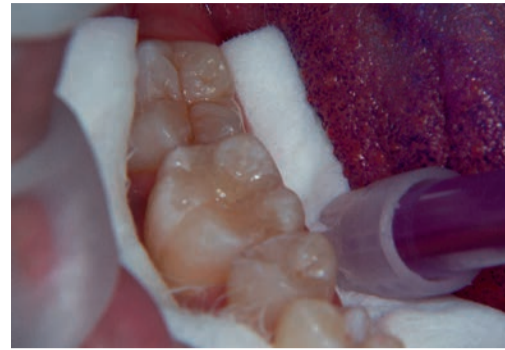


Fig. 7c



Fig. 8a

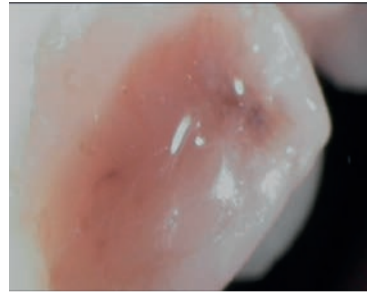


Fig. 8b

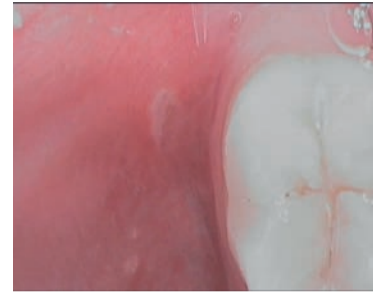


Fig. 9a



Fig. 9b

< pagina 26

sulla mucosa geniena di forma ovalare in regione 4.7, di aspetto crateriforme, di 1 cm di diametro, di colore grigiastro, caratterizzata da un'area di necrosi superficiale ricoperta da una membrana fibrino-purulenta e circondata da un alone eritematoso infiammatorio. Il paziente riferisce intensa sintomatologia algica e sanguinamento mesiale della superficie occlusale del 4.6, immagine in modalità daylight e con ingrandimento 100X (Figg. 4a,4b). In modalità Cario il sistema evidenzia la presenza di carie smalto-dentinali, già a partire dallo stadio 1 (codice ICDAS II) (Fig. 5).

Il trattamento ha inizio con una seduta d'igiene orale professionale, con utilizzo di ablatore Mectron Multypiezo Pro, in modalità soft, e air polish con polvere di glicina. Le zone interdentali della sezione frontale, dove è presente un affollamento, sono deterse con l'aiuto del filo interdentale. Le immagini in real view della videocamera riescono a migliorare la compliance al corretto utilizzo dei presidi per l'igiene interprossimale (Figg. 6a, 6b: tecnica di spazzolamento personalizzata da Nardi e collaboratori con strumenti Sunstar). Col fine di diminuire l'indice di rischio e facilitare le procedure di igiene orale a livello delle superfici occlusali dei primi molari inferiori, presentanti entrambi solchi multipli molto accentuati ed acuti difficili da detergere, abbiamo preferito eseguire la sigillatura dei solchi e delle fossette. Questa è una metodica di prevenzione della carie conosciuta e applicata in tutto il mondo ormai da molti decenni (Simonsen, 2002; Mejare et al., 2003; Ahovuo-Saloranta et al., 2004; Kitchens, 2005; Hiri et al., 2006). Ab-

biamo scelto di usare il sigillante Control Seal (Voco), un prodotto altamente riempitivo e contenente fluoro, la cui caratteristica è la trasparenza, che permette un controllo costante del sigillo. Con un contenuto di riempitivi del 55% in peso, Control Seal è l'unico sigillante per fessure sul mercato che combina la trasparenza con la stabilità di un sigillante opaco. Inoltre, la trasparenza di questo prodotto permette l'uso di metodi diagnostici basati sulla fluorescenza laser, così che la carie possa essere diagnosticata e monitorata quando necessario anche sotto lo strato di sigillante. Prima di iniziare la procedura per la sigillatura abbiamo deterso le superfici con la polvere Prophylaxis powder con Airflow Combi Mectron. Asciugate le superfici abbiamo applicato il gel mordenzante Vococid e lasciato agire per 15-30 secondi, risciacquato con abbondante getto d'acqua e asciugato. Abbiamo applicato il sigillante Control Seal nella cavità e lasciato penetrare per 15-20 secondi, rimossi gli eccessi con una spugnetta e polimerizzato per 20-30 secondi. Per remineralizzare le zone mordenzate che non sono state coperte dal sigillante abbiamo ritenuto opportuno applicare uno strato di Voco Profluorid, vernice a base di fluoro, per sigillare i tubuli dentinali e per desensibilizzare l'area. Si è proceduto alla remineralizzazione dello smalto con mousse remineralizzante a base di 140 ppm NaF idrossiapatite e xilitolo (Remin Pro, Voco), per favorire il rinforzo dello smalto e prevenire l'eventuale ipersensibilità post igiene orale professionale. (Figg. 7a-7c).

Le aree di demineralizzazione dei molari superiori, di forma crateriformi, non presentano aree di rammollimento, vengono perciò trattate in modo

diretto con Ivoclar Fluor protector S. Usando un pennellino la vernice è stata distribuita uniformemente in uno strato sottile, coprendo l'intera superficie della lesione. Questa vernice tollera la presenza di umidità e aderisce spontaneamente alle superfici umide del dente (Figg. 8a, 8b). Dopo il corretto assorbimento, è stato consigliato al pa-

ziente di evitare cibi duri, alcol, spazzolamento o l'uso del filo interdentale per le 4 ore successive all'applicazione. Per il trattamento della lesione aftosa, invece, ci si avvale dell'Oralmedic®, un dispositivo medico realizzato con tecnologia HybenX®, indicato nel trattamento topico delle lesioni ulcerate del cavo orale. La mono sommi-

nistrazione della soluzione determina una rapida riduzione del dolore e del discomfort del paziente. Il prodotto agisce attraverso dei processi fisico-chimici che determinano la denaturazione dei tessuti superficiali. Vieni così favorita la naturale guarigione dell'area affetta attraverso la deposizione di una sottile barriera costituita da materiale organico precipitato con funzione protettiva. Dopo aver asciugato la zona, si utilizza un apposito tampone predosato contenente la soluzione, mantenendolo in situ per 5-10 secondi. Successivamente si risciacqua e si asciuga la zona (Figg. 9a, 9b).

Il paziente è stato visitato a distanza di una settimana, la lesione aftosa non è più visibile. Il paziente riferisce che la sintomatologia algica dovuta alla lesione aftosa, risultava notevolmente diminuita sin dal giorno seguente, come anche le sue dimensioni.

La visione della telecamera intraorale Acteon SoprCare™ ha permesso di fare una attenta disamina clinica, interagendo con il paziente e motivandolo a una maggiore attenzione di efficacia del controllo domiciliare del biofilm batterico e all'importanza del follow up, per rivedere la situazione clinica e confrontarla con le immagini archiviate della visita precedente.

25th ANNIVERSARY
SIMIT
DENTAL

SOPROCARE

LA RIVELAZIONE

SOPROCARE risponde a svariate esigenze di profilassi fornendo una rapida diagnosi della salute orale del paziente.

- **Modalità PERIO** : Evidenzia la presenza di placca dentale e di infiammazioni gengivali, anche se presenti in uno stadio iniziale.
- **Modalità CARIO** : Evidenzia la presenza di carie smalto-dentinali, dallo stadio 1 (Codice ICDAS II), in maniera semplice.
- **Modalità DAYLIGHT** : La macrovisione/magnificazione rende visibile anche i dettagli impercettibili e consente il controllo di eventuali micro lesioni e la loro evoluzione.





www.soprocure.com

NEW TECHNOLOGY

Get Your Hygiene Patients “Off the Fence”!

Fluorescing Camera for Early Detection and Recognition of Caries, Dental Plaque, and Gingival Inflammation

Dental caries and periodontal disease are transmittable bacterial infections of the teeth and gums.^{1,2} Each infection has unique characteristics, yet both share the common source of infection—oral biofilms (Figure 1). Both diseases have been implicated as inflammatory diseases.³⁻⁴ Inflammatory diseases affect our systemic health and contribute to the aging process.⁵⁻⁶ Incidence of dental caries and periodontal disease are both rising.^{7,8} Despite these compelling facts, motivating patients to seek treatment for painless pathology can be frustrating. Clinicians can benefit by using additional ways to detect, reveal, and oblige our patients to treatment.

Use of disclosing dyes have a mainstay for revealing biofilm accumulation, but this is a messy and “old fashioned” process. There are several new technologies appearing in the market, improving our ability to detect biofilm, inflammation, and dental caries. One company, ACTEON North America, has developed a high-performance intraoral camera (SoproCARE) that can highlight dental plaque, gingival inflammation, and effectively assists in enamel-dentinal caries detection (Figure 2). This camera can connect to any image management program and is easy for the dentist and hygienist to use. Intraoral cameras have been used for years to communicate various clinical situations. We have been involved in the clinical use of this fluorescence light-induced camera used for evaluation of biofilm, caries, and gingival inflammation.

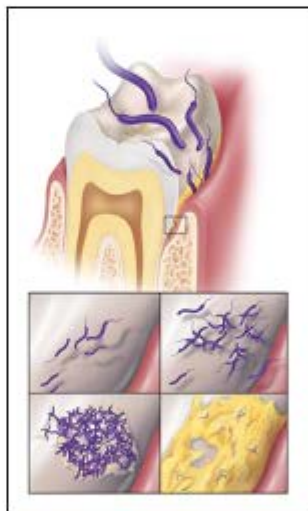


Figure 1. Dental caries and periodontal disease are biofilm induced.



Figure 2. SoproCARE intraoral camera (ACTEON North America).



Jeffrey M.
Rosenberg, DDS



Joann Papanier,
RDH, LLA



Beverly B. Abdullah,
RDH, LLA

This article will describe a protocol we have developed for daily use of this technology during the prophylaxis appointment.

THE PREMISE

Treatment acceptance is no longer just based on relationship building skills. Most patients enjoy a trusting relationship with dental offices and engage in prevention through prophylactic “check-up” visits. Yet many people’s behavior has changed as their culture has



Figure 3. PERIO mode. Schematic illustration of the colors produced: at the neck, white indicates soft deposits; above that, orange indicates calcified deposits and tartar; and on the gum, red indicates inflamed areas.



Figure 4. CARIO mode. Schematic illustration of the colors produced: the areas warning of carious activity appear red.



Figure 5. Intraoral view, in CARIO mode, of a fractured restoration.



Figure 6. Pre-op view in Daylight mode at the start of check-up visit.



Figure 7. Pre-op view in PERIO mode.



Figure 8. Post-op view in Daylight mode confirming effectiveness and value of the prophylaxis appointment.



Figure 9. Pre-op view (upper left) of biofilm and apparent stain in Daylight mode.



Figure 10. View (same as Figure 9) in PERIO mode. Soft bacterial deposits are white, calcified deposits are orange-yellow, inflamed tissues are purplish-pink-red.



Figure 11. View of suspicious grooves in magnified Daylight mode. Caries present?

changed. Fifty seven percent of people say they talk more online than they do in real life (in households with income of \$75k or more).⁹ Even when personal recommendations are made, online research cements the decision for service providers and purchase decisions. This is the digital age.

In order to best serve our patients, it is important that you develop a comprehensive, integrated, user-friendly platform to facilitate communication and address patient preferences. The visual communication provided by an intraoral camera fits into this digital consciousness.

THE TECHNOLOGY: FLUORESCENCE

The SoproCARE intraoral camera is a high-quality, high-magnification camera (up to 110x) that uses white and blue LEDs projected into the oral tissues and biofilm which is then absorbed and reflected back in the form of fluorescence. Dental tissues have fluorescent molecules that absorb light, and then emit the energy back as fluorescent light. This is called autofluorescence.¹⁰ The device uses selective chromatic amplification of the fluorescent chroma to reveal caries, calcified and noncalcified dental plaque, and gingival inflammation.

The camera is unique in that it has 3

modes. It has a Daylight mode for natural high quality image of the tissues, a CARIO mode that uses the blue light to amplify the fluorescent chroma for visual detection of dental caries, and a PERIO mode that combines the blue and white lights to highlight any biofilm and inflammation that may be present (Figures 3 and 4).

It is now possible to layer, upon the high quality intraoral pictures, a graphic color interpretation of what these conditions mean to the patient with regard to home care, cavities, and periodontal inflammation.

What remains to be discussed is a system to implement the process.

THE IMPLEMENTATION PROTOCOL

It starts with an auxiliary driven (nonthreatening personnel) approach—"Mrs. Smith, the doctor asked me to take a preliminary look in your mouth for any potential problem areas. We are now using the latest technology for early detection of cavities and gum disease. This report card is a color-coded guide to rating your risk. We want you to be involved in decisions about your own health, so we will be showing you and telling you what we see as we go along. Let's get started!"

Use the SoprocARE camera in the Daylight mode. Start with the teeth first (cavities are still king). Identify stained fissures, cracks in teeth, or restorations and wear. Then switch the camera over to the CARIO mode to grade if the lesions identified are carious. Finally, use the PERIO mode to view existing biofilm, mature biofilm (calculus), and any tissue inflammation.

*Follow this with the doctor's examination—*The exam should not begin with, "Are you having any problems?" The hygienist or assistant has already done this. Instead, greet the patient and turn to the hygienist/assistant and ask, "Please bring me up to date. What are your findings?"

*The hygienist/assistant should brief the doctor—*on medical history/blood pressure. Remember that caries and periodontal pathology affect systemic health, and the examination should reflect this relevance!

*Patient concerns—*The periodontal condition and recommendations. "No pockets over 3 mm other than x. Areas still in need of attention. Last scaling."

Recall/home care—"I recommended Mrs. Smith come back in 3 months."

Today I noted these findings with the SoprocARE Display the images from the Daylight, CARIO, and PERIO modes.

Previous recommendations: "I noted in the chart you are concerned about tooth No. 4 [you will have that image]. It looks like if that continues to be a problem, and we'd likely recommend a crown, but we'll see."

Review radiographic data, cosmetic issues, bite/wear, etc.

After a few repetitions of this suggested protocol, you will find it to be an efficient, comprehensive, codiscovery experience that supports the concepts of oral-systemic health, preventative health, and early disease detection.

APPLICATIONS

*Communication—*The intraoral camera is

the fastest, most effective way to communicate to patients their oral status. The projection of intraoral images on to a large screen monitor fosters patients through the codiscovery process. We know that most dental treatment starts out asymptomatic, so a picture of a painless, fractured restoration helps the patient (and dental team) in the treatment decision process (Figure 5).

*Home care evaluation; presence of biofilm—*The prophylaxis appointment is the portal to patient education and motivation. With the continuing discoveries of interrelationships between oral and systemic disease, the dental team needs to present a meaningful depiction of the patient's oral health status. If inflammation is the common mechanism connecting periodon-

Our Experience With SoprocARE Technology

Joann "Jodi" Papanier, RDH, LLA

Have you ever been "on the fence" during a dental examination with a new or existing patient at your dental practice? At our dental practice, The Dental Healthcare Group, we are not in the habit of saying, "Let's just put a watch on this tooth and check it again in a few months," or "Let's just watch your gums and see if the bleeding subsides by the time you are due to come back for your next cleaning." All of our patients receive a complete diagnosis and a comprehensive treatment plan. Our goal is to deliver optimal treatment plans so our patients can make fully informed and knowledgeable decisions regarding their dental health and their overall health.

In our opinion, there are 4 critical steps to successfully achieving patient compliance and acceptance of dental treatment: communication, comprehension, diagnosis, and treatment planning. In order to adhere to our goal of delivering optimal treatment planning, we rely heavily on utilizing accurate tools both at the chair and in our consultation room.

The SoprocARE intraoral camera (ACTEON North America) has become a necessary aid in our office. This instrument is fast and easy to operate, and the level of accuracy (compared to other intraoral cameras) is paramount for the proper diagnosis of oral conditions. My coworker and dental hygienist of 30 years, Beverly Abdullah, RDH, LLA, was the first to experience the accuracy and simplicity of this system. After using the SoprocARE on every patient for several months, Beverly found that she was significantly more successful in the diagnosis of caries and inflammation. This technology also helped her increase the level of patient compliance and patient acceptance of any treatments suggested.

Although maintaining the health of hard tissue (teeth, bone, etc) is of significant importance, as hygienists, Beverly and I obviously make it our priority to pay close and specific attention to the soft tissue (gingiva, mucosa, etc). With the regular and repeated use of the SoprocARE intraoral camera, Beverly and I have made charting and following the pattern of inflammation a mandatory protocol for every visit for all of our patients. Most importantly, these findings and patterns of inflammation are documented and kept on file for review for future comparisons. Without the use of this technology, we would not be able to follow and diagnose the periodontal status of our patients with such accuracy, certainty, and confidence.

When comparing the SoprocARE camera with other intraoral cameras, I have experienced and discovered false caries detection and inaccurate levels of inflammation with the others. This can occur especially if a patient has not had a recent and complete oral hygiene cleaning immediately prior to using other intraoral cameras. The SoprocARE intraoral camera has a more sophisticated accuracy that limits this false detection from occurring simply due to an unclean mouth.

Get "off the fence" during your dental examinations! Make it your personal challenge to deliver optimal treatment plans to all of your patients. In our opinion, based on our clinical experiences, this would not be achievable without SoprocARE intraoral camera technology.



Figure 12. The biofilm is removed from the occlusal grooves with air polishing to complete the evaluation; caries are red (CARIO mode).



Figure 13. A cervical lesion may be treated in a variety of approaches; the presence of red (indicating caries) aids in the treatment decision.



Figure 14. View of marginal ridge fracture unapparent to the patient, as seen during the examination process.



Figure 15. Quick shift to CARIO mode indicates the presence of an active lesion.

tal disease and cardiovascular disease, a picture of the oral biofilm with adjacent tissue inflammation can be a compelling way to communicate the importance of tissue management and homecare. High magnification as well as selective chromatic amplification also allow the clinician to evaluate the successful removal of deposits (Figures 6 to 10).

EARLY LESION DETECTION AND LESION EVALUATION

Light-induced fluorescence facilitates earlier caries lesion detection and subsequent less invasive treatment.¹⁷ In the protocol presented, the patient is alerted to the presence of caries by referring to the risk assessment card indicating dental caries as red in color with the SoproCARE device. Suspicious grooves can be evaluated as to the need for preventive treatment such as sealants versus more invasive preparation (Figures 11 and 12). The status of cervical lesions can be evaluated to determine the course treatment—preparation versus fluoride varnish, remineralizing pastes, etc (Figure 13). Proximal fractures can be evaluated as to the presence of active caries in real time as the patient sees the clinical conditions as the dentist or auxiliary conducts the examination (Figures 14 and 15).

IN SUMMARY

The days of handing patients a mirror to show their oral health status are long gone. Intraoral cameras (such as SoproCARE), used with the suggested protocol outlined in this article, facilitate the codiscovery process through technology which is “cognitively familiar” to today’s digitally aware dental patients.

Doctor-patient communication is streamlined, and patient education and motivation is facilitated with this protocol. In addition, early detection of caries and inflammation is also made possible with this technology; and reinforcement of previously diagnosed clinical conditions can be brought back into our patients’ focus.

Implementing the latest intraoral camera technology in to the dental practice clinical protocol can also give value-added factors to “wow” patients, prevent buyer’s remorse, and can also be used to boost reputation in today’s social media markets. ♦

References

1. Caufield PW. Dental caries: an infectious and transmissible disease. Where have we been and where are we going? *N Y State Dent J*. 2005;71:23-27.
2. Van Winkelhoff AJ, Boutaga K. Transmission of periodontal bacteria and models of infection. *J Clin Periodontol*. 2005;32(suppl 6):16-27.
3. Southward K. The systemic theory of dental caries. *Gen Dent*. 2011;59:367-375.
4. Ramamoorthy RD, Nallasamy V, Reddy R, et al. A review of C-reactive protein: a diagnostic indicator in periodontal med-

- icine. *J Pharm Biomed Sci*. 2012;4(suppl 2):S422-S426.
5. Nakano K, Nemoto H, Nomura R, et al. Detection of oral bacteria in cardiovascular specimens. *Oral Microbiol Immunol*. 2009;24:64-68.
6. Abranches J, Miller JH, Martinez AR, et al. The collagen-binding protein Cnm is required for *Streptococcus mutans* adherence to and intracellular invasion of human coronary artery endothelial cells. *Infect Immun*. 2011;79:2277-2284.
7. Bagamian RA, Garcia-Godoy F, Volpe AR. The global increase in dental caries. A pending public health crisis. *Am J Dent*. 2009;22:3-8.
8. Papanian PN. The prevalence of periodontitis in the US: forget what you were told. *J Dent Res*. 2012;91:907-908.
9. Pickard M. Power to the people. *Think Quarterly*. September 2011. google.com/think/articles/power-to-the-people.html. Accessed November 12, 2013.
10. Terer E, Koubi S, Dionne A, et al. A new concept in restorative dentistry: light-induced fluorescence evaluator for diagnosis and treatment. Part 1: Diagnosis and treatment of initial occlusal caries. *J Contemp Dent Pract*. 2009;10:E086-E094.
11. Rosenberg JM, Shuman L, Morgan A. Technology enhances caries diagnosis and treatment. *Dent Today*. 2011;30:162-166.

Dr. Rosenberg maintains a private practice in Philadelphia, Pa, emphasizing restorative and esthetic dentistry. He is a fellow of the AGD and holds associations with various restorative, esthetic, and orthodontic organizations. He publishes in this field to increase awareness of high-tech materials and procedures and performing dentistry more efficiently and with higher quality. Dr. Rosenberg places hundreds of bonded restorations monthly and has a patent pending in the area of nonmetal dental restorations. He is also the head of The Dental Healthcare Group, which provides high-quality continuing education in the Philadelphia area. He can be reached at (215) 592-4747 or via e-mail at djreff@philadelphiasdentist.com.

Disclosure: Dr. Rosenberg discloses that the SoproLIFE camera was provided by ACTEON North America.

Ms. Papanier is a registered dental hygienist with The Dental Healthcare Group located in Philadelphia, Pa. Practicing dental hygiene since 1987, she is licensed to administer local anesthesia and strongly prefers treating patients who are periodontally involved. She strives to develop a professional and personal rapport with every patient she meets/treats as this has shown to be the best method of successful treatment and compliance between herself and her patients. She participates in many continuing education courses in order to stay on the cutting edge. She can be reached at jodipapanier@aol.com.

Disclosure: Ms. Papanier discloses that the SoproLIFE camera was provided by ACTEON North America.

Ms. Abdullah is a registered dental hygienist (RDH) with The Dental Healthcare Group in Philadelphia, Pa, and has more than 30 years of experience in the field. She earned her degree at the Community College of Philadelphia in 1984. Prior to obtaining her RDH degree, Ms. Abdullah was a clinical dental assistant. She is licensed in local anesthesia and participates in numerous educational courses to advance her clinical skills, including soft-tissue management (phases 1 and 2), scaling and root planing, and utilizing ultrasonic instruments. She is also certified as a myofunctional therapist. She also has extensive training in Botox and Juvederm therapy. She has participated in various dental trials for companies such as Proctor and Gamble/Warner Lambert as well. She can be reached via e-mail at the address bev_dhcg@yahoo.com.

Disclosure: Ms. Abdullah discloses that the SoproLIFE camera was provided by ACTEON North America.

Performance of a light fluorescence device for the detection of microbial plaque and gingival inflammation

Peter Rechmann¹ · Shasan W. Liou² · Beate M. T. Rechmann¹ · John D. B. Featherstone¹

Received: 29 November 2014 / Accepted: 15 April 2015 / Published online: 28 April 2015
© Springer-Verlag Berlin Heidelberg (outside the USA) 2015

Abstract

Objectives The hypothesis to be tested was that using the SOPROCARE system in fluorescence perio-mode allows scoring of microbial plaque that is comparable to the Turesky modification of the Quigley Hein plaque index (T-QH) and scoring of gingival inflammation comparable to the Silness and Løe gingival inflammation index (GI).

Materials and methods Fifty-five subjects with various amounts of microbial plaque were recruited. The T-QH and GI index were recorded. SOPROCARE pictures were recorded in fluorescence perio-mode and in daylight mode. Finally, conventional digital photographs were taken. All pictures were assessed using the same criteria as described for the clinical indices.

Results The average T-QH was 1.1 ± 1.2 (mean \pm SD). Scoring with SOPROCARE perio-mode led to a slightly higher average than the T-QH scores. SOPROCARE daylight mode and digital photography showed the highest plaque scores. The average GI index was 0.7 ± 0.9 . SOPROCARE in perio-mode scored slightly lower. Linear regression fits between the different clinical indices and SOPROCARE scores were significantly different from zero demonstrating high goodness of fit.

Conclusions The study demonstrated that the SOPROCARE fluorescence assessment tool in perio-mode allows reliable judgment of microbial plaque and gingival inflammation levels similar to the established Turesky-modified Quigley Hein index and the Silness and Løe gingival inflammation index. Training on plaque-free teeth will actually reduce scoring errors.

Clinical relevance The SOPROCARE fluorescence tool in perio-mode provides reliable evaluation of microbial plaque and gingival inflammation for the dental clinician.

Keywords 450-nanometer wavelength · Gingival inflammation · Microbial plaque · Detection · Clinical study · SOPROCARE · Orthodontic brackets · Gingival pigmentation

Introduction

Gingival inflammation due to microbial plaque and calculus may lead to advanced periodontal disease [1, 2] with non-physiological gingival pocket formation [3]. If left untreated, loss of attachment and bone loss might be the consequences. Removal of microbial plaque in the gingivitis stage generally restores gingival health [4, 5]. Often, the white yellow microbial plaque on teeth is difficult to see clinically. The dental professional may use artificial plaque disclosing methods [6–10] or probes the surface of each tooth for adherent plaque [11].

Illumination with blue light has been shown to induce fluorescence from the dentin body and caries lesions, respectively, supporting the classifications of early caries lesions in the precavitated stage [12, 13]. Fluorescence is a property of some manmade and natural materials that absorb energy at certain wavelengths and emit light at longer wavelengths. Several caries detection methods utilize fluorescence. When a caries lesion is illuminated with, for instance, red laser light at 655 nm

✉ Peter Rechmann
rechmannp@dentistry.ucsf.edu

¹ Department of Preventive and Restorative Dental Sciences, School of Dentistry, University of California at San Francisco, 707 Parnassus, San Francisco, CA 94143, USA

² Department of Orofacial Sciences, School of Dentistry, University of California at San Francisco, 707 Parnassus, San Francisco, CA 94143, USA

(DIAGNOdent, KaVo, Biberach, Germany), organic molecules that have penetrated porous regions of the tooth, especially metabolites from oral bacteria, will create an infrared fluorescence. This fluorescence is believed to originate from porphyrins related to oral bacteria [14–17]. Other caries detection tools use ultraviolet light sources to induce fluorescence from caries lesions (quantitative light fluorescence (QLF), Inspektor™ Pro, Amsterdam, Netherlands [18–21]; Spectra Caries Detection Aid (AIR TECHNIQUES, Melville, NY) [22]).

A caries detection tool (SOPROLIFE, SOPRO, ACTEON Group, La Ciotat, France) illuminates with intense blue light (450 nm), and consequently, the dentin body fluoresces back in green. The green light excites the porphyrins involved in the caries process, which then show fluorescence in the red spectrum [12]. Blue light illumination might also help to make microbial plaque and calculus visible due to fluorescence caused by its porphyrin content. Microbial plaque adjacent to the gingiva releases exotoxins that induce gingival inflammation.

Gingivitis starts with localized inflammation of the marginal gingiva followed by inflammation of the circumferential marginal area. The host reaction to bacteria and toxins results in pain, redness, and swelling. The observed redness is a direct consequence of increased blood flow since inflammation includes a response of vascular tissue. The red blood cell component hemoglobin is an iron-containing oxygen-transport metalloprotein and is the best-known porphyrin. Since these blood-related porphyrins will absorb incoming light and show fluorescence, inflamed gingiva should show more fluorescence than healthy gingiva.

The SOPROCARE camera system used in the present study is closely related to the SOPROLIFE caries detection tool. It also emits blue light at 450-nm wavelength using three blue diodes.

The hypothesis to be tested in this study was that using the SOPROCARE camera in fluorescence perio-mode allows detecting, visualizing, and scoring of microbial plaque and also permits a comparison to the Turesky modification of the Quigley Hein plaque index. Furthermore, the use of the system allows detecting, visualizing, and scoring of gingival inflammation and facilitates scoring of the inflammation comparable to a clinical scoring engaging the Silness and Løe gingival inflammation index.

Materials and methods

Study subjects, inclusion and exclusion criteria, stratified recruitment

Approval for the study was obtained from the Committee on Human Research at UCSF (IRB approval number: 13–10575). Inclusion criteria to be eligible for the study were a subject age of 13 years and older and having a dentition with at least six anterior teeth.

Subjects were excluded from the study if they were suffering from systemic diseases, had a significant past or medical history with conditions that may affect oral health (i.e., diabetes, HIV, heart conditions that require antibiotic prophylaxis), or were taking medications that may affect the oral flora (e.g., antibiotic use in the past 3 months). Subjects were also excluded if they had multiple front teeth crowned, major areas of the buccal tooth surface filled, or frank caries lesions on buccal surfaces of several teeth. Subjects had to be willing to sign the “Authorization for Release of Personal Health Information and Use of Personally Unidentified Study Data for Research” form. There were no gender restrictions. Subjects who met the selection criteria were asked to provide verbal/written assent/consent themselves and/or their parent/guardian.

Fifty-five subjects were recruited for the study, including 23 females and 32 males, with an average age of 36.9 ± 17.8 year (age range 14.0 to 83.4 years). Subjects wearing brackets or having dark gingiva were also recruited in order to study the influence of dark-pigmented gingiva and orthodontic brackets on the fluorescence. To study subjects with various amounts of plaque including the range of no, low, moderate, and high amounts of plaque, a stratified recruitment based on a clinical screening of the presented plaque amount covering the front teeth was performed.

Study tests

The Turesky modification of the Quigley Hein plaque index (T-QH) [23, 24] and the Silness and Løe [25, 26] gingiva inflammation index were recorded. Pictures were recorded with the SOPROCARE system in fluorescence perio-mode and in daylight mode. Conventional digital photographs were also taken. All recorded pictures were later on assessed using the same criteria as described for the plaque and the gingival inflammation index (as defined in section T-QH and Silness & Løe (GI) for the clinical indexing). For the scoring of the recorded pictures, the pictures comprising three teeth per quadrant were magnified on a computer screen to 22 cm in width and evaluated from a distance of 60 cm.

Turesky modification of the Quigley Hein plaque index (TQ-H)

A plaque index was performed to register the amount of microbial plaque on the study teeth. The T-QH does not use a plaque disclosing agent. A score of 0 to 5 is assigned to each facial and lingual non-restored surface of all the teeth except third molars, as described in Table 1 (in this study, we only assigned plaque scores to the facial surfaces of the front teeth selected for the study). Clinically, the T-QH index is performed by probing over the tooth surface beginning from the tip of the tooth in direction to the gingival margin. The

Table 1 Criteria for Turesky modification of the Quigley and Hein plaque index

Scores	Criteria
0	No plaque
1	Separate flecks of plaque at the cervical margin of the tooth
2	A thin continuous band of plaque (up to 1 mm) at the cervical margin of the tooth
3	A band of plaque wider than 1 mm but covering less than one third of the crown of the tooth
4	Plaque covering at least one third but less than two thirds of the crown of the tooth
5	Plaque covering two thirds or more of the crown of the tooth

moment when plaque occurs at the probe tip is registered, and the according score is assigned.

Silness and Löe Gingival index (GI)

The Silness and Löe GI was assigned to register the degree of gingival inflammation. Using this index, the absence of inflammation and three levels of gingival inflammation, respectively, were registered for the facial surface of each study tooth (Table 2).

SOPROCARE perio-mode fluorescence and daylight mode pictures

The SOPROCARE camera system emits in perio-mode fluorescence mode blue light at 450-nm wavelength using three blue diodes (SOPRO Acteon Imaging, La Ciotat, France). The tooth (dentin body) fluoresces due to the blue light and is simultaneously illuminated with four white LEDs. Electronically, the image obtained through fluorescence is superimposed over the anatomic image resulting from the white light, creating a visible representation of the plaque level and tissue conditions, which are, otherwise, invisible under

Table 2 Criteria for Silness and Löe gingival index

Scores	Criteria
0	Normal, healthy gingival with sharp, non-inflamed margins
1	Marginal gingivitis with minimal inflammation and edema at the free gingiva. No bleeding on probing
2	Moderate gingivitis with a wider band of inflammation and bleeding upon probing
3	Advanced gingivitis with severe inflammation, tendency to spontaneous bleeding

white light alone. New plaque is highlighted by its white and grainy characteristics, and old plaque is revealed as shades of yellow and orange (Fig. 1a). Marginal inflammation appears as enhanced red/pink coloration [27].

In daylight mode, the white LEDs permit taking a picture without fluorescence influence. Microbial plaque on the tooth is visible as white accumulation, but gingival tissue appears pale (Fig. 1b).

In this present study, the system was used in the intra-oral mode imaging three teeth in one picture (cuspid to central incisor). The images were recorded with the SOPRO imaging software. A HP 620 Notebook (HP, Palo Alto, CA; Windows 7, Microsoft Redmond, WA) was used to collect the pictures.

Digital photography

Digital photographs were taken to allow an independent examiner to make judgments at a later point in time (Canon EOS 10D, Macro Ring Lite MR-14EX, Canon Macro Lens EF 100 mm, F1:2.8, USM, Melville, NY). Each picture included the central incisor to a cuspid area. Figure 1c shows the same tooth as in Fig. 1a, b, but the picture was taken with the digital camera.

Blinding

The junior examiner (WS) was blind to the clinical scores when evaluating the archived SOPROCARE perio-mode fluorescence and daylight mode pictures and the digital photographs. The senior examiner, who had assessed the clinical scores, performed the evaluations of archived pictures after the clinical part of the study had been finished for at least 4 weeks.

Statistical analyses

The data were analyzed by multiple statistical methods (one-way ANOVA, Newman-Keuls multiple comparison test, linear regression analysis) to compare results from the SOPROCARE daylight mode and fluorescence perio-mode assessments, the digital photography, and the clinical indices. Two examiners, one senior more experienced (PR) and one junior less-experienced (WS) examiner, assessed SOPROCARE and digital photography scores. Table 3 shows the kappa evaluations for each examiner separately (intra-examiner reliability) and between examiners (inter-examiner reliability) [28]. The reliabilities were determined for the plaque index evaluations with SOPROCARE perio-mode and daylight mode, and digital photography. Kappa values were also calculated for the GI assessments using SOPROCARE perio-mode and digital photography.

Kappa as “exact matches” and weighted kappa [29], which also considers “close matches” and accounts for how far apart the two ratings are, were calculated. The strength of agreement was also described as “poor,” “fair,” “moderate,” “good,” and “very good” [30, 31].

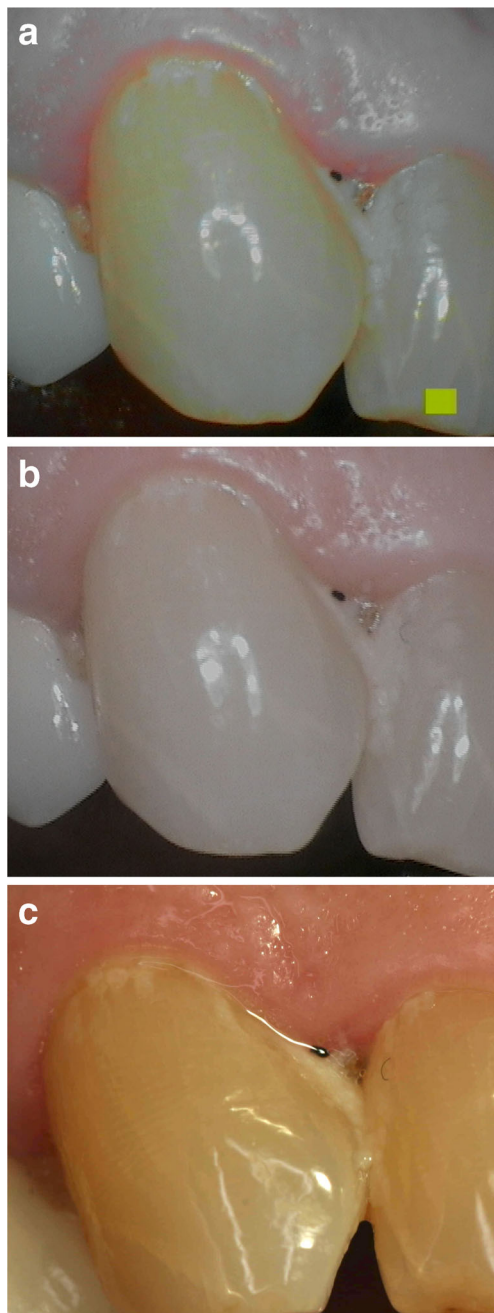


Fig. 1 **a** SPROCARE fluorescence perio-mode picture. New plaque appears *white* and *granny*, old plaque is more *yellow*, and marginal inflammation appears as enhanced *red/pink*. **b** SPROCARE daylight mode picture, same tooth as in Fig. 1a. Microbial plaque appears *white* and no red inflammation is visible. **c** Digital photography of the same tooth as in Fig. 1a, b

Results

Of the 55 recruited subjects, 8 subjects had dark gingival pigmentation, 11 were wearing orthodontic brackets, and 3 had brackets and dark gingival pigmentation. The stratified recruitment, based on the presented plaque amount covering the front teeth, provided a relatively even distribution of

subjects with different levels of microbial plaque and represented all stages of gingival inflammation (amount of plaque/number of recruited subjects; no 18, low 16, moderate 10, high 11). Table 4 shows the number of teeth with T-QH score 0 to 5 and GI score 0 to 3.

Turesky-modified Quigley Hein plaque index—averages

Six hundred and thirty-eight teeth were available for scoring with the Turesky-modified Quigley Hein criteria. The average plaque score was 1.1 ± 1.2 (mean \pm standard deviation [SD]). Figure 2 demonstrates the average registered Turesky-modified Quigley Hein plaque index. Additionally, it showed the plaque index as judged from the stored pictures captured with the SPROCARE system in fluorescence perio-mode, in daylight mode, and with digital photography.

The plaque scoring with SPROCARE in perio-mode led to a slightly higher average score than the T-QH scores. SPROCARE daylight mode plaque evaluation resulted in an even higher average plaque score, while digital photography showed the highest scores. The last two scores were significantly higher than the clinical T-QH score (SPROCARE daylight mode $P=0.013$, digital photography $P<0.0001$).

For the 33 subjects without brackets and without dark gingival pigmentation, the plaque score average was at a similar level (1.0 ± 1.1). For those showing dark gingival pigmentation, the average was slightly lower (0.9 ± 1.1), and for those wearing brackets, the plaque index was higher with an average of (1.6 ± 1.4). Nevertheless, the observed differences were not statistically significant (significance level $P>0.05$).

Linear regression fits for the clinically evaluated Turesky-modified Quigley Hein plaque index and the other assessment methods

To evaluate for each assessment method, the capacity for discrimination between two different consecutive scores, linear regression curves were calculated for each tool. Figure 3 shows the linear regression fit for the clinically evaluated T-QH plaque index versus SPROCARE perio-mode, daylight mode, and the digital photography scores. All linear regression fits were significantly different from zero. The highest goodness of fit was found for the digital photography with an $r^2=0.96$, followed by for SPROCARE daylight mode with $r^2=0.94$ and $r^2=0.92$ for SPROCARE perio-mode.

Linear regression showed that there was a “setoff” for all three methods. The Y -axis intercept describes at which level a clinically determined score of “0” is judged by an evaluation system. While the Y -axis intercept for the digital photography was the highest (1.17 ± 0.2), the Y -axis intercept for the SPROCARE daylight mode was slightly lower and lowest for the SPROCARE perio-mode evaluation (0.66 ± 0.25). All three methods lead to higher scoring values than the

Table 3 Inter- and intra-examiner reliability kappa values (kappa and weighted kappa) for assessment methods used

Method	Index	Intra-examiner kappa PR	Intra-examiner weighted kappa PR	Intra-examiner kappa WS	Intra-examiner weighted kappa WS	Inter-examiner kappa	Inter-examiner weighted kappa
SOPROCARE perio	Plaque	0.474 moderate	0.649 good	0.659 good	0.767 good	0.274 fair	0.451 moderate
	GI	0.594 moderate	0.691 good	0.013 poor	0.119 poor	0.471 moderate	0.522 moderate
SOPROCARE day	Plaque	0.613 good	0.731 good	0.070 poor	0.219 fair	0.233 fair	0.333 fair
Digital photography	Plaque	0.427 moderate	0.614 good	0.428 moderate	0.615 good	0.139 poor	0.300 fair
	GI	0.752 good	0.838 very good	0.347 fair	0.493 moderate	0.485 moderate	0.548 moderate

clinical T-QH value. Slopes of those fits, determining the capacity to differentiate between two consecutive scores, were for the digital photography fit 0.65, 95 % confidence interval (CI) (0.46, 0.83), SOPROCARE daylight mode 0.54, 95 % CI (0.36, 0.72), and for SOPROCARE perio-mode 0.53, 95 % CI (0.31, 0.76).

Figure 4 shows linear regression curves for the two examiners demonstrating that the above-mentioned setoff was smaller for the senior and larger for junior examiner for the SOPROCARE fluorescence mode evaluation.

Both linear regression fits were significantly different from zero with high goodness for fit ($r^2=0.9683$ senior and 0.9152 junior examiner). Nevertheless, the slope of those fits, the capacity to differentiate between two consecutive scores, was low (0.32, 95 % CI (0.24, 0.40)) for “SOPROCARE junior examiner” and higher for “SOPROCARE senior examiner” (0.53, 95 % CI (0.31, 0.76)). At the highest plaque levels (T-QH 5), both linear fits were at a similar level. At lower plaque levels, the SOPROCARE junior examiner regression line stayed at high levels and intercepts with the Y-axis at a score twice as high as SOPROCARE senior examiner.

A reason for a larger setoff, specifically at lower clinical plaque scores, was that at “plaque-free” patients, yellow lines at the gingival margins were visible. These yellow lines possibly mislead the examiner in scoring plaque. Figure 5a, b

shows SOPROCARE perio-mode pictures of a clinically plaque-free patient.

Silness and Löe gingival inflammation index—averages

All 638 teeth were available for evaluating the Silness and Löe GI. For all subjects, the average GI was 0.7 ± 0.9 (mean \pm SD). Subjects with brackets showed a slightly higher inflammation index (0.8 ± 1.0). The index was lower for the subjects with gingival pigmentations and no brackets (0.3 ± 0.7), but differences between all groups were not statistically significant.

Figure 6 depicts the comparison between the clinically evaluated Silness and Löe GI and the indices evaluated on SOPROCARE perio-mode, daylight mode, and digital photography pictures for all 55 subjects. Evaluated with SOPROCARE perio-mode, the GI was with 0.6 ± 0.9 slightly lower than the clinically evaluated Silness and Löe plaque index.

Table 4 Number of teeth with T-QH scores 0 to 5 and GI scores 0 to 3

T-QH score	No. of teeth	GI score	No. of teeth
0	267	0	382
1	165	1	134
2	112	2	81
3	60	3	41
4	27		
5	7		

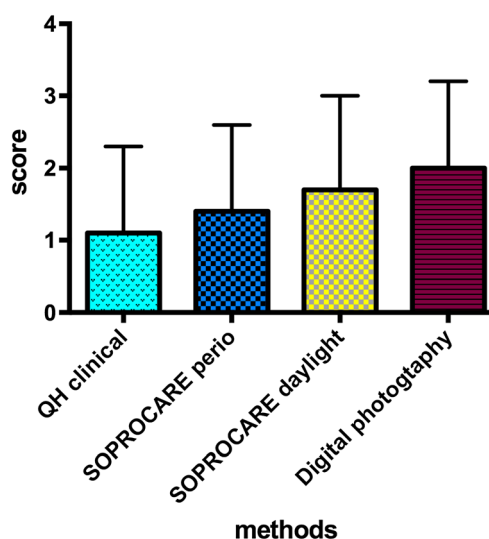


Fig. 2 Average Turesky-modified Quigley Hein plaque index, clinically registered and scored on SOPROCARE perio-mode, SOPROCARE daylight mode, and digital photography pictures (mean \pm SD)

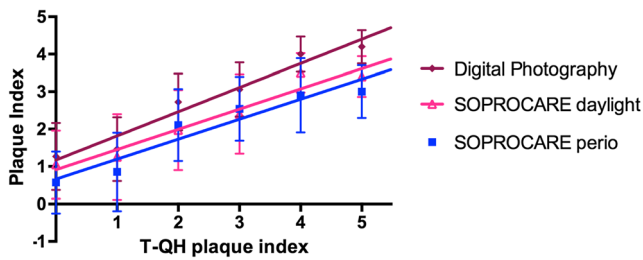


Fig. 3 Linear regression fits for Turesky-modified Quigley Hein plaque index and the plaque indices evaluated by SOPROCARE perio-mode, SOPROCARE daylight mode, and digital photography (mean±SD)

The results for scoring on digital photography pictures showed slightly lower averages than the clinical evaluation. Nevertheless, the observed differences were not statistically significant.

The data also showed that none of the evaluation tools was significantly influenced in determining a GI by the presence or absence of dark gingival pigmentation or the presence or absence of orthodontic brackets. The group with dark gingival pigmentations showed an overall lower clinical Silness and Løe GI than the other groups, but all evaluation tools for this group showed a similar lower GI.

Linear regression fits for the Silness and Løe gingival index and two other assessment methods

To evaluate for the assessment methods SOPROCARE perio-mode and digital photography, the discrimination between two different consecutive scores, again linear regression fit curves were calculated (Fig. 7). The linear regression fits were significantly different from zero with high goodness of fit values for both methods ($r^2=0.96$ for both methods). The slopes for those fits were highest for the digital photography (0.76, 95 % CI (0.33, 1.19)) and only slightly lower for SOPROCARE perio-mode (0.66, 95 % CI (0.27, 1.05)). The linear regression demonstrated that there is only a slight setoff for both methods.

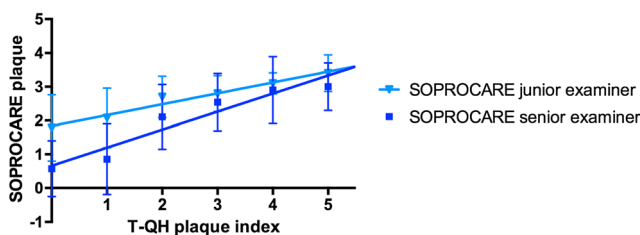


Fig. 4 Linear regression fits for clinically evaluated Turesky-modified Quigley Hein plaque index and plaque indices evaluated by SOPROCARE in perio-mode fluorescence mode, for a junior and a senior examiner (mean±SD)

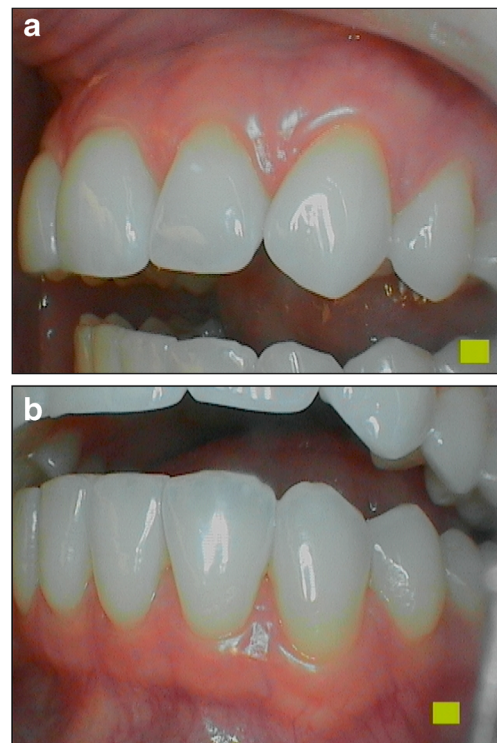


Fig. 5 The pictures represent a clinically plaque-free patient: **a** upper left and **b** lower left side with a T-QH score 0, S&L score 0; notice the “yellow” line at the gingival margin—possibly misleading a less-trained examiner to assume that microbial plaque is present

Discussion

The use of clinical photography among general dentist is common. Photographs can be an important and accurate part of patient records specifically with respect to litigations [32].

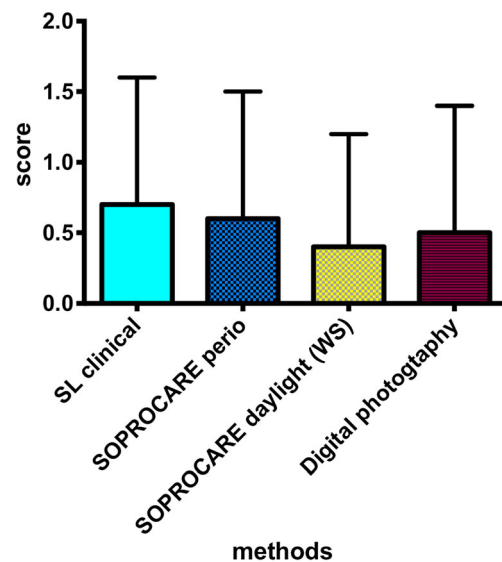


Fig. 6 Average gingival inflammation index evaluated with the different evaluation methods. All applied methods show slightly lower values than the clinically evaluated Silness and Løe gingival index. The observed differences were not statistically significant (mean±SD)

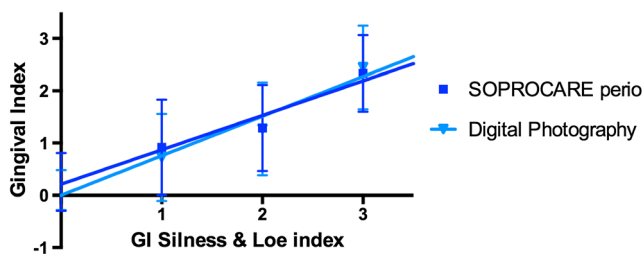


Fig. 7 Linear regression fits for Silness and Loe Gingival index scores and the gingival indices evaluated by SOPROCARE perio-mode and digital photography (mean±SD)

Digital photography simplifies the process of picture taking [33] for treatment planning and patient instruction and motivation [34–36].

Clinical studies have shown that digital photography is superior in intra-oral reliability testing when compared to unaided visual examination and an operating microscope by improving the restorative treatment decisions of the occlusal surfaces on posterior teeth [37, 38]. Digital photography can enhance objectivity and inter-professional communication [39, 40]. Another study reported that sensitivity, specificity, and the likelihood ratio of scoring caries on photographs made with an intra-oral camera were favorable. The inter- and intra-observer reliability for caries was good to excellent suggesting the use of intra-oral photographs in clinical practice and large epidemiological studies [41]. Several fluorescence camera systems have been employed for early caries detection [12, 42, 43], but there has been no system that images microbial plaque and gingival inflammation using natural blue light fluorescence and an intra-oral camera.

Microbial plaque

Dental plaque traditionally has been made clinically visible by using disclosing agents like erythrosine and fluorescein [8, 44]. Cameras using ultraviolet light sources with and without fluorescein dye application [7, 44, 45] have also been employed for plaque documentation at patients. In contrast, the SOPROCARE system uses LED light that emits in the visible blue spectra and does not require any cumbersome use of disclosing agents.

Evaluating the SOPROCARE detection camera system in comparison to a typical clinical plaque indexing method revealed the capacity of the SOPROCARE fluorescence system in perio-mode to assess and score microbial plaque levels. Blue light has been used in laboratory settings for detection of dental calculus [46] as well as for selective removal of microbial plaque and calculus [47–49].

The observed minimal higher scoring of microbial plaque using the SOPROCARE system in daylight mode or the professional digital camera system equipped with a ring flash might simply be explained by the magnification all systems offer. In addition in the fluorescence mode, the white plaque

typically is colored and contrasts better to the white enamel background.

At the beginning of this study, it was speculated that orthodontic brackets might show strong reflections of the illuminating (blue) light and thus interfere with the fluorescence picture received from microbial plaque. Nevertheless, orthodontic brackets that were resin-bonded to the buccal surfaces of the anterior teeth of the 14 subjects in orthodontic treatment did not influence the capturing of the pictures or analyzing the stored pictures. Obviously, the light intensities of the new system are below causing serious reflections from metal objects.

All systems tested in this study have the capacity to easily discriminate between two scores. The linear regression fits underline that the SOPROCARE perio-mode method shows a slight setoff in positive direction, but less than the SOPROCARE daylight mode or even the digital photography. Since the microbial plaque evaluation with SOPROCARE fluorescence tool in perio-mode showed that the plaque level was marginally overestimated and thus scored at slightly elevated levels, the use of the tool might be specifically indicated in patient education and motivation by dentist and dental hygienists.

This study also showed that the slopes of the regression fits for the junior evaluator were typically less steep with a higher setoff. It is possible that when only a small amount of microbial plaque is present on the tooth surface, the score is overestimated. If there is a large amount of microbial plaque present easily pictured by the fluorescence system, the correct score is more accurately attainable. To prevent overestimation with overscoring of plaque, training on teeth with no or low plaque is needed. Consequently, the risk that each yellowish change of a tooth especially visible at the gingival margin is scored as positive for existing microbial plaque would be reduced. These yellow lines most probably originate from porphyrins derived from periodontal bacteria that are stored in porosities of the cervical enamel and root dentin structure.

Gingival inflammation

To study inflammation, Doppler flowmetry [50] and spectral imaging to identify erythema distribution in the gingival tissue [51] have been discussed but only in laboratory settings. Digital camera systems have also been tried to assess gingival inflammation and overgrowth [52].

This study here demonstrated the ability of the SOPROCARE fluorescence camera system in perio-mode to detect gingival inflammation, which helped in scoring inflammation levels. Despite possible fluorescence from the inflamed tissues possibly helping the fluorescence system, the clinical scoring revealed a slightly higher index. The results showed that, obviously, when using the fluorescence tool, no overscoring occurred.

Scoring inflammation with digital photography and SOPROCARE daylight mode showed even lower values than the clinical scoring. Since signs of inflammation include the absence or presence of visible “redness” of the gingiva, which assists a clinician in weighting inflammation [53–55], the SOPROCARE daylight mode system is at a disadvantage in assessing gingival inflammation. The daylight mode significantly suppresses the red gingiva color by using the additional white light. Nevertheless, since all observed differences were very small and not statistically significant, they appear not be clinically relevant.

Subgroups with no orthodontic brackets and no dark gingival pigmentation, and those with dark gingival pigmentation but no brackets, showed no differences in the scoring distribution patterns over the three systems. While those with dark-pigmented gingiva showed clinically a much lower Silness and Løe inflammation index, all different levels of gingival inflammation were present and could be differentiated. It may be appropriate to conclude that dark-pigmented gingiva does not impede the SOPROCARE fluorescence perio-mode camera system in the detection of an accurate gingiva inflammation level.

As already discussed above, training may reduce overscoring. The need for a basic training with all different assessment tools became again obvious when looking at the intra-examiner kappa values. The senior examiner showed better intra-examiner reliability than the less-experienced junior examiner when the intra-examiner reliability was compared between the two examiners. Training will improve the intra-examiner reliability. Since the inter-examiner reliability compares how well two examiners agree on a score, it is not surprising that the inter-examiner agreement in this study due to different experience levels was also low.

Conclusion

Within the limitations of this study, the SOPROCARE fluorescence assessment tool in perio-mode allows reliable evaluation of microbial plaque and gingival inflammation levels. This scoring of microbial plaque and gingival inflammation level is consistent with the established Turesky-modified Quigley Hein and the Silness and Løe GI. Training on plaque-free teeth will actually reduce overscoring errors. Evaluation of plaque and gingival inflammation levels can also be performed on stored pictures. Those pictures can be used for patient education and motivation but also may be consulted and compared by the dentist and dental hygienist at a patient recall visit.

Acknowledgments This work presented was supported by a grant from Acteon, France, through the Contracts & Grants Division at UCSF representing the Regents of the University of California. The authors want to thank Dr. John Kornak, Department of Epidemiology and Biostatistics, UCSF, for his statistical advices and Dr. Richard Kinsel, Preventive and Restorative Dental Sciences, School of Dentistry, UCSF, for his editorial assistance.

Conflict of interest The authors declare that they have no conflict of interest.

References

1. Brook I (2003) Microbiology and management of periodontal infections. *Gen Dent* 51(5):424–428
2. Neely AL, Holford TR, Loe H, Anerud A, Boysen H (2001) The natural history of periodontal disease in man. Risk factors for progression of attachment loss in individuals receiving no oral health care. *J Periodontol* 72(8):1006–1015
3. Schatzle M, Loe H, Burgin W et al (2003) Clinical course of chronic periodontitis. I. Role of gingivitis. *J Clin Periodontol* 30(10):887–901
4. Loe H, Theilade E, Jensen SB (1965) Experimental gingivitis in man. *J Periodontol* 36:177–187
5. Theilade E, Wright WH, Jensen SB, Loe H (1966) Experimental gingivitis in man. II. A longitudinal clinical and bacteriological investigation. *J Periodontol* 1:1–13
6. Sharma NC, Qaqish J, Klukowska M, Grender J, Rooney J (2011) The plaque removal efficacy of a novel power brush head. *J Clin Dent* 22(1):19–22
7. Raggio DP, Braga MM, Rodrigues JA et al (2010) Reliability and discriminatory power of methods for dental plaque quantification. *J Appl Oral Sci: Rev FOB* 18(2):186–193
8. Claydon N, Yates R, Labello R et al (2004) A methodology using subjective and objective measures to compare plaque inhibition by toothpastes. *J Clin Periodontol* 31(12):1106–1109
9. Gillings BR (1977) Recent developments in dental plaque disclosants. *Aust Dent J* 22(4):260–266
10. Gallagher IH, Fussell SJ, Cutress TW (1977) Mechanism of action of a two-tone plaque disclosing agent. *J Periodontol* 48(7):395–396
11. Lim LP, Tay FB, Waite IM, Comick DE (1986) A comparison of 4 techniques for clinical detection of early plaque formed during different dietary regimes. *J Clin Periodontol* 13(7):658–665
12. Rechmann P, Charland D, Rechmann BM, Featherstone JD (2012) Performance of laser fluorescence devices and visual examination for the detection of occlusal caries in permanent molars. *J Biomed Opt* 17(3):036006
13. Rechmann P, Rechmann BM, Featherstone JD (2012) Caries detection using light-based diagnostic tools. *Compend Contin Educ Dent* 33(8):582–584, 86, 88–93; quiz 94, 96
14. Lussi A, Imwinkelried S, Pitts N, Longbottom C, Reich E (1999) Performance and reproducibility of a laser fluorescence system for detection of occlusal caries in vitro. *Caries Res* 33(4):261–266
15. König K, Flemming G, Hibst R (1998) Laser-induced autofluorescence spectroscopy of dental caries. *Cell Mol Biol* 44(8):1293–1300
16. Lussi A, Hibst R, Paulus R (2004) DIAGNOdent: an optical method for caries detection. *J Dent Res*. 83 Spec No C:C80-3
17. Verdonchot EH, van der Veen MH (2002) Lasers in dentistry 2. Diagnosis of dental caries with lasers. *Ned Tijdschr Tandheelkd* 109(4):122–126

18. de Josselin de Jong E, Sundstrom F, Westerling H et al (1995) A new method for in vivo quantification of changes in initial enamel caries with laser fluorescence. *Caries Res* 29(1):2–7
19. Tranaeus S, Al-Khateeb S, Bjorkman S, Twetman S, Angmar-Mansson B (2001) Application of quantitative light-induced fluorescence to monitor incipient lesions in caries-active children. A comparative study of remineralisation by fluoride varnish and professional cleaning. *Eur J Oral Sci* 109(2):71–75
20. Tranaeus S, Shi XQ, Lindgren LE, Trollsas K, Angmar-Mansson B (2002) In vivo repeatability and reproducibility of the quantitative light-induced fluorescence method. *Caries Res* 36(1):3–9
21. Yin W, Feng Y, Hu D, Ellwood RP, Pretty IA (2007) Reliability of quantitative laser fluorescence analysis of smooth surface lesions adjacent to the gingival tissues. *Caries Res* 41(3):186–189
22. Jablonski-Momeni A, Heinzel-Gutenbrunner M, Klein SM (2014) In vivo performance of the VistaProof fluorescence-based camera for detection of occlusal lesions. *Clin Oral Investig* 18(7):1757–1762
23. Turesky S, Gilmore ND, Glickman I (1970) Reduced plaque formation by the chloromethyl analogue of vitamin C. *J Periodontol* 41(1):41–43
24. Quigley GA, Hein JW (1962) Comparative cleansing efficiency of manual and power brushing. *J Am Dent Assoc* 65:26–29
25. Loe H, Silness J (1963) Periodontal disease in pregnancy. I. Prevalence and severity. *Acta Odontol Scand* 21:533–551
26. Loe H (1967) The gingival index, the plaque index and the retention index systems. *J Periodontol* 38(6):Suppl:610–616
27. Acteon-Sopro SOPROCARE The Revelation (2012) <http://www.soprocare.fr/wp-content/uploads/2012/05/Plaq-Soprocare-UK.pdf>
28. Cohen J (1960) A coefficient of agreement for nominal scales. *Educ Psychol Meas* 20(1):37–46
29. Cohen J (1968) Weighted kappa: nominal scale agreement with provision for scaled disagreement or partial credit. *Psychol Bull* 70(4):213–220
30. GraphPad. Quantify agreement with Kappa—assess how well two observers classify subjects into groups. In: Kappa QAW (ed) GraphPad software incorporated; 2011. p. QuickCalcs Online Calculators for Scientists
31. Landis JR, Koch GG (1977) The measurement of observer agreement for categorical data. *Biometrics* 33(1):159–174
32. Wander P, Ireland RS (2014) Dental photography in record keeping and litigation. *Br Dent J* 217(3):133–137
33. Sharland MR (2004) Digital imaging for the general dental practitioner: 2. Intra-oral imaging. *Dent Update* 31(6):328–332
34. Morse GA, Haque MS, Sharland MR, Burke FJ (2010) The use of clinical photography by UK general dental practitioners. *Br Dent J* 208(1), E1, discussion 14–5
35. Freedman G (2002) Intraoral cameras: patient education and motivation. *Dent Today* 21(4):126–131
36. McLaren EA, Garber DA, Figueira J (2013) The Photoshop smile design technique (part 1): digital dental photography. *Compend Contin Educ Dent* 34(10):772, 74, 76 passim
37. Erten H, Uctasli MB, Akarslan ZZ, Uzun O, Semiz M (2006) Restorative treatment decision making with unaided visual examination, intraoral camera and operating microscope. *Oper Dent* 31(1):55–59
38. Erten H, Uctasli MB, Akarslan ZZ, Uzun O, Baspinar E (2005) The assessment of unaided visual examination, intraoral camera and operating microscope for the detection of occlusal caries lesions. *Oper Dent* 30(2):190–194
39. Staudt CB, Kinzel S, Hassfeld S et al (2001) Computer-based intraoral image analysis of the clinical plaque removing capacity of 3 manual toothbrushes. *J Clin Periodontol* 28(8):746–752
40. Gallegos AG (2001) Enhancing interprofessional communication through digital photography. *J Calif Dent Assoc* 29(10):752–757
41. Elfrink ME, Veerkamp JS, Aartman IH, Moll HA, Ten Cate JM (2009) Validity of scoring caries and primary molar hypomineralization (DMH) on intraoral photographs. *Eur Arch Paediatr Dent* 10(Suppl 1):5–10
42. Amaechi BT, Ramalingam K (2014) Evaluation of fluorescence imaging with reflectance enhancement technology for early caries detection. *Am J Dent* 27(2):111–116
43. Tassery H, Levallois B, Terrer E et al (2013) Use of new minimum intervention dentistry technologies in caries management. *Aust Dent J* 58(Suppl 1):40–59
44. Baab DA, Broadwell AH, Williams BL (1983) A comparison of antimicrobial activity of four disclosant dyes. *J Dent Res* 62(7):837–841
45. Checchi L, Forteleoni G, Pelliccioni GA, Loriga G (1997) Plaque removal with variable instrumentation. *J Clin Periodontol* 24(10):715–717
46. Qin Y, Luan X, Bi L et al (2007) Real-time detection of dental calculus by blue-LED-induced fluorescence spectroscopy. *J Photochem Photobiol B Biol* 87(2):88–94
47. Schoenly JE, Seka W, Featherstone JD, Rechmann P (2012) Near-UV laser treatment of extrinsic dental enamel stains. *Lasers Surg Med* 44(4):339–345
48. Schoenly JE, Seka W, Rechmann P (2014) Pulsed laser ablation of dental calculus in the near ultraviolet. *J Biomed Opt* 19(2):028003
49. Rechmann P, Hennig T (2001) Lasers in periodontology, today and tomorrow. *Med Laser Appl* 16(3):223–230
50. Orekhova LY, Barmasheva AA (2013) Doppler flowmetry as a tool of predictive, preventive and personalised dentistry. *EPMA J* 4(1):21
51. Zakian C, Pretty I, Ellwood R, Hamlin D (2008) In vivo quantification of gingival inflammation using spectral imaging. *J Biomed Opt* 13(5):054045
52. Smith RN, Lath DL, Rawlinson A, Karmo M, Brook AH (2008) Gingival inflammation assessment by image analysis: measurement and validation. *Int J Dent Hyg* 6(2):137–142
53. Winkel EG, Abbas F, Van der Velden U et al (1987) Experimental gingivitis in relation to age in individuals not susceptible to periodontal destruction. *J Clin Periodontol* 14(9):499–507
54. Baumgartner WJ, Weis RP, Reyher JL (1966) The diagnostic value of redness in gingivitis. *J Periodontol* 37(4):294–297
55. Seshan H, Shwetha M (2012) Gingival inflammation assessment: image analysis. *J Indian Soc Periodontol* 16(2):231–234